# MECHANISMS OF VESSEL DEVELOPMENT: FROM A PRIMITIVE DRAFT TO A MATURE VASCULATURE

EDITED BY: Tullio Genova, Sara Petrillo, Anna Rita Cantelmo and Luca Munaron

PUBLISHED IN: Frontiers in Physiology

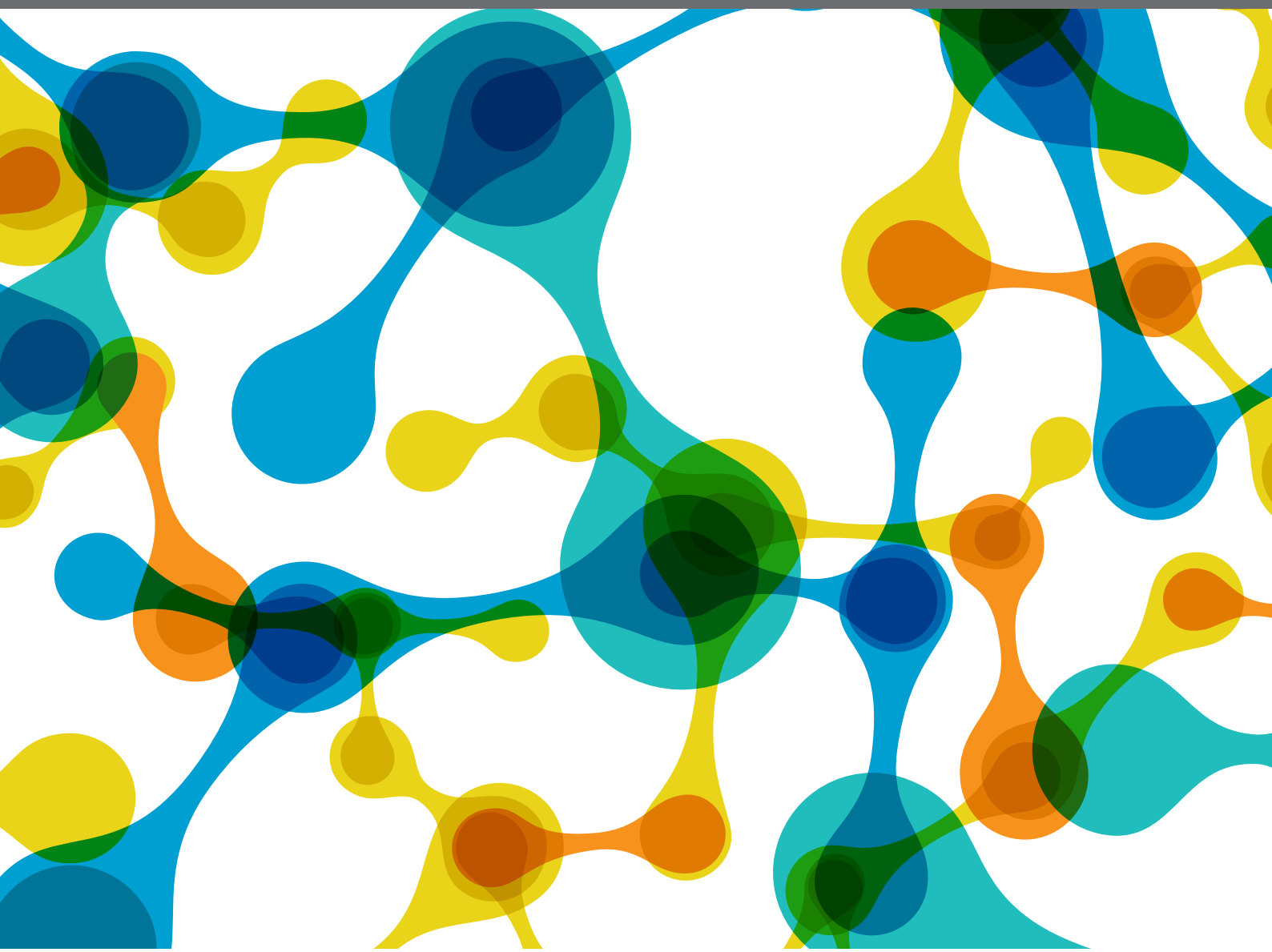

frontiers Research Topics

# frontiers



ISSN 1664-8714
ISBN 978-2-88971-335-6
DOI 10.3389/978-2-88971-335-6

## About Frontiers

Frontiers is more than just an open-access publisher of scholarly articles: it is a pioneering approach to the world of academia, radically improving the way scholarly research is managed. The grand vision of Frontiers is a world where all people have an equal opportunity to seek, share and generate knowledge. Frontiers provides immediate and permanent online open access to all its publications, but this alone is not enough to realize our grand goals.

## Frontiers Journal Series

The Frontiers Journal Series is a multi-tier and interdisciplinary set of open-access, online journals, promising a paradigm shift from the current review, selection and dissemination processes in academic publishing. All Frontiers journals are driven by researchers for researchers; therefore, they constitute a service to the scholarly community. At the same time, the Frontiers Journal Series operates on a revolutionary invention, the tiered publishing system, initially addressing specific communities of scholars, and gradually climbing up to broader public understanding, thus serving the interests of the lay society, too.

## Dedication to Quality

Each Frontiers article is a landmark of the highest quality, thanks to genuinely collaborative interactions between authors and review editors, who include some of the world's best academicians. Research must be certified by peers before entering a stream of knowledge that may eventually reach the public - and shape society; therefore, Frontiers only applies the most rigorous and unbiased reviews.
Frontiers revolutionizes research publishing by freely delivering the most outstanding research, evaluated with no bias from both the academic and social point of view. By applying the most advanced information technologies, Frontiers is catapulting scholarly publishing into a new generation.

## What are Frontiers Research Topics?

Frontiers Research Topics are very popular trademarks of the Frontiers Journals Series: they are collections of at least ten articles, all centered on a particular subject. With their unique mix of varied contributions from Original Research to Review Articles, Frontiers Research Topics unify the most influential researchers, the latest key findings and historical advances in a hot research area! Find out more on how to host your own Frontiers Research Topic or contribute to one as an author by contacting the Frontiers Editorial Office: frontiersin.org/about/contact

# MECHANISMS OF VESSEL DEVELOPMENT: FROM A PRIMITIVE DRAFT TO A MATURE VASCULATURE

Topic Editors:
**Tullio Genova,** University of Turin, Italy
**Sara Petrillo,** University of Turin, Italy
**Anna Rita Cantelmo,** Université Lille Nord de France, France
**Luca Munaron,** University of Turin, Italy

**Citation:** Genova, T., Petrillo, S., Cantelmo, A. R., Munaron, L., eds. (2021). Mechanisms of Vessel Development: From a Primitive Draft to a Mature Vasculature. Lausanne: Frontiers Media SA. doi: 10.3389/978-2-88971-335-6

# Table of Contents

frontiers in Physiology

EDITORIAL
published: 16 July 2021
doi: 10.3389/fphys.2021.725531

# Editorial: Mechanisms of Vessel Development: From a Primitive Draft to a Mature Vasculature

*Sara Petrillo*[1]*, *Anna Rita Cantelmo*[2], *Tullio Genova*[3] and *Luca Munaron*[3]

[1] Department of Molecular Biotechnology and Health Sciences, Molecular Biotechnology Center (MBC), University of Turin, Turin, Italy, [2] University Lille, Inserm, U1003—PHYCEL—Physiologie Cellulaire, Lille, France, [3] Department of Life Sciences and Systems Biology, University of Turin, Turin, Italy

**Keywords: endothelial cell heterogeneity, vascular remodeling, vascular maturation, blood flow, vessel enlargement**

**Editorial on the Research Topic**

**Mechanisms of Vessel Development: From a Primitive Draft to a Mature Vasculature**

## TISSUE-SPECIFIC ENDOTHELIAL CELL HETEROGENEITY

Vascular heterogeneity has become a hot topic over the past 5 years. New and advanced molecular techniques, such as single-cell sequencing (scRNA-seq), have contributed to answer fundamental questions on how the different phenotypes adopted by endothelial cells (ECs) in the organ in which they reside shape the architecture and function of the vasculature. Understanding tissue-specific EC heterogeneity is crucial for targeted therapies which aim to deliver therapeutic agents to specific organs. Although vessel heterogeneity is defined by signals from the tissue microenvironment, the picture is much more complex than anticipated as gene expression patterns have been found shared among different tissue types. In this regard, Fleischer et al. provided an extensive overview of the structural and functional properties of ECs among tissue-specific vascular beds, highlighting the contribution of EC plasticity to pathological angiogenesis.

Endocrine signals ensure a peculiar vascular niche that is directly involved in the temporal control of hormone secretion and entry into the bloodstream (Stucker et al.). The complex interplay between endothelial and endocrine cells underlies the endocrine function. Consequently, vascular alterations may lead to endocrine disorders. Among the endocrine organs, the adipose tissue and its dense vascular network, have gained attention. Herold and Kalucka highlighted the role of the vascular system in the regulation of adipocyte function and adipogenesis. Interestingly, obesity is characterized by an angiogenesis-dependent rapid expansion of the adipose tissue: such dysfunctional environment is sustained by alterations in the paracrine signaling that governs the crosstalk between adipocytes and ECs. This evidence suggests that angiogenesis may be targeted for therapeutic purpose to ameliorate the complications and comorbidities associated to obesity.

Alfaidy et al. gave us another example of how a deep comprehension of the mechanisms involved in tissue-specific angiogenesis can provide novel tools for the treatment of human diseases. They discussed in detail the contribution of endocrine gland derived-vascular endothelial growth factor (EG-VEGF) in placental vascularization during pregnancy. Importantly, EG-VEGF is a member of the prokineticin family and a placental pro-angiogenic factor that has been proposed as a biomarker in preeclampsia, one of the most threatening pregnancy disorders.

Several zebrafish and mouse model systems contributed to the understanding of the complex brain vessel patterning. Brain ECs show many peculiarities, especially in light of their interaction with astrocytes and neurons within the neurovascular unit. Although significant progress has so far been made in characterizing brain endothelium, yet much is unknown regarding how brain

OPEN ACCESS

***Edited and reviewed by:***
*Gerald A. Meininger, University of Missouri, United States*

***Correspondence:**
*Sara Petrillo*
*sara.petrillo@unito.it*

***Specialty section:***
*This article was submitted to Vascular Physiology, a section of the journal Frontiers in Physiology*

***Received:*** *15 June 2021*
***Accepted:*** *22 June 2021*
***Published:*** *16 July 2021*

***Citation:***
*Petrillo S, Cantelmo AR, Genova T and Munaron L (2021) Editorial: Mechanisms of Vessel Development: From a Primitive Draft to a Mature Vasculature. Front. Physiol. 12:725531. doi: 10.3389/fphys.2021.725531*

vessels organize. Gupta et al. comprehensively summarized all the established, new and emerging concepts in brain vascular development. A crucial issue in the study of brain ECs concerns the difficulty to obtain reliable *in vitro* models that mimic the physiological complexity of the blood brain barrier. Indeed, mammalian primary brain ECs easily lose their barrier function upon culture. A rigorous phenotypic characterization is therefore fundamental to assess the value of EC culture models. Lu et al. addressed this point in depth and clearly demonstrated that human pluripotent stem cells (hPSCs)-derived brain microvascular ECs (iBMEC) are not phenotypically comparable to primary human brain microvascular cells (BMECs), but rather display the features of an epithelial barrier. The need for single-cell level analysis as scRNA-seq for proper characterization of hPSCs-derived ECs also emerges from the work of Helle et al. Indeed, they showed that despite hPSC-derived ECs can adequately respond to flow-induced shear stress, they nevertheless retain an immature nature and tendency to transdifferentiate, making them different from primary ECs.

Vascular alterations in the central nervous system (CNS) are very detrimental and often not compatible with life. Moreover, vessels modifications are involved in the pathophysiology of glioblastoma (GB), one of the most aggressive CNS tumors in adults. The morphological and functional features of the brain tumor vasculature in GB have been extensively described by Guyon et al. Interestingly, the authors provided an excursus of useful tools that allow reproducing and studying tumor-stroma interactions and can be exploited for therapeutic applications. Among them, tissue-engineered blood vessels and 3D co-culture models represent an attractive alternative to animal models and may be used in drug-screening to identify improved therapies.

## CELL DYNAMICS IN SHAPING VASCULAR REMODELING

Newly formed vessels are immature, and they must undergo remodeling to achieve a functional network. Microvascular remodeling is a dynamic process, which reflects the dynamic nature of blood flow. Santamaría et al. provided a comprehensive description of the mechanisms that drive remodeling, from the crucial role of flow forces to the chemical signals and mechanical cues involved. To reach an adequate vascular patterning, ECs integrate mechanical and chemical signals and translate them into functional behaviors. Interestingly, Vion et al. showed that vascular endothelial growth factor receptor 2 (VEGFR2) is a sensor able to integrate chemical and mechanical information and control cell shape.

Importantly, blood flow is a master regulator of vascular remodeling not only by promoting vessel pruning or splitting, but also by regulating vessel enlargement. The critical role played by vessel enlargement during both development and adulthood has been discussed by Gifre-Renom and Jones, who highlighted the mechanisms involved in the process, yet pointing out the need for further studies that may open new translational opportunities.

A deeper understanding of the molecular factors which dynamically shape the transcriptional landscape of ECs under different environmental and developmental conditions, is also fundamental. In the last years, several molecular players involved in vascular maturation and remodeling have been identified. In their review, Doronzo et al. summarized the latest advances on the transcription factor EB (TFEB), which acts as a hub in vessel remodeling and maturation by activating specific genetic programs currently under investigation.

Finally, an interesting perspective and promising strategy for therapeutic angiogenesis comes from emerging studies on resident endothelial progenitors' dynamics. Endothelial colony forming cells (ECFCs) are endothelial progenitors that are mobilized in the peripheral blood to maintain endothelial homeostasis and/or facilitate neovascularization in diseased tissue. Moccia et al. addressed this topic, and reported the most advanced strategies enrolled to boost the regenerative potential of ECFCs, including intracellular calcium mobilization upon stimulation with light.

## AUTHOR CONTRIBUTIONS

All authors listed have made a substantial, direct and intellectual contribution to the work, and approved it for publication.

## ACKNOWLEDGMENTS

We are grateful to all contributors of this Research Topic. Furthermore, we thank the reviewers who helped us to create an interesting and high-quality Research Topic. We hope that readers will enjoy reading this Research Topic as much as we have enjoyed editing it.

**Conflict of Interest:** The authors declare that the research was conducted in the absence of any commercial or financial relationships that could be construed as a potential conflict of interest.

frontiers in Physiology

ORIGINAL RESEARCH
published: 15 October 2020
doi: 10.3389/fphys.2020.591450

# Flow-Induced Transcriptomic Remodeling of Endothelial Cells Derived From Human Induced Pluripotent Stem Cells

*Emmi Helle[1,2†], Minna Ampuja[1†], Laura Antola[1] and Riikka Kivelä[1,3*]*

[1] Stem Cells and Metabolism Research Program, Faculty of Medicine, University of Helsinki, Helsinki, Finland, [2] New Children's Hospital, and Pediatric Research Center Helsinki University Hospital, Helsinki, Finland, [3] Wihuri Research Institute, Helsinki, Finland

The vascular system is essential for the development and function of all organs and tissues in our body. The molecular signature and phenotype of endothelial cells (EC) are greatly affected by blood flow-induced shear stress, which is a vital component of vascular development and homeostasis. Recent advances in differentiation of ECs from human induced pluripotent stem cells (hiPSC) have enabled development of *in vitro* experimental models of the vasculature containing cells from healthy individuals or from patients harboring genetic variants or diseases of interest. Here we have used hiPSC-derived ECs and bulk- and single-cell RNA sequencing to study the effect of flow on the transcriptomic landscape of hiPSC-ECs and their heterogeneity. We demonstrate that hiPS-ECs are plastic and they adapt to flow by expressing known flow-induced genes. Single-cell RNA sequencing showed that flow induced a more homogenous and homeostatically more stable EC population compared to static cultures, as genes related to cell polarization, barrier formation and glucose and fatty acid transport were induced. The hiPS-ECs increased both arterial and venous markers when exposed to flow. Interestingly, while in general there was a greater increase in the venous markers, one cluster with more arterial-like hiPS-ECs was detected. Single-cell RNA sequencing revealed that not all hiPS-ECs are similar even after sorting, but exposing them to flow increases their homogeneity. Since hiPS-ECs resemble immature ECs and demonstrate high plasticity in response to flow, they provide an excellent model to study vascular development.

**Keywords: endothelial cells, induced pluripotent stem cells, shear stress, flow, single-cell RNA sequencing, RNA sequencing**

OPEN ACCESS

***Edited by:***
*Tullio Genova, University of Turin, Italy*

***Reviewed by:***
*Shijun Hu, Soochow University, China*
*Ngan F. Huang, Stanford University, United States*

****Correspondence:***
*Riikka Kivelä*
*riikka.kivela@helsinki.fi*

*† These authors have contributed equally to this work*

***Specialty section:***
*This article was submitted to Vascular Physiology, a section of the journal Frontiers in Physiology*

***Received:*** *04 August 2020*
***Accepted:*** *16 September 2020*
***Published:*** *15 October 2020*

***Citation:***
*Helle E, Ampuja M, Antola L and Kivelä R (2020) Flow-Induced Transcriptomic Remodeling of Endothelial Cells Derived From Human Induced Pluripotent Stem Cells. Front. Physiol. 11:591450. doi: 10.3389/fphys.2020.591450*

## INTRODUCTION

Endothelial cells (ECs) are present in all tissues, and they regulate the development, growth and function of all organs. Endothelial dysfunction has been implicated as a major cause of many developmental defects and several adulthood diseases (Feng et al., 2002). Human induced pluripotent stem cell-derived endothelial cells (hiPS-EC) show great promise for disease modeling, drug discovery and regenerative medicine, as they can be obtained from healthy individuals as well

as from patients harbouring genetic variants or diseases of interest. A number of protocols have been described to derive ECs from hiPSCs. When compared to primary ECs, hiPS-ECs have more embryonic-like gene signatures, but they demonstrate similar functional properties as primary ECs, such as 3D tube formation, barrier function and response to inflammatory stimuli (Orlova et al., 2014a,b; Halaidych et al., 2018).

ECs are constantly exposed to shear stress *in vivo*. Shear stress regulates diverse physiological processes in health and disease. Laminar shear stress induced by blood flow is an essential regulator of blood vessel development (Campinho et al., 2020), and it promotes endothelial cell quiescence, which is required for vascular homeostasis (Baeyens et al., 2016). Multiple pathways classically known to be involved in embryonic development, such as BMP–TGFβ, WNT, NOTCH, HIF1α, TWIST1, and HOX family genes, are regulated by shear stress in adult arteries. Mechanical activation of these pathways likely evolved to orchestrate vascular development, but they can also drive atherosclerosis upon disturbed flow and low shear stress.

Even though hiPSC-derived ECs do not fully recapitulate the phenotype and function of adult ECs, they provide an excellent tool to model tissue development *in vitro*. While several studies have demonstrated the transcriptomic effects of shear stress in primary ECs, data on effects of flow on hiPS-EC are still scarce. In this study, we examined how hiPS-ECs respond and adapt to flow, and used single-cell RNA sequencing (scRNASeq) to evaluate the heterogeneity of response. This is important as hiPS-ECs are increasingly studied for both *in vitro* modeling as well as for transplantation to patients with vascular diseases.

# MATERIALS AND METHODS

## Data Availability

The RNA sequencing datasets generated for this study are deposited in the Gene Expression Omnibus (GEO) database with accession numbers GSE150741 and GSE150740.

## hiPS Cell Lines

Three healthy human induced pluripotent stem cell lines (HEL47.2, HEL46.11, and HEL24.3) were obtained from the Biomedicum Stem Cell Center. The cell lines were created by using retroviral/Sendai virus transduction of Oct3/4, Sox2, Klf4, and c-Myc, as described previously (Trokovic et al., 2015a,b; Saarimäki-Vire et al., 2017). In addition, the hiPSC line K1 was a kind gift from Prof. Anu Wartiovaara group.

## hiPSC Culture

hiPSCs were maintained in Essential 8 media (A1517001, Thermo Fisher Scientific) on thin-coated Matrigel (354277, dilution 1:200; Corning, Corning, NY, United States). The cells were passaged using EDTA.

## hiPS-EC Differentiation

Endothelial cell differentiation was conducted based on the protocol by Giacomelli et al. (2017) with slight modifications. The BPEL medium ingredients were purchased from the same vendors as mentioned in the article, except for BSA (A7030, Sigma) and PVA (362607, Sigma). Briefly, 125,000 – 175,000 cells/well in a 6-well plate were plated on day 0. On day 1, the medium was changed to BPEL with 20 ng/ml BMP4 (120-05ET, Peprotech), 20 ng/ml Activin A (AF-120-14E–50 μg, Peprotech) and 4 μmol/L CHIR (S2924, Selleckhem). On day 3, the medium was changed to BPEL with 50 ng/ml VEGF (produced in-house) and 5 μmol/L IWR-1 (I0161, Sigma). On day 6, medium was changed to BPEL with 50 ng/ml VEGF and the cells were maintained in this medium until they were sorted. 50 ng/ml VEGF was maintained in all hiPS-ECs cultures unless otherwise indicated.

## hiPS-EC Sorting

After differentiation, hiPS-ECs were sorted using magnetic beads with an antibody against CD31 (130-091-935, Miltenyi Biotec), according to the manufacturer's protocol. The concentration of the cells was counted with Bio-Rad TC10 or TC20 Automated Cell Counter. The cells were immediately used for experiments.

## hiPS-EC Exposure to Flow

After sorting, 2.5–3.5 × 10^5 hiPS-ECs were plated on an Ibidi μ-Slide I Luer (80176, Ibidi). 4.0–6.0 × 10^5 hiPS-ECs were plated in one well in 6-well plate (static control). After 24 h, the cells on Ibidi slide were subjected to laminar shear stress of 15 dyn/cm$^2$ by using the Ibidi Pump System (10902, Ibidi). After 24 h of exposure to flow, the cells were processed either for bulk RNA-sequencing or single-cell RNA-sequencing. The static control cells were processed at the same time. For bulk RNA-sequencing, the cells were collected into the RA1 lysis buffer and extracted using the Nucleospin RNA Plus Extraction kit (740984, Macherey-Nagel). Each experiment (whether for scRNASeq or bulk RNASeq) consists of one differentiation round from each hiPS cell line.

## Immunofluorescence Staining

Cells were fixed with 4% PFA and stained with VE-cadherin (2500, Cell Signaling Technology). Nuclei were visualized with DAPI or Hoechst. Stained cells were imaged with fluorescent or confocal microscopes (Zeiss AxioImager and Zeiss LSM 780).

## Matrigel Tube Assay

48-well plate was coated with 100 μl of Matrigel per well. After gelling of Matrigel, 90,000 hiPS-ECs/well (HEL24.3 and HEL47.2) or 30,000 HUVECs/well were added on top of the Matrigel-covered wells. The cells were allowed to attach and grow. Phase-contrast images were taken at 24, 48, and 72 h.

## LDL Uptake

Atto-labeled LDL oxidized with 10 μmol/L CuSO4 (20 h, 37C°) (courtesy of Dr. Katariina Öörni lab) was applied to hiPS-ECs on coverslips in a 24-well plate for 20 h (7.5 μg/well). The coverslips were fixed and imaged with a Zeiss LSM 780 confocal microscope.

## Processing of Cells for Single-Cell RNA-Sequencing

The cells were detached using Accutase (A6964, Sigma) and concentration of the cell suspension was measured. The cells were washed once with PBS containing 0.04% BSA, and then resuspended in PBS with 0.04% BSA to a final concentration of 0.79–1.0 × 10^6 cells/ml. The cells were passed through a 35 μm strainer (352235, Corning) and kept on ice until processing for the 10X Genomics Single Cell Protocol at the Institute of Molecular Medicine Finland (FIMM). At FIMM, the concentration and viability of cells was calculated one more time with Luna Automated Cell Counter and 4000 cells/sample were processed.

## Single-Cell RNA-Sequencing

Single-cell gene expression profiles were studied using the 10× Genomics Chromium Single Cell 3′RNAseq platform. The Chromium Single Cell 3′RNAseq run and library preparation were done using the Chromium Single Cell 3′ Reagent version 2 chemistry. The sample libraries were sequenced on Illumina NovaSeq 6000 system. 4000 cells and 50,000 PE/cell were analyzed.

Data processing and analysis were performed using 10× Genomics Cell Ranger v2.1.1 pipelines. The "cellranger mkfastq" pipeline was used to produce FASTQ (raw data) files. The "cellranger count" was used to perform alignment, filtering and UMI counting. mkfastq was run using the Illumina bcl2fastq v2.2.0 and alignment was done against human genome GRCh38. Cellranger aggr pipeline was used to combine data from multiple samples into an experiment-wide gene-barcode matrix and analysis.

Analyses were performed with Seurat R package version 3.0.1 (Butler et al., 2018). Cells, in which more than 1000 genes were detected, were included. Seurat function CellCycleScoring was used to assign cell cycle scores (iG2/M scores and S scores), which then were used to regress out cell cycle effect. Normalization and variance stabilization was done with SCTransform in Seurat (vars.to.regress was used to remove confounding sources of variation including mitochondrial mapping percentage, and cell cycle scores) (Hafemeister and Satija, 2019). Principal component analysis (PCA) was performed on the highly variable genes. The first 30 PCs were used for uniform manifold approximation (UMAP). Differential expression for each subpopulation in the scRNASeq data was performed using the FindAllMarkers function (Wilcoxon Rank Sum test) in Seurat, and FindMarkers was used to distinguish different conditions. Cells were clustered based on their expression profile setting the resolution to 0.5, which led to 11 clusters which were quite clearly distinguished in the UMAP. Established markers on The Human Protein Atlas and published literature were used to annotate cell types.

## Single-Cell RNA-Sequencing – Data Presentation

For clarity, we present the scRNASeq results in the main figures for the cell line HEL47.2. Only results, which were statistically significant in both cell lines, are presented, unless otherwise stated. The corresponding results for the cell line HEL24.3 are presented in the **Supplementary Material**.

## Bulk RNA-Sequencing

RNA samples were sequenced at Biomedicum Functional Genomics Unit (FuGU) with Illumina NextSeq sequencer (Illumina, San Diego, CA, United States) in High output run using NEBNext® Ultra™ II Directional RNA Library Prep Kit for Illumina. The sequencing was performed as single-end sequencing for read length 75 bp. The count data was used to calculate differential expression statistics with the DESeq2 software in the R environment. Genes with an adjusted $p$-value for the log2-fold change $<0.05$ were considered significant. Gene Ontology (GO) analysis was performed using DAVID Bioinformatics Resources 6.8.

# RESULTS

## hiPS-EC Characterization

Immunofluorescence staining of the hiPS-ECs showed strong expression of VE-cadherin and PECAM1 in cell-cell junctions (**Figure 1A**). In addition, the hiPS-ECs were able to take up oxidized LDL (**Figure 1A**), demonstrating their functionality. Matrigel tube assay showed that the hiPS-ECs formed tubes in 3D Matrigel assay similarly to HUVECs (**Figure 1B**). Interestingly, although the hiPS-EC tubes were not as uniform, they lasted longer than the HUVEC-derived structures. In 2D culture, the hiPS-ECs had a cobblestone-like morphology similar to primary ECs, and upon exposure to shear stress they aligned in response to flow (**Figure 1C**).

## Single Cell Profiling of hiPS-ECs Grown in Static Conditions and Under Flow

To analyze the heterogeneity and identity of the hiPS-ECs, we performed scRNASeq in two independent hiPS cell lines from healthy donors (HEL47.2 and HEL24.3). The results from HEL47.2 are presented in the main figures and the results from HEL24.3 in the **Supplementary Material**. In general, the results were highly similar in both cell lines and only genes and pathways found to be affected in both lines are reported.

A total of 11 clusters were identified in the aggregated data of both flow and static conditions (**Figures 2A–C**). Most hiPS-ECs had high expression of the endothelial cell markers *CD34*, *PECAM1*, *KDR*, and *CDH5* (**Figures 2D,E**). The expression of lymphatic EC genes (*PROX1* and *PDPN*) was very low or absent, demonstrating that the protocol used in our study does not produce lymphatic ECs (**Figure 2D**). Static hiPS-ECs formed five distinct clusters, of which one consisted of proliferating cells with high expression of the cell cycle genes *MKI67*, *TOP2A*, and *BIRC5* (Proliferating) and one with markedly lower EC gene expression, which we named as Poorly differentiated (**Figures 2B,C**). The proliferating cell cluster contained almost exclusively cells from the static culture, reflecting the flow-induced inhibition of EC proliferation. The other three clusters were labeled as Static EC 1–3. Five distinct flow clusters were identified (EC Flow 1–5). Finally, a very small cluster containing few cells from both

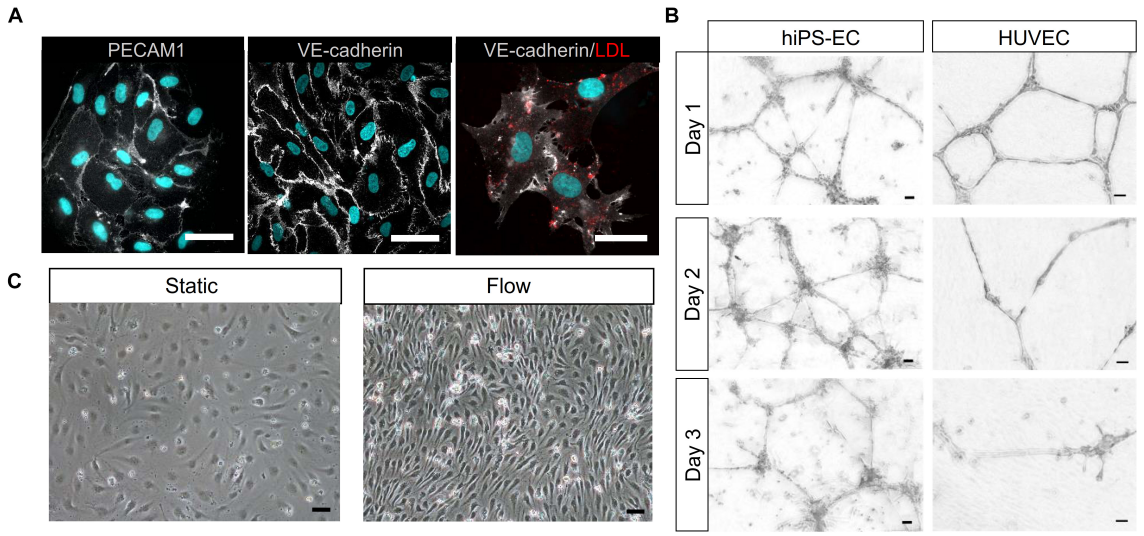


**FIGURE 1 |** Characterization of hiPS-ECs. **(A)**, PECAM1 and VE-cadherin IF staining of hiPS-ECs (white) and uptake of oxLDL by hiPS-ECs (red). Nuclei are shown in blue. Scale bar 50 μm. **(B)**, Matrigel tube assay of hiPS-ECs and HUVECs (scale bar 50 μm). The cells were plated on Matrigel and imaged every day for 72 h. **(C)**, Phase-contrast images of hiPS-ECs after 24 h exposure to flow-induced shear stress and under static conditions. The cells in both conditions are from the same differentiation batch and images have been taken at the same time point just before processing them for scRNASeq. Scale bar 50 μm.

conditions expressed a mesenchymal cell phenotype with high expression of *TAGLN*, and *ACTA2* (MC, Mesenchymal cells) (**Figure 2B**). Clustering of the HEL24.3 hiPS-ECs is presented in the **Supplementary Figure S1**.

## Single-Cell and Bulk RNA Sequencing Reveal Similar Responses in hiPS-ECs Compared to Primary ECs

Flow induced upregulation of 171 genes, and downregulation of 136 genes in the scRNASeq analysis (genes significantly changed in both cell lines, **Supplementary Table S1A**). The flow-experiment was replicated with four hiPS-EC-lines (HEL47.2, HEL24.3, HEL46.11, and K1), and analyzed with bulk RNASeq with deeper sequencing depth, allowing detection of low-abundant genes. In the bulk RNASeq analysis, 656 significantly upregulated and 525 downregulated genes in response to flow were identified (**Supplementary Table S1B**). The most highly induced genes in both analyses included several known flow-responsive genes such as *KLF2* and *CYP1B1*, demonstrating that the hiPS-ECs responded to flow in a similar manner as primary ECs (**Figure 2C** and **Supplementary Tables S1A–C**). When the scRNASeq and bulk RNASeq data were analyzed together, in total 99 genes were upregulated and 54 genes were downregulated in all data sets, forming a core of the flow-induced genes in hiPS-ECs (**Supplementary Table S1C**).

## Single-Cell RNA-Sequencing of Flow-Exposed Cells Identifies Arterial- and Venous-Like hiPS-ECs

According to the scRNASeq analysis, flow increased the expression of characteristic EC markers (**Figures 2D,E**), and both arterial and venous EC markers. HEL47.2 EC Flow clusters 1–2 and 4–5 had higher expression of venous genes (**Figure 3A**), while the cluster EC Flow 3 had a higher expression of arterial genes (**Figure 3B**). Similar clustering was found in the HEL24.3 hiPS-ECs with one arterial-like cluster (**Supplementary Figure S2**). In the bulk RNASeq data, where the effects of flow were studied as a single population, significant upregulation was found in the venous markers *NRP2*, *FTH1*, and *EPHB4*, and the arterial marker *NOTCH1* (**Supplementary Table S1B**). Except for the scRNASeq clusters EC Flow 3 in the HEL47.2 cell line and EC Flow 5 in the HEL24.3 cell line, which showed more arterial phenotype, the expression of other arterial genes than *NOTCH1* were not significantly changed in the flow hiPS-ECs compared to static hiPS-ECs. Interestingly, these arterial-like clusters showed smaller responses to flow than the other flow clusters based on the expression of the flow-induced genes *KLF2*, *CYP1B1*, and *IGFBP5* (**Figure 2C**). However, these cells still clearly differed from the static cells (**Figure 2C**). Compared to the other flow clusters, these cells had increased expression of arterial (*ACKR3, CXCR4, HEY1, GJA1*, and *HES1*) and EC activation markers (*ANGPT2, ESM1*, and *PGF*) (**Figure 3C**). These findings demonstrate the power of scRNASeq, as the arterial-like cluster was relatively small, and these differences cannot be detected from the bulk RNASeq data.

## Flow-Exposed hiPS-ECs Represent a More Stable and Homeostatic EC Phenotype

Shear stress activated pathways associated with blood vessel development, cell migration, cell communication, cell-cell adhesion, and fluid shear stress responses, and these replicated in both scRNASeq (HEL47.2 and HEL24.3 combined) and bulk RNASeq analyses (**Figures 4A–C**). The repressed gene ontologies (GO) in scRNASeq included angiogenesis, reactive oxygen species metabolism, hypoxia response, cell cycle regulation and response to stress. In the bulk RNASeq, in

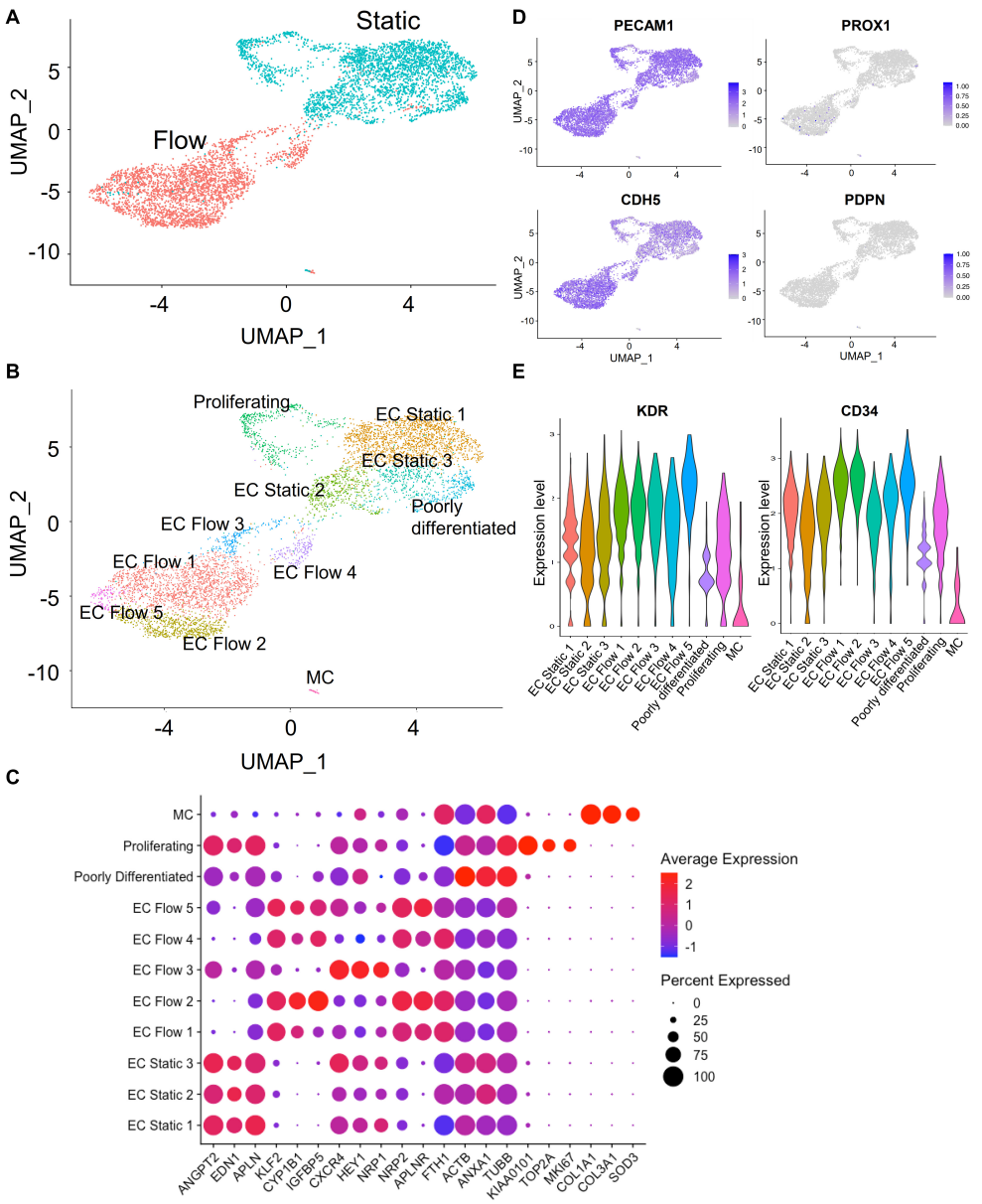


**FIGURE 2 |** Characterization of single-cell RNA sequencing clusters (HEL47.2 cells). **(A)**, UMAP (Uniform Manifold Approximation and Projection) plot of flow and static cells. **(B)**, UMAP plot of the delineated clusters. **(C)**, Dot plot for marker genes of the delineated clusters. **(D)**, Feature plot of blood EC (*PECAM1, CDH5*) and lymphatic EC (*PROX1, PDPN*) EC marker gene expression. **(E)**, Violin plot of EC marker genes (*KDR, CD34*) in all identified clusters.

addition to these, pathways related to protein translation and RNA catabolism were significantly downregulated (**Figure 4B**). In the scRNASeq GO analysis, two categories came up among both upregulated and downregulated genes (blood vessel development and regulation of cell migration) with different affected genes (**Figure 4D**). Upregulated genes represented flow-response and stabilization of the vasculature and downregulated genes were related to EC activation and proliferation.

The expression of known flow-induced genes *KLF2*, *KLF4*, and *eNOS* (*NOS3*), which regulate vascular tone (Sangwung et al., 2017), were highly upregulated in flow (**Figure 5A** and **Supplementary Tables S1A–C**). In addition, the expression of anti-atherogenic genes (*CYP1A1*, *CYP1B1*, and *PLPP3*) (Conway et al., 2009; Mueller et al., 2019), genes that promote vascular homeostasis and EC survival (*SLC9A3R2, PODXL*, and *ADAM15*) (Bhattacharya et al., 2012; Horrillo et al., 2016; Babendreyer et al., 2019) and stress response markers (*HMOX1* and *NQO1*) (Dinkova-Kostova and Talalay, 2000; Issan et al., 2014) were upregulated by flow (**Figure 5A** and **Supplementary Tables S1A–C**). In contrast, shear stress significantly downregulated the vascular tone regulator *EDN1*

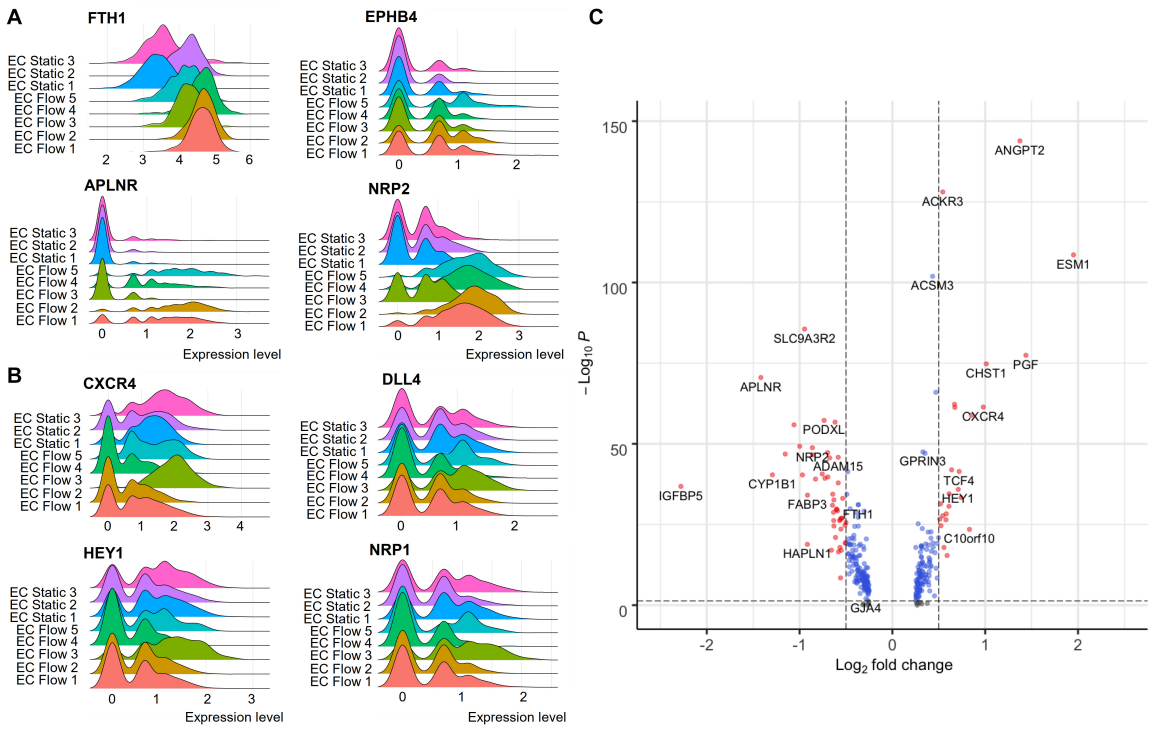


**FIGURE 3 |** The expression of venous and arterial genes in hiPSC-ECs flow and static clusters (HEL47.2). **(A)**, Venous genes. **(B)**, Arterial genes. **(C)**, Volcano plot on the differential expression of flow arterial-like cluster 3 genes compared to all the other flow clusters.

(Yanagisawa et al., 1988) in all flow clusters (**Figure 5B** and **Supplementary Tables S1A–C**).

Flow promoted quiescence in hiPS-ECs, demonstrated by downregulation of several angiogenesis and EC activation marker genes (*APLN, ANGPT2*, *CITED2, DDAH1* and *THBS1*) (Freedman et al., 2003; Smadja et al., 2011; Trittmann et al., 2019; Masoud et al., 2020) (**Figure 5B** and **Supplementary Tables S1A–C**) and by the upregulation of *TEK* (*TIE2*), that contributes to the maintenance of vascular quiescence (Augustin et al., 2009) (**Supplementary Tables S1A–C**). Vascular endothelial protein tyrosine phosphatase (*VE-PTP*, also known as *PTPRB*), that regulates blood vessel remodeling and angiogenesis (Küppers et al., 2014), was also markedly induced by flow together with other PTPs *PTPRG* and *PTPRE* (**Supplementary Tables S1A–C** and **Figure 6A**).

Also, several other genes that are implicated in vascular health and regeneration (*PRCP*, *APLNR*, *PLVAP*, and *HAPLN1*) (Wirrig et al., 2007; Adams et al., 2013; Deshwar et al., 2016; Guo et al., 2016) were induced by flow (**Figure 5A** and **Supplementary Tables S1A–C**). Moreover, shear stress induced downregulation of atherogenic *CAV1* (Melchionna et al., 2005; Fernández-Hernando et al., 2010) and *SOD2* (Ohashi et al., 2006) (**Figure 5B** and **Supplementary Table S1A**). A small GTPase *RALA*, which has previously been shown to be repressed by *KLF2* (Dekker et al., 2005), was the most downregulated gene by flow in the bulk RNASeq (**Figure 6A** and **Supplementary Table S1B**). In addition, *BMP4* (Helbing et al., 2017) and *PDGFB* (Tisato et al., 2013), which are related to inflammatory responses in ECs, were among the most repressed genes by flow (**Figure 6B** and **Supplementary Table S1B**).

Flow also affected metabolic genes in hiPS-ECs, as it increased the expression of glucose transporters *GLUT1* (*SLC2A1*) and *GLUT3* (*SLC2A3*) as well as fatty acid handling genes *FABP3* and *PLIN2* (**Supplementary Tables S1A–C**).

The respective results for the HEL24.3 cell line are presented in the **Supplementary Figure S3**.

## Flow Induces NOTCH-Signaling Especially in Arterial-Like hiPS-ECs

Shear stress is a known NOTCH-pathway activator inducing increased *NOTCH1* expression. NOTCH1 has recently been identified as an important mechanosensor in ECs (Mack et al., 2017; Polacheck et al., 2017). Compared to static hiPS-ECs, altered expression of several NOTCH pathway genes were observed in the hiPS-ECs exposed to flow. Interestingly, the effects were different in the venous-like (EC Flow 1–2, 4–5) and arterial-like (EC Flow 3) clusters. The expression levels of *NOTCH1* were upregulated in all flow hiPS-EC clusters, but *NOTCH4* only in the arterial-like cluster. The notch-ligand *DLL4* was upregulated in the arterial-like hiPS-ECs in flow, whereas the expression level was repressed in the venous-like hiPS-ECs compared to hiPS-ECs in static conditions (**Figure 7A**). Likewise, the expression of the NOTCH-targets *HEY1*, *HES1*, and *GJA1* was induced in the arterial-like Flow EC 3. The respective results for HEL24.3 cells are presented in **Supplementary Figure S4**.

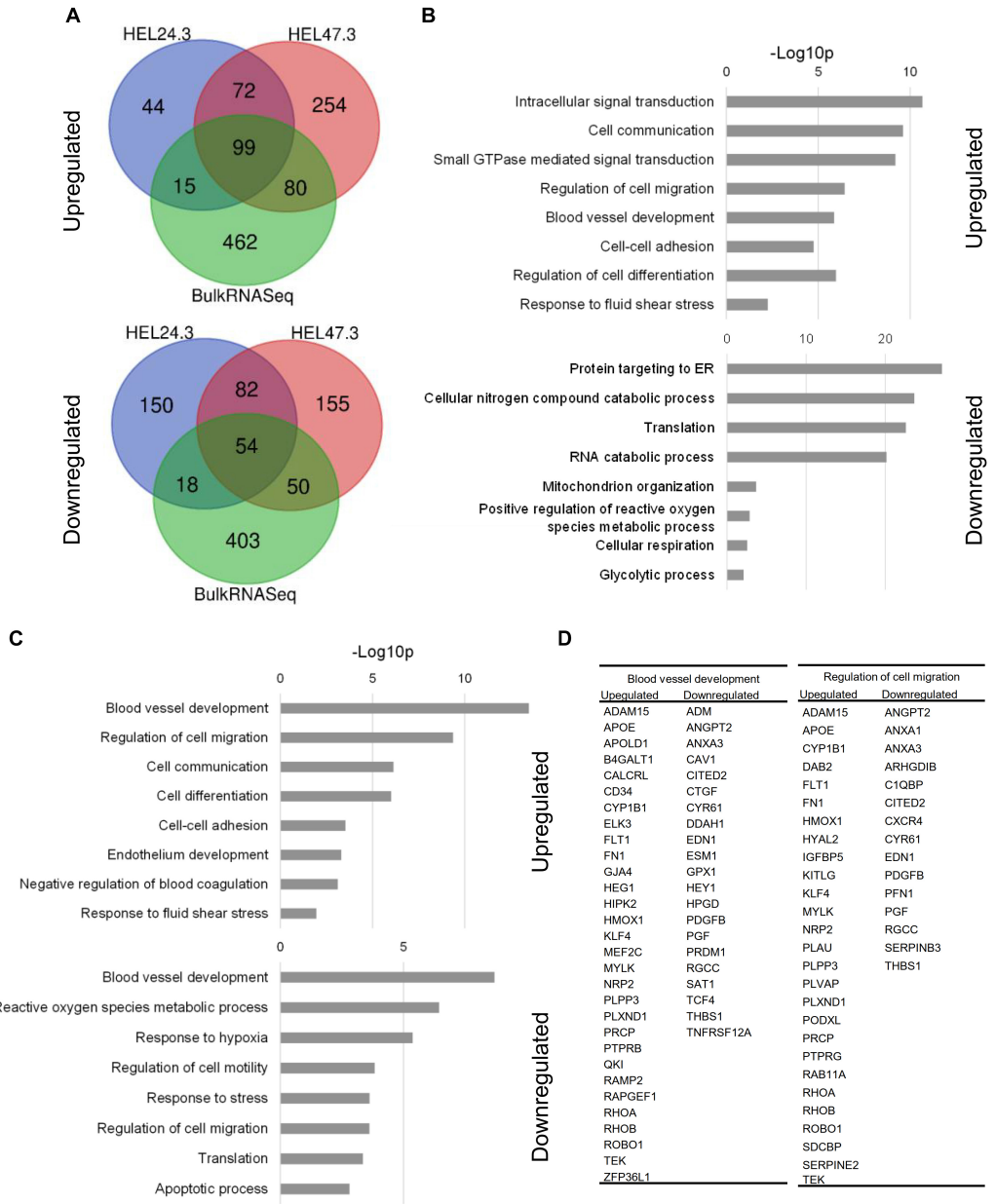


**FIGURE 4 |** Gene Ontology (GO) analysis of the scRNASeq and bulk RNASeq data (DAVID Bioinformatics Resources). **(A)**, Venn diagram of upregulated and downregulated genes shared between scRNASeq and bulk RNASeq. **(B)**, Upregulated and downregulated GO terms in bulk RNASeq data **(C)**, Upregulated and downregulated GO terms in scRNASeq data. **(D)**, A list of genes included in the GO term categories that were both upregulated and downregulated.

## Flow Altered the Expression of VEGF Signaling Pathway Genes

Markedly reduced expression of the VEGF pathway ligand *PGF* was observed in flow compared to static hiPS-ECs (**Figure 7B**), whereas *VEGFC* was upregulated by flow, except in the Flow EC 3 cluster. The VEGF receptors *FLT1* (*VEGFR1*), *KDR* (*VEGFR2*), and *FLT4* (*VEGFR3*) tended to be induced by flow in most clusters (**Figure 7B**). The VEGF co-receptor *NRP2* was upregulated in all flow clusters, whereas *NRP1* was increased specifically in Flow EC 3 cluster (the arterial type cluster). The respective results for HEL24.3 cells are presented in **Supplementary Figure S4**.

# DISCUSSION

Patient derived hiPS-ECs are increasingly used in disease modeling to study specific disease related phenotypes and genotype-phenotype correlations. However, hiPS-ECs do not gain full maturity and identity compared to ECs *in vivo*,

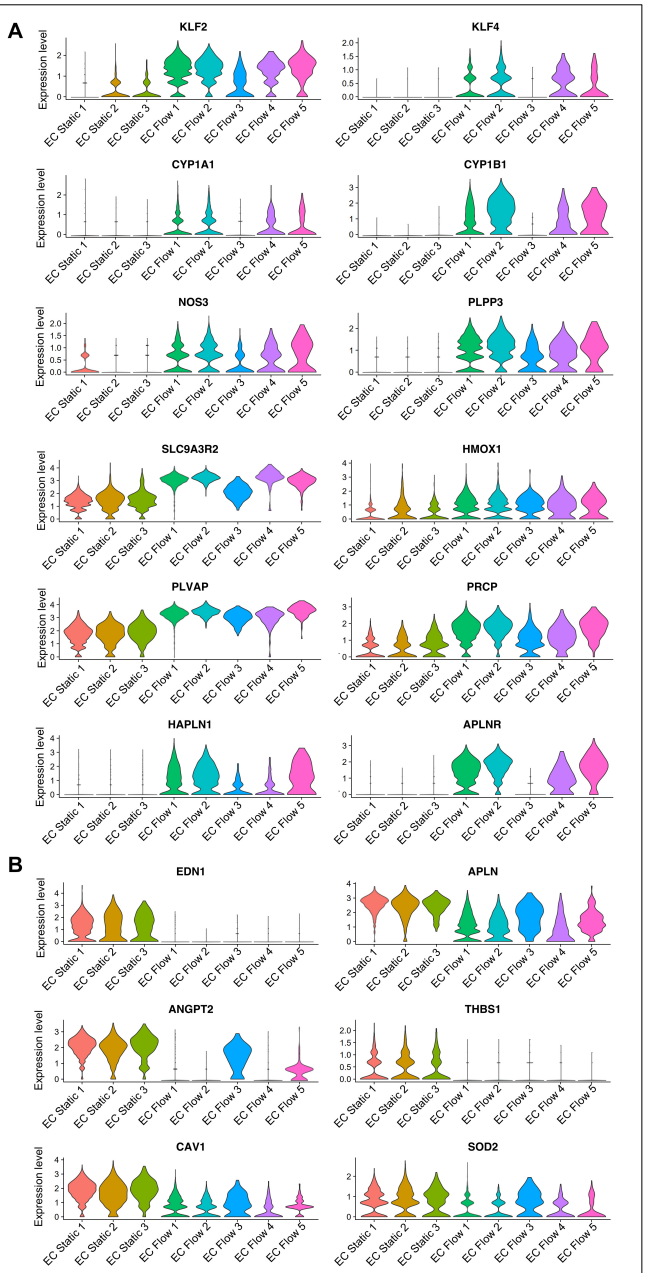


**FIGURE 5 |** The effect of flow on hiPS-EC gene expression (HEL47.2). **(A)**, Violin plots for selected genes upregulated by flow. **(B)**, Downregulated genes in response to flow.

where ECs are exposed to mechanical forces of blood flow such as shear stress and pulsatile pressure, and paracrine signals from neighboring parenchymal cells. In addition, the efficiency of differentiation as well as maturity of cells vary depending on the protocol used. Here we demonstrate that differentiating hiPSCs to hiPS-ECs results in a population of cells with cobble-stone morphology and high expression of EC molecular markers. In addition, these cells are able to form vascular tube structures in 3D and take up oxidized LDL. We show that the hiPS-ECs have high plasticity as they adapt to laminar flow-induced shear stress by entering quiescence and presenting with a more homogenous and homeostatically stable phenotype. Interestingly, the expression of both arterial and venous genes increased in flow, and single-cell analysis and clustering revealed flow-exposed subpopulations with transcriptomic profiles toward either a more venous or arterial identity. Our results highlight the importance of single-cell RNA sequencing to distinguish different phenotypes of hiPSC-derived ECs.

Based on their gene expression profiles, hiPS-ECs are more similar to embryonic ECs when compared to primary ECs (Rufaihah et al., 2013; Orlova et al., 2014a; Vazão et al., 2017). The expression levels of the endothelial progenitor marker *CD34* were high in our hiPS-ECs, demonstrating an immature nature of these cells. This feature potentially results in plasticity to further develop to, or even transfer between arterial and venous phenotypes according to various external cues (Rufaihah et al., 2013; Ikuno et al., 2017). This is an advantage when modeling the development and maturation of ECs and vasculature. In addition, due to these properties, hiPS-ECs can potentially provide a relevant model for screening for embryonic vascular toxicity (Vazão et al., 2017), to model diseases associated with immature vasculature, or to study the effect of EC responses to abnormal flow conditions during development.

hiPS-ECs cultured in static conditions expressed more arterial than venous markers, which is consistent with previous reports (Paik et al., 2018; Vilà-González et al., 2019). However, the cells did not cluster according to arterial or venous phenotype in static culture. Single-cell sequencing of flow-exposed hiPS-ECs revealed increased expression of several arterial and venous genes, with higher induction seen in venous markers, which is in accordance with previous studies of hiPS-ECs (Ohtani-Kaneko et al., 2017). The expression pattern was replicated in the bulk RNASeq data for the venous markers *NRP2, FTH1*, and *EPHB4*, and the arterial marker *NOTCH1*. Importantly, single-cell RNA-sequencing revealed several hiPS-EC-subclusters in the flow exposed cells, of which one was clearly arterial-like and the others venous-like, underlining the responsiveness of the cells to external stimuli and also the heterogeneity of the phenotypic change. When compared to primary ECs *in vivo*, hiPS-ECs in culture do not show organotypic features or clear separation of arterial, venous or capillary ECs (Kalucka et al., 2020), thus the clusters are not directly comparable to *in vivo* primary EC clusters. The expression levels of the lymphatic EC markers *PROX1* and *PDPN* were very low, indicating that there were no lymphatic ECs among the hiPS-ECs. A small number of cells expressed the smooth muscle cell marker *ACTA2*, and these cells clustered far from other hiPS-ECs and were discarded in further analyses.

As expected, flow activated known vascular tone regulators, such as *KLF2* (Dekker et al., 2002) and *KLF4* (Sangwung et al., 2017), and shear responsive anti-atherogenic genes, such as *CYP1A1*, *CYP1B1*, and *PLPP3* (Conway et al., 2009; Mueller et al., 2019). This demonstrates that the hiPS-ECs

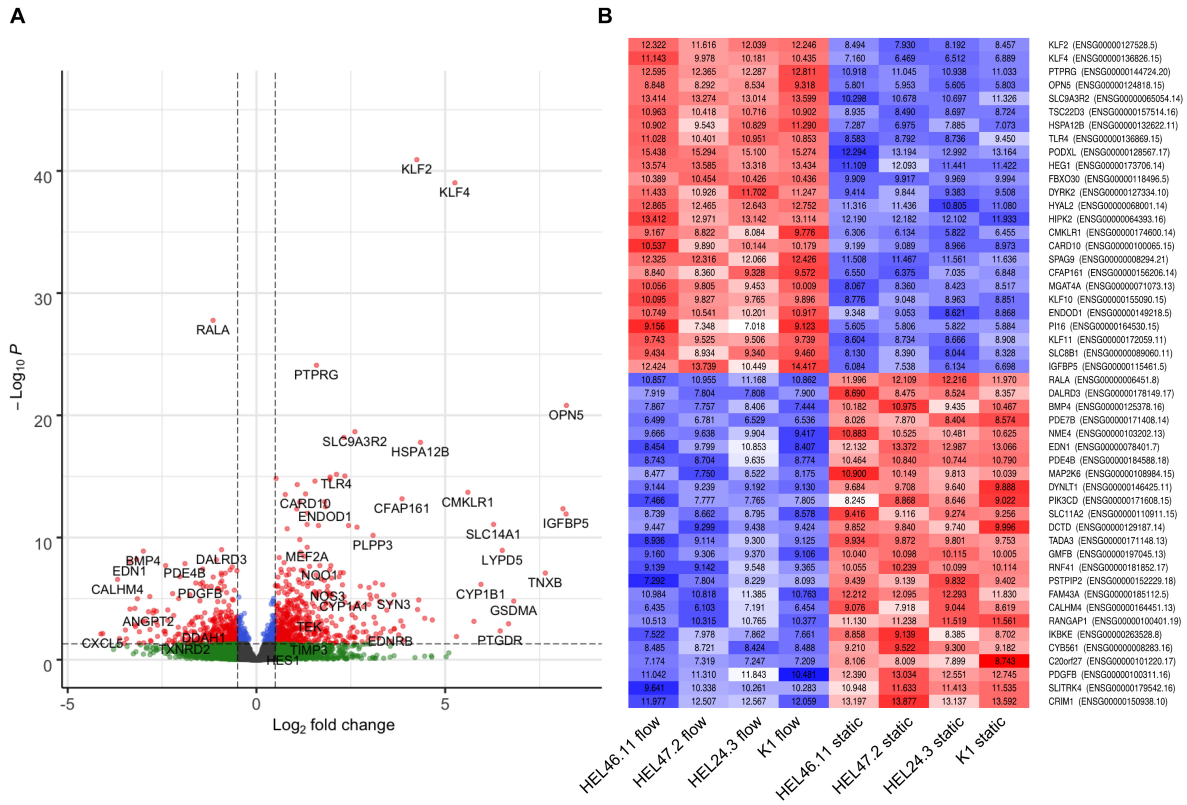


**FIGURE 6 |** Bulk RNASeq analysis of the effect of flow compared to static condition. **(A)**, A volcano plot of differentially expressed genes in flow compared to static hiPS-ECs. **(B)**, Heat map of the 50 most significantly changed genes by flow. Red denotes upregulation and blue downregulation.

are plastic and can adapt to flow-induced changes similarly to primary ECs. Interestingly, the cells, which had the lowest response to flow. e.g., attenuated upregulation of *KLF2* and *CYP1B1*, acquired more of an arterial-like phenotype. In primary ECs and *in vivo*, KLF2 has been shown as a positive transcriptional regulator of shear-dependent endothelial function for example through upregulation of endothelial nitric oxide synthase (*eNOS*), and downregulation of the vasoconstrictor *EDN1* and small GTPase *RALA* (Bhattacharya et al., 2005; Dekker et al., 2005). These effects were also observed in the present study.

Other changes indicating a stabilizing effect of flow were also seen, such as the downregulation of *SOD2*, *PGF*, and *CAV1*. SOD2 protects against oxidative stress and endothelial dysfunction (Ohashi et al., 2006). Hypoxia increases PGF expression in human myocardium (Torry et al., 2009), and pathological cardiac conditions such as ischemic cardiomyopathy or acute myocardial infarction result in elevated plasma levels of PGF (Iwama et al., 2006; Nakamura et al., 2006). Overexpression of the structural protein CAV-1 in mouse ECs lead to progression of atherosclerosis, while the absence of it reduces the progression of atherosclerosis (Fernández-Hernando et al., 2010). Three protein tyrosine phosphatases (*PTPRB*, *PTPRG*, and *PTPRE*) were strongly induced by flow. PTPRB (VE-PTP) activity enhances VE-cadherin-mediated adhesion and promotes endothelial barrier function (Nawroth et al., 2002), and it is also an important regulator of TEK, VEGFR2 and PECAM1 activity (Küppers et al., 2014), indicating EC stabilization. We also identified *SLC9A3R2 (NHERF2)* as a novel flow-response gene by both single-cell and bulk RNASeq. It has previously been shown to be expressed specifically in ECs (Wallgard et al., 2008) and to regulate vascular homeostasis (Bhattacharya et al., 2012; Schrimpf et al., 2012). Interestingly, in kidney MDCK cells, NHERF2 was shown to bind to podocalyxin (PODXL), another gene significantly induced by flow in our model, and to regulate epithelial cell polarization (Meder et al., 2005). It is likely that these genes act together also in ECs mediating the flow-induced cellular polarization. Thus, our findings show that many genes necessary for stability, barrier function, polarization and regeneration are highly responsive to flow in hiPS-ECs.

Laminar shear stress -induced KLF2 activation has been shown to modulate EC metabolism by reducing glucose uptake and glycolysis, which contributes to EC quiescence (Doddaballapur et al., 2015). Pathway analysis of the bulk RNASeq data revealed that flow repressed glycolysis-related genes also in hiPS-ECs. However, we observed increased expression of glucose transporters *GLUT1* and *GLUT3* as well as fatty acid handling genes *FATP3* and *PLIN2* in flow-exposed hiPS-ECs in all three experiments (**Supplementary Tables S1A–C**). As

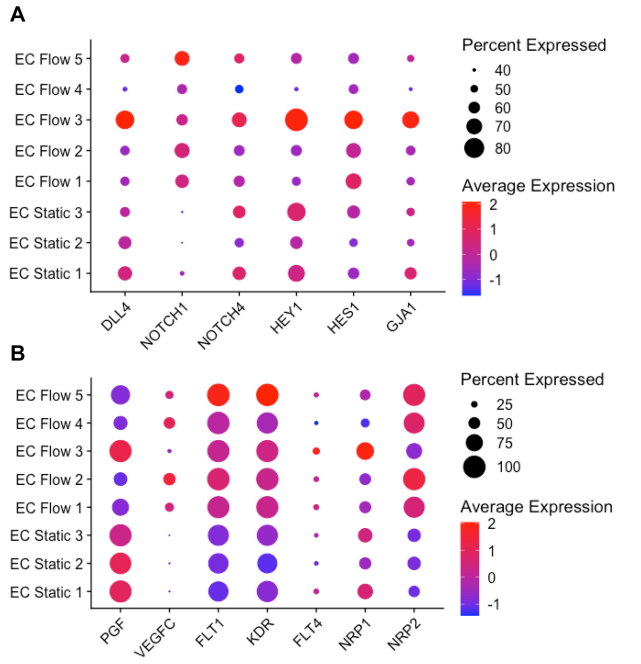


**FIGURE 7 |** NOTCH and VEGF pathway gene expressions in scRNASeq (HEL47.2). **(A)**, NOTCH pathway gene expression in flow and static clusters. **(B)**, VEGF pathway genes in flow and static clusters.

glucose uptake is mainly regulated by translocation of GLUTs to cell membrane, and not by transcription, we think that the upregulation of glucose and fatty acid transport/storage genes mainly reflect the maturation of flow-exposed hiPS-ECs compared to the static cells, and not regulation of glucose uptake or glycolysis.

VEGF and NOTCH signaling are both essential for blood and lymphatic vasculature growth and specification. Our data showed that the VEGF receptors *FLT1* and *KDR* were highly expressed in all hiPS-ECs. Flow induced significant repression of *PGF* and a slight upregulation of *VEGFC*. In addition, the co-receptor *NRP2* was markedly induced in the venous-like clusters, whereas *NRP1* was upregulated specifically in the arterial-like cluster. Furthermore, markers of EC activation and proliferation were significantly repressed by flow. These changes indicate a more stable and quiescent EC phenotype. *NOTCH1*, which has been shown to act as a mechanosensor in ECs (Mack et al., 2017), was highly upregulated by shear stress in all flow clusters in hiPS-ECs. The NOTCH pathway ligands and effectors *DLL4*, *HEY1*, *HES1*, and *GJA1* were induced only in the arterial-like Flow EC 3 cluster, but were found to be expressed in all clusters to some level. Recently, NOTCH activation was found to be important for cell cycle arrest and arterial specification in ECs (Fang et al., 2017).

Analysis at the single-cell level shows that as a group, the flow-stimulated ECs are more homogenous as compared to hiPS-ECs grown in static conditions. The clusters that were identified as poorly differentiated were absent in the flow-exposed cells. It is possible that flow results in further improved differentiation of these cells, or that subpopulations of the iPS-ECs in static conditions have transdifferentiation properties, which are suppressed by flow. This is an important finding considering e.g., disease modeling, as the comparison between healthy and diseased cells would have much less noise in the data when studied under flow conditions. This also mimics better the *in vivo* environment, as ECs are constantly exposed to shear stress.

This study is limited by the number of iPS-cell lines used, mainly due to the high costs of single-cell RNA-sequencing. However, the obtained results were highly reproducible in scRNASeq analysis of both cell lines as well as in a replication experiment with bulk RNAseq of 4 different hiPS cell lines. The disadvantages of using iPSC-derived ECs compared to primary ECs or cell lines is the immature nature of the cells, their tendency for transdifferentiation, the low proliferation capacity over passaging and the costs to produce them. However, in disease modeling they are superior to study the interactions between cell types, as all cell types can be derived from the same patient carrying the same genetic variants. This is why the development of better iPS-EC models are highly needed. Our study demonstrates the importance of flow for the stability and homeostasis of hiPS-ECs.

In summary, our study showed that exposing hiPS-ECs to laminar shear stress promotes a more stable and quiescent EC phenotype, which was more homogenous than hiPS-ECs grown under static conditions. The immature nature of hiPS-ECs is an advantage for modeling the effects of flow on EC phenotype and maturation. Our results also demonstrate that the flow responses are highly consistent in different healthy hiPS-EC lines, similarly to what was previously shown for barrier function and inflammatory responses (Halaidych et al., 2018).

## DATA AVAILABILITY STATEMENT

The datasets presented in this study can be found in online repositories. The names of the repository/repositories and accession number(s) can be found below: https://www.ncbi.nlm.nih.gov/geo/, GSE150741 https://www.ncbi.nlm.nih.gov/geo/, GSE150740.

## ETHICS STATEMENT

The studies involving human participants were reviewed and approved by the Ethics Committee of Helsinki and Uusimaa Hospital District. The patients/participants provided their written informed consent to participate in this study.

## AUTHOR CONTRIBUTIONS

EH and RK contributed to the conceptualization, funding acquisition, and supervision. EH contributed to the data curation, formal analysis, project administration, and software. MA, EH, and LA contributed to the investigation. EH and MA contributed to the methodology and visualization. EH and RK

contributed to the resources. EH, RK, and MA contributed to the writing of the original draft. EH, MA, and RK contributed to the writing – review and editing. All authors contributed to the article and approved the submitted version.

## FUNDING

This work has been funded by Finnish Medical Foundation (EH), Finnish Foundation for Pediatric Research (EH), Finnish Foundation for Cardiovascular Research (EH and RK), University of Helsinki (EH), Academy of Finland (grant 297245, RK), Jenny and Antti Wihuri Foundation, Sigrid Jusélius Foundation (RK), Finnish Cultural Foundation (EH and RK), and University of Helsinki Pediatric Research Center (EH).

## ACKNOWLEDGMENTS

We thank Ilse Paetau for her help in the cell culture and administrative support. We thank Professor Timo Otonkoski and Docent Ras Trokovic at Biomedicum Stem Cell Center for providing us with three control hiPS-cell lines and Professor Anu Suomalainen-Wartiovaara for the gift of the hiPSC line K1. We are grateful to Maija Atuegwu and Docent Katariina Öörni for providing us with oxidized-LDL and help with the LDL uptake assay. Biomedicum Functional Genomics Unit (FuGU) is acknowledged for providing the bulk RNASeq service and Institute of Molecular Medicine Finland (FIMM) for providing the scRNASeq service. We thank Biomedicum Molecular Imaging Unit for the imaging facilities.

## SUPPLEMENTARY MATERIAL

The Supplementary Material for this article can be found online at: https://www.frontiersin.org/articles/10.3389/fphys.2020.591450/full#supplementary-material

**Supplementary Figure 1 |** Characterization of single-cell RNA sequencing clusters in HEL24.3 cells. **(A)** UMAP (Uniform Manifold Approximation and Projection) plot of flow and static cells. **(B)** UMAP plot of the delineated clusters. **(C)** Dot plot of the marker genes in delineated clusters. **(D)** Feature plot of blood (*PECAM1, CDH5*) and lymphatic (*PROX1, PDPN*) EC marker gene expression. **(E)** Violin plot of EC marker genes in all identified clusters.

**Supplementary Figure 2 |** The expression of venous and arterial genes in hiPSC-EC flow and static clusters (HEL24.3). **(A)** Venous genes. **(B)** Arterial genes.

**Supplementary Figure 3 |** The effect of flow on hiPSC-EC gene expression (HEL24.3). **(A)** Selected genes upregulated by the exposure to flow. **(B)** Genes downregulated in response to flow.

**Supplementary Figure 4 |** NOTCH and VEGF pathway gene expression in scRNASeq (HEL24.3). **(A)** NOTCH pathway genes expressed in flow and static clusters. **(B)** VEGF pathway genes expressed in flow and static clusters.

**Supplementary Table 1 |** List of differentially expressed genes upon flow exposure in **(A)** bulk RNASeq data, **(B)** scRNASeq data and **(C)** in combined analysis of bulk and single-cell RNASeq data.

## REFERENCES

Adams, G. N., Stavrou, E. X., Fang, C., Merkulova, A., Alaiti, M. A., Nakajima, K., et al. (2013). Prolylcarboxypeptidase promotes angiogenesis and vascular repair. *Blood* 122, 1522–1531. doi: 10.1182/blood-2012-10-460360

Augustin, H. G., Koh, G. Y., Thurston, G., and Alitalo, K. (2009). Control of vascular morphogenesis and homeostasis through the angiopoietin–Tie system. *Nat. Rev. Mol. Cell Biol.* 10, 165–177. doi: 10.1038/nrm2639

Babendreyer, A., Molls, L., Simons, I. M., Dreymueller, D., Biller, K., Jahr, H., et al. (2019). The metalloproteinase ADAM15 is upregulated by shear stress and promotes survival of endothelial cells. *J. Mol. Cell. Cardiol.* 134, 51–61. doi: 10.1016/j.yjmcc.2019.06.017

Baeyens, N., Bandyopadhyay, C., Coon, B. G., Yun, S., and Schwartz, M. A. (2016). Endothelial fluid shear stress sensing in vascular health and disease. *J. Clin. Invest.* 126, 821–828. doi: 10.1172/jci83083

Bhattacharya, R., Senbanerjee, S., Lin, Z., Mir, S., Hamik, A., Wang, P., et al. (2005). Inhibition of vascular permeability factor/vascular endothelial growth factor-mediated angiogenesis by the Kruppel-like factor KLF2. *J. Biol. Chem.* 280, 28848–28851. doi: 10.1074/jbc.c500200200

Bhattacharya, R., Wang, E., Dutta, S. K., Vohra, P. K., Guangqi, E., Prakash, Y. S., et al. (2012). NHERF-2 maintains endothelial homeostasis. *Blood* 119, 4798–4806. doi: 10.1182/blood-2011-11-392563

Butler, A., Hoffman, P., Smibert, P., Papalexi, E., and Satija, R. (2018). Integrating single-cell transcriptomic data across different conditions, technologies, and species. *Nat. Biotechnol.* 36, 411–420. doi: 10.1038/nbt.4096

Campinho, P., Vilfan, A., and Vermot, J. (2020). Blood flow forces in shaping the vascular system: a focus on endothelial cell behavior. *Front. Physiol.* 11:552. doi: 10.3389/fphys.2020.00552

Conway, D. E., Sakurai, Y., Weiss, D., Vega, J. D., Taylor, W. R., Jo, H., et al. (2009). Expression of CYP1A1 and CYP1B1 in human endothelial cells: regulation by fluid shear stress. *Cardiovasc. Res.* 81, 669–677. doi: 10.1093/cvr/cvn360

Dekker, R. J., van Soest, S., Fontijn, R. D., Salamanca, S., de Groot, P. G., VanBavel, E., et al. (2002). Prolonged fluid shear stress induces a distinct set of endothelial cell genes, most specifically lung Krüppel-like factor (KLF2). *Blood* 100, 1689–1698. doi: 10.1182/blood-2002-01-0046

Dekker, R. J., van Thienen, J. V., Rohlena, J., de Jager, S. C., Elderkamp, Y. W., Seppen, J., et al. (2005). Endothelial KLF2 links local arterial shear stress levels to the expression of vascular tone-regulating genes. *Am. J. Pathol.* 167, 609–618. doi: 10.1016/s0002-9440(10)63002-7

Deshwar, A. R., Chng, S. C., Ho, L., Reversade, B., and Scott, I. C. (2016). The Apelin receptor enhances Nodal/TGFβ signaling to ensure proper cardiac development. *eLife* 5:e13758. doi: 10.7554/eLife.13758

Dinkova-Kostova, A. T., and Talalay, P. (2000). Persuasive evidence that quinone reductase type 1 (DT diaphorase) protects cells against the toxicity of electrophiles and reactive forms of oxygen. *Free Radic. Biol. Med.* 29, 231–240.

Doddaballapur, A., Michalik, K. M., Manavski, Y., Lucas, T., Houtkooper, R. H., You, X., et al. (2015). Laminar shear stress inhibits endothelial cell metabolism via KLF2-mediated repression of PFKFB3. *Arterioscler. Thromb. Vasc. Biol.* 35, 137–145. doi: 10.1161/atvbaha.114.304277

Fang, J. S., Coon, B. G., Gillis, N., Chen, Z., Qiu, J., Chittenden, T. W., et al. (2017). Shear-induced Notch-Cx37-p27 axis arrests endothelial cell cycle to enable arterial specification. *Nat. Commun.* 8:2149.

Feng, Q., Song, W., Lu, X., Hamilton, J. A., Lei, M., Peng, T., et al. (2002). Development of heart failure and congenital septal defects in mice lacking endothelial nitric oxide synthase. *Circulation* 106, 873–879. doi: 10.1161/01.cir.0000024114.82981.ea

Fernández-Hernando, C., Yu, J., Dávalos, A., Prendergast, J., and Sessa, W. C. (2010). Endothelial-specific overexpression of caveolin-1 accelerates atherosclerosis in apolipoprotein E-deficient mice. *Am. J. Pathol.* 177, 998–1003. doi: 10.2353/ajpath.2010.091287

Freedman, S. J., Sun, Z.-Y. J., Kung, A. L., France, D. S., Wagner, G., and Eck, M. J. (2003). Structural basis for negative regulation of hypoxia-inducible factor-1α by CITED2. *Nat. Struct. Mol. Biol.* 10, 504–512. doi: 10.1038/nsb936

Giacomelli, E., Bellin, M., Orlova, V. V., and Mummery, C. L. (2017). Co-differentiation of human pluripotent stem cells-derived cardiomyocytes and endothelial cells from cardiac mesoderm provides a three-dimensional model of cardiac microtissue. *Curr. Protoc. Hum. Genet.* 95, 21.9.1–21.9.22.

Guo, L., Zhang, H., Hou, Y., Wei, T., and Liu, J. (2016). Plasmalemma vesicle-associated protein: a crucial component of vascular homeostasis. *Exp. Ther. Med.* 12, 1639–1644. doi: 10.3892/etm.2016.3557

Hafemeister, C., and Satija, R. (2019). Normalization and variance stabilization of single-cell RNA-seq data using regularized negative binomial regression. *Genome Biol.* 20:296.

Halaidych, O. V., Freund, C., van den Hil, F., Salvatori, D. C. F., Riminucci, M., Mummery, C. L., et al. (2018). Inflammatory responses and barrier function of endothelial cells derived from human induced pluripotent stem cells. *Stem Cell Rep.* 10, 1642–1656. doi: 10.1016/j.stemcr.2018.03.012

Helbing, T., Arnold, L., Wiltgen, G., Hirschbihl, E., Gabelmann, V., Hornstein, A., et al. (2017). Endothelial BMP4 regulates leukocyte diapedesis and promotes inflammation. *Inflammation* 40, 1862–1874. doi: 10.1007/s10753-017-0627-0

Horrillo, A., Porras, G., Ayuso, M. S., and González-Manchón, C. (2016). Loss of endothelial barrier integrity in mice with conditional ablation of podocalyxin (Podxl) in endothelial cells. *Eur. J. Cell Biol.* 95, 265–276. doi: 10.1016/j.ejcb.2016.04.006

Ikuno, T., Masumoto, H., Yamamizu, K., Yoshioka, M., Minakata, K., Ikeda, T., et al. (2017). Efficient and robust differentiation of endothelial cells from human induced pluripotent stem cells via lineage control with VEGF and cyclic AMP. *PLoS One* 12:e0173271. doi: 10.1371/journal.pone.0173271

Issan, Y., Kornowski, R., Aravot, D., Shainberg, A., Laniado-Schwartzman, M., Sodhi, K., et al. (2014). Heme oxygenase-1 induction improves cardiac function following myocardial ischemia by reducing oxidative stress. *PLoS One* 9:e92246. doi: 10.1371/journal.pone.0092246

Iwama, H., Uemura, S., Naya, N., Imagawa, K.-I., Takemoto, Y., Asai, O., et al. (2006). Cardiac expression of placental growth factor predicts the improvement of chronic phase left ventricular function in patients with acute myocardial infarction. *J. Am. Coll. Cardiol.* 47, 1559–1567. doi: 10.1016/j.jacc.2005.11.064

Kalucka, J., de Rooij, L. P. M. H., Goveia, J., Rohlenova, K., Dumas, S. J., Meta, E., et al. (2020). Single-cell transcriptome atlas of murine endothelial cells. *Cell* 180, 764–779.

Küppers, V., Vockel, M., Nottebaum, A. F., and Vestweber, D. (2014). Phosphatases and kinases as regulators of the endothelial barrier function. *Cell Tissue Res.* 355, 577–586. doi: 10.1007/s00441-014-1812-1

Mack, J. J., Mosqueiro, T. S., Archer, B. J., Jones, W. M., Sunshine, H., Faas, G. C., et al. (2017). NOTCH1 is a mechanosensor in adult arteries. *Nat. Commun.* 8:1620.

Masoud, A. G., Lin, J., Azad, A. K., Farhan, M. A., Fischer, C., Zhu, L. F., et al. (2020). Apelin directs endothelial cell differentiation and vascular repair following immune-mediated injury. *J. Clin. Invest.* 130, 94–107. doi: 10.1172/jci128469

Meder, D., Shevchenko, A., Simons, K., and Füllekrug, J. (2005). Gp135/podocalyxin and NHERF-2 participate in the formation of a preapical domain during polarization of MDCK cells. *J. Cell Biol.* 168, 303–313. doi: 10.1083/jcb.200407072

Melchionna, R., Porcelli, D., Mangoni, A., Carlini, D., Liuzzo, G., Spinetti, G., et al. (2005). Laminar shear stress inhibits CXCR4 expression on endothelial cells: functional consequences for atherogenesis. *FASEB J.* 19, 629–631.

Mueller, P. A., Yang, L., Ubele, M., Mao, G., Brandon, J., Vandra, J., et al. (2019). Coronary artery disease risk-associated Plpp3 gene and its product lipid phosphate phosphatase 3 regulate experimental atherosclerosis. *Arterioscler. Thromb. Vasc. Biol.* 39, 2261–2272. doi: 10.1161/atvbaha.119.313056

Nakamura, T., Funayama, H., Kubo, N., Yasu, T., Ishikawa, S.-E., and Momomura, S.-I. (2006). Elevation of plasma placental growth factor in the patients with ischemic cardiomyopathy. *J. Card. Fail.* 12:S177. doi: 10.1016/j.cardfail.2006.08.162

Nawroth, R., Poell, G., Ranft, A., Kloep, S., Samulowitz, U., Fachinger, G., et al. (2002). VE-PTP and VE-cadherin ectodomains interact to facilitate regulation of phosphorylation and cell contacts. *EMBO J.* 21, 4885–4895. doi: 10.1093/emboj/cdf497

Ohashi, M., Runge, M. S., Faraci, F. M., and Heistad, D. D. (2006). MnSOD deficiency increases endothelial dysfunction in ApoE-deficient mice. *Arterioscler. Thromb. Vasc. Biol.* 26, 2331–2336. doi: 10.1161/01.atv.0000238347.77590.c9

Ohtani-Kaneko, R., Sato, K., Tsutiya, A., Nakagawa, Y., Hashizume, K., and Tazawa, H. (2017). Characterisation of human induced pluripotent stem cell-derived endothelial cells under shear stress using an easy-to-use microfluidic cell culture system. *Biomed. Microdevices* 19:91.

Orlova, V. V., Drabsch, Y., Freund, C., Petrus-Reurer, S., van den Hil, F. E., Muenthaisong, S., et al. (2014a). Functionality of endothelial cells and pericytes from human pluripotent stem cells demonstrated in cultured vascular plexus and zebrafish xenografts. *Arterioscler. Thromb. Vasc. Biol.* 34, 177–186. doi: 10.1161/atvbaha.113.302598

Orlova, V. V., van den Hil, F. E., Petrus-Reurer, S., Drabsch, Y., Ten Dijke, P., and Mummery, C. L. (2014b). Generation, expansion and functional analysis of endothelial cells and pericytes derived from human pluripotent stem cells. *Nat. Protoc.* 9, 1514–1531. doi: 10.1038/nprot.2014.102

Paik, D. T., Tian, L., Lee, J., Sayed, N., Chen, I. Y., Rhee, S., et al. (2018). Large-scale single-cell RNA-Seq reveals molecular signatures of heterogeneous populations of human induced pluripotent stem cell-derived endothelial cells. *Circ. Res.* 123, 443–450. doi: 10.1161/circresaha.118.312913

Polacheck, W. J., Kutys, M. L., Yang, J., Eyckmans, J., Wu, Y., Vasavada, H., et al. (2017). A non-canonical Notch complex regulates adherens junctions and vascular barrier function. *Nature* 552, 258–262. doi: 10.1038/nature24998

Rufaihah, A. J., Huang, N. F., Kim, J., Herold, J., Volz, K. S., Park, T. S., et al. (2013). Human induced pluripotent stem cell-derived endothelial cells exhibit functional heterogeneity. *Am. J. Transl. Res.* 5, 21–35.

Saarimäki-Vire, J., Balboa, D., Russell, M. A., Saarikettu, J., Kinnunen, M., Keskitalo, S., et al. (2017). An activating STAT3 mutation causes neonatal diabetes through premature induction of pancreatic differentiation. *Cell Rep.* 19, 281–294. doi: 10.1016/j.celrep.2017.03.055

Sangwung, P., Zhou, G., Nayak, L., Chan, E. R., Kumar, S., Kang, D.-W., et al. (2017). KLF2 and KLF4 control endothelial identity and vascular integrity. *JCI Insight* 2:e91700.

Schrimpf, C., Xin, C., Campanholle, G., Gill, S. E., Stallcup, W., Lin, S.-L., et al. (2012). Pericyte TIMP3 and ADAMTS1 modulate vascular stability after kidney injury. *J. Am. Soc. Nephrol.* 23, 868–883. doi: 10.1681/asn.2011080851

Smadja, D. M., d'Audigier, C., Bièche, I., Evrard, S., Mauge, L., Dias, J.-V., et al. (2011). Thrombospondin-1 is a plasmatic marker of peripheral arterial disease that modulates endothelial progenitor cell angiogenic properties. *Arterioscler. Thromb. Vasc. Biol.* 31, 551–559. doi: 10.1161/atvbaha.110.220624

Tisato, V., Zamboni, P., Menegatti, E., Gianesini, S., Volpi, I., Zauli, G., et al. (2013). Endothelial PDGF-BB produced ex vivo correlates with relevant hemodynamic parameters in patients affected by chronic venous disease. *Cytokine* 63, 92–96. doi: 10.1016/j.cyto.2013.04.018

Torry, R. J., Tomanek, R. J., Zheng, W., Miller, S. J., Labarrere, C. A., and Torry, D. S. (2009). Hypoxia increases placenta growth factor expression in human myocardium and cultured neonatal rat cardiomyocytes. *J. Heart Lung Transplant.* 28, 183–190. doi: 10.1016/j.healun.2008.11.917

Trittmann, J. K., Almazroue, H., Jin, Y., and Nelin, L. D. (2019). DDAH1 regulates apoptosis and angiogenesis in human fetal pulmonary microvascular endothelial cells. *Physiol. Rep.* 7:e14150.

Trokovic, R., Weltner, J., and Otonkoski, T. (2015a). Generation of iPSC line HEL24.3 from human neonatal foreskin fibroblasts. *Stem Cell Res.* 15, 266–268. doi: 10.1016/j.scr.2015.05.012

Trokovic, R., Weltner, J., and Otonkoski, T. (2015b). Generation of iPSC line HEL47.2 from healthy human adult fibroblasts. *Stem Cell Res.* 15, 263–265. doi: 10.1016/j.scr.2015.05.013

Vazão, H., Rosa, S., Barata, T., Costa, R., Pitrez, P. R., Honório, I., et al. (2017). High-throughput identification of small molecules that affect human embryonic vascular development. *Proc. Natl. Acad. Sci. U S A.* 114, E3022–E3031. doi: 10.1073/pnas.1617451114

Vilà-González, M., Kelaini, S., Magee, C., Caines, R., Campbell, D., Eleftheriadou, M., et al. (2019). Enhanced function of induced pluripotent stem cell-derived endothelial cells through ESM1 signaling. *Stem Cells* 37, 226–239. doi: 10.1002/stem.2936

Wallgard, E., Larsson, E., He, L., Hellström, M., Armulik, A., Nisancioglu, M. H., et al. (2008). Identification of a core set of 58 gene transcripts with broad and specific expression in the microvasculature. *Arterioscler. Thromb. Vasc. Biol.* 28, 1469–1476. doi: 10.1161/atvbaha.108.165738

Wirrig, E. E., Snarr, B. S., Chintalapudi, M. R., O'neal, J. L., Phelps, A. L., Barth, J. L., et al. (2007). Cartilage link protein 1 (Crtl1), an extracellular matrix component playing an important role in heart development. *Dev. Biol.* 310, 291–303. doi: 10.1016/j.ydbio.2007.07.041

Yanagisawa, M., Kurihara, H., Kimura, S., Tomobe, Y., Kobayashi, M., Mitsui, Y., et al. (1988). A novel potent vasoconstrictor peptide produced by vascular endothelial cells. *Nature* 332, 411–415. doi: 10.1038/332411a0

**Conflict of Interest:** The authors declare that the research was conducted in the absence of any commercial or financial relationships that could be construed as a potential conflict of interest.

frontiers in Physiology

REVIEW
published: 15 October 2020
doi: 10.3389/fphys.2020.586852

# Remodeling of the Microvasculature: May the Blood Flow Be With You

*Ricardo Santamaría[1†], María González-Álvarez[2†], Raquel Delgado[1], Sergio Esteban[1] and Alicia G. Arroyo[1,2*]*

[1] Department of Vascular Pathophysiology, Centro Nacional de Investigaciones Cardiovasculares (CNIC), Madrid, Spain,
[2] Department of Molecular Biomedicine, Centro de Investigaciones Biológicas Margarita Salas (CIB-CSIC), Madrid, Spain

The vasculature ensures optimal delivery of nutrients and oxygen throughout the body, and to achieve this function it must continually adapt to varying tissue demands. Newly formed vascular plexuses during development are immature and require dynamic remodeling to generate well-patterned functional networks. This is achieved by remodeling of the capillaries preserving those which are functional and eliminating other ones. A balanced and dynamically regulated capillary remodeling will therefore ensure optimal distribution of blood and nutrients to the tissues. This is particularly important in pathological contexts in which deficient or excessive vascular remodeling may worsen tissue perfusion and hamper tissue repair. Blood flow is a major determinant of microvascular reshaping since capillaries are pruned when relatively less perfused and they split when exposed to high flow in order to shape the microvascular network for optimal tissue perfusion and oxygenation. The molecular machinery underlying blood flow sensing by endothelial cells is being deciphered, but much less is known about how this translates into endothelial cell responses as alignment, polarization and directed migration to drive capillary remodeling, particularly *in vivo*. Part of this knowledge is theoretical from computational models since blood flow hemodynamics are not easily recapitulated by *in vitro* or *ex vivo* approaches. Moreover, these events are difficult to visualize *in vivo* due to their infrequency and briefness. Studies had been limited to postnatal mouse retina and vascular beds in zebrafish but new tools as advanced microscopy and image analysis are strengthening our understanding of capillary remodeling. In this review we introduce the concept of remodeling of the microvasculature and its relevance in physiology and pathology. We summarize the current knowledge on the mechanisms contributing to capillary regression and to capillary splitting highlighting the key role of blood flow to orchestrate these processes. Finally, we comment the potential and possibilities that microfluidics offers to this field. Since capillary remodeling mechanisms are often reactivated in prevalent pathologies as cancer and cardiovascular disease, all this knowledge could be eventually used to improve the functionality of capillary networks in diseased tissues and promote their repair.

**Keywords: microvascular remodeling, capillary pruning, capillary splitting, blood flow, shear stress, endothelial cells, 3D-confocal microscopy, microfluidics**

OPEN ACCESS

***Edited by:***
*Anna Rita Cantelmo, Université Lille Nord de France, France*

***Reviewed by:***
*Oliver Baum, Charité – Universitätsmedizin Berlin, Germany*
*Anne-Clémence Vion, INSERM U1087 L'Unité de Recherche de l'Institut Duthorax, France*

***Correspondence:**
*Alicia G. Arroyo*
*agarroyo@cib.csic.es*

*[†] These authors have contributed equally to this work*

***Specialty section:***
*This article was submitted to Vascular Physiology, a section of the journal Frontiers in Physiology*

***Received:*** *24 July 2020*
***Accepted:*** *09 September 2020*
***Published:*** *15 October 2020*

***Citation:***
*Santamaría R, González-Álvarez M, Delgado R, Esteban S and Arroyo AG (2020) Remodeling of the Microvasculature: May the Blood Flow Be With You. Front. Physiol. 11:586852. doi: 10.3389/fphys.2020.586852*

## DYNAMIC MICROVASCULAR REMODELING IN PHYSIOLOGY AND PATHOPHYSIOLOGY

The microvasculature constantly adjusts to tissue metabolic demands through functional and structural adaptations (Pries and Secomb, 2014). This is attained by dynamic remodeling of the capillaries preserving and expanding those which are functional and eliminating redundant or poorly efficient ones. We will refer in this review as microvascular or capillary remodeling to the dynamic gain or loss of capillaries for increasing or decreasing the complexity of the microvascular network in order to optimize oxygen and nutrient distribution into the tissue. Two main processes determine microvascular reshaping in several organs and tissues during their growth and development: i) capillary pruning or regression, the elimination of non-functional capillaries to form a functional hierarchically branched network; and ii) duplication of highly perfused capillaries which results in the quick expansion of the microvasculature. Duplication can occur via intussusceptive angiogenesis, recognized as the division of a large lumen within a sinus, or by splitting in tubular capillaries, the process in which we will mainly focus this review (**Figure 1**).

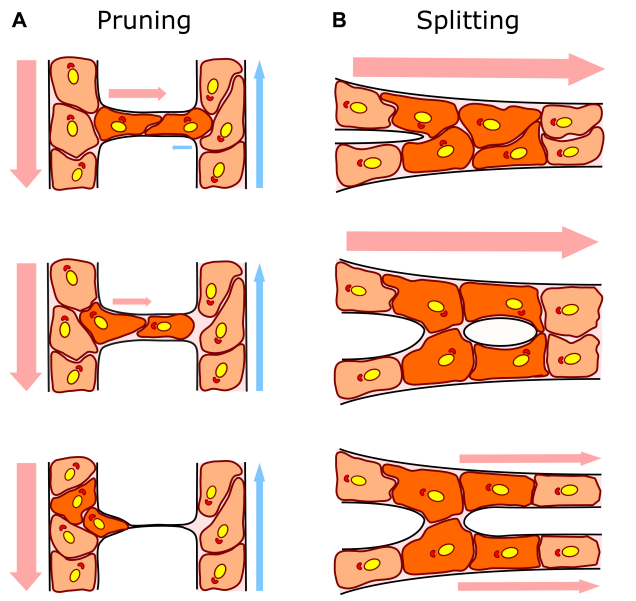


**FIGURE 1 |** Capillary remodeling by pruning/regression and splitting/duplication. **(A)** In capillary pruning the poorly perfused vessel is selected to regress, its lumen collapses and the endothelial cells inside (dark orange) polarized against flow and migrate toward the higher flow adjacent vessel. **(B)** In capillary splitting, highly perfused vessels vasodilate and endothelial cells nearby the intersections (Y bifurcation; dark orange) reorganize their cytoskeleton, migrate toward the lumen and form an intraluminal pillar that will eventually split the vessel forming two daughter vessels. Arrows indicate the direction and intensity of the blood flow (arterial flow in red and venous flow in blue). Endothelial cell nuclei and Golgi are colored in yellow and red, respectively, to show endothelial cell polarization preferentially against the flow.

Once immature vascular plexuses are formed mostly by sprouting angiogenesis, capillary remodeling becomes essential to preserve tissue homeostasis in physiological contexts during development but also in adult tissues. Capillary regression takes place in all developmental stages during embryogenesis after the formation of the first primitive vasculature as in the chicken yolk sac and limb embryo (Feinberg et al., 1986; Lee et al., 2011) or the brain and intersegmental vessels in the zebrafish (Chen et al., 2012; Kochhan et al., 2013; Franco et al., 2015), but also right after birth like in the postnatal mouse retina (Connolly et al., 1988). Vascular regression can also be associated not only to optimization of the blood flow network but also to the elimination of unneeded tissue like in hyaloid regression after birth (Lang et al., 1994; Ito and Yoshioka, 1999; Lobov et al., 2005) or in involution of post-lactation mammary gland and ovarian luteolysis in the adult (Goede et al., 1998; Andres and Djonov, 2010); in these contexts endothelial cell apoptosis is considered the main mechanism and will not be discussed further in this review (Watson et al., 2017). Capillary duplication promotes expansion of the microvasculature during embryo and organ development as observed in the chicken chorioallantoic membrane (Patan et al., 1993) and in a variety of tissues after birth as the lung, heart, intestine, liver or kidney (Patan et al., 1992). It also contributes to capillary growth upon increasing tissue demands as in the exercising skeletal muscle (Prior et al., 2003; Mentzer and Konerding, 2014). Notably these vascular reshaping mechanisms are often reactivated or defective in prevalent pathologies leading generally to a dysfunctional microvasculature which aggravates damage and hinders tissue repair. Although altered capillary pruning has been described in tumors (Holash et al., 1999), it may also occur in ischemic disorders as myocardial infarction (Luttun et al., 2002; Gkontra et al., 2019), hypertension (Boudier, 1999), and age-related neurodegeneration or Alzheimer's disease (Wu et al., 2005; Bell and Zlokovic, 2009; Sagare et al., 2012) exacerbating the hypo-perfusion of the damaged tissue. Capillary splitting has been observed among others in inflammatory bowel disease (Mori et al., 2005; Ravnic et al., 2007; Esteban et al., 2020), tumors (Patan et al., 1996b; Ribatti and Djonov, 2012), lung dysplasia of prematurity (De Paepe et al., 2015, 2017) and other syndromes (Giacomini et al., 2015) contributing to disease progression. Impaired endothelial cell responses involved in microvascular remodeling can also result in the persistence or arteriovenous shunts, the basis for arteriovenous malformations (AVM) (Red-Horse and Siekmann, 2019).

Capillary remodeling events are dynamic, occurring in hours to a few days and involve active endothelial cell rearrangements and quick morphological changes of the microvasculature, often without compromising its integrity since the basement membrane is preserved (Ricard and Simons, 2015). The current model for capillary pruning proposes a multi-staged model to explain the dynamics of the vessel regression process observed in the postnatal mouse retina and intersegmental vessels in zebrafish (Franco et al., 2015, 2016; Franco and Gerhardt, 2017). Firstly, there is a blood flow-driven selection of the regressing vascular branch which triggers the subsequent morphological alterations. The selected vessel receiving low flow constricts

leading to lumen stenosis or even collapse. Then, endothelial cells retract along with junctional remodeling and migrate intraluminally from the regressing segment to the higher-flow adjacent vessel (Franco et al., 2015; Barbacena et al., 2016). The final resolution step involves the complete integration of endothelial cells from the regressing branch into the neighbor vessel leaving an empty basement membrane surrounded by pericytes which is called "empty sleeve" and considered a hallmark of vessel regression (Barbacena et al., 2016). The number of regressed segments increased only slightly and did not accumulate from P4 to P8 during remodeling of the postnatal retinal microvasculature indicating that in spite of the limitation of the analysis in still images, these pruning events seem dynamic and with a limited lifetime (Franco et al., 2015). Accordingly, live microscopy of the intersegmental vessels of zebrafish embryos showed that endothelial cell dynamics during segment regression occur in about 24 h (Franco et al., 2015).

In the context of capillary duplication by splitting or intussusceptive angiogenesis observed for example in the chicken chorioallantoic membrane, the rat skeletal muscle and the mouse inflamed intestine, the division of the vascular plexus takes place through the formation and expansion of intraluminal pillars. Increased blood flow in the capillary bed causes vasodilation of the blood vessels. The endothelial cells of the vessel reorganize their cytoskeleton, develop luminal filopodia mostly from the inter-junctional area and migrate toward the vascular lumen until they join the opposite side and rearrange their junctions (Patan et al., 1996a; Burri et al., 2004; Williams et al., 2006a). The cells form a cell bridge in the center of the vessel, rich in parallel actin filaments. These steps in the nascent pillar have been visualized by microscopy techniques, but it remains unknown how filopodia grow and fuse under high blood flow that would impose a mechanical barrier to the process. Pillars form in vessels with an intact basement membrane (Mentzer and Konerding, 2014), and subsequently, a 1–5 μm-pore forms in the center of the capillary which is invaded by surrounding tissue pericytes and myofibroblasts. These cells deposit collagen fibers stabilizing the formation of the pillar. Finally, the pillars grow in diameter and join other pillars splitting the capillary into two parallel vessels in the form of loops and duplications (Burri et al., 2004; Karthik et al., 2018). Of note, pillar formation in the chorioallantoic membrane initiated 40 min to few hours after vasodilation and in the inflamed ear model full capillary splitting was achieved in 3 days (Styp-Rekowska et al., 2011). Recently a pioneer study has analyzed the dynamics of vessel splitting by live microscopy imaging in the caudal vein plexus of zebrafish and showed that pillar formation and fusion can occur in just a few hours (Karthik et al., 2018). In this study, new data obtained by 3D reconstruction of scanning electron microscopy images have shown with unprecedented resolution the process of formation of intraluminal pillars and their fusion and highlighted the need of understanding the dynamics and cellular events of the loss of endothelial cell polarity, cytoskeleton rearrangement and establishment of new endothelial cell junctions at the pillar (Karthik et al., 2018).

# BLOOD FLOW-DRIVEN CAPILLARY REGRESSION AND SPLITTING: TWO SIDES OF THE SAME COIN?

The dynamic nature of microvascular remodeling closely reflects the dynamically changing nature of blood flow, constantly responding to physicochemical cues in the tissues (Pries and Secomb, 2014). Pioneer studies in the embryo yolk sac established the essential role of blood flow in vascular remodeling (le Noble et al., 2004) and put the foundations about the dynamic responses induced by blood flow in endothelial cells as their directed migration from small capillaries to larger arteries (Udan et al., 2013). In addition to influencing angiogenic endothelial cell sprouting (Campinho et al., 2020), blood flow governs microvascular remodeling by promoting pruning of capillaries when not constantly perfused and expanding them when exposed to high flow in order to shape the microvascular network for optimal blood flow distribution (**Figure 2A**). However, the concept that low flow drives pruning and high flow triggers splitting is an oversimplification since it is not the magnitude but the gradients of blood flow that rule both remodeling processes as discussed in more detail in the following sections.

## Blood Flow Basics

Blood flow refers to the movement of the blood through the vessels. Flow is typically characterized based on certain physical parameters yielding different types of flow (Chiu and Chien, 2011). The flow is considered laminar, that is smooth and continuous, when all the fluid particles flow in parallel fluid layers. Otherwise, flow is defined as turbulent when it experiences irregularities and chaotic motion as it occurs at high velocities or in certain geometries such as big curvatures, bifurcations, anastomoses or stenotic sites. In general, the microcirculation responds to a steady and laminar flow. However, this assumption cannot be made in larger vessels like arteries where the flow is pulsatile due to the heart beat. Another type of flow observed in the vasculature and maybe relevant for remodeling events is reciprocating flow. In reciprocating or oscillatory flow, the velocity oscillates back and forth with a given frequency, resulting in a minimal forward net blood flow. Impinging flow can be found mainly at arterial bifurcation apices. This type of flow has classically a T-shaped geometry, where the inlet with high velocity collapses against a wall generating a stagnation point (Ostrowski et al., 2014).

Wall shear stress (referred as shear stress hereon) is the force per unit area acting on the vessel wall performed by the blood flowing through the vessel. It has pressure units (Pascal, Pa, in IS; in vascular research dyn/cm$^2$). This force is tangential and depends on two parameters: the viscosity of blood and the rate at which the velocity of blood changes along the vessel radius (shear rate). The shear rate could be in theory correlated with vessel diameter, but only taking into consideration the instantaneous volumetric flow rate and velocity field through that vessel. In addition, since the blood is in reality a non-Newtonian fluid, its viscosity will change depending on this shear rate (Eckmann et al., 2000). Recent computational efforts have also shown the

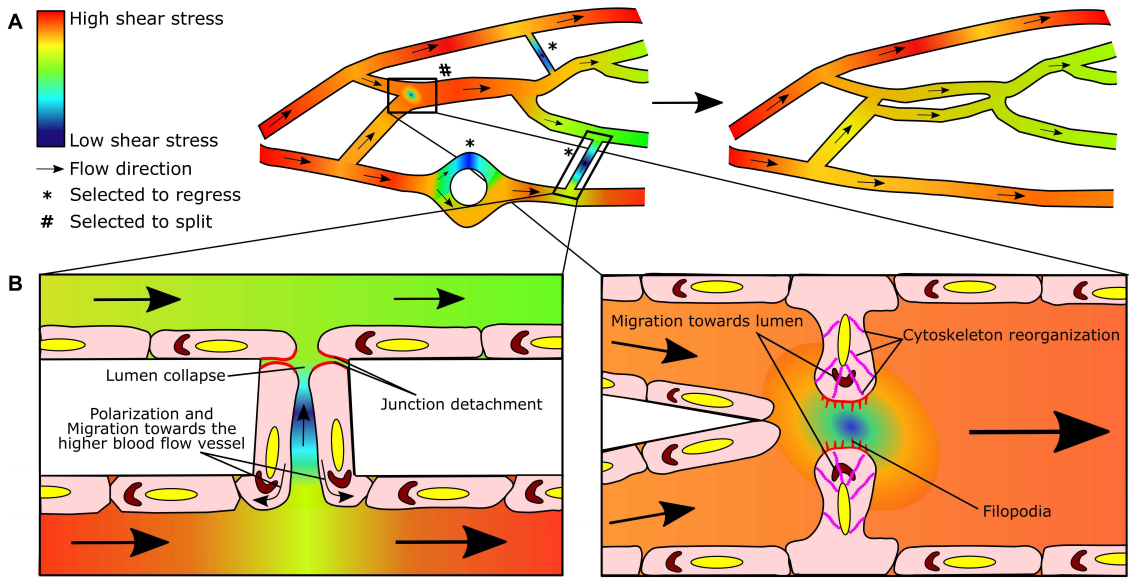


**FIGURE 2 |** Blood flow-driven capillary pruning and splitting: two sides of the same coin. **(A)** Heterogeneous flow distribution in dynamic microvascular networks results in shear stress gradients (left). As a consequence, lower perfused segments will be selected to regress (*) and highly perfused segments to split (#) in order to redistribute flow in a more efficient manner in the remodeled network (right). **(B)** Endothelial cells sense the blood flow and shear stress gradients and respond by elongating and aligning in the direction of flow. In the case of pruning, endothelial cells in the regressing segment (left panel) detach from their neighbors (red) during lumen collapse, polarize (Golgi in brown) and migrate toward the region of higher flow in the adjacent vessel (curved arrows). In capillary splitting (right panel), endothelial cells close to shear stress gradient at the bifurcation, reorganize their cytoskeleton (pink), protrude luminal filopodia (red), and polarize (Golgi in brown) and migrate toward the lumen to form the intraluminal pillar; note the area drawn with low blood flow/shear stress at the nascent pillar which could be permissive for filopodia growth and fusion. Heat map colors indicate the predicted/simulated shear stress values in the modeled microvascular network. Straight arrows indicate the flow direction. Adapted from Chen et al. (2012).

essential role of circulating cells, often disregarded in theoretical *in silico* simulations, in modulating blood viscosity and regional shear stress (Zhou et al., 2020). Moreover, the geometry of the microvascular network also influences shear stress patterns and values, particularly at curvatures and bifurcations (Chiu and Chien, 2011). Therefore, even though in principle shear stress could be expected to be high in small vessels, in regressing capillaries (with net blood flow practically null) and duplicating capillaries (with altered blood flow related to the geometry), shear stress values are rather low. In fact, shear stress and fluid velocity are simulated together and correlate in the retina and other vascular plexus (Filipovic et al., 2009; Szczerba et al., 2009; Bernabeu et al., 2014). In **Table 1** shear stress values at different vascular territories and developmental stages are included as a reference.

Shear stress is sensed by the endothelial cells in the inner lining of the vessels and it is a major determinant of endothelial cell behavior (Chiu and Chien, 2011). But it is not only the magnitude of shear stress but its fluctuations that determine the responses of endothelial cells and therefore influence capillary remodeling. Time-related parameters as duration, ramping rate and frequency/oscillations of shear stress have differential impact on endothelial cell morphology and behavior (Yoshino et al., 2017). As an example, long exposure to disturbed instead of laminar flow upregulates pro-inflammatory genes and proliferation, which predisposes to atherosclerosis (Chiu and Chien, 2011; Mack et al., 2017), but short exposure to changing shear stress direction may underlie endothelial cell morphological changes relevant to capillary remodeling (Wang et al., 2013). And abrupt increase in shear stress augments endothelial cell membrane fluidity while gradual increase does not (Butler et al., 2002). Local changes and the 3D geometry of the network also generate shear stress spatial gradients between adjacent or nearby endothelial cells *in vitro* (Mack et al., 2017) or vascular segments *in vivo* (Franco et al., 2015). The pattern of shear stress is different in straight, branched and curved regions of the vasculature (Karino and Goldsmith, 1980; Karino et al., 1987; Nerem, 1993; Colangelo et al., 1994; Chien, 2003) and this can be related with the preference for Y and polygonal geometries in capillary splitting (Filipovic et al., 2009; Karthik et al., 2018) and H or O (loop) geometries in capillary regression (Bernabeu et al., 2014; Barbacena et al., 2016).

## Blood Flow and Capillary Pruning

Early reports pointed to endothelial cell apoptosis as the main actor in vessel regression (Meeson et al., 1999; Hahn et al., 2005; Lobov et al., 2005; Wang et al., 2011; Simonavicius et al., 2012). More recent works in the mouse yolk sac and postnatal retina among others have shown however that blood flow is critical to induce dynamic endothelial cell responses (le Noble et al., 2004; Udan et al., 2013; Franco et al., 2015). In particular, endothelial cells elongate and align along shear stress axis and gradients of shear stress induce endothelial cell polarization and directed migration toward the higher blood flow adjacent vessel during

**TABLE 1 |** Shear stress in microvascular remodeling. Summary of shear stress (SS) values in selected vascular territories under homeostatic and microvascular remodeling conditions *in vivo*. Note that capillary shear stress values obtained by computational approaches are based on theoretical input pressure values into the simulated network and may not accurately reflect *in vivo* physiological values.

| Vascular bed | SS (dyn/cm$^2$) | Comments | References |
|---|---|---|---|
| **Physiological shear stress values** | | | |
| **Human** | | | |
| Arteries (various tissues) | 1–7 | | Chiu and Chien (2011) |
| Veins (various tissues) | 0.6–1.1 | | |
| Vascular geometries | <4 | Arterial branch points and curvatures | |
| **Mouse** | | | |
| Embryo | ≈5 | | Udan et al. (2013) |
| Retinal Arteriole (p5 and p6) | 0–200 | Based on computational simulations | Bernabeu et al. (2014), Franco et al. (2015) |
| Retinal Arteriole (8-12 weeks) | 70 | Using a network modeling | Ganesan et al. (2010) |
| Retinal Venule (p5) | 0–100 | Based on computational simulations | Bernabeu et al. (2014) |
| Retinal Venule (p6) | 0–150 | Based on computational simulations | Franco et al. (2015) |
| Retinal Venule (8–12 weeks) | 55 | Using a network modeling | Ganesan et al. (2010) |
| Retinal Capillaries (p5 and p6) | 0–200 | Based on computational simulations | Bernabeu et al. (2014), Franco et al. (2015) |
| Retinal vessels order 1–3 (arterial) | 40–110 | Using a network modeling | Ganesan et al. (2010) |
| Retinal vessels order 1–3 (venous) | 25–90 | Using a network modeling | Ganesan et al. (2010) |
| Postnatal and adult mouse aorta | 60–250 | Mean SS in postnatal: 140 dyn/cm$^2$<br>Mean SS in adult: 95 dyn/cm$^2$ | Trachet et al. (2009) |
| **Zebrafish** | | | |
| Caudal Plexus Vein 25–42 hpf | 0–22.5 | Computational simulations | Karthik et al. (2018) |
| | 0–15 | At the pillar/splitting zone | |
| Intersegmental Vessels 5 dpf | 1.2 ± 0.2 | Pruning usually occurring | Choi et al. (2017) |
| **Chicken chorioallantoic membrane (CAM)** | | | |
| Chicken CAM Arterioles | 4.47 ± 2.7 | Mathematical simulations | Maibier et al. (2016) |
| Chicken CAM Venules | 4.65 ± 3.4 | Mathematical simulations | |
| **Rat** | | | |
| Skeletal muscle | 5.6 ± 0.8 | | Hudlicka et al. (2006) |
| **Capillary pruning and splitting shear stress values** | | | |
| **Pruning** | | | |
| Retina (p6) | 0–1 | Computational simulation pruned vessel | Bernabeu et al. (2014) |
| Retina (p6) | ≈0 | Computational simulation pruned vessel | Franco et al. (2015) |
| Zebrafish Brain (3 dpf) | 0.55 ± 0.05<br>0.18 ± 0.02 | Computational simulation of pruned vessel (2 different events) | Chen et al. (2012) |
| | 1 ± 0.2<br>1 | Computational simulation of unpruned adjacent vessel (2 different events) | |
| **Splitting** | | | |
| Zebrafish CVP (25–42 hpf) | 0.4 and 1 | Computational simulation after pillar appearance (values of 2 different pillars) | Karthik et al. (2018) |
| | 1.6 and 5 | Computational simulation before pillar appearance (linked with above pillars) | |
| | 11 | Computational simulation, 5 μm to pillar | |
| | 0.8 | Computational simulation in the shortest distance to the same pillar above | |
| Chick CAM | <0.3 and <0.6 | In the zone of the first intravascular pillar and in the interpillar surfaces | Lee et al. (2010) |
| Murine colitis | 15–45 | Computational simulations | Filipovic et al. (2009) |
| Murine colitis (and CAM) | <1 | Dead zone where pillars form | |
| Rat skeletal muscle (2 day-activity) | 11.4 ± 1.0 | Prior to splitting | Hudlicka et al. (2006) |

capillary pruning (Franco et al., 2015; Barbacena et al., 2016) (**Figure 2B**). Moreover, studies such as those performed in the brain vasculature of zebrafish suggest the existence of a flow threshold for vessel regression (Chen et al., 2012).

This new concept establishes that, contrary to expected, capillary endothelial cells are not quiescent, but subjected to flow changes that regulate their polarization and migratory behavior. It has been proposed that differential blood flow/shear stress

patterns in juxtaposed vessels drive asymmetries in cellular movements causing endothelial cells to migrate toward high flow neighboring vessels, thus favoring regression and pruning of the low blood flow capillaries (Lucitti et al., 2007; Chen et al., 2012; Kochhan et al., 2013; Franco et al., 2015). Strong flow/high shear stress seemed to attract endothelial cells making them polarize and migrate against blood flow (Tzima et al., 2002; Franco et al., 2015; Chang et al., 2017). Indeed, linear regression analysis identified a strong correlation between high shear stress values and cell polarization (Franco et al., 2015). But, how is blood flow and shear stress in the regressing segment? Quantification of blood flow and shear stress *in vivo* is challenging in particular in mouse models, and most information about shear stress values and patterns *in vivo*, in particular in capillaries, is derived from computational analysis and simulations. These models provide cues about these values in vascular networks with active capillary pruning as the mouse postnatal retina or the brain and the intersegmental vessels in zebrafish (Chen et al., 2012; Franco et al., 2015, 2016). In the postnatal mouse retina simulations predicted shear stress values up to 200 dyn/cm$^2$ at arterioles, 100–150 dyn/cm$^2$ at venules and 200 dyn/cm$^2$ in normal capillaries to values near 0 dyn/cm$^2$ in regressing capillaries which correlated with the percentage of cells aligned and polarized in each of these territories (Franco et al., 2015). Indeed, although dynamic quantification of shear stress cannot be analyzed, comparison of simulated distribution of blood flow and shear stress between P5 and P6 neonatal retinas suggest the presence of spatial and temporal gradients that could underlie pruning events (Bernabeu et al., 2014). Moreover, in the brain zebrafish vasculature capillaries with blood flow below a certain value were selected to regress (Chen et al., 2012). **Table 1** shows shear stress values observed or simulated in the context of vessel regression. Of note, live-imaging in zebrafish brain vasculature demonstrated that regressing vessel segments exhibit low or reciprocating flow, which decreased irreversibly prior to the onset of regression (Chen et al., 2012). The shear stress threshold to enter the regression program seems variable and depends on relative levels on juxtaposed vessel segments indicating the need for spatial shear stress gradients (Chen et al., 2012). In relation to this, vascular segments with lower shear stress segments in a range between 2.5 and 10 dyn/cm$^2$ often contained endothelial cells with very low axial or misaligned polarity vectors in the intersegmental vessels of zebrafish (Franco et al., 2015). However, in this state, endothelial cells were able to sense the onset of flow and responded dynamically polarizing against the direction of flow and migrating toward the highly perfused neighboring vessel. This paradoxical phenomenon, also observed in capillary splitting, underscores the relevance of shear stress ramping and gradients to trigger endothelial cell responses leading to microvascular remodeling. Finally, it has been observed that pruning of capillary segments often occurs at locations with H or O (loop) geometries, usually in flat vascular networks, but how bifurcations and intersections affect shear stress and thus endothelial cell migration and how capillary pruning may occur in 3D complex networks remains poorly characterized.

## Blood Flow and Capillary Splitting

Tiny holes representative of intraluminal pillars during intussusceptive angiogenesis were visible in vascular segments that were dilated and at triple or quadruple branching points in several tissues and organs (Patan et al., 1992), already indicating that blood flow and shear stress magnitude or gradients were relevant for this remodeling process. Indeed, a sustained increase in blood flow of between 50 and 60% in the chorioallantoic membrane of chicken was reported to increase shear stress and stimulate the creation of intraluminal pillars, leading to the division of the vascular sinus (Burri et al., 2004). Moreover, the increased vascular volume in the skeletal muscle induced by exercise or the administration of vasodilators as prazosin also led to capillary splitting (Zhou et al., 1998). In the zebrafish caudal vein plexus, blood flow is an essential requirement for vessel duplication as demonstrated by its occurrence only in perfused areas and by enhanced or reduced pillar formation observed with pharmacological strategies that increase (adrenergic agonist) or decrease (muscle contractility inhibitor) blood flow (Karthik et al., 2018). In models of experimental colitis, vasodilation of the intestine feeding arterioles has been reported (Mori et al., 2005) and impairing vasodilation prevents capillary splitting in the inflamed intestine (Esteban et al., 2020). Therefore, increased blood flow is considered a prerequisite for initiation of capillary splitting aimed to restore blood flow and shear stress in the duplicated segments (Egginton, 2011). Indeed shear stress will promote cellular events such as loss of apical-basal endothelial cell polarity, cytoskeleton and membrane rearrangements and filopodia protrusion to form the intraluminal pillars (Karthik et al., 2018) (**Figure 2B**). Although this review is focused on the role of shear stress in capillary remodeling, it is worth mentioning that increased blood flow may trigger splitting by elevating not only shear stress but also circumferential wall stress, which is similarly sensed by capillary endothelial cells (Lu and Kassab, 2011). How the increased blood flow induces the endothelial cell intraluminal rearrangements needed for the formation of pillars is far from being understood yet.

Since blood flow and shear stress cannot be quantified in the capillaries of the mucosa vascular plexus in the intestine, computational modeling has helped understand their contribution to capillary splitting. Previous computational studies of shear stress maps indicated that formation of new intravascular pillars was limited to regions of lower shear stress, less than 1 dyn/cm$^2$, that were constrained between high shear stress in the pillar midportion and the lateral vessel wall (Filipovic et al., 2009) (**Table 1**). In parallel, flow modeling showed that these pillars were favored in areas with high flow (Szczerba et al., 2009). Consequently, the accepted paradigm is that development of the pillars is caused by increased flow but it occurs in low shear/turbulent flow areas (Djonov et al., 2002; Lee et al., 2010). This paradox (similar to capillary pruning) could be explained if the high flow was not continuous or whether it occurred after a period of decreased flow as observed in the rabbit ear (Styp-Rekowska et al., 2011). These observations would suggest a role for shear stress gradients and ramping in capillary splitting, so that, perhaps, sharp gradients of both

shear stress and flow promote capillary duplication in areas which normally have very low shear stress. Indeed, this has been confirmed in an elegant study performed in zebrafish in which blood flow velocity and shear stress profiles have been simulated from live microscopy videos of the caudal vein plexus (Karthik et al., 2018). The authors observed that there was a steep drop in shear stress (about 2.5–5 dyn/cm$^2$) in the region of pillar formation and initial fusion and then, as the pillar grows and splitting occurs, shear stress increased gradually (between 10 and 12.5 dyn/cm$^2$).

## Beyond Blood Flow in Capillary Remodeling

At first, it was unclear how hemodynamic forces promoted endothelial cell migration in the mouse yolk sac (Udan et al., 2013), but it was proposed that endothelial cells could be responding to shear stress or substrate tension gradients (mechanotaxis) (Chiu and Chien, 2011) and/or to chemical signals released by cells sensing the force (chemotaxis). In microvascular remodeling, previous reports indicated that although blood flow is a critical driver, it needs to be coupled with other physical, chemical and cellular cues (Georgieva et al., 2019).

In the context of capillary pruning in the mouse postnatal retina, computational modeling studies stated that soluble signals such as VEGF (induced in low perfused regions) will complement blood flow actions in the vascular regression process (Watson et al., 2012). In addition to its role in optimizing network functionality, microvascular remodeling also aims at preventing the formation and persistence of preferential arteriovenous shunts which would negatively impact oxygen distribution (Pries and Secomb, 2014). In computational simulations during the remodeling of pillars into a differentiated network, it was predicted the need of a chemical inhibitor to avoid arteriovenous shunts (Szczerba et al., 2009). More recently, blood flow has been shown to act in coordination with endothelial cell collective migration for maintenance or avoidance of bifurcations which together with molecular signals and network geometry will contribute to capillary remodeling (Edgar et al., 2020).

In mouse experimental colitis, computational models pointed to the relevance of mechanical and chemical cues such as oxygen, metabolites and growth factors to fully explain capillary splitting together with blood flow and shear stress (Szczerba et al., 2009). It was proposed that tissue mechanical properties would regulate shear stress and lead to endothelial responses (recently reviewed in Gordon et al., 2020), but also to the secretion of chemical signals that will contribute to the splitting process and to the crosstalk with supporting cells (Szczerba et al., 2009; Egginton, 2011). These secreted chemical signals could promote or inhibit pillar growth fine-tuning the remodeling of the network. Most interestingly, they predicted the properties of such soluble factors which should have a diffusion coefficient between $10^{-9}$ and $10^{-12}$ m$^2$/s and a molecular mass of 1 to 100 kD. The influence of mechanical tension on the process of capillary splitting has directly been demonstrated in the chorioallantoic membrane in which stretching stimulated capillary splitting (Belle et al., 2014).

Interstitial flow also leads to shear stress and other pressure forces on blood vessels that endothelial cells are able to sense and that may be contributing to some extent to the remodeling of the vascular tree. The role of interstitial flow has mostly been studied in the context of vascular morphogenesis and sprouting angiogenesis. However, although shear stress produced by interstitial flow is in the order of $10^{-3}$ dyn/cm$^2$ (Rutkowski and Swartz, 2007; Shirure et al., 2017), orders of magnitude below those produced by blood flow, significant endothelial cell elongation and actin filament rearrangement has been reported for shear stress between $5.15 \times 10^{-2}$ and $2.15 \times 10^{-1}$ dyn/cm$^2$ (Vickerman and Kamm, 2012), suggesting that interstitial flow may also contribute to capillary remodeling events. The effect of interstitial flow through the vessel wall (transmural) or around the vessel wall through the surrounding endothelial cells has been analyzed in different angiogenic contexts and in combination with VEGF actions (Song and Munn, 2011; Vickerman and Kamm, 2012). Interstitial flow was concluded to drive endothelial cell migration toward vessels that have higher microvascular pressure, a phenomenon reminding of capillary regressing events. Another relevant effect is the elimination of morphogen gradients since physiological values of interstitial fluid could dissipate morphogen gradients within hours in a magnitude-dependent manner (Shirure et al., 2017). Through these actions on endothelial cell migration and on the distribution of the biomolecular endothelial cell environment, interstitial flow may constitute an underestimated player in capillary remodeling.

## Common Features in Capillary Pruning and Splitting

Therefore, both modes of capillary remodeling rely on blood flow forces. In particular, on spatial-temporal gradients of shear stress established at particular network geometries as the intersections between capillaries and adjacent larger vessels (in pruning) or between adjacent capillaries (in splitting). These gradients coupled with capillary caliber changes drive endothelial cell rearrangements leading to cell migration toward the high flow/shear stress region either the adjacent highly perfused larger vessel (in pruning) or the lumen (in splitting). In addition, although both pruning and splitting events occur at sites of local lower shear stress, the observations point to high blood flow as the main driver, indicating that dynamics and ramping of shear stress changes are critical drivers. Finally, chemical signals as oxygen or VEGF and mechanical cues as tissue stiffness or interstitial flow can also contribute to both capillary pruning and splitting.

The co-existence of both remodeling processes can be envisioned in the entity called intussusceptive pruning in which pillar extension occurs in non-axial directions (Mentzer and Konerding, 2014); this has been observed in the extraembryonic vessels of chick embryos (Lee et al., 2011) and at the branch angles of bifurcating vessels in experimental mouse colitis (Ackermann et al., 2013). Moreover, reported images of the vascular plexus behind the sprouting front in the postnatal mouse retina show holes that could remind of intraluminal pillars (Turner et al., 2017), supporting the possible co-occurrence of both remodeling processes in this capillary plexus. Nevertheless, capillary splitting

and pruning are still often considered independent and distinct processes. However, common hemodynamic regulatory cues together with the subsequent changes in the number and perfusion of microvascular segments lead us to propose that pruning and splitting could be the two sides of the same coin. That is, two different mechanisms of microvascular remodeling that are coordinated in time and space in response to changes in tissue oxygen demand and in blood flow distribution with the final aim to achieve an optimized and refined vascular network. It would not be unexpected that molecular mechanisms are also shared.

## MECHANISMS IN BLOOD FLOW-DRIVEN CAPILLARY REMODELING

Shear stress sensed by endothelial cells induces different cellular responses that would finally lead to capillary remodeling *in vivo* (Davies, 1995; Wang et al., 2013). *In vitro* studies showed firstly that endothelial cells elongate and align in a shear stress-dependent manner with alignment requiring longer exposure times (Levesque and Nerem, 1985), and secondly that the higher the laminar flow and shear stress the larger the proportion of endothelial cells that polarize and migrate against flow direction (**Table 2**). These findings would suggest that endothelial cell elongation, alignment and polarization and migration against blood flow are sequential responses to higher and longer shear stress values, but the reality is more complex and depends on the endothelial cell type, the onset of blood flow (*in vitro* is usually abrupt) and the kinetics of the process under investigation (Dieterich et al., 2000) (**Table 2**). And what is it known about values of shear stress and endothelial cell responses *in vivo*? Without disregarding the potential effect of vessel caliber and geometry as well as matrix composition in endothelial cell elongation and orientation *in vivo* (Campinho et al., 2020; Gordon et al., 2020), previous reports (Tkachenko et al., 2013; Franco et al., 2015, 2016; Chang et al., 2017; Poduri et al., 2017) and our own observations indicate that endothelial cell elongation and polarization against the flow direction positively correlate with the shear stress magnitude estimated in different arterial beds and in capillaries during pruning (**Table 1**). These findings emphasize the influence of spatiotemporal regulation of blood flow/shear stress and the possible existence of threshold shear stress values for differential endothelial cell responses *in vivo* (**Table 2**).

Molecular actors involved in blood flow-mediated endothelial cell responses, in particular the mechanosensor complex formed by PECAM-1/VE-cadherin/VEGFR2 at the junctions, have already been reviewed (Korn and Augustin, 2015; Campinho et al., 2020; Gordon et al., 2020). In this review, we will comment only some of the molecular pathways known to be regulated by shear stress and that seem to be relevant to endothelial cell responses in the context of blood flow-driven pruning and splitting (**Tables 3**, **4**).

The new concepts in capillary remodeling predict that the molecular pathways related to sensing blood flow/shear stress by endothelial cells and its transduction into extracellular and intracellular gradients will be of special relevance to modulate the process. The non-canonical Wnt signaling pathway (Wnt11 and Wnt5a) regulates vessel regression in the mouse retina by affecting the sensitivity of the vasculature to shear stress (Franco et al., 2016). The role of BMP signals can be more complex since BMP9 cooperates with the primary cilium to prevent vessel regression under low shear stress (Vion et al., 2018) but the absence of endothelial BMP-SMAD1/5 signals results in reduced vessel regression with aberrant vascular loops and arteriovenous malformations in areas with high blood flow in the mouse retina (Benn et al., 2020). Endoglin, a TGFβ/BMP co-receptor, is required to couple flow-mediated mechanical cues with endothelial cell migration and shape modulating final vessel remodeling (Lobov et al., 2011; Boriushkin et al., 2019). The role of novel mechanosensors (in addition to the well-known PECAM-1/VE-cadherin/VEGFR2 complex) in driving polarized endothelial cell responses is also an active field of research (see review by Campinho et al., 2020). Among these mechanosensors, Piezo 1 increases intracellular calcium in response to shear stress and regulates endothelial cell migration via nitric oxide production and its absence leads to defects in embryonic vascular remodeling suggestive of defective pruning (Li et al., 2014; Ranade et al., 2014). Downstream of Piezo 1, the transcriptional factor Yap/Taz, responsive to both shear stress and endothelial cell stretching (Nakajima et al., 2017; Neto et al., 2018), has been proved to be active during capillary remodeling by inducing actin polymerization; this resulted in a decrease in vascular regression when Yap/Taz pathway is silenced (Nagasawa-Masuda and Terai, 2017). Endothelial $K^+$ channel Kir2.1 has recently been identified as a shear stress sensor whose absence led to decreased endothelial alignment in retinal endothelium and reduced capillary pruning near the angiogenic front of postnatal retinas (Boriushkin et al., 2019). The quick response of these mechanosensors to shear stress (**Table 3**) underscores their role as initial upstream regulators of early endothelial cell responses as alignment and polarization required for capillary pruning (**Table 4**). Of interest is the transcription factor Dach 1 that is regulated by laminar flow specifically, being expressed in arteries subjected to low flow in which it stimulates endothelial cell migration against blood flow (Chang et al., 2017) suggesting a similar not-yet investigated role during capillary pruning. The actions of Notch pathway in capillary pruning seem more complex and pleiotropic; inhibition of Dll4/Notch was shown to prevent retinal capillary regression in the mouse retina by regulating vasoconstriction and blood flow (Lobov et al., 2011) and deletion or loss of its inhibitor Nrapr resulted in enhanced vessel regression, likely by the additional modulation of Wnt signaling (Phng et al., 2009). Moreover, since lower Notch activity correlated with more mobile VE-cadherin at endothelial junctions (Bentley et al., 2014a), differential Notch activity may coordinate endothelial cell arrangements during polarized migration in capillary regression (Franco et al., 2015). Accordingly, endothelial Notch1 was demonstrated to be responsive to shear stress and necessary for the maintenance of junctional integrity induced by laminar shear stress (Mack et al., 2017). However, shear stress sensing needs to be transduced into polarized intracellular signals to promote alignment, polarization

**TABLE 2 |** Shear stress-induced endothelial cell responses.

| EC Type | SS (dyn/cm$^2$) | Exposure Time | EC response | Comments | References |
|---|---|---|---|---|---|
| **Elongation** | | | | | |
| HUVEC | 10 | 12 h | Elongation | Enhanced at 24 h | Steward et al. (2015) |
| HUVEC | 20 | 12 h | Elongation | | Ohta et al. (2015) |
| HAEC | 10 | | Elongation | | Mack et al. (2017) |
| | 26 | | | | |
| BAEC | 15.2 | 3 h | Elongation | | Galbraith et al. (1998) |
| BAEC | 30 | 24 h | Elongation | | Levesque and Nerem (1985) |
| **Alignment** | | | | | |
| HUVEC | 20 | 24 h | Alignment | | Ohta et al. (2015) |
| HMVEC | 9 | 21 h | Alignment | Non-oriented EC near the stagnation point and parallel to flow far from the center | Ostrowski et al. (2014) |
| | 34 and 68 | | | Azimuthal EC orientation at radial distances and parallel to flow far from SS peak | |
| | 210 | | | EC detachment near the flow orifice, and remaining EC with azimuthal orientation | |
| | Impinging | | | Model of Impinging flow | |
| MAEC | 15 | 12 h | Alignment | | Magid et al. (2003) |
| PAEC | <12 | | No alignment | Low effect on orientation | Dieterich et al. (2000) |
| | 68 | | Alignment | Orientation within 10 min | |
| **Polarization (against flow unless indicated)** | | | | | |
| HUVEC | 3 | 15 min | Polarization | ≈50% subconfluent EC polarized (lamellipodia in flow direction) | Wojciak-Stothard and Ridley (2003) |
| HUVEC | 20 | 4 h | Polarization | More than 60% of cells polarized | Franco et al. (2016) |
| HUVEC | Static and 4 | 24 h | Random orientation | | Sonmez et al. (2020) |
| | 7.2 | 3 h | Polarization | Different time of exposure | |
| | 4.4, 18.6, and 40.2 | 24 h | Polarization | 95% polarized (against flow at higher SS values, 18.6 and 40.2) | |
| HCAEC | 14 | 24 h | Polarization | 70–80% | Poduri et al. (2017) |
| **Migration** | | | | | |
| HUVEC | 7.5 | 24 h | Migration | Smooth migration and long distances with flow vs pulsatile flow or static | Blackman et al. (2002) |
| HMVEC | 9, 34, 68, and 210 Impinging flow | 21 h | Migration | Faster migration at higher flow up to 68 dyn/cm$^2$. At 210 dyn/cm$^2$, pushed outward and then adapt, change direction, and migrate upstream after ∼16.7 h | Ostrowski et al. (2014) |
| HCAEC | 35 | 72 h | Migration | Most migrating against the flow direction | Poduri et al. (2017) |
| **Other cellular responses** | | | | | |
| HUVEC | ≈0.5 + 4 Reciprocating | | Round shape<br>Random and short actin filaments at periphery<br>Slow migration<br>High permeability | Model of reciprocating flow | Chiu and Chien (2011) |
| | >10 Laminar | | Alignment<br>Long and parallel stress fibers at center<br>Fast migration<br>Low permeability | Compared with the reciprocating flow model | |
| MAEC | ± 15 Reciprocating | 12 h | No alignment | Model of reciprocating flow | Magid et al. (2003) |

*(Continued)*

**TABLE 2 |** Continued

| EC Type | SS (dyn/cm$^2$) | Exposure Time | EC response | Comments | References |
|---|---|---|---|---|---|
| BAEC | 0.5 ± 4 Reciprocating | | Discontinuous VE-cadherin (similar to disturbed flow) | Model of reciprocating flow | Chien (2008) |
| BAEC | 15.2 | 3 h | Thicker junctions | | Galbraith et al. (1998) |
| | | | More stress fibers | | |
| | | | More apical F-actin | | |
| | | 6 h | MTOC and nuclei reorganization | | |
| RFPEC | 15 | 30 min | Filopodia protrusion | | Zeng and Tarbell (2014) |
| PAEC | 15 | 8 h | F-actin reorganization | | Noria et al. (2004) |

*Representative selected reports showing endothelial cell responses to distinct shear stress values and patterns in vitro. Values of shear stress correspond to laminar flow unless otherwise indicated. ECs, endothelial cells; HUVEC, human umbilical vein ECs; HCAEC, human coronary artery ECs; MAEC, mouse aorta ECs; BAEC, bovine aorta ECs; RFPEC, rat fat pad ECs; PAEC, pig pulmonary artery ECs.*

(with the Golgi in front of the nucleus toward the migrating edge) and directed migration. In this line, the small GTPase Rac1, regulator of actin polymerization and cell migration, is required for vessel regression in the zebrafish brain (Chen et al., 2012) and polarized Rac1 subcellular gradients are induced by laminar (15 dyn/cm$^2$) but not disturbed flow in endothelial cells *in vitro* (Shao et al., 2017). Similarly, phosphoinositide gradients are required for a balanced capillary pruning induced by VEGF since the absence of CDP-diacylglycerol synthase-2 (CDS2), a metabolic enzyme that controls phosphoinositide recycling, in mouse and zebrafish showed increased endothelial cell migration and vessel regression (Zhao et al., 2019). VEGF was considered an essential player in vascular regression occurring after deprivation of VEGF or VEGF-induced signals which led to endothelial cell apoptosis in different tissues and contexts (Meeson et al., 1999; Tang et al., 2004; Baffert et al., 2006). Previous *in vivo* and *in silico* analysis in the postnatal mouse retina pointed to VEGF as a complementary actor together with blood flow in capillary pruning in this context (Watson et al., 2012). However, how VEGF precisely participates in endothelial cell migration against blood flow during capillary pruning remains undefined.

Much less is known about the mechanisms underlying capillary splitting or duplication since there is no optimal *in vitro* model for its study and the endothelial cell processes involved are less understood. In a pioneer attempt to understand the molecular pathways involved in capillary splitting, Egginton's group aimed at identifying genes differentially expressed in the context of capillary splitting (vasodilator-treated) versus sprouting (agonist-excised) in the skeletal muscle and they found that endothelial nitric oxide synthase (eNOS) and neuropilin-1 were upregulated (Egginton, 2011). Nitric oxide is a downstream target of the laminar flow-induced transcription factor Klf2 (Nayak et al., 2011) but also by shear stress-stimulated glycocalyx on endothelial apical side (Bartosch et al., 2017). Indeed, nitric oxide produced by the endothelial cells is essential not only to induce the endothelial cell rearrangements required for intraluminal pillar formation and splitting, in particular luminal filopodia protruding mostly from the inter-junctional regions, but for capillary splitting to occur as demonstrated in the skeletal muscle of vasodilator-treated eNOS-deficient mice (Baum et al., 2004; Williams et al., 2006a). A recent report from our group has added a layer to nitric oxide regulation showing that TSP1 cleavage by the protease MT1-MMP promotes endothelial cell production of nitric oxide favoring vasodilation and capillary splitting during experimental colitis (Esteban et al., 2020); whether in this model nitric oxide mainly acts by inducing vasodilation of the feeding arterioles or has additional actions in the endothelial cell rearrangements to form the pillars during capillary splitting still needs to be established. Of note, nitric oxide is a soluble factor with properties close to those predicted for the soluble factor required for refining capillary splitting according to *in silico* models (Filipovic et al., 2009). The role of VEGF in the process is supported by its expression in the chorioallantoic membrane microvasculature and the delay in capillary splitting when VEGF was inhibited (Baum et al., 2010) and by the induction at high doses of dysfunctional capillaries by splitting (Gianni-Barrera et al., 2013); VEGF actions in this context can be modulated by PDGFB and EphrinB2/EphB4 pathways (Gianni-Barrera et al., 2018; Groppa et al., 2018). Novel actors include the inhibitor of proteases RECK which regulates non-sprouting (likely splitting) vascular remodeling during embryonic development (Chandana et al., 2010) and Notch (Dimova et al., 2013) and endoglin, whose inhibition led to enhanced capillary splitting by distinct mechanisms (Hlushchuk et al., 2017).

Of course, the cellular and molecular understanding of capillary remodeling and its regulation is far from being complete. Other possible cues not much investigated yet, but with possible roles in regulation of endothelial cell morphology, include endothelial cell junction components that may be a critical factor to explain rearrangements during both regression and splitting. In particular, VE-cadherin forms part of the mechanosensory complex together with PECAM-1 and VEGFR2 (Tzima et al., 2005) and, it has been reported that short-term reciprocating flow reduces VE-cadherin localization at the junctions while sustained exposure to pulsatile flow reinforces it (Miao et al., 2005). Since reciprocating flow is observed at the regressing segment (Chen et al., 2012), subsequent reduction in junctional VE-cadherin may favor destabilization of endothelial junctions and allow endothelial cell migration to the adjacent

**TABLE 3 |** Shear stress regulation of molecular effectors.

| EC type | SS (dyn/cm$^2$) | Exposure time | Molecular response | References |
|---|---|---|---|---|
| **Mechanosensors** | | | | |
| HUVEC | 20 | 10 min | Increase Piezo 1-dependent $Ca^2$ peaks | Li et al. (2014) |
| MAEC | 15 | | Piezo 1-dependent alignment | Ranade et al. (2014) |
| HPAEC | 15 | 20–50 min | Polarized Piezo 1 to leading edge | Ranade et al. (2014) |
| HPAEC | 15 | 10 min | YAP nuclear translocation and acto-myosin reorganization | Nakajima et al. (2017) |
| BAEC | 5 | | 40% Kir2.1 current increase | Jacobs et al. (1995) |
| **Notch, Wnt, BMP** | | | | |
| HAEC | 20 | 24 h | Maximum Notch1 mRNA | Mack et al. (2017) |
| HAEC | 26 | | Plateau Notch1 nuclear translocation and polarization | Mack et al. (2017) |
| HUVEC | 20 | 4 h | Increased alignment against flow direction (in absence of Wnt5a/Wnt11) | Franco et al. (2016) |
| HUVEC | 12 | 45 min | Smad1 translocation | Baeyens et al. (2016) |
| HUVEC | 12 | 24 h | BMP9, Klf2, Klf4 expression | Baeyens et al. (2016) |
| HCAEC | 15 | 24 h | Increased endoglin expression | Chu and Peters (2008) |
| HUVEC | 12 | 15 min | Association endoglin/Alk1 and enhanced BMP9 sensitivity | Baeyens et al. (2016) |
| HUVEC | 10–20 | | Smad1/5 maximally activated | Baeyens et al. (2015) |
| **Signal transducers** | | | | |
| HCAEC | 5 | | Decreased Dach1 expression (gradient SS maintains its expression) | Chang et al. (2017) |
| HUVEC | 1.5 or 15 | 3 h | Increase in APJ protein (also after an acute change to higher flow) | Busch et al. (2015) |
| BAEC | 3.5–35 | 25 min | Increase in Erk5 activity | Yan et al. (1999) |
| BAEC | 12 | 20 min–2 h | Increase in Erk5 activity | Yan et al. (1999) |
| HUVEC | 14 | 2 h | Increase in Erk5 activity (continuous, pulsatile or to-an-fro flow) | Shalaby et al. (2017) |
| HUVEC | 22 | | Increase in Ins1,4,5P3 (0.5 up to 6 min) | Nollert et al. (1990) |
| HUVEC | 0.4, 1.4, and 22 | 30 min | Decrease in PI, PE, PA at 10-30 s and increase in DAG, free arachidonate and Ins1,4,5P3. IP3 peak at 10 min | Bhagyalakshmi et al. (1992) |
| BAEC | 12 | 30 min | Increased Rac1 activity at 30 min | Tzima et al. (2002) |
| BAEC | 15 | 30 min | Polarized Rac1 activity | Shao et al. (2017) |
| Zebrafish Brain | Decreased blood flow | | Increased Rac1 activity | Chen et al. (2012) |
| HUVEC | 23 | 1–20 min | pp130Cas/Crk association | Okuda et al. (1999) |
| PAEC | 20 | 5 min | Polarized decrease in pp130Cas in edge opposite to flow | Zaidel-Bar et al. (2005) |
| BAEC | 12 | 5 – 60 min | No recruitment of Nck to VEGFR2 (in contrast to VEGF 10 ng/ml) | Wang et al. (2007) |
| **ECM-related** | | | | |
| μvascular rat EC | 14 | 4 – 8 h | Decreased MT1-MMP expression (in contrast to cyclic strain) | Yun et al. (2002) |
| HUVEC | 5.3 + S1P | | Increase in MT1-MMP activity and EC membrane recruitment (in 3D collagen matrices) | Kang et al. (2011) |
| HUVEC | 13 | 2 h | Enhanced TSP1 secretion to ECM | Gomes et al. (2005) |
| Prazosin in muscle | Increases blood flow | | Increased ECM TSP1 *in vivo* | Bongrazio et al. (2006) |
| Yolk sac | Flow restauration | 30 min–4 h | Recovers Nrp1 arterial expression | le Noble et al. (2004) |
| Muscle | Increased blood flow | | Increase in Npr1 | Williams et al. (2006b) |
| Mouse EC | 20 | 24 h | Nrp1 association to PLXND1 and VEGFR2 mechanosensor | Mehta et al. (2020) |
| **Soluble factors** | | | | |
| Umbilical Vessels | 24 vs 4 | 1.5, 3, and 6 h | Biphasic down, up and down VEGF regulation | Gan et al. (2000) |
| HUVEC | 10 (orbital shaker) | 72 h | Increased VEGF165/VEGFR2/pVEGFR2 | dela Paz et al. (2012) |
| HUVEC | 20 | 38 h | eNOs (not under pulsatile flow) | Voyvodic et al. (2012) |
| HUVEC | 8, 2–8 (periodic, 15 min) and 12.4 (reciprocating) | | Increase in nitric oxide synthesis (in contrast to turbulent flow (1.2 to 11.7 dyn/cm$^2$) | Noris et al. (1995) |

*List of selected reports showing the regulation of molecular effectors in endothelial cells by distinct shear stress values and patterns in vitro and in vivo. ECs, endothelial cells; HUVEC, human umbilical vein ECs; HCAEC, human coronary artery ECs; PAEC, human pulmonary artery ECs; MAEC, mouse aorta ECs; PTEC, pulmonary trunk ECs; BAEC, bovine aorta ECs; S1P, sphingosine-1-phosphate.*

**TABLE 4 |** Molecular actors in capillary remodeling *in vivo*.

| | | |
|---|---|---|
| **Capillary pruning** | | |
| **Mechanosensors** | | |
| Piezo 1 | LOF, probable decreased vessel regression in mouse retina | Ranade et al. (2014) |
| YAP/TAZ | Nuclear location required for vessel regression in zebrafish | Nagasawa-Masuda and Terai (2017) |
| $K^+$ channel Kir2.1 | LOF, reduced EC alignment and vessel regression in mouse retina | Boriushkin et al. (2019) |
| **Notch, Wnt, BMP** | | |
| Notch | LOF, EC elongation and decreased capillary regression in mouse retina | Lobov et al. (2011), Mack et al. (2017) |
| Non-canon Wnt | LOF, increased sensitivity to SS-induced regression *in vivo* | Franco et al. (2016) |
| Alk1 | LOF, hyper-vascularization and AV malformations in mouse retina | Larrivee et al. (2012) |
| Endoglin | LOF, EC shape changes (no alignment), directed migration and AV shunts | Jin et al. (2017); Sugden et al. (2017) |
| Smad1/5 | LOF, reduced vessel regression and loop formation in mouse retina | Benn et al. (2020) |
| IFT88 | LOF, premature and random vessel regression in mouse retina | Vion et al. (2018) |
| **Signal transducers** | | |
| CDS2 | LOF, increased vessel regression in zebrafish and postnatal mouse retina | Zhao et al. (2019) |
| Rac1 | LOF, EC migration *in vivo* and defective vessel pruning in zebrafish brain | Chen et al. (2012) |
| **Soluble factors** | | |
| VEGF | Predicted contribution to capillary pruning in mouse retina | Watson et al. (2012) |
| **Capillary splitting** | | |
| **ECM-related** | | |
| MT1-MMP | LOF, decreased vessel splitting during mouse colitis *in vivo* | Esteban et al. (2020) |
| TSP1 | LOF, decreased vessel splitting in mouse colitis | Esteban et al. (2020) |
| **Soluble factors** | | |
| VEGF | Promotes vessel splitting in skeletal muscle and CAM | Baum et al. (2010); Gianni-Barrera et al. (2013) |
| Nitric oxide/eNOS | LOF, reduces capillary splitting in the skeletal muscle and correlates with less capillary splitting in mouse colitis | Esteban et al. (2020), Williams et al. (2006a) |
| **Other vascular remodeling events** | | |
| **Signal transducers** | | |
| Dach1 | GOF/LOF, EC polarization, alignment and migration against flow and LOF, impaired embryonic arterial patterning | Chang et al. (2017) |
| ApelinR | Required for EC polarization *in vitro* and *in vivo* in zebrafish | Kwon et al. (2016) |
| Erk5 | LOF, Disorganized and rounded ECs *in vivo* | Nithianandarajah-Jones et al. (2014), Spiering et al. (2009) |
| Nck | LOF, impaired EC front-rear polarity and VEGF-directed migration *in vivo*; no impact in vessel regression in retina | Chaki and Rivera (2013), Dubrac et al. (2016) |
| p130Cas | LOF, less focal adhesion turnover and EC directed migration *in vitro* | Spiering et al. (2009), Zaidel-Bar et al. (2005) |
| **ECM-related** | | |
| Nrp1 | Enables EC filopodia via cdc42 in zebrafish and mouse retina and regulates EC shape, cell contacts, and actin in collective migration in zebrafish | Fantin et al. (2015), Hamm et al. (2016) |

*Representative molecular players with reported or suggested actions in capillary regression, splitting or other vascular remodeling events in vivo. EC, endothelial cells; GOF, gain-of-function; LOF, loss-of-function.*

high flow vessels. Cues from the basement membrane on which directed endothelial cell migration takes place toward the adjacent vessel can also be important as suggested by recent studies with gradients of a collagen IV peptide *in vitro* (Du and Gao, 2019). Actin cytoskeleton may be an additional actor since short exposure to laminar flow induces apical F-actin reorganization and filopodia (Galbraith et al., 1998; Zeng and Tarbell, 2014) (**Table 2**) and actin filaments are visualized in the pillars during capillary splitting although their ability to generate the required force for intraluminal protrusions under blood flow is still unclear (Paku et al., 2011; Mentzer and Konerding, 2014). Finally, other players in endothelial directed migration as the Apelin GPCR (Kwon et al., 2016), the actin cytoskeleton regulators cdc42 (Lavina et al., 2018) and Nck (Chaki and Rivera, 2013), the atypical MAP kinase Erk5 (Spiering et al., 2009), the TGFβ/BMP receptor Alk1 (Rochon et al., 2016) or the adapter p130Cas (Evans et al., 2017) could also be good candidates to participate in capillary remodeling *in vivo* (**Tables 3**, **4**).

## NEW METHODOLOGICAL APPROACHES AND TOOLS TO UNDERSTAND CAPILLARY REMODELING *IN VIVO* AND *IN VITRO*

It is clear that capillary remodeling events depend largely on local spatiotemporal gradients of blood flow, but also cellular

gradients (molecular signals) and luminal and tissue gradients (soluble factors), which forces us to change the paradigm of how to analyze cellular and molecular actors involved in these processes. Remodeling cannot be analyzed in bulk approaches but at single cell level as also recently reviewed (Campinho et al., 2020). This need demands advanced imaging techniques (with reporters and probes to track possible actors and signals) *in vitro*, *ex vivo*, and *in vivo* but also screening for new players by single-cell and spatial techniques for protein changes and modifications since some of these events occur in a time-scale that would not allow major gene changes (Lundberg and Borner, 2019).

## Single-Vessel and Single-Cell Image Analysis

Although *in vitro* models have provided relevant cues about cellular and molecular mechanisms involved in endothelial cell responses to changes in blood flow gradients, *in vivo* models allow a closer look at the endothelial cell behavior in the real physiological context. *In vivo* models used in the context of microvascular remodeling have typically focused on either immature microvascular networks during development or in pathological scenarios. Most advances have been made by the use of animal models such as the postnatal mouse retina (Connolly et al., 1988) and the intersegmental vessels and the brain vasculature in the transparent zebrafish (Chen et al., 2012; Franco et al., 2015) for segment pruning and the choriollantoic membrane of the chicken (Feinberg et al., 1986), the caudal venous plexus of the zebrafish (Karthik et al., 2018), the skeletal muscle (Hudlicka et al., 2006) and the experimental mouse colitis (Esteban et al., 2020) for capillary duplication.

Once endothelial cell migration triggered by changes in the blood flow sensing was established as the main actor in the vascular remodeling, markers implicated in the migration of the cells became an ideal target to monitor the behavior of these cells and also identify the potential vessels involved in this process. Thus, transgenic reporter animals became an essential tool in the investigation of vascular remodeling. Transgenic lines carrying endothelial cell fluorescence reporters have allowed live-imaging and visualization of the dynamics of the process in zebrafish (Scheer and Campos-Ortega, 1999; Lawson and Weinstein, 2002; Chen et al., 2012). More recently, Franco's group has generated the GNrep transgenic mouse line with a double fluorescence reporter for the Golgi apparatus and the endothelial cell nucleus which allows a direct analysis of endothelial cell polarization in vascular territories undergoing remodeling (Barbacena et al., 2019). Notably, the use of the Raichu Rac1 FRET sensor established the role for the activity of this small GTPase in regulating directed endothelial cell migration during capillary pruning in the brain vasculature of zebrafish (Chen et al., 2012). LifeAct reporter has recently been used for visualization of endothelial cell filopodia and dynamics in the postnatal mouse retina *ex vivo* (Riedl et al., 2008; Prahst et al., 2020) and it could be a useful tool to analyze cytoskeletal rearrangements of endothelial cells during capillary remodeling. A better knowledge of the molecular actors involved in each step of segment pruning or splitting could help designing new fluorescent reporter animal lines.

In addition to time-lapse microscopy in amenable models as zebrafish, confocal microscopy and 3D image analysis have largely advanced our understanding of capillary remodeling events (Campinho et al., 2020). Confocal microscopy in the quasi-2D flat mount postnatal retina has allowed precise quantification and characterization of "empty sleeves" (collagen IV positive, endothelial cell negative), the hallmark of capillary pruning events (**Figure 3A**). The challenge of exploring capillary pruning in more complex 3D vascular plexus remains and novel confocal microscopy-based 3D image processing tools and algorithms may help comprehend this process (Gkontra et al., 2018, 2019). Likewise, confocal microscopy of vessel-stained tissues such as whole-mount inflamed intestine combined with 3D-image rendering has turned into an approach that provides sufficient resolution to identify and quantify capillary holes/pillars, loops, and duplications (**Figure 3B**) (Karthik et al., 2018; Esteban et al., 2020), all hallmarks of capillary splitting, circumventing the limitations of previously used corrosion cast techniques and electron microscopy (Nowak-Sliwinska et al., 2018). Light-sheet fluorescent microscopy (LSFM) has recently been applied to the quantitative 3D and 4D analysis of endothelial cell motility and filopodia dynamics in blood flow-free *ex vivo* postnatal mouse retina (Prahst et al., 2020). Advanced microscopy techniques will undoubtedly improve our knowledge about capillary remodeling in more complex vascular beds what combined with the use of fluorescent reporter animal lines may provide unprecedented visualization and information about these events.

Novel mathematical and computational tools can also be of great value to understand the changes and actions of blood flow and shear stress, specially their gradients and dynamic changes. Although continuous blood flow models can provide some information about blood flow fluctuations and drop pressure changes in the microvascular network by means of permeability tensors (Gkontra et al., 2019), capillary remodeling research will most benefit from discontinuous or segment-based models and simulations. This has been the base for the efforts made to simulate the complexity of the hemodynamic forces even in simple networks as the postnatal retina vasculature (Bernabeu et al., 2014) and the development of new tools such as PolNet (an open-source software; Bernabeu et al., 2018) which aimed at facilitating the combined analysis of blood flow and shear stress with cell polarization in order to understand their influence in capillary remodeling by comparison of values between neighbor segments and at different developmental stages. This tool is available and useful for the study of blood flow in low complexity network as retinas. It is worth mentioning that computational modelization of particles has just uncovered the essential role of circulating red blood cells in generating regional shear stress differences and thus in regulating vascular remodeling by modulation of blood viscosity (Zhou et al., 2020). Of note, new advances in mathematical approaches in the multidisciplinary field of Adaptive Systems could also help decipher the dynamic changes of endothelial cells responding

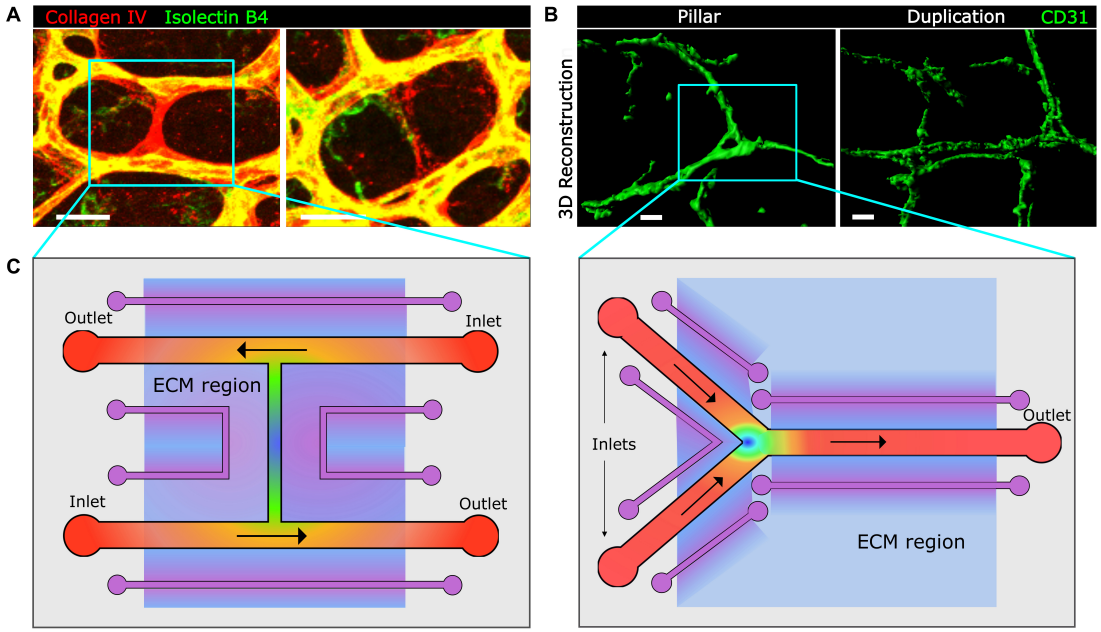


**FIGURE 3 |** Image-based approaches to capillary remodeling *in vivo* and proposed device-based simulation *in vitro*. **(A, B)** Examples of whole-mount staining and confocal microscopy for the visualization and analysis of capillary pruning in the mouse postnatal retina **(A)** and of capillary splitting in the inflamed mouse intestine by means of 3D reconstruction with Imaris software. Scale bar, 20 μm. **(C)** Top view of proposed microfluidic chips for the study of capillary regression in an H-type geometry (left panel) and of capillary splitting in Y-type geometry (right panel), mimicking the geometries found in microvascular networks (blue boxes in panels **A** and **B**). Inlets and outlets for flow are indicated and are exchangeable depending on the preferred direction of flow in the different segments. Vessel channels are covered with a basement membrane and endothelial cells. In purple auxiliary channels for creating biochemical gradients along the extracellular matrix (ECM)-like hydrogel region (light blue). This hydrogel could also incorporate cells for co-culture analysis. Heat map color represent theoretical shear stress values (as in **Figure 2**) for established flow gradient profiles and shading represent biochemical gradients along the ECM. The rest of the microfluidic chip would be made of PDMS.

to a variety of environmental signals in order to adopt the best network architecture possible (Bentley et al., 2014b).

## *In vitro* Systems for Analysis of Microvascular Remodeling Under Flow: Microfluidics as a Promising Technology

*In vitro* flow chambers could be considered the preludes of microfluidic-based devices as they mimic hemodynamic shear stress in macroscale flow chambers with 2D endothelial cell monolayers. The two main models of *in vitro* flow chambers are the parallel plate flow chamber and the cone and plate viscometer with its corresponding modifications; in both cases, cells are cultured on a two-dimensional stiff surface and fluid is flown over the culture. While the parallel plate system has several advantages as its simplicity or its compatibility with imaging modalities, the effects of shear stress cannot be discriminated from those due to hydrostatic pressure. On the other hand, the cone and plate viscometer does allow to separate both effects but it has other limitations as its difficult combination with imaging and the need of continuously supply the culture with fresh medium (Papadaki and McLntire, 1999). The most popular commercial versions of flow chambers are the family products Bioflux (multi-well format with small fluid reservoir) and Ibidi (varied plate formats with larger fluid reservoir for longer experiments) which are widely used among researchers in the field. They are relatively easy to implement and offer advantages as its high reproducibility, good cell viability and technical support on-hand. But they come with limitations since they are not very versatile (fixed geometries and fluid properties) and they are expensive (disposable and non-reusable plates and consumables) (Roest et al., 2011). These type of 2D systems are mostly interesting to examine the role of shear stress exerted by different types of flow including laminar, pulsatile and reciprocating flow (Usami et al., 1993; Chien, 2007) but, in addition to the limitations already discussed, they do not incorporate the remodeling of the extracellular matrix (ECM) nor its mechanical properties, failing to fully recapitulate the complex 3D environment, geometries or the shear stress gradients found *in vivo* (Coluccio et al., 2019; Gordon et al., 2020).

Microfluidic chips are characterized by having channel sizes of tens to thousands of micrometers and dealing with volumes in the microliter to picoliter range; in fact, they are considered such when one or more channels have at least one dimension smaller than 1 mm. Switching from the macroscale to the microscale offers new advantages for researchers including a big reduction in the amount of reagents but more importantly a huge versatility for exploring new geometries and flow conditions (van Duinen et al., 2015). The main advantages of this technology are that it provides the possibility of isolating and controlling fluid properties, physical, chemical and biological stimuli while being compatible with several imaging modalities including time-lapse microscopy (Hsu et al., 2013). They can also be used in a

high throughput manner so several conditions can be tested simultaneously (Hsu et al., 2013). Among the applications of interest in the miocrovascular remodeling field is the analysis of vascular cell responses to shear stress (Wong et al., 2012). Even though microfluidic technology is usually applied for quasi-2D models with laminar flow, in the last years new techniques implemented fully 3D models that offer a more physiological environment.

Microfluidic devices are typically built in PDMS (polydimethylsiloxane) because being it transparent, permeable to oxygen and compatible with soft-lithography and rapid prototyping techniques, it is a good option to build biocompatible devices for research with custom-made geometries. Nevertheless, further demands for deeper understanding of vascular phenomena made PDMS-hydrogel hybrid devices emerge as a better option for the study of angiogenesis and vascular remodeling (Bogorad et al., 2015; Gordon et al., 2020). This type of devices incorporates a hydrogel region surrounding the endothelial cell-covered microchannels which can be remodeled by cells and whose mechanical properties resemble much better the endothelial microenvironment. In addition, with the hydrogel regions, different types of biochemical gradients can be incorporated throughout the device. The possibility to control and model computationally both the biochemical and physical gradients (Nguyen et al., 2013) and the flow and shear stress distribution, timing and ramping along the device (Chiu and Chien, 2011) makes it possible to establish correlations between the different types of stimuli and the endothelial cell response. Given that intraluminal endothelial migration occurs in contact with the preserved basement membrane during capillary remodeling, it is worth mentioning that microfluidic systems including a basement membrane have been implemented for the study of endothelial cell permeability or cancer metastasis (Han et al., 2015; Kim et al., 2019; Coughlin and Kamm, 2020).

One drawback of lithographic techniques commonly used to produce the PDMS structure is the limitation to rectangular cross-sections rather than the natural cylindrical shape (Akbari et al., 2017), that could influence the outcome of the experiments due to pulling and traction forces at the corners of polygonal shapes (Rauff et al., 2019). Cylindrical cross-sections have been achieved with 3D microvessel templates by cross-linking the hydrogel around a needle or rod that is then removed. However, this technique is limited to linear geometries and larger diameters (60–200 μm). The report of a grid geometry for microvessel networks that resemble the highly branched native plexus, where blood passes from capillaries to arterioles and venules, could be of interest as a retina model since in both cases blood flow diverges and decelerates as it branches, and consequently it creates different shear stress patterns (Zheng et al., 2015). Going even further, fully hydrogel embedded systems that can incorporate other cell types such as pericytes in co-culture, are the most accurate at resembling the three-dimensional physiological microenvironment.

PDMS-hydrogel hybrid devices can incorporate branching and bifurcating regions of special interest for capillary splitting and other remodeling events due to the different flow patterns occurring at these sites. This type of devices have recently been used to produce impinging bifurcating fluid flow, laminar shear stress and transvascular fluid flow (Akbari et al., 2018) and also controllable disturbed flow patterns for the study of its effects on actin stress fiber and endothelial cell orientation (Tovar-Lopez et al., 2019). But how exactly does the direction, slope and average magnitude of shear stress gradients affect endothelial cell biological and molecular responses needs still to be understood. Due to the geometrical versatility and high reproducibility and control that microfluidic devices offer, this technology springs as a promising tool for a better understanding of these events. For example, a recent microfluidic device was able to produce areas with three different constant shear stress values and six different shear stress gradients and showed that human endothelial cell upstream orientation depends on gradient direction (Sonmez et al., 2020). Following a top-down approach (Hesh et al., 2019), we propose two prototypes of hybrid devices that on one hand are inspired on real microvascular networks in which capillary pruning and splitting occurs (**Figure 3A,B**), mimicking their preferential H and Y geometries; and on the other, they incorporate predicted shear stress values and spatiotemporal gradients, as discussed along this review, whose tuning and dynamics could only be recapitulated in these systems (**Figure 3C**). These prototypes could even represent better the *in vivo* microvascular remodeling context by including a physiologically relevant ECM, a basement membrane and supporting cells in co-culture.

Microfluidic devices offer several advantages. The influence of the environment on the microvasculature, in particular chemical factors, can be tested not only controlling its concentration but its gradients for example of WNTs, Notch-related molecules, VEGF, all with important roles in vessel pruning (Wong et al., 2012; Korn and Augustin, 2015). The possibility of time-lapse imaging allows to study the dynamics of microvascular remodeling events (Wong et al., 2012). Some devices can incorporate supporting cells such as pericytes (Rauff et al., 2019), contributors to microvascular remodeling. *In vitro* microfluidic models designed using solely human components may serve as a translational bridge between experimental animal models and human applications given the much larger shear stress values found in mouse compared to human vessels (Chiu and Chien, 2011; Zheng et al., 2015). Microfluidic models can also offer a platform to test and refine computational models. Mathematical and computational models require tight boundary conditions (like flow parameters at the inlet and outlet or pre-defined values at certain locations) that are impossible to control or measure *in vivo*. Since flow parameters can be tuned by the user in microfluidic chips and they are compatible with several imaging modalities and measuring techniques, microfluidic platforms could be a great complement to feed these theoretical models.

A bit aside from the classical microfluidic chips that have been described so far, but that may be relevant in the field, are organ mimetic microdevices and organ-on-a-chip devices. These technologies combine microfluidic technology with other culture systems as bioreactors and microchambers and computer control systems (Huh et al., 2011).

Even though the advantages of microfluidics versus macroscale flow chambers are vast, the fact that it has recently

started to be exploited for biological research poses some difficulties related to their implementation by researchers. Protocols for biochemical assays and cellular cultures are established for macroscale conditions where the surface to volume ratio is small and the culture media to cell ratio is large. These conditions have to be carefully adjusted to the microscale to avoid artifacts and cell death and comparison with the results obtained in macroscale systems and classical biochemical assays have to be made with care. For PDMS devices, attention has to be paid with the surface coating for proper cell attachment (which is different to that in glass or polystyrene). Also, $CO_2$ concentration and pH needs to be checked since, even though it is permeable to gases, too thick PDMS layers can hinder proper ventilation of the culture. The perfusion system (that can be gravity-driven, external syringes or on-chip peristaltic pumps, all of them having been proved to allow more than 1 week perfusion) has to be carefully configured to ensure both adequate nutrient flow at the flow rate required for the shear stress pattern to be studied and bubble-free fluid flow (Kim et al., 2007). Fluid control can become specially challenging in self-organized microvessels due to their random nature. Lastly, it has to be mentioned that often microfluidic control systems are rather complex to use and researchers may not be familiar with its handling (Halldorsson et al., 2015).

All in all, we believe that the microfluidic technology needs still to be exploited to reach its full potential in the study of vascular remodeling events because of the many advantages it offers in comparison to other *in vitro* systems and that standardization of this type of experiments will overcome many of the difficulties it may pose nowadays.

## CONCLUSIONS AND PERSPECTIVES

Tissues continuously adjust their oxygen and nutrient demands and for that they require the dynamic adaption of the microvasculature in order to optimize blood flow distribution. This is achieved by means of capillary remodeling, eliminating poorly functional or redundant segments by pruning, or duplicating segments to expand the microvasculature by splitting. Defective or excessive capillary remodeling will deprive tissue regions of appropriate perfusion leading to tissue damage or limiting its repair. This process has therefore attracted a lot of recent interest not only to understand vascular homeostasis but also to propose new strategies devoted to prevent disease and promote tissue repair (Georgieva et al., 2019).

Active research on the basic mechanisms of capillary remodeling beyond blood flow-driven endothelial cell migration can help identifying novel actors and modulators with potential use in preventing or ameliorating diseases related to excessive or defective capillary splitting or pruning as for example inflammatory bowel diseases, lung dysplasia, myocardial infarction or Alzheimer's disease among others. As an example, the small GTPase Rac1 has been involved in capillary pruning in the brain zebrafish microvasculature and it is tempting to speculate that Rac1 inhibitors may help prevent excessive brain capillary pruning associated for example with aging or Alzheimer's disease (Garkavtsev et al., 2011; Chen et al., 2012). On the other hand, excessive capillary splitting has been shown to contribute to the progression of inflammatory bowel disease and targeting recently identified actors as the molecular axis MT1-MMP/TSP1/eNOS by delivery of inhibitory antibodies or competitive peptides was shown to ameliorate the progression of the disease in mice (Esteban et al., 2020). Since failed microvascular remodeling can also lead to the presence of undesired arteriovenous shunts, recent identification of endoglin as a key regulator of endothelial cell responses for preventing AVM, can shed light about mechanistic links between endothelial cell responses to blood flow and disease. Furthermore, provocatively considering capillary pruning and splitting as two coordinated processes which continuously translate blood flow/shear stress fluctuations into microvascular adaptations can also help advance our understanding of these vascular events.

Finally, research efforts should be encouraged for the development and implementation of approaches and tools which more closely recapitulate the dynamics, geometries and flow conditions and the biochemical microenvironment of *in vivo* capillary remodeling in order to guarantee a wider comprehension of this process in near future.

## AUTHOR CONTRIBUTIONS

RS and SE obtained microscopy images. RS and MG-Á prepared the figures. RS, MG-Á, and AGA wrote the text and all authors revised it. All authors contributed to the article and approved the submitted version.

## FUNDING

The work in this manuscript has been funded by a grant from the Spanish Ministry of Science and Innovation (SAF2017-83229-R to AGA) and a fellowship from the FPI-Severo Ochoa program (to RS). The CNIC is supported by the Instituto de Salud Carlos III (ISCIII), the Ministerio de Ciencia e Innovación (MCIN) and the Pro CNIC Foundation, and was a Severo Ochoa Center of Excellence (SEV-2015-0505). We acknowledge support of the publication fee by the CSIC Open Access Publication Support Initiative through its Unit of Information Resources for Research (URICI).

## REFERENCES

Ackermann, M., Tsuda, A., Secomb, T. W., Mentzer, S. J., and Konerding, M. A. (2013). Intussusceptive remodeling of vascular branch angles in chemically-induced murine colitis. *Microvasc. Res.* 87, 75–82. doi: 10.1016/j.mvr.2013.02.002

Akbari, E., Spychalski, G. B., Rangharajan, K. K., Prakash, S., and Song J. W. (2018). Flow dynamics control endothelial permeability in a microfluidic vessel bifurcation model. *Lab. Chip.* 18, 1084–1093. doi: 10.1039/C8LC00130H

Akbari, E., Spychalski, G. B., and Song, J. W. (2017). Microfluidic approaches to the study of angiogenesis and the microcirculation. *Microcirculation* 24:e12363. doi: 10.1111/micc.12363

Andres, A. C., and Djonov, V. (2010) The mammary gland vasculature revisited. *J. Mammary Gland Biol. Neoplasia* 15, 319–328. doi: 10.1007/s10911-010-9186-9

Baeyens, N., Bandyopadhyay, C., Coon, B. G., Yun, S., and Schwartz, M. A. (2016). Endothelial fluid shear stress sensing in vascular health and disease. *J. Clin. Invest.* 126, 821–828. doi: 10.1172/JCI83083

Baeyens, N., Nicoli, S., Coon, B. G., Ross, T. D., Van den Dries, K., Han, J., et al. (2015). Vascular remodeling is governed by a VEGFR3-dependent fluid shear stress set point. *eLife* 4:e04645. doi: 10.7554/eLife.04645

Baffert, F., Le, T., Sennino, B., Thurston, G., Kuo, C. J., Hu-Lowe, D., et al. (2006). Cellular changes in normal blood capillaries undergoing regression after inhibition of VEGF signaling. *Am. J. Physiol. Heart Circ. Physiol.* 290, H547–H559. doi: 10.1152/ajpheart.00616.2005

Barbacena, P., Carvalho, J. R., and Franco, C. A. (2016). Endothelial cell dynamics in vascular remodelling. *Clin. Hemorheol. Microcirc.* 64, 557–563. doi: 10.3233/CH-168006

Barbacena, P., Ouarne, M., Haigh, J. J., Vasconcelos, F. F., Pezzarossa, A., and Franco, C. A. (2019). GNrep mouse: a reporter mouse for front-rear cell polarity. *Genesis* 57:e23299. doi: 10.1002/dvg.23299

Bartosch, A. M. W., Mathews, R., and Tarbell, J. M. (2017). Endothelial glycocalyx-mediated nitric oxide production in response to selective AFM pulling. *Biophys. J.* 113, 101–108. doi: 10.1016/j.bpj.2017.05.033

Baum, O., Da Silva-Azevedo, L., Willerding, G., Wockel, A., Planitzer, G., Gossrau, R., et al. (2004). Endothelial NOS is main mediator for shear stress-dependent angiogenesis in skeletal muscle after prazosin administration. *Am. J. Physiol. Heart Circ. Physiol.* 287, H2300–H2308. doi: 10.1152/ajpheart.00065.2004

Baum, O., Suter, F., Gerber, B., Tschanz, S. A., Buergy, R., Blank, F., et al. (2010). VEGF-A promotes intussusceptive angiogenesis in the developing chicken chorioallantoic membrane. *Microcirculation* 17, 447–457. doi: 10.1111/j.1549-8719.2010.00043.x

Bell, R. D., and Zlokovic, B. V. (2009). Neurovascular mechanisms and blood-brain barrier disorder in Alzheimer's disease. *Acta Neuropathol.* 118, 103–113. doi: 10.1007/s00401-009-0522-3

Belle, J., Ysasi, A., Bennett, R. D., Filipovic, N., Nejad, M. I., Trumper, D. L., et al. (2014). Stretch-induced intussusceptive and sprouting angiogenesis in the chick chorioallantoic membrane. *Microvasc. Res.* 95, 60–67. doi: 10.1016/j.mvr.2014.06.009

Benn, A., Alonso, F., Mangelschots, J., Genot, E., Lox, M., and Zwijsen, A. (2020). BMP-SMAD1/5 signaling regulates retinal vascular development. *Biomolecules* 10:488. doi: 10.3390/biom10030488

Bentley, K., Franco, C. A., Philippides, A., Blanco, R., Dierkes, M., Gebala, V., et al. (2014a). The role of differential VE-cadherin dynamics in cell rearrangement during angiogenesis. *Nat. Cell Biol.* 16, 309–321. doi: 10.1038/ncb2926

Bentley, K., Philippides, A., and Ravasz Regan, E. (2014b). Do endothelial cells dream of eclectic shape? *Dev. Cell.* 29, 146–158. doi: 10.1016/j.devcel.2014.03.019

Bernabeu, M. O., Jones, M. L., Nash, R. W., Pezzarossa, A., Coveney, P. V., Gerhardt, H., et al. (2018). PolNet: a tool to quantify network-level cell polarity and blood flow in vascular remodeling. *Biophys. J.* 114, 2052–2058. doi: 10.1016/j.bpj.2018.03.032

Bernabeu, M. O., Jones, M. L., Nielsen, J. H., Kruger, T., Nash, R. W., Groen, D., et al. (2014). Computer simulations reveal complex distribution of haemodynamic forces in a mouse retina model of angiogenesis. *J. R. Soc. Interface* 11:20140543. doi: 10.1098/rsif.2014.0543

Bhagyalakshmi, A., Berthiaume, F., Reich, K. M., and Frangos, J. A. (1992). Fluid shear stress stimulates membrane phospholipid metabolism in cultured human endothelial cells. *J. Vasc. Res.* 29, 443–449. doi: 10.1159/000158963

Blackman, B. R., Garcia-Cardena, G., and Gimbrone, M. A. Jr. (2002). A new in vitro model to evaluate differential responses of endothelial cells to simulated arterial shear stress waveforms. *J. Biomech. Eng.* 124, 397–407. doi: 10.1115/1.1486468

Bogorad, M. I., DeStefano, J., Karlsson, J., Wong, A. D., Gerecht, S., and Searson, P. C. (2015). Review: in vitro microvessel models. *Lab. Chip.* 15, 4242–4255. doi: 10.1039/C5LC00832H

Bongrazio, M., Da Silva-Azevedo, L., Bergmann, E. C., Baum, O., Hinz, B., Pries, A. R., et al. (2006). Shear stress modulates the expression of thrombospondin-1 and CD36 in endothelial cells in vitro and during shear stress-induced angiogenesis in vivo. *Int. J. Immunopathol. Pharmacol.* 19, 35–48. doi: 10.1177/205873920601900104

Boriushkin, E., Fancher, I. S., and Levitan, I. (2019). Shear-stress sensitive inwardly-rectifying K(+) channels regulate developmental retinal angiogenesis by vessel regression. *Cell Physiol. Biochem.* 52, 1569–1583. doi: 10.33594/000000109

Boudier, H. A. (1999). Arteriolar and capillary remodelling in hypertension. *Drugs* 58, 37–40.

Burri, P. H., Hlushchuk, R., and Djonov, V. (2004). Intussusceptive angiogenesis: its emergence, its characteristics, and its significance. *Dev. Dyn.* 231, 474–488. doi: 10.1002/dvdy.20184

Busch, R., Strohbach, A., Pennewitz, M., Lorenz, F., Bahls, M., Busch, M. C., et al. (2015). Regulation of the endothelial apelin/APJ system by hemodynamic fluid flow. *Cell Signal.* 27, 1286–1296. doi: 10.1016/j.cellsig.2015.03.011

Butler, P. J., Tsou, T. C., Li, J. Y., Usami, S., and Chien, S. (2002). Rate sensitivity of shear-induced changes in the lateral diffusion of endothelial cell membrane lipids: a role for membrane perturbation in shear-induced MAPK activation. *FASEB J.* 16, 216–218. doi: 10.1096/fj.01-0434fje

Campinho, P., Vilfan, A., and Vermot, J. (2020). Blood flow forces in shaping the vascular system: a focus on endothelial cell behavior. *Front. Physiol.* 11:552. doi: 10.3389/fphys.2020.00552

Chaki, S. P., and Rivera, G. M. (2013). Integration of signaling and cytoskeletal remodeling by Nck in directional cell migration. *Bioarchitecture* 3, 57–63. doi: 10.4161/bioa.25744

Chandana, E. P., Maeda, Y., Ueda, A., Kiyonari, H., Oshima, N., Yamamoto, M., et al. (2010). Involvement of the Reck tumor suppressor protein in maternal and embryonic vascular remodeling in mice. *BMC Dev. Biol.* 10:84. doi: 10.1186/1471-213X-10-84

Chang, A. H., Raftrey, B. C., D'Amato, G., Surya, V. N., Poduri, A., Chen, H. I., et al. (2017). DACH1 stimulates shear stress-guided endothelial cell migration and coronary artery growth through the CXCL12-CXCR4 signaling axis. *Genes Dev.* 31, 1308–1324. doi: 10.1101/gad.301549.117

Chen, Q., Jiang, L., Li, C., Hu, D., Bu, J. W., Cai, D., et al. (2012). Haemodynamics-driven developmental pruning of brain vasculature in zebrafish. *PLoS Biol.* 10:e1001374. doi: 10.1371/journal.pbio.1001374

Chien, S. (2003). Molecular and mechanical bases of focal lipid accumulation in arterial wall. *Prog. Biophys. Mol. Biol.* 83, 131–151. doi: 10.1016/S0079-6107(03)00053-1

Chien, S. (2007). Mechanotransduction and endothelial cell homeostasis: the wisdom of the cell. *Am. J. Physiol. Heart Circ. Physiol.* 292, H1209–H1224. doi: 10.1152/ajpheart.01047.2006

Chien, S. (2008). Effects of disturbed flow on endothelial cells. *Ann. Biomed. Eng.* 36, 554–562. doi: 10.1007/s10439-007-9426-3

Chiu, J. J., and Chien, S. (2011). Effects of disturbed flow on vascular endothelium: pathophysiological basis and clinical perspectives. *Physiol. Rev.* 91, 327–387. doi: 10.1152/physrev.00047.2009

Choi, W., Kim, H. M., Park, S., Yeom, E., Doh, J., and Lee SJ. (2017). Variation in wall shear stress in channel networks of zebrafish models. *J. R. Soc. Interface* 14:20160900. doi: 10.1098/rsif.2016.0900

Chu, T. J., and Peters, D. G. (2008). Serial analysis of the vascular endothelial transcriptome under static and shear stress conditions. *Physiol. Genomics* 34, 185–192. doi: 10.1152/physiolgenomics.90201.2008

Colangelo, S., Langille, B. L., and Gotlieb AI. (1994). Three patterns of distribution characterize the organization of endothelial microfilaments at aortic flow dividers. *Cell Tissue Res.* 278, 235–242. doi: 10.1007/BF00414165

Coluccio, M. L., D'Attimo, M. A., Cristiani, C. M., Candeloro, P., Parrotta, E., Dattola, E., et al. (2019). A passive microfluidic device for chemotaxis studies. *Micromachines* 10:551 doi: 10.3390/mi10080551

Connolly, S. E., Hores, T. A., Smith, L. E., and D'Amore, P. A. (1988). Characterization of vascular development in the mouse retina. *Microvasc. Res.* 36, 275–290. doi: 10.1016/0026-2862(88)90028-3

Coughlin, M. F., and Kamm, R. D. (2020). The use of microfluidic platforms to probe the mechanism of cancer cell extravasation. *Adv. Health Mater.* 9:e1901410. doi: 10.1002/adhm.201901410

Davies, P. F. (1995). Flow-mediated endothelial mechanotransduction. *Physiol. Rev.* 75, 519–560. doi: 10.1152/physrev.1995.75.3.519

De Paepe, M. E., Benny, M. K. V., Priolo, L., Luks, F. I., and Shapiro, S. (2017). Florid intussusceptive-like microvascular dysangiogenesis in a preterm lung. *Pediatr. Dev. Pathol.* 20, 432–439. doi: 10.1177/1093526616686455

De Paepe, M. E., Chu, S., Hall, S. J., McDonnell-Clark, E., Heger, N. E, Schorl, C., et al. (2015). Intussusceptive-like angiogenesis in human fetal lung xenografts: link with bronchopulmonary dysplasia-associated microvascular dysangiogenesis? *Exp. Lung Res.* 41, 477–488. doi: 10.3109/01902148.2015.1080321

dela Paz, N. G., Walshe, T. E., Leach, L. L., Saint-Geniez, M., and D'Amore, P. A. (2012). Role of shear-stress-induced VEGF expression in endothelial cell survival. *J. Cell Sci.* 125(Pt 4), 831–843. doi: 10.1242/jcs.084301

Dieterich, P., Odenthal-Schnittler, M., Mrowietz, C., Kramer, M., Sasse, L., and Oberleithner, H., et al. (2000). Quantitative morphodynamics of endothelial cells within confluent cultures in response to fluid shear stress. *Biophys. J.* 79, 1285–1297. doi: 10.1016/S0006-3495(00)76382-X

Dimova, I., Hlushchuk, R., Makanya, A., Styp-Rekowska, B., Ceausu, A., Flueckiger, S., et al. (2013). Inhibition of Notch signaling induces extensive intussusceptive neo-angiogenesis by recruitment of mononuclear cells. *Angiogenesis* 16, 921–937. doi: 10.1007/s10456-013-9366-5

Djonov, V. G., Kurz, H., and Burri, P. H. (2002). Optimality in the developing vascular system: branching remodeling by means of intussusception as an efficient adaptation mechanism. *Dev. Dyn.* 224, 391–402. doi: 10.1002/dvdy.10119

Du, W., and Gao, C. (2019). Selective adhesion and directional migration of endothelial cells guided by Cys-Ala-Gly peptide density gradient on antifouling polymer brushes. *Macromol. Biosci.* 19:e1900292. doi: 10.1002/mabi.201900292

Dubrac, A., Genet, G., Ola, R., Zhang, F., Pibouin-Fragner, L., Han J, et al. (2016). Targeting NCK-mediated endothelial cell front-rear polarity inhibits neovascularization. *Circulation* 133, 409–421. doi: 10.1161/CIRCULATIONAHA.115.017537

Eckmann, D. M., Bowers, S., Stecker, M., and Cheung, A. T. (2000). Hematocrit, volume expander, temperature, and shear rate effects on blood viscosity. *Anesth. Analg.* 91, 539–545. doi: 10.1213/00000539-200009000-00007

Edgar, L. T., Franco, C. A., Gerhardt, H., and Bernabeu, M. O. (2020). On the preservation of vessel bifurcations during flow-mediated angiogenic remodelling. *bioRxiv [Preprint]* doi: 10.1101/2020.02.07.938522

Egginton, S. (2011). In vivo shear stress response. *Biochem. Soc. Trans.* 39, 1633–1638. doi: 10.1042/BST20110715

Esteban, S., Clemente, C., Koziol, A., Gonzalo, P., Rius, C., Martinez, F., et al. (2020). Endothelial MT1-MMP targeting limits intussusceptive angiogenesis and colitis via TSP1/nitric oxide axis. *Embo Mol Med.* 12:e10862. doi: 10.15252/emmm.201910862

Evans, I. M., Kennedy, S. A., Paliashvili, K., Santra, T., Yamaji, M., Lovering, R. C., et al. (2017). Vascular endothelial growth factor (VEGF) promotes assembly of the p130Cas interactome to drive endothelial chemotactic signaling and angiogenesis. *Mol. Cell. Proteomics* 16, 168–180. doi: 10.1074/mcp.M116.064428

Fantin, A., Lampropoulou, A., Gestri, G., Raimondi, C., Senatore, V., Zachary, I., et al. (2015). NRP1 regulates CDC42 activation to promote filopodia formation in endothelial tip cells. *Cell Rep.* 11, 1577–1590. doi: 10.1016/j.celrep.2015.05.018

Feinberg, R. N., Latker, C. H., and Beebe, D. C. (1986). Localized vascular regression during limb morphogenesis in the chicken embryo. I. Spatial and temporal changes in the vascular pattern. *Anat. Rec.* 214, 405–409. doi: 10.1002/ar.1092140411

Filipovic, N., Tsuda, A., Lee, G. S., Miele, L. F., Lin, M., Konerding, M. A., et al. (2009). Computational flow dynamics in a geometric model of intussusceptive angiogenesis. *Microvasc. Res.* 78, 286–293. doi: 10.1016/j.mvr.2009.08.004

Franco, C. A., and Gerhardt, H. (2017). Morph or move? How distinct endothelial cell responses to blood flow shape vascular networks. *Dev. Cell.* 41, 574–576. doi: 10.1016/j.devcel.2017.06.008

Franco, C. A., Jones, M. L., Bernabeu, M. O., Geudens, I., Mathivet, T., Rosa, A., et al. (2015). Dynamic endothelial cell rearrangements drive developmental vessel regression. *PLoS Biol.* 13:e1002125. doi: 10.1371/journal.pbio.1002125

Franco, C. A., Jones, M. L., Bernabeu, M. O., Vion, A. C., Barbacena, P., Fan, J., et al. (2016). Non-canonical Wnt signalling modulates the endothelial shear stress flow sensor in vascular remodelling. *eLife* 5:e07727. doi: 10.7554/eLife.07727

Galbraith, C. G., Skalak, R., and Chien, S. (1998). Shear stress induces spatial reorganization of the endothelial cell cytoskeleton. *Cell Motil. Cytoskeleton* 40, 317–330. doi: 10.1002/(SICI)1097-0169(1998)40:4<317::AID-CM1>3.0.CO;2-8

Gan, L., Miocic, M., Doroudi, R., Selin-Sjogren, L., and Jern, S. (2000). Distinct regulation of vascular endothelial growth factor in intact human conduit vessels exposed to laminar fluid shear stress and pressure. *Biochem. Biophys. Res. Commun.* 272, 490–496. doi: 10.1006/bbrc.2000.2663

Ganesan, P., He, S., and Xu, H. (2010). Development of an image-based network model of retinal vasculature. *Ann. Biomed. Eng.* 38, 1566–1585. doi: 10.1007/s10439-010-9942-4

Garkavtsev, I., Chauhan, V. P., Wong, H. K., Mukhopadhyay, A., Glicksman, M. A., Peterson, R. T., et al. (2011). Dehydro-alpha-lapachone, a plant product with antivascular activity. *Proc. Natl. Acad. Sci. U.S.A.* 108, 11596–11601. doi: 10.1073/pnas.1104225108

Georgieva, P. B., Marchuk, D. A., Gerhardt, H., and Leducq, A. C. (2019). Attract. *Circ. Res.* 125, 262–264. doi: 10.1161/CIRCRESAHA.119.315198

Giacomini, A., Ackermann, M., Belleri, M., Coltrini, D., Nico, B., Ribatti, D., et al. (2015). Brain angioarchitecture and intussusceptive microvascular growth in a murine model of Krabbe disease. *Angiogenesis* 18, 499–510. doi: 10.1007/s10456-015-9481-6

Gianni-Barrera, R., Butschkau, A., Uccelli, A., Certelli, A., Valente, P., Bartolomeo, M., et al. (2018). PDGF-BB regulates splitting angiogenesis in skeletal muscle by limiting VEGF-induced endothelial proliferation. *Angiogenesis* 21, 883–900. doi: 10.1007/s10456-018-9634-5

Gianni-Barrera, R., Trani, M., Fontanellaz, C., Heberer, M., Djonov, V., Hlushchuk, R., et al. (2013). VEGF over-expression in skeletal muscle induces angiogenesis by intussusception rather than sprouting. *Angiogenesis* 16, 123–136. doi: 10.1007/s10456-012-9304-y

Gkontra, P., El-Bouri, W. K., Norton, K. A., Santos, A., Popel, A. S., Payne, S. J., et al. (2019). Dynamic changes in microvascular flow conductivity and perfusion after myocardial infarction shown by image-based modeling. *J. Am. Heart Assoc.* 8:e011058. doi: 10.1161/JAHA.118.011058

Gkontra, P., Norton, K. A., Zak, M. M., Clemente, C., Agüero, J., Ibáñez, B., et al. (2018). Deciphering microvascular changes after myocardial infarction through 3D fully automated image analysis. *Sci. Rep.* 8:1854. doi: 10.1038/s41598-018-32598-6

Goede, V., Schmidt, T., Kimmina, S., Kozian, D., and Augustin, H. G. (1998). Analysis of blood vessel maturation processes during cyclic ovarian angiogenesis. *Lab. Invest.* 78, 1385–1394.

Gomes, N., Legrand, C., and Fauvel-Lafeve, F. (2005). Shear stress induced release of von Willebrand factor and thrombospondin-1 in HUVEC extracellular matrix enhances breast tumour cell adhesion. *Clin. Exp Metast.* 22, 215–223. doi: 10.1007/s10585-005-7359-5

Gordon, E., Schimmel, L., and Frye, M. (2020). The importance of mechanical forces for in vitro endothelial cell biology. *Front. Physiol.* 11:684. doi: 10.3389/fphys.2020.00684

Groppa, E., Brkic, S., Uccelli, A., Wirth, G., Korpisalo-Pirinen, P., Filippova, M., et al. (2018). EphrinB2/EphB4 signaling regulates non-sprouting angiogenesis by VEGF. *Embo Rep.* 19:e45054. doi: 10.15252/embr.201745054

Hahn, P., Lindsten, T., Tolentino, M., Thompson, C. B., Bennett, J., and Dunaief, J. L. (2005). Persistent fetal ocular vasculature in mice deficient in bax and bak. *Arch. Ophthalmol.* 123, 797–802. doi: 10.1001/archopht.123.6.797

Han, S., Shin, Y., Jeong, H. E., Jeon, J. S., Kamm, R. D., Huh, D., et al. (2015). Constructive remodeling of a synthetic endothelial extracellular matrix. *Sci. Rep.* 5:18290. doi: 10.1038/srep18290

Halldorsson, S., Lucumi, E., Gomez-Sjoberg, R., and Fleming, R. M. T. (2015). Advantages and challenges of microfluidic cell culture in polydimethylsiloxane devices. *Biosens. Bioelectron.* 63, 218–231. doi: 10.1016/j.bios.2014.07.029

Hamm, M. J., Kirchmaier, B. C., and Herzog, W. (2016). Sema3d controls collective endothelial cell migration by distinct mechanisms via Nrp1 and PlxnD1. *J. Cell Biol.* 215, 415–430. doi: 10.1083/jcb.201603100

Hesh, C. A., Qiu, Y., and Lam, W. A. (2019). Vascularized microfluidics and the blood-endothelium interface. *Micromachines* 11:18. doi: 10.3390/mi11010018

Hlushchuk, R., Styp-Rekowska, B., Dzambazi, J., Wnuk, M., Huynh-Do, U., Makanya, A., et al. (2017). Endoglin inhibition leads to intussusceptive angiogenesis via activation of factors related to COUP-TFII signaling pathway. *PLoS One* 12:e0182813. doi: 10.1371/journal.pone.0182813

Holash, J., Maisonpierre, P. C., Compton, D., Boland, P., Alexander, C. R., Zagzag, D., et al. (1999). Vessel cooption, regression, and growth in tumors mediated by angiopoietins and VEGF. *Science* 284, 1994–1998. doi: 10.1126/science.284.5422.1994

Hsu, Y. H., Moya, M. L., Hughes, C. C., George, S. C., and Lee, A. P. (2013). A microfluidic platform for generating large-scale nearly identical human microphysiological vascularized tissue arrays. *Lab. Chip.* 13, 2990–2998. doi: 10.1039/c3lc50424g

Hudlicka, O., Brown, M. D., May, S., Zakrzewicz, A., and Pries, A. R. (2006). Changes in capillary shear stress in skeletal muscles exposed to long-term activity: role of nitric oxide. *Microcirculation* 13, 249–259. doi: 10.1080/10739680600556951

Huh, D., Hamilton, G. A., and Ingber, D. E. (2011). From 3D cell culture to organs-on-chips. *Trends Cell Biol.* 21, 745–754. doi: 10.1016/j.tcb.2011.09.005

Ito, M., and Yoshioka, M. (1999). Regression of the hyaloid vessels and pupillary membrane of the mouse. *Anat. Embryol.* 200, 403–411. doi: 10.1007/s004290050289

Jacobs, E. R., Cheliakine, C., Gebremedhin, D., Birks, E. K., Davies, P. F., and Harder, D. R. (1995). Shear activated channels in cell-attached patches of cultured bovine aortic endothelial cells. *Pflugers Arch.* 431, 129–131. doi: 10.1007/BF00374386

Jin, Y., Muhl, L., Burmakin, M., Wang, Y., Duchez, A. C., Betsholtz, C., et al. (2017). Endoglin prevents vascular malformation by regulating flow-induced cell migration and specification through VEGFR2 signalling. *Nat. Cell Biol.* 19, 639–652. doi: 10.1038/ncb3534

Kang, H., Kwak, H. I., Kaunas, R., and Bayless, K. J. (2011). Fluid shear stress and sphingosine 1-phosphate activate calpain to promote membrane type 1 matrix metalloproteinase (MT1-MMP) membrane translocation and endothelial invasion into three-dimensional collagen matrices. *J. Biol. Chem.* 286, 42017–42026. doi: 10.1074/jbc.M111.290841

Karino, T., and Goldsmith, H. L. (1980). Disturbed flow in models of branching vessels. *Trans. Am. Soc. Artif. Intern. Organs.* 26, 500–506.

Karino, T., Goldsmith, H. L., Motomiya, M., Mabuchi, S., and Sohara, Y. (1987). Flow patterns in vessels of simple and complex geometries. *Ann. N. Y. Acad. Sci.* 516, 422–441. doi: 10.1111/j.1749-6632.1987.tb33063.x

Karthik, S., Djukic, T., Kim, J. D., Zuber, B., Makanya, A., Odriozola, A., et al. (2018). Synergistic interaction of sprouting and intussusceptive angiogenesis during zebrafish caudal vein plexus development. *Sci. Rep.* 8:9840. doi: 10.1038/s41598-018-27791-6

Kim, L., Toh, Y. C., Voldman, J., and Yu, H. (2007). A practical guide to microfluidic perfusion culture of adherent mammalian cells. *Lab. Chip.* 7, 681–694. doi: 10.1039/b704602b

Kim, H., Chung, H., Kim, J., Choi, D. H., Shin, Y., Kang, Y. G., et al. (2019). Macrophages-triggered sequential remodeling of endothelium-interstitial matrix to form pre-metastatic niche in microfluidic tumor microenvironment. *Adv. Sci.* 6:1900195. doi: 10.1002/advs.201900195

Kochhan, E., Lenard, A., Ellertsdottir, E., Herwig, L., Affolter, M., Belting, H. G., et al. (2013). Blood flow changes coincide with cellular rearrangements during blood vessel pruning in zebrafish embryos. *PLoS One* 8:e75060. doi: 10.1371/journal.pone.0075060

Korn, C., and Augustin, H. G. (2015). Mechanisms of vessel pruning and regression. *Dev. Cell.* 34, 5–17. doi: 10.1016/j.devcel.2015.06.004

Kwon, H. B., Wang, S., Helker, C. S., Rasouli, S. J., Maischein, H. M., Offermanns, S. (2016). In vivo modulation of endothelial polarization by Apelin receptor signalling. *Nat Commun.* 7:11805. doi: 10.1038/ncomms11805

Lang, R., Lustig, M., Francois, F., Sellinger, M., and Plesken, H. (1994). Apoptosis during macrophage-dependent ocular tissue remodelling. *Development* 120, 3395–3403.

Larrivee, B., Prahst, C., Gordon, E., del Toro, R., Mathivet, T., Duarte, A., et al. (2012). ALK1 signaling inhibits angiogenesis by cooperating with the Notch pathway. *Dev Cell.* 22, 489–500. doi: 10.1016/j.devcel.2012.02.005

Lavina, B., Castro, M., Niaudet, C., Cruys, B., Alvarez-Aznar, A., Carmeliet, P., et al. (2018). Defective endothelial cell migration in the absence of Cdc42 leads to capillary-venous malformations. *Development* 145: dev161182. doi: 10.1242/dev.161182

Lawson, N. D., and Weinstein, B. M. (2002). In vivo imaging of embryonic vascular development using transgenic zebrafish. *Dev Biol.* 248, 307–318. doi: 10.1006/dbio.2002.0711

le Noble, F., Moyon, D., Pardanaud, L., Yuan, L., Djonov, V., Matthijsen, R., et al. (2004). Flow regulates arterial-venous differentiation in the chick embryo yolk sac. *Development* 131, 361–375. doi: 10.1242/dev.00929

Lee, G. S., Filipovic, N., Lin, M., Gibney, B. C., Simpson, D. C., Konerding, M. A., et al. (2011). Intravascular pillars and pruning in the extraembryonic vessels of chick embryos. *Dev. Dyn.* 240, 1335–1343. doi: 10.1002/dvdy.22618

Lee, G. S., Filipovic, N., Miele, L. F., Lin, M., Simpson, D. C., Giney, B., et al. (2010). Blood flow shapes intravascular pillar geometry in the chick chorioallantoic membrane. *J. Angiogenes Res.* 2:11. doi: 10.1186/2040-2384-2-11

Levesque, M. J., and Nerem, R. M. (1985). The elongation and orientation of cultured endothelial cells in response to shear stress. *J. Biomech. Eng.* 107, 341–347. doi: 10.1115/1.3138567

Li, J., Hou, B., Tumova, S., Muraki, K., Bruns, A., Ludlow, M. J., et al. (2014). Piezo1 integration of vascular architecture with physiological force. *Nature* 515, 279–282. doi: 10.1038/nature13701

Lobov, I. B., Cheung, E., Wudali, R., Cao, J., Halasz, G., Wei, Y., et al. (2011). The Dll4/Notch pathway controls postangiogenic blood vessel remodeling and regression by modulating vasoconstriction and blood flow. *Blood* 117, 6728–6737. doi: 10.1182/blood-2010-08-302067

Lobov, I. B., Rao, S., Carroll, T. J., Vallance, J. E., Ito, M., Ondr, J. K., et al. (2005). WNT7b mediates macrophage-induced programmed cell death in patterning of the vasculature. *Nature* 437, 417–421. doi: 10.1038/nature03928

Lu, D., and Kassab, G. S. (2011). Role of shear stress and stretch in vascular mechanobiology. *J. R. Soc. Interface* 8, 1379–1385. doi: 10.1098/rsif.2011.0177

Lucitti, J. L., Jones, E. A., Huang, C., Chen, J., Fraser, S. E., and Dickinson, M. E. (2007). Vascular remodeling of the mouse yolk sac requires hemodynamic force. *Development* 134, 3317–3326. doi: 10.1242/dev.02883

Lundberg, E., and Borner, G. H. H. (2019). Spatial proteomics: a powerful discovery tool for cell biology. *Nat. Rev. Mol. Cell Biol.* 20, 285–302. doi: 10.1038/s41580-018-0094-y

Luttun, A., Tjwa, M., Moons, L., Wu, Y., Angelillo-Scherrer, A., Liao, F., (2002). Revascularization of ischemic tissues by PlGF treatment, and inhibition of tumor angiogenesis, arthritis and atherosclerosis by anti-Flt1. *Nat Med.* 8, 831–840. doi: 10.1038/nm731

Mack, J. J., Mosqueiro, T. S., Archer, B. J., Jones, W. M., Sunshine, H., Faas, G. C., et al. (2017). NOTCH1 is a mechanosensor in adult arteries. *Nat. Commun.* 8:1620. doi: 10.1038/s41467-017-01741-8

Magid, R., Martinson, D., Hwang, J., Jo, H., and Galis, Z. S. (2003). Optimization of isolation and functional characterization of primary murine aortic endothelial cells. *Endothelium* 10, 103–109. doi: 10.1080/10623320303364

Maibier, M., Reglin, B., Nitzsche, B., Xiang, W., Rong, W. W., Hoffmann, B., et al. (2016). Structure and hemodynamics of vascular networks in the chorioallantoic membrane of the chicken. *Am. J. Physiol. Heart Circ. Physiol.* 311, H913–H926. doi: 10.1152/ajpheart.00786.2015

Meeson, A. P., Argilla, M., Ko, K., Witte, L., and Lang, R. A. (1999). VEGF deprivation-induced apoptosis is a component of programmed capillary regression. *Development* 126, 1407–1415.

Mehta, V., Pang, K. L., Rozbesky, D., Nather, K., Keen, A., Lachowski, D., et al. (2020). The guidance receptor plexin D1 is a mechanosensor in endothelial cells. *Nature* 578, 290–295. doi: 10.1038/s41586-020-1979-4

Mentzer, S. J., and Konerding, M. A. (2014). Intussusceptive angiogenesis: expansion and remodeling of microvascular networks. *Angiogenesis* 17, 499–509. doi: 10.1007/s10456-014-9428-3

Miao, H., Hu, Y. L., Shiu, Y. T., Yuan, S., Zhao, Y., Kaunas, R., et al. (2005). Effects of flow patterns on the localization and expression of VE-cadherin at vascular endothelial cell junctions: in vivo and in vitro investigations. *J. Vasc. Res.* 42, 77–89. doi: 10.1159/000083094

Mori, M., Stokes, K. Y., Vowinkel, T., Watanabe, N., Elrod, J. W., Harris, N. R., et al. (2005). Colonic blood flow responses in experimental colitis: time course and underlying mechanisms. *Am. J. Physiol. Gastrointest. Liver Physiol.* 289, G1024–G1029. doi: 10.1152/ajpgi.00247.2005

Nagasawa-Masuda, A., and Terai, K. (2017). Yap/Taz transcriptional activity is essential for vascular regression via Ctgf expression and actin polymerization. *PLoS One* 12:e0174633. doi: 10.1371/journal.pone.0174633

Nakajima, H., Yamamoto, K., Agarwala, S., Terai, K., Fukui, H., Fukuhara, S., et al. (2017). Flow-dependent endothelial YAP regulation contributes to vessel maintenance. *Dev Cell.* 40, 523.e6–536.e6. doi: 10.1016/j.devcel.2017.02.019

Nayak, L., Lin, Z., and Jain, M. K. (2011). "Go with the flow": how Kruppel-like factor 2 regulates the vasoprotective effects of shear stress. *Antioxid. Redox Signal.* 15, 1449–1461. doi: 10.1089/ars.2010.3647

Nerem, R. M. (1993). Hemodynamics and the vascular endothelium. *J. Biomech. Eng.* 115, 510–514. doi: 10.1115/1.2895532

Neto, F., Klaus-Bergmann, A., Ong, Y. T., Alt, S., Vion, A. C., Szymborska, A., et al. (2018). YAP and TAZ regulate adherens junction dynamics and endothelial cell distribution during vascular development. *eLife* 7:e31037. doi: 10.7554/eLife.31037

Nguyen, D. H., Stapleton, S. C., Yang, M. T., Cha, S. S., Choi, C. K., Galie, P. A., et al. (2013). Biomimetic model to reconstitute angiogenic sprouting morphogenesis in vitro. *Proc. Natl. Acad. Sci. U.S.A.* 110, 6712–6717. doi: 10.1073/pnas.1221526110

Nithianandarajah-Jones, G. N., Wilm, B., Goldring, C. E., Muller, J., Cross, M. J. (2014). The role of ERK5 in endothelial cell function. *Biochem. Soc. Trans.* 42, 1584–1589. doi: 10.1042/BST20140276

Nollert, M. U., Eskin, S. G., and McIntire, L. V. (1990). Shear stress increases inositol trisphosphate levels in human endothelial cells. *Biochem. Biophys. Res. Commun.* 170, 281–287. doi: 10.1016/0006-291X(90)91271-S

Noria, S., Xu, F., McCue, S., Jones, M., Gotlieb, A. I., Langille, B. L. (2004). Assembly and reorientation of stress fibers drives morphological changes to endothelial cells exposed to shear stress. *Am. J. Pathol.* 164, 1211–1223. doi: 10.1016/S0002-9440(10)63209-9

Noris, M., Morigi, M., Donadelli, R., Aiello, S., Foppolo, M., Todeschini, M., et al. (1995). Nitric oxide synthesis by cultured endothelial cells is modulated by flow conditions. *Circ. Res.* 76, 536–543. doi: 10.1161/01.RES.76.4.536

Nowak-Sliwinska, P., Alitalo, K., Allen, E., Anisimov, A., Aplin, A. C., Auerbach, R., et al. (2018). Consensus guidelines for the use and interpretation of angiogenesis assays. *Angiogenesis* 21, 425–532 doi: 10.1007/s10456-018-9613-x

Ohta, S., Inasawa, S., Yamaguchi, Y. (2015). Alignment of vascular endothelial cells as a collective response to shear flow. *J. Phys. D Appl. Phys.* 48, 245–401. doi: 10.1088/0022-3727/48/24/245401

Okuda, M., Takahashi, M., Suero, J., Murry, C. E., Traub, O., Kawakatsu, H., et al. (1999). Shear stress stimulation of p130(cas) tyrosine phosphorylation requires calcium-dependent c-Src activation. *J. Biol. Chem.* 274, 26803–26809. doi: 10.1074/jbc.274.38.26803

Ostrowski, M. A., Huang, N. F., Walker, T. W., Verwijlen, T., Poplawski, C., Khoo, A. S., et al. (2014). Microvascular endothelial cells migrate upstream and align against the shear stress field created by impinging flow. *Biophys. J.* 106, 366–374. doi: 10.1016/j.bpj.2013.11.4502

Paku, S., Dezso, K., Bugyik, E., Tovari, J., Timar, J., Nagy, P, et al. (2011). A new mechanism for pillar formation during tumor-induced intussusceptive angiogenesis: inverse sprouting. *Am. J. Pathol.* 179, 1573–1585. doi: 10.1016/j.ajpath.2011.05.033

Papadaki, M., and McLntire, L. V. (1999). Quantitative measurement of shear-stress effects on endothelial cells. *Methods Mol. Med.* 18,577–593. doi: 10.1385/0-89603-516-6:577

Patan, S., Alvarez, M. J., Schittny, J. C., Burri, P. H. (1992). Intussusceptive microvascular growth: a common alternative to capillary sprouting. *Arch. Histol. Cytol.* 55, 65–75. doi: 10.1679/aohc.55.Suppl_65

Patan, S., Haenni, B., and Burri, P. H. (1993). Evidence for intussusceptive capillary growth in the chicken chorio-allantoic membrane (CAM). *Anat. Embryol.* 187, 121–130. doi: 10.1007/BF00171743

Patan, S., Haenni, B., and Burri PH. (1996a). Implementation of intussusceptive microvascular growth in the chicken chorioallantoic membrane (CAM): 1. pillar formation by folding of the capillary wall. *Microvasc. Res.* 51, 80–98. doi: 10.1006/mvre.1996.0009

Patan, S., Munn, L. L., and Jain, R. K. (1996b). Intussusceptive microvascular growth in a human colon adenocarcinoma xenograft: a novel mechanism of tumor angiogenesis. *Microvasc. Res.* 51, 260–272. doi: 10.1006/mvre.1996.0025

Phng, L. K., Potente, M., Leslie, J. D., Babbage, J., Nyqvist, D., Lobov, I., et al. (2009). Nrarp coordinates endothelial Notch and Wnt signaling to control vessel density in angiogenesis. *Dev. Cell.* 16, 70–82. doi: 10.1016/j.devcel.2008.12.009

Poduri, A., Chang, A. H., Raftrey, B., Rhee, S., Van, M., and Red-Horse, K. (2017). Endothelial cells respond to the direction of mechanical stimuli through SMAD signaling to regulate coronary artery size. *Development* 144, 3241–3252. doi: 10.1242/dev.150904

Prahst, C., Ashrafzadeh, P., Mead, T., Figueiredo, A., Chang, K., Richardson, D., et al. (2020). Mouse retinal cell behaviour in space and time using light sheet fluorescence microscopy. *eLife* 9: e49779. doi: 10.7554/eLife.49779

Pries, A. R., and Secomb, T. W. (2014). Making microvascular networks work: angiogenesis, remodeling, and pruning. *Physiology* 29, 446–455. doi: 10.1152/physiol.00012.2014

Prior, B. M., Lloyd, P. G., Yang, H. T., and Terjung, R. L. (2003). Exercise-induced vascular remodeling. *Exerc. Sport Sci. Rev.* 31, 26–33. doi: 10.1097/00003677-200301000-00006

Ranade, S. S., Qiu, Z., Woo, S. H., Hur, S. S., Murthy, S. E., Cahalan, S. M., et al. (2014). Piezo1, a mechanically activated ion channel, is required for vascular development in mice. *Proc. Natl. Acad. Sci. U.S.A.* 111, 10347–10352. doi: 10.1073/pnas.1409233111

Rauff, A., LaBelle, S. A., Strobel, H. A., Hoying, J. B., and Weiss, J. A. (2019). Imaging the dynamic interaction between sprouting microvessels and the extracellular matrix. *Front. Physiol.* 10:1011. doi: 10.3389/fphys.2019.01011

Ravnic, D. J., Konerding, M. A., Tsuda, A., Huss, H. T., Wolloscheck, T., Pratt, J. P., et al. (2007). Structural adaptations in the murine colon microcirculation associated with hapten-induced inflammation. *Gut* 56, 518–523. doi: 10.1136/gut.2006.101824

Red-Horse, K., and Siekmann, A. F. (2019). Veins and arteries build hierarchical branching patterns differently: bottom-up versus top-down. *Bioessays* 41:e1800198. doi: 10.1002/bies.201800198

Ribatti, D., and Djonov, V. (2012). Intussusceptive microvascular growth in tumors. *Cancer Lett.* 316, 126–131. doi: 10.1016/j.canlet.2011.10.040

Ricard, N., and Simons, M. (2015). When it is better to regress: dynamics of vascular pruning. *PLoS Biol.* 13:e1002148. doi: 10.1371/journal.pbio.1002148

Riedl, J., Crevenna, A. H., Kessenbrock, K., Yu, J. H., Neukirchen, D., Bista, M., et al. (2008). Lifeact: a versatile marker to visualize F-actin. *Nat. Methods* 5, 605–607. doi: 10.1038/nmeth.1220

Rochon, E. R., Menon, P. G., and Roman, B. L. (2016). Alk1 controls arterial endothelial cell migration in lumenized vessels. *Development* 143, 2593–2602. doi: 10.1242/dev.135392

Roest, M., Reininger, A., Zwaginga, J. J., King, M. R., Heemskerk, J. W., Biorheology Subcommittee of the SSCotI (2011). Flow chamber-based assays to measure thrombus formation in vitro: requirements for standardization. *J. Thromb. Haemost.* 9, 2322–2324. doi: 10.1111/j.1538-7836.2011.04492.x

Rutkowski, J. M., and Swartz, M. A. (2007). A driving force for change: interstitial flow as a morphoregulator. *Trends Cell Biol.* 17, 44–50. doi: 10.1016/j.tcb.2006.11.007

Sagare, A. P., Bell, R. D., and Zlokovic, B. V. (2012). Neurovascular dysfunction and faulty amyloid beta-peptide clearance in Alzheimer disease. *Cold Spring Harb. Perspect. Med.* 2:a011452 doi: 10.1101/cshperspect.a011452

Scheer, N., and Campos-Ortega, J. A. (1999). Use of the Gal4-UAS technique for targeted gene expression in the zebrafish. *Mech. Dev.* 80, 153–158. doi: 10.1016/S0925-4773(98)00209-3

Shalaby, S. Y., Chitragari, G., Sumpio, B. J., and Sumpio, B. E. (2017). Shear stress induces change in extracellular signal-regulated kinase 5 levels with sustained activation under disturbed and continuous laminar flow. *Int. J. Angiol.* 26, 109–115. doi: 10.1055/s-0037-1599057

Shao, S., Xiang, C., Qin, K., Ur Rehman Aziz, A., Liao, X., and Liu, B. (2017). Visualizing the spatiotemporal map of Rac activation in bovine aortic endothelial cells under laminar and disturbed flows. *PLoS One* 12:e0189088. doi: 10.1371/journal.pone.0189088

Shirure, V. S., Lezia, A., Tao, A., Alonzo, L. F., and George, S. C. (2017). Low levels of physiological interstitial flow eliminate morphogen gradients and guide angiogenesis. *Angiogenesis* 20, 493–504. doi: 10.1007/s10456-017-9559-4

Simonavicius, N., Ashenden, M., van Weverwijk, A., Lax, S., Huso, D. L., Buckley, C. D., et al. (2012). Pericytes promote selective vessel regression to regulate vascular patterning. *Blood* 120, 1516–1527. doi: 10.1182/blood-2011-01-332338

Song, J. W., and Munn, L. L. (2011). Fluid forces control endothelial sprouting. *Proc. Natl. Acad. Sci. U.S.A.* 108, 15342–15347. doi: 10.1073/pnas.1105316108

Sonmez, U. M., Cheng, Y.-W., Simon, C. W., Beth, L. R., and Lance, A. D. (2020). Endothelial cell polarization and orientation to flow in a novel microfluidic multimodal shear stress generator. *bioRxiv [Preprint]* doi: 10.1101/2020.07.10.197244

Spiering, D., Schmolke, M., Ohnesorge, N., Schmidt, M., Goebeler, M., Wegener, J., et al. (2009). MEK5/ERK5 signaling modulates endothelial cell migration and focal contact turnover. *J. Biol. Chem.* 284, 24972–24980. doi: 10.1074/jbc.M109.042911

Steward, R. Jr., Tambe, D., Hardin, C. C., Krishnan, R., and Fredberg, JJ. (2015). Fluid shear, intercellular stress, and endothelial cell alignment. *Am. J. Physiol. Cell Physiol.* 308, C657–C664. doi: 10.1152/ajpcell.00363.2014

Styp-Rekowska, B., Hlushchuk, R., Pries, A. R., and Djonov, V. (2011). Intussusceptive angiogenesis: pillars against the blood flow. *Acta Physiol.* 202, 213–223. doi: 10.1111/j.1748-1716.2011.02321.x

Sugden, W. W., Meissner, R., Aegerter-Wilmsen, T., Tsaryk, R., Leonard, E. V., Bussmann, J., et al. (2017). Endoglin controls blood vessel diameter through endothelial cell shape changes in response to haemodynamic cues. *Nat. Cell Biol.* 19, 653–665. doi: 10.1038/ncb3528

Szczerba, D., Kurz, H., and Szekely, G. (2009). A computational model of intussusceptive microvascular growth and remodeling. *J. Theor. Biol.* 261, 570–583. doi: 10.1016/j.jtbi.2009.09.018

Tang, K., Breen, E. C., Gerber, H. P., Ferrara, N. M., and Wagner, P. D. (2004). Capillary regression in vascular endothelial growth factor-deficient skeletal muscle. *Physiol. Genomics* 18, 63–69. doi: 10.1152/physiolgenomics.00023.2004

Tkachenko, E., Gutierrez, E., Saikin, S. K., Fogelstrand, P., Kim, C., Groisman, A., et al. (2013). The nucleus of endothelial cell as a sensor of blood flow direction. *Biol. Open.* 2, 1007–1012. doi: 10.1242/bio.20134622

Tovar-Lopez, F., Thurgood, P., Gilliam, C., Nguyen, N., Pirogova, E., Khoshmanesh, K., et al. (2019). A microfluidic system for studying the effects of disturbed flow on endothelial cells. *Front. Bioeng. Biotechnol.* 7:81. doi: 10.3389/fbioe.2019.00081

Trachet, B., Swillens, A., Van Loo, D., Casteleyn, C., De Paepe, A., Loeys, B., et al. (2009). The influence of aortic dimensions on calculated wall shear stress in the mouse aortic arch. *Comput. Methods Biomech. Biomed. Engin.* 12, 491–499. doi: 10.1080/10255840802695445

Turner, C. J., Badu-Nkansah, K., and Hynes, R. O. (2017). Endothelium-derived fibronectin regulates neonatal vascular morphogenesis in an autocrine fashion. *Angiogenesis* 20, 519–531. doi: 10.1007/s10456-017-9563-8

Tzima, E., Del Pozo, M. A., Kiosses, W. B., Mohamed, S. A., Li, S., Chien, S., et al. (2002). Activation of Rac1 by shear stress in endothelial cells mediates both cytoskeletal reorganization and effects on gene expression. *Embo J.* 21, 6791–6800. doi: 10.1093/emboj/cdf688

Tzima, E., Irani-Tehrani, M., Kiosses, W. B., Dejana, E., Schultz, D. A., Engelhardt, B., et al. (2005). A mechanosensory complex that mediates the endothelial cell response to fluid shear stress. *Nature* 437, 426–431. doi: 10.1038/nature03952

Udan, R. S., Vadakkan, T. J., Dickinson, M. E. (2013). Dynamic responses of endothelial cells to changes in blood flow during vascular remodeling of the mouse yolk sac. *Development* 140, 4041–4050. doi: 10.1242/dev.096255

Usami, S., Chen, H. H., Zhao, Y., Chien, S., and Skalak, R. (1993). Design and construction of a linear shear stress flow chamber. *Ann. Biomed. Eng.* 21, 77–83. doi: 10.1007/BF02368167

van Duinen, V., Trietsch, S. J., Joore, J., Vulto, P., and Hankemeier, T. (2015). Microfluidic 3D cell culture: from tools to tissue models. *Curr. Opin. Biotechnol.* 35, 118–126. doi: 10.1016/j.copbio.2015.05.002

Vickerman, V., and Kamm, R. D. (2012). Mechanism of a flow-gated angiogenesis switch: early signaling events at cell-matrix and cell-cell junctions. *Integr. Biol.* 4, 863–874. doi: 10.1039/c2ib00184e

Vion, A. C., Alt, S., Klaus-Bergmann, A., Szymborska, A., Zheng, T., Perovic, T., et al. (2018). Primary cilia sensitize endothelial cells to BMP and prevent excessive vascular regression. *J. Cell Biol.* 217, 1651–1665. doi: 10.1083/jcb.201706151

Voyvodic, P. L., Min, D., and Baker, A. B. (2012). A multichannel dampened flow system for studies on shear stress-mediated mechanotransduction. *Lab. Chip.* 12, 3322–3330. doi: 10.1039/c2lc40526a

Wang, C., Baker, B. M., Chen, C. S., and Schwartz, M. A. (2013). Endothelial cell sensing of flow direction. *Arterioscler. Thromb. Vasc. Biol.* 33, 2130–2136. doi: 10.1161/ATVBAHA.113.301826

Wang, S., Park, S., Fei, P., and Sorenson, C. M. (2011). Bim is responsible for the inherent sensitivity of the developing retinal vasculature to hyperoxia. *Dev. Biol.* 349, 296–309. doi: 10.1016/j.ydbio.2010.10.034

Wang, Y., Chang, J., Chen, K. D., Li, S., Li, J. Y., Wu, C., et al. (2007). Selective adapter recruitment and differential signaling networks by VEGF vs. shear stress. *Proc. Natl. Acad. Sci. U.S.A.* 104, 8875–8879. doi: 10.1073/pnas.0703088104

Watson, E. C., Grant, Z. L., and Coultas, L. (2017). Endothelial cell apoptosis in angiogenesis and vessel regression. *Cell Mol. Life Sci.* 74, 4387–4403. doi: 10.1007/s00018-017-2577-y

Watson, M. G., McDougall, S. R., Chaplain, M. A., Devlin, A. H., and Mitchell, C. A. (2012). Dynamics of angiogenesis during murine retinal development: a coupled in vivo and in silico study. *J. R. Soc Interface* 9, 2351–2364. doi: 10.1098/rsif.2012.0067

Williams, J. L., Cartland, D., Hussain, A., and Egginton, S. (2006a). A differential role for nitric oxide in two forms of physiological angiogenesis in mouse. *J. Physiol.* 570(Pt 3):445–454. doi: 10.1113/jphysiol.2005.095596

Williams, J. L., Weichert, A., Zakrzewicz, A., Da Silva-Azevedo, L., Pries, A. R., Baum, O., et al. (2006b). Differential gene and protein expression in abluminal sprouting and intraluminal splitting forms of angiogenesis. *Clin. Sci.* 110, 587–595. doi: 10.1042/CS20050185

Wojciak-Stothard, B., and Ridley, A. J. (2003). Shear stress-induced endothelial cell polarization is mediated by Rho and Rac but not Cdc42 or PI 3-kinases. *J. Cell Biol.* 161, 429–439. doi: 10.1083/jcb.200210135

Wong, K. H., Chan, J. M., Kamm, R. D., and Tien, J. (2012). Microfluidic models of vascular functions. *Annu. Rev. Biomed. Eng.* 14, 205–230. doi: 10.1146/annurev-bioeng-071811-150052

Wu, Z., Guo, H., Chow, N., Sallstrom, J., Bell, R. D., Deane, R. (2005). Role of the MEOX2 homeobox gene in neurovascular dysfunction in Alzheimer disease. *Nat Med.* 11, 959–965. doi: 10.1038/nm1287

Yan, C., Takahashi, M., Okuda, M., Lee, J. D., and Berk, B. C. (1999). Fluid shear stress stimulates big mitogen-activated protein kinase 1 (BMK1) activity in endothelial cells. Dependence on tyrosine kinases and intracellular calcium. *J. Biol. Chem.* 274, 143–150. doi: 10.1074/jbc.274.1.143

Yoshino, D., Sakamoto, N., and Sato M. (2017). Fluid shear stress combined with shear stress spatial gradients regulates vascular endothelial morphology. *Integr. Biol.* 9, 584–594. doi: 10.1039/C7IB00065K

Yun, S., Dardik, A., Haga, M., Yamashita, A., Yamaguchi, S., Koh, Y., et al. (2002). Transcription factor Sp1 phosphorylation induced by shear stress inhibits membrane type 1-matrix metalloproteinase expression in endothelium. *J. Biol. Chem.* 277, 34808–34814. doi: 10.1074/jbc.M205417200

Zaidel-Bar, R., Kam, Z., and Geiger, B. (2005). Polarized downregulation of the paxillin-p130CAS-Rac1 pathway induced by shear flow. *J. Cell Sci.* 118(Pt 17), 3997–4007. doi: 10.1242/jcs.02523

Zeng, Y., and Tarbell, J. M. (2014). The adaptive remodeling of endothelial glycocalyx in response to fluid shear stress. *PLoS One* 9:e86249. doi: 10.1371/journal.pone.0086249

Zhao, W., Cao, L., Ying, H., Zhang, W., Li, D., Zhu, X., et al. (2019). Endothelial CDS2 deficiency causes VEGFA-mediated vascular regression and tumor inhibition. *Cell Res.* 29, 895–910. doi: 10.1038/s41422-019-0229-5

Zheng, Y., Chen, J., Lopez, J. A. (2015). Flow-driven assembly of VWF fibres and webs in in vitro microvessels. *Nat. Commun.* 6:7858. doi: 10.1038/ncomms8858

Zhou, A., Egginton, S., Hudlicka, O., and Brown, M. D. (1998). Internal division of capillaries in rat skeletal muscle in response to chronic vasodilator treatment with alpha1-antagonist prazosin. *Cell Tissue Res.* 293, 293–303. doi: 10.1007/s004410051121

Zhou, Q., Perovic, T., Fechner, I., Edgar, L. T., snmHoskins, P. R., Gerhardt, H., et al. (2020). Association between erythrocyte dynamics and vessel remodelling in developmental vascular networks. *bioRxiv [Preprint]* doi: 10.1101/2020.05.21.106914

**Conflict of Interest:** The authors declare that the research was conducted in the absence of any commercial or financial relationships that could be construed as a potential conflict of interest.

frontiers in Physiology

REVIEW
published: 11 November 2020
doi: 10.3389/fphys.2020.591901

# Vascular Heterogeneity With a Special Focus on the Hepatic Microenvironment

*Johannes Robert Fleischer, Chiara Angelina Jodszuweit, Michael Ghadimi, Tiago De Oliveira and Lena-Christin Conradi**

*Department of General, Visceral and Pediatric Surgery, University Medical Center Göttingen, Göttingen, Germany*

Utilizing single-cell sequencing, recent studies were able to analyze at a greater resolution the heterogeneity of the vasculature and its complex composition in different tissues. Differing subpopulations have been detected, distinguishable only by their transcriptome. Designed to provide further insight into the heterogeneity of the functional vascular tissue, endothelial cells have been the main target of those studies. This review aims to present a synopsis of the variability of the different vascular beds, their endothelial variety, and the supporting cells that allow the vessels to serve their various purposes. Firstly, we are going to chart vascular tissue heterogeneity on a cellular level, describing endothelial diversity as well as stromal microenvironmental variety and interaction in a physiological setting. Secondly, we will summarize the current knowledge of pathological vessel formation in the context of cancer. Conventional anti-tumor therapeutic targets as well as anti-angiogenetic therapy is frequently limited by poor response of the tumor tissue. Reasons for moderate response and resistance to treatment can be found through different drivers of angiogenesis, different mechanisms of blood supply, but also in poorly understood tissue diversity. Based on this, we are comparing how pathologies alter the normal structure of vascular tissues highlighting the involved mechanisms. Lastly, illustrating the concept above, we will focus on the hepatic microenvironment, an organ of frequent metastatic spreading (e.g., from colorectal, breast, and lung cancers). We will address how the hepatic vasculature usually develops and subsequently we will describe how common liver metastases vary in their vasculature and the way they supply themselves (e.g., angiogenesis versus vessel co-option).

**Keywords: vasculature, heterogeneity, microenvironment, liver metastases, angiogenesis, vessel co-option**

OPEN ACCESS

***Edited by:***
*Sara Petrillo,*
*University of Turin, Italy*

***Reviewed by:***
*Andreas Pircher,*
*Innsbruck Medical University, Austria*
*Carmen Clapp,*
*National Autonomous University of Mexico, Mexico*

***Correspondence:**
*Lena-Christin Conradi*
*lena.conradi@med.uni-goettingen.de*

***Specialty section:***
*This article was submitted to Vascular Physiology, a section of the journal Frontiers in Physiology*

***Received:*** *05 August 2020*
***Accepted:*** *28 September 2020*
***Published:*** *11 November 2020*

***Citation:***
*Fleischer JR, Jodszuweit CA, Ghadimi M, De Oliveira T and Conradi L-C (2020) Vascular Heterogeneity With a Special Focus on the Hepatic Microenvironment. Front. Physiol. 11:591901. doi: 10.3389/fphys.2020.591901*

## PHYSIOLOGICAL VESSEL HETEROGENEITY

Heterogeneity of the vasculature can be determined and discussed on different levels within the vascular tree and with respect to multi-omics analyses. This review first wants to recapitulate microscopic features of the body's vessels as a brief introduction to the topic of vascular heterogeneity by connecting it to familiar knowledge. Secondly, we want to focus on the transcriptome level of heterogeneity, as we understand single-cell RNA sequencing (scRNAseq) as the current state-of-the-art technique in high-throughput analyses.

## Basic Composition of the Vasculature

All blood vessels can be characterized according to their function in transporting blood and nutrients (Pawlina, 2020). The largest arteries, in closest proximity to the heart, experience the highest pressure gradient and are tasked in transforming those pressure peaks into an even flow (Drake et al., 2015). These elastic arteries exhibit polygonal endothelial cells that are aligned in the direction of flow, and are reinforced with a strong cytoskeleton and actin filaments anchoring the cells to the basement membrane to cope the shear stress. To withstand and level out pressure peaks, elastic arteries are equipped with strong concentric muscular lamellae variegated with elastic fibers, assuming high volume compliance to store up to half of the cardiac output and discharge it during low-pressure states (see **Figure 1A**; Boron and Boulpaep, 2003; Pape et al., 2014; Welsch et al., 2014).

These arteries turn into their muscular counterparts, which are less elastic with the primary focus on withstanding the blood pressure. Consequently, the intima of those vessels closely resembles the previously described phenotype, however, the media is lacking elastic fibers. The connective tissue, holding the arteries in place is strongly developed (see **Figure 1B**; Welsch et al., 2014; Drake et al., 2015).

In the microcirculation small arterioles regulate the perfusion of the vascular bed. Ordinarily, constriction of the thin smooth muscle lamellae allows only 25% of the capillary bed to be perfused (Boron and Boulpaep, 2003; Drake et al., 2015). Creating the main body of vascular resistance leads to their name of resistance arteries. This interaction is tightly coordinated, hence a dense neural plexus can be found in their adventitia (see **Figure 1C**; Welsch et al., 2014; Pawlina, 2020). These vessel subtypes display a prominent membrana elastica interna that can be utilized to distinguish arteries from veins by using histochemistry stainings, such as Verhoeff's elastica stain or more specifically resorcin-fuchsin (Puchtler and Waldrop, 1979).

Capillaries are ubiquitously found in the body, given that oxygen can only traverse 2 mm through tissue (Griffith et al., 2005). Needing to fulfill every tissue specific demand, more structural heterogeneity is observed in all parts of the human body. Tissues like the brain, heart, and skeletal muscle have little physiological need to exchange big particles. However, some sensitive organs have a high need for protection against harmful substances (e.g., the blood–brain-barrier, blood–testis-barrier). Thus, a continuous endothelium with varying levels of occluding junctions is present in those areas. Endocrine organs, bowel mucosa, or adipose tissue have a higher need for facilitated diffusion, which is met by capillaries with fenestrated endothelium and diaphragms closing the fenestrations. Liver lobules, the bone marrow, or the glomeruli of the kidneys have the highest need for vessel permeability, thus displaying

**Abbreviations:** miR-126, microRNA 126; A2m, alpha-2-macroglobulin; Acta2, actin alpha 2, smooth muscle; Alk1, ALK receptor tyrosine kinase 1; Anpep, alanyl aminopeptidase, membrane; Aplnr, apelin receptor; aSMA, alpha smooth muscle actin; Atp13a5, ATPase 13A5; Baiap3, BAI1 associated protein 3; BMEC, bone marrow endothelial cells; Bmx, BMX non-receptor tyrosine kinase; BRAF, B-Raf proto-oncogene, serine/threonine kinase; CCND1, cyclin D1; CD13, cluster of differentiation 13; CD146, cluster of differentiation 146; CD31, cluster of differentiation 31; CD34, cluster of differentiation 34; CD34, cluster of differentiation 34; CD36, cluster of differentiation 36; CD4, cluster of differentiation 4; CD45, cluster of differentiation 45; Cdh5, cadherin 5; CDKN1A, cyclin dependent kinase inhibitor 1A; Cldn5, claudin 5; Clec4g, C-type lectin domain family 4 member G; Cnn1, calponin 1; CNV, choroidal neovascularizations; CSF-1, colony stimulating factor 1; CSF2, colony stimulating factor 2; Cspg4, chondroitin sulfate proteoglycan 4; Cxcl1, C-X-C motif chemokine ligand 1; Cytl1, cytokine like 1; DARC, Duffy antigen chemokine receptor; Depp, DEPP1 autophagy regulator; Des, desmin; Dll4, delta like canonical notch ligand 4; Dnase113, deoxyribonuclease 113; E2F1, E2F transcription factor 1; ECs, endothelial cells; Efnb2, ephrin B2; EGF, epidermal growth factor; Ehd3, EH domain containing 3; Emcn, endomucin; EPAS1, endothelial PAS domain protein 1; EVP, endovascular progenitor cell; EZH2, enhancer of zeste 2 polycomb repressive complex 2 subunit; Fabp4, fatty acid binding protein 4; Fam167b, family with sequence similarity 167 member B; Fbln5, fibulin 5; Fcgr2b, Fc fragment of IgG receptor IIb; FGF-2, fibroblast growth factor 2; Flt4, Fms related receptor tyrosine kinase 4; FOXM1, forkhead box M1; Gata5, GATA binding protein 5; GPR56, G protein-coupled receptor 56; Hand2, heart and neural crest derivatives expressed 2; HB-EGF, heparin binding epidermal growth factor; hBFGF, human basic fibroblast growth factor; hEGF, human epidermal growth factor; Hey1, hes related family BHLH transcription factor with YRPW motif 1; Hey2, hes related family BHLH transcription factor with YRPW motif 2; HGF, hepatocyte growth factor; HIF1, hypoxia inducible factor 1; HIF2, hypoxia inducible factor 2; Higd1b, HIG1 hypoxia inducible domain family member 1B; Hoxa7, homeobox A7; Ifitm1, interferon induced transmembrane protein 1; Il33, interleukin 33; IL-6, interleukin 6; Il6st, interleukin 6 signal transducer; Itgbl1, integrin subunit beta like 1; Itm2a, integral membrane protein 2A; Jag1, jagged canonical notch ligand 1; Junb, JunB proto-oncogene, AP-1 transcription factor subunit; Kdr, kinase insert domain receptor; KRAS, KRAS proto-oncogene, GTPase; Krtdap, keratinocyte differentiation associated protein; Lcn2, lipocalin 2; Lgr5, leucine rich repeat containing G protein-coupled receptor 5; Ly6a, stem cells antigen-1; Mcam, melanoma cell adhesion molecule; MET, MET proto-oncogene, receptor tyrosine kinaseID1 KISS1; Mfsd2a, major facilitator superfamily domain containing 2A; miR-335, microRNA 335; Myc, Myc proto oncogene; Myh11, myosin heavy chain 11; Myocd, myocardin; NG2, neuron-glial antigen 2; Npr3, natriuretic peptide receptor 3; Nr2f2, nuclear receptor subfamily 2 group F member 2; Nr4a2, nuclear receptor subfamily 4 group A member 2; NRAS, NRAS proto-oncogene, GTPase; Nrp1, neuropilin 1; PCs, pericytes; PCV, postcapillary venules; Pde1c, phosphodiesterase 1C; PDGF, platelet derived growth factor; Pdgfra, platelet derived growth factor receptor alpha; Pdgfrb, platelet derived growth factor receptor beta; Pecam1, platelet and endothelial cell adhesion molecule 1; PFKFB3, 6-phosphofructo-2-kinase/fructose-2,6-biphosphatase 3; Pgf, placental growth factor; Pglyrp1, peptidoglycan recognition protein 1; PIK3CA, phosphatidylinositol-4,5-bisphosphate 3-kinase catalytic subunit alpha; PVE, portal vein embolization; RABL6, RAB, member RAS oncogene family like 6; Rad54b, RAD54 homolog B; RB1, retinoblastoma 1; RRM2, ribonucleotide reductase regulatory subunit M2; S1pr3, sphingosine-1-phosphate receptor 3; SCA-1, stem cells antigen-1; scRNAseq, single cell RNA sequencing; Sema3g, semaphorin 3G; Slc16a1, solute carrier family 16 member 1; Slc2a1, solute carrier family 2 member 1; Slco1c1, solute carrier organic anion transporter family member 1C1; Smad1, SMAD family member 1; SMC, smooth muscle cell; SNAI1, snail family transcriptional repressor 1; SNAI2, snail family transcriptional repressor 2; Sox4, SRY-box transcription factor 4; Sox9, SRY-box transcription factor 9; SPIN, sorting points in neighborhood; Ssh2, slingshot protein phosphatase 2; Stab2, stabilin 2; Tagln, transgelin; Tfrc, transferrin receptor; TGF-α, transforming growth factor α; TGF-β, transforming growth factor β; TGF-β1, transforming growth factor β1; Tgif1, TGFB induced factor homeobox 1; Tie1, tyrosine kinase with immunoglobulin like and EGF like domains 1; Tmem100, transmembrane protein 100; Tmem132e, transmembrane protein 132E; TP53, tumor protein 53; Trgj1, T cell receptor gamma joining 1; Trim29, tripartite motif containing 29; Trp53, tumor protein P53; TWIST1, twist family BHLH transcription factor 1; Ush1g, USH1 protein network component sans; Vcam-1, vascular cell adhesion molecule 1; VE-cadherin, vascular endothelial cadherin; VEGF, vascular endothelial growth factor; Vegfc, vascular endothelial growth factor C; VEGFR1, vascular endothelial growth factor receptor 1; VEGFR2, vascular endothelial growth factor receptor 2; VEGFR3, vascular endothelial growth factor receptor 3; Vtn, vitronectin; vWF, von Willebrand factor; Wnt9b, Wnt family member 9B; Zic3, Zic family member 3. Source: https://www.genecards.org retrieved on August 5, 2020.

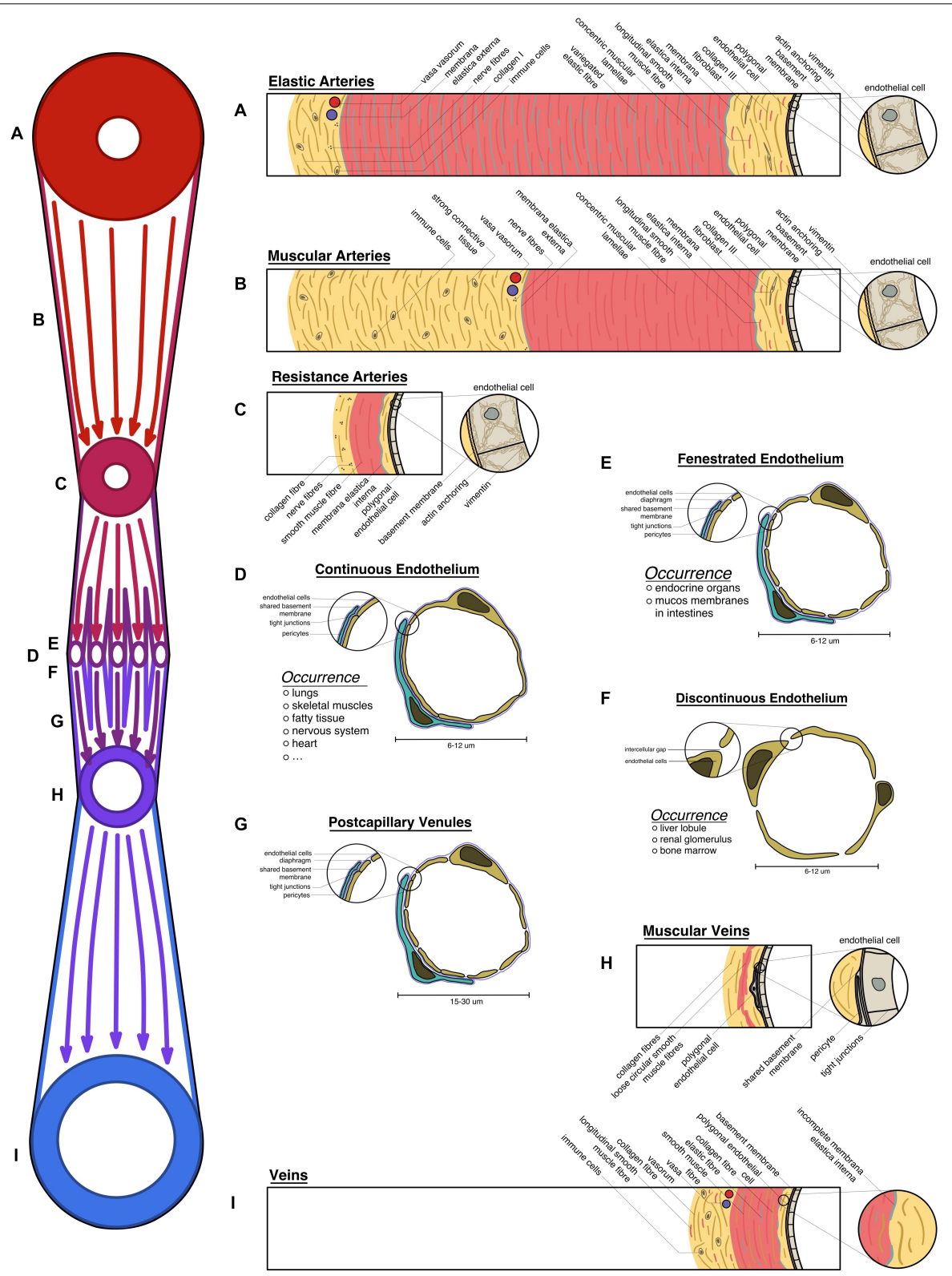


**FIGURE 1 |** Overview of the vascular system: schematic transversal depiction of the structural elements of all vessels under homeostatic conditions: **(A)** elastic arteries, expressing strong muscular lamellae with variegated elastic fibers; **(B)** muscular arteries with strong connective tissue; **(C)** resistance arteries; **(D)** continuous endothelium; **(E)** fenestrated endothelium; **(F)** discontinuous endothelium; **(G)** postcapillary venules; **(H)** muscular veins; **(I)** large veins exhibiting longitudinal muscle fibers in their connective tissue. **(A–I)** All vessel types are laid on the schematic vascular tree (on the left), according to their physiological position.

a discontinuous endothelium with intercellular gaps (see **Figures 1D–F**; Welsch et al., 2014; Pawlina, 2020).

Recollecting and supplying the blood back to the heart, venules are bigger capillaries at first, with fenestrations, allowing immune cells to trespass into the surrounding tissue (diapedesis) (see **Figure 1G**). In secondary lymphoid tissue, high endothelial venules can be found that facilitate recirculation of naive lymphocytes through lymphoid organs (see **Figure 1G**; Veerman et al., 2019).

Closer to the heart, those venules start to exhibit loose circular smooth muscle fibers and strong connective tissue, embedding the vessel into its environment (see **Figure 1H**; Welsch et al., 2014).

Big veins almost reassemble the structure of the arteries that they are running with. Contrarily, they have a bigger lumen compared to arteries and store up to 80% of the total blood volume. They have in general thinner structures, as they do not have to withstand the high pressure levels present in the arterial system. However, as veins can experience negative pressure, longitudinal smooth muscle fibers can be found in the adventitia, allowing them to keep the lumen open during low-pressure states (see **Figure 1I**). Depending on the location those structures vary as venules and veins embedded into tight connective tissue, like the dura mater, do not show any musculature as they are not in need to regulate their wall pressure. Veins located in the lower extremities often exhibit venous valves to inhibit backflow (Welsch et al., 2014; Pawlina, 2020).

## Latest Insights Into Vessel Heterogeneity

### Endothelial Cell Heterogeneity

Endothelial cells (ECs) are the innermost lining of all blood vessels. Approximations put the length of all vessels combined above 100.000 km. Dysfunctional ECs are a predictor for cardiovascular disease (Widlansky et al., 2003) but are also a relevant contributor component to other diseases, as observed in newly formed aberrant cancer vessels. Therefore, a profound understanding of their pathophysiology is necessary to provide patients with better therapies. It is well established that ECs are heterogeneous and vary between different tissue types, within the vascular tree of an organ and even between neighboring (Aird, 2012), yet an exhaustive and in-depth understanding is still not established. With the emerge of single-cell sequencing techniques in the last years, the resolution in which we can detect heterogeneity has been increased noticeably (Sabbagh et al., 2018; Vanlandewijck et al., 2018; Lukowski et al., 2019; Goveia et al., 2020; Jambusaria et al., 2020; Kalucka et al., 2020; Rohlenova et al., 2020). We are going to review and consider recent findings on EC diversity, and compare them to the available knowledge.

#### *General EC makers*

Although ECs are heterogeneous, they can be identified in a mixture of cell types by sorting for conserved features that all ECs express. The platelet-endothelial cell adhesion molecule 1 (*Pecam1*) also known as cluster of differentiation 31 (*CD31*) can be used to distinguish ECs. As *Pecam1/CD31* co-stains immune cells, additional sorting for *CD34*, von Willebrand factor (*vWF*), or vascular E-Cadherin (VE-cadherin) has to be done to securely identify ECs (Ghilardi et al., 2008; Cleuren et al., 2019). Another study has used an expression pattern of *Pecam1, Cdh5,* and *Tie1* to identify ECs (Feng et al., 2019; see **Table 1**).

#### *Inter-tissue heterogeneity*

As cells that line the inner surface of the body's blood vessels, ECs are the key regulatory cells in the crosstalk between tissue and the overall systemic circulation. They face systemic challenges such as regulation of the blood pressure, mediation of the immune response, or initiation of hemostasis, but also tasks such as facilitated diffusion or cellular barrier functions. Consecutively, it seems only natural that ECs, which have to meet such heterogeneous tasks, differ on all levels of multi-omics. Several recent studies have contributed to a further understanding of how heterogeneous ECs from different organs are (Sabbagh et al., 2018; Cleuren et al., 2019; Feng et al., 2019; Goveia et al., 2020; Kalucka et al., 2020). The following paragraph reports on these findings. However, the origin of ECs (wild type mice, transgenic mice, *ex vivo*), the methods of how the single-cell level was achieved (enzymatic, mechanical, or both) and the general study designs differ. As proven by Cleuren et al. (2019), those factors significantly impact the transcriptome, hence differences in the experimental methodology limit the comparability and implementation between these studies.

ECs in the brain, eye and testis are part of the blood–brain barrier, blood-retinal barrier or blood–testis barrier and express the highest degree of occlusion in continuous endothelium that can be found in the vascular system (Daneman and Prat, 2015; Mruk and Cheng, 2015; Díaz-Coránguez et al., 2017). Using scRNAseq on murine tissue samples, Kalucka et al. (2020) were able to verify previous reports (Su et al., 2011; Sweeney et al., 2019) that those ECs express differentially overexpressed gene sets involved in transmembrane transport. When performing differential analysis on 11 different murine organs, they identified *Pglyrp1* and *Lcn2* (related to the innate immune response) as novel marker genes that where solely expressed in brain and testis ECs, respectively (Kalucka et al., 2020). Feng et al. (2019) found *Slc2a1* and *Itm2a* to be uniquely expressed by brain ECs (Feng et al., 2019), while Cleuren et al. (2019) additionally described the genes *Rad54b, Zic3,* and *Slco1c1* as distinctive brain EC markers (Cleuren et al., 2019). Additionally, another single-cell study comparing ECs from four different murine tissues found that brain ECs upregulates the expression of genes encoding the membrane transporters *Mfsd2a, Slc2a1*, and *Slco1c1* (Sabbagh et al., 2018).

Transcriptomes of ECs from skeletal muscle tissue and the heart showed high expression of gene sets that were involved in membrane transport and redox homeostasis fitting to the abundance of oxygen and their resulting highly oxidative environment (Kalucka et al., 2020). In skeletal muscle, *Ssh2,* and *Nrp1* were found highly expressed (Kalucka et al., 2020).

In the heart, ECs not only line the coronary vessels, but also form the endocardium and the adjacent part of the ascending aorta. Here, Feng et al. (2019) show a high expression of the fatty acid transporting genes *Fabp4* and *Cd36* in the coronaries, *Npr3* (atrial natriuretic peptide receptor), and *Cytl1* in the endocardial ECs, and *Ehd3* and *Fam167b* in the aortic ECs (Feng et al., 2019).

**TABLE 1 |** General EC marker genes.

| Marker | Remarks | Associated function | Species | Study |
|---|---|---|---|---|
| **General EC marker genes** | | | | |
| *Pecam1* | Co-stains immune cells | Adhesion molecule | mouse | Ghilardi et al., 2008; Cleuren et al., 2019; Feng et al., 2019 |
| *CD34* | | Adhesion molecule | mouse | Ghilardi et al., 2008; Cleuren et al., 2019 |
| *vWF* | Mostly expressed in cells from large vessels | Glycoprotein involved in hemostasis | mouse | Ghilardi et al., 2008; Cleuren et al., 2019 |
| *VE-cadherin* | | Adherends junctions | mouse | Ghilardi et al., 2008; Cleuren et al., 2019; Feng et al., 2019 |
| *Tie1* | | Angiopoietin receptor | mouse | Feng et al., 2019 |

Also, *A2m* and *Itgbl1* have been described as endocardial EC marker genes (Cleuren et al., 2019). In synopsis with other sequencing data, varying levels of *Ehd3* expression in the aortic EC clusters are observed (Feng et al., 2019; Lukowski et al., 2019). Still, the origin of this variance remains to be determined, but as previously mentioned, differences in the techniques utilized in the workflow/analysis (e.g., underlying confounders) should be taken into consideration.

When observing the gene signature of lung ECs, MHC II genes were highly differentially expressed, suggesting their role in immune surveillance. This finding aligns with results from another recent single-cell study (Goveia et al., 2020). *Tmem100*, a transmembrane protein responsible for developmental endothelial differentiation and vascular morphogenesis and regulation of nociception, was identified as a marker gene to be exclusively expressed in lung tissue (Kalucka et al., 2020). Additionally, Cleuren et al. (2019) identified the immune system-related genes *Trgj1* and *Trim29* to be highly expressed in lung ECs. An interesting finding, reported by Feng et al. (2019), is the apparent heterogeneity between lung ECs, which can be traced back to the sex of the mouse that the ECs were harvested from. This gender difference was found in several organs, while others, such as brain ECs did not show this behavior.

Interestingly, comparing ECs from four different murine tissues, Sabbagh et al. (2018) found that liver ECs express genes that encode for scavenging receptors like *Fcgr2b, Stab2*, and *Clec4g* in line with the specializations of the tissue in question. *Dnase113* was found to be another liver EC marker, whereas *Clec4g* was confirmed by another independent group (Feng et al., 2019). Nevertheless, *Tmem132e, Ush1g,* and *Wnt9b* were described by Cleuren et al. (2019) as specific hepatic markers.

Karaiskos et al. (2018) focused on characterizing the heterogeneity within the murine renal glomerulus. They have established the existence of several subclusters within the glomerular ECs. The authors further detected an upregulation of *Ehd3*, which was suggested as a gene-specific marker to glomerular ECs by previous studies (George et al., 2011; Karaiskos et al., 2018). Summarizing, the relevant data presented by those studies (Feng et al., 2019; Lukowski et al., 2019) has to be taken into account in the execution and analysis of future scientific approaches. Nevertheless, *Ehd3* can be used as a glomerular EC marker gene within kidney cells. Other subpopulations showed the expression of *Jag1*, connected to EC pericyte (PC) crosstalk, as well as *Fbln5, Cxcl1,* and *Cldn5*, related to the regulation of angiogenesis, endothelial activation, and response to complement activation, respectively (Karaiskos et al., 2018). Other groups have also established *Gata5, Krtdap,* and *Lgr5* as genes upregulated in renal ECs (Cleuren et al., 2019).

Kalucka et al. (2020) conducted hierarchical clustering, a technique that establishes a pyramidal scheme that allows to examine relations between the different cell clusters. Including all identified subclusters, the authors found the tissue of origin accounting for most of the heterogeneity between the subtypes rather than the affiliation of different parts of the vascular tree. These findings indicate that capillary ECs are very adaptive to their environment expressing tissue-specific markers rather than generally conserved markers. This presumption is supported by another independent study (Cleuren et al., 2019).

While reporting on the heterogeneity of ECs within different tissues and vascular beds it is especially important to emphasize the finding that arterial and venous ECs of different tissues express congruent markers between 80 and 100% of all examined tissues (Kalucka et al., 2020). This finding implies a conservational phenomenon in these areas of the vascular tree. As capillaries express more heterogeneous markers, it seems that those vessels are more adaptive to their tissue environment (Kalucka et al., 2020).

For a comprehensive listing of all marker genes named see **Table 2** and **Figure 2**.

### *Intra-tissue heterogeneity/heterogeneity within the vascular tree*

The fact that ECs of different parts of the vascular hierarchy are heterogeneous is also well established (Yamamoto et al., 1998; Gustavsson et al., 2010). For example, *Vcam-1* and *vWF* expression correlates to vessel size, being almost absent in small capillaries and most abundant in the big vessels (Yamamoto et al., 1998; Gustavsson et al., 2010). However, the exact relation of the different ECs was at the time of the discovery unclear. Using the sorting points in neighborhood method (SPIN; Tsafrir et al., 2005), a form of pseudo-time trajectory, Vanlandewijck et al. (2018) established a one-dimensional trajectory using ECs of murine brain. When analyzing the trajectory for previously described marker genes, they found the arterial markers *Bmx, Efnb2, Vegfc,* and *Sema3g* (Ekman et al., 1997; Wang et al., 1998; Hogan et al., 2009; Kutschera et al., 2011) to be expressed at one end, presumed to be the arterial end. The venous marker *Nr2f2* (Hirashima and Suda, 2006) peaked at the opposing

**TABLE 2 |** Differentially expressed genes in different tissues.

| Organ | Marker | Remarks | Associated function | Species | Study |
|---|---|---|---|---|---|
| **Inter-tissue heterogeneity** | | | | | |
| Testis | *Lcn2* | Marker gene | Innate immune response | mouse | Kalucka et al., 2020 |
| Brain | *Pglyrp1* | Marker gene | Innate immune response | mouse | Kalucka et al., 2020 |
| Brain | *Mfsd2a* | | Transporter | mouse | Sabbagh et al., 2018 |
| Brain | *Slc2a1* | | Transporter | mouse | Sabbagh et al., 2018; Feng et al., 2019 |
| Brain | *Slco1c1* | | Transporter | mouse | Sabbagh et al., 2018; Cleuren et al., 2019 |
| Brain | *Itm2a* | | Integral membrane protein/Immune activation | mouse | Feng et al., 2019 |
| Brain | *Rad54b* | | DEAD-like helicase superfamily | mouse | Cleuren et al., 2019 |
| Brain | *Zic3* | | Cerebellum ZIC family | mouse | Cleuren et al., 2019 |
| Skeletal muscle | *Ssh2* | | Protein phosphatase slingshot homolog 2 | mouse | Kalucka et al., 2020 |
| Skeletal muscle | *Nrp1* | | Neuropilin 1, role in angiogenesis, cell survival migration, and invasion | mouse | Kalucka et al., 2020 |
| Coronaries | *Fabp4* | | Carrier protein fatty acids | mouse | Feng et al., 2019 |
| Coronaries | *CD36* | | Fatty acid translocase | mouse | Feng et al., 2019 |
| Endocardial ECs | *Npr3* | | Atrial natriuretic peptide receptor | mouse | Feng et al., 2019 |
| Endocardial ECs | *Cytl1* | | Cytokine-like 1 | mouse | Feng et al., 2019 |
| Endocardial ECs | *A2m* | | Antiprotease | mouse | Cleuren et al., 2019 |
| Endocardial ECs | *Itgbl1* | | Integrin subunit beta like 1 | mouse | Cleuren et al., 2019 |
| Aortic ECs | *Fam167b* | | | mouse | Feng et al., 2019 |
| Aortic ECs | *Ehd3* | Debatable! | Endocytic trafficking, moonlighting protein | mouse | Feng et al., 2019; Lukowski et al., 2019 |
| Lung | *Tmem100* | Marker gene | Transmembrane protein 100 | mouse | Kalucka et al., 2020 |
| Lung | *Trgj1* | | T-cell receptor joining 1 | mouse | Cleuren et al., 2019 |
| Lung | *Trim29* | | TRIM protein family | mouse | Cleuren et al., 2019 |
| Liver | *Fcgr2b* | | Scavenging receptor | mouse | Sabbagh et al., 2018 |
| Liver | *Stab2* | | Scavenging receptor | mouse | Sabbagh et al., 2018 |
| Liver | *Clec4g* | | Scavenging receptor | mouse | Sabbagh et al., 2018; Feng et al., 2019 |
| Liver | *Dnase113* | | | mouse | Feng et al., 2019 |
| Liver | *Tmem132e* | | Transmembrane protein | mouse | Cleuren et al., 2019 |
| Liver | *Ush1g* | | | mouse | Cleuren et al., 2019 |
| Liver | *Wnt9b* | | Wnt Family Member 9B | mouse | Cleuren et al., 2019 |
| Glomerular kidney | *Ehd3* | Marker gene | Endocytic trafficking, moonlighting protein | mouse | George et al., 2011; Karaiskos et al., 2018 |
| Kidney | *Gata5* | | Transcription factor | mouse | Cleuren et al., 2019 |
| Kidney | *Krtdap* | | Keratinocyte differentiation-associated protein | mouse | Cleuren et al., 2019 |
| Kidney | *Lgr5* | | Member Wnt signaling pathway | mouse | Cleuren et al., 2019 |

end of the range, while the capillary marker *Mfsd2a* (Nguyen et al., 2014) was found to be expressed in the middle of the trajectory (Vanlandewijck et al., 2018). Therefore, the expression pattern of *Vcam-1* and *vWf* at the opposing sides of the range, but not the middle (denoted as the capillary region), fitted to the description that they are only expressed in arteries and veins. *Tfrc* and *Slc16a1* were found to be expressed on the middle left part of the trajectory, fitting to the previously described expression in capillaries and veins (Vanlandewijck et al., 2018). The gradual decline in expression of genes along with the projection proved that ECs are exhibiting a continuous phenotype, coined zonation (Vanlandewijck et al., 2018), rather than showing discreet phenotypes.

Other patterns of markedly expressed genes that can be found in arteries are *Ephrin B2, Alk1, Dll4, NRP1, Depp, Hey1* and *Hey2, EPAS1* while veins express a pattern of *Ephrin B2, Eph B4, NRP2,* and *COUP−TFII* (Cheng et al., 2002; Aird, 2007; Ribatti et al., 2020).

For a comprehensive listing of all named genes see **Table 3** and **Figure 3**.

It was also found that transcription factors such as *Hey2, Junb,* or *Nr4a2* which are involved in arterial endothelial cell differentiation, regulation of cell proliferation and response to hypoxia respectively, were significantly expressed in the arterial ECs, while transporter genes dominated in capillaries and veins, suggesting that the prominent trans-endothelial transport is increased in those regions (Vanlandewijck et al., 2018).

Recently, the heterogeneity within bone marrow endothelial cells (BMEC) has been evaluated (Baryawno et al., 2019). BMECs expressed the established markers *Pecam1, Cdh5, Kdr,*

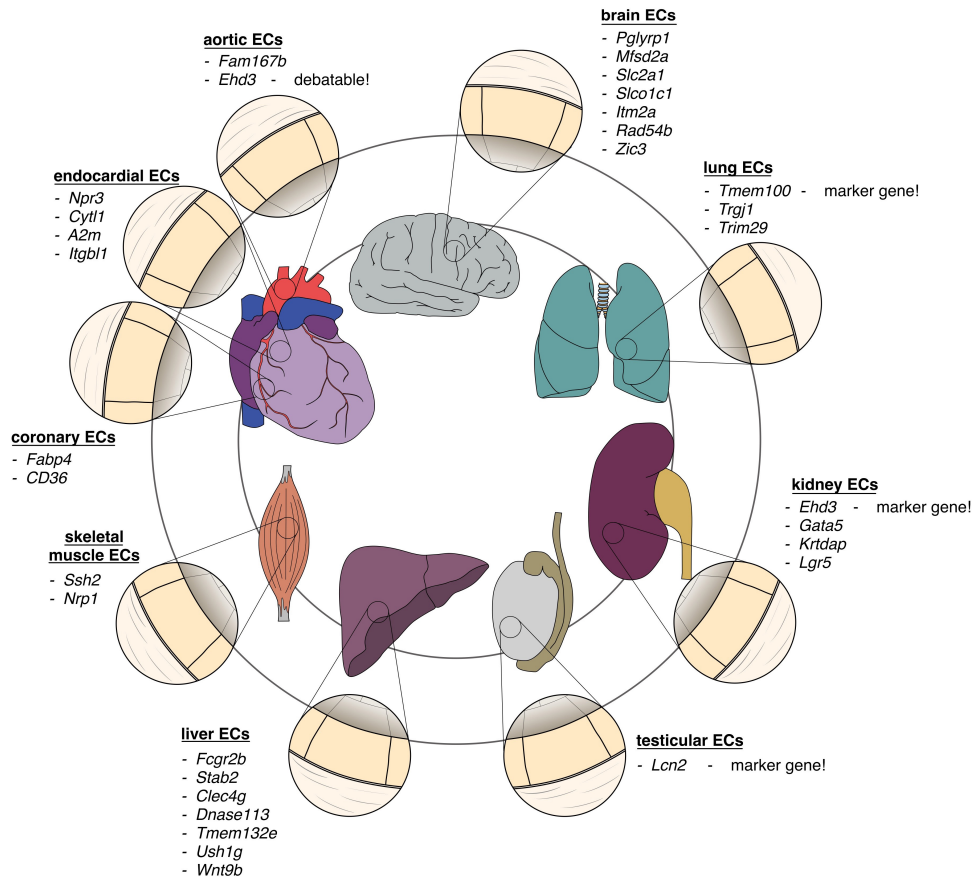


**FIGURE 2 |** Vascular heterogeneity between different organs and tissues: chart of genes differentially upregulated in endothelial cells in various tissues of the body.

and *Emcn* (Rafii et al., 2016) and are related to each other on a continuous trajectory. Sinusoidal BMECs show a pattern of high *Flt4* expression (encoding for VEGFR3) and low *Ly6a* expression (SCA-1). The cluster of arteriolar BMECs could be distinguished from the sinusoidal BMEC by an inverted pattern of low *Flt4* expression and high *Ly6a* expression (Baryawno et al., 2019). Those findings align with previously published reports (Hooper et al., 2009; Itkin et al., 2016). The third cluster that was identified was understood to be a subcluster of the arteriolar BMECs. Those ECs showed an exclusive but heterogeneous expression of *vWF*. Furthermore, CD34 which has been described as an associated marker for arteriolar BMECs, was found in the third identified cluster (Coutu et al., 2017), interestingly lacking the expression of the sinusoidal marker *Il6st* (Baryawno et al., 2019).

### *Intra-tissue heterogeneity/cell-to-cell variation*

Recently, Lukowski et al. (2019) paid special attention to cell-to-cell heterogeneity in EC populations within the murine aorta, a phenomenon already described (Eichmann et al., 2005; Adams and Alitalo, 2007). Previously, Patel et al. (2017) described the existence of endovascular progenitor cells (EVP) within the vascular beds. Those cells are in contrast to definitive differentiated ECs which represent a successive cell type. Later, it was confirmed that all ECs where related to each other on a seamless trajectory rather than expressing a discreet and isolated phenotype (Patel et al., 2017; Donovan et al., 2019). EVPs express a stringent surface marker profile $CD34^{+}$ $CD45^{-}$ $CD31^{lo}$ $VEGFR2^{-}$ and increased expression of *VEGFR2* and *CD31* when transitioning to definitive differentiated ECs (Lukowski et al., 2019). Through differential analysis, definitive differentiated ECs could be characterized by an increase in *Pecam1* and *Cdh5* expression, while EVPs expressed high levels of *Pdgfra, Il33,* and *Sox9* (Lukowski et al., 2019).

## Heterogeneity in Pericytes

In an effort to study heterogeneity within PCs, Vanlandewijck et al. (2018) identified PCs among other cell types within murine brain samples by applying known PC gene patterns to their data set. Sorting for the presence of canonical PC markers such as *Pdgfrb, Cspg4,* and *Des* and excluding cells expressing smooth muscle cell (SMC) markers like *Acta2* and *TagIn*, as well as fibroblast markers

**TABLE 3 |** Differentially expressed marker genes in the vascular tree.

| Vascular tree | Marker | Name/function | Species | Study |
|---|---|---|---|---|
| **vascular tree heterogeneity** | | | | |
| Large vessels | *Vcam-1* | Vascular cell adhesion molecule 1 | Mouse | Yamamoto et al., 1998; Gustavsson et al., 2010 |
| Large vessels | *Vwf* | von Willebrand factor | Mouse | Yamamoto et al., 1998; Gustavsson et al., 2010 |
| Arteries | *Bmx* | Cytoplasmic tyrosine kinase | Mouse, human | Ekman et al., 1997 |
| Arteries | *Efnb2* | Transmembrane protein (receptor) | Mouse | Wang et al., 1998 |
| Arteries | *Vegfc* | Vascular endothelial growth factor C | Zebrafish | Hogan et al., 2009 |
| Arteries | *Sema3g* | Endothelial cell-expressed class 3 semaphorin | Mouse | Kutschera et al., 2011 |
| Arteries | *EphB2* | Ephrin type-B receptor 2 | Mouse | Cheng et al., 2002; Aird, 2007; Ribatti et al., 2020 |
| Arteries | *Alk1* | Cell-surface receptor | Mouse | Cheng et al., 2002; Aird, 2007; Ribatti et al., 2020 |
| Arteries | *Dll4* | Notch ligand | Mouse | Cheng et al., 2002; Aird, 2007; Ribatti et al., 2020 |
| Arteries | *Nrp1* | Neuropilin 1 | Mouse | Cheng et al., 2002; Aird, 2007; Ribatti et al., 2020 |
| Arteries | *Depp* | Decidual protein induced by progesterone | Mouse | Cheng et al., 2002; Aird, 2007; Ribatti et al., 2020 |
| Arteries | *Hey1* | Transcription factor | Mouse | Cheng et al., 2002; Aird, 2007; Ribatti et al., 2020 |
| Arteries | *Hey2* | Transcription factor | Mouse | Cheng et al., 2002; Aird, 2007; Ribatti et al., 2020 |
| Arteries | *Epas1* | Endothelial PAS domain-containing protein 1 | Mouse | Cheng et al., 2002; Aird, 2007; Ribatti et al., 2020 |
| Capillaries, veins | *Tfrc* | Transferrin receptor | Mouse | Vanlandewijck et al., 2018 |
| Capillaries, veins | *Slc16a1* | Solute carrier 16a1 | Mouse | Vanlandewijck et al., 2018 |
| Veins | *Nr2f2* | COUP-TFII | Mouse, human, zebrafish | Hirashima and Suda, 2006 |
| Veins | *EphB2* | Ephrin type-B receptor 2 | Mouse | Cheng et al., 2002; Aird, 2007; Ribatti et al., 2020 |
| Veins | *EphB4* | Ephrin type-B receptor 4 | Mouse | Cheng et al., 2002; Aird, 2007; Ribatti et al., 2020 |
| Veins | *Nrp2* | Neuropilin 2 | Mouse | Cheng et al., 2002; Aird, 2007; Ribatti et al., 2020 |

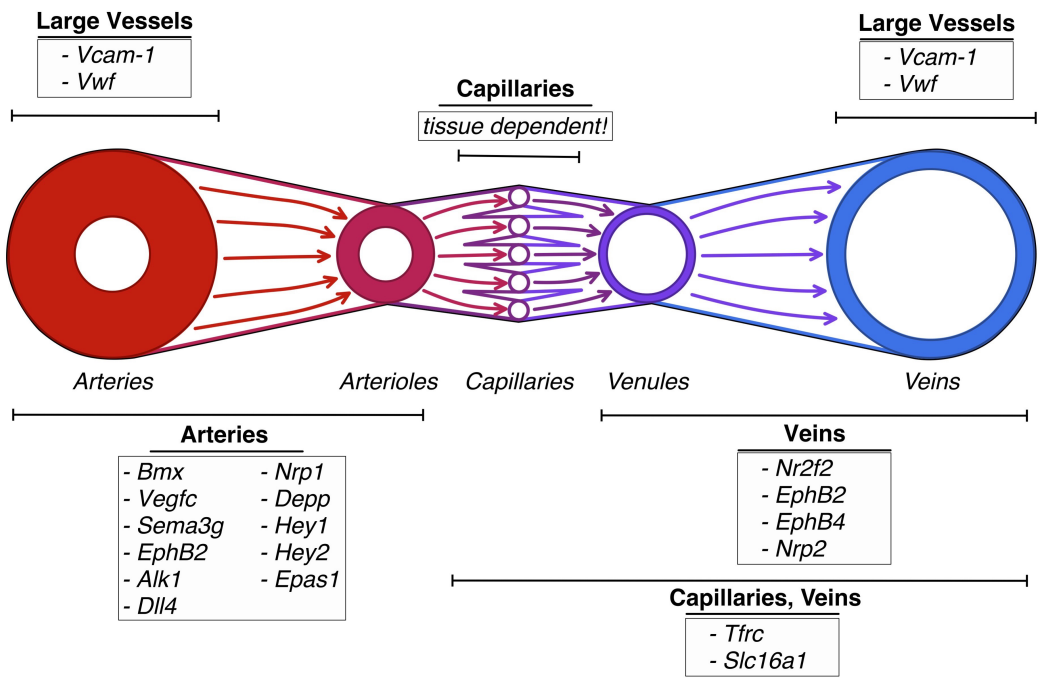


**FIGURE 3 |** Vascular heterogeneity between sections of the vascular tree: schematic depiction of genes differentially upregulated in endothelial cells in the different sections of the vascular tree.

*Pdgfra, Lum,* and *Dcn*, the authors established a likely PC population within their murine brain sample. Moreover, they noted the shortcomings of this procedure which are that *Acta2* and *TagIn* which are not expressed by capillaries, venules, and only faint by large veins, making them indistinguishable from PCs (Vanlandewijck et al., 2018). Performing further analysis on this population, no subclusters were identified, suggesting that within one tissue type pericytes are very uniform and show little heterogeneity (Vanlandewijck et al., 2018).

Vanlandewijck et al. (2018) went further on to examine whether murine PCs from different tissue samples show heterogeneity, by comparing them to murine lung tissue. Both cell populations expressed conserved markers, such as *Vtn, Higd1b, S1pr3, Mcam, Ifitm1, Baiap3,* and *Ehd3* (Vanlandewijck et al., 2018), suggesting close relation to each other. By performing further differential analysis, they singled out *Anpep* and *Atp13a5* as specific marker for brain PCs. Thus proving that pericytes express heterogeneity *between* different tissue types.

These findings however, can only be understood as assumptions in the intense debate on the definition of PC characteristics (Ferland-Mccollough et al., 2017), as their generally accepted characterization only broadly defines them as cells embedded within the vascular basement membrane (Crisan et al., 2008; Armulik et al., 2011; Ferland-Mccollough et al., 2017) – leaving out the possibility to define different sets of cells as pericytes.

According to Crisan et al. (Crisan et al., 2008, 2012), arterial pericytes express neural/glial antigen 2 (*NG2*) as well as α*SMA,* while capillary pericytes lacked these markers (Crisan et al., 2012; Ferland-Mccollough et al., 2017), again indicating the existence of a heterogeneous PC population rather than uniformity within the same organ. Moreover, Smyth et al. (2018) reported that capillary-associated PCs express *Pdgfrb, NG2, CD13,* and *CD146,* diverging from the previously cited reports (Crisan et al., 2008, 2012; Armulik et al., 2011; Ferland-Mccollough et al., 2017; Smyth et al., 2018; Vanlandewijck et al., 2018).

The reasons for such differing results remain unclear. Whilst Smyth et al. (Smyth et al., 2018) used human brain tissue, Crisan et al. (Crisan et al., 2008) used multiple human tissues from adult and fetal specimen (including the brain), and Vanlandewijck et al. (2018) employed a model of murine brain PCs (Crisan et al., 2008; Smyth et al., 2018; Vanlandewijck et al., 2018).

It remains to be further investigated if the differences originate from a real heterogeneous population, or rather the deviation can be accounted to diverging methodology and models. For that, it should be taken into consideration if pericytes in the different tissues have a common denominator, or whether they should be considered independent cell types of their own in each tissue. Consecutively, a redefinition of already accepted markers and features will need to take place for a deeper and concise PC characterization.

### Mural Vessel Zonation

Examining murine brain vessel samples, Vanlandewijck et al. (2018) studied the transcriptional identity of mural vessel cells such as pericytes and SMC. *Cnn1* was used as a marker for arterial SMC with a diameter larger than 13 μm. *Acta2* and *TagIn* were used to identify arterial SMCs present in vessels with diameters larger than 8μm. Interestingly, *Acta2* and *TagIn* were absent in capillaries pericytes and venules, and hardly detectable in large veins. Conducting an interspecies comparison, the authors proved that *TagIn* was also markedly expressed in zebrafish brain arteries, suggesting mural cell heterogeneity to be evolutionarily conserved (Vanlandewijck et al., 2018). Lastly, *Abcc9*, which was used as a marker for murine venous SMC and pericytes, was also found in a zebrafish line labeling mural cells in capillaries and veins, backing the conservation mechanism (Vanlandewijck et al., 2018).

Liu and Gomez (2019) reviewed, that an expression pattern *of Myh11, Acta2, Tagln,* and *Myocd* can be utilized to identify SMC, congruent with the findings of Dobnikar et al. (2018). In their study, scRNAseq of murine aorta found the existence of seven subclusters within the designated SMC population, supporting the understanding that SMCs are highly heterogeneous. They further identified that single subclusters are locally expressed, describing *Pde1c* and *Hand2* as marker genes of SMC for the aortic arch region, whilst *Hoxa7* was expressed in the descending thoracic aorta (Dobnikar et al., 2018). These findings suggest that SMCs are not only heterogeneous between different sections of the vascular tree, but also differ within the same vessel.

In stark contrast to the seamless continuum in ECs, mural cells sorted on a trajectory did not follow anatomical directions. When examined for transcriptional relatedness using the SPIN method, pericytes where most closely related to venous SMCs that then neighbored arteriolar SMCs on the trajectory, and lastly arterial SMCs which were closest related to the arteriolar SMCs (Tsafrir et al., 2005; Vanlandewijck et al., 2018). Two discreet subclusters were detected, one formed by pericytes and venous SMCs, that merged gradually by loss of PC markers and gain of venous SMC markers. The other subcluster, separated by an abrupt transition between venous SMC and arteriolar SMC, was formed by arteriolar SMC that merged into arterial SMC by gradually expressing markers denoting them as arterial SMCs. The transition between the two clusters happens abruptly from one cell to another (Vanlandewijck et al., 2018).

### Key Points

ECs are proven to differ not only between different sections of the vascular tree, but also on a cell-to-cell basis within the same vessel. Capillary ECs are more heterogeneous and express markers according to their surrounding tissue, while large vessels express little heterogeneity and present more conserved markers, independently of their position in the body. Endothelial cells relate to each other on a consistent, seamless trajectory, without expressing distinct, isolated phenotypes. Moreover, key evidences suggest that the gender of the individual also accounts for additional heterogeneity. Contrarily, identification criteria of PCs are not universally accepted, hence comparing results from different authors is hardly possible. Finally, SMCs are highly heterogeneous, express distinct subpopulations, and differ also within the same vessel. However, they appear to not present a confluent trajectory, but rather express distinct isolated subgroups which are confluent within themselves. Limitations to the novel marker gene identification should be kept in mind, as consolidating orthogonal studies confirming the *in silico* findings are yet to be published.

## PATHOLOGICAL VESSEL HETEROGENEITY

It is evident that new vessels are formed physiologically but this phenomenon is also observed in many other pathologies,

including cancer (Carmeliet, 2003). Therefore, to fully comprehend pathological vessel heterogeneity, we will first review the initial steps of vessel formation.

In the embryonic stage of development, the formation of the heart and primitive vascular plexus is called vasculogenesis. Postpartum, development, remodeling, and expansion of blood vessels and their network is called angiogenesis (Patan, 2004). Angiogenesis can be distinguished in two main different processes: intussusceptive microvascular growth (Ribatti and Djonov, 2012) and sprouting angiogenesis. Further forms are known, such as vasculogenesis by endothelial progenitor cells and vascular mimicry. Amongst all, sprouting angiogenesis receives most of the attention and is the prime model, on how growing tissues sustain themselves with nutrients and oxygen. This process can be summarized as the formation of endothelial sprouts that denote expansive growth from pre-existing vessels which then form collateral bridges (Carmeliet, 2003). Once the vasculature has reached its maximum extent and supplies all cells, ECs go into quiescence, where they remain for most of the life as a relatively stable cell population (Risau, 1997; Blanco and Gerhardt, 2013). Physiologically, the turnover of quiescent ECs is measured in years (Bergers and Benjamin, 2003). There are some physiological examples for sprouting angiogenesis, such as wound healing (Tonnesen et al., 2000) and the female reproductive cycle (Rizov et al., 2017). Sprouting angiogenesis has also been named one of the hallmarks of cancer, thus underlining, that this physiological process is highjacked in many pathologies.

## Mechanism – Sprouting Angiogenesis

As new vessel formation has been already extensively reviewed, our objective is to illustrate how pathological vessels come into existence and how they differ from their counterparts. Hence, only a summary of the process of neoangiogenesis will be addressed (for further reading see references Carmeliet, 2003; Blanco and Gerhardt, 2013; Minami et al., 2019).

In a physiological setting, neo-angiogenesis is tightly regulated by a balance of pro- and anti-angiogenic signals (Bergers and Benjamin, 2003). Vital for new vessel sprouting is the local production of vascular-specific pro-angiogenic factors, such as vascular endothelial growth factor (VEGF; Blanco and Gerhardt, 2013), which is induced by hypoxic conditions (triggering HIF1 & 2 expression) but also by cytokines, growth factors, hormones, or oncogenes (Dvorak, 2005). VEGF stimulates physiological and pathological angiogenesis in a strict dose-depending manner, creating a gradient that leads the direction (Carmeliet, 2003). It is relevant to mention that on a cellular level, sprouting angiogenesis requires the local break down of the vessel wall, the disintegration of the basement membrane, the change in cellular phenotype, and the invasion of the surrounding tissue (Blanco and Gerhardt, 2013). So-called tip cells that spearhead the sprouts and process cues of the microenvironment to define the route of the new vessel, are responsible for this process which utilizes the help of newly formed filopodia (Gerhardt et al., 2003; Blanco and Gerhardt, 2013). They also create new connections between different sprouts to generate a functional network (Isogai et al., 2003).

Tip cells are followed by so-called stalk cells which lack the expression of many filopodia, but are highly proliferative. They establish the adhesions to create a stable inner lining of the newly formed vessel (Blanco and Gerhardt, 2013). Endothelial cells express several relevant cell surface receptors, such as Dll4, VEGFR1, and VEGFR2 – to mention a few relevant ones (Claxton and Fruttiger, 2004; Blanco and Gerhardt, 2013). To accomplish their functions, ECs are highly self-organized and those receptors are of crucial importance. Whilst VEGFR2 activation leads to high kinase activity, VEGFR1 does not trigger an intracellular response to that extension and acts as a decoy receptor preventing exacerbated vessel sprout formation by taking up excess VEGF (Park et al., 1994). Blanco and Gerhardt (2013) showed that VEGFR levels translate directly to Dll4 expression, a ligand that induces Notch signaling in adjacent cells, suppressing the development of a tip cell phenotype, and successively leading to the development of the stalk-like behavior (Blanco and Gerhardt, 2013). This phenomenon is best described by the concept of "lateral inhibition," a phenomenon well-known from neuronal cells (see **Figure 4**). This inhibition is vital in organizing appropriate spacing between new sprouts, as several studies have shown that inhibition of DLL4/Notch signaling leads to a dramatic increase in sprouting, vessel branching, and formation of filopodia (Hellström et al., 2007; Lobov et al., 2007; Suchting et al., 2007; Blanco and Gerhardt, 2013). Conversely, it has been shown that Notch gain of function leads to decreased branching (Hellström et al., 2007). Alongside to Notch signaling (Blanco and Gerhardt, 2013), metabolism has shown to have important effects on angiogenesis (De Bock et al., 2013). It was recently discovered that glycolysis has a significant effect on the potency of ECs to acquire tip cell features. As ECs are highly glycolytic and glycolysis is used to cover up to 85% of their energy need, knock-down of the glycolytic activator enzyme PFKFB3 was proven to decrease the length and number of vessel sprouts. *Vice versa*, hypermutation of PFKFB3 leads to unorganized hyper sprouting (De Bock et al., 2013). To summarize, the "battle for the lead" (Blanco and Gerhardt, 2013) is decided by stochastic differences between cells which express VEGFR2 and the local VEGF levels and their metabolic capacity that provides individual cells the advantage over their competitive neighboring cells in acquiring the tip cell phenotype (De Bock et al., 2013). VEGFR2 expressing cells become tip cells, VEGFR1 expressing cells follow a stalk-like behavior (Blanco and Gerhardt, 2013). On a final note, tip and stalk features do not represent a final but rather a dynamic differentiational flux, which can be altered when microenvironmental signals are changing (Bentley et al., 2009; Blanco and Gerhardt, 2013).

## General Differences From Physiological Vessels – Vessel Remodeling

What sets apart the physiological and pathological pattern of vessel formation can easily be summarized into one phrase: "Cancer represents a dysregulation of the body's normal controlled cellular programs" (Farnsworth et al., 2014). Newly formed tumor vessels lack the tight regulation and hierarchically ordered patterning that can be found in the healthy body.

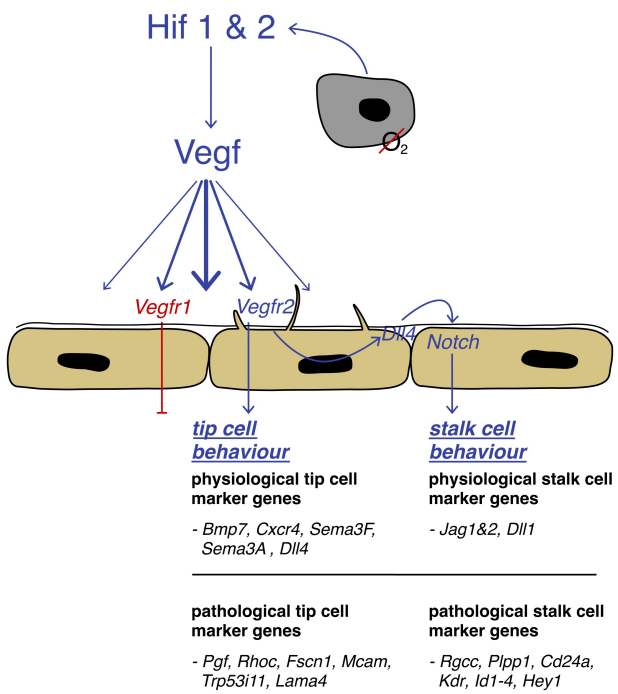


**FIGURE 4 |** Triggers of neoangiogenesis: schematic depiction of the activation pathway of neoangiogenesis, strongly mediated by HIF1/2 and VEGF and the involvement of tip cells that are leading stalk cells to the hypoxic area by filopodia guidance with their differentially expressed genes.

Tumor vessels are heterogeneous, irregularly branched, differ in circumference, are typically enlarged, and often hyperpermeable (Bergers and Benjamin, 2003; Nagy et al., 2006; Carmeliet and Jain, 2011b; Nagy and Dvorak, 2012; Sun et al., 2018). This remodeling process leads to altered EC-PC interaction and abnormal, oscillating blow flow (Bergers and Benjamin, 2003; see **Figure 5**). Expression of different angiogenetic growth factors leads to distinct patterns of angiogenesis, which can be observed in diverse tumors (Farnsworth et al., 2014). As observed in some tumors originating from the lung, colon, or brain, these can show a lower vessel density then the normal healthy tissue (Eberhard et al., 2000; Bergers and Benjamin, 2003). However, vessel density cannot be taken as a predictor for the aggressiveness of the tumor, as grade I pilocytic brain tumors are highly angiogenic, but are slow-growing and do not metastasize (Tomlinson et al., 1994; Bergers and Benjamin, 2003), whilst tumors such as chondrosarcomas are very aggressive but show a very low vessel density (Brem et al., 1972; Bergers and Benjamin, 2003). Certain tumor entities rely on the mobilization of endothelial progenitor cells, known as vasculogenesis (Lyden et al., 2001). Others, such as low-grade astrocytomas utilize a completely different approach, connecting themselves up to pre-existent vessels in a poorly understood process called vessel co-option. Hence, they are generally considered non-angiogenic tumors (Bergers and Benjamin, 2003).

Growth of tumor vasculature is not only driven by VEGF, but a dysregulated ensemble of many factors, such as angiopoietins, platelet-derived growth factor, and transforming growth factor families (Carmeliet and Jain, 2011a). As a result of this uncontrolled angiogenic process, mechanisms that normally ensure strong and occluding endothelial cell junctions are lost. Consecutively, tumor ECs show excessive permeability which can be, amongst other things, explained by the low EC to perivascular cell ratio. Pericytes that usually take part in vessel regulation are not only scarce in tumor-associated vessels, but also shown to be mutated, leading to vascular malformations (Morikawa et al., 2002; Bergers and Song, 2005; Viallard and Larrivée, 2017). Additionally, tumor vessels' basement membrane is commonly found altered (Baluk et al., 2003), contributing to leaky vessels. Tumor vessels lack the typical cobblestone-like lining of ECs which can occasionally be found multi-layered. A vascular tree cannot be distinguished, and their arterial or venous identity is lost. Nevertheless, shunts can be found (Potente et al., 2011). In pathological angiogenesis, large transient mother vessels are the first to form, arising from capillaries (Farnsworth et al., 2014). Those mother vessels are characterized by their large diameter as well as their thin and permeable walls. These vascular malformations later obtain an irregular coat of smooth muscle fibers and reassemble abnormally large veins (Nagy et al., 2010). Although tumor vessels remodeling is often characterized by the physical repositioning of the cellular components, molecular alterations often accompany the process (Farnsworth et al., 2014). Illustrating this concept, we present the genetic differences of marker genes in physiological and pathological tip and stalk cells in **Figure 4** (Hofmann and Luisa Iruela-Arispe, 2007; Strasser et al., 2010; Rohlenova et al., 2020).

## Recent Findings in Pathological Vessel Heterogeneity

### Retinal Vessel Sprouting in a Murine Model

Recently, a study focused on the differences between healthy choroidal ECs and choroidal neovascularization (CNV), in the context of wet age-related macular disease (Rohlenova et al., 2020). Utilizing a pre-clinical murine model of laser-induced CNV they obtained tissue which was consecutively sequenced at single-cell resolution. When comparing healthy murine ECs and ECs from eyes that underwent laser treatment they observed the existence of a distinct subcluster in CNV. Further gene signature analysis proved the existence of proliferating ECs and tip cells, but also three new EC populations. One population showed signatures of transitioning from a postcapillary venule (PCV) to an angiogenic phenotype, whilst the other two populations were termed immature and maturing ECs (Rohlenova et al., 2020). Interestingly, proliferating cells showed increased expression of the transcription factor *Trp53*. Tip cells upregulated the disease restricted angiogenic factor *Pgf* and showed that the transcription factor *Tgif1* was involved in EC designation, whilst immature ECs did not present specific upregulation of marker genes, but more unspecific patterns of activation markers. The authors also showed that the transcription factors *Smad1* and *Sox4* are involved in EC

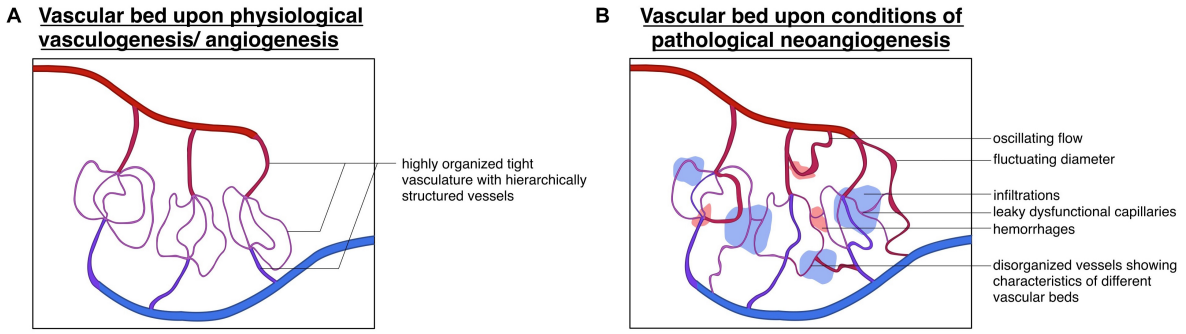


**FIGURE 5 |** Divergence of physiological and pathological vascular beds: schematic depiction of the **(A)** vascular bed upon the physiological processes of vasculogenesis/angiogenesis displaying a highly organized vessel hierarchy and **(B)** vascular bed upon conditions of pathological neoangiogenesis, showing a highly unorganized structure with (hemorrhagic) infiltrations oscillating flow patterns and fluctuating vessel diameters.

development (Rohlenova et al., 2020). Maturing cells, which are also termed phalanx cells, overexpressed a Notch signaling signature. Rohlenova et al. (2020) showed that activated and transitioning PCV cells upregulated *Nr2f2*, which is in line with previous reports (Jeong et al., 2017; Rohlenova et al., 2020). When performing pseudotime analysis, Rohlenova et al. (2020) showed the existence of a seamless trajectory within this additional cluster which starts with activated PCV cells that evolve to CNV transitioning cells, and are followed by immature EC cells, tip cells, and mature phalanx cells. These findings indicate that neovascularization might originate in PCVs as previously predicted by morphological evidences (Folkman, 1982; Rohlenova et al., 2020). The same study further evaluated commonly shared markers, which are also overexpressed in different tumor ECs originating in different tissues (Rohlenova et al., 2020). When performing combined differential analysis between their data set of CNV and a previously generated data set on lung tumor ECs (Goveia et al., 2020), the authors found proliferation, hypoxia, and extracellular matrix formation pathways to be commonly upregulated (Rohlenova et al., 2020) and identified *Aplnr* as a congruent marker between these EC populations. *Aplnr* is an angiogenic and vasculoprotective gene that regulates EC metabolism (Rohlenova et al., 2020). Importantly, when pseudo-time analysis was performed on lung tumor ECs that were previously collected by an affiliated author (Goveia et al., 2020), the same trajectory was found as in Rohlenovas' (Rohlenova et al., 2020) CNV-EC samples. Lung tumor ECs that expressed the gene pattern of veins were at the start of the trajectory, which then changed their gene expression profile, differentiating to PCV immature ECs. These cells then further developed into tip cells, losing their previous marker genes. Along the pseudo time trajectory, they then express markers of neo-phalanx cells, and lastly markers of activated arteries. These findings indicate that the neoangiogenic process follows a conserved pattern of stages in at least two different tissue types (Goveia et al., 2020; Rohlenova et al., 2020).

## Pathological Vessels in Human Lung Carcinoma

Recent studies focused on the comparison of EC heterogeneity of non-small lung cancer to the healthy peri-tumoral vasculature. Goveia et al. (2020) sequenced the transcriptome of eight different human lung cancer EC specimens on a single-cell level and compared the transcriptome to their healthy counterparts. As the vasculature is rather quiescent under normal circumstances, the authors only found the transcriptome patterns of classical angiogenic phenotypes in tumor samples involving tip and proliferating ECs (the latter only being sparsely transcribed). Tip cells expressed genes involved in VEGF signaling, EC migration matrix remodeling, and the disease-specific molecule *pgf* [which was also detected by Rohlenova et al. (2020) in CNV] (Goveia et al., 2020). Interestingly, the authors describe the existence of an immature EC phenotype, which reassembled stalk-like cells, showing up-regulation of gene related to vessel maturing, vessel barrier integrity and notch signaling (Goveia et al., 2020). Also, they found another tumor restricted phenotype, which they termed "activated post-capillary veins," as these ECs upregulated immunomodulatory factors and reassembled features of high endothelial venules (Goveia et al., 2020). Besides detecting the transcriptome signature of previously described EC subpopulations, Goveia et al. (2020) identified two novel capillary phenotypes, which were suspected to be induced by tumor-derived cytokines. In accordance with their gene signature, they were termed "scavenging ECs" (scavenging receptors, macrophage associated genes, and antigen processing) and "activated capillaries" (activation markers). As Zhao et al. (2018) described the phenomenon of tip cells showing different markers in different tumor models, Goveia et al. (2020) made use of a mouse model to further cross-validate their findings. In this analysis, the authors found that the sparsely detected proliferating ECs were more abundant, and that these ECs could be traced back to faster-growing murine carcinomas and a possibly different type of tumor vascularization (Goveia et al., 2020). Moreover, the presence of neophalanx cells, an even more mature angiogenic cell population that expressed capillary and arteriole markers (Goveia et al., 2020), was observed. Surprisingly, the authors found the presence of a previously unknown population, which upregulated tip EC, and VEGF-associated basement and collagen remodeling markers, later named "breach" and "pre-breach" cells (Seano et al., 2014).

## LIVER VASCULATURE

This review section aims to take a closer look at the development of the hepatic vasculature in both its embryonic and adult stages. Furthermore, this section also addresses how primary tumors may metastasize into the liver and how metastatic cells can present different behaviors within the hepatic microenvironment. A better understanding of these points is crucial to the development of new therapeutic options in the treatment of liver metastases.

### Normal Hepatic Vasculature Development and Sinusoids' Microenvironment

The liver is considered the largest mass of glandular tissue in the human body and its development starts at the beginning of the fourth embryonal week (Pawlina, 2020). At the 10th-week hepatic vasculogenesis starts. Interestingly, the hepatic vasculature arises from different embryological layers. Intra-hepatic arteries are seen first in the 10th-week in the central portal tracts and in the 15th-week also in the peripheral part of the liver. They are formed by neoangiogenesis, this process beginning in the perihilar region and advancing toward the peripheral region (Gouysse et al., 2002; Pawlina, 2020). The sinusoids differentiate from capillary vessels of the septum transversum, whilst portal veins differentiate from vitelline veins (Gouysse et al., 2002). The intraportal vessels differentiate from mesenchymal precursor cells (Gouysse et al., 2002). Their corresponding endothelial cell subpopulations exhibit a high degree of cellular differentiation, especially those forming the sinusoids (Gouysse et al., 2002).

Vascular development and differentiation during organogenesis are driven by different aspects like cytokine activity (e.g., by VEGF, Interleukins), and the cellular microenvironment composition, including components of the extracellular matrix-like integrins (Risau, 1997). As already mentioned, the angiogenic profile of the endothelial cells will differ depending on their belonging tissue (Rafii et al., 2016). From the 5th- to 10th-week of embryonal development the existing vessels are derived from pre-existing vessels with a low differentiation status (Gouysse et al., 2002). A low differentiation status means that the endothelial cells are not highly specialized as are endothelial cells from hepatic sinusoids, which exhibit certain structural and functional characteristics like cytoplasmatic fenestration and a gain of differentiation markers like CD4 (Gouysse et al., 2002). ECs of large embryonic vessels like the precursors of portal veins express CD34 and are surrounded by a tenascin-rich matrix, whereas the precursors of sinusoids, such as the capillary vessels of septum transversum, still behave like a continuous endothelium and are generally surrounded by a laminin-1-rich matrix (Gouysse et al., 2002). As previously noticed, pericytes surround vessels and are externally located on their wall. These cells are also considered mesenchymal stem cells and can be detected by their CD146 expression (Shenoy and Bose, 2018). In mice, hepatic pericytes can be differentiated in two main types: (i) a subpopulation with myogenic features and (ii) a second population with fibrogenic behavior. Whilst myogenic pericytes form multinucleated myotubes, fibrogenic pericytes develop into myofibroblasts (Shenoy and Bose, 2018). In humans, vascular hepatic pericytes can be differentiated according to their cluster of differentiation. Whilst pericytes surrounding the portal vein and hepatic artery express consistently CD146, pericytes in other hepatic areas express low levels of CD146 (Strauss et al., 2017).

As discussed in "Pathological vessel heterogeneity," vasculogenesis is seen in the embryonal development. During adulthood, hepatic vascularization is mainly triggered by lower blood flow which leads to an increase in VEGF release and consecutive proliferation of hepatic ECs. In this scenario, new collateral vessels are formed (Dirscherl et al., 2020). These ECs show specific differentiation markers like CD4, which is specific for the discontinuous endothelium of sinusoids. The sinusoidal hepatic endothelial cells also take an important role in pathological conditions such as liver fibrosis and cirrhosis (DeLeve and Maretti-Mira, 2017). Moreover, liver sinusoidal endothelial cells can release anti-inflammatory cytokines, like TGF-β which can inhibit the inflammatory response in these conditions (Ni et al., 2017).

Cancer and its tumor-associated microenvironment not only affects tumor progression but also has a high impact on the development of metastases (Zhang et al., 2018). The hepatic microenvironment is composed by a complex and interconnected group of highly specialized cells. Surrounding the liver sinusoids we can observe Kupffer cells, which are a part of the mononuclear phagocytotic system, and are involved in the final elimination of erythrocytes and in the recycling of its fragments and ferritin (Pawlina, 2018). We also observe hepatic stellate cells in the liver parenchyma. These cells can store vitamin A and, in pathologic conditions, like chronic inflammation, are also able to transdifferentiate into myofibroblasts and further synthesize collagen (Pawlina, 2018).

It is important to understand the interaction between the tumor or metastases and the microenvironment, to develop new therapeutic approaches. Recent findings have shed a light on the underlining mechanisms involving hepatic stellate cells and angiogenesis (Dirscherl et al., 2020). It has been shown that hepatic stellate cells have the ability to sense hypoxia and subsequently release VEGF which further increases angiogenesis. Additionally, an increase of vWF and CD34-positive endothelium was seen in hypoxia-exposed liver tissue (Dirscherl et al., 2020). Thus, these in vitro results show an important interaction between the hepatic microenvironment and angiogenesis which might, in a transformed, malignant scenario, promote tumor growth.

The afferent blood supply of the adult liver is made up mainly by the portal vein and the hepatic artery (Pawlina, 2018). At the *porta hepatis*, both enter the liver and supply the capillary networks. Most of the liver's blood supply comes from the portal vein (approx. 75%), with low oxygen levels, as it has previously collected the blood from the digestive tract, pancreas, and spleen (Pawlina, 2018). Derived from intra-hepatic mesenchymal precusors, interlobular vessels, accompanied by bile ducts, form the portal triad, draining their blood into the sinusoids (Gouysse et al., 2002). The sinusoids are highly specialized capillary vessels

that transport arterial and venous blood (see **Figure 6**). In the definition of a classic liver lobule, the blood flows from the portal vein and hepatic artery right into a sinusoid. The sinusoids send blood into the central vein (Pawlina, 2018). Hepatic sinusoidal endothelial cells show a fenestrated endothelium, however, during inflammatory conditions this fenestra are reduced in size, and the amount of endothelial cells and the basement membrane becomes discontinuous (Ni et al., 2017). The central vein further enters a sub lobular vein which finally flows into the inferior vena cava. Sinusoids show a discontinuous basal membrane and big fenestrae without diaphragms within the ECs (Pawlina, 2018).

### Hepatic Regeneration

The hepatic tissue exhibits the unique capability to regenerate itself after injury (Michalopoulos, 2007; Mao et al., 2014; Tao et al., 2017). After toxic damage or loss of hepatic tissue, the liver enters, a still not completely understood, process that cumulates in its restorage in size, via hyperplastic growth (Mao et al., 2014). Starting at the portal field (hepatic lobules), a front of hepatocytes enters into mitosis advancing toward the central vein (Rabes, 1977). Interestingly, all hepatocytes undergo mitosis, contrary to other regenerative scenarios, such as in the skin or intestine, where a group of proliferating stem cells creates the mass of new cells (Michalopoulos, 2007). This peculiar regenerative behavior leads to the observation that the hepatocyte plates grow to almost twice their normal size (Michalopoulos and DeFrances, 1997), with the liver reaching its former volume after 8–15 days past injury (Michalopoulos, 2007). Basically, the hepatic regenerative process can be summarized in three stages. First, the activation of more than 100 genes which are generally silenced during homeostasis can be observed. Surprisingly, IL-6 is suggested to be responsible for approximately 40% of this regulatory mechanism. Second, a massive proliferation wave (also called progression phase) begins and the majority of all hepatocytes enters into mitosis. Crucial mitogenic factors for this phase are HGF, TGF-α, EGF, and HB-EGF. Finally, homeostasis is achieved and the process is terminated. Although this final process still remains poorly understood, recent findings suggested that TGF-β1 might be directly involved in its conclusion (Mao et al., 2014). Strikingly, all these phases take place whilst the liver maintains its homeostatic functions (Michalopoulos, 2007). This astonishing performance gives rise to different medical practices, such as dividing graft organs between recipients or resecting large metastatic areas. In this specific oncological situation, it is imperative that after the resection of the metastatic site the future remnant liver can cope with its normal homeostatic functions and hemodynamic stress. To achieve that, the use of hepatic portal vein embolization (PVE) has been employed since the 1990's (Makuuchi et al., 1990). Briefly, the procedure redirects the hepatic blood flow to segments of the future liver remnant which ultimately results in hepatic hypertrophy. Recent RNA-seq profiling data of liver regeneration models contributed to the identification of a molecular signature and regenerative signaling pathways involved in hepatic regeneration in rats, upon surgical procedures (Colak et al., 2020a,b). The authors' analyses evidenced transcriptomic changes in genes associated with cell cycle (e.g., *TP53, RB1, CCND1*), transcription factors (e.g., *Myc, E2F1, FOXM1*), DNA replication regulators (e.g., *EZH2, CDKN1A, RRM2*), G1/S- transition regulators (e.g., *RABL6, CCND1*), growth factors and cytokines (e.g., *CSF2, HGF, IL-6*). Nevertheless, the participation and active cross-talking between cells of the hepatic milieu, like hepatic stellate cells, has been already confirmed (Dirscherl et al., 2020). Notably, also ECs can directly contribute to hepatic regeneration, as *in vivo* data generated with Id-1-deficient mice show, which present reduced number of liver sinusoidal EC, demonstrated that upon hepatic damage this population releases angiocrine factors, such as Wnt2 and HGF, triggering hepatocyte proliferation and liver regeneration (Ding et al., 2010).

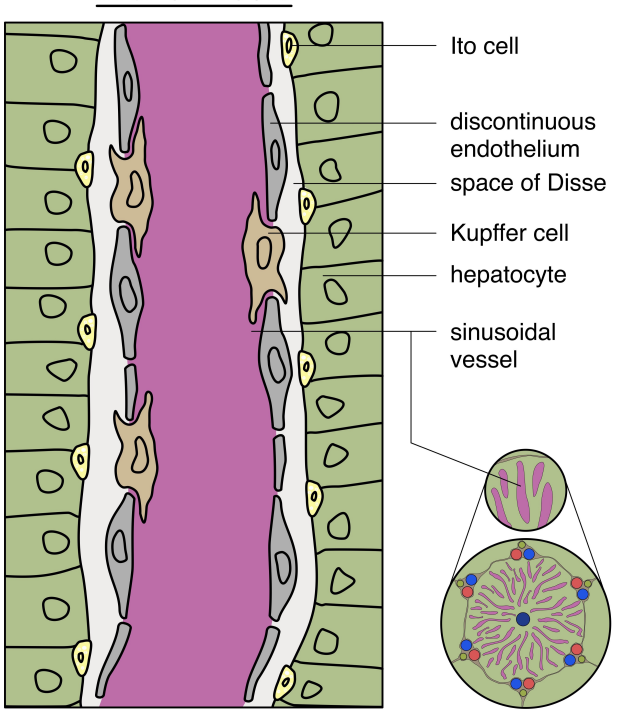


**FIGURE 6 |** Structure of liver sinusoids: schematic depiction of a typical liver sinusoid showing a discontinuous endothelium with intercalated Kupffer cells in the vessel wall, with additional glimpse of the hepatic lobule (on the bottom, right).

## Mechanisms of Hepatic Tumor Dissemination

### Intra-Hepatic Tumor Angiogenesis

As reported in "Mechanism – Sprouting Angiogenesis" and "General Differences From Physiological Vessels – Vessel Remodeling," angiogenesis is a tightly regulated process that is highjacked in an unorganized manner by the tumor environment. Neoangiogenic vessels that develop during carcinogenic processes are different from those that are generated in the physiological process of angiogenesis (Jain, 2014). It has been previously shown that one possible reason

for this difference is that tumor endothelial cells are exposed to extremely high amounts of VEGF from tumor cells and tumor-associated fibroblasts (Jain, 2014). Additionally, angiopoietin, PDGF-B, and TGF-ß are also responsible for the development of less functional vessels in tumors (Viallard and Larrivée, 2017). Tumor blood vessels show a very atypical morphology, the vessels are dilated and disorganized and are leaky (Jain, 2014; Viallard and Larrivée, 2017). This leakiness can cause edema due to plasma extravasation which can significantly slow down blood flow as erythrocytes concentrated and interstitial hypertension increases (Jain, 2014). Nevertheless, tumor endothelial cells are also highly glycolytic, therefore they generally differentiate into tip cells that are responsible for sprouting, rather than into stalk cells, which give vessels stability. This deficit in stability and aberrant architecture leads to an unordered and less effective vascularization and consequently higher hypoxia levels and worse tumor nutrition (Jain, 2014).

## Heterogeneity Within Metastases

Several different types of solid tumors and their metastases overexpress one or more types of growth factors of the VEGF family which help them to achieve their vascular supply. The sprouting of vessels starts at a very early carcinogenic stage, generally when tumors reach 2–3 $mm^3$ in size (Vasudev and Reynolds, 2014). This suggests that an anti-angiogenic treatment can affect most types of solid tumors and their metastases (Vasudev and Reynolds, 2014; Itatani et al., 2018). Conflicting, it has been already proven that some solid tumors and their metastases do not benefit from anti-angiogenic therapy (Hurwitz et al., 2004). According to the IMPOwer 150 (NCT02366143) study, patients from all subgroups with metastasized non-squamous NSCLC, which were previously defined by their PD-L1 expression, benefited from additional treatment with bevacizumab. This is of high clinical relevance, as the first line monotherapy with PD-L1 inhibitors is actually limited for patients with a high PD-L1 expression. Interestingly, those synergistic effects could not be observed in other two recent clinical trials [IMPOwer132 (NCT02657434) (Papadimitrakopoulou et al., 2018) and IMPOwer130 (NCTT02367781) (West et al., 2019)], highlighting the complex hepatic environment, where traditional VEGF inhibition in addition to immune-oncological therapy show clear benefits. These results further support new treatment options with PD-L1 inhibitors for patients with hepatic metastatic disease, even for patients who exhibit low PD-L1 expression (Socinski et al., 2018).

As patients with metastases can often not be treated curatively by surgery, therapeutical options that slow down tumor growth are of extreme importance. In addition to VEGF blockade, the use of tyrosine kinase inhibitors show positive effects on advanced hepatocellular carcinoma and advanced pancreatic neuroendocrine tumors, and is a promising option in pancreatic adenocarcinoma (Vasudev and Reynolds, 2014; Daneshmanesh et al., 2018).

These varying results denote the need to find new biomarkers or other prognostic features to predict the response of patients to an anti-angiogenic therapy. New biomarkers could also improve the further understanding why metastases respond differently to anti-angiogenic therapy. Colorectal cancer is well-known to often spread into the liver due to the intestinal drainage system. Also, lung, brain, pancreatic and cervical tumors present this chemotactic predilection (Yachida et al., 2010; Assoun et al., 2017; Tewari et al., 2017). Besides drainage, there are other mechanisms which can favor hepatic metastatic colonization. It has been already shown that tumor cells favor certain types of endothelial interaction which would explain the reason they metastasize into certain organs more often than into others (Nguyen et al., 2009; Dasgupta et al., 2017). Analysis of the genetic determinants involved in this process revealed the participation of genes related to cell motility, epithelial-to-mesenchymal transition, extracellular matrix degradation, and bone marrow progenitor mobilization, such as *TWIST1, SNAI1, SNAI2, MET, ID1 KISS1, miR-126, miR-335, DARC*, and *GPR56* (Nguyen et al., 2009).

Regarding colorectal cancer liver metastasis, genotyping of tumor specimens is becoming a standard diagnostic practice, with the evaluation of several relevant oncogenes, such as *KRAS, BRAF, PIK3CA*, and *NRAS* (Huang et al., 2018; Sagaert et al., 2018). This information allows the prediction of therapy response and can set patient's prognosis. Interestingly, some degree of inter-metastatic heterogeneity is observed in some patients. In a study evaluating KRAS mutational status, it was observed that 6.8% of the evaluated metastatic sites differ between themselves. The same study also observed heterogeneity in the status of BRAF mutations (Turajlic et al., 2020).

## Different Mechanisms of Blood Irrigation

It is already well described that liver metastases can present different growth patterns (Frentzas et al., 2016; van Dam et al., 2017; Hoppener et al., 2019). The most prevalent type in pre-existing colorectal cancer liver metastases after chemotherapy in combination with bevacizumab is the desmoplastic growth pattern – where the tumor cells are surrounded by a desmoplastic rim, composed mainly by fibroblasts and immune cells (Frentzas et al., 2016; van Dam et al., 2017; Hoppener et al., 2019). The desmoplastic growth pattern utilizes neoangiogenesis to supply tumor cells with nutrients and oxygen (Frentzas et al., 2016). Generally, these metastases produce high levels of VEGF which then induce vessel sprouting. Another hepatic metastatic growth pattern, which also uses the mechanism of neoangiogenesis to obtain its blood supply, is the pushing growth pattern (Hoppener et al., 2019). In this growth pattern, which accounts for approximately 5% of the observed patterns, also in pre-existing colorectal cancer liver metastases after chemotherapy in combination with bevacizumab, the tumor cells push the healthy liver parenchyma aside, without building a desmoplastic rim (Frentzas et al., 2016; van Dam et al., 2017).

Yet, according to Frentzas et al. (2016), the second most prevalent metastatic growth pattern, accounting for approximately 45% of the detected growth patterns, is the replacement type (see **Figure 7**; Frentzas et al., 2016; van Dam et al., 2017; Galjart et al., 2019). In this situation metastases access their blood supply via co-option, meaning that tumor cells receive oxygen and nutrients from pre-existing vessels, like e.g., the hepatic sinusoids (van Dam et al., 2017). Interestingly, the

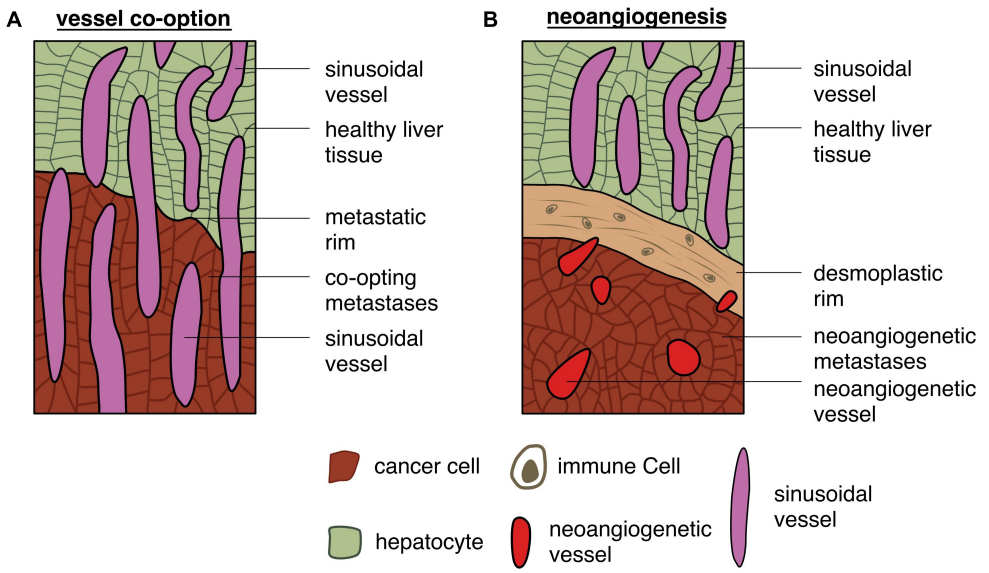


**FIGURE 7 |** Different capabilities of gaining access to the vasculature: schematic depiction of **(A)** tumor cells gaining access to vessels by co-option and **(B)** tumor cells accessing vessels by triggering neoangiogenesis.

replacement growth pattern increases from approximately 55% in untreated patients to approximately 85% in recurrent liver metastases after treatment with chemotherapy in combination with bevacizumab (Frentzas et al., 2016). Nevertheless, tumor hepatic growth patterns can present a degree of heterogeneity with patients exhibiting hepatic metastatic sites with different growth patterns (Frentzas et al., 2016). This can be considered one reason why patients with metastatic colorectal cancer respond in an unpredictable way to anti-angiogenic therapy, as the metastatic growth pattern is usually not determined in patients (van Dam et al., 2017). As expected, patients with desmoplastic growth pattern respond better to an anti-angiogenic therapy than patients with the replacement type, relying on co-option (Hoppener et al., 2019). Nevertheless, what makes liver metastases grow in one or another histological growth pattern is still a central question that needs to be further investigated.

Besides the histopathological growth patterns other markers that indicate the response to anti-angiogenic therapy have been already described (van Dam et al., 2017; Incio et al., 2018). Previously, a study has shown that high levels of circulating VEGF-A predicts a survival benefit for anti-angiogenic therapy in patients with metastatic breast and gastric cancer (Vasudev and Reynolds, 2014). This is justified as those tumors will respond better to anti-angiogenic therapy. Further exploring this scenario, Ma et al. (2019) investigated the impact of VEGF-A in primary liver cancers, showing that a high level of VEGF-A expressed by malignant cells leads to a more divers tumor microenvironment which was correlated to a significantly worse overall survival. Two other factors that cause a resistance to anti-angiogenic therapy are IL-6 and FGF-2 that are upregulated under obesity conditions (Incio et al., 2018). Frequently, acquired resistance to anti-VEGF therapy is observed in a significative fraction of patients (Hurwitz et al., 2004). However, a fraction of patients shows innate, intrinsic resistance to anti-angiogenic therapy. This alteration in therapy response also echoes to the different types of growth patterns, as changes from the desmoplastic to replacement type can be observed in patients undergoing anti-angiogenic treatment (van Dam et al., 2018; Hoppener et al., 2019).

Tumor cells heterogeneity is not the only variable which has been described as a possible mechanism that could influence anti-angiogenic therapy resistance. The host organ microenvironment, especially the immune cells, have also been suggested to play a crucial role in in the process of metastasis (Quail and Joyce, 2013; Dagogo-Jack and Shaw, 2018). Macrophages, which usually are critical effector cells in immune response, can support tumor progression (Quail and Joyce, 2013). It has been already shown that tumor-associated macrophages release tumor-derived CSF-1 and macrophage-derived EGF through a paracrine manner, further promoting therapy resistance (Quail and Joyce, 2013). Therefore, CSF-1 might be a new possible target in oncology. Yet, the underlying mechanisms which influence macrophages phenotype switch from a tumor-suppressing to a pro-tumorigenic type are still unclear. However, it is presumed that conditions within the tumor microenvironment, like hypoxia, might cause phenotypical changes (Jain, 2014). High levels of VEGF and endothelin-2 serve as chemoattractants and could be responsible for the recruitment of these cells to hypoxic regions, leading to their correlation with neoangiogenesis and invasion (Quail and Joyce, 2013; Albini et al., 2018). Lastly, regarding tumor microenvironment cells, it is important to reinforce the participation of tumor-associated fibroblasts in the promotion and growth of malignant cells and metastases (Quail and Joyce, 2013). Normal fibroblasts instead promote the growth of healthy endothelial cells and suppress the growth

of tumor cells (Quail and Joyce, 2013). Currently, the exact origin of tumor-associated fibroblasts is controverse. It has been suggested that they arise from the endothelial-to-mesenchymal transition (EMT). *In vivo* mouse experiments with melanoma and neuroendocrine cells showed that the tumor-associated fibroblasts are derived from endothelial cells, accumulating in the tumor microenvironment and are activated by several growth factors and cytokines, which ultimately support they cellular turn over (Quail and Joyce, 2013).

### Key Points

We can recapitulate that angiogenesis is a crucial aspect in the process of metastasis. Many tumors metastasize especially in the liver, where they are confronted with a highly specialized vascular system. The tumor cells instrumentalize different mechanisms to gain access to the blood system. One of the most common is neoangiogenesis, which is driven mainly by VEGF. The metastases are highly dependent on nutrition via the blood vessels which has made neoangiogenesis an interesting target for anti-angiogenetic therapy. Unfortunately, thanks to their heterogeneity, tumors are able to adapt to severe changes in their environment, evidencing the current limitations of anti-angiogenetic therapeutical approaches.

## CONCLUSION AND FUTURE PERSPECTIVES

This review summarizes the main aspects involved in developmental and pathological angiogenesis. From the start of embryogenesis to the establishment and maintenance of the human mature adult body, vascularization is vital for all processes. Not long ago, the extensive lack of information regarding the molecular signature of the vascular system started to be revised and filled by elegant, well-designed studies which helped us to better comprehend the complexity of this system. As described in this review, new and advanced molecular techniques, such as single-cell sequencing certainly brought relevant missing pieces of information, which are used not only to deepen our knowledge on molecular mechanisms underlying vascular physiology and pathogenesis, but also to generate new promising therapeutical approaches such as EC metabolic inhibition and tumor-vessel normalization (Schoors et al., 2014; Cantelmo et al., 2016). Those scientific insights are crucial to help us overcome the current setbacks observed in e.g., vascular regeneration and anti-angiogenic therapy. The concepts proposed at the beginning of the angiogenesis research by Judah Folkmann in 1971 (Folkman, 1971), which were heavily criticized and not acknowledged at that time, have never been so extensively tested and recognized. Therefore, the further uncovering and comprehension of the human endothelial and mural cell heterogeneity and their involvement in disease at the molecular and metabolic level, are decisive factors to improve future therapeutic strategies.

## AUTHOR CONTRIBUTIONS

JF and CJ drafted the manuscript. TD and L-CC conceptualized the review article. JF designed the figures. All authors revised and discussed the manuscript.

## REFERENCES


Adams, R. H., and Alitalo, K. (2007). Molecular regulation of angiogenesis and lymphangiogenesis. *Nat. Rev. Mol. Cell Biol.* 8, 464–478. doi: 10.1038/nrm2183

Aird, W. C. (2007). Phenotypic Heterogeneity of the Endothelium. *Circ. Res.* 100, 174–190. doi: 10.1161/01.res.0000255690.03436.ae

Aird, W. C. (2012). Endothelial Cell Heterogeneity. *Cold Spring Harb. Perspect. Med.* 2:a006429.

Albini, A., Bruno, A., Noonan, D. M., and Mortara, L. (2018). Contribution to Tumor Angiogenesis From Innate Immune Cells Within the Tumor Microenvironment: Implications for Immunotherapy. *Front. Immunol.* 9:527. doi: 10.3389/fimmu.2018.00527

Armulik, A., Genové, G., and Betsholtz, C. (2011). Pericytes: Developmental. Physiological, and Pathological Perspectives, Problems, and Promises. *Dev. Cell* 21, 193–215. doi: 10.1016/j.devcel.2011.07.001

Assoun, S., Brosseau, S., Steinmetz, C., Gounant, V., and Zalcman, G. (2017). Bevacizumab in advanced lung cancer: state of the art. *Future Oncol.* 13, 2515–2535. doi: 10.2217/fon-2017-0302

Baluk, P., Morikawa, S., Haskell, A., Mancuso, M., and McDonald, D. M. (2003). Abnormalities of Basement Membrane on Blood Vessels and Endothelial Sprouts in Tumors. *Am. J. Pathol.* 163, 1801–1815. doi: 10.1016/s0002-9440(10)63540-7

Baryawno, N., Przybylski, D., Kowalczyk, M. S., Kfoury, Y., Severe, N., Gustafsson, K., et al. (2019). A Cellular Taxonomy of the Bone Marrow Stroma in Homeostasis and Leukemia. *Cell* 177, 1915–1932.e16.

Bentley, K., Mariggi, G., Gerhardt, H., and Bates, P. A. (2009). Tipping the Balance: Robustness of Tip Cell Selection. *Migr. Fusion Angiogenesis* 5:e1000549. doi: 10.1371/journal.pcbi.1000549

Bergers, G., and Benjamin, L. E. (2003). Tumorigenesis and the angiogenic switch. *Nat. Rev. Cancer* 3, 401–410. doi: 10.1038/nrc1093

Bergers, G., and Song, S. (2005). The role of pericytes in blood-vessel formation and maintenance. *Neuro Oncol.* 7, 452–464. doi: 10.1215/s1152851705000232

Blanco, R., and Gerhardt, H. (2013). VEGF and Notch in Tip and Stalk Cell Selection. *Cold Spring Harb. Perspect. Med.* 3:a006569. doi: 10.1101/cshperspect.a006569

Boron, W. F., and Boulpaep, E. L. (2003). *Medical Physiology*. Philadelphia: Elsevier Inc.

Brem, S., Cotran, R., and Folkman, J. (1972). Tumor angiogenesis: a quantitative method for histologic grading. *J. Natl. Cancer Inst.* 48, 347–356.

Cantelmo, A. R., Conradi, L. C., Brajic, A., Goveia, J., Kalucka, J., Pircher, A., et al. (2016). Inhibition of the Glycolytic Activator PFKFB3 in Endothelium Induces Tumor Vessel Normalization, Impairs Metastasis, and Improves Chemotherapy. *Cancer Cell* 30, 968–985. doi: 10.1016/j.ccell.2016.10.006

Carmeliet, P. (2003). Angiogenesis in health and disease. *Nat. Med.* 9, 653–660.

Carmeliet, P., and Jain, R. K. (2011a). Molecular mechanisms and clinical applications of angiogenesis. *Nature* 473, 298–307. doi: 10.1038/nature10144

Carmeliet, P., and Jain, R. K. (2011b). Principles and mechanisms of vessel normalization for cancer and other angiogenic diseases. *Nat. Rev. Drug Discov.* 10, 417–427. doi: 10.1038/nrd3455

Cheng, N., Brantley, D. M., and Chen, J. (2002). The ephrins and Eph receptors in angiogenesis. *Cytokine Growth Factor Rev.* 13, 75–85. doi: 10.1016/s1359-6101(01)00031-4

Claxton, S., and Fruttiger, M. (2004). Periodic Delta-like 4 expression in developing retinal arteries. *Gene. Expr. Patterns* 5, 123–127. doi: 10.1016/j.modgep.2004.05.004

Cleuren, A. C. A., Van Der Ent, M. A., Jiang, H., Hunker, K. L., Yee, A., Siemieniak, D. R., et al. (2019). The in vivo endothelial cell translatome is highly heterogeneous across vascular beds. *Proc. Natl. Acad. Sci.* 116, 23618–23624. doi: 10.1073/pnas.1912409116

Colak, D., Al-Harazi, O., Mustafa, O. M., Meng, F., Assiri, A. M., Dhar, D. K., et al. (2020a). Publisher Correction: RNA-Seq transcriptome profiling in three liver regeneration models in rats: comparative analysis of partial hepatectomy. *ALLPS PVL. Sci. Rep.* 10:7502.

Colak, D., Al-Harazi, O., Mustafa, O. M., Meng, F., Assiri, A. M., Dhar, D. K., et al. (2020b). RNA-Seq transcriptome profiling in three liver regeneration models in rats: comparative analysis of partial hepatectomy. *ALLPS PVL. Sci. Rep.* 10:5213.

Coutu, D. L., Kokkaliaris, K. D., Kunz, L., and Schroeder, T. (2017). Three-dimensional map of nonhematopoietic bone and bone-marrow cells and molecules. *Nat. Biotechnol.* 35, 1202–1210. doi: 10.1038/nbt.4006

Crisan, M., Corselli, M., Chen, W. C. W., and Péault, B. (2012). Perivascular cells for regenerative medicine. *J. Cell. Mole. Med.* 16, 2851–2860. doi: 10.1111/j.1582-4934.2012.01617.x

Crisan, M., Yap, S., Casteilla, L., Chen, C.-W., Corselli, M., Park, T. S., et al. (2008). A Perivascular Origin for Mesenchymal Stem Cells in Multiple Human Organs. *Cell Stem Cell* 3, 301–313. doi: 10.1016/j.stem.2008.07.003

Dagogo-Jack, I., and Shaw, A. T. (2018). Tumour heterogeneity and resistance to cancer therapies. *Nat. Rev. Clin. Oncol.* 15, 81–94. doi: 10.1038/nrclinonc.2017.166

Daneman, R., and Prat, A. (2015). The Blood–Brain Barrier. *Cold Spring Harb. Perspect. Biol.* 7:a020412.

Daneshmanesh, A. H., Hojjat-Farsangi, M., Ghaderi, A., Moshfegh, A., Hansson, L., Schultz, J., et al. (2018). A receptor tyrosine kinase ROR1 inhibitor (KAN0439834) induced significant apoptosis of pancreatic cells which was enhanced by erlotinib and ibrutinib. *PLoS One* 13:e0198038. doi: 10.1371/journal.pone.0198038

Dasgupta, A., Lim, A. R., and Ghajar, C. M. (2017). Circulating and disseminated tumor cells: harbingers or initiators of metastasis? *Mol. Oncol.* 11, 40–61. doi: 10.1002/1878-0261.12022

De Bock, K., Georgiadou, M., Schoors, S., and Kuchnio, A. (2013). Brian, Anna, et al. Role of PFKFB3-Driven Glycolysis in Vessel Sprouting. *Cell* 154, 651–663. doi: 10.1016/j.cell.2013.06.037

DeLeve, L. D., and Maretti-Mira, A. C. (2017). Liver Sinusoidal Endothelial Cell: An Update. *Semin. Liver Dis.* 37, 377–387. doi: 10.1055/s-0037-1617455

Díaz-Coránguez, M., Ramos, C., and Antonetti, D. A. (2017). The inner blood-retinal barrier: Cellular basis and development. *Vision Res.* 139, 123–137. doi: 10.1016/j.visres.2017.05.009

Ding, B. S., Nolan, D. J., Butler, J. M., James, D., Babazadeh, A. O., Rosenwaks, Z., et al. (2010). Inductive angiocrine signals from sinusoidal endothelium are required for liver regeneration. *Nature* 468, 310–315. doi: 10.1038/nature09493

Dirscherl, K., Schlapfer, M., Roth Z'graggen, B., Wenger, R. H., Booy, C., Flury-Frei, R., et al. (2020). Hypoxia sensing by hepatic stellate cells leads to VEGF-dependent angiogenesis and may contribute to accelerated liver regeneration. *Sci. Rep.* 10:4392.

Dobnikar, L., Taylor, A. L., Chappell, J., Oldach, P., Harman, J. L., Oerton, E., et al. (2018). Disease-relevant transcriptional signatures identified in individual smooth muscle cells from healthy mouse vessels. *Nat. Comm.* 9:4567

Donovan, P., Patel, J., Dight, J., Wong, H. Y., Sim, S. L., Murigneux, V., et al. (2019). Endovascular progenitors infiltrate melanomas and differentiate towards a variety of vascular beds promoting tumor metastasis. *Nat. Commun.* 1:18.

Drake, R. L., Vogl, A. W., and Mitchell, A. W. M. (2015). *Gray's Anatomy for Students*, 3 Edn. Philadelphia: Churchill Livingstone.

Dvorak, H. F. (2005). Angiogenesis: update 2005. *J. Thromb. Haemost.* 3, 1835–1842. doi: 10.1111/j.1538-7836.2005.01361.x

Eberhard, A., Kahlert, S., Goede, V., Hemmerlein, B., Plate, K. H., and Augustin, H. G. (2000). Heterogeneity of angiogenesis and blood vessel maturation in human tumors: implications for antiangiogenic tumor therapies. *Cancer Res.* 60, 1388–1393.

Eichmann, A., Yuan, L., Moyon, D., Lenoble, F., Pardanaud, L., and Breant, C. (2005). Vascular development: from precursor cells to branched arterial and venous networks. *Int. J. Dev. Biol.* 49, 259–267. doi: 10.1387/ijdb.041941ae

Ekman, N., Lymboussaki, A., Västrik, I., Sarvas, K., Kaipainen, A., and Alitalo, K. (1997). Bmx tyrosine kinase is specifically expressed in the endocardium and the endothelium of large arteries. *Circulation* 96, 1729–1732. doi: 10.1161/01.cir.96.6.1729

Farnsworth, R. H., Lackmann, M., Achen, M. G., and Stacker, S. A. (2014). Vascular remodeling in cancer. *Oncogene* 33, 3496–3505.

Feng, W., Chen, L., Nguyen, P. K., Wu, S. M., and Li, G. (2019). Single Cell Analysis of Endothelial Cells Identified Organ-Specific Molecular Signatures and Heart-Specific Cell Populations and Molecular Features. *Front. Cardiovasc. Med.* 6:165 doi: 10.3389/fcvm.2019.00165

Ferland-Mccollough, D., Slater, S., Richard, J., Reni, C., and Mangialardi, G. (2017). Pericytes, an overlooked player in vascular pathobiology. *Pharmacol. Ther.* 171, 30–42. doi: 10.1016/j.pharmthera.2016.11.008

Folkman, J. (1971). Tumor angiogenesis: therapeutic implications. *N. Engl. J. Med.* 285, 1182–1186.

Folkman, J. (1982). Angiogenesis: initiation and control. *Ann. N. Y. Acad. Sci.* 401, 212–227. doi: 10.1111/j.1749-6632.1982.tb25720.x

Frentzas, S., Simoneau, E., Bridgeman, V. L., Vermeulen, P. B., Foo, S., Kostaras, E., et al. (2016). Vessel co-option mediates resistance to anti-angiogenic therapy in liver metastases. *Nat. Med.* 22, 1294–1302. doi: 10.1038/nm.4197

Galjart, B., Nierop, P. M. H., van der Stok, E. P., van den Braak, R., Hoppener, D. J., Daelemans, S., et al. (2019). Angiogenic desmoplastic histopathological growth pattern as a prognostic marker of good outcome in patients with colorectal liver metastases. *Angiogenesis* 22, 355–368. doi: 10.1007/s10456-019-09661-5

George, M., Rainey, M. A., Naramura, M., Foster, K. W., Holzapfel, M. S., Willoughby, L. L., et al. (2011). Renal Thrombotic Microangiopathy in Mice with Combined Deletion of Endocytic Recycling Regulators EHD3 and EHD4. *PLoS One* 6:e17838. doi: 10.1371/journal.pone.0017838

Gerhardt, H., Golding, M., Fruttiger, M., Ruhrberg, C., Lundkvist, A., Abramsson, A., et al. (2003). VEGF guides angiogenic sprouting utilizing endothelial tip cell filopodia. *J. Cell Biol.* 161, 1163–1177. doi: 10.1083/jcb.200302047

Ghilardi, C., Chiorino, G., Dossi, R., Nagy, Z., Giavazzi, R., and Bani, M. (2008). Identification of novel vascular markers through gene expression profiling of tumor-derived endothelium. *BMC Genom.* 9:201. doi: 10.1186/1471-2164-9-201

Gouysse, G., Couvelard, A., Frachon, S., Bouvier, R., Nejjari, M., Dauge, M. C., et al. (2002). Relationship between vascular development and vascular differentiation during liver organogenesis in humans. *J. Hepatol.* 37, 730–740. doi: 10.1016/s0168-8278(02)00282-9

Goveia, J., Rohlenova, K., Taverna, F., Treps, L., Conradi, L. C., Pircher, A., et al. (2020). An Integrated Gene Expression Landscape Profiling Approach to Identify Lung Tumor Endothelial Cell Heterogeneity and Angiogenic Candidates. *Cancer Cell* 37:21–36.e13.

Griffith, C. K., Miller, C., Sainson, R. C., Calvert, J. W., Jeon, N. L., Hughes, C. C., et al. (2005). Diffusion limits of an in vitro thick prevascularized tissue. *Tissue Eng.* 11, 257–266. doi: 10.1089/ten.2005.11.257

Gustavsson, C., Agardh, C.-D., Zetterqvist, A. V., Nilsson, J., Agardh, E., and Gomez, M. F. (2010). Vascular Cellular Adhesion Molecule-1 (VCAM-1) Expression in Mice Retinal Vessels Is Affected by Both Hyperglycemia and Hyperlipidemia. *PLoS One* 5:e12699. doi: 10.1371/journal.pone.0012699

Hellström, M., Phng, L.-K., Hofmann, J. J., Wallgard, E., Coultas, L., Lindblom, P., et al. (2007). Dll4 signalling through Notch1 regulates formation of tip cells during angiogenesis. *Nature* 445, 776–780. doi: 10.1038/nature05571

Hirashima, M., and Suda, T. (2006). Differentiation of arterial and venous endothelial cells and vascular morphogenesis. *Endothelium* 13, 137–145.

Hofmann, J. J.,and Luisa Iruela-Arispe, M. (2007). Notch expression patterns in the retina: An eye on receptor-ligand distribution during angiogenesis. *Gene. Expr. Patterns* 7, 461–470.

Hogan, B. M., Herpers, R., Witte, M., Heloterä, H., Alitalo, K., Duckers, H. J., et al. (2009). Vegfc/Flt4 signalling is suppressed by Dll4 in developing zebrafish intersegmental arteries. *Development* 136, 4001–4009. doi: 10.1242/dev.039990

Hooper, A. T., Butler, J. M., Nolan, D. J., Kranz, A., Iida, K., Kobayashi, M., et al. (2009). Engraftment and reconstitution of hematopoiesis is dependent on

VEGFR2-mediated regeneration of sinusoidal endothelial cells. *Cell Stem Cell* 4, 263–274. doi: 10.1016/j.stem.2009.01.006

Hoppener, D. J., Nierop, P. M. H., Herpel, E., Rahbari, N. N., Doukas, M., Vermeulen, P. B., et al. (2019). Histopathological growth patterns of colorectal liver metastasis exhibit little heterogeneity and can be determined with a high diagnostic accuracy. *Clin. Exp. Metastasis* 36, 311–319. doi: 10.1007/s10585-019-09975-0

Huang, D., Sun, W., Zhou, Y., Li, P., Chen, F., Chen, H., et al. (2018). Mutations of key driver genes in colorectal cancer progression and metastasis. *Cancer Metastasis Rev.* 37, 173–187. doi: 10.1007/s10555-017-9726-5

Hurwitz, H., Fehrenbacher, L., Novotny, W., Cartwright, T., Hainsworth, J., Heim, W., et al. (2004). Bevacizumab plus irinotecan, fluorouracil, and leucovorin for metastatic colorectal cancer. *N. Engl. J. Med.* 350, 2335–2342.

Incio, J., Ligibel, J. A., McManus, D. T., Suboj, P., Jung, K., Kawaguchi, K., et al. (2018). Obesity promotes resistance to anti-VEGF therapy in breast cancer by up-regulating IL-6 and potentially FGF-2. *Sci. Transl. Med.* 10:eaag0945 doi: 10.1126/scitranslmed.aag0945

Isogai, S., Lawson, N. D., Torrealday, S., Horiguchi, M., and Weinstein, B. M. (2003). Angiogenic network formation in the developing vertebrate trunk. *Development* 130, 5281–5290. doi: 10.1242/dev.00733

Itatani, Y., Kawada, K., Yamamoto, T., and Sakai, Y. (2018). Resistance to Anti-Angiogenic Therapy in Cancer-Alterations to Anti-VEGF Pathway. *Int. J. Mol. Sci.* 19:1232 doi: 10.3390/ijms19041232

Itkin, T., Gur-Cohen, S., Spencer, J. A., Schajnovitz, A., Ramasamy, S. K., Kusumbe, A. P., et al. (2016). Distinct bone marrow blood vessels differentially regulate haematopoiesis. *Nature* 532, 323–328. doi: 10.1038/nature17624

Jain, R. K. (2014). Antiangiogenesis strategies revisited: from starving tumors to alleviating hypoxia. *Cancer Cell* 26, 605–622. doi: 10.1016/j.ccell.2014.10.006

Jambusaria, A., Hong, Z., Zhang, L., Srivastava, S., Jana, A., Toth, P. T., et al. (2020). Endothelial heterogeneity across distinct vascular beds during homeostasis and inflammation. *eLife* 9:e51413

Jeong, H.-W., Hernández-Rodríguez, B., Kim, J., Kim, K.-P., Enriquez-Gasca, R., Yoon, J., et al. (2017). Transcriptional regulation of endothelial cell behavior during sprouting angiogenesis. *Nat. Comm.* 8:726

Kalucka, J., de Rooij, L., Goveia, J., Rohlenova, K., Dumas, S. J., Meta, E., et al. (2020). Single-Cell Transcriptome Atlas of Murine Endothelial Cells. *Cell* 180, 764–779.e20.

Karaiskos, N., Rahmatollahi, M., Boltengagen, A., Liu, H., Hoehne, M., Rinschen, M., et al. (2018). A Single-Cell Transcriptome Atlas of the Mouse Glomerulus. *J. Am. Soc. Nephrol.* 29, 2060–2068. doi: 10.1681/asn.2018030238

Kutschera, S., Weber, H., Weick, A., De Smet, F., Genove, G., Takemoto, M., et al. (2011). Differential endothelial transcriptomics identifies semaphorin 3G as a vascular class 3 semaphorin. *Arterioscler. Thromb. Vasc. Biol.* 31, 151–159. doi: 10.1161/atvbaha.110.215871

Liu, M., and Gomez, D. (2019). Smooth Muscle Cell Phenotypic Diversity. *Arterioscler. Thromb. Vasc. Biol.* 39, 1715–1723. doi: 10.1161/atvbaha.119.312131

Lobov, I. B., Renard, R. A., Papadopoulos, N., Gale, N. W., Thurston, G., Yancopoulos, G. D., et al. (2007). Delta-like ligand 4 (Dll4) is induced by VEGF as a negative regulator of angiogenic sprouting. *Proc. Natl. Acad. Sci.* 104, 3219–3224. doi: 10.1073/pnas.0611206104

Lukowski, S. W., Patel, J., Andersen, S. B., Sim, S.-L., Wong, H. Y., Tay, J., et al. (2019). Single-Cell Transcriptional Profiling of Aortic Endothelium Identifies a Hierarchy from Endovascular Progenitors to Differentiated Cells. *Cell Rep.* 27, 2748–2758.e3.

Lyden, D., Hattori, K., Dias, S., Costa, C., Blaikie, P., Butros, L., et al. (2001). Impaired recruitment of bone-marrow-derived endothelial and hematopoietic precursor cells blocks tumor angiogenesis and growth. *Nat. Med.* 7, 1194–1201. doi: 10.1038/nm1101-1194

Ma, L., Hernandez, M. O., Zhao, Y., Mehta, M., Tran, B., Kelly, M., et al. (2019). Tumor Cell Biodiversity Drives Microenvironmental Reprogramming in Liver Cancer. *Cancer Cell* 36:418–430.e6.

Makuuchi, M., Thai, B. L., Takayasu, K., Takayama, T., Kosuge, T., Gunven, P., et al. (1990). Preoperative portal embolization to increase safety of major hepatectomy for hilar bile duct carcinoma: a preliminary report. *Surgery* 107, 521–527.

Mao, S. A., Glorioso, J. M., and Nyberg, S. L. (2014). Liver regeneration. *Trans. Res.* 163, 352–362.

Michalopoulos, G. K. (2007). Liver regeneration. *J. Cell Physiol.* 213, 286–300.

Michalopoulos, G. K., and DeFrances, M. C. (1997). Liver regeneration. *Science* 276, 60–66.

Minami, T., Muramatsu, M., and Kume, T. (2019). Organ/Tissue-Specific Vascular Endothelial Cell Heterogeneity in Health and Disease. *Biol. Pharmaceutical Bull.* 42, 1609–1619. doi: 10.1248/bpb.b19-00531

Morikawa, S., Baluk, P., Kaidoh, T., Haskell, A., Jain, R. K., and McDonald, D. M. (2002). Abnormalities in Pericytes on Blood Vessels and Endothelial Sprouts in Tumors. *Am. J. Pathol.* 160, 985–1000. doi: 10.1016/s0002-9440(10)64920-6

Mruk, D. D., and Cheng, C. Y. (2015). The Mammalian Blood-Testis Barrier: Its Biology and Regulation. *Endocr. Rev.* 36, 564–591. doi: 10.1210/er.2014-1101

Nagy, J. A., and Dvorak, H. F. (2012). Heterogeneity of the tumor vasculature: the need for new tumor blood vessel type-specific targets. *Clin. Exp. Metastasis* 29, 657–662. doi: 10.1007/s10585-012-9500-6

Nagy, J. A., Feng, D., Vasile, E., Wong, W. H., Shih, S. C., Dvorak, A. M., et al. (2006). Permeability properties of tumor surrogate blood vessels induced by VEGF-A. *Lab. Invest.* 86, 767–780. doi: 10.1038/labinvest.3700436

Nagy, J., Chang, S.-H., Shih, S.-C., Dvorak, A., and Dvorak, H. (2010). Heterogeneity of the Tumor Vasculature. *Sem. Thromb. Hemost.* 36, 321–331. doi: 10.1055/s-0030-1253454

Nguyen, D. X., Bos, P. D., and Massague, J. (2009). Metastasis: from dissemination to organ-specific colonization. *Nat. Rev. Cancer* 9, 274–284. doi: 10.1038/nrc2622

Nguyen, L. N., Ma, D., Shui, G., Wong, P., Cazenave-Gassiot, A., Zhang, X., et al. (2014). Mfsd2a is a transporter for the essential omega-3 fatty acid docosahexaenoic acid. *Nature* 509, 503–506. doi: 10.1038/nature13241

Ni, Y., Li, J. M., Liu, M. K., Zhang, T. T., Wang, D. P., Zhou, W. H., et al. (2017). Pathological process of liver sinusoidal endothelial cells in liver diseases. *World J. Gastroenterol.* 23, 7666–7677.

Papadimitrakopoulou, V., Cobo, M., Bordoni, R., Dubray-Longeras, P., Szalai, Z., Ursol, G., et al. (2018). OA05.07 IMpower132: PFS and Safety Results with 1L Atezolizumab + Carboplatin/Cisplatin + Pemetrexed in Stage IV Non-Squamous NSCLC. *J. Thorac. Oncol.* 13, S332–S333.

Pape, H.-C., Kurtz, A., and Silbernagl, S. (2014). *Physiologie. 7 ed. Stuttgart*.Stuttgart: Georg Thieme Verlag KG.

Park, J. E., Chen, H. H., Winer, J., Houck, K. A., and Ferrara, N. (1994). Placenta growth factor. Potentiation of vascular endothelial growth factor bioactivity, in vitro and in vivo, and high affinity binding to Flt-1 but not to Flk-1/KDR. *J. Biol. Chem.* 269, 25646–25654.

Patan, S. (2004). Vasculogenesis and angiogenesis. *Cancer Treat Res.* 117, 3–32.

Patel, J., Seppanen, E. J., Rodero, M. P., Wong, H. Y., Donovan, P., Neufeld, Z., et al. (2017). Functional Definition of Progenitors Versus Mature Endothelial Cells Reveals Key SoxF-Dependent Differentiation Process. *Circulation* 135, 786–805. doi: 10.1161/circulationaha.116.024754

Pawlina, W. (2018). *Histology: A Text and Atlas: With Correlated Cell and Molecular Biology*. Alphen aan den Rijn: Wolters Kluwer.

Pawlina, W. (2020). *Histology : a text and atlas : with correlated cell and molecular biology*, 8 Edn. Philadelphia: Wolters Kluwer.

Potente, M., Gerhardt, H., and Carmeliet, P. (2011). Basic and Therapeutic Aspects of Angiogenesis. *Cell* 146, 873–887. doi: 10.1016/j.cell.2011.08.039

Puchtler, H., and Waldrop, F. S. (1979). On the mechanism of Verhoeff's elastica stain: a convenient stain for myelin sheaths. *Histochemistry* 62, 233–247. doi: 10.1007/bf00508352

Quail, D. F., and Joyce, J. A. (2013). Microenvironmental regulation of tumor progression and metastasis. *Nat. Med.* 19, 1423–1437. doi: 10.1038/nm.3394

Rabes, H. M. (1977). Kinetics of hepatocellular proliferation as a function of the microvascular structure and functional state of the liver. *Ciba Found. Symp.* 55, 31–53.

Rafii, S., Butler, J. M., and Ding, B.-S. (2016). Angiocrine functions of organ-specific endothelial cells. *Nature* 529, 316–325.

Ribatti, D., and Djonov, V. (2012). Intussusceptive microvascular growth in tumors. *Cancer Lett.* 316, 126–131.

Ribatti, D., Tamma, R., Ruggieri, S., Annese, T., and Crivellato, E. (2020). Surface markers: An identity card of endothelial cells. *Microcirculation* 27:e12587

Risau, W. (1997). Mechanisms of angiogenesis. *Nature* 386, 671–674.

Rizov, M., Andreeva, P., and Dimova, I. (2017). Molecular regulation and role of angiogenesis in reproduction. *Taiwanese J. Obstet. Gynecol.* 56, 127–132.

Rohlenova, K., Goveia, J., Garcia-Caballero, M., Subramanian, A., Kalucka, J., Treps, L., et al. (2020). Single-Cell RNA Sequencing Maps Endothelial Metabolic Plasticity in Pathological Angiogenesis. *Cell Metab.* 31, 862–77.e14.

Sabbagh, M. F., Heng, J. S., Luo, C., Castanon, R. G., Nery, J. R., Rattner, A., et al. (2018). Transcriptional and epigenomic landscapes of CNS and non-CNS vascular endothelial cells. *eLife* 7:e36187 doi: 10.7554/eLife.36187

Sagaert, X., Vanstapel, A., and Verbeek, S. (2018). Tumor Heterogeneity in Colorectal Cancer: What Do We Know So Far? *Pathobiology* 85, 72–84. doi: 10.1159/000486721

Schoors, S., De Bock, K., Cantelmo, A. R., Georgiadou, M., Ghesquiere, B., Cauwenberghs, S., et al. (2014). Partial and transient reduction of glycolysis by PFKFB3 blockade reduces pathological angiogenesis. *Cell Metab.* 19, 37–48. doi: 10.1016/j.cmet.2013.11.008

Seano, G., Chiaverina, G., Gagliardi, P. A., Di Blasio, L., Puliafito, A., Bouvard, C., et al. (2014). Endothelial podosome rosettes regulate vascular branching in tumour angiogenesis. *Nat. Cell Biol.* 16, 931–941. doi: 10.1038/ncb3036

Shenoy, P. S., and Bose, B. (2018). Hepatic perivascular mesenchymal stem cells with myogenic properties. *J. Tissue Eng. Regen. Med.* 12, e1297–e1310. doi: 10.1002/term.2503

Smyth, L. C. D., Rustenhoven, J., Scotter, E. L., Schweder, P., Faull, R. L. M., Park, T. I. H., et al. (2018). Markers for human brain pericytes and smooth muscle cells. *J. Chem. Neuroanat.* 92, 48–60. doi: 10.1016/j.jchemneu.2018.06.001

Socinski, M. A., Jotte, R. M., Cappuzzo, F., Orlandi, F., Stroyakovskiy, D., Nogami, N., et al. (2018). Atezolizumab for First-Line Treatment of Metastatic Nonsquamous NSCLC. *N. Engl. J. Med.* 378, 2288–2301. doi: 10.1056/NEJMoa1716948

Strasser, G. A., Kaminker, J. S., and Tessier-Lavigne, M. (2010). Microarray analysis of retinal endothelial tip cells identifies CXCR4 as a mediator of tip cell morphology and branching. *Blood* 115, 5102–5110. doi: 10.1182/blood-2009-07-230284

Strauss, O., Phillips, A., Ruggiero, K., Bartlett, A., and Dunbar, P. R. (2017). Immunofluorescence identifies distinct subsets of endothelial cells in the human liver. *Sci. Rep. UK* 7:44356 doi: 10.1038/srep44356

Su, L., Mruk, D. D., and Cheng, C. Y. (2011). Drug transporters, the blood-testis barrier, and spermatogenesis. *J. Endocrinol.* 208, 207–223. doi: 10.1677/JOE-10-0363

Suchting, S., Freitas, C., Le Noble, F., Benedito, R., Breant, C., Duarte, A., et al. (2007). The Notch ligand Delta-like 4 negatively regulates endothelial tip cell formation and vessel branching. *Proc. Natl. Acad. Sci. U S A* 104, 3225–3230. doi: 10.1073/pnas.0611177104

Sun, Z., Wang, C.-Y., Lawson, D. A., Kwek, S., Velozo, H. G., Owyong, M., et al. (2018). Single-cell RNA sequencing reveals gene expression signatures of breast cancer-associated endothelial cells. *Oncotarget* 9, 10945–10961. doi: 10.18632/oncotarget.23760

Sweeney, M. D., Zhao, Z., Montagne, A., Nelson, A. R., and Zlokovic, B. V. (2019). Blood-Brain Barrier: From Physiology to Disease and Back. *Physiol. Rev.* 99, 21–78. doi: 10.1152/physrev.00050.2017

Tao, Y., Wang, M., Chen, E., and Tang, H. (2017). Liver Regeneration: Analysis of the Main Relevant Signaling Molecules. *Mediat. Inflamm.* 2017, 1–9. doi: 10.1155/2017/4256352

Tewari, K. S., Sill, M. W., Penson, R. T., Huang, H., Ramondetta, L. M., Landrum, L. M., et al. (2017). Bevacizumab for advanced cervical cancer: final overall survival and adverse event analysis of a randomised, controlled, open-label, phase 3 trial (Gynecologic Oncology Group 240). *Lancet* 390, 1654–1663. doi: 10.1016/S0140-6736(17)31607-0

Tomlinson, F. H., Scheithauer, B. W., Hayostek, C. J., Parisi, J. E., Meyer, F. B., Shaw, E. G., et al. (1994). The significance of atypia and histologic malignancy in pilocytic astrocytoma of the cerebellum: a clinicopathologic and flow cytometric study. *J. Child Neurol.* 9, 301–310. doi: 10.1177/088307389400900317

Tonnesen, M. G., Feng, X., and Clark, R. A. F. (2000). Angiogenesis in Wound Healing. *J. Investig. Dermatol. Symp. Proc.* 5, 40–46. doi: 10.1046/j.1087-0024.2000.00014.x

Tsafrir, D., Tsafrir, I., Ein-Dor, L., Zuk, O., Notterman, D. A., and Domany, E. (2005). Sorting points into neighborhoods (SPIN): data analysis and visualization by ordering distance matrices. *Bioinformatics* 21, 2301–2308. doi: 10.1093/bioinformatics/bti329

Turajlic, S., Sottoriva, A., Graham, T., and Swanton, C. (2020). Author Correction: Resolving genetic heterogeneity in cancer. *Nat. Rev. Genet.* 21:65. doi: 10.1038/s41576-019-0188-1

van Dam, P. J., Daelemans, S., Ross, E., Waumans, Y., Van Laere, S., Latacz, E., et al. (2018). Histopathological growth patterns as a candidate biomarker for immunomodulatory therapy. *Semin. Cancer Biol.* 52, 86–93. doi: 10.1016/j.semcancer.2018.01.009

van Dam, P. J., van der Stok, E. P., Teuwen, L. A., Van den Eynden, G. G., Illemann, M., Frentzas, S., et al. (2017). International consensus guidelines for scoring the histopathological growth patterns of liver metastasis. *Br. J. Cancer* 117, 1427–1441. doi: 10.1038/bjc.2017.334

Vanlandewijck, M., He, L., Mäe, M. A., Andrae, J., Ando, K., Del Gaudio, F., et al. (2018). A molecular atlas of cell types and zonation in the brain vasculature. *Nature* 554, 475–480. doi: 10.1038/nature25739

Vasudev, N. S., and Reynolds, A. R. (2014). Anti-angiogenic therapy for cancer: current progress, unresolved questions and future directions. *Angiogenesis* 17, 471–494. doi: 10.1007/s10456-014-9420-y

Veerman, K., Tardiveau, C., Martins, F., Coudert, J., and Girard, J.-P. (2019). Single-cell analysis reveals heterogeneity of high endothelial venules and different regulation of genes controlling lymphocyte entry to lymph nodes. *Cell Rep.* 26, 3116.e–3131.e. doi: 10.1016/j.celrep.2019.02.042

Viallard, C., and Larrivée, B. (2017). Tumor angiogenesis and vascular normalization: alternative therapeutic targets. *Angiogenesis* 20, 409–426. doi: 10.1007/s10456-017-9562-9

Wang, H. U., Chen, Z. F., and Anderson, D. J. (1998). Molecular distinction and angiogenic interaction between embryonic arteries and veins revealed by ephrin-B2 and its receptor Eph-B4. *Cell* 93, 741–753. doi: 10.1016/S0092-8674(00)81436-1

Welsch, U., Kummer, W., and Deller, T. (2014). *Lehrbuch Histologie. München.*Munich: Urban and Fischer Verlag, 699.

West, H., McCleod, M., Hussein, M., Morabito, A., Rittmeyer, A., Conter, H. J., et al. (2019). Atezolizumab in combination with carboplatin plus nab-paclitaxel chemotherapy compared with chemotherapy alone as first-line treatment for metastatic non-squamous non-small-cell lung cancer (IMpower130): a multicentre, randomised, open-label, phase 3 trial. *Lancet Oncol.* 20, 924–937. doi: 10.1016/S1470-2045(19)30167-6

Widlansky, M. E., Gokce, N., Keaney, J. F., and Vita, J. A. (2003). The clinical implications of endothelial dysfunction. *J. Am. Coll. Cardiol.* 42, 1149–1160. doi: 10.1016/S0735-1097(03)00994-X

Yachida, S., Jones, S., Bozic, I., Antal, T., Leary, R., Fu, B., et al. (2010). Distant metastasis occurs late during the genetic evolution of pancreatic cancer. *Nature* 467, 1114–1117. doi: 10.1038/nature09515

Yamamoto, K., de Waard, V., Fearns, C., and Loskutoff, D. J. (1998). Tissue distribution and regulation of murine von Willebrand factor gene expression in vivo. *Blood* 92, 2791–2801. doi: 10.1182/blood.V92.8.2791

Zhang, Q., Lou, Y., Bai, X. L., and Liang, T. B. (2018). Immunometabolism: A novel perspective of liver cancer microenvironment and its influence on tumor progression. *World J. Gastroenterol.* 24, 3500–3512. doi: 10.3748/wjg.v24.i31.3500

Zhao, Q., Eichten, A., Parveen, A., Adler, C., Huang, Y., Wang, W., et al. (2018). Single-Cell Transcriptome Analyses Reveal Endothelial Cell Heterogeneity in Tumors and Changes following Antiangiogenic Treatment. *Cancer Res.* 78, 2370–2382. doi: 10.1158/0008-5472.CAN-17-2728

**Conflict of Interest:** The authors declare that the research was conducted in the absence of any commercial or financial relationships that could be construed as a potential conflict of interest.

frontiers in Physiology

MINI REVIEW
published: 12 November 2020
doi: 10.3389/fphys.2020.591850

# The Emerging Role of the Prokineticins and Homeobox Genes in the Vascularization of the Placenta: Physiological and Pathological Aspects

*Nadia Alfaidy[1,2,3]*, Sophie Brouillet[4], Gayathri Rajaraman[5], Bill Kalionis[6], Pascale Hoffmann[1,2,3], Tiphaine Barjat[7], Mohamed Benharouga[8] and Padma Murthi[6,9]*

*[1] Unité 1036, Institut National de la Santé et de la Recherche Médicale, Grenoble, France, [2] Department of Biology, University of Grenoble Alpes, Grenoble, France, [3] Commissariat à l'Energie Atomique et aux Energies Alternatives (CEA), Biosciences and Biotechnology Institute of Grenoble, Grenoble, France, [4] INSERM U1203, Department of Reproductive Biology, University of Montpellier, Montpellier, France, [5] Faculty of Health and Biomedicine, First Year College, Victoria University, St. Albans, VIC, Australia, [6] Department of Maternal-Fetal Medicine, Obstetrics and Gynaecology, Pregnancy Research Centre, Royal Women's Hospital, The University of Melbourne, Parkville, VIC, Australia, [7] Unité 1059, Saint-Etienne Hospital, Institut National de la Santé et de la Recherche Médicale, Saint-Étienne, France, [8] Unité Mixte de Recherche 5249, Laboratoire de Chimie et Biologie des Métaux, Centre National de la Recherche Scientifique (CNRS), Grenoble, France, [9] Department of Pharmacology, The Ritchie Centre, Monash Biomedicine Discovery Institute, Hudson Institute of Medical Research, Monash University, Clayton, VIC, Australia*

OPEN ACCESS

**Edited by:**
*Luca Munaron, University of Turin, Italy*

**Reviewed by:**
*Martina Rudnicki, York University, Canada*
*Martha Sosa-Macías, National Polytechnic Institute (IPN), Mexico*

***Correspondence:**
*Nadia Alfaidy*
*nadia.alfaidy-benharouga@cea.fr*

**Specialty section:**
*This article was submitted to Vascular Physiology, a section of the journal Frontiers in Physiology*

**Received:** *05 August 2020*
**Accepted:** *13 October 2020*
**Published:** *12 November 2020*

**Citation:**
*Alfaidy N, Brouillet S, Rajaraman G, Kalionis B, Hoffmann P, Barjat T, Benharouga M and Murthi P (2020) The Emerging Role of the Prokineticins and Homeobox Genes in the Vascularization of the Placenta: Physiological and Pathological Aspects. Front. Physiol. 11:591850. doi: 10.3389/fphys.2020.591850*

Vasculogenesis and angiogenesis are key processes of placental development, which occur throughout pregnancy. Placental vasculogenesis occurs during the first trimester of pregnancy culminating in the formation of hemangioblasts from intra-villous stem cells. Placental angiogenesis occurs subsequently, forming new blood vessels from existing ones. Angiogenesis also takes place at the fetomaternal interface, allowing essential spiral arteriole remodeling to establish the fetomaternal circulation. Vasculogenesis and angiogenesis in animal models and in humans have been studied in a wide variety of *in vitro*, physiological and pathological conditions, with a focus on the pro- and anti-angiogenic factors that control these processes. Recent studies revealed roles for new families of proteins, including direct participants such as the prokineticin family, and regulators of these processes such as the homeobox genes. This review summarizes recent advances in understanding the molecular mechanisms of actions of these families of proteins. Over the past decade, evidence suggests increased production of placental anti-angiogenic factors, as well as angiogenic factors are associated with fetal growth restriction (FGR) and preeclampsia (PE): the most threatening pathologies of human pregnancy with systemic vascular dysfunction. This review also reports novel clinical strategies targeting members of these family of proteins to treat PE and its consequent effects on the maternal vascular system.

**Keywords: vessel development, endothelial cells, angiogenesis, prokineticins, homeobox genes, vascularization, pregnancy, EG-VEGF**

## INTRODUCTION

The placenta is the key organ for a successful pregnancy. It acts as a semi-permeable barrier to control nutrient and gasses exchanges and regulate waste produced by developing fetus. This hemochorial villous organ develops earlier during pregnancy, following the erosion of nearby maternal capillaries by the lytic activity of the syncytiotrophoblast. Around the 11th-12th day post-conception, the primitive uteroplacental circulation is launched (Gude et al., 2004). The establishment of this circulation is based on two key processes, the first one takes place within the placental villi and is governed by the intra-villi vasculogenesis and angiogenesis; the second one occurs at the fetomaternal interface and is governed by the extravillous trophoblasts (EVT) that remodel maternal spiral arteries to establish the fetomaternal circulation (Velicky et al., 2016).

Villous vascularization is an important process in organogenesis and is essential for the placenta to function efficiently (Zygmunt et al., 2003). At the end of the 3rd week post-conception, intra-villous stem cells differentiate into connective tissue culminating in the formation of hemangioblasts. The differentiation of the hemangioblasts into angioblasts and hematopoietic cells allows the formation of new blood vessels that connect with those of the embryo to form the primitive capillary network (Gude et al., 2004). Placental vasculogenesis is followed by two phases of angiogenesis; branching angiogenesis in immature villi where new vessels form by sprouting, and non-branching angiogenesis in the stem villi, where capillary loops form through elongation. These processes increase the surface area to volume ratio (Charnock-Jones, 2002; Chaddha et al., 2004; Zou et al., 2011) and enhance diffusional exchange between the maternal and fetal circulations (Kingdom et al., 2000; Kaufmann et al., 2004). The second type of angiogenesis, occurring at the fetomaternal interface is mainly ensured by EVTs. By the end of first trimester of pregnancy, the EVTs acquire an invasive phenotype along with markers of endothelial cells. These features allow them to colonize maternal spiral arteries, through the replacement of maternal endothelial cells, culminating in an increase in diameter of these vasculature, which allow more oxygenated maternal blood in the intervillous space (Burton and Jaunaiux, 2001; Burton, 2009).

## IMPAIRED PLACENTAL ANGIOGENESIS AND PREGNANCY-ASSOCIATED DISORDERS

The spectrum of vascular defects associated with clinically significant pregnancy disorders including fetal growth restriction (FGR) and preeclampsia (PE), attests to the close relationship between the placental angiogenesis and embryonic development. Villi from placentae where intrauterine embryonic death and blighted ova exhibit aberrant vascular characteristics with significantly decreased vascular density, fibrosis and hydropic degeneration (Meegdes et al., 1988).

Studies using stereological techniques have reported that in placentae from FGR pregnancies, the number, surface area and volume of terminal villi were significantly reduced in FGR compared with placentae from uncomplicated pregnancies. Villous vessels exhibited fewer branches with slender and uncoiled vessels (Chen et al., 2002; Mayhew, 2003; Mayhew et al., 2003). Reduced capability of branching angiogenesis (non-branching angiogenesis) in FGR was strongly associated with a reduced supply of oxygen and nutrients to the fetus, and a subsequent delay in fetal growth (Kingdom et al., 2000; Salafia et al., 2006). Whether the vascular defects cause human FGR, or whether these changes are a consequence of aberrant biological mechanisms in the placentae from FGR pregnancies (Maulik et al., 2006) is unknown. To address this, it is vital to understand the molecular regulation of angiogenesis in the human placenta.

## MOLECULAR REGULATION OF ANGIOGENESIS

The processes of angiogenesis involve distinct changes in the phenotype of endothelial cells (ECs), which comprise the basic organizational units of vascular structures. The stimuli for these complex processes of placental angiogenesis are temporally coordinated by the microenvironment surrounding the EC surface (Patel et al., 2005). At the molecular level, *in vitro* and *in vivo* studies reported several growth factors and receptors that activate critical signaling pathways (Arderiu et al., 2007). Vascular endothelial growth factor (VEGF), placental growth factor (PlGF), and angiopoietins together with their primary receptors, VEGF receptor-1 (VEGFR-1) and VEGF receptor-2 (VEGFR-2) and PlGF that binds only to VEGFR-1, were identified as key candidates by Patel et al. (2005). VEGF is a potent stimulator of EC proliferation, migration, and production of plasminogen activators that are required for degradation of the basement membrane (Regnault et al., 2002).

In uncomplicated pregnancies, placental expression of key growth factors correlates with their established roles. For example, expression of VEGF and VEGFR-2 is highest during early gestation, which coincides with vasculogenesis and branching angiogenesis, but expression declines with advancing pregnancy (Jackson et al., 1994). Conversely, PlGF and VEGFR-1 expression is highest toward term, coinciding with non-branching angiogenesis (Clark et al., 1996).

Although differential expression of these angiogenic factors have been implicated in the development in PE and FGR (Ahmed and Perkins, 2000; Tsatsaris et al., 2003), new families of proteins have been identified and reported to play key roles in the control of these angiogenic processes. These include two important families of proteins; the prokineticins and the nuclear transcription factors including homeobox genes/homeodomain proteins.

## PROKINETICIN FAMILY IN THE CONTROL OF PLACENTAL ANGIOGENESIS

Recent studies from our group provided evidence for the direct role of a new placental angiogenic called prokineticin 1 (PROK1)

in normal and FGR pregnancies (Hoffmann et al., 2006, 2009; Brouillet et al., 2012b, 2013b; Murthi et al., 2015; Sergent et al., 2016). Due to its similarities of action with VEGF (LeCouter et al., 2001), PROK1 is also called as endocrine gland derived-vascular endothelial growth factor (EG-VEGF). EG-VEGF belongs to the prokineticin family that includes two key members PROK1 and PROK2, also called BV8 (≈ 8 kDa) (LeCouter et al., 2001; Lin et al., 2002). These circulating ligands show differential expression patterns in humans depending on the organ/tissue types. For example, PROK1/EG-VEGF is highly expressed in peripheral tissues (specifically in steroidogenic organs such as human ovary, placenta and adrenal gland), whereas PROK2/Bv8 is widely expressed in the central nervous system and non-steroidogenic cells of the testes (LeCouter et al., 2001; Lin et al., 2002; Traboulsi et al., 2015). EG-VEGF and BV8 activate two G-protein linked receptors namely prokineticin receptor 1 (PROKR1) and -2 (PROKR2). The signaling pathways include, cAMP, Akt, and p42-p44 MAP-kinases phosphorylation and calcium mobilization. PROKs regulate a stunning array of biological functions such as gastrointestinal motility (LeCouter et al., 2001; Lin et al., 2002), circadian rhythm regulation, neurogenesis, angiogenesis, pain perception, mood regulation, and reproduction (Brouillet et al., 2010, 2012b; Alfaidy et al., 2016; Zhao et al., 2019). Dysregulation of PROKs/PROKRs signaling pathways have been reported in a variety of diseases, such as cancer, abnormal angiogenesis and pregnancy pathologies (Brouillet et al., 2010, 2012b; Alfaidy et al., 2016; Traboulsi et al., 2017; Zhao et al., 2019).

Throughout normal human pregnancy, a dynamic expression of circulating EG-VEGF is found in the serum of pregnant women, with a five-fold increase during the first trimester (≈250 pg/ml) (Hoffmann et al., 2009). The placental expression of EG-VEGF is high during the first trimester of human pregnancy, with a peak at 8–11 weeks of gestation (Hoffmann et al., 2009). PROKR1 and PROKR2 are highly expressed in villous cytotrophoblasts (VCT) as well as micro- and macrovascular placental endothelial cells (Brouillet et al., 2010). At the cellular level, EG-VEGF is expressed in the syncytiotrophoblast (ST), VCT, fetal endothelium, and Hofbauer cells (Ho) (Hoffmann et al., 2006; Holloway et al., 2014; Garnier et al., 2015).

## PROKINETICINS EXPRESSION IN MICRO- AND MACROVASCULAR PLACENTAL ECs

Lang et al. (2003) reported distinct morphogenetic, antigenic and functional differences between the two EC types present in the placenta, with respect to the secretion of vasoactive substances and the proliferative response to cytokines. The dissimilar responses of micro- and macrovascular ECs to various stimuli (Lang et al., 2003; Brouillet et al., 2010) most likely reflect differences in the activation of transcription factors, **Figure 1**. Despite these differences, HUVEC are the predominant cell type used to model placental vasculogenic and angiogenic processes (Demir et al., 1989). Microvascular ECs, despite being the predominant cell type that vascularize the placental villi are less well understood. Importantly, these cells play critical role in placental disorders such as FGR and PE (Demir et al., 1989; Kingdom et al., 2000; Lang et al., 2003).

Endocrine gland derived-vascular endothelial growth factor enhances angiogenesis within the placental villi during the first trimester of human pregnancy (Brouillet et al., 2010). It controls various angiogenic processes including endothelial cell proliferation, survival, migration, tube organization, sprouting, permeability, and paracellular transport (Brouillet et al., 2010). Interestingly, EG-VEGF also displays stronger effects on the placental microvascular endothelial cells, the PLEC cells compare to its effects on the macrovascular cells, the HUVEC (Human umbilical vessel endothelial cells) (Brouillet et al., 2010). Via its PROKR1 receptor, EG-VEGF increases PLEC proliferation, migration and sprouting and controls their permeability via PROKR2. Importantly, EG-VEGF effects on PLEC cells were stronger compare to the VEGF effects on the same cells (Brouillet et al., 2010). At the feto-maternal interface, we demonstrated that EG-VEGF controls extra-villi angiogenesis through the inhibition of precocious invasion of EVT into the maternal spiral arteries (Hoffmann et al., 2009).

Recent studies from our own group and from others demonstrated that increased expression of EG-VEGF is associated with PE and FGR development (Hoffmann et al., 2006; Alfaidy, 2016; Inan et al., 2018). Our group also demonstrated that the concentration of EG-VEGF is significantly increased in both pathologies (Hoffmann et al., 2006; Murthi et al., 2015; Alfaidy, 2016). More recently, a study confirmed the increase in EG-VEGF levels in PE and proposed this factor as a biomarker for the diagnosis of PE patients (Inan et al., 2018).

## KEY REGULATORS OF PROKINETICINS FOR SUCCESSFUL PLACENTAL ANGIOGENESIS

Since its identification EG-VEGF has been associated with the control of placental angiogenesis during the first trimester of pregnancy and the reactivation of its receptors in the placenta of patients with pregnancy pathologies such as PE and FGR (Brouillet et al., 2010, 2012a, 2013a, 2014a,b; Garnier et al., 2015; Alfaidy, 2016; Sergent et al., 2016). The reactivation of angiogenic processes was meant to compensate for the associated deleterious vascularization. In these pathologies, EG-VEGF and receptors contribute to neoangiogenesis processes that allow pregnancy to progress. To fulfill these functions, EG-VEGF and its receptors have been reported to be regulated by key actors of vasculogenesis and angiogenesis within the placenta. The first supposed regulator of EG-VEGF expression was oxygen. This was reported by Ferrara et al. (LeCouter et al., 2001), as HIF1α response element was identified in the promoter region of EG-VEGF and BV8. In 2006, we demonstrated that EG-VEGF and its PROKR1 receptor were upregulated by hypoxia in the human placenta (Hoffmann et al., 2006). EG-VEGF upregulation by hypoxia substantiated its role during the first trimester, as placental development and vascularization occur in hypoxic

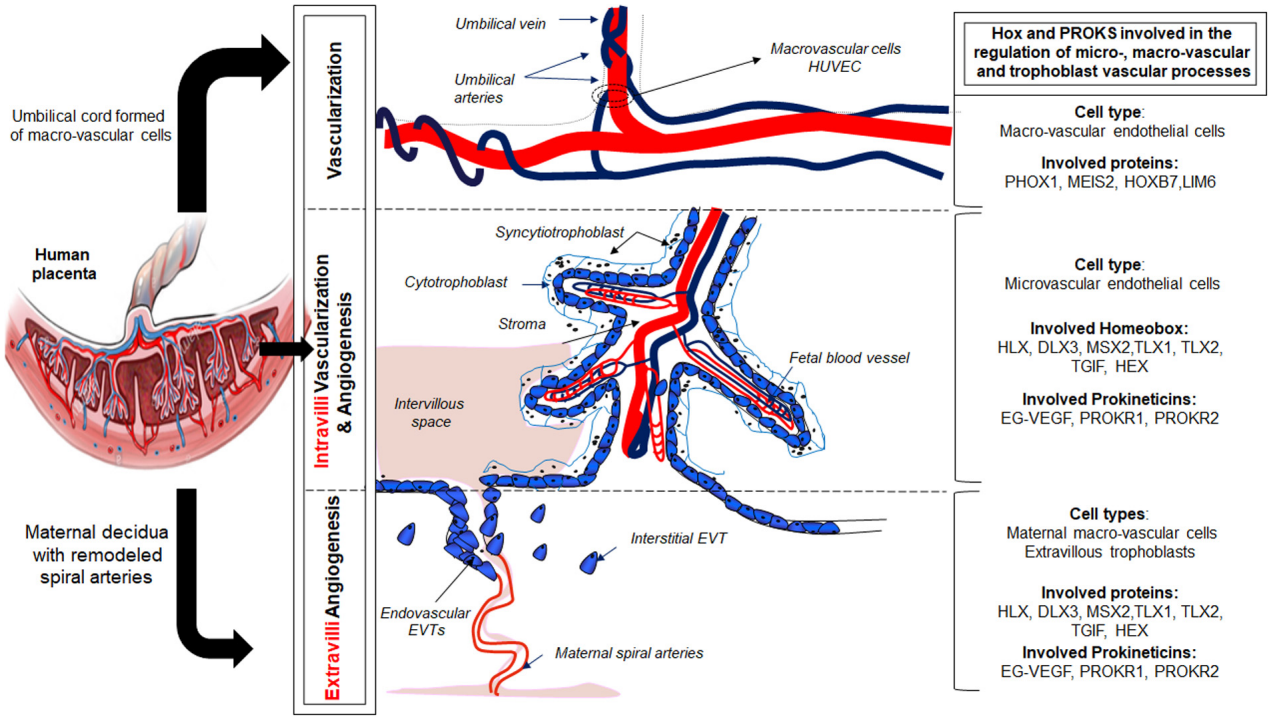


**FIGURE 1 |** Illustration of the role of the prokineticin and HOX family members in the control of placental vascularization and angiogenesis.

environment during this period (Burton, 2009). In 2012, we demonstrated that another key actor of placental development, the human chorionic gonadotropin (βhCG) upregulates the expression of EG-VEGF and its receptors (Brouillet et al., 2012b). Importantly, in 2013, glycosylated-hCG has been reported to regulate another actor of angiogenesis, the TGFb (Berndt et al., 2013). These finding suggest that EG-VEGF belongs to a complex of placenta proteins that are controlled by the master hormone, βhCG to fulfill a well orchestrated angiogenesis. In the same lane, we have also demonstrated in 2015 that part of the effects of the transcription factor PPARγ on placental angiogenesis are mediated by EG-VEGF, suggesting that the placental defects observed in the PPARγ knockout mice might well be due to deregulations in the EG-VEGF/PROKR functions (Garnier et al., 2015).

## TRANSCRIPTIONAL FACTORS IN THE CONTROL OF PLACENTAL ANGIOGENESIS

Cells respond to cues from growth factors and signaling molecules, allowing them to either maintain or alter their state of differentiation during angiogenesis (Irving and Lala, 1995). However, EC nuclear transcription factors determine how these cues are interpreted and drive the cellular response. Many different types of transcription factors play essential roles in placental cell differentiation, including endothelial and trophoblast cells (Cross et al., 2002). Most transcription factors have common protein structural motifs allowing them to be placed into a few large families (e.g., zinc finger, leucine zipper, helix-loop-helix and helix-turn-helix) (Johnson and McKnight, 1989; Woodside et al., 2004). This review will mainly focus on members of the "homeobox" gene family of transcription factors.

## HOMEOBOX GENES AND HOMEODOMAIN PROTEINS

Homeobox genes are frequently present as clusters of related homeobox genes called "HOX" cluster genes, but there are also individual, divergent HOX-like genes. Homeobox genes contain a highly conserved 180 base pair DNA sequence, which encodes a 60 amino acid "homeodomain" and contains a helix-turn-helix DNA binding motif. Although homeodomain proteins have similar DNA binding specificity, they regulate highly diverse and context-dependent cellular functions (Levine and Hoey, 1988), which includes the processes of vasculogenesis and angiogenesis.

## HOMEOBOX GENES IN MURINE AND HUMAN PLACENTAL DEVELOPMENT

Targeted deletion of specific homeobox genes in murine models provides genetic proof of homeobox gene regulation of placental development during pregnancy (Rossant and Cross, 2001; Myers and Capper, 2002; Gorski and Leal, 2003; Gorski and Walsh, 2003). For example, targeted deletion of Esx1

(Fohn and Behringer, 2001) and Dlx3 (Morasso et al., 1999) resulted in disruption of the vascular network in the placental labyrinthine layer (Cross et al., 2003). Mutant embryos in both cases were growth-restricted, and Dlx3-/- mutants were embryonic lethal due to adequate placental circulation (Morasso et al., 1999). These studies show homeobox genes are specific regulators of placental vascular development.

Recent studies from our laboratory provided comprehensive analyses of homeobox genes in human placental pathologies. We carried out the first screening of a 32-weeks placental cDNA library for homeobox genes, which led to the isolation of DLX4, MSX2, GAX and HLX (Quinn et al., 1997). Immunohistochemical analyses localized these homeobox genes/homeodomain proteins to trophoblasts and ECs (Murthi et al., 2006; Rajaraman et al., 2008; Chui et al., 2010). We also reported decreased homeobox gene HLX expression in ECs and trophoblast cells in FGR-affected placentae (Murthi et al., 2006). Homeobox genes DLX4 and DLX3 showed increased expression in FGR-affected placentae (Murthi et al., 2006), whereas GAX and MSX2 showed no significant difference in expression.

## HOMEOBOX GENE EXPRESSION IN MICRO- AND MACROVASCULAR PLACENTAL ECs

In our studies, primary PLEC were used to identify homeobox genes expressed in the placental microvasculature, and to compare that with macrovascular HUVEC. We detected mRNA expression of homeobox genes HLX, MSX2, DLX3, DLX4, and GAX and in both PLEC and HUVEC. Notably, HLX mRNA in HUVEC was significantly lower compared with PLEC (Murthi et al., 2007). These data provided evidence of heterogeneity in homeobox gene expression between microvascular PLEC and macrovascular HUVEC, which most likely reflects significant differences in EC function in the two different cellular environments, **Table 1**.

## FUNCTIONAL SIGNIFICANCE OF HOMEOBOX GENES IN MICRO- AND MACROVASCULAR ECs

We detected high HLX mRNA expression in PLEC, which are also proliferative cell types compared with their macrovascular counterparts (Murthi et al., 2007). Moreover, in response to placental growth factor (PlGF), PLEC have more proliferative activity compared with HUVEC (Lang et al., 2003; Brouillet et al., 2010). Together, these data suggest a possible role for HLX in the proliferative capacity of microvascular ECs. The role(s), if any, of homeobox genes HLX, MSX2, DLX3, DLX4, and GAX in the transcriptional regulation of other PLEC function such as migration and invasion is yet to be explored. Quinn et al. (2000) proposed that co-expression of a combination of homeobox genes (i.e., HLX, MSX2, and GAX) may play a role in the regulation of epithelial-mesenchymal interactions in the placenta. Thus, co-expression of the homeobox genes in both trophoblast and endothelium may also be important in coordinating villous outgrowth and angiogenesis within the terminal villi. Other studies showed that Homeobox genes regulate numerous key genes such as, CDKN1, RB, GATA2, PPARg, ITGAV, NRP-1, ANGPT-1, and 2 (Rajaraman et al., 2008; Chui et al., 2013; Novakovic et al., 2017; Harris et al., 2019; **Table 1**).

The repertoire of homeobox genes expressed in PLEC, was further investigated by microarray expression profiling of ECs (Murthi et al., 2008). We identified homeobox genes TLX1, TLX2, TGIF, HEX, PHOX1, MEIS2, HOXB7, and LIM6 in PLEC. Importantly, our studies reported that these homeobox genes were differentially expressed in macro- compared with microvascular ECs, **Figure 1**. Functional studies in cultured ECs are underway in our laboratory to determine the role of these novel endothelial homeobox genes.

## GROWTH FACTOR REGULATION OF HOMEOBOX GENES IN THE PLACENTA

Many EC growth factors and signal transduction pathways are involved in the maintenance of an efficient uteroplacental vasculature (Thaete et al., 2004). Our previous studies have demonstrated that HLX expression in *in vitro* models of human EVT, HTR8-SV neo and SGH-PL4 was significantly upregulated by HGF (Rajaraman et al., 2010) and CSF-1 (Rajaraman et al., 2007, 2008). Recent studies also showed that the homeobox gene HOXB7 is regulated by DKK1 and the Wnt-1/b-catenin (Huang et al., 2019; **Table 1**).

In 2015, our group demonstrated that the canonical member of the prokineticin family, EG-VEGF, controls homeobox genes expression in normal human placenta and in placenta from FGR pregnancies (Murthi et al., 2015). This regulation was observed in whole placenta explants, including endothelial, stroma and trophoblast cells. In particular, EG-VEGF up-regulated the following homeobox genes, HOXA9, HOXC8, HOXC10, HOXD1, HOXD8, HOXD9, and HOXD11, while downregulating the expression of NKX 3.1. Further investigations using an *in vitro* model of trophoblast cells, we demonstrated that reduced NKX3.1 expression significantly enhanced premature differentiation and apoptosis in the syncytiotrophoblast cell line, the BeWo, while significantly reduced migration and invasive potential of the HTR8-SV neo cells (Murthi et al., 2015). This study was the first to demonstrate that the new placental angiogenic factor exhibits part of its effects on trophoblast invasion and differentiation through the NKX3.1 homeobox gene. The demonstration that growth factors such as EG-VEGF regulate homeobox genes in the trophoblast lineage, especially the EVT, involved in extravillous angiogenesis, opens new perspectives into the potential involvement of homeobox genes in the cross talk between trophoblast and extra-villi and intra-villi endothelial cells to fulfill placental angiogenesis throughout pregnancy. Ongoing validations of the newly discovered EG-VEGF-regulated homeobox genes should bring more insights into the role of these homeobox genes in the control of angiogenic processes at both intra-villi and extra-villi sites, throughout human pregnancy, **Figure 1**.

**TABLE 1 |** Summarizes the localizations of the prokineticin and HOX members within the placenta, their respective roles in the control of the angiogenesis in macro and microvascular blood vessels and lists their local regulators.

| Placental prokineticins and homeobox genes | Role in the placenta | Type of placenta associated structure | Regulated genes in the placenta | | Placental regulators | Associated placental vascular pathologies | References |
|---|---|---|---|---|---|---|---|
| EG-VEGF, PROKR1 and PROKR2 | Angiogenesis, inflammation Placental development | Trophoblast cells, micro and macrovascular systems, Hofbauer cells | HOXD1, 8, 9, and 11 HOX A9 and HOXC8, 10 | | Nicotine, Hypoxia, βhCG, PPARg | FGR, Hydatidiform moles, Choriocarcinoma and PE | Hoffmann et al., 2006, 2009; Brouillet et al., 2012a,b, 2013b; Holloway et al., 2014; Garnier et al., 2015; Murthi et al., 2015; Traboulsi et al., 2015, 2017; Sergent et al., 2016 |
| HLX, DLX3, DLX4, MSX2, GAX,TLX1,TLX2 | Cell Invasion, migration and proliferation Stem cell proliferation and differentiation | Microvascular system | CDKN1C (+) RB (+) GATA2, PPAR g ITGAV,NRP-1, ANPGT-1 and 2 | VEGF, PLGF, HGF, CSF-1 Angiopoietins, PPARg, IGF-II, Endoglin, TGFb | IGFR2 (-) PLGF (+) | FGR and PE | Murthi et al., 2007, 2008; Rajaraman et al., 2008, 2010; Chui et al., 2013; Liang et al., 2016; Novakovic et al., 2017; Harris et al., 2019 |
| TGIF | | Micro and macrovascular systems | | | | FGR (+) | Pathirage et al., 2013; Gunatillak et al., 2016 |
| HEX | Role in hematopoiesis | Vascular system | | | | | Unpublished data |
| PHOX1 | | Macrovascular system | | | | | Unpublished data |
| MEIS2 | Control of mouse placental vascularization | Macrovascular system | Activin and Inhibin | | | | Unpublished data |
| LIM6 | | Macrovascular system | VEGF | | | | Unpublished data |
| HOXB7 | Endothelial differentiation | Macrovascular system | | | DKK1 (–) Wnt1/b catenin (–) | FGR (+) | Huang et al., 2019 |
| NKX3.1 | Role in trophoblast differentiation and proliferation | Trophoblast lineage | | | EG-VEGF (–) | | Murthi et al., 2015 |
| HOXD1, 8, 9, and 11 HOX A9 and HOXC8, 10 | | | HOXA9 upregulates MMP14, EphB4, eNOS, VEGFR2 | | EG-VEGF (+) | FGR (+) | Murthi et al., 2015 |

*Also reports their associated placental vascular pathologies.*

## PROKINETICINS AND/OR HOMEOBOX GENES AS POTENTIAL TARGETS IN FGR AND PE PATHOLOGIES

Numerous studies from our team have clearly demonstrated that EG-VEGF and its receptors are directly involved in normal placental vascularization and angiogenesis during the first trimester of pregnancy and that maintenance of increased circulating levels of placental EG-VEGF over that trimester is associated with the development of PE and FGR (Hoffmann et al., 2006, 2009; Brouillet et al., 2012b; Murthi et al., 2015; Traboulsi et al., 2015). These finding strongly suggest that antagonisation of EG-VEGF signaling might contribute to the attenuation of vascular-pregnancy pathologies. Importantly, we have recently demonstrated that treatment of animal model of choriocarcinoma with PROKR2 antagonist significantly reduced tumor growth, vascularization and metastasis (Traboulsi et al., 2017). Hence, one can speculate that the benefit upon the antagonisation of the prokineticin signaling might well trigger an upstream regulation of the EG-VEGF-dependent homeobox genes including NKX3.1, HOXA9, HOXC8, HOXC10, HOXD1, HOXD8, HOXD9, and HOXD11 as potential target genes for aberrant angiogenesis associated with the pathogenesis of PE and FGR. Further studies are needed to better characterize the relationship between placental angiogenic factors and the homeobox genes to fulfill successful pregnancy outcomes.

## AUTHOR CONTRIBUTIONS

NA and PM designed the manuscript, supervised the progress of the review, and verified the English aspects. SB, GR, and BK wrote the different parts of the review. MB, TB, and PH helped with the clinical aspects and performed the figure and table. All authors contributed to the article and approved the submitted version.

## FUNDING

We acknowledge the following sources of funding: Institut National de la Santé et de la Recherche Médicale (U1036), University of Grenoble Alpes, Commissariat à l'Energie Atomique (DSV/iRTSV/BCI), Région Auvergne-Rhône-Alpes "CLARA, Oncostarter," Ligue Nationale Contre le Cancer and Ligue Départementale (Savoie) Contre le Cancer, Inserm Transfert.

## REFERENCES

Ahmed, A., and Perkins, J. (2000). Angiogenesis and intrauterine growth restriction. *Baillieres Best Pract. Res. Clin. Obstet. Gynaecol.* 14, 981–998. doi: 10.1053/beog.2000.0139

Alfaidy, N. (2016). Prokineticin1 and pregnancy. *Ann. Endocrinol.* 77, 101–104. doi: 10.1016/j.ando.2016.04.014

Alfaidy, N., Hoffmann, P., Gillois, P., Gueniffey, A., Lebayle, C., Garcin, H., et al. (2016). PROK1 level in the follicular microenvironment: a new noninvasive predictive biomarker of embryo implantation. *J. Clin. Endocrinol. Metab.* 101, 435–444. doi: 10.1210/jc.2015-1988

Arderiu, G., Cuevas, I., Chen, A., Carrio, M., East, L., and Boudreau, N. J. (2007). HoxA5 stabilizes adherens junctions via increased Akt1. *Cell Adh. Migr.* 1, 185–195. doi: 10.4161/cam.1.4.5448

Berndt, S., Blacher, S., Munaut, C., Detilleux, J., Perrier d'Hauterive, S., Huhtaniemi, I., et al. (2013). Hyperglycosylated human chorionic gonadotropin stimulates angiogenesis through TGF-beta receptor activation. *FASEB J.* 27, 1309–1321. doi: 10.1096/fj.12-213686

Brouillet, S., Dufour, A., Prot, F., Feige, J. J., Equy, V., Alfaidy, N., et al. (2014a). Influence of the umbilical cord insertion site on the optimal individual birth weight achievement. *Biomed. Res. Int.* 2014:341251. doi: 10.1155/2014/341251

Brouillet, S., Hoffmann, P., Alfaidy, N., and Feige, J. J. (2014b). [Prokineticins: new regulatory peptides in human reproduction]. *Med. Sci.* 30, 274–279. doi: 10.1051/medsci/20143003015

Brouillet, S., Hoffmann, P., Benharouga, M., Salomon, A., Schaal, J. P., Feige, J. J., et al. (2010). Molecular characterization of EG-VEGF-mediated angiogenesis: differential effects on microvascular and macrovascular endothelial cells. *Mol. Biol. Cell* 21, 2832–2843. doi: 10.1091/mbc.E10-01-0059

Brouillet, S., Hoffmann, P., Chauvet, S., Salomon, A., Chamboredon, S., Sergent, F., et al. (2012a). Revisiting the role of hCG: new regulation of the angiogenic factor EG-VEGF and its receptors. *Cell Mol. Life Sci.* 69, 1537–1550. doi: 10.1007/s00018-011-0889-x

Brouillet, S., Hoffmann, P., Feige, J. J., and Alfaidy, N. (2012b). EG-VEGF: a key endocrine factor in placental development. *Trends Endocrinol. Metab.* 23, 501–508. doi: 10.1016/j.tem.2012.05.006

Brouillet, S., Hoffmann, P., Thomas-Cadi, C., Bergues, U., Feige, J. J., Alfaidy, N., et al. (2013a). [PROK1, prognostic marker of embryo implantation?]. *Gynecol. Obstet. Fertil.* 41, 562–565. doi: 10.1016/j.gyobfe.2013.07.007

Brouillet, S., Murthi, P., Hoffmann, P., Salomon, A., Sergent, F., De Mazancourt, P., et al. (2013b). EG-VEGF controls placental growth and survival in normal and pathological pregnancies: case of fetal growth restriction (FGR). *Cell Mol. Life Sci.* 70, 511–525. doi: 10.1007/s00018-012-1141-z

Burton, G. J. (2009). Oxygen, the Janus gas; its effects on human placental development and function. *J. Anat.* 215, 27–35. doi: 10.1111/j.1469-7580.2008.00978.x

Burton, G. J., and Jaunaiux, E. (2001). Maternal vascularisation of the human placenta: does the embryo develop in a hypoxic environment? *Gynecol. Obstet. Fertil.* 29, 503–508. doi: 10.1016/s1297-9589(01)00179-5

Chaddha, V., Viero, S., Huppertz, B., and Kingdom, J. (2004). Developmental biology of the placenta and the origins of placental insufficiency. *Semin. Fetal Neonatal. Med.* 9, 357–369. doi: 10.1016/j.siny.2004.03.006

Charnock-Jones, D. S. (2002). Soluble flt-1 and the angiopoietins in the development and regulation of placental vasculature. *J. Anat.* 200, 607–615. doi: 10.1046/j.1469-7580.2002.00063.x

Chen, C. P., Bajoria, R., and Aplin, J. D. (2002). Decreased vascularization and cell proliferation in placentas of intrauterine growth-restricted fetuses with abnormal umbilical artery flow velocity waveforms. *Am. J. Obstet. Gynecol.* 187, 764–769. doi: 10.1067/mob.2002.125243

Chui, A., Kalionis, B., Abumaree, M., Cocquebert, M., Fournier, T., Evain-Brion, D., et al. (2013). Downstream targets of the homeobox gene DLX3 are differentially expressed in the placentae of pregnancies affected by human idiopathic fetal growth restriction. *Mol. Cell. Endocrinol.* 377, 75–83. doi: 10.1016/j.mce.2013.06.032

Chui, A., Pathirage, N. A., Johnson, B., Cocquebert, M., Fournier, T., Evain-Brion, D., et al. (2010). Homeobox gene distal-less 3 is expressed in proliferating and differentiating cells of the human placenta. *Placenta* 31, 691–697. doi: 10.1016/j.placenta.2010.05.003

Clark, D. E., Smith, S. K., Sharkey, A. M., and Charnock-Jones, D. S. (1996). Localization of VEGF and expression of its receptors flt and KDR in human placenta throughout pregnancy. *Hum. Reprod.* 11, 1090–1098. doi: 10.1093/oxfordjournals.humrep.a019303

Cross, J. C., Baczyk, D., Dobric, N., Hemberger, M., Hughes, M., Simmons, D. G., et al. (2003). Genes, development and evolution of the placenta. *Placenta* 24, 123–130. doi: 10.1053/plac.2002.0887

Cross, J. C., Hemberger, M., Lu, Y., Nozaki, T., Whiteley, K., Masutani, M., et al. (2002). Trophoblast functions, angiogenesis and remodeling of the maternal vasculature in the placenta. *Mol. Cell. Endocrinol.* 187, 207–212. doi: 10.1016/s0303-7207(01)00703-1

Demir, R., Kaufmann, P., Castellucci, M., Erbengi, T., and Kotowski, A. (1989). Fetal vasculogenesis and angiogenesis in human placental villi. *Acta Anat.* 136, 190–203. doi: 10.1159/000146886

Fohn, L. E., and Behringer, R. R. (2001). ESX1L, a novel X chromosome-linked human homeobox gene expressed in the placenta and testis. *Genomics* 74, 105–108. doi: 10.1006/geno.2001.6532

Garnier, V., Traboulsi, W., Salomon, A., Brouillet, S., Fournier, T., Winkler, C., et al. (2015). PPARgamma controls pregnancy outcome through activation of EG-VEGF: new insights into the mechanism of placental development. *Am. J. Physiol. Endocrinol. Metab.* 309, E357–E369. doi: 10.1152/ajpendo.00093.2015

Gorski, D. H., and Leal, A. J. (2003). Inhibition of endothelial cell activation by the homeobox gene Gax. *J. Surg. Res.* 111, 91–99. doi: 10.1016/s0022-4804(03)00042-8

Gorski, D. H., and Walsh, K. (2003). Control of vascular cell differentiation by homeobox transcription factors. *Trends Cardiovasc. Med.* 13, 213–220. doi: 10.1016/s1050-1738(03)00081-1

Gude, N. M., Roberts, C. T., Kalionis, B., and King, R. G. (2004). Growth and function of the normal human placenta. *Thromb. Res.* 114, 397–407. doi: 10.1016/j.thromres.2004.06.038

Harris, L. K., Pantham, P., Yong, H. E. J., Pratt, A., Borg, A. J., Crocker, I., et al. (2019). The role of insulin-like growth factor 2 receptor-mediated homeobox gene expression in human placental apoptosis, and its implications in idiopathic fetal growth restriction. *Mol. Hum. Reprod.* 25, 572–585. doi: 10.1093/molehr/gaz047

Hoffmann, P., Feige, J. J., and Alfaidy, N. (2006). Expression and oxygen regulation of endocrine gland-derived vascular endothelial growth factor/prokineticin-1 and its receptors in human placenta during early pregnancy. *Endocrinology* 147, 1675–1684. doi: 10.1210/en.2005-0912

Hoffmann, P., Saoudi, Y., Benharouga, M., Graham, C. H., Schaal, J. P., Mazouni, C., et al. (2009). Role of EG-VEGF in human placentation: physiological and pathological implications. *J. Cell Mol. Med.* 13, 2224–2235. doi: 10.1111/j.1582-4934.2008.00554.x

Holloway, A. C., Salomon, A., Soares, M. J., Garnier, V., Raha, S., Sergent, F., et al. (2014). Characterization of the adverse effects of nicotine on placental development: in vivo and in vitro studies. *Am. J. Physiol. Endocrinol. Metab.* 306, E443–E456. doi: 10.1152/ajpendo.00478.2013

Huang, L., Ying, H., Chen, Z., Zhu, Y. L., Gu, Y., Hu, L., et al. (2019). Down-regulation of DKK1 and Wnt1/beta-catenin pathway by increased homeobox B7 resulted in cell differentiation suppression of intrauterine fetal growth retardation in human placenta. *Placenta* 80, 27–35. doi: 10.1016/j.placenta.2019.03.001

Inan, C., Varol, F. G., Erzincan, S. G., Uzun, I., Sutcu, H., and Sayin, N. C. (2018). Use of prokineticin-1 (PROK1), pregnancy-associated plasma protein A (PAPP-A) and PROK1/PAPP-A ratio to predict adverse pregnancy outcomes in the first trimester: a prospective study. *J. Matern. Fetal Neonatal Med.* 31, 2685–2692. doi: 10.1080/14767058.2017.1351536

Irving, J. A., and Lala, P. K. (1995). Functional role of cell surface integrins on human trophoblast cell migration: regulation by TGF-beta, IGF-II, and IGFBP-1. *Exp. Cell Res.* 217, 419–427. doi: 10.1006/excr.1995.1105

Jackson, M. R., Carney, E. W., Lye, S. J., and Ritchie, J. W. (1994). Localization of two angiogenic growth factors (PDECGF and VEGF) in human placentae throughout gestation. *Placenta* 15, 341–353. doi: 10.1016/0143-4004(94)90002-7

Johnson, P. F., and McKnight, S. L. (1989). Eukaryotic transcriptional regulatory proteins. *Annu. Rev. Biochem.* 58, 799–839. doi: 10.1146/annurev.bi.58.070189.004055

Kaufmann, P., Mayhew, T. M., and Charnock-Jones, D. S. (2004). Aspects of human fetoplacental vasculogenesis and angiogenesis. II. Changes during normal pregnancy. *Placenta* 25, 114–126. doi: 10.1016/j.placenta.2003.10.009

Kingdom, J., Huppertz, B., Seaward, G., and Kaufmann, P. (2000). Development of the placental villous tree and its consequences for fetal growth. *Eur. J. Obstet. Gynecol. Reprod. Biol.* 92, 35–43. doi: 10.1016/s0301-2115(00)00423-1

Lang, I., Pabst, M. A., Hiden, U., Blaschitz, A., Dohr, G., Hahn, T., et al. (2003). Heterogeneity of microvascular endothelial cells isolated from human term placenta and macrovascular umbilical vein endothelial cells. *Eur. J. Cell Biol.* 82, 163–173. doi: 10.1078/0171-9335-00306

LeCouter, J., Kowalski, J., Foster, J., Hass, P., Zhang, Z., Dillard-Telm, L., et al. (2001). Identification of an angiogenic mitogen selective for endocrine gland endothelium. *Nature* 412, 877–884. doi: 10.1038/35091000

Levine, M., and Hoey, T. (1988). Homeobox proteins as sequence-specific transcription factors. *Cell* 55, 537–540. doi: 10.1016/0092-8674(88)90209-7

Liang, H., Zhang, Q., Lu, J., Yang, G., Tian, N., Wang, X., et al. (2016). MSX2 Induces Trophoblast Invasion in Human Placenta. *PLoS One* 11:e0153656. doi: 10.1371/journal.pone.0153656

Lin, D. C., Bullock, C. M., Ehlert, F. J., Chen, J. L., Tian, H., and Zhou, Q. Y. (2002). Identification and molecular characterization of two closely related G protein-coupled receptors activated by prokineticins/endocrine gland vascular endothelial growth factor. *J. Biol. Chem.* 277, 19276–19280. doi: 10.1074/jbc.M202139200

Maulik, D., Frances Evans, J., and Ragolia, L. (2006). Fetal growth restriction: pathogenic mechanisms. *Clin. Obstet. Gynecol.* 49, 219–227. doi: 10.1097/00003081-200606000-00005

Mayhew, T. M. (2003). Changes in fetal capillaries during preplacental hypoxia: growth, shape remodelling and villous capillarization in placentae from high-altitude pregnancies. *Placenta* 24, 191–198. doi: 10.1053/plac.2002.0895

Mayhew, T. M., Ohadike, C., Baker, P. N., Crocker, I. P., Mitchell, C., and Ong, S. S. (2003). Stereological investigation of placental morphology in pregnancies complicated by pre-eclampsia with and without intrauterine growth restriction. *Placenta* 24, 219–226. doi: 10.1053/plac.2002.0900

Meegdes, B. H., Ingenhoes, R., Peeters, L. L., and Exalto, N. (1988). Early pregnancy wastage: relationship between chorionic vascularization and embryonic development. *Fertil. Steril.* 49, 216–220. doi: 10.1016/s0015-0282(16)59704-0

Morasso, M. I., Grinberg, A., Robinson, G., Sargent, T. D., and Mahon, K. A. (1999). Placental failure in mice lacking the homeobox gene Dlx3. *Proc. Natl. Acad. Sci. U.S.A.* 96, 162–167. doi: 10.1073/pnas.96.1.162

Murthi, P., Brouillet, S., Pratt, A., Borg, A., Kalionis, B., Goffin, F., et al. (2015). An EG-VEGF-dependent decrease in homeobox gene NKX3.1 contributes to cytotrophoblast dysfunction: a possible mechanism in human fetal growth restriction. *Mol. Med.* 21, 645–656. doi: 10.2119/molmed.2015.00071

Murthi, P., Hiden, U., Rajaraman, G., Liu, H., Borg, A. J., Coombes, F., et al. (2008). Novel homeobox genes are differentially expressed in placental microvascular endothelial cells compared with macrovascular cells. *Placenta* 29, 624–630. doi: 10.1016/j.placenta.2008.04.006

Murthi, P., Said, J. M., Doherty, V. L., Donath, S., Nowell, C. J., Brennecke, S. P., et al. (2006). Homeobox gene DLX4 expression is increased in idiopathic human fetal growth restriction. *Mol. Hum. Reprod.* 12, 763–769. doi: 10.1093/molehr/gal087

Murthi, P., So, M., Gude, N. M., Doherty, V. L., Brennecke, S. P., and Kalionis, B. (2007). Homeobox genes are differentially expressed in macrovascular human umbilical vein endothelial cells and microvascular placental endothelial cells. *Placenta* 28, 219–223. doi: 10.1016/j.placenta.2006.02.012

Myers, L. J., and Capper, W. L. (2002). A transmission line model of the human foetal circulatory system. *Med. Eng. Phys.* 24, 285–294. doi: 10.1016/s1350-4533(02)00019-x

Novakovic, B., Fournier, T., Harris, L. K., James, J., Roberts, C. T., Yong, H. E. J., et al. (2017). Increased methylation and decreased expression of homeobox genes TLX1, HOXA10 and DLX5 in human placenta are associated with trophoblast differentiation. *Sci. Rep.* 7:4523. doi: 10.1038/s41598-017-04776-5

Patel, N. S., Li, J. L., Generali, D., Poulsom, R., Cranston, D. W., and Harris, A. L. (2005). Up-regulation of delta-like 4 ligand in human tumor vasculature and the role of basal expression in endothelial cell function. *Cancer Res.* 65, 8690–8697. doi: 10.1158/0008-5472.CAN-05-1208

Quinn, L. M., Johnson, B. V., Nicholl, J., Sutherland, G. R., and Kalionis, B. (1997). Isolation and identification of homeobox genes from the human placenta including a novel member of the Distal-less family, DLX4. *Gene* 187, 55–61. doi: 10.1016/s0378-1119(96)00706-8

Quinn, L. M., Latham, S. E., and Kalionis, B. (2000). The homeobox genes MSX2 and MOX2 are candidates for regulating epithelial-mesenchymal cell interactions in the human placenta. *Placenta* 21(Suppl. A), S50–S54. doi: 10.1053/plac.1999.0514

Rajaraman, G., Murthi, P., Brennecke, S. P., and Kalionis, B. (2010). Homeobox gene HLX is a regulator of HGF/c-met-mediated migration of human trophoblast-derived cell lines. *Biol. Reprod.* 83, 676–683. doi: 10.1095/biolreprod.109.078634

Rajaraman, G., Murthi, P., Leo, B., Brennecke, S. P., and Kalionis, B. (2007). Homeobox gene HLX1 is a regulator of colony stimulating factor-1 dependent trophoblast cell proliferation. *Placenta* 28, 991–998. doi: 10.1016/j.placenta.2007.03.011

Rajaraman, G., Murthi, P., Quinn, L., Brennecke, S. P., and Kalionis, B. (2008). Homeodomain protein HLX is expressed primarily in cytotrophoblast cell types in the early pregnancy human placenta. *Reprod. Fertil. Dev.* 20, 357–367. doi: 10.1071/rd07159

Regnault, T. R., Galan, H. L., Parker, T. A., and Anthony, R. V. (2002). Placental development in normal and compromised pregnancies– a review. *Placenta* 23(Suppl. A), S119–S129. doi: 10.1053/plac.2002.0792

Rossant, J., and Cross, J. C. (2001). Placental development: lessons from mouse mutants. *Nat. Rev. Genet.* 2, 538–548. doi: 10.1038/35080570

Salafia, C. M., Charles, A. K., and Maas, E. M. (2006). Placenta and fetal growth restriction. *Clin. Obstet. Gynecol* 49, 236–256. doi: 10.1097/00003081-200606000-00007

Sergent, F., Hoffmann, P., Brouillet, S., Garnier, V., Salomon, A., Murthi, P., et al. (2016). Sustained endocrine gland-derived vascular endothelial growth factor levels beyond the first trimester of pregnancy display phenotypic and functional changes associated with the pathogenesis of pregnancy-induced hypertension. *Hypertension* 68, 148–156. doi: 10.1161/HYPERTENSIONAHA.116.07442

Thaete, L. G., Dewey, E. R., and Neerhof, M. G. (2004). Endothelin and the regulation of uterine and placental perfusion in hypoxia-induced fetal growth restriction. *J. Soc. Gynecol. Investig.* 11, 16–21. doi: 10.1016/j.jsgi.2003.07.001

Traboulsi, W., Brouillet, S., Sergent, F., Boufettal, H., Samouh, N., Aboussaouira, T., et al. (2015). Prokineticins in central and peripheral control of human reproduction. *Horm. Mol. Biol. Clin. Investig.* 24, 73–81. doi: 10.1515/hmbci-2015-0040

Traboulsi, W., Sergent, F., Boufettal, H., Brouillet, S., Slim, R., Hoffmann, P., et al. (2017). Antagonism of EG-VEGF Receptors as Targeted Therapy for Choriocarcinoma Progression In Vitro and In Vivo. *Clin Cancer Res* 23, 7130–7140. doi: 10.1158/1078-0432.CCR-17-0811

Tsatsaris, V., Goffin, F., Munaut, C., Brichant, J. F., Pignon, M. R., Noel, A., et al. (2003). Overexpression of the soluble vascular endothelial growth factor receptor in preeclamptic patients: pathophysiological consequences. *J. Clin. Endocrinol. Metab.* 88, 5555–5563. doi: 10.1210/jc.2003-030528

Velicky, P., Knofler, M., and Pollheimer, J. (2016). Function and control of human invasive trophoblast subtypes: intrinsic vs. maternal control. *Cell Adh. Migr.* 10, 154–162. doi: 10.1080/19336918.2015.1089376

Woodside, K. J., Shen, H., Muntzel, C., Daller, J. A., Sommers, C. L., and Love, P. E. (2004). Expression of Dlx and Lhx family homeobox genes in fetal thymus and thymocytes. *Gene Expr. Patterns* 4, 315–320. doi: 10.1016/j.modgep.2003.10.003

Zhao, Y., Wu, J., Wang, X., Jia, H., Chen, D. N., and Li, J. D. (2019). Prokineticins and their G protein-coupled receptors in health and disease. *Prog. Mol. Biol. Transl. Sci.* 161, 149–179. doi: 10.1016/bs.pmbts.2018.09.006

Zou, J., Luo, H., Zeng, Q., Dong, Z., Wu, D., and Liu, L. (2011). Protein kinase CK2alpha is overexpressed in colorectal cancer and modulates cell proliferation and invasion via regulating EMT-related genes. *J. Transl. Med.* 9:97. doi: 10.1186/1479-5876-9-97

Zygmunt, M., Herr, F., Munstedt, K., Lang, U., and Liang, O. D. (2003). Angiogenesis and vasculogenesis in pregnancy. *Eur. J. Obstet. Gynecol. Reprod. Biol.* 110(Suppl. 1), S10–S18. doi: 10.1016/s0301-2115(03)00168-4

**Conflict of Interest:** The authors declare that the research was conducted in the absence of any commercial or financial relationships that could be construed as a potential conflict of interest.

frontiers in Physiology

PERSPECTIVE
published: 20 January 2021
doi: 10.3389/fphys.2020.616189

# Towards Novel Geneless Approaches for Therapeutic Angiogenesis

*Francesco Moccia[1†], Maria Rosa Antognazza[2†] and Francesco Lodola[2,3*]*

[1]Department of Biology and Biotechnology "L. Spallanzani", University of Pavia, Pavia, Italy, [2]Center for Nano Science and Technology @PoliMi, Istituto Italiano di Tecnologia, Milan, Italy, [3]Department of Biotechnology and Biosciences, University of Milano-Bicocca, Milan, Italy

Cardiovascular diseases are the leading cause of mortality worldwide. Such a widespread diffusion makes the conditions affecting the heart and blood vessels a primary medical and economic burden. It, therefore, becomes mandatory to identify effective treatments that can alleviate this global problem. Among the different solutions brought to the attention of the medical-scientific community, therapeutic angiogenesis is one of the most promising. However, this approach, which aims to treat cardiovascular diseases by generating new blood vessels in ischemic tissues, has so far led to inadequate results due to several issues. In this perspective, we will discuss cutting-edge approaches and future perspectives to alleviate the potentially lethal impact of cardiovascular diseases. We will focus on the consolidated role of resident endothelial progenitor cells, particularly endothelial colony forming cells, as suitable candidates for cell-based therapy demonstrating the importance of targeting intracellular $Ca^{2+}$ signaling to boost their regenerative outcome. Moreover, we will elucidate the advantages of physical stimuli over traditional approaches. In particular, we will critically discuss recent results obtained by using optical stimulation, as a novel strategy to drive endothelial colony forming cells fate and its potential in the treatment of cardiovascular diseases.

**Keywords: cardiovascular disease, therapeutic angiogenesis, endothelial colony forming cells, intracellular $Ca^{2+}$ signaling, transient receptor potential vanilloid 1, cell fate, optical stimulation, conjugated polymers**

OPEN ACCESS

***Edited by:***
*Sara Petrillo,*
*University of Turin, Italy*

***Reviewed by:***
*Andrea Gerbino,*
*National Research Council, Italy*
*Roberto Berra-Romani,*
*Benemérita Universidad Autónoma de Puebla, Mexico*
*Anna Laurenzana,*
*University of Florence, Italy*

***Correspondence:**
*Francesco Lodola*
*francesco.lodola@unimib.it*

*[†]These authors have contributed equally to this work*

***Specialty section:***
*This article was submitted to Vascular Physiology, a section of the journal Frontiers in Physiology*

***Received:*** *11 October 2020*
***Accepted:*** *08 December 2020*
***Published:*** *20 January 2021*

***Citation:***
*Moccia F, Antognazza MR and Lodola F (2021) Towards Novel Geneless Approaches for Therapeutic Angiogenesis. Front. Physiol. 11:616189. doi: 10.3389/fphys.2020.616189*

## INTRODUCTION

The vascular network is indispensable for all organisms to distribute oxygen ($O_2$) and nutrients to the tissues and to remove carbon dioxide and other metabolic waste products (Heinke et al., 2012). Additionally, the circulatory system serves to maintain homeostasis by stabilizing body temperature and avoiding pH unbalance, to facilitate inter-organ humoral communication, and finally, to guide immune cells towards sites of inflammation or infection (Heinke et al., 2012; Udan et al., 2013). Insufficient vascularization or impairment of regional blood flow due to local vessel obstruction results in ischemia, thereby promoting coronary artery disease, acute myocardial infarction, peripheral artery disease, stroke, pre-eclampsia, and obesity- or neurodegenerative associated disorders (Draoui et al., 2017; Potente and Mäkinen, 2017). Cardiovascular disease (CVD) induced by disruption of the vascular network in heart, limbs and brain is, therefore, regarded as a global medical and economic issue with high prevalence

and mortality rates (Benjamin et al., 2019). The World Health Organization and Global Burden Disease have listed CVD as the first cause of death worldwide (Mensah et al., 2019). Therapeutic angiogenesis (TA) represents a promising strategy that aims at reconstructing the damaged vascular network by stimulating the regrowth of the endothelial cell layer that lines the inner lumen of blood vessels and plays a crucial role in adjusting blood supply according to local energy demand (Qadura et al., 2018; Prasad et al., 2020). Endothelial colony forming cells (ECFCs), which represent the only known truly endothelial precursor (Medina et al., 2017), are mobilized in peripheral circulation to maintain endothelial homeostasis throughout postnatal life and to rescue local blood flow upon an ischemic insult (D'Alessio et al., 2015; Tasev et al., 2016; O'Neill et al., 2018). A wealth of *in vitro* and *in vivo* studies has been recently carried out to design an effective strategy to stimulate endogenous ECFCs' regenerative potential for therapeutic purposes, thereby alleviating the life-threatening impact of CVD (Tasev et al., 2016; Moccia et al., 2018a; O'Neill et al., 2018; Paschalaki and Randi, 2018).

In this perspective, we will briefly describe how endothelial precursors generate the primitive vascular plexus and can, therefore, be exploited for TA. Then, we will explain the rationale for targeting the $Ca^{2+}$ handling machinery, which delivers a crucial pro-angiogenic signaling input. Finally, we will review recent approaches, based on the use of physical stimuli in place of chemical cues. Specifically, we will report on the use of visible light pulses to stimulate ECFCs' proliferation and bidimensional tube formation. Optical modulation could provide an effective strategy to rescue ECFCs' vasoreparative potential in patients affected by CVD and to circumvent the main hurdles associated to autologous stem cell therapy.

## THE ROLE OF ECFCs IN VASCULAR DEVELOPMENT AND HOMEOSTASIS: ORIGIN, CHARACTERIZATION, AND SUITABILITY OF THERAPEUTIC ANGIOGENESIS

The circulatory system is the first functional organ to develop (already during gastrulation) with the purpose to supply growing tissues with $O_2$ and nutrients and thereby sustain organism growth (Udan et al., 2013; Potente and Mäkinen, 2017). Embryonic blood vessels arise from endothelial progenitor cells (EPCs), also known as angioblasts, which differentiate from multipotent mesodermal precursors. EPCs coalesce and assembly into a primitive capillary plexus, according to a process known as vasculogenesis. This is followed by further expansion of the vascular network *via* angiogenesis, which may occur through either sprouting or splitting of pre-existing vessels (Udan et al., 2013; Potente and Mäkinen, 2017). The endothelial monolayer retains a state of proliferative quiescence for years, but it may undergo sprouting angiogenesis to meet local metabolic demand under hypoxia, i.e., during skeletal muscle exercise, or in the cycling ovary and in the placenta during pregnancy (Potente and Mäkinen, 2017). Furthermore, EPCs may be released on demand by cytokines released from hypoxic/injured tissues to support local angiogenesis and rescue local blood flow (Moccia et al., 2012; O'Neill et al., 2018). Since the landmark discovery of a population of endothelial precursors circulating in peripheral blood (Asahara et al., 1997), multiple EPC subtypes were isolated, characterized and probed for their therapeutic potential (Asahara et al., 2011; Keighron et al., 2018). Nevertheless, ECFCs were recently presented as the most suitable cellular substrate for regenerative therapy of CVD (Moccia et al., 2015; Tasev et al., 2016; Medina et al., 2017; Paschalaki and Randi, 2018; O'Leary et al., 2019). Unlike other myeloid EPC subtypes, which stimulate neovessel growth in a paracrine manner, ECFCs display the following properties: (1) they are truly endothelial progenitors, able to assembly into capillary-networks *in vitro* and to form patent vessels *in vivo*; (2) display high clonogenic potential and may be replated into secondary and tertiary colonies; (3) rescue injured vascular networks by physically engrafting within neovessels and by releasing pro-angiogenic signals; (4) interact with perimural cells, which ensures neovessel stability; and (5) are more amenable for pharmacological and genetic manipulation aiming at improving their vasoreparative phenotype (Moccia et al., 2015, 2018a,b; Tasev et al., 2016; Medina et al., 2017; Paschalaki and Randi, 2018; O'Leary et al., 2019).

## INTRACELLULAR $Ca^{2+}$ SIGNALING DRIVES ECFCs' ANGIOGENIC ACTIVITY

A finely tuned spatio-temporal increase in intracellular $Ca^{2+}$ concentration $[(Ca^{2+})_i]$ in vascular endothelial cells has long been known to stimulate angiogenesis (Fiorio Pla and Munaron, 2014; Moccia et al., 2014, 2019; Negri et al., 2020a). Endothelial $Ca^{2+}$ signals may indeed mediate the pro-angiogenic effect of multiple growth factors, including vascular endothelial growth factor (VEGF; Potenza et al., 2014; Yokota et al., 2015; Savage et al., 2019), and epidermal growth factor (Moccia et al., 2003), inflammatory mediators, such as ATP (Moccia et al., 2001), and pleiotropic hormones, such as erythropoietin (Yu et al., 2017). Likewise, a recent series of reports documented that intracellular $Ca^{2+}$ signals stimulate ECFCs to undergo angiogenesis both *in vitro* (Zuccolo et al., 2016; Lodola et al., 2017a; Wu et al., 2017) and *in vivo* (Zuccolo et al., 2018; Balbi et al., 2019). For instance, VEGF-induced intracellular $Ca^{2+}$ oscillations stimulated ECFC proliferation and tube formation by promoting the nuclear translocation of the $Ca^{2+}$-sensitive transcription factor, nuclear factor-κB (NF-κB; Dragoni et al., 2015b; Lodola et al., 2017a), whereas biphasic $Ca^{2+}$ signals favored stromal derived factor-1α (SDF-1α)-induced ECFC homing to injured tissues by recruiting the extracellular signal-regulated kinase (ERK) and phosphoinositide 3-kinases (PI3K)/Akt (Zuccolo et al., 2018). The $Ca^{2+}$ response to these pro-angiogenic cues was initiated by endogenous $Ca^{2+}$ release from the endoplasmic reticulum (ER) through inositol-1,4,5-trisphosphate ($InsP_3$) receptors ($InsP_3Rs$), followed by store-operated $Ca^{2+}$ entry (SOCE) activation (Lodola et al., 2017a; Zuccolo et al., 2018; **Figure 1**). SOCE is activated upon $InsP_3$-induced ER $Ca^{2+}$

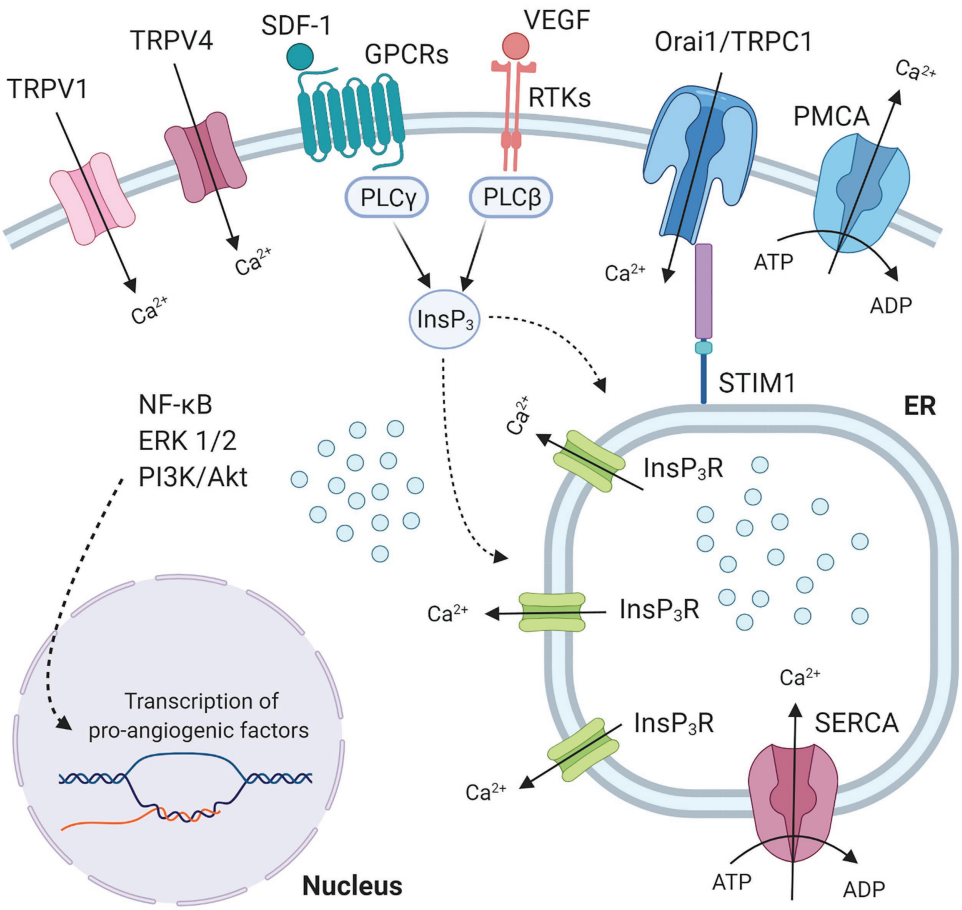


**FIGURE 1 |** Endothelial colony forming cells (ECFCs) $Ca^{2+}$ machinery and pro-angiogenic $Ca^{2+}$ signals. Growth factors (like VEGF or IGF2) and chemokines (like SDF-1) bind to Receptor tyrosine kinases (RTKs) and G protein-coupled receptors (GPCRs) respectively, thus activating specific PLC isoforms, which in turn leads to production of inositol 1,4,5-trisphosphate ($InsP_3$). $InsP_3$ binds to $InsP_3$ receptors ($InsP_3R$) bearing the release of $Ca^{2+}$ from the endoplasmic reticulum (ER) pool. The $Ca^{2+}$ store depletion, detected by $Ca^{2+}$ sensor Stromal interaction molecule 1 (STIM1), is the signal for store-operated calcium entry (SOCE) activation. SOCE, the major $Ca^{2+}$ entry pathway in ECFCs, is mediated by the interaction among STIM1 and the proteins Orai1 and Transient receptor potential canonical 1 (TRPC1). These plasma membrane pore channels allow $Ca^{2+}$ entry from the extracellular space that will be subsequently transported from the cytosol within the SR by the Sarco-Endoplasmic Reticulum Calcium ATPase (SERCA), while Plasma membrane Calcium ATPase (PMCA) contributes to clear cytosolic $Ca^{2+}$ levels. Transient receptor potential vanilloid (TRPV) channels (TRPV1 and TRPV4) also represent an alternative pathway for extracellular $Ca^{2+}$ entry in ECFCs. These intracellular $Ca^{2+}$ signals evoke pathways (NF-κB, ERK1/2, PI3K/Akt) that lead to nuclear transcription of pro-angiogenic factors.

depletion to refill the ER with $Ca^{2+}$ and is mediated by the interplay among STIM1, Orai1, and Transient Receptor Potential (TRP) Canonical 1 in ECFCs (Lodola et al., 2012; **Figure 1**). TRP channels provide an alternative pathway for extracellular $Ca^{2+}$ entry in both vascular endothelial cells (Negri et al., 2020a) and ECFCs (Inoue and Xiong, 2009; Hofmann et al., 2014; Dragoni et al., 2015a; **Figure 1**). Endothelial cells use TRP channels to sense the local microenvironment in which they reside, thereby adapting to subtle changes in the chemical composition of the extracellular milieu and/or in the mechanical forces acting on the vascular wall (Genova et al., 2020; Negri et al., 2020a). For instance, the endothelial TRPV1 is sensitive to an increase in local temperature above 43°C (Negri et al., 2020b) and/or in local hydrogen peroxide ($H_2O_2$; DelloStritto et al., 2016), whereas TRPV4 is sensitive to physical stimuli, such as shear stress (Schierling et al., 2011) and pulsatile stretch (Thodeti et al., 2009), and to arachidonic acid (AA) production (Fiorio Pla et al., 2008). Recent studies suggested that TRP channels may also stimulate ECFCs' angiogenic activity. For instance, TRPV1-mediated uptake of anandamide stimulates ECFC migration (Hofmann et al., 2014), whereas TRPV4-mediated nitric oxide release promotes the pro-angiogenic effects of AA (Zuccolo et al., 2016). It has, therefore, been suggested that targeting TRP channels could represent an efficient strategy to boost ECFCs' regenerative potential (Moccia et al., 2015, 2018a). Indeed, TRP channels are physically coupled to specific $Ca^{2+}$-dependent effectors which translate extracellular $Ca^{2+}$ entry through specific pathways into precise biological outputs which differentially affect endothelial cell fate (Smani et al., 2018; Genova et al., 2020; Negri et al., 2020a).

## CURRENT LIMITATIONS OF ECFCs FOR THERAPEUTIC ANGIOGENESIS

ECFCs hold great promise for TA. Conversely, clinical trials clearly showed that cell therapy based upon transplantation of myeloid EPCs fail to induce a remarkable improvement in capillary density and local blood flow in patients affected by CVD (Moccia et al., 2012; Prasad et al., 2020). Indeed, an array of hurdles hampered the enthusiasm towards ECFC introduction in therapy. Firstly, the frequency of circulating ECFCs is rather low, ranging from 0.28 to 15 ECFCs/$10^7$ mononuclear cells, which is insufficient to achieve a therapeutically relevant outcome (Moccia et al., 2017, 2018a). Secondly, ECFCs' angiogenic activity is severely compromised by CVD (Sung et al., 2013; Mauge et al., 2014; Su et al., 2017; Komici et al., 2020) and by cardiovascular risk factors (Shelley et al., 2012; Jarajapu et al., 2014; Mena et al., 2018), which may ultimately lead to ischemia-related disorders. Thirdly, ECFCs' angiogenic activity could be further reduced once they reach the harsh microenvironment of ischemic tissues. For instance, ECFC proliferation and tube formation are affected in the presence of elevated pro-inflammatory signaling (Mena et al., 2018), oxidative stress (Gremmels et al., 2017), and hypoxia (He et al., 2018; Tasev et al., 2018). As recently reviewed (Faris et al., 2020), the therapeutic use of umbilical cord blood-derived ECFCs, which display a greater pro-angiogenic potential as compared to circulating ECFCs, is currently not feasible for the high cost of their processing and banking and potential immune complications. It has, therefore, been proposed that the therapeutic outcome of ECFCs-based treatment of CVD could be remarkably improved by boosting the specific pro-angiogenic signaling pathways of circulating ECFCs (Tasev et al., 2016; Moccia et al., 2018a,b; Paschalaki and Randi, 2018).

## STRATEGIES TO BOOST ANGIOGENESIS BASED ON PHYSICAL STIMULI

The evidence that ECFC harvested from CVD patients often present a dysfunctional phenotype with low proliferative potential and reduced vasculogenic and angiogenic capability boosted numerous efforts to improve ECFC therapeutic efficacy (Paschalaki and Randi, 2018). The large majority of these trials relies on a chemical approach, and include epigenetic activation through stimulation of proangiogenic signaling pathways by specific drugs, as well as administration of bioactive compounds (i.e. fucoidan, genistein, globular adiponectin; Tasev et al., 2016). Very recently, acidic preconditioning has been also reported to have positive effects on ECFC adhesion, vascular density and inflammation reduction (Mena et al., 2018). Chemically controlled methods proved to be successful in many cases. Unfortunately, they are mostly considered to be still insufficient to modulate ECFCs' activity and to promote TA in a fully satisfactory way. In more detail, their critical limitations consist in limited spatial and temporal resolution of administration, as well as lack of reversibility. Thus, the opportunity to employ physical stimuli has been emerging in the latest years as an alternative, innovative tool to control ECFC fate. Several possibilities are being explored in this direction. First, the effects of micropatterning and nano-patterning and, more generally, of mechanical cues, is under intensive investigation. The hypothesis that the direct micropatterning of ECFCs induces morphological elongation, cytoskeletal alignment, and changes in immunogenic and thrombogenic–related gene expression, is being tested. It was recently reported that ECFCs cultured on top of micropatterned polyurethane substrates show sizable alignment to the underlying substrate geometry, accompanied by the alignment of actin fibers and microtubules. However, this did not correspond to significant cellular elongation in the case of ECFCs, nor to sizable changes in the expression of the transcription factor Krüppel-like Factor 2 (KLF-2) or its downstream targets (Hagen and Hinds, 2020). Conversely, in another work, cells patterned on 25 μm-wide lanes, created by alternating collagen-I and a blocking polymer, clearly displayed elongation, and actin alignment. Micropatterning increased their packing densities, without affecting the apoptotic rate, and KLF-2 gene expression was increased in micropatterned relative to non-patterned ECFCs after 50 h. No significant differences were seen in the other genes tested (Hagen and Hinds, 2019). Lower, sub-micrometric scale was also addressed; patterning of ECFCs in this case lead to a decrease in the ECFC area and perimeter, as well as to an increase in their filopodial outgrowth, associated with a modulation of the focal adhesions and overexpression of the ROCK gene (Cui et al., 2018). Overall, however, the number of studies addressing the use of mechanical stimuli on ECFCs is still very limited and does not allow for sketching a complete picture of their effects.

A second possible approach, still in the early stages, is the use of electromagnetic stimulation. It was reported that electrical stimulation, provided by a wearable solar cell, favored the secretion of angiogenic growth factors and EPC migration (Jeong et al., 2017). Moreover, electrical stimulation promoted the formation of capillaries and arterioles in a mouse model of ischemia, while attenuating muscle necrosis and fibrosis and eventually preventing loss of the injured limb. Interestingly, it was also reported that electrical stimulation significantly increases, among other effects, the number of EPCs in the peripheral blood of rats subjected to fluid percussion injury (Zheng et al., 2017). Magnetic field-guided transplantation of silica-coated magnetic iron oxide nanoparticle-labeled EPCs was associated with their enhanced aggregation in the infarcted border zone (Zhang et al., 2019). These initial, promising results are expected to boost the investigation of electromagnetic stimulation in the field of TA, and in more detail the investigation of the effects of a localized electromagnetic field on ECFC activity.

Thirdly, the use of light stimuli may be perfectly suited for TA. In the last decade, the scientific community has exploited the use of light to control the activity of different cell types genetically modified to express light-sensitive ion channels, thus gaining an unprecedented control in terms of selectivity

and reversibility (Knollmann, 2010; Deisseroth, 2011). An alternative strategy, that obviates the need of viral gene transfer is based on the use of hybrid interfaces between living cells and organic semiconductors (OS), used as artificial light transducers (Rivnay et al., 2017; Di Maria et al., 2018; Fang et al., 2020; Ohayon and Inal, 2020). OS, and thiophene-based materials in particular, have emerged as promising tools for biological application, thanks to a series of key-enabling characteristics: they are soft materials with a high degree of mechanical conformability; they are highly biocompatible and very well tolerated within *in vivo* conditions; they support both electronic and ionic charge conduction; they are sensitive to visible and near-infrared light; they are easily processed from solution. Among other materials, it has been demonstrated that optical excitation of regioregular Poly (3-hexyl-thiophene), P3HT, reliably and efficiently modulates the activity of living cells, tissues and systems, including non-excitable (Benfenati et al., 2014; Martino et al., 2015) and excitable cells (Ghezzi et al., 2011; Feyen et al., 2016; Lodola et al., 2019b), retinal explants (Ghezzi et al., 2013), as well as invertebrate (Tortiglione et al., 2017) and mammal animal models (Maya-Vetencourt et al., 2017). It has been also reported that illumination of thiophene thin films leads to a functional interplay with cytochrome C protein, opening the path to selective targeting of sub-cellular organelles (Abdel Aziz et al., 2020).

## OPTICAL CONTROL OF ECFC FATE MEDIATED BY P3HT

Interestingly, it was demonstrated that optical excitation of P3HT leads to sizable modulation of TRPV1 channels, in TRPV1 Stable Cell Line-HEK-293 (Lodola et al., 2017b). Moreover, we unambiguously proved that optical excitation of thiophene-based materials leads to non-toxic activation of photoelectrochemical phenomena (Tullii et al., 2017; Abdel Aziz et al., 2020), i.e., reactive oxygen species (ROS) generation and subsequent modulation of $Ca^{2+}$ dynamics (Bossio et al., 2018; Moros et al., 2018). Indeed, reduction of the oxygen present in the extracellular medium in consequence to the polymer photoexcitation leads to the formation of superoxide ($O_2^-$), intermediate ROS and ends up with spatially and temporally controlled generation of $H_2O_2$, which, in turn, can permeate the plasma membrane, thereby causing an increase in the cytosolic $H_2O_2$ levels, which can activate TRPV1 and induced extracellular $Ca^{2+}$ entry (DelloStritto et al., 2016; Lodola et al., 2019a). A local reduction in extracellular pH because of polymer photoexcitation could also gate TRPV1 (Negri et al., 2020b), but its role in P3HT-mediated TRPV1 activation remains to be investigated.

This experimental evidence prompted us to investigate whether a similar optically-triggered approach could have a beneficial effect on the modulation of ECFC's angiogenic activity.

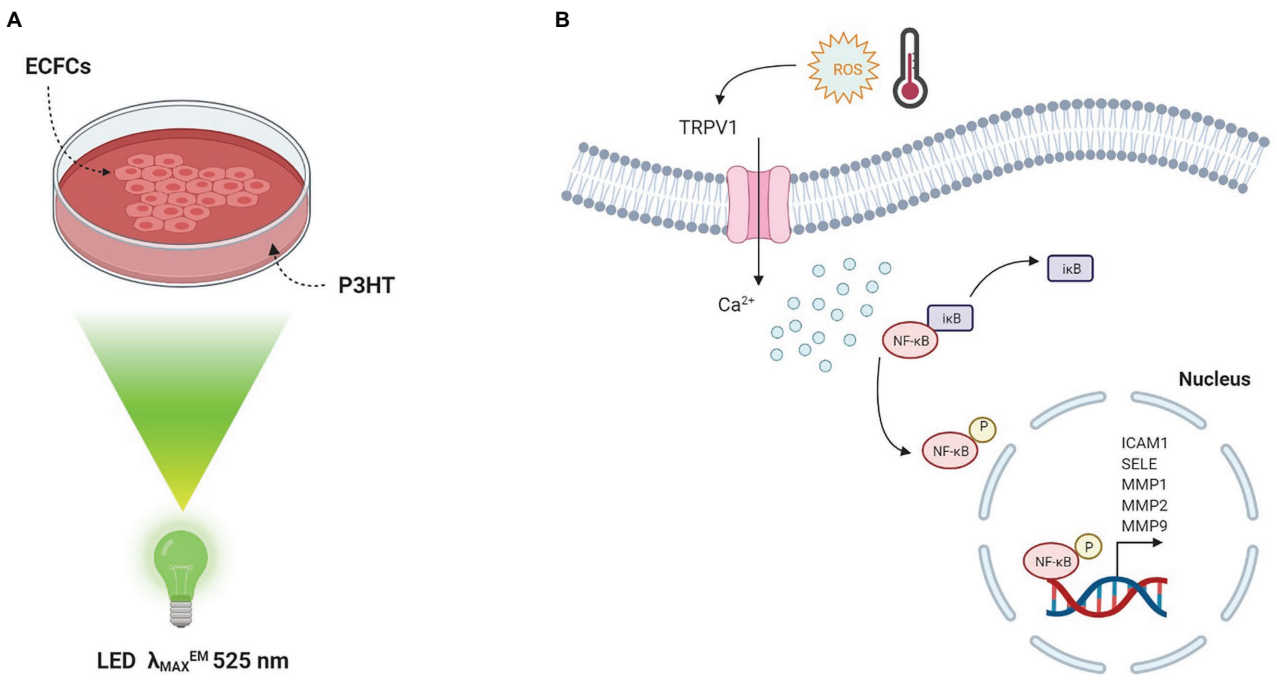


**FIGURE 2 |** Conjugated polymers optically drive the fate of Endothelial Colony Forming Cells. **(A)** Sketch of the polymer device used for cell optical activation. ECFCs are cultured on top of P3HT thin films, deposited on glass substrates. Optical excitation is provided by a green LED ($\lambda_{MAX}^{EM}$ 525 nm). **(B)** Photo-thermal and photo-electrochemical reactions occur at the interface between material and ECFC membrane. The latter is the predominant mechanism triggering TRPV1 activation. A subsequent increase in $[Ca^{2+}]_i$ results in the degradation of IκB, the inhibitory sub-unit of the transcriptional factor NF-κB. As a consequence, the p65 NF-κB subunit is released from IκB inhibition and translocates into the nucleus leading to a robust up-regulation of angiogenic genes, which are under NF-κB-dependent transcriptional control.

To this purpose, circulating ECFCs were seeded on top of P3HT and subjected to light stimulation in the green visible region (**Figure 2A**). We observed that P3HT excitation leads to spatiotemporally resolved modulation of the $Ca^{2+}$ permeable TRPV1 channel, as well as increased ECFC proliferation and tubulogenesis (Lodola et al., 2019a). The interplay among these experimental evidences was clarified by means of a detailed pharmacological analysis: TRPV1 inhibition and manipulation of intracellular free $Ca^{2+}$ levels by selective drugs impaired the pro-angiogenic effect of P3HT excitation thus highlighting the pivotal role of TRPV1-mediated $Ca^{2+}$ influx in ECFC proliferation and tube formation. Moreover, we experimentally identified the phototransduction effect as due to a temporally and spatially localized activation of photoelectrochemical reactions at the interface between the conjugated polymer surface and the cell membrane. Finally, we depicted the molecular scenario observing that polymer photoexcitation led to a significant nuclear translocation of the $Ca^{2+}$-sensitive transcription factor NF-kB and subsequent up-regulated the mRNA levels of specific pro-angiogenic genes (**Figure 2B**). Overall, these results start paving the way towards the use of conjugated polymers as reliable and efficient functional materials for precise and reversible optically-driven modulation of ECFC physiological activity.

## CONCLUSION

In this perspective, we have summarized the most recent outcomes in the field of TA. ECFCs are emerging as suitable candidates for cell-based therapy, but to achieve clinically relevant results it is pivotal to ameliorate current treatment limitations (i.e., insufficient circulating ECFCs frequency, impaired angiogenic activity in CVD, low engraftment, survival and integration within the inhospitable environment of damaged myocardium). The use of physical stimuli, a still less beaten path that should ideally receive increasing attention in the forthcoming years, may allow to overcome these drawbacks. The development of novel biohybrid interfaces between ECFC and materials endowed with electrical, photoacoustic, piezoelectric, magnetic, and/or optical properties may reveal a successful route for selective stimulation of pro-angiogenic signaling pathways. The portfolio of different possibilities is still fully open and among them, the use of optical stimuli represents a minimally invasive strategy, able to trigger the desired biophysical pathways with unprecedented selectivity and spatial resolution. In particular, the promising results shown by ECFC optical stimulation using light-sensitive conjugated polymers (Lodola et al., 2019a) may be further exploited in multiple directions. Optical stimulation could be harnessed to stimulate also capillary endothelial cells nearby the injury site, thereby promoting local angiogenesis. Besides circulating ECFCs, TRPV1 is largely expressed and drives proliferation and tube formation in vascular endothelial cells (Negri et al., 2020a,b). Light active materials can be easily patterned with micro- and sub-micrometer resolution, and processed in three-dimensional architectures (Tullii et al., 2020). Another possible action consists in the development of optically active beads, eventually functionalized with specific moieties, for the selective targeting of ECFCs. Polymer nanoparticles can be easily internalized within cells, can target subcellular organelles, show excellent photocatalytic properties, and are able to modulate intracellular $Ca^{2+}$ dynamics and display optimal *in vivo* biocompatibility properties (Bossio et al., 2018; Maya-Vetencourt et al., 2020). Thus, they may serve as sub-micrometer active sites for local triggering of ECFC pathways relevant for TA. Moreover, conjugated polymers are prone to chemical functionalization with specific drugs, opening the possibility to couple optical excitation with on-demand pharmacological treatment. Many crucial issues should be carefully addressed in detail before any preclinical test can be envisaged: (i) understand the complex interplay among materials, physical stimuli and ECFCs biophysical pathways, e.g., the investigation of additional ROS-sensitive pro-angiogenic channels, such as TRP Melastatin 2 (Mittal et al., 2015); (ii) critically evaluate the dose-response efficiency and reliability of the different approaches and stimulation devices; (iii) assess any possible biocompatibility issue and adverse side effects; (iv) develop suitable tools for implantation and *in vivo* chronic use (i.e., engineering of proper waveguides as well as implementation of microscopic, minimally invasive light sources already optimized for optogenetics). Experimental studies in this direction, though highly promising, are currently at a very embryonal stage, and in our opinion would deserve supra-disciplinary efforts from the bioengineering, materials science, and physics communities. We believe the effort will be worth taking and will pay off in time.

## DATA AVAILABILITY STATEMENT

The original contributions presented in the study are included in the article/supplementary material, further inquiries can be directed to the corresponding author.

## AUTHOR CONTRIBUTIONS

All authors listed have made a substantial, direct and intellectual contribution to the work and approved it for publication.

## FUNDING

The authors gratefully acknowledge financial support from: Italian Ministry of Education, University and Research (MIUR): Dipartimenti di Eccellenza Program (2018–2022) - Dept. of Biology and Biotechnology "L. Spallanzani", University of Pavia (FM); Fondo Ricerca Giovani from the University of Pavia (FM); European Research Council (ERC) under the European Union's Horizon 2020 research and innovation program 'LINCE', grant agreement n. 803621 (MA); EU Horizon 2020 FETOPEN-2018-2020 Programme 'LION-HEARTED', grant agreement n. 828984 (FM, MA, and FL).

## ACKNOWLEDGMENTS

Figures created with BioRender.com.

## REFERENCES


Abdel Aziz, I., Malferrari, M., Roggiani, F., Tullii, G., Rapino, S., and Antognazza, M. R. (2020). Light-triggered electron transfer between a conjugated polymer and cytochrome C for optical modulation of redox signaling. *iScience* 23:101091. doi: 10.1016/j.isci.2020.101091

Asahara, T., Kawamoto, A., and Masuda, H. (2011). Concise review: circulating endothelial progenitor cells for vascular medicine. *Stem Cells* 29, 1650–1655. doi: 10.1002/stem.745

Asahara, T., Murohara, T., Sullivan, A., Silver, M., van der Zee, R., Li, T., et al. (1997). Isolation of putative progenitor endothelial cells for angiogenesis. *Science* 275, 964–966. doi: 10.1126/science.275.5302.964

Balbi, C., Lodder, K., Costa, A., Moimas, S., Moccia, F., van Herwaarden, T., et al. (2019). Supporting data on in vitro cardioprotective and proliferative paracrine effects by the human amniotic fluid stem cell secretome. *Data Brief* 25:104324. doi: 10.1016/j.dib.2019.104324

Benfenati, V., Martino, N., Antognazza, M. R., Pistone, A., Toffanin, S., Ferroni, S., et al. (2014). Organic polymers: photostimulation of whole-cell conductance in primary rat neocortical astrocytes mediated by organic semiconducting thin films (Adv. Healthcare mater. 3/2014). *Adv. Healthc. Mater.* 3:306. doi: 10.1002/adhm.201470013

Benjamin, E. J., Muntner, P., Alonso, A., Bittencourt, M. S., Callaway, C. W., Carson, A. P., et al. (2019). Heart disease and stroke statistics—2019 update: a report from the American Heart Association. *Circulation* 139, e56–e528. doi: 10.1161/CIR.0000000000000659

Bossio, C., Abdel Aziz, I., Tullii, G., Zucchetti, E., Debellis, D., Zangoli, M., et al. (2018). Photocatalytic activity of polymer nanoparticles modulates intracellular calcium dynamics and reactive oxygen species in HEK-293 cells. *Front. Bioeng. Biotechnol.* 6:114. doi: 10.3389/fbioe.2018.00114

Cui, L. -H., Joo, H. J., Kim, D. H., Seo, H. -R., Kim, J. S., Choi, S. -C., et al. (2018). Manipulation of the response of human endothelial colony-forming cells by focal adhesion assembly using gradient nanopattern plates. *Acta Biomater.* 65, 272–282. doi: 10.1016/j.actbio.2017.10.026

D'Alessio, A., Moccia, F., Li, J. -H., Micera, A., and Kyriakides, T. R. (2015). Angiogenesis and vasculogenesis in health and disease. *Bio. Med. Res. Int.* 2015, 1–2. doi: 10.1155/2015/126582

Deisseroth, K. (2011). Optogenetics. *Nat. Methods* 8, 26–29. doi: 10.1038/nmeth.f.324

DelloStritto, D. J., Connell, P. J., Dick, G. M., Fancher, I. S., Klarich, B., Fahmy, J. N., et al. (2016). Differential regulation of TRPV1 channels by H2O2: implications for diabetic microvascular dysfunction. *Basic Res. Cardiol.* 111:21. doi: 10.1007/s00395-016-0539-4

Di Maria, F., Lodola, F., Zucchetti, E., Benfenati, F., and Lanzani, G. (2018). The evolution of artificial light actuators in living systems: from planar to nanostructured interfaces. *Chem. Soc. Rev.* 47, 4757–4780. doi: 10.1039/C7CS00860K

Dragoni, S., Guerra, G., Pla, A. F., Bertoni, G., Rappa, A., Poletto, V., et al. (2015a). A functional transient receptor potential Vanilloid 4 (TRPV4) channel is expressed in human endothelial progenitor cells: TRPV4 EXPRESSION IN EPCs. *J. Cell. Physiol.* 230, 95–104. doi: 10.1002/jcp.24686

Dragoni, S., Reforgiato, M., Zuccolo, E., Poletto, V., Lodola, F., Ruffinatti, F. A., et al. (2015b). Dysregulation of VEGF-induced proangiogenic $Ca^{2+}$ oscillations in primary myelofibrosis-derived endothelial colony-forming cells. *Exp. Hematol.* 43, 1019–1030.e3. doi: 10.1016/j.exphem.2015.09.002

Draoui, N., de Zeeuw, P., and Carmeliet, P. (2017). Angiogenesis revisited from a metabolic perspective: role and therapeutic implications of endothelial cell metabolism. *Open Biol.* 7:170219. doi: 10.1098/rsob.170219

Fang, Y., Meng, L., Prominski, A., Schaumann, E. N., Seebald, M., and Tian, B. (2020). Recent advances in bioelectronics chemistry. *Chem. Soc. Rev.* 49, 7978–8035. doi: 10.1039/D0CS00333F

Faris, P., Negri, S., Perna, A., Rosti, V., Guerra, G., and Moccia, F. (2020). Therapeutic potential of endothelial colony-forming cells in ischemic disease: strategies to improve their regenerative efficacy. *Int. J. Mol. Sci.* 21:7406. doi: 10.3390/ijms21197406

Feyen, P., Colombo, E., Endeman, D., Nova, M., Laudato, L., Martino, N., et al. (2016). Light-evoked hyperpolarization and silencing of neurons by conjugated polymers. *Sci. Rep.* 6:22718. doi: 10.1038/srep22718

Fiorio Pla, A., Grange, C., Antoniotti, S., Tomatis, C., Merlino, A., Bussolati, B., et al. (2008). Arachidonic acid-induced $Ca^{2+}$ entry is involved in early steps of tumor angiogenesis. *Mol. Cancer Res.* 6, 535–545. doi: 10.1158/1541-7786.MCR-07-0271

Fiorio Pla, A., and Munaron, L. (2014). Functional properties of ion channels and transporters in tumour vascularization. *Philos. Trans. R. Soc. B Biol. Sci.* 369:20130103. doi: 10.1098/rstb.2013.0103

Genova, T., Gaglioti, D., and Munaron, L. (2020). Regulation of vessel permeability by TRP channels. *Front. Physiol.* 11:421. doi: 10.3389/fphys.2020.00421

Ghezzi, D., Antognazza, M. R., Dal Maschio, M., Lanzarini, E., Benfenati, F., and Lanzani, G. (2011). A hybrid bioorganic interface for neuronal photoactivation. *Nat. Commun.* 2:166. doi: 10.1038/ncomms1164

Ghezzi, D., Antognazza, M. R., Maccarone, R., Bellani, S., Lanzarini, E., Martino, N., et al. (2013). A polymer optoelectronic interface restores light sensitivity in blind rat retinas. *Nat. Photonics* 7, 400–406. doi: 10.1038/nphoton.2013.34

Gremmels, H., de Jong, O. G., Hazenbrink, D. H., Fledderus, J. O., and Verhaar, M. C. (2017). The transcription factor Nrf2 protects angiogenic capacity of endothelial colony-forming cells in high-oxygen radical stress conditions. *Stem Cells Int.* 2017, 1–11. doi: 10.1155/2017/4680612

Hagen, M. W., and Hinds, M. T. (2019). Static spatial growth restriction micropatterning of endothelial colony forming cells influences their morphology and gene expression. *PLoS One* 14:e0218197. doi: 10.1371/journal.pone.0218197

Hagen, M., and Hinds, M. T. (2020). The effects of topographic micropatterning on endothelial colony forming cells. *Tissue Eng. Part A*. doi: 10.1089/ten.TEA.2020.0066 [Epub ahead of print]

He, M., Ma, S., Cai, Q., Wu, Y., Shao, C., Kong, H., et al. (2018). Hypoxia induces the dysfunction of human endothelial colony-forming cells via HIF-1α signaling. *Respir. Physiol. Neurobiol.* 247, 87–95. doi: 10.1016/j.resp.2017.09.013

Heinke, J., Patterson, C., and Moser, M. (2012). Life is a pattern: vascular assembly within the embryo. *Front. Biosci.* 30, 2269–2288. doi: 10.2741/541

Hofmann, N. A., Barth, S., Waldeck-Weiermair, M., Klec, C., Strunk, D., Malli, R., et al. (2014). TRPV1 mediates cellular uptake of anandamide and thus promotes endothelial cell proliferation and network-formation. *Biol. Open* 3, 1164–1172. doi: 10.1242/bio.20149571

Inoue, K., and Xiong, Z. -G. (2009). Silencing TRPM7 promotes growth/proliferation and nitric oxide production of vascular endothelial cells via the ERK pathway. *Cardiovasc. Res.* 83, 547–557. doi: 10.1093/cvr/cvp153

Jarajapu, Y. P. R., Hazra, S., Segal, M., LiCalzi, S., Jhadao, C., Qian, K., et al. (2014). Vasoreparative dysfunction of CD34+ cells in diabetic individuals involves hypoxic desensitization and impaired autocrine/paracrine mechanisms. *PLoS One* 9:e93965. doi: 10.1371/journal.pone.0093965

Jeong, G. -J., Oh, J. Y., Kim, Y. -J., Bhang, S. H., Jang, H. -K., Han, J., et al. (2017). Therapeutic angiogenesis via solar cell-facilitated electrical stimulation. *ACS Appl. Mater. Interfaces* 9, 38344–38355. doi: 10.1021/acsami.7b13322

Keighron, C., Lyons, C. J., Creane, M., O'Brien, T., and Liew, A. (2018). Recent advances in endothelial progenitor cells toward their use in clinical translation. *Front. Med.* 5:354. doi: 10.3389/fmed.2018.00354

Knollmann, B. C. (2010). Pacing lightly: optogenetics gets to the heart. *Nat. Methods* 7, 889–891. doi: 10.1038/nmeth1110-889

Komici, K., Faris, P., Negri, S., Rosti, V., García-Carrasco, M., Mendoza-Pinto, C., et al. (2020). Systemic lupus erythematosus, endothelial progenitor cells and intracellular $Ca^{2+}$ signaling: a novel approach for an old disease. *J. Autoimmun.* 112:102486. doi: 10.1016/j.jaut.2020.102486

Lodola, F., Laforenza, U., Bonetti, E., Lim, D., Dragoni, S., Bottino, C., et al. (2012). Store-operated $Ca^{2+}$ entry is remodelled and controls in vitro angiogenesis in endothelial progenitor cells isolated from tumoral patients. *PLoS One* 7:e42541. doi: 10.1371/journal.pone.0042541

Lodola, F., Laforenza, U., Cattaneo, F., Ruffinatti, F. A., Poletto, V., Massa, M., et al. (2017a). VEGF-induced intracellular $Ca^{2+}$ oscillations are down-regulated and do not stimulate angiogenesis in breast cancer-derived endothelial colony forming cells. *Oncotarget* 8, 95223–95246. doi: 10.18632/oncotarget.20255

Lodola, F., Martino, N., Tullii, G., Lanzani, G., and Antognazza, M. R. (2017b). Conjugated polymers mediate effective activation of the mammalian ion channel transient receptor potential Vanilloid 1. *Sci. Rep.* 7:8477. doi: 10.1038/s41598-017-08541-6

Lodola, F., Rosti, V., Tullii, G., Desii, A., Tapella, L., Catarsi, P., et al. (2019a). Conjugated polymers optically regulate the fate of endothelial colony-forming cells. *Sci. Adv.* 12:eaav4620. doi: 10.1126/sciadv.aav4620

Lodola, F., Vurro, V., Crasto, S., Di Pasquale, E., and Lanzani, G. (2019b). Optical pacing of human-induced pluripotent stem cell-derived cardiomyocytes mediated by a conjugated polymer Interface. *Adv. Healthc. Mater.* 8:1900198. doi: 10.1002/adhm.201900198

Martino, N., Feyen, P., Porro, M., Bossio, C., Zucchetti, E., Ghezzi, D., et al. (2015). Photothermal cellular stimulation in functional bio-polymer interfaces. *Sci. Rep.* 5:8911. doi: 10.1038/srep08911

Mauge, L., Sabatier, F., Boutouyrie, P., D'Audigier, C., Peyrard, S., Bozec, E., et al. (2014). Forearm ischemia decreases endothelial colony-forming cell angiogenic potential. *Cytotherapy* 16, 213–224. doi: 10.1016/j.jcyt.2013.09.007

Maya-Vetencourt, J. F., Ghezzi, D., Antognazza, M. R., Colombo, E., Mete, M., Feyen, P., et al. (2017). A fully organic retinal prosthesis restores vision in a rat model of degenerative blindness. *Nat. Mater.* 16, 681–689. doi: 10.1038/nmat4874

Maya-Vetencourt, J. F., Manfredi, G., Mete, M., Colombo, E., Bramini, M., Di Marco, S., et al. (2020). Subretinally injected semiconducting polymer nanoparticles rescue vision in a rat model of retinal dystrophy. *Nat. Nanotechnol.* 15, 698–708. doi: 10.1038/s41565-020-0696-3

Medina, R. J., Barber, C. L., Sabatier, F., Dignat-George, F., Melero-Martin, J. M., Khosrotehrani, K., et al. (2017). Endothelial progenitors: a consensus statement on nomenclature: endothelial progenitors nomenclature. *Stem Cells Transl. Med.* 6, 1316–1320. doi: 10.1002/sctm.16-0360

Mena, H. A., Zubiry, P. R., Dizier, B., Schattner, M., Boisson-Vidal, C., and Negrotto, S. (2018). Acidic preconditioning of endothelial colony-forming cells (ECFC) promote vasculogenesis under proinflammatory and high glucose conditions in vitro and in vivo. *Stem Cell Res Ther* 9:120. doi: 10.1186/s13287-018-0872-7

Mensah, G. A., Roth, G. A., and Fuster, V. (2019). The global burden of cardiovascular diseases and risk factors. *J. Am. Coll. Cardiol.* 74, 2529–2532. doi: 10.1016/j.jacc.2019.10.009

Mittal, M., Urao, N., Hecquet, C. M., Zhang, M., Sudhahar, V., Gao, X., et al. (2015). Novel role of reactive oxygen species–activated *trp* melastatin channel-2 in mediating angiogenesis and postischemic neovascularization. *Arterioscler. Thromb. Vasc. Biol.* 35, 877–887. doi: 10.1161/ATVBAHA.114.304802

Moccia, F., Baruffi, S., Spaggiari, S., Coltrini, D., Berra-Romani, R., Signorelli, S., et al. (2001). P2Y1 and P2Y2 receptor-operated $Ca^{2+}$ signals in primary cultures of cardiac microvascular endothelial cells. *Microvasc. Res.* 61, 240–252. doi: 10.1006/mvre.2001.2306

Moccia, F., Berra-Romani, R., and Rosti, V. (2018a). Manipulating intracellular $Ca^{2+}$ signals to stimulate therapeutic angiogenesis in cardiovascular disorders. *Curr. Pharm. Biotechnol.* 19, 686–699. doi: 10.2174/1389201019666180808165309

Moccia, F., Berra-Romani, R., Tritto, S., Signorelli, S., Taglietti, V., and Tanzi, F. (2003). Epidermal growth factor induces intracellular $Ca^{2+}$ oscillations in microvascular endothelial cells. *J. Cell. Physiol.* 194, 139–150. doi: 10.1002/jcp.10198

Moccia, F., Bonetti, E., Dragoni, S., Fontana, J., Lodola, F., Berra Romani, R., et al. (2012). Hematopoietic progenitor and stem cells circulate by surfing on intracellular $Ca^{2+}$ waves: a novel target for cell-based therapy and anti-cancer treatment? *Curr. Signal Transduct. Ther.* 7, 161–176. doi: 10.2174/157436212800376672

Moccia, F., Fotia, V., Tancredi, R., Porta, M. G. D., Rosti, V., Bonetti, E., et al. (2017). Breast and renal cancer-derived endothelial colony forming cells share a common gene signature. *Eur. J. Cancer* 77, 155–164. doi: 10.1016/j.ejca.2017.01.025

Moccia, F., Lucariello, A., and Guerra, G. (2018b). TRPC3-mediated $Ca^{2+}$ signals as a promising strategy to boost therapeutic angiogenesis in failing hearts: the role of autologous endothelial colony forming cells. *J. Cell. Physiol.* 233, 3901–3917. doi: 10.1002/jcp.26152

Moccia, F., Ruffinatti, F. A., and Zuccolo, E. (2015). Intracellular $Ca^{2+}$ signals to reconstruct a broken heart: still a theoretical approach? *Curr. Drug Targets* 16, 793–815. doi: 10.2174/1389450116666141219121723

Moccia, N., Shekha, F., and Guerra, (2019). Endothelial $Ca^{2+}$ signaling, angiogenesis and vasculogenesis: just what it takes to make a blood vessel. *Int. J. Mol. Sci.* 20:3962. doi: 10.3390/ijms20163962

Moccia, F., Tanzi, F., and Munaron, L. (2014). Endothelial remodelling and intracellular calcium machinery. *Curr. Mol. Med.* 14, 457–480. doi: 10.2174/1566524013666131118113410

Moros, M., Lewinska, A., Onorato, G., Antognazza, M. R., Di Maria, F., Blasio, M., et al. (2018). Light-triggered modulation of cell antioxidant defense by polymer semiconducting nanoparticles in a model organism. *MRS Commun.* 8, 918–925. doi: 10.1557/mrc.2018.104

Negri, S., Faris, P., Berra-Romani, R., Guerra, G., and Moccia, F. (2020a). Endothelial transient receptor potential channels and vascular remodeling: extracellular Ca2 + entry for angiogenesis, arteriogenesis and vasculogenesis. *Front. Physiol.* 10:1618. doi: 10.3389/fphys.2019.01618

Negri, S., Faris, P., Rosti, V., Antognazza, M. R., Lodola, F., and Moccia, F. (2020b). Endothelial TRPV1 as an emerging molecular target to promote therapeutic angiogenesis. 30.

O'Leary, O. E., Canning, P., Reid, E., Bertelli, P. M., McKeown, S., Brines, M., et al. (2019). The vasoreparative potential of endothelial colony-forming cells in the ischemic retina is enhanced by cibinetide, a non-hematopoietic erythropoietin mimetic. *Exp. Eye Res.* 182, 144–155. doi: 10.1016/j.exer.2019.03.001

O'Neill, C. L., McLoughlin, K. J., Chambers, S. E. J., Guduric-Fuchs, J., Stitt, A. W., and Medina, R. J. (2018). The vasoreparative potential of endothelial colony forming cells: a journey through pre-clinical studies. *Front. Med.* 5:273. doi: 10.3389/fmed.2018.00273

Ohayon, D., and Inal, S. (2020). Organic bioelectronics: from functional materials to next-generation devices and power sources. *Adv. Mater.* 32:2001439. doi: 10.1002/adma.202001439

Paschalaki, K. E., and Randi, A. M. (2018). Recent advances in endothelial colony forming cells toward their use in clinical translation. *Front. Med.* 5:295. doi: 10.3389/fmed.2018.00295

Potente, M., and Mäkinen, T. (2017). Vascular heterogeneity and specialization in development and disease. *Nat. Rev. Mol. Cell Biol.* 18, 477–494. doi: 10.1038/nrm.2017.36

Potenza, D. M., Guerra, G., Avanzato, D., Poletto, V., Pareek, S., Guido, D., et al. (2014). Hydrogen sulphide triggers VEGF-induced intracellular $Ca^{2+}$ signals in human endothelial cells but not in their immature progenitors. *Cell Calcium* 56, 225–234. doi: 10.1016/j.ceca.2014.07.010

Prasad, M., Corban, M. T., Henry, T. D., Dietz, A. B., Lerman, L. O., and Lerman, A. (2020). Promise of autologous CD34+ stem/progenitor cell therapy for treatment of cardiovascular disease. *Cardiovasc. Res.* 116, 1424–1433. doi: 10.1093/cvr/cvaa027

Qadura, M., Terenzi, D. C., Verma, S., Al-Omran, M., and Hess, D. A. (2018). Concise review: cell therapy for critical limb ischemia: an integrated review of preclinical and clinical studies: stem cell therapy for critical limb ischemia. *Stem Cells* 36, 161–171. doi: 10.1002/stem.2751

Rivnay, J., Wang, H., Fenno, L., Deisseroth, K., and Malliaras, G. G. (2017). Next-generation probes, particles, and proteins for neural interfacing. *Sci. Adv.* 3:e1601649. doi: 10.1126/sciadv.1601649

Savage, A. M., Kurusamy, S., Chen, Y., Jiang, Z., Chhabria, K., MacDonald, R. B., et al. (2019). tmem33 is essential for VEGF-mediated endothelial calcium oscillations and angiogenesis. *Nat. Commun.* 10:732. doi: 10.1038/s41467-019-08590-7

Schierling, W., Troidl, K., Apfelbeck, H., Troidl, C., Kasprzak, P. M., Schaper, W., et al. (2011). Cerebral arteriogenesis is enhanced by pharmacological as well as fluid-shear-stress activation of the Trpv4 calcium channel. *Eur. J. Vasc. Endovasc. Surg.* 41, 589–596. doi: 10.1016/j.ejvs.2010.11.034

Shelley, W. C., Leapley, A. C., Huang, L., Critser, P. J., Zeng, P., Prater, D., et al. (2012). Changes in the frequency and in vivo vessel-forming ability of rhesus monkey circulating endothelial colony–forming cells across the lifespan (birth to aged). *Pediatr. Res.* 71, 156–161. doi: 10.1038/pr.2011.22

Smani, T., Gómez, L. J., Regodon, S., Woodard, G. E., Siegfried, G., Khatib, A. -M., et al. (2018). TRP channels in angiogenesis and other endothelial functions. *Front. Physiol.* 9:1731. doi: 10.3389/fphys.2018.01731

Su, S. -H., Wu, C. -H., Chiu, Y. -L., Chang, S. -J., Lo, H. -H., Liao, K. -H., et al. (2017). Dysregulation of vascular endothelial growth factor receptor-2 by multiple miRNAs in endothelial colony-forming cells of coronary artery disease. *J. Vasc. Res.* 54, 22–32. doi: 10.1159/000449202

Sung, S. -H., Wu, T. -C., Chen, J. -S., Chen, Y. -H., Huang, P. -H., Lin, S. -J., et al. (2013). Reduced number and impaired function of circulating endothelial progenitor cells in patients with abdominal aortic aneurysm. *Int. J. Cardiol.* 168, 1070–1077. doi: 10.1016/j.ijcard.2012.11.002

Tasev, D., Dekker-Vroling, L., van Wijhe, M., Broxterman, H. J., Koolwijk, P., and van Hinsbergh, V. W. M. (2018). Hypoxia impairs initial outgrowth of endothelial colony forming cells and reduces their proliferative and sprouting potential. *Front. Med.* 5:356. doi: 10.3389/fmed.2018.00356

Tasev, D., Koolwijk, P., and van Hinsbergh, V. W. M. (2016). Therapeutic potential of human-derived endothelial colony-forming cells in animal models. *Tissue Eng. Part B Rev.* 22, 371–382. doi: 10.1089/ten.teb.2016.0050

Thodeti, C. K., Matthews, B., Ravi, A., Mammoto, A., Ghosh, K., Bracha, A. L., et al. (2009). TRPV4 channels mediate cyclic strain–induced endothelial cell reorientation through integrin-to-integrin signaling. *Circ. Res.* 104, 1123–1130. doi: 10.1161/CIRCRESAHA.108.192930

Tortiglione, C., Antognazza, M. R., Tino, A., Bossio, C., Marchesano, V., Bauduin, A., et al. (2017). Semiconducting polymers are light nanotransducers in eyeless animals. *Sci. Adv.* 3:e1601699. doi: 10.1126/sciadv.1601699

Tullii, G., Desii, A., Bossio, C., Bellani, S., Colombo, M., Martino, N., et al. (2017). Bimodal functioning of a mesoporous, light sensitive polymer/electrolyte interface. *Org. Electron.* 46, 88–98. doi: 10.1016/j.orgel.2017.04.007

Tullii, G., Donini, S., Bossio, C., Lodola, F., Pasini, M., Parisini, E., et al. (2020). Micro- and nanopatterned silk substrates for antifouling applications. *ACS Appl. Mater. Interfaces* 12, 5437–5446. doi: 10.1021/acsami.9b18187

Udan, R. S., Culver, J. C., and Dickinson, M. E. (2013). Understanding vascular development: understanding vascular development. *Wiley Interdiscip. Rev. Dev. Biol.* 2, 327–346. doi: 10.1002/wdev.91

Wu, Y., He, M. -Y., Ye, J. -K., Ma, S. -Y., Huang, W., Wei, Y. -Y., et al. (2017). Activation of ATP-sensitive potassium channels facilitates the function of human endothelial colony-forming cells *via* Ca $^{2+}$/Akt/eNOS pathway. *J. Cell. Mol. Med.* 21, 609–620. doi: 10.1111/jcmm.13006

Yokota, Y., Nakajima, H., Wakayama, Y., Muto, A., Kawakami, K., Fukuhara, S., et al. (2015). Endothelial $Ca^{2+}$ oscillations reflect VEGFR signaling-regulated angiogenic capacity in vivo. *eLife* 4:e08817. doi: 10.7554/eLife.08817

Yu, Y. -B., Su, K. -H., Kou, Y. R., Guo, B. -C., Lee, K. -I., Wei, J., et al. (2017). Role of transient receptor potential vanilloid 1 in regulating erythropoietin-induced activation of endothelial nitric oxide synthase. *Acta Physiol.* 219, 465–477. doi: 10.1111/apha.12723

Zhang, B., Jiang, H., Chen, J., Hu, Q., Yang, S., and Liu, X. (2019). Silica-coated magnetic nanoparticles labeled endothelial progenitor cells alleviate ischemic myocardial injury and improve long-term cardiac function with magnetic field guidance in rats with myocardial infarction. *J. Cell. Physiol.* 234, 18544–18559. doi: 10.1002/jcp.28492

Zheng, Z., Dong, X., Li, Y., Gao, W., Zhou, Y., Jiang, R., et al. (2017). Electrical stimulation improved cognitive deficits associated with traumatic brain injury in rats. *Brain Behav.* 7:e00667. doi: 10.1002/brb3.667

Zuccolo, E., Di Buduo, C., Lodola, F., Orecchioni, S., Scarpellino, G., Kheder, D. A., et al. (2018). Stromal cell-derived factor-1α promotes endothelial colony-forming cell migration through the Ca $^{2+}$-dependent activation of the extracellular signal-regulated kinase 1/2 and phosphoinositide 3-kinase/AKT pathways. *Stem Cells Dev.* 27, 23–34. doi: 10.1089/scd.2017.0114

Zuccolo, E., Dragoni, S., Poletto, V., Catarsi, P., Guido, D., Rappa, A., et al. (2016). Arachidonic acid-evoked $Ca^{2+}$ signals promote nitric oxide release and proliferation in human endothelial colony forming cells. *Vasc. Pharmacol.* 87, 159–171. doi: 10.1016/j.vph.2016.09.005

**Conflict of Interest:** The authors declare that the research was conducted in the absence of any commercial or financial relationships that could be construed as a potential conflict of interest.

frontiers in Physiology

MINI REVIEW
published: 09 February 2021
doi: 10.3389/fphys.2020.624903

# Angiogenesis in Adipose Tissue: The Interplay Between Adipose and Endothelial Cells

*Jacqueline Herold*[1] *and Joanna Kalucka*[1,2]*

[1]*Department of Biomedicine, Aarhus University, Aarhus, Denmark,* [2]*Aarhus Institute of Advanced Studies (AIAS), Aarhus University, Aarhus, Denmark*

Obesity is a worldwide health problem, and as its prevalence increases, so does the burden of obesity-associated co-morbidities like type 2 diabetes or cardiovascular diseases (CVDs). Adipose tissue (AT) is an endocrine organ embedded in a dense vascular network. AT regulates the production of hormones, angiogenic factors, and cytokines. During the development of obesity, AT expands through the increase in fat cell size (hypertrophy) and/or fat cell number (hyperplasia). The plasticity and expansion of AT is related to its angiogenic capacities. Angiogenesis is a tightly orchestrated process, which involves endothelial cell (EC) proliferation, migration, invasion, and new tube formation. The expansion of AT is accelerated by hypoxia, inflammation, and structural remodeling of blood vessels. The paracrine signaling regulates the functional link between ECs and adipocytes. Adipocytes can secrete both pro-angiogenic molecules, e.g., tumor necrosis factor-alpha (TNF-α), interleukin-6 (IL-6), or vascular endothelial growth factor (VEGF), and anti-angiogenic factors, e.g., serpins. If the pro-angiogenic molecules dominate, the angiogenesis is dysregulated and the endothelium becomes dysfunctional. However, if anti-angiogenic molecules are overexpressed relative to the angiogenic regulators, the angiogenesis is repressed, and AT becomes hypoxic. Furthermore, in the presence of chronic nutritional excess, endothelium loses its primary function and contributes to the inflammation and fibrosis of AT, which increases the risk for CVDs. This review discusses the current understanding of ECs function in AT, the cross-talk between adipose and ECs, and how obesity can lead to its dysfunction. Understanding the interplay of angiogenesis with AT can be an approach to therapy obesity and obesity-related diseases such as CVDs.

**Keywords: adipocytes, adipose tissue, angiogenesis, endothelial cells, obesity**

OPEN ACCESS

***Edited by:***
*Tullio Genova,*
*University of Turin, Italy*

***Reviewed by:***
*Gabriella Doronzo,*
*University of Turin, Italy*
*Constantinos Marios Mikelis,*
*Texas Tech University Health Sciences Center, United States*

***Correspondence:**
*Joanna Kalucka*
*joanna.kalucka@aias.au.dk*

***Specialty section:***
*This article was submitted to Vascular Physiology, a section of the journal Frontiers in Physiology*

***Received:*** *01 November 2020*
***Accepted:*** *29 December 2020*
***Published:*** *09 February 2021*

***Citation:***
*Herold J and Kalucka J (2021) Angiogenesis in Adipose Tissue: The Interplay Between Adipose and Endothelial Cells. Front. Physiol. 11:624903. doi: 10.3389/fphys.2020.624903*

## INTRODUCTION

Recent findings have led us to reconsider the notion of adipose tissue (AT) being a mere storage depot for body energy. Instead, ATs are emerging as endocrine and immunologically active organs with multiple effects on the regulation of systemic energy homeostasis (Lee et al., 2013). AT is classified as either white (WAT), brown (BAT), or beige/brite based on whether it functions as energy storage or thermogenic organ. Adipocytes in BAT are rich in mitochondria and generate chemical energy in the form of heat (Sun et al., 2020). BAT expands when

an organism is exposed to prolonged cold conditions and is linked with increased insulin sensitivity (Cypess et al., 2009; Van Marken Lichtenbelt et al., 2009). WAT stores energy in the form of triglycerides in lipid droplets and is an endocrine organ that releases hormones, growth factors, and adipokines such as leptin and adiponectin. AT consists of not only adipocytes (40–50%) but also connective tissue matrix, vascular and neural cells, and non-adipocyte cells called stromal vascular fraction (SVF). SVF includes preadipocytes, immune cells (macrophages, natural killer cells, B-lymphocytes, and T-lymphocytes), endothelial cells (ECs), vascular progenitors, fibroblasts, and mesenchymal stem cells (Rosenwald and Wolfrum, 2014). The WAT is mainly divided into two types based on its distribution site, the subcutaneous (SAT) and visceral AT (VAT). During overnutrition, the surplus energy is stored as triglycerides in the SAT leading to AT expansion. AT generates new adipocytes (hyperplasia) and enlarges existing adipocytes (hypertrophy; Hafidi et al., 2019). These processes change the structure and function of AT, and these events are defined as "AT remodeling" (Longo et al., 2019).

The prevalence of obesity has increased all over the world during the last 50 years and more than 650 million obese adults were reported in 2016. According to the World Health Organization (WHO), obesity is an "abnormal or excessive fat accumulation that may impair health." The general measurement of obesity is the body mass index (BMI). Subjects with a BMI $\geq$ 25 kg/m$^2$ are classified to be overweight, while those with a BMI $\geq$ 30 kg/m$^2$ are considered obese. A major cause of obesity is the imbalance between energy intake and expenditure, resulting in the storage of triglycerides in AT. Many factors, including genetics, epigenetics, ethnicity, and environmental factors are involved in the complex pathogenesis of obesity (Rohde et al., 2019). Obesity is a critical risk factor for many diseases, including type 2 diabetes, non-alcoholic fatty liver disease, hypertension, and cardiovascular disease (CVD); it is also linked to several cancers (Ungefroren et al., 2015). In obesity, alteration in AT remodeling may induce the dysregulation of AT-secreted adipokines and cytokines, and the increased secretion of pro-inflammatory molecules may promote systemic low-grade inflammations (Mancuso, 2016). This results in macrophage and T-cell infiltration into AT (Huh et al., 2014). However, AT remodeling does not necessarily lead to these obesity-related diseases; several studies have reported that a subgroup of obese individuals are metabolically "healthy" and display normal physiology and biomarker profiles (Blüher, 2010). This suggests the presence of differences in pathways that regulate AT dysfunction, which further leads to dysfunction in other organs.

The vascular circulatory system forms an extensive network of arteries, veins, and capillaries and is important for continuous supply and delivery of nutrients and oxygen to all tissues (Aird, 2004). The blood vessels are lined with a thin layer of ECs, the main drivers of sprouting angiogenesis (Eelen et al., 2018). In healthy adult tissue, ECs remain quiescent. The switch from quiescent to proliferative/angiogenic ECs is mediated by changes in metabolism and angiogenic factors (Draoui et al., 2017; Kalucka et al., 2018). Angiogenesis requires a balance between pro-angiogenic and anti-angiogenic molecules. Overexpression of pro-angiogenic molecules can also lead to EC dysfunction. Dysfunctional ECs cannot induce normal angiogenesis, which leads to lesser blood vessel formation. Lower vascular density is a high-risk factor for hypoxia and inflammation and is associated with various diseases, such as CVDs, obesity, and cancer (Eelen et al., 2018; Nijhawans et al., 2020).

Obesity is accompanied by EC dysfunction and decreased vascular density (**Figure 1**). This is mainly due to disbalance and overexpression of pro-angiogenic and pro-inflammatory stimulus. Therefore, understanding the precise relationship between adipocytes and ECs are of significant importance. In this review, we have discussed the function of ECs in AT with respect to the influence of obesity on angiogenesis, the crosstalk between adipocytes and ECs, and how obesity can influence ECs (dys)function.

## ANGIOGENESIS IN HEALTHY ADIPOSE TISSUE

Adipose tissue is a highly vascularized tissue, and the density of blood vessels is important for the regulation of adipocyte function and adipogenesis. In addition to nutrients and oxygen, the vessels also transport growth factors, cytokines, and hormones that are required for adipocyte function, growth, and survival (Cao, 2013). Furthermore, the vessels regulate the transport of adipokines, cytokines, and growth factors from the AT to other organs and thus promote the endocrine function of the AT. The vascular system controls alteration in the AT microenvironment, including acidosis and hypoxia, which influences the adipocyte function, preadipocyte differentiation, and the AT mass (Cao, 2013; **Figure 1**). There are different possible triggers for angiogenesis in AT, the angiogenic expansion may be due to signals emanating from proliferating and enlarging adipocytes or it may be triggered by metabolic signals with the enlargement of adipocytes as a parallel phenomenon (Corvera and Gealekman, 2014). These processes are not mutually exclusive, and a combination of the two is most probably responsible for angiogenesis. The expansion of AT is angiogenesis-dependent (Rupnick et al., 2002). With a high nutrient availability, the adipocytes store lipids in lipid droplets, and as their size expands oxygen availability is reduced. This mild hypoxic status can induce angiogenesis and remodeling of extracellular matrix to reduce hypoxia (Crewe et al., 2017). In healthy AT, the vessels are lined by a single monolayer of quiescent ECs, which can rapidly switch to the angiogenic/proliferative state in the presence of angiogenic and metabolic signals to form new blood vessels (Draoui et al., 2017). AT produces and secretes various angiogenic factors such as angiopoietin-2 (Angpt2) and vascular endothelial growth factor (VEGF) as well as adipokines such as leptin and adiponectin, which influence and modulate angiogenesis and the vascular structure (Cao, 2010; Sorop et al., 2017). This suggests an autoregulatory function for angiogenesis in AT (Cao, 2007).

Interestingly, studies show the presence of precursor cells in the vessel wall, which have the capacity to differentiate into ECs and/or adipocytes in WAT and BAT depots (Tran et al., 2012). Tang et al. identified the presence of white adipocyte progenitors

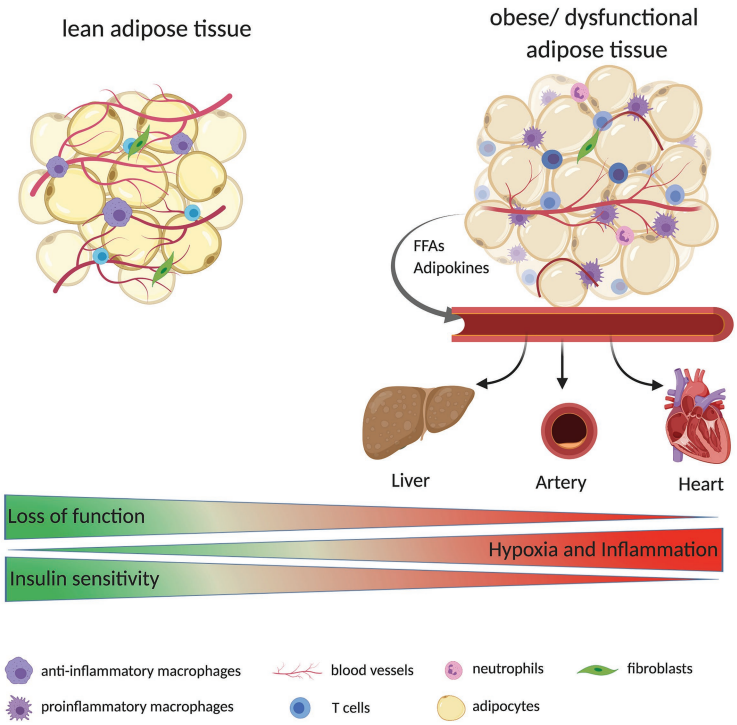


**FIGURE 1 |** Adipose tissue (AT) is composed of multiple cells, including adipocytes, immune cells (e.g., macrophages, T cells, and neutrophils), fibroblasts, and endothelial cells (ECs; building blocks of blood vessels). During the development of obesity, AT expands quickly. Due to decreased tissue vascularization, increased hypoxia, and inflammation, AT might become dysfunctional. Dysfunctional AT releases high levels of free fatty acids (FFAs) and adipokines (e.g., leptin) to the bloodstream, reaching other organs such as liver, heart, and large arteries. Ultimately this can result in a higher fat accumulation in these tissues and alter their function e.g., the organs are less insulin sensitive or display an increase in immune cell infiltration/inflammation.

in the mural compartment of adipose vasculature, but not in the vasculature of other tissues. These mural cells had high adipogenic potential (Tang et al., 2008). These results indicate a link between ECs and adipocytes in terms of their interchangeability in the presence of a possible "switch" and the cell–cell interaction.

## ANGIOGENESIS IN OBESITY

Obesity is characterized by a rapid expansion of AT, which affects tissue vascularization. The lack of vessels leads to decreased oxygen supply in adipocytes, which leads to hypoxia that promotes inflammation (Hodson et al., 2013), and inadequate vessel maintenance and growth. During hypoxia, the hypoxia-inducible factors (HIFs) signaling is activated (Wood et al., 2009). Once translocated to the nucleus, HIF1α dimerizes with HIF1β and forms the functional transcription factor HIF1. HIF1 can bind to hypoxia response elements of target genes, including VEGFA and Angpt2, which induce angiogenic response (Tahergorabi and Khazaei, 2013). HIF1α is reportedly increased in the AT of obese patients and its expression was found to be reduced after surgery-induced weight loss (Lemoine et al., 2013). Genetic deletion of HIF1α in adipocytes decreases the risk of obesity-induced inflammation and insulin resistance (Lee et al., 2014). Hypoxia stimulates inflammation and results in the accumulation of macrophages and other immune cells (Murdoch et al., 2005). Activation of HIF-signaling pathways in macrophages in obese mice leads to induction of platelet-derived growth factor (PDGF) expression, which is likely to induce the tube formation of ECs to improve vascular density (Pang et al., 2008). During inflammation, several factors released from immune cells, such as tumor necrosis factor alpha (TNFα; Madge and Pober, 2001), act on ECs activating the signaling pathway of factor nuclear kappa B (NFκB; Benelli et al., 2007). Additionally, with an increase in angiogenesis, more blood vessels are formed to provide oxygen and nutrients for the metabolic needs of the cells present at the inflammatory sites (Costa et al., 2007).

During obesity, there is a higher release in free fatty acids (FFAs) from adipocytes into the bloodstream, owing to a saturated storage capacity and dysfunctional adipocyte metabolism (Hafidi et al., 2019; **Figure 1**). The FFAs can be taken up by ECs through either fatty acid transport proteins 3 and 4 (FATP3/FATP4) or the scavenger receptor cluster of differentiation CD36 (CD36) and can be converted into hydrophilic acyl-CoAs. These are involved in several processes, including the synthesis of ceramides, which are membrane components. Furthermore, FFAs can activate the NF-κB through

Toll-like receptor (TLR) signaling (Goldberg and Bornfeldt, 2013), which in turn can activate the process of inflammation (Theodorou and Boon, 2018).

The VEGF/VEGF-receptor (VEGFR) system is the main regulator of the angiogenic activity in AT and is expressed in the SVF and mature adipocytes (Lemoine et al., 2013). In a murine model with a *VEGF* deletion in AT, the reduced vascular density accompanied by enhanced hypoxia, inflammation, and apoptosis was observed (Sung et al., 2013). VEGF binds to its tyrosine kinase receptors VEGFR1 and VEGFR2 in order to perform various biological functions. VEGFA plays the role in AT angiogenesis and its expression is increased during the adipocyte differentiation (Fukumura et al., 2003). VEGF secreted by AT also stimulates the proliferation of vascular smooth muscle cells (VSMCs). Schlich et al. (2013) demonstrated that VSMC cultivated in the adipocyte-conditioned medium had a higher VEGFR1 and VEGFR2 expression, as well as higher VEGF secretion. Although VEGF binds to both receptors, VEGFR2 mediates most of the cellular responses to induce migration, survival, and proliferation of ECs (Costa et al., 2007). Blocking VEGFR2 limits diet-induced AT expansion by decreasing angiogenesis and adipogenesis (Tam et al., 2009). However, VEGFR2 has an opposite effect in lymphatic vessels (Zhang et al., 2018). Mice with a genetic deletion of neuropilin 1 (Nrp1) and Vegfr1 are resistant to diet-induced obesity by reduced lacteal chylomicron uptake. The inhibition of Vegfr2 restores the permeable junction and rescued chylomicron transport and the mice are not resistant to diet-induced obesity anymore (Zhang et al., 2018).

Overexpression of VEGF in WAT and BAT in mice led to increased number and size of blood vessels, increased insulin sensitivity, and improved glucose tolerance (Elias et al., 2012). The transgenic mice were protected from diet-induced obesity and local hypoxia, which was indicated by decreased expression of HIF1. Lu and Zheng (2013) reported that VEGF repression in mice also leads to resistance of diet-induced obesity and surprisingly higher expression of BAT markers, including uncoupling protein 1 (UCP1) and Cell Death Inducing DFFA Like Effector A (CIDEA; Lu et al., 2012). VEGFB was found to be expressed in ECs of the skeletal muscles, heart, and BAT. It binds to VEGFR1 and Nrp1 and increases the expression of FATP3/FATP4 to induce the FFA uptake (Hagberg et al., 2010). Another study demonstrated that the binding of VEGFB to VEGFR1 results in the activation of VEGF/VEGFR2 pathway and improves the capillary density and insulin signaling in AT (Robciuc et al., 2016).

Genetic deletion, as well as pharmacological inhibition of endothelial VEGFR1, increased adipose angiogenesis and browning of SAT, leading to elevated thermogenesis (Seki et al., 2018). Additionally, the anti-VEGFR1 treatment led to higher expression levels of UCP1 and smaller adipocyte size in WAT (Seki et al., 2018). This implied the beginning of browning in WAT, which effected the energy expenditure. A high-fat diet in transgenic mice with a deletion of VEGFR1 in ECs resulted in reduced body weight and body fat mass. Furthermore, the VEGFR1 knockout significantly ameliorated obesity-induced dysfunction by lowering the levels of FFAs, glycerol, triglyceride, glucose, and insulin in the blood of these mice (Seki et al., 2018). These results demonstrate the regulatory role and crosstalk between the different VEGF-members and their receptors that are involved in various mechanisms (Elias et al., 2013). Also, the potential of anti-angiogenic compounds for the treatment of obesity was investigated. Angiostatin and endostatin, two inhibitors of angiogenesis, inhibit weight gain in ob/ob mice and diet-induced obesity (Rupnick et al., 2002). Endostatin inhibits dietary-induced obesity and adipogenesis *via* decreased expression of mTOR. Furthermore, treatment with endostatin had a preventive effect on obesity-induced complication such as glucose intolerance (Hui et al., 2015).

In addition to VEGF, other angiogenic factors are expressed in AT. For example, PDGF is expressed in all cell types of AT (preadipocytes, adipocytes, macrophages, and ECs), however, its expression levels may differ (Engin, 2017). Preadipocytes express more PDGF than mature adipocytes. However, since in obesity, most of the preadipocytes are differentiated into mature adipocytes, the number of preadipocytes is reduced and thus the local PDGF level decreases. To meet the demand for PDGF, AT macrophages increase the PDGF production. In obese subject, in response to the reduced vascular density in AT and increased hypoxia, macrophages express PDGF to facilitate capillary formation. It is mandatory that the balance between these two angiogenic factors is maintained in order to form functional new capillaries. Angiogenesis is coordinated by VEGF and PDGF through their related receptors on ECs and VSMCs, respectively (Greenberg et al., 2008). The expression of another angiogenic factor, fibroblast growth factor-2 (FGF-2), is increased during adipocyte differentiation and during the induction of obesity by high-fat diet in mice. In AT, FGF2 enhanced the inflammation response through NLRP3 inflammasome activation (ZhuGe et al., 2020).

Peroxisome proliferator-activated receptor gamma (PPARγ), the master regulator of adipocyte differentiation, can influence the angiogenesis. Multiple studies demonstrate that PPARγ inhibits proliferation of ECs, however, in AT angiogenesis was enhanced by PPARγ activators (Gealekman et al., 2008). AT obtained from mice and humans treated with PPARγ agonist *rosiglitazone* were found to exhibit increased capillary density and capillary sprouting (Gealekman et al., 2012). Co-culture experiments of adipocytes and ECs demonstrated that the PPARγ expression levels were lower in EC–adipocyte coculture than that in the adipocyte-only control, and smaller lipid droplets per adipocyte were found in the latter (Hammel and Bellas, 2020). Other studies described anti-inflammatory effects of PPARγ in ECs including inhibition of NF-κB signaling, decreased expression of chemokines, and proinflammatory adhesion molecules, including intercellular adhesion molecule (ICAM)-1 and vascular cell adhesion molecule (VCAM)-1 (Mehrotra et al., 2014). Mice with a knockdown of PPARγ in ECs that were fed a high-fat diet were found to have decreased SAT and VAT mass but increased spleen and liver weights compared to those in control mice, in spite of same body weight in both groups. Moreover, the adipocyte size was 25% lower in VAT from PPARγ knockdown mice compared to control mice (Kanda et al., 2009). Furthermore, the knockdown mice had lower glucose and insulin

levels and were more insulin sensitive. However, these mice showed a higher concentration of circulating FFA, increased hepatic CD36 expression, and increased very low-density lipoprotein (vLDL) production. Taken together, these studies demonstrate that PPARγ in ECs contributes to metabolic response in various organs.

## METABOLIC DISORDERS RELATED TO OBESITY AND CARDIOVASCULAR COMPLICATIONS

With the development of obesity, AT becomes dysfunctional. In obesity, a higher release of FFAs from the adipocytes into the bloodstream is observed. FFAs from the VAT can drain directly to the liver *via* the portal circulation, where they affect the hepatocytes. The FFAs reduce insulin degradation, resulting in hyperinsulinemia, and induce insulin resistance thereby increasing glucose production in the liver (Lee et al., 2013). Furthermore, the higher amount of circulating FFAs provides more substrate for triglyceride synthesis leading to a higher production of vLDL, which is atherogenic (Cepeda-Valery et al., 2011), thus contributing to hyperlipidemia, hepatic steatosis, and nonalcoholic fatty liver diseases (Hijona et al., 2010). The higher production of vLDL and low-density lipoproteins (LDL) results in a higher release of these molecules to the circulation, which in turn leads to their retention in the intima within the artery wall; further, the oxidation of LDL contributes to EC activation (Hansson, 2005). The adhesion of leukocytes in the artery wall and a superficial erosion of ECs, leads to the formation of a platelet thrombus. The microvessels become more and more fragile and are potential locations for hemorrhage and thrombosis (Costa et al., 2007). This eventually leads to atherosclerosis. As previously mentioned, absorbed FFAs in ECs are converted to acyl-CoAs that are involved in the synthesis of ceramides and sphingolipids (De Lima et al., 2019). These lipid classes were reported to be positively correlated with cardiovascular disease and cardiovascular-related death in a subcohort of the Long-Term Intervention with Pravastatin in Ischemic Disease (LIPID) study, which included individuals with a myocardial infarction or hospital admission for unstable angina, for a randomized trial of *pravastatin* (Mundra et al., 2018). Fatty acid uptake by the ECs involves crosstalk between the ECs and AT. Bae et al. (2020) showed that Angpt2, which is highly expressed in SAT, can regulate the fatty acid uptake in ECs; ECs treated with Angpt2 showed increased fatty acid uptake *via* the scavenger receptor CD36 and FATP3 in SAT. Angpt2 activates the integrin α5β1 signaling pathway, which results in a translocation of CD36 and FATP3, thereby improving the fatty acid uptake in SAT. Moreover, Angpt2 overexpression in AT results in an increased expression of angiogenic and endothelial markers, VEGFA and CD31, and an increased vascular density in SAT (An et al., 2017). Furthermore, under a high-fat diet, mice with endothelial-specific knockout of Angpt2 exhibited in improved glucose clearance and insulin sensitivity, as shown by oral glucose tolerance test (oGTT) and insulin tolerance test (ITT). The Notch signaling *via* Rbp-jκ activation plays a role in fatty acid transport in the heart. The inhibition of Notch signaling results in decreased expression of endothelial lipase, CD36, and FATP4 (Jabs et al., 2018). This alteration leads to a switch from fatty acids to glucose as sources for energy production, which is known from several animal models of heart failure.

Obesity is also associated with diabetes, and the expression of p53 in ECs was found to be increased in the diabetic state. Under the high-calorie diet, the EC-specific p53 knockout mice showed improved insulin sensitivity and glucose tolerance along with lower plasma insulin levels as well as VAT and SAT (Yokoyama et al., 2014). The deletion of p53 results in higher oxygen consumption and higher glucose uptake in skeletal muscles and BAT through the upregulated endothelial expression of glucose transporter (Glut)1. Moreover, the deletion of p53 resulted in higher expression of genes related to mitochondrial biogenesis, such as PPARγ coactivator-1α (PGC1α), *via* higher phosphorylation of endothelial nitric oxide synthase (eNOS) in skeletal muscles. Conversely, the upregulation of endothelial p53 caused metabolic abnormalities. PGC1α has widespread functions in different tissues and cell types (Sawada et al., 2014), and diabetes induces the expression of PGC1α in ECs (Carmeliet and Jain, 2011). Endothelial-specific PGC1α-overexpression resulted in significantly repressed EC migration, a hallmark of EC function, as measured by transwell migration assays. This inhibition of EC migration is induced by the activation of Notch-signaling and inhibition of Rac/Akt/eNOS signaling, suggesting that PGC1α mediates, in part, the vascular dysfunction caused by diabetes.

Under the high-fat diet, the insulin signaling in ECs is impaired, showing a reduction in insulin receptor substrate-2 (Irs2) and insulin-induced eNOS phosphorylation. This leads to a further reduction in insulin-induced glucose uptake by the skeletal muscles triggered by decreased capillary recruitment and interstitial insulin concentration in the skeletal muscles (Kubota et al., 2011). The reduction of Irs2 in ECs also influences the insulin secretion in the pancreatic β-cells by impairing islet blood flow (Hashimoto et al., 2015). The insulin increase NO synthesis, *via* Phosphoinositide 3-kinase (PI3-K), in ECs, and platelets and in VSMCs. Mediated by nitric oxide, insulin increases the protein expression and secretion of VEGF (Doronzo et al., 2004). Hasan et al. (2020) demonstrated that obesity leads to higher activation of Notch signaling in ECs. This results in decreased insulin sensitivity and lower glucose uptake in the muscles. These effects are mediated by inhibition of genes involved in caveolae formation, such as caveolar protein caveolin 1 (Cav1), and results in a diminished insulin transport to the muscles.

Extracellular vesicles (EVs) can be involved in cell-to-cell and organ-to-organ communication *via* metabolic signals. This has been demonstrated for e.g., adipose-derived stem cells EVs by Zhao et al. (2018). Obese mice treated with these exosomes showed improved insulin sensitivity. EVs of AT macrophages from lean mice injected to obese mice

caused whole-body insulin sensitivity and glucose tolerance, as determined by GTT and ITT (Ying et al., 2017). Conversely, EVs from obese mice injected to lean mice led to insulin resistance, lower glucose tolerance, and increased inflammation. This outcome was induced by miRNA155, which targets PPARγ and impairs the expression of Glut4. Crewe et al. (2018) demonstrated crosstalk between ECs and adipocytes, *via* Cav1-containing adipocyte EVs that are taken up by ECs (**Figure 2**). This transfer is dependent on metabolic status and increases during fasting. Proteomic analysis of the EVs showed an increase in the expression of proteins involved in polyamine metabolism, antioxidant response, and transport of small molecules during the fasted state. However, a decrease in molecules involved in lipid and amino acid metabolism was observed (Crewe et al., 2018). There is further evidence of direct crosstalk between ECs and adipocytes/AT. The endothelial-specific knockdown of the transcription factor Forkhead Box O1 (FoxO1) led to a higher vascular density in AT (Rudnicki et al., 2018). Under the high-fat diet, VAT displays a higher expression of Pecam1, higher capillary number per adipocyte, reduced triglycerides in blood and less hepatic lipid accumulation. FoxO1 depletion increases the ECs proliferation by upregulating glycolytic markers, including Glut1, hexokinase 2, and phosphofructokinase. The suppression of argonaute (AGO1), a regulator of the endothelial hypoxia response, leads to a desuppression of VEGFA and thereby contributing to hypoxia-induced angiogenesis (Chen et al., 2013). The EC-specific AGO1 knockout in mice resulted in lower body weight gain under a high-fat high-sucrose diet, which could be explained by the lower SAT and BAT mass (Tang et al., 2020; **Figure 2**). The knockout mice had lower fasting glucose level and higher insulin sensitivity, as confirmed by oGTT, ITT, and higher phosphorylation levels of AKT and AMPK, hallmarks of insulin sensitivity, in SAT and BAT. Furthermore, browning in SAT was observed, as indicated by increased expression levels of UCP1 and its regulator PGC1α. Moreover, AGO1 deletion led to increased levels of VEGFA and higher CD31+ staining in SAT (Tang et al., 2020).

## CONCLUSION

Obesity can lead to many complications and comorbidities. It affects not only the AT but also several organs such as the liver or cardiovascular system. EC dysfunction is a hallmark of obesity. For a long time, it was thought that only the AT affects the EC function. However, several studies have demonstrated that changes in EC functions and signaling pathways influence adipocyte metabolism and can improve the obesity-induced dysfunction (**Figure 2**). These first insights and differences in the metabolism of healthy and dysfunctional ECs could provide a basis for further studies that may target ECs for therapeutic benefits. The EC-specific treatment can potentially have direct effects on the metabolism of adipocytes and/or AT. However, further studies are necessary to understand

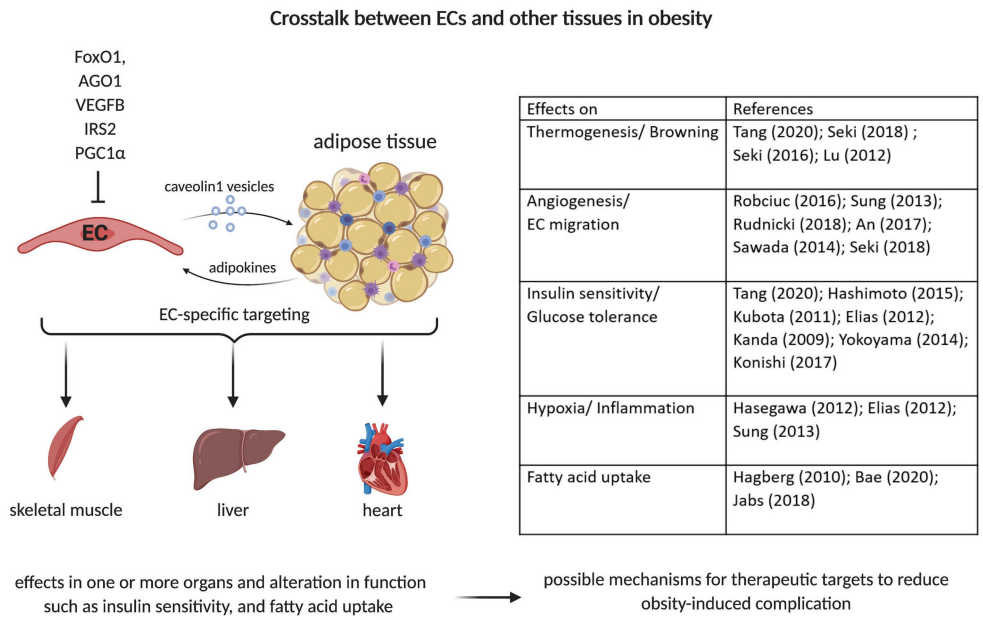


| Effects on | References |
|---|---|
| Thermogenesis/ Browning | Tang (2020); Seki (2018) ; Seki (2016); Lu (2012) |
| Angiogenesis/ EC migration | Robciuc (2016); Sung (2013); Rudnicki (2018); An (2017); Sawada (2014); Seki (2018) |
| Insulin sensitivity/ Glucose tolerance | Tang (2020); Hashimoto (2015); Kubota (2011); Elias (2012); Kanda (2009); Yokoyama (2014); Konishi (2017) |
| Hypoxia/ Inflammation | Hasegawa (2012); Elias (2012); Sung (2013) |
| Fatty acid uptake | Hagberg (2010); Bae (2020); Jabs (2018) |

**FIGURE 2 |** Crosstalk between ECs and adipocytes/adipose tissue. Caveolin 1 (Cav1)-vesicle can transport small molecules from ECs to adipocytes. The EC-specific depletion/deletion of various proteins such as Forkhead Box O1 (FoxO1), Argonaute (AGO1), vascular endothelial growth factor (VEGF), Insulin Receptor Substrate 2 (IRS2), or PPARG Coactivator 1 Alpha (PGC1α) can alter adipocytes' function. This can result in changes of fatty acid uptake, insulin signaling, and glucose homeostasis. This can further induce alterations in other organs' functions, such as liver, heart, and skeletal muscle. The crosstalk with other organs is a possible therapeutic target mechanism to reduce obesity-induced complications, e.g., insulin resistance and fat accumulation in other organs.

the direct crosstalk between ECs and adipocytes as well as the organ-to-organ communication that may help develop strategies to reduce the obesity-induced complications and alteration to whole body metabolism.

## AUTHOR CONTRIBUTIONS

JH and JK selected the literature, wrote the manuscripts, and prepared the figures. All authors contributed to the article and approved the submitted version.

## FUNDING

JK is supported by the Lundbeck Fonden R307-2018-3667, by AIAS-COFUNDII:GA: MSCA: 754513 and Steno Diabetes Center Aarhus.

## ACKNOWLEDGMENTS

We apologize for not being able to cite the work of all other studies related to this topic because of space restrictions. The figures were created with BioRender.com.

## REFERENCES


Aird, W. C. (2004). Endothelium as an organ system. *Crit. Care Med.* 32, S271–S279. doi: 10.1097/01.ccm.0000129669.21649.40

An, Y. A., Sun, K., Joffin, N., Zhang, F., Deng, Y., Donzé, O., et al. (2017). Angiopoietin-2 in white adipose tissue improves metabolic homeostasis through enhanced angiogenesis. *Elife* 6:e24071. doi: 10.7554/eLife.24071

Bae, H., Hong, K. Y., Lee, C. K., Jang, C., Lee, S. J., Choe, K., et al. (2020). Angiopoietin-2–integrin α5β1 signaling enhances vascular fatty acid transport and prevents ectopic lipid-induced insulin resistance. *Nat. Commun.* 11:2980. doi: 10.1038/s41467-020-16795-4

Benelli, R., Lorusso, G., Albini, A., and Noonan, D. (2007). Cytokines and chemokines as regulators of angiogenesis in health and disease. *Curr. Pharm. Des.* 12, 3101–3115. doi: 10.2174/138161206777947461

Blüher, M. (2010). The distinction of metabolically "healthy" from "unhealthy" obese individuals. *Curr. Opin. Lipidol.* 21, 38–43. doi: 10.1097/MOL.0b013e3283346ccc

Cao, Y. (2007). Angiogenesis modulates adipogenesis and obesity. *J. Clin. Invest.* 117, 2362–2368. doi: 10.1172/JCI32239

Cao, Y. (2010). Adipose tissue angiogenesis as a therapeutic target for obesity and metabolic diseases. *Nat. Rev. Drug Discov.* 9, 107–115. doi: 10.1038/nrd3055

Cao, Y. (2013). Angiogenesis and vascular functions in modulation of obesity, adipose metabolism, and insulin sensitivity. *Cell Metab.* 18, 478–489. doi: 10.1016/j.cmet.2013.08.008

Carmeliet, P., and Jain, R. K. (2011). Molecular mechanisms and clinical applications of angiogenesis. *Nature* 473, 298–307. doi: 10.1038/nature10144

Cepeda-Valery, B., Pressman, G. S., Figueredo, V. M., and Romero-Corral, A. (2011). Impact of obesity on total and cardiovascular mortality-fat or fiction? *Nat. Rev. Cardiol.* 8, 233–237. doi: 10.1038/nrcardio.2010.209

Chen, Z., Lai, T. C., Jan, Y. H., Lin, F. M., Wang, W. C., Xiao, H., et al. (2013). Hypoxia-responsive miRNAs target argonaute 1 to promote angiogenesis. *J. Clin. Invest.* 123, 1057–1067. doi: 10.1172/JCI65344

Corvera, S., and Gealekman, O. (2014). Adipose tissue angiogenesis: impact on obesity and type-2 diabetes. *Biochim. Biophys. Acta Mol. Basis Dis.* 1842, 463–472. doi: 10.1016/j.bbadis.2013.06.003

Costa, C., Incio, J., and Soares, R. (2007). Angiogenesis and chronic inflammation: cause or consequence? *Angiogenesis* 10, 149–166. doi: 10.1007/s10456-007-9074-0

Crewe, C., An, Y. A., and Scherer, P. E. (2017). The ominous triad of adipose tissue dysfunction: inflammation, fibrosis, and impaired angiogenesis. *J. Clin. Invest.* 127, 74–82. doi: 10.1172/JCI88883

Crewe, C., Joffin, N., Rutkowski, J. M., Kim, M., Zhang, F., Towler, D. A., et al. (2018). An endothelial-to-adipocyte extracellular vesicle axis governed by metabolic state. *Cell* 175, 695–708.e13. doi: 10.1016/j.cell.2018.09.005

Cypess, A. M., Lehman, S., Williams, G., Tal, I., Rodman, D., Goldfine, A. B., et al. (2009). Identification and importance of brown adipose tissue in adult humans. *N. Engl. J. Med.* 360, 1509–1517. doi: 10.1056/NEJMoa0810780

De Lima, J. C., Moura-Assis, A., Cintra, R. M., Quinaglia, T., Velloso, L. A., and Sposito, A. C. (2019). Central role of obesity in endothelial cell dysfunction and cardiovascular risk. *Rev. Assoc. Med. Bras.* 65, 87–97. doi: 10.1590/1806-9282.65.1.87

Doronzo, G., Russo, I., Mattiello, L., Anfossi, G., Bosia, A., and Trovati, M. (2004). Insulin activates vascular endothelial growth factor in vascular smooth muscle cells: influence of nitric oxide and of insulin resistance. *Eur. J. Clin. Investig.* 34, 664–673. doi: 10.1111/j.1365-2362.2004.01412.x

Draoui, N., De Zeeuw, P., and Carmeliet, P. (2017). Angiogenesis revisited from a metabolic perspective: role and therapeutic implications of endothelial cell metabolism. *Open Biol.* 7:170219. doi: 10.1098/rsob.170219

Eelen, G., de Zeeuw, P., Treps, L., Harjes, U., Wong, B. W., and Carmeliet, P. (2018). Endothelial cell metabolism. *Physiol. Rev.* 98, 3–58. doi: 10.1152/physrev.00001.2017

Elias, I., Franckhauser, S., and Bosch, F. (2013). Response to comment on: Elias et al. Adipose tissue overexpression of vascular endothelial growth factor protects against diet-induced obesity and insulin resistance. Diabetes 2012;61:1801-1813. *Diabetes* 62:e4. doi: 10.2337/db12-1274

Elias, I., Franckhauser, S., Ferré, T., Vilà, L., Tafuro, S., Muñoz, S., et al. (2012). Adipose tissue overexpression of vascular endothelial growth factor protects against diet-induced obesity and insulin resistance. *Diabetes* 61, 1801–1813. doi: 10.2337/db11-0832

Engin, A. (2017). "Adipose tissue hypoxia in obesity and its impact on preadipocytes and macrophages: hypoxia hypothesis" in *Advances in experimental medicine and biology*. New York LLC: Springer, 305–326.

Fukumura, D., Ushiyama, A., Duda, D. G., Xu, L., Tam, J., Krishna, V., et al. (2003). Paracrine regulation of angiogenesis and adipocyte differentiation during in vivo adipogenesis. *Circ. Res.* 93, e88–e97. doi: 10.1161/01.RES.0000099243.20096.FA

Gealekman, O., Burkart, A., Chouinard, M., Nicoloro, S. M., Straubhaar, J., and Corvera, S. (2008). Enhanced angiogenesis in obesity and in response to PPARγ activators through adipocyte VEGF and ANGPTL4 production. *Am. J. Physiol. Endocrinol. Metab.* 295, E1056–E1064. doi: 10.1152/ajpendo.90345.2008

Gealekman, O., Guseva, N., Gurav, K., Gusev, A., Hartigan, C., Thompson, M., et al. (2012). Effect of rosiglitazone on capillary density and angiogenesis in adipose tissue of normoglycaemic humans in a randomised controlled trial. *Diabetologia* 55, 2794–2799. doi: 10.1007/s00125-012-2658-2

Goldberg, I. J., and Bornfeldt, K. E. (2013). Lipids and the endothelium: bidirectional interactions. *Curr. Atheroscler. Rep.* 15:365. doi: 10.1007/s11883-013-0365-1

Greenberg, J. I., Shields, D. J., Barillas, S. G., Acevedo, L. M., Murphy, E., Huang, J., et al. (2008). A role for VEGF as a negative regulator of pericyte function and vessel maturation. *Nature* 456, 809–814. doi: 10.1038/nature07424

Hafidi, M. E., Buelna-Chontal, M., Sánchez-Muñoz, F., and Carbó, R. (2019). Adipogenesis: a necessary but harmful strategy. *Int. J. Mol. Sci.* 20:3657. doi: 10.3390/ijms20153657

Hagberg, C. E., Falkevall, A., Wang, X., Larsson, E., Huusko, J., Nilsson, I., et al. (2010). Vascular endothelial growth factor B controls endothelial fatty acid uptake. *Nature* 464, 917–921. doi: 10.1038/nature08945

Hammel, J. H., and Bellas, E. (2020). Endothelial cell crosstalk improves browning but hinders white adipocyte maturation in 3D engineered adipose tissue. *Integr. Biol.* 12, 81–89. doi: 10.1093/intbio/zyaa006

Hansson, G. K. (2005). Inflammation, atherosclerosis, and coronary artery disease. *N. Engl. J. Med.* 352, 1685–1695. doi: 10.1056/NEJMra043430

Hasan, S. S., Jabs, M., Taylor, J., Wiedmann, L., Leibing, T., and Nordström, V., et al. (2020). Endothelial notch signaling controls insulin transport in muscle. *EMBO Mol. Med.* 12:e09271. doi:10.15252/emmm.201809271.

Hashimoto, S., Kubota, N., Sato, H., Sasaki, M., Takamoto, I., Kubota, T., et al. (2015). Insulin receptor substrate-2 (Irs2) in endothelial cells plays a crucial role in insulin secretion. *Diabetes* 64, 876–886. doi: 10.2337/db14-0432

Hijona, E., Hijona, L., Arenas, J. I., and Bujanda, L. (2010). Inflammatory mediators of hepatic steatosis. *Mediat. Inflamm.* 2010, 1–7. doi: 10.1155/2010/837419

Hodson, L., Humphreys, S. M., Karpe, F., and Frayn, K. N. (2013). Metabolic signatures of human adipose tissue hypoxia in obesity. *Diabetes* 62, 1417–1425. doi: 10.2337/db12-1032

Huh, J. Y., Park, Y. J., Ham, M., and Kim, J. B. (2014). Crosstalk between adipocytes and immune cells in adipose tissue inflammation and metabolic dysregulation in obesity. *Mol. Cell* 37, 365–371. doi: 10.14348/molcells.2014.0074

Hui, W., Chen, Y., Lu, X. A., Liu, G., Fu, Y., and Luo, Y. (2015). Endostatin prevents dietary-induced obesity by inhibiting adipogenesis and angiogenesis. *Diabetes* 64, 2442–2456. doi: 10.2337/db14-0528

Jabs, M., Rose, A. J., Lehmann, L. H., Taylor, J., Moll, I., Sijmonsma, T. P., et al. (2018). Inhibition of endothelial notch signaling impairs fatty acid transport and leads to metabolic and vascular remodeling of the adult heart. *Circulation* 137, 2592–2608. doi: 10.1161/CIRCULATIONAHA.117.029733

Kalucka, J., Bierhansl, L., Conchinha, N. V., Missiaen, R., Elia, I., Brüning, U., et al. (2018). Quiescent endothelial cells upregulate fatty acid β-oxidation for vasculoprotection via redox homeostasis. *Cell Metab.* 28, 881–894. doi: 10.1016/j.cmet.2018.07.016

Kanda, T., Brown, J. D., Orasanu, G., Vogel, S., Gonzalez, F. J., Sartoretto, J., et al. (2009). PPARγ in the endothelium regulates metabolic responses to high-fat diet in mice. *J. Clin. Invest.* 119, 110–124. doi: 10.1172/JCI36233

Kubota, T., Kubota, N., Kumagai, H., Yamaguchi, S., Kozono, H., Takahashi, T., et al. (2011). Impaired insulin signaling in endothelial cells reduces insulin-induced glucose uptake by skeletal muscle. *Cell Metab.* 13, 294–307. doi: 10.1016/j.cmet.2011.01.018

Lee, M. J., Wu, Y., and Fried, S. K. (2013). Adipose tissue heterogeneity: implication of depot differences in adipose tissue for obesity complications. *Mol. Asp. Med.* 34, 1–11. doi: 10.1016/j.mam.2012.10.001

Lee, Y. S., Kim, J. W., Osborne, O., Oh, D. Y., Sasik, R., Schenk, S., et al. (2014). Increased adipocyte $O_2$ consumption triggers HIF-1α, causing inflammation and insulin resistance in obesity. *Cell* 157, 1339–1352. doi: 10.1016/j.cell.2014.05.012

Lemoine, A. Y., Ledoux, S., and Larger, E. (2013). Adipose tissue angiogenesis in obesity. *Thromb. Haemost.* 110, 661–669. doi: 10.1160/TH13-01-0073

Longo, M., Zatterale, F., Naderi, J., Parrillo, L., Formisano, P., Raciti, G. A., et al. (2019). Adipose tissue dysfunction as determinant of obesity-associated metabolic complications. *Int. J. Mol. Sci.* 20:2358. doi: 10.3390/ijms20092358

Lu, X., Ji, Y., Zhang, L., Zhang, Y., Zhang, S., An, Y., et al. (2012). Resistance to obesity by repression of VEGF gene expression through induction of brown-like adipocyte differentiation. *Endocrinology* 153, 3123–3132. doi: 10.1210/en.2012-1151

Lu, X., and Zheng, Y. (2013). Comment on: Elias et al. Adipose tissue overexpression of vascular endothelial growth factor protects against diet-induced obesity and insulin resistance. Diabetes 2012; 61:1801-1813. *Diabetes* 62:e3. doi: 10.2337/db12-1130

Madge, L. A., and Pober, J. S. (2001). TNF signaling in vascular endothelial cells. *Exp. Mol. Pathol.* 70, 317–325. doi: 10.1006/exmp.2001.2368

Mancuso, P. (2016). The role of adipokines in chronic inflammation. *Immuno Targets Ther.* 5, 47–56. doi: 10.2147/ITT.S73223

Mehrotra, D., Wu, J., Papangeli, I., and Chun, H. J. (2014). Endothelium as a gatekeeper of fatty acid transport. *Trends Endocrinol. Metab.* 25, 99–106. doi: 10.1016/j.tem.2013.11.001

Mundra, P. A., Barlow, C. K., Nestel, P. J., Barnes, E. H., Kirby, A., Thompson, P., et al. (2018). Large-scale plasma lipidomic profiling identifies lipids that predict cardiovascular events in secondary prevention. *JCI Insight* 3:e121326. doi: 10.1172/jci.insight.121326

Murdoch, C., Muthana, M., and Lewis, C. E. (2005). Hypoxia regulates macrophage functions in inflammation. *J. Immunol.* 175, 6257–6263. doi: 10.4049/jimmunol.175.10.6257

Nijhawans, P., Behl, T., and Bhardwaj, S. (2020). Angiogenesis in obesity. *Biomed. Pharmacother.* 126:110103. doi: 10.1016/j.biopha.2020.110103

Pang, C., Gao, Z., Yin, J., Zhang, J., Jia, W., and Ye, J. (2008). Macrophage infiltration into adipose tissue may promote angiogenesis for adipose tissue remodeling in obesity. *Am. J. Physiol. Endocrinol. Metab.* 295, 313–322. doi: 10.1152/ajpendo.90296.2008

Robciuc, M. R., Kivelä, R., Williams, I. M., De Boer, J. F., Van Dijk, T. H., Elamaa, H., et al. (2016). VEGFB/VEGFR1-induced expansion of adipose vasculature counteracts obesity and related metabolic complications. *Cell Metab.* 23, 712–724. doi: 10.1016/j.cmet.2016.03.004

Rohde, K., Keller, M., la Cour Poulsen, L., Blüher, M., Kovacs, P., and Böttcher, Y. (2019). Genetics and epigenetics in obesity. *Metabolism* 92, 37–50. doi: 10.1016/j.metabol.2018.10.007

Rosenwald, M., and Wolfrum, C. (2014). The origin and definition of brite versus white and classical brown adipocytes. *Adipocytes* 3, 4–9. doi: 10.4161/adip.26232

Rudnicki, M., Abdifarkosh, G., Nwadozi, E., Ramos, S. V., Makki, A., Sepa-Kishi, D. M., et al. (2018). Endothelial-specific FoxO1 depletion prevents obesity-related disorders by increasing vascular metabolism and growth. *Elife* 7:e39780. doi: 10.7554/eLife.39780

Rupnick, M. A., Panigrahy, D., Zhang, C. Y., Dallabrida, S. M., Lowell, B. B., Langer, R., et al. (2002). Adipose tissue mass can be regulated through the vasculature. *Proc. Natl. Acad. Sci. U. S. A.* 99, 10730–10735. doi: 10.1073/pnas.162349799

Sawada, N., Jiang, A., Takizawa, F., Safdar, A., Manika, A., Tesmenitsky, Y., et al. (2014). Endothelial PGC-1α mediates vascular dysfunction in diabetes. *Cell Metab.* 19, 246–258. doi: 10.1016/j.cmet.2013.12.014

Schlich, R., Willems, M., Greulich, S., Ruppe, F., Knoefel, W. T., Ouwens, D. M., et al. (2013). VEGF in the crosstalk between human adipocytes and smooth muscle cells: depot-specific release from visceral and perivascular adipose tissue. *Mediat. Inflamm.* 2013, 1–10. doi: 10.1155/2013/982458

Seki, T., Hosaka, K., Fischer, C., Lim, S., Andersson, P., Abe, M., et al. (2018). Ablation of endothelial VEG FR1 improves metabolic dysfunction by inducing adipose tissue browning. *J. Exp. Med.* 215, 611–626. doi: 10.1084/jem.20171012

Sorop, O., Olver, T. D., Van DeWouw, J., Heinonen, I., Van Duin, R. W., Duncker, D. J., et al. (2017). Themicrocirculation: a key player in obesity-associated cardiovascular disease. *Cardiovasc. Res.* 113, 1035–1045. doi: 10.1093/cvr/cvx093

Sun, W., Dong, H., Balaz, M., Slyper, M., Drokhlyansky, E., Colleluori, G., et al. (2020). Single-nucleus RNA-Seq reveals a new type of brown adipocyte regulating thermogenesis. bioRxiv [Preprint]. doi: 10.1101/2020.01.20.890327

Sung, H. K., Doh, K. O., Son, J. E., Park, J. G., Bae, Y., Choi, S., et al. (2013). Adipose vascular endothelial growth factor regulates metabolic homeostasis through angiogenesis. *Cell Metab.* 17, 61–72. doi: 10.1016/j.cmet.2012.12.010

Tahergorabi, Z., and Khazaei, M. (2013). The relationship between inflammatory markers, angiogenesis, and obesity. *ARYA Atheroscler* 9, 247–253.

Tam, J., Duda, D. G., Perentes, J. Y., Quadri, R. S., Fukumura, D., and Jain, R. K. (2009). Blockade of VEGFR2 and not VEGFR1 can limit diet-induced fat tissue expansion: role of local versus bone marrow-derived endothelial cells. *PLoS One* 4:e4974. doi: 10.1371/journal.pone.0004974

Tang, W., Zeve, D., Suh, J. M., Bosnakovski, D., Kyba, M., Hammer, R. E., et al. (2008). White fat progenitor cells reside in the adipose vasculature. *Science* 322, 583–586. doi: 10.1126/science.1156232

Tang, X., Miao, Y., Luo, Y., Sriram, K., Qi, Z., Lin, F. -M., et al. (2020). Suppression of endothelial AGO1 promotes adipose tissue browning and improves metabolic dysfunction. *Circulation* 142, 365–379. doi: 10.1161/CIRCULATIONAHA.119.041231

Theodorou, K., and Boon, R. A. (2018). Endothelial cell metabolism in atherosclerosis. *Front. Cell Dev. Biol.* 6:82. doi: 10.3389/fcell.2018.00082

Tran, K. -V., Gealekman, O., Frontini, A., Zingaretti, M. C., Morroni, M., Giordano, A., et al. (2012). The vascular endothelium of the adipose tissue gives rise to both white and brown fat cells. *Cell Metab.* 15, 222–229. doi: 10.1016/j.cmet.2012.01.008

Ungefroren, H., Gieseler, F., Fliedner, S., and Lehnert, H. (2015). Obesity and cancer. *Horm. Mol. Biol. Clin. Invest.* 21, 5–15. doi: 10.1515/hmbci-2014-0046

Van Marken Lichtenbelt, W. D., Vanhommerig, J. W., Smulders, N. M., Drossaerts, J. M. A. F. L., Kemerink, G. J., Bouvy, N. D., et al. (2009). Cold-activated brown adipose tissue in healthy men. *N. Engl. J. Med.* 360, 1500–1508. doi: 10.1056/NEJMoa0808718

Wood, I. S., De Heredia, F. P., Wang, B., and Trayhurn, P. (2009). Cellular hypoxia and adipose tissue dysfunction in obesity. *Proc. Nutr. Soc.* 68, 370–377. doi: 10.1017/S0029665109990206

Ying, W., Riopel, M., Bandyopadhyay, G., Dong, Y., Birmingham, A., and Seo, J. B., et al. (2017). Adipose tissue macrophage-derived exosomal miRNAs can modulate in vivo and in vitro insulin sensitivity. *Cell* 171, 372–384. doi: 10.1016/j.cell.2017.08.035.

Yokoyama, M., Okada, S., Nakagomi, A., Moriya, J., Shimizu, I., Nojima, A., et al. (2014). Inhibition of endothelial p53 improves metabolic abnormalities related to dietary obesity. *Cell Rep.* 7, 1691–1703. doi: 10.1016/j.celrep.2014.04.046

Zhang, F., Zarkada, G., Han, J., Li, J., Dubrac, A., Ola, R., et al. (2018). Lacteal junction zippering protects against diet-induced obesity. *Science* 361, 599–603. doi: 10.1126/science.aap9331

Zhao, H., Shang, Q., Pan, Z., Bai, Y., Li, Z., Zhang, H., et al. (2018). Exosomes from adipose-derived stem cells attenuate adipose inflammation and obesity through polarizing M2 macrophages and beiging in white adipose tissue. *Diabetes* 67, 235–247. doi: 10.2337/db17-0356

ZhuGe, D. L., Javaid, H. M. A., Sahar, N. E., Zhao, Y. Z., and Huh, J. Y. (2020). Fibroblast growth factor 2 exacerbates inflammation in adipocytes through NLRP3 inflammasome activation. *Arch. Pharm. Res.* 43, 1311–1324. doi: 10.1007/s12272-020-01295-2

**Conflict of Interest:** The authors declare that the research was conducted in the absence of any commercial or financial relationships that could be construed as a potential conflict of interest.

frontiers in Physiology

REVIEW
published: 12 February 2021
doi: 10.3389/fphys.2021.636736

# Established, New and Emerging Concepts in Brain Vascular Development

*Ankan Gupta[1], Kevin R. Rarick[2] and Ramani Ramchandran[1]**

[1] Department of Pediatrics, Division of Neonatology, Developmental Vascular Biology Program, Children's Research Institute (CRI), Medical College of Wisconsin, Milwaukee, WI, United States, [2] Department of Pediatrics, Division of Critical Care, Children's Research Institute (CRI), Medical College of Wisconsin, Milwaukee, WI, United States

In this review, we discuss the state of our knowledge as it relates to embryonic brain vascular patterning in model systems zebrafish and mouse. We focus on the origins of endothelial cell and the distinguishing features of brain endothelial cells compared to non-brain endothelial cells, which is revealed by single cell RNA-sequencing methodologies. We also discuss the cross talk between brain endothelial cells and neural stem cells, and their effect on each other. In terms of mechanisms, we focus exclusively on Wnt signaling and the recent developments associated with this signaling network in brain vascular patterning, and the benefits and challenges associated with strategies for targeting the brain vasculature. We end the review with a discussion on the emerging areas of meningeal lymphatics, endothelial cilia biology and novel cerebrovascular structures identified in vertebrates.

**Keywords: endothelial cell, brain, blood–brain barrier, neurovascular disease, neural stem cell, neuron, wnt**

OPEN ACCESS

***Edited by:***
*Sara Petrillo,*
*University of Turin, Italy*

***Reviewed by:***
*Naoki Mochizuki,*
*National Cerebral and Cardiovascular Center (Japan), Japan*
*Sathish Srinivasan,*
*Oklahoma Medical Research Foundation, United States*

***Correspondence:**
*Ramani Ramchandran*
*rramchan@mcw.edu*

***Specialty section:***
*This article was submitted to Vascular Physiology, a section of the journal Frontiers in Physiology*

***Received:*** *01 December 2020*
***Accepted:*** *15 January 2021*
***Published:*** *12 February 2021*

***Citation:***
*Gupta A, Rarick KR and Ramchandran R (2021) Established, New and Emerging Concepts in Brain Vascular Development. Front. Physiol. 12:636736. doi: 10.3389/fphys.2021.636736*

## INTRODUCTION

Normal physiological function of the brain depends upon adequate supply of oxygen and nutrients. Cells in the brain rely on the brain vasculature for their supply of oxygen and nutrients, which are carried out by the macrovasculature (arteries and veins) and microvasculature (arterioles, capillaries, and venules). To meet the growing needs of the neural tissue, the brain concomitantly expands and remodels its vasculature. Alteration in the central nervous system (CNS) vascularization results in the progressive destruction of tissue, especially at the subventricular zone, which eventually leads to embryonic lethality (Raab et al., 2004). The brain vasculature develops exclusively via angiogenesis; a process of new vessel formation from existing established vasculature in contrast to *de novo* vasculogenesis, a process that involves assembly of vessels from endothelial precursor cells. In most tissues, vasculogenesis and angiogenesis processes work together to determine vessel expansion and remodeling (Risau, 1997; Louissaint et al., 2002). However in the brain, angiogenesis is the main process responsible for vascular development that results in 600 kilometer (∼372 miles) network of capillaries (Zlokovic, 2005). Brain endothelial cells (ECs) that line the vasculature are distinct from peripheral ECs in that they are in contact with more cell types (astrocytes and neurons) in addition to smooth muscle-like mural cells referred to as pericytes. Brain ECs also do not align to shear stress like the large caliber human umbilical vein ECs do and the shear stress encountered by the brain vessels are much different than those encountered by the peripheral vasculature (DeStefano et al., 2017). Further, the brain microvasculature is made up of capillaries and postcapillary venules which carries out its microcirculatory function. Brain

capillaries are also structurally distinct from capillaries of the skin, lung, and liver in that they are continuous and non-fenestrated (lack of pores) with tight junctions that makes solute transport highly restrictive and regulated (Daneman and Prat, 2015; Zhao et al., 2015). Thus, the brain vasculature possesses distinct properties, which is suited to the unique cellular environment that the brain ECs reside in. In this review, we focus on the brain ECs and its interaction with cell types in the brain in both embryonic and adult life, the underlying mechanisms associated with this process, and the areas of emerging research in the brain.

## BRAIN VASCULAR DEVELOPMENT: LESSONS FROM VERTEBRATE AND MAMMALIAN DEVELOPMENT

We will discuss our current understanding of brain vessel formation from studies in vertebrate zebrafish (**Figures 1A,B**) and mammalian mouse (**Figures 2A,B**) model systems (Tata et al., 2015). We focus on vascular development in the hindbrain and forebrain regions of the brain. Zebrafish, a freshwater fish from the Ganges river has contributed immensely to our understanding of vascular development primarily because: embryos develop fairly rapidly *ex vivo* and are transparent in embryonic stage, and genetic manipulation is relatively straightforward with injection of RNA, DNA and oligonucleotides feasible at the 1-cell stage. The genetic engineering methods facilitated the development of tissue-specific fluorescent reporter gene expressing transgenic lines, which when combined with confocal and 2-photon microscopy, provided deep insights into the vascular assembly processes in the developing brain. Early studies on mutants identified in the ethylnitrosurea (enu)-induced mutagenesis screens reported *violet beauregarde* (*vbg*) (causative allele: *activin-receptor-like kinase, ALK1*), which showed increased ECs numbers in the brain at 2–2.25 days post fertilization (dpf) (Roman et al., 2002). Using the vascular-specific transgenic reporter line (*etv2*:GFP), time-lapse imaging revealed onset of two major clusters of cells in the 12 hour post fertilization (hpf) embryonic brain namely the rostral organizing center and the midbrain organizing center. By 24 h, these two cell clusters give rise to the most rostral and posterior cranial vessels, respectively (Proulx et al., 2010) (**Figures 1A,B**). Subsequently, using two different vascular transgenic lines (*kdrl*:GFP & *fli1a*:EGFP), additional details of the hindbrain vascular patterning process were identified (Fujita et al., 2011; Ulrich et al., 2011). Two sets of precursor cells (24–28 hpf), one from the anterior end, primordial midbrain-derived and second from posterior end namely anterior cardinal vein-derived, migrate and form the primordial hindbrain channels (PHBCs) (Ulrich et al., 2011) (**Figure 1B**). At 26–28 hpf, basilar artery, the major blood vessel that supplies the hindbrain is formed by medial sprouting and migration of ECs from the bilateral pair of PHBCs veins (Fujita et al., 2011) (**Figures 1A,B**). A second wave of sprouting (30–42 hpf) occurs from PHBCs that gives rise to central arteries (CtAs) (**Figure 1B**), which penetrate and vascularize the hindbrain at the rhombomere (segment of the developing neural tube) boundaries (Fujita et al., 2011; Ulrich et al., 2011). Flow, which commences between 25 and 28 hpf in the developing zebrafish brain has been implicated as a critical feature that ensures the proper formation of arterial-venous connection and the establishment of a functional circulatory loop (Bussmann et al., 2011). Between 36 and 48 hpf, a subset of hindbrain vessels has aligned proximally to neuron clusters and axon tracts suggesting cross-communication between these cell types during development (Ulrich et al., 2011). Moving posteriorly, the integration of the vascular systems between the hindbrain and spinal cord was determined using time lapse imaging in 3–4 dpf *fli1a*:EGFP & *fli1a*:nEGFP lines (Kimura et al., 2015).

In the zebrafish forebrain, much of our knowledge of vascular patterning has emerged from high-resolution time-lapse imaging of the palatocerebral artery (PLA), which forms via angiogenesis (Lenard et al., 2013). PLA runs along the base of the forebrain and connects two cranial internal carotid artery that encapsulate the optic cup on each side of the embryonic head. PLA forms through fusion of two lumenized angiogenic sprouts, and blood flow influences the transcellular lumen formation. *VE-cadherin* (a pivotal EC junction marker) plays a critical role in the initial steps of the vessel fusion process (Lenard et al., 2013). Vessel anastomosis (fusion) and establishment of ECs polarity are coordinated processes, which occur in a stepwise manner.

The brain development in mouse (**Figure 2A**) begins as early as embryonic day 7.5 (E7.5), when the formation of neural tube begins. At E9.5, dorsoventral patterning of neural tube progenitors is established (Dessaud et al., 2008). During this time, neurons and glial cells differentiate from progenitor cells and begin migrating, an event that coincides with the development of the brain vasculature. Vascularization of spinal cord and brain is initiated before birth through the angiogenic sprouting networks, specifically, the perineural vascular plexus (PNVP) and the periventricular plexus (PVP) (Ruhrberg and Bautch, 2013). PNVP arises from mesoderm-derived angioblasts (endothelial precursor cells) and covers the entire CNS by E9.0 (Hogan et al., 2004; Engelhardt and Liebner, 2014) (**Figure 2A**). Half a day later, the mouse hindbrain vascularization begins. Vascular sprouts emerge from PNVP and grow in a radial direction toward the ventricular zone in the direction of the neural progenitor cell location, which are thought to secrete vascular growth factors that stimulate the radial migration of ECs (Fantin et al., 2010). At E10.25, radial vessels extend at 90° angle and parallel to the hindbrain surface when they intersect with neighboring radial vessels and anastomose to become the sub-ventricular vascular plexus (SVP). This anastomosis process is facilitated by macrophages (precursors of microglia) (Fantin et al., 2010). At E12.5, an extensive vascular network has emerged from SVP, which sprouts and penetrates deep into the brain based on cues from neural glial cells (**Figure 2B**). For additional details on the brain anatomy and vessel location in mouse brain, we refer the reader to a detailed review on this subject (Puelles et al., 2019).

The mouse forebrain vascularization commences at E9.5, which also occurs from the PNVP and progresses across the entire rostro-caudal axis in a ventrolateral or dorsomedial direction. At E10.0, the ventral forebrain is vascularized by PNVP while the dorsal region is largely avascular. Intriguingly, vasculature in the dorsal forebrain does not arise from dorsal

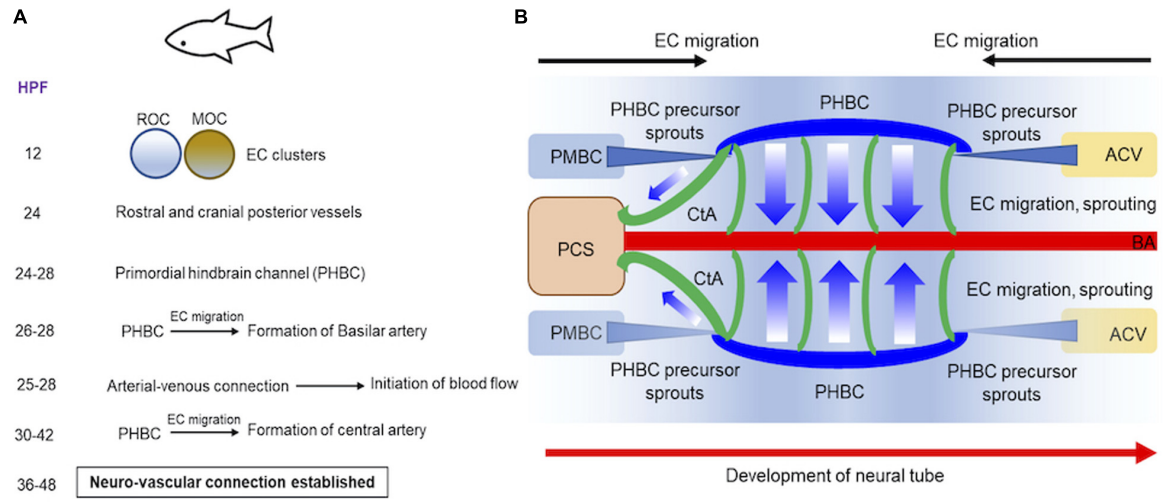


**FIGURE 1 |** Progression of vascular development in brain of embryonic zebrafish. **(A)** A summary of the timeline of events demonstrating how two endothelial cell (ECs) clusters in rostral or midbrain organizing centers give rise to blood vessels in embryonic zebrafish is provided. **(B)** Schematics demonstrate how blood vessels in brain are formed at 24–48 hpf during embryonic development. Precursor cells sprout from PMBC or ACV that ultimately form PHBC (blue). ECs migration and sprouting occurs from PHBC to first establish BA (red) and subsequently CA (green). Direction of neural tube development is also shown (red arrow). **ACV,** Anterior cardinal vein; **BA**, basilar artery; **CA**, central artery; **ECs,** endothelial cells; **HPF,** hours post fertilization; **MOC,** midbrain organizing center; **PMBC,** primordial midbrain channel; **PHBC,** primordial hindbrain channel; **PCS,** posterior communicating segment; **ROC,** rostral organizing center.

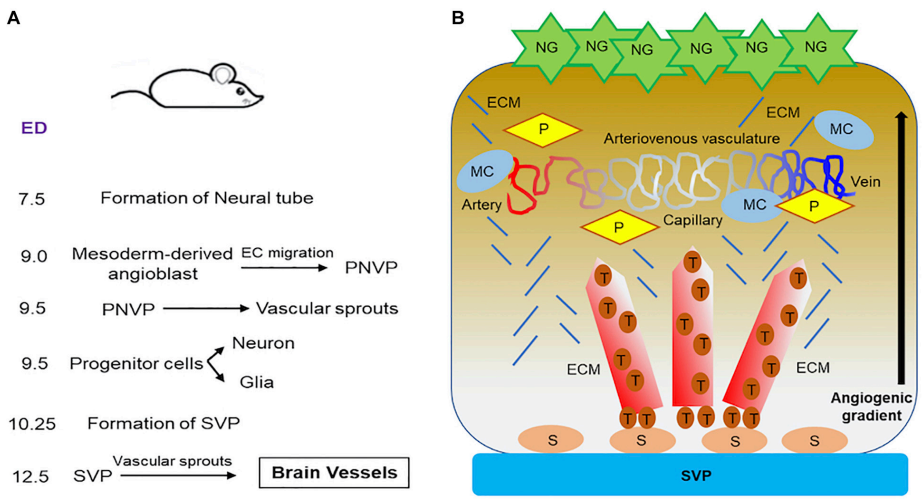


**FIGURE 2 |** Progression of vascular development in brain of embryonic mouse. **(A)** A summary of the timeline of events showing how brain vessel is formed and synchronized to neural development in embryonic mouse is provided. **(B)** Schematics demonstrate how blood vessels in brain are formed and stabilized. During neurovascular development in embryonic mouse brain, neuroglia (NG) release proangiogenic factors. Vascular sprouts emerges from SVP as stalk cells differentiate into tip cells along the angiogenic gradient as established by neuroglia. These sprouting form the brain vessels, which are stabilized by the recruitment of ECM, mural cells and pericytes. The stable brain vessels eventually give rise to mature arteriovenous vasculature in the ventricular area of embryonic mouse hindbrain at E12.5 and beyond. **ECM**, extra cellular matrix; **ED,** embryonic days; **MC**, mural cell; **NG**, neuroglia; **P**, pericyte; **PNVP,** perineural vascular plexus; **S**, stalk cell; **SVP,** sub-ventricular vascular plexus; **T**, tip cell.

PNVP but instead, it is derived from the SVP of the ventral compartment (Vasudevan et al., 2008). By E11.0, SVP is formed in both ventral and dorsal areas of the forebrain including the dorsal medial wall region. In addition to PNVP, vascularization of the embryonic forebrain also occurs from the PVP. The PVP vascularization process is regulated by EC-derived transcription factors (Vasudevan et al., 2008). EC migrates from the surrounding PNVP into the neuroepithelium and initiates CNS vascularization, and also migrate from the pial surface toward the subventricular zone. As ECs migrate into these avascular regions, they adopt specific phenotypes (Haigh et al., 2003; Mancuso et al., 2008). As the neural tissue expands, the blood vessels grow into vast networks and remodels into arterial and venous vasculature.

The nascent brain vasculature continues to develop with cues from surrounding brain resident cells, and is stabilized via the recruitment of mural cells, and establishment of extracellular matrix (Jain, 2003). This growth and maturation of the brain vasculature coincides with the generation of different neural cell types and establishment of the neural circuit (Vasudevan et al., 2008; Ulrich et al., 2011; Tata et al., 2016). The timing of this vascular maturation is critical toward serving the metabolic need of developing neural tissue and the expansion of various neural cells in the brain (Knobloch and Jessberger, 2017). Thus, coordination of the neural and vascular development processes in the brain is necessary and suggests that crosstalk between these two cellular systems are critical for physiological brain development.

## EVOLUTION AND GENETIC SIGNATURE OF A BRAIN ENDOTHELIAL CELL – INSIGHTS FROM SINGLE CELL SEQUENCING DATA ANALYSIS

The origin of brain ECs in mammals is not well understood and understudied. The long-standing hypothesis in the field is that brain-derived ECs are unique with respect to distinct transcriptome and gene expression signatures, and function. Clues for brain ECs origin have emerged from studying the expression of a transcription factor Sox2, which is a key regulator of neuronal differentiation and brain development (Amador-Arjona et al., 2015). Flk1$^{+}$ Sox2$^{+}$ ECs were identified adjacent to the developing brain cells that only express Sox2 at E10.5 and E14.0 (Bostrom et al., 2018). At E12.5, Sox2$^{+}$ VE-cadherin$^{+}$ EC sub-population were observed, which was absent at E18.5 upon development of the vasculature. These data collectively suggest that Sox2-marked cells are undergoing sub-selection for vascular lineage specification, leading to progressive temporal expression of vascular markers Flk1 and VE-cadherin. Knowledge from these initial observations has expanded further with the advent of single cell RNA sequencing technologies (scRNA-seq) (Picelli, 2017; Potter, 2018). Profiling of individual brain ECs suggested great heterogeneity in this population and extensive molecular changes during embryonic development (Hupe et al., 2017). Using scRNA-seq method, 15 distinct cell sub-types of mouse brain ECs have been observed compared to 17 distinct cell sub-types of mouse lung ECs (He et al., 2018). Not surprisingly, mouse embryonic brain ECs show more features related to BBB differentiation, while post-natal brain ECs reveal distinct relationships between cell types (for example, arteries and tip cells, veins, and mitotic cells) (Sabbagh et al., 2018). When EC-specific translating ribosome affinity purification (EC-TAP) was combined with scRNA-seq methodology, additional low abundance transcripts were revealed (Cleuren et al., 2019), and marked differences across vascular beds was observed when host was challenged with stress factors (lipopolysaccharides). The scRNA-seq studies also revealed that organ-specific ECs typically show expression patterns that mimic the site that they reside in Jambusaria et al. (2020). For example, brain ECs express synaptic vesicle genes or cardiac ECs express contractile genes. This tissue-specific heterogeneity of EC expression pattern is also conserved during disease conditions such as inflammation. Further, brain- and liver-specific ECs cluster strongly by tissue of residence while others, adipose- and heart-specific ECs overlap with ECs from other tissues (Paik et al., 2020).

In a comprehensive study of >32,000 single EC transcriptomes from 11 mouse tissues revealed some interesting insights (Kalucka et al., 2020). First, ECs from somewhat unsuspected pairs of tissue (brain/testis, liver/spleen, small intestine/colon, and skeletal muscle/heart) show partially overlapping gene expression. Second, tissue rather than vessel type contributed to the EC heterogeneity. Third, capillary ECs in a tissue are more heterogenous in gene expression than arterial, venous, and lymphatic ECs in that tissue. Fourth, transcriptomes of metabolic gene products showed distinct patterns across vessel types in a given tissue and was reflective of the respective tissue function. Additional scRNA-seq studies also revealed during aging that hippocampal brain capillary ECs undergo the greatest transcriptional changes, upregulate innate immunity and oxidative stress response pathways compared to hippocampal arterial or venous brain ECs (Chen et al., 2020b). Further, senescent EC numbers increases by 10% in the mouse cerebral microcirculation (Kiss et al., 2020). Thus, transcriptional age of brain ECs are sensitive to age-related circulatory cues (Chen et al., 2020b). Another noteworthy connection that emerged from scRNA-seq analysis is the one between tip cells and aortic ECs (Sabbagh et al., 2018). Tip cells are front line cells of the plexus and act as "sensor" of growth factor gradients, and rarely proliferate. Stalk cells, which are located behind the tip cells, proliferate, form the vascular lumen and help extend the length of the growing sprout (Gerhardt et al., 2003; Ridley et al., 2003; Mancuso et al., 2008). Brain capillary EC clusters identified by scRNA-seq are enriched for cells expressing catecholamine DOPA Decarboxylase (Ddc), which was previously reported to express in aortic ECs (Sorriento et al., 2012). Similarly, CXCR4 receptor (tip cell marker) (Strasser et al., 2010) was observed in brain-derived EC clusters, and its ligand CXCL12 was enriched in the arterial EC cluster. These data collectively suggest that a communication signal may exist between endothelial sprouting tip cells and arterial ECs in the brain. These examples highlight the ability of scRNA-seq method to provide unexpected insights and spur new areas of EC biology.

## ENDOTHELIAL CELL AND ITS EFFECT ON NEURAL STEM CELLS IN THE DEVELOPING AND ADULT BRAIN

In the embryonic CNS, the vascular and neural compartments develop concomitantly (Karakatsani et al., 2019). The mammalian neocortex is defined by six layers of neurons that develops from a single layer of neuroepithelial cells called radial glial cells (RGs), also referred to as neural stem cells (NSCs). RGs undergo extensive symmetric division to expand, followed by differentiation into neurons or basal progenitors, and finally symmetric division to generate post-mitotic pyramidal neurons, which migrate to attain their terminal position in the

cortex. All these processes occur between E10.5 and E17.5 in the mouse embryonic brain (Gotz and Huttner, 2005). The early embryonic brain is hypoxic because of lack of vasculature, and in this hypoxic microenvironment, NSCs proliferation is abundant (Mohyeldin et al., 2010). Positional proximity of developing vasculature in brain sets the microenvironment conducive for the expansion of neural progenitors (Javaherian and Kriegstein, 2009; Nie et al., 2010). Interestingly, the relief of hypoxia by angiogenesis promotes NSCs differentiation (Lange et al., 2016b). Premature neuronal differentiation at the expense of reduced self-renewal of NSCs occurs in a reduced angiogenic state (Tata et al., 2016). Thus, the vasculature that develops from the PVVP (E8.5–E10.0) and PNVP (E11.0–E12.5) provide nourishment to growing stem cell niches and balance the expansion vs differentiation of NSCs. ECs effect on NSCs and the reverse effect of NSCs on ECs have been well documented. For example, ECs when co-cultured with embryonic NSCs, promote stem cell maintenance through unknown paracrine factors (Gama Sosa et al., 2007; Vissapragada et al., 2014), and enhance NSC survival and preserve their pluripotency (Lowry et al., 2008). On the contrary, conditioned media from RGs decreases brain ECs proliferation (da Silva et al., 2019), promotes migration and formation of vessel-like structures *in vitro* (Siqueira et al., 2018). Also, in an autopsy of telencephalon from 22-week old human embryo, a defined $Gfap^{+}$ $Cx43^{+}$ $CXCL12^{+}$ RG population appeared to establish physical contact and interaction with angiogenic-activated ($CD105^{+}$) ECs (Errede et al., 2014). These specialized contacts, recognizable on both perforating radial vessels and growing collaterals, appeared as CXCL12-reactive. In absence of RG cells, a significant reduction has been observed of cortical thickness and the regression of nascent brain vessels, *via* the inhibition of EC-specific Wnt signaling in a contact and stage-dependent manner (Ma et al., 2013). In the adult, similar to embryonic stage, the vasculature is required not only for transporting oxygen and nutrients but also for trophic support of the neuronal compartment (Licht and Keshet, 2015; Ramasamy et al., 2015). The ECs are located adjacent to self-renewing multipotent NSCs populations in sub-ventricular zone (SVZ) and sub-granular zone (SGZ) both in the adult (Gage, 2000; Alvarez-Buylla and Lim, 2004). ECs indeed promote NSCs proliferation and differentiation (Han et al., 2015) via secretion of VEGF-C that act on its cognate receptor VEGFR-3 expressed on NSCs. Further, the EC's role in maintaining NSCs quiescence was suggested as cell-cell contact mediated, with ephrinB2 and Jagged1 identified as molecules that were responsible for this process (Ottone et al., 2014). Thus, ECs and NSCs depend on the other for sustenance during embryonic and adult stages.

## SIGNALING MOLECULES: FOCUS ON EMERGING WNT-β CATENIN SIGNALING PATHWAY TO SHAPE BRAIN VASCULAR DEVELOPMENT

A survey of the literature for signaling pathways impacting the brain vasculature formation shows that VEGF, TGF-β, and Wnt signaling are repeated themes that emerge. Both VEGF and TGF-β signaling pathway in the context of brain development have been extensively reviewed elsewhere (Rodriguez-Martinez and Velasco, 2012; Lange et al., 2016a). In this review, we emphasize Wnt signaling and its role in brain vascular patterning. Wnt signaling (**Figure 3**) is one of the pivotal evolutionarily conserved networks that orchestrates cell–cell communication during the embryonic development of multicellular organisms (Clevers, 2006; MacDonald et al., 2009; Clevers and Nusse, 2012). The Wnt signaling pathway directs cell proliferation, cell polarity, and cell fate determination during embryonic development (Logan and Nusse, 2004). Mutations in the Wnt pathway are often linked to congenital defects (Clevers, 2006). The developmental importance of Wnt protein was first demonstrated in larval development of *Drosophila*, where Wnt1 homolog was shown to regulate segment polarity (Nusslein-Volhard and Wieschaus, 1980). The study on developmental significance of Wnt signaling cascade was further extended in *Drosophila* as well as in *Xenopus* (McMahon and Moon, 1989; Siegfried et al., 1992; Noordermeer et al., 1994; Peifer et al., 1994). Once gastrulation is commenced, Wnt/β-catenin signaling activates a defined transcriptional program that directs anteroposterior axis development, leading to the development of head structures and formation of tail (Green et al., 2015). In the last four decades, "canonical" Wnt signaling has been extensively studied and emerged as a major Wnt pathway that regulates key developmental gene expression programs (MacDonald et al., 2009). In the absence of ligand Wnt ("Wnt switch off"), the cytoplasmic β-catenin protein is degraded by an Axin protein complex, which includes ademotous polyposis coli gene (*APC*), casein kinase 1 (*CK1*), and glycogen synthase 3 (*GSK3*). CK1 and GSK3 phosphorylates specific amino acid residues in β-catenin in a specific sequence, which leads to its recognition by β-Trcp, an *E3* ubiquitin ligase subunit that targets β-catenin protein for proteasomal degradation (**Figure 3**). In the presence of ligand Wnt, it binds to a seven pass-transmembrane Frizzled (Fz) receptor and co-receptor low-density lipoprotein receptor-related protein 6 (LRP6) complex leading to recruitment of the scaffolding protein Dishevelled (Dvl) resulting in LRP6 phosphorylation. This results in inhibition of Axin-mediated β-catenin phosphorylation leading to β-catenin stabilization, accumulation of β-catenin in the cytoplasm, followed by entry into the nucleus. In the nucleus, β-catenin engages with DNA-bound TCF transcription factors (Behrens et al., 1996; Molenaar et al., 1996) to activate Wnt target genes ("Wnt switch on") (Lee et al., 2009; Hikasa et al., 2010) (**Figure 3**). In the "Wnt switch off" condition, TCFs interact with specific transcriptional repressors (Cavallo et al., 1998; Roose et al., 1998) preventing the gene transcription. *Axin2* gene is a global transcriptional target of Wnt and is therefore considered a "generic" index of Wnt pathway activity (Lustig et al., 2002).

In mammals, Wnt signaling is facilitated by 19 ligands (MacDonald et al., 2009), targets several genes (Vlad et al., 2008), and the effects are cell or context-specific (Logan and Nusse, 2004). Apart from canonical Wnt signaling cascade, there are two additional pathways that are also known to be activated following Wnt receptor activation (Clevers, 2006), a noncanonical planar cell polarity (PCP) pathway (Seifert and Mlodzik, 2007; Wang

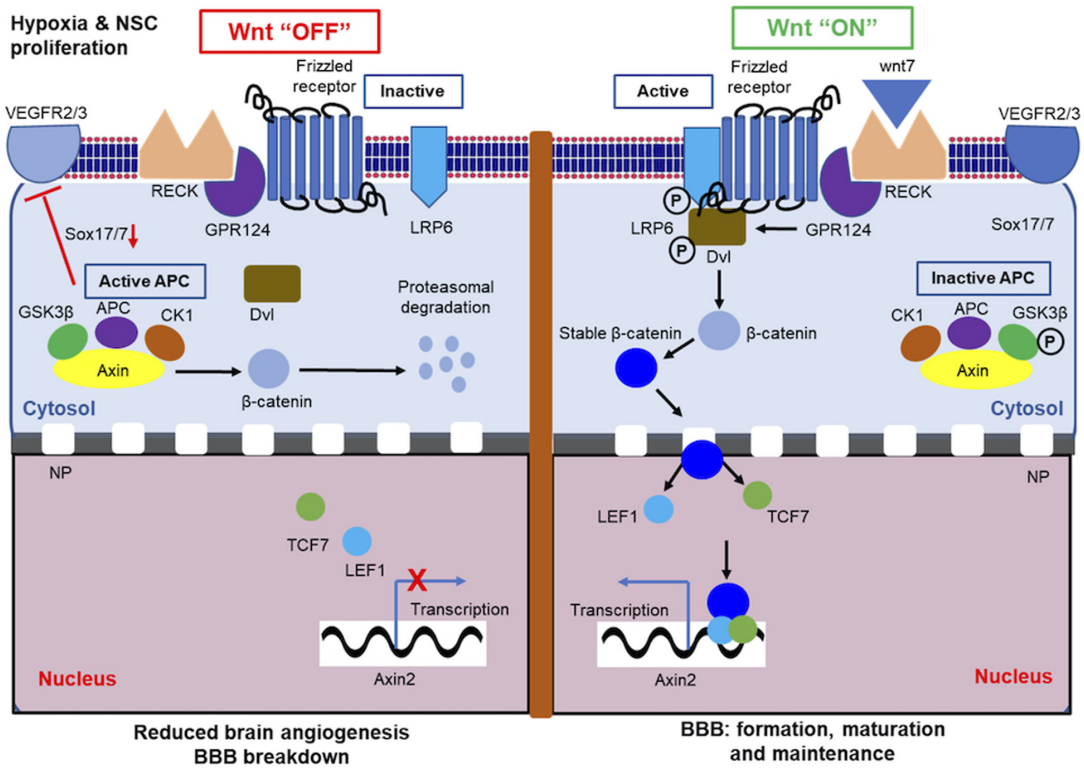


**FIGURE 3 |** Canonical Wnt pathway in brain endothelial cells (ECs). In absence of its cognate ligand, canonical Wnt pathway remains inactive or "OFF" state. In the OFF state, cytosolic axin protein complex (APC) prevents stabilization of β-catenin and promotes its proteasomal degradation. In the Wnt "OFF" condition, axin indirectly downregulates VEGFR2 or VEGFR3 by inhibiting Sox17/7 and abrogates CNS angiogenesis. In active or Wnt "ON" state, Wnt binds to its receptor located in the surface of brain ECs, which causes the stabilization of cytosolic β-catenin. Stable β-catenin is then translocated to nucleus to promote transcription of downstream target genes. **P,** phosphorylation; **NP,** nuclear pore. In brain ECs Wnt OFF state, hypoxic condition is ensued, which in turn influences neural stem cell (NSC) proliferation.

and Nathans, 2007), and a Wnt/$Ca^{2+}$ pathway (Kohn and Moon, 2005). In the non-canonical pathway, Wnts bind to Fz receptors and activate Dvl, independent of GSK-3β or β-catenin. Other signaling proteins involved in the non-canonical pathway activation include small GTPases, the heterotrimeric G proteins, and, in some cases, *C*-Jun *N*-terminal kinase (Mlodzik, 2002; Fanto and McNeill, 2004; Montcouquiol et al., 2006). In the second non-canonical pathway, certain combination of Wnts and Fzs can activate intracellular calcium, which in turn induces calcium-calmodulin-dependent kinase (CAMKII) and protein kinase C (Moon et al., 1993; Du et al., 1995; Sheldahl et al., 1999; Kuhl et al., 2000). Thus, Wnt signaling has several ways to trigger signaling cascades associated with specific phenotypic readouts, which makes it a prime candidate for fine tuning of brain angiogenesis in the developing and adult vasculature.

Several Wnt family members are expressed in the neural tube, which coincides with neural tube angiogenesis (Parr et al., 1993). Enrichment of high mobility group transcription factors Lef1 and Tcf7 are indicators of active canonical Wnt signaling in brain ECs (Cadigan and Waterman, 2012; Sabbagh et al., 2018). Impaired endothelial β-catenin signaling in experimental animal model results in abrogated ECs proliferation and sprouting that ultimately causes hypo-vascularization of the brain (Martowicz et al., 2019). ECs with and without β-catenin formed tip cell suggesting that endothelial β-catenin is not absolutely needed for tip cell formation. However, the tip cell's ability to compete for the tip cell position was compromised. Notably, impaired endothelial β-catenin signaling abrogated the expression of the VEGFR2 (tip cell selection marker) and VEGFR3 in brain microvessels but not in the lung endothelium, suggesting that the β-catenin-EC-specific functional implication are specific to brain ECs (CNS) compared to peripheral ECs (non-CNS) (Martowicz et al., 2019). Several lines of evidence support the theory of restriction of Wnt signaling to the CNS versus non-CNS tissue. Spatial distribution of Wnt ligands in CNS and non-CNS tissues were investigated using EC-specific (*Tie2-Cre*) mouse line that was crossed to Wnt reporter (*R26-Tcf/Lef-LoxPSTOPLoxP-H2B-GFP-6xMYC*) mice (Sabbagh et al., 2018). In this model, Cre recombinase enzyme-mediated excision of a *LoxP*-flanked transcription stop cassette allows for visualization of active Wnt signaling in ECs wherein the multimerized TCF/LEF motifs, together with a minimal promoter drives the expression of a nuclear-localized histone *H2B-GFP-6xMYC* fusion protein (Cho et al., 2017a). The nuclear accumulation of LEF1, which is both a mediator and a marker of canonical Wnt signaling was confined to the CNS and perineural ECs. This observation implies that the canonical

wnt signaling is active in ECs of CNS but not elsewhere. In a second-independent approach (Daneman et al., 2009), a Wnt reporter *TOP-GAL* transgenic mice was used that expresses the *lacZ* transgene under the control of *Tcf* promoters, a downstream effector of Wnt signaling. Thus, *LacZ* expression occurs in cells where canonical Wnt/catenin signaling is activated. Activated Wnt signaling was co-localized with the transgenic EC marker (*Tie2*-GFP) only in the CNS, but not in peripheral tissues. To implicate β-catenin function in Wnt signaling in ECs, an EC-specific β-catenin knock-out mice (*Tie2 cre*$^{+/-}$ β-*catenin*$^{flox/flox}$) was generated. Normal vascular pattern in non-neural tissues was retained while major vascular defects were observed in the CNS of all knockout mice. No capillaries were formed throughout the developing forebrain and the PNVP was significantly thickened. In terms of Wnt signaling and its role in BBB, EC-specific β-catenin activation *in vivo* was necessary for formation and maintenance of BBB, and enhanced barrier maturation, while inactivation of this pathway contributed to BBB breakdown (Liebner et al., 2008).

To date, how brain ECs respond and react in the brain microenvironment is not fully understood but recent studies are beginning to shed some light on this process. In the first zebrafish study, GPI-anchored MMP inhibitor Reversion Inducing Cysteine Rich Protein with Kazal Motifs (RECK) was identified as critical for cerebrovascular development and promotes canonical Wnt signaling (Ulrich et al., 2016). A second zebrafish study suggested that an orphan G-protein coupled receptor (GPCR) Gpr124 along with RECK worked together as integral components of the Wnt-specific signaling complex to facilitate brain angiogenesis (tip cell development) and dorsal root sensory neurogenesis (Vanhollebeke et al., 2015). This GPR124-RECK-WNT signaling axes was also later confirmed in the mouse CNS angiogenesis (Cho et al., 2017b). GPR124, an orphan GPCR has been previously reported by several groups as essential for CNS vascularization (embryonic and adult) (Kuhnert et al., 2010; Anderson et al., 2011), establishment of the BBB (Cullen et al., 2011; Zhou and Nathans, 2014), and BBB integrity (Chang et al., 2017). Biochemical studies reveal that GPR124 through its ectodomain binds to RECK, and RECK binds to Wnt7A and 7B ligands but not Wnt3A ligand (Vallon et al., 2018). Further, RECK binds with low micromolar affinity to the disordered region of Wnt7 ligand (Eubelen et al., 2018). This interaction leads to Wnt receptor Frizzled signaling, which is dependent in part on the interaction between GPR124 and Dvl, a downstream phosphoprotein from the Frizzled receptor (**Figure 3**). Thus, RECK is a selective Wnt receptor that mediates GPR124/Frizzled/LRP-dependent canonical Wnt-β-catenin signaling. The extracellular interactions are partly associated with controlling the bioavailability of Wnt ligand for signaling (Eubelen et al., 2018; Vallon et al., 2018) and is a key regulatory step in this mechanism. Intracellularly, GPR124 contains a PDZ domain that is responsible partly for Wnt7-stimulated β-catenin signaling in brain ECs (Posokhova et al., 2015). Taken together, several studies have made inroads into our understanding of the genetic and biochemical mechanisms associated with Wnt signaling in the brain vasculature. Collectively, these studies imply that canonical Wnt-β-catenin signaling is active, functions in a cell autonomous manner in brain ECs, specific to the CNS, and facilitates BBB formation and maintenance through specific protein–protein interactions.

## EMERGING TOPICS, FUTURE DIRECTIONS, AND PERSPECTIVES

Thus far, we have extensively discussed the brain ECs and the underlying mechanism that is involved in their inception and development. In this section, we will discuss emerging topics of interest to the brain vascular field including meningeal lymphatic ECs, the role of brain microvascular EC cilia to vascular stability and the discovery of a new cerebrovascular structure in vertebrates.

## ENDOTHELIAL CELLS OF THE MENINGEAL LYMPHATIC SYSTEM

The recent discovery of a meningeal lymphatic vascular system in the dura mater adds to the ongoing controversy surrounding brain waste clearance that includes glymphatic, paravascular, and perivascular pathways (Szentistvanyi et al., 1984; Iliff et al., 2012; Morris et al., 2016; Bacyinski et al., 2017). While there is evidence to support the existence of each of these distinct routes, the total contribution of each pathway to waste clearance under physiologic and pathologic conditions remains to be determined. In this section we will briefly discuss the development of meningeal lymphatics, provide a comparison with peripheral lymphatics, and present their role in emerging areas of interest. Additional, in-depth reviews have previously been published on origins and development of lymphatic ECs and meningeal lymphatic vessels (Balint et al., 2019; Gutierrez-Miranda and Yaniv, 2020). Studies in mice have determined that peripheral lymphatic vessels develop out of venous ECs from the common cardinal vein. Around embryonic day E9.5 to E10, venous ECs start to express prospero homeobox protein 1 transcription factor (PROX1) (Antila et al., 2017). After this, vascular endothelial growth factor receptor 3 (VEGFR3)$^{+}$ lymphatic EC progenitors begin to sprout from the common cardinal vein to develop the first peripheral lymphatic plexus. Additional sprouting in response to the paracrine action of VEGF-C expands the lymphatic vascular tree (i.e., lymphangiogenesis). The identification of these specific lymphatic endothelial cell (LEC) markers allowed for the discovery of the meningeal lymphatic system. CNS lymphatic vessels positive for the classic lymphatic EC markers PROX1, VEGFR3, and podoplanin (PDPN) were recently identified using whole-mount preparations of dissected mouse brain meninges (Aspelund et al., 2015; Louveau et al., 2015). With this technique, Louveau et al. (2015) demonstrated the existence of independent vessel structures that run parallel to the dural sinus veins within the meningeal layer. These vessel structures were confirmed to be lymphatic vessels since they were lined with cells positive for lymphatic vessel endothelial hyaluronan receptor 1 (LYVE1) and were not connected to the cardiovascular circulation as they were not labeled by intravenous injection of fluorescent lectin. Furthermore, Aspelund et al. (2015) demonstrated the entirety of

the network of lymphatic vessels within the CNS and surrounding meninges by analyzing *Prox1*-GFP and *Vegfr3*+/*LacZ* reporter mice. While no lymphatic vessels were observed on the brain parenchyma or the pia mater, lymphatic vessels were visualized along the superior sagittal sinus, the transverse sinus, the rostral rhinal veins, the middle meningeal artery, as well as exiting the skull along the meningeal portions of the pterygopalatine artery and cranial nerves (Aspelund et al., 2015). Like peripheral lymphatic vessels, the meningeal lymphatics also function to transport fluid and immune cells allowing for waste clearance and immune surveillance of the CNS. Unlike ECs of the blood brain barrier, meningeal LECs are characterized by fenestrated endothelium and absence of a basal membrane. Also, the meningeal lymphatics do not have valves to prevent back flow like their peripheral counterparts with the noted exception of some vessel segments located near the base of the skull (Aspelund et al., 2015). RNAseq analysis comparing meningeal LECs to those obtained from peripheral lymphatics of the diaphragm and skin showed high similarity in LEC-specific gene sets. However, gene set enrichment analysis suggested that the specific microenvironment of the LECs influences cell phenotype as multiple pathways related to extracellular matrix, focal adhesion, angiogenesis, and response to endogenous and exogenous stimuli were uniquely altered (Louveau et al., 2018). This theme of tissue environment influencing LECs gene expression is reminiscent to that observed for blood ECs in brain and other tissues described earlier in this review. Efficient brain waste clearance of molecules such as amyloid beta and tau is considered an important mechanism to alleviate neuronal injury and degeneration in Alzheimer's disease and after traumatic brain injury (Iliff et al., 2012, 2014; Peng et al., 2016; de Leon et al., 2017). In addition to waste molecules, meningeal lymphatics have a role in regulating CNS immune responses as a route for antigen and immune cell drainage and for clearing red blood cells from the subarachnoid space after hemorrhagic stroke (Louveau et al., 2018; Chen et al., 2020a). Interfering with the normal clearance function of the meningeal lymphatic pathway has been shown to cause cognitive impairment in mice, increase pathology in experimental autoimmune encephalomyelitis (EAE) models of multiple sclerosis, and increase edema and infarction volume in an ischemic stroke rat model (Si et al., 2006; Radjavi et al., 2014; Louveau et al., 2018). Importantly, CSF drainage via meningeal lymphatic vessels to the deep cervical lymph nodes has been demonstrated in humans and non-human primates using contrast enhanced MRI scans further suggesting that meningeal lymphatic pathways are an emerging area of important clinical relevance for multiple CNS injury and neurodegenerative diseases (Absinta et al., 2017; Eide et al., 2018; Wu et al., 2020).

## BRAIN MICROVASCULAR ENDOTHELIAL CELL CILIA

Growing evidence in the literature suggests that a microtubule-based cell organelle called cilia that projects from the apical surface of ECs into the lumen (Goetz et al., 2014), is thought to function as a cellular antenna and a central processing unit (Malicki and Johnson, 2017) and signaling center (Goetz and Anderson, 2010). Recently, endothelial cilia is thought to play an important role in brain vascular barrier function (Ma and Zhou, 2020), which is an emerging area of research in brain vascular biology. Cilia are found in most cells (Goetz and Anderson, 2010), and defects in cilia are often collectively referred to as "ciliopathies." In ECs, cilia are widely considered as a flow sensor (Nauli et al., 2008; Egorova et al., 2012) and often reported as mechanosensors (Luu et al., 2018) wherein they convert mechanical input (flow-mediated) into chemical signaling inside the cell. The prevailing theory is that upon blood flow, cilia bends at an angle of 45° (Goetz et al., 2014), which triggers the release of calcium into the cells (Nauli et al., 2008; Ando and Yamamoto, 2013; Goetz et al., 2014), and subsequent cellular signaling effects (Hierck et al., 2008). Cilia is often considered a low-flow sensor (Goetz et al., 2014; Vion et al., 2018), and upon high flow, they have been shown to be lost from macrovessel (Iomini et al., 2004). Cilia expression and function in brain vessels have not been comprehensively investigated, until recently. We showed using confocal imaging of zebrafish vasculature that cilia are found in brain ECs prior to flow, during flow, and post establishment of high flow (Eisa-Beygi et al., 2018). We also found cilia in vasculogenic, and angiogenic vessels in the brain, and during various distinct processes associated with the vessel growth such as sprouting, anastomosis and lumen formation. Thus, these data collectively suggest that brain EC-cilia have functions beyond just sensing flow (Norris and Santoro, 2018). Knocking out or knocking down proteins in cilia causes the brain vessels to rupture followed by intracranial hemorrhage (Kallakuri et al., 2015; Eisa-Beygi et al., 2018; Pollock et al., 2020). These hemorrhages are exacerbated by enhanced shear stress (Eisa-Beygi et al., 2018). Similarly, polycystic kidney mutant fish and *ciliary intraflagellar transport (IFT)* protein mutant fish show intracranial vessel hemorrhage (Kallakuri et al., 2015; Pollock et al., 2020). Re-expressing of the IFT protein in the brain ECs rescued the hemorrhage phenotype thus arguing for a cell autonomous function for cilia in vascular stabilization (Eisa-Beygi et al., 2018). Similarly, mouse mutants *Ift172* (Gorivodsky et al., 2009) and *Ift122* (Cortellino et al., 2009), both show cranial neural tube defects and bleeding, and ECs isolated from *Ift88* mice with polycystic kidney disease show higher permeability to dextran (Jones et al., 2012). In addition to its role in promoting vascular stability through ECs junctional integrity, EC-cilia has also been recently implicated to recruit support cells such as mural cells that stabilizes the brain vasculature (Chen et al., 2017). Thus, we hypothesize that cilia role in vascular barrier formation and the underlying mechanisms associated with cilia-mediated vascular stability are perhaps the next areas of brain vascular integrity research. Given the propensity for cerebrovascular incidents in several patient populations including sickle cell disease (Hirtz and Kirkham, 2019), preeclampsia (Miller, 2019) and others, it will not be surprising if brain EC-cilia emerges as a key signaling center that contributes to the cerebral vessel pathogenesis. Finally, in relation to lymphatics ECs, it is unknown whether cilia are expressed in LECs and if so, what their potential function is? These and

other emerging questions will keep scientists from numerous multi-disciplines busy.

## NEW TRANSIENT CEREBROVASCULAR STRUCTURE IN VERTEBRATES

In a recent zebrafish study (Kugler et al., 2019), using time series light sheet microscopy of brain vessels in 3 days old fish, the authors observed a spherical EC membrane structure that is transient in nature and protrudes from the cerebral vessel. This structure dubbed "*kugeln*" (German for sphere) was observed as early as 3 days post fertilization (dpf), and as late as 28 dpf. On an average, *kugeln* was observed to exist for 23 min, formed in the absence of flow, and does not communicate with vessel lumen. *Kugeln* also contains little to no cytoplasm, no nuclei but is filled with nitric oxide. Further, *kugeln* does not interact with brain lymphatic ECs, or with macrophage cells in the brain nor was it observed in peripheral trunk vessels. Inhibition of VEGF signaling or Wnt signaling dysregulation increases *kugeln* formation, and inhibition of actin polymerization, myosin II or Notch signaling decreases *kugeln* formation. The obvious question of *kugeln*'s role and function remains unknown, and a congruent *kugeln* structure in mammalian brain vessels has not been identified to date. The presence of such dynamic structures in cerebral vessels emphasizes the point that so much is still unknown regarding how brain vessels pattern. These and other such discoveries will bring fresh and novel perspectives to the field of brain vascular biology.

## CONCLUSION

Considerable progress in our understanding of the developing brain vascular patterning process has been made in vertebrates, and more is yet to come especially at the mechanistic level. In this review, we discussed the contributions of the zebrafish and the mouse model systems to the brain vessel patterning process. The contribution of various cell types in the brain to the ECs-driven vascular patterning process is an untapped area of research. Mechanisms associated with vasculogenesis, angiogenesis and the origin of brain ECs are beginning to emerge. Single cell sequencing technology is providing a framework for new questions such as the similarity of ECs between brain and testis. Details related to various molecules that participate together to mechanistically control Wnt signaling in brain vascular development is coming to focus. Finally, meningeal lymphatics, brain EC-cilia and a new brain-specific vascular structure *kugeln* are emerging areas of research that will offer new insights into brain vascular patterning and homeostasis. These basic science studies are likely to contribute to better understanding of vascular compromise states in several clinical conditions that afflict the brain.

## AUTHOR CONTRIBUTIONS

AG partly conceptualized, wrote, and edited the manuscript. KR assisted in writing parts of the manuscript. RR provided the conceptual input, wrote, edited, and provided funding for the manuscript. All authors contributed to the article and approved the submitted version.

## FUNDING

AG, KR, and RR were partly supported by R61HL154254 grant from the National Institutes of Health.

## ACKNOWLEDGMENTS

We attempted to consolidate the brain vascular literature, specifically, the role of ECs in the brain vascular patterning process. This was a challenging process, and due to space limitations, please note that we could not include all the primary papers of many outstanding scientists and their contributions. We hope that the scientific community will find this review useful to formulate new questions in their research projects.

## REFERENCES

Absinta, M., Ha, S. K., Nair, G., Sati, P., Luciano, N. J., Palisoc, M., et al. (2017). Human and nonhuman primate meninges harbor lymphatic vessels that can be visualized noninvasively by MRI. *Elife* 6:, e29738.

Alvarez-Buylla, A., and Lim, D. A. (2004). For the long run: maintaining germinal niches in the adult brain. *Neuron* 41, 683–686.

Amador-Arjona, A., Cimadamore, F., Huang, C. T., Wright, R., Lewis, S., Gage, F. H., et al. (2015). SOX2 primes the epigenetic landscape in neural precursors enabling proper gene activation during hippocampal neurogenesis. *Proc. Natl. Acad. Sci. U. S. A.* 112, E1936–E1945.

Anderson, K. D., Pan, L., Yang, X. M., Hughes, V. C., Walls, J. R., Dominguez, M. G., et al. (2011). Angiogenic sprouting into neural tissue requires Gpr124, an orphan G protein-coupled receptor. *Proc. Natl. Acad. Sci. U. S. A.* 108, 2807–2812. doi: 10.1073/pnas.1019761108

Ando, J., and Yamamoto, K. (2013). Flow detection and calcium signalling in vascular endothelial cells. *Cardiovasc. Res.* 99, 260–268. doi: 10.1093/cvr/cvt084

Antila, S., Karaman, S., Nurmi, H., Airavaara, M., Voutilainen, M. H., Mathivet, T., et al. (2017). Development and plasticity of meningeal lymphatic vessels. *J. Exp. Med.* 214, 3645–3667. doi: 10.1084/jem.20170391

Aspelund, A., Antila, S., Proulx, S. T., Karlsen, T. V., Karaman, S., Detmar, M., et al. (2015). lymphatic vascular system that drains brain interstitial fluid and macromolecules. *J. Exp. Med.* 212, 991–999. doi: 10.1084/jem.20142290

Bacyinski, A., Xu, M., Wang, W., and Hu, J. (2017). The paravascular pathway for brain waste clearance: current understanding, significance and controversy. *Front. Neuroanat.* 11:101. doi: 10.3389/fnana.2017.00101

Balint, L., Ocskay, Z., Deak, B. A., Aradi, P., and Jakus, Z. (2019). Lymph flow induces the postnatal formation of mature and functional meningeal lymphatic vessels. *Front Immunol* 10:3043. doi: 10.3389/fimmu.2019.03043

Behrens, J., von Kries, J. P., Kuhl, M., Bruhn, L., Wedlich, D., Grosschedl, R., et al. (1996). Functional interaction of beta-catenin with the transcription factor LEF-1. *Nature* 382, 638–642. doi: 10.1038/382638a0

Bostrom, K. I., Yao, J., Wu, X., and Yao, Y. (2018). Endothelial cells may have tissue-specific origins. *J. Cell Biol. Histol.* 1:, 104.

Bussmann, J., Wolfe, S. A., and Siekmann, A. F. (2011). Arterial-venous network formation during brain vascularization involves hemodynamic regulation of chemokine signaling. *Development* 138, 1717–1726. doi: 10.1242/dev.059881

Cadigan, K. M., and Waterman, M. L. (2012). TCF/LEFs and Wnt signaling in the nucleus. *Cold Spring Harb. Perspect. Biol.* 4:, a007906. doi: 10.1101/cshperspect.a007906

Cavallo, R. A., Cox, R. T., Moline, M. M., Roose, J., Polevoy, G. A., Clevers, H., et al. (1998). *Drosophila* Tcf and Groucho interact to repress Wingless signalling activity. *Nature* 395, 604–608. doi: 10.1038/26982

Chang, J., Mancuso, M. R., Maier, C., Liang, X., Yuki, K., Yang, L., et al. (2017). Gpr124 is essential for blood-brain barrier integrity in central nervous system disease. *Nat. Med.* 23, 450–460.

Chen, J., Wang, L., Xu, H., Xing, L., Zhuang, Z., Zheng, Y., et al. (2020a). Meningeal lymphatics clear erythrocytes that arise from subarachnoid hemorrhage. *Nat. Commun.* 11:, 3159.

Chen, M. B., Yang, A. C., Yousef, H., Lee, D., Chen, W., Schaum, N., et al. (2020b). Brain endothelial cells are exquisite sensors of age-related circulatory cues. *Cell Rep. 30* 441:, e4.

Chen, X., Gays, D., Milia, C., and Santoro, M. M. (2017). Cilia control vascular mural cell recruitment in vertebrates. *Cell Rep.* 18, 1033–1047. doi: 10.1016/j.celrep.2016.12.044

Cho, C., Smallwood, P. M., and Nathans, J. (2017a). Reck and Gpr124 are essential receptor cofactors for Wnt7a/Wnt7b-specific signaling in mammalian CNS angiogenesis and blood-brain barrier regulation. *Neuron 95* 105:, e5.

Cho, C., Smallwood, P. M., and Nathans, J. (2017b). Reck and Gpr124 are essential receptor cofactors for Wnt7a/Wnt7b-specific signaling in mammalian CNS angiogenesis and blood-brain barrier regulation. *Neuron* 95, 1221–1225. doi: 10.1016/j.neuron.2017.08.032

Cleuren, A. C. A., van der Ent, M. A., Jiang, H., Hunker, K. L., Yee, A., Siemieniak, D. R., et al. (2019). The in vivo endothelial cell translatome is highly heterogeneous across vascular beds. *Proc. Natl. Acad. Sci. U. S. A.* 116, 23618–23624. doi: 10.1073/pnas.1912409116

Clevers, H. (2006). Wnt/beta-catenin signaling in development and disease. *Cell* 127, 469–480. doi: 10.1016/j.cell.2006.10.018

Clevers, H., and Nusse, R. (2012). Wnt/beta-catenin signaling and disease. *Cell* 149, 1192–1205.

Cortellino, S., Wang, C., Wang, B., Bassi, M. R., Caretti, E., Champeval, D., et al. (2009). Defective ciliogenesis, embryonic lethality and severe impairment of the Sonic Hedgehog pathway caused by inactivation of the mouse complex A intraflagellar transport gene Ift122/Wdr10, partially overlapping with the DNA repair gene Med1/Mbd4. *Dev. Biol.* 325, 225–237. doi: 10.1016/j.ydbio.2008.10.020

Cullen, M., Elzarrad, M. K., Seaman, S., Zudaire, E., Stevens, J., Yang, M. Y., et al. (2011). GPR124, an orphan G protein-coupled receptor, is required for CNS-specific vascularization and establishment of the blood-brain barrier. *Proc. Natl. Acad. Sci. U. S. A.* 108, 5759–5764. doi: 10.1073/pnas.1017192108

da Silva, S. M., Campos, G. D., Gomes, F. C. A., and Stipursky, J. (2019). Radial glia-endothelial cells' bidirectional interactions control vascular maturation and astrocyte differentiation: impact for blood-brain barrier formation. *Curr. Neurovasc. Res.* 16, 291–300. doi: 10.2174/1567202616666191014120156

Daneman, R., Agalliu, D., Zhou, L., Kuhnert, F., Kuo, C. J., and Barres, B. A. (2009). Wnt/beta-catenin signaling is required for CNS, but not non-CNS, angiogenesis. *Proc. Natl. Acad. Sci. U. S. A.* 106, 641–646. doi: 10.1073/pnas.0805165106

Daneman, R., and Prat, A. (2015). The blood-brain barrier. *Cold Spring Harb. Perspect Biol.* 7:, a020412.

de Leon, M. J., Li, Y., Okamura, N., Tsui, W. H., Saint-Louis, L. A., Glodzik, L., et al. (2017). Cerebrospinal fluid clearance in alzheimer disease measured with dynamic PET. *J. Nucl. Med.* 58, 1471–1476. doi: 10.2967/jnumed.116.187211

Dessaud, E., McMahon, A. P., and Briscoe, J. (2008). Pattern formation in the vertebrate neural tube: a sonic hedgehog morphogen-regulated transcriptional network. *Development* 135, 2489–2503. doi: 10.1242/dev.009324

DeStefano, J. G., Xu, Z. S., Williams, A. J., Yimam, N., and Searson, P. C. (2017). Effect of shear stress on iPSC-derived human brain microvascular endothelial cells (dhBMECs). *Fluids Barriers CNS* 14:, 20.

Du, S. J., Purcell, S. M., Christian, J. L., McGrew, L. L., and Moon, R. T. (1995). Identification of distinct classes and functional domains of Wnts through expression of wild-type and chimeric proteins in Xenopus embryos. *Mol. Cell Biol.* 15, 2625–2634. doi: 10.1128/mcb.15.5.2625

Egorova, A. D., van der Heiden, K., Poelmann, R. E., and Hierck, B. P. (2012). Primary cilia as biomechanical sensors in regulating endothelial function. *Differentiation* 83, S56–S61.

Eide, P. K., Vatnehol, S. A. S., Emblem, K. E., and Ringstad, G. (2018). Magnetic resonance imaging provides evidence of glymphatic drainage from human brain to cervical lymph nodes. *Sci. Rep.* 8:, 7194.

Eisa-Beygi, S., Benslimane, F. M., El-Rass, S., Prabhudesai, S., Abdelrasoul, M. K. A., Simpson, P. M., et al. (2018). Characterization of endothelial cilia distribution during cerebral-vascular development in Zebrafish (Danio rerio). *Arterioscler. Thromb. Vasc. Biol.* 38, 2806–2818. doi: 10.1161/atvbaha.118.311231

Engelhardt, B., and Liebner, S. (2014). Novel insights into the development and maintenance of the blood-brain barrier. *Cell Tissue Res.* 355, 687–699. doi: 10.1007/s00441-014-1811-2

Errede, M., Girolamo, F., Rizzi, M., Bertossi, M., Roncali, L., and Virgintino, D. (2014). The contribution of CXCL12-expressing radial glia cells to neuro-vascular patterning during human cerebral cortex development. *Front. Neurosci.* 8:324. doi: 10.3389/fnins.2014.00324

Eubelen, M., Bostaille, N., Cabochette, P., Gauquier, A., Tebabi, P., Dumitru, A. C., et al. (2018). A molecular mechanism for Wnt ligand-specific signaling. *Science* 361:, eaat1178. doi: 10.1126/science.aat1178

Fantin, A., Vieira, J. M., Gestri, G., Denti, L., Schwarz, Q., Prykhozhij, S., et al. (2010). Tissue macrophages act as cellular chaperones for vascular anastomosis downstream of VEGF-mediated endothelial tip cell induction. *Blood* 116, 829–840. doi: 10.1182/blood-2009-12-257832

Fanto, M., and McNeill, H. (2004). Planar polarity from flies to vertebrates. *J. Cell Sci.* 117, 527–533. doi: 10.1242/jcs.00973

Fujita, M., Cha, Y. R., Pham, V. N., Sakurai, A., Roman, B. L., Gutkind, J. S., et al. (2011). Assembly and patterning of the vascular network of the vertebrate hindbrain. *Development* 138, 1705–1715. doi: 10.1242/dev.058776

Gage, F. H. (2000). Mammalian neural stem cells. *Science* 287, 1433–1438. doi: 10.1126/science.287.5457.1433

Gama Sosa, M. A., De Gasperi, R., Rocher, A. B., Perez, G. M., Simons, K., Cruz, D. E., et al. (2007). Interactions of primary neuroepithelial progenitor and brain endothelial cells: distinct effect on neural progenitor maintenance and differentiation by soluble factors and direct contact. *Cell Res.* 17, 619–626. doi: 10.1038/cr.2007.53

Gerhardt, H., Golding, M., Fruttiger, M., Ruhrberg, C., Lundkvist, A., Abramsson, A., et al. (2003). VEGF guides angiogenic sprouting utilizing endothelial tip cell filopodia. *J. Cell Biol.* 161, 1163–1177. doi: 10.1083/jcb.200302047

Goetz, J. G., Steed, E., Ferreira, R. R., Roth, S., Ramspacher, C., Boselli, F., et al. (2014). Endothelial cilia mediate low flow sensing during zebrafish vascular development. *Cell Rep.* 6, 799–808. doi: 10.1016/j.celrep.2014.01.032

Goetz, S. C., and Anderson, K. V. (2010). The primary cilium: a signalling centre during vertebrate development. *Nat. Rev. Genet.* 11, 331–344. doi: 10.1038/nrg2774

Gorivodsky, M., Mukhopadhyay, M., Wilsch-Braeuninger, M., Phillips, M., Teufel, A., Kim, C., et al. (2009). Intraflagellar transport protein 172 is essential for primary cilia formation and plays a vital role in patterning the mammalian brain. *Dev. Biol.* 325, 24–32. doi: 10.1016/j.ydbio.2008.09.019

Gotz, M., and Huttner, W. B. (2005). The cell biology of neurogenesis. *Nat. Rev. Mol. Cell Biol.* 6, 777–788.

Green, D., Whitener, A. E., Mohanty, S., and Lekven, A. C. (2015). Vertebrate nervous system posteriorization: Grading the function of Wnt signaling. *Dev. Dyn.* 244, 507–512. doi: 10.1002/dvdy.24230

Gutierrez-Miranda, L., and Yaniv, K. (2020). Cellular origins of the lymphatic endothelium: implications for cancer lymphangiogenesis. *Front. Physiol.* 11:577584. doi: 10.3389/fphys.2020.577584

Haigh, J. J., Morelli, P. I., Gerhardt, H., Haigh, K., Tsien, J., Damert, A., et al. (2003). Cortical and retinal defects caused by dosage-dependent reductions in VEGF-A paracrine signaling. *Dev. Biol.* 262, 225–241. doi: 10.1016/s0012-1606(03)00356-7

Han, J., Calvo, C. F., Kang, T. H., Baker, K. L., Park, J. H., Parras, C., et al. (2015). Vascular endothelial growth factor receptor 3 controls neural stem cell activation in mice and humans. *Cell Rep.* 10, 1158–1172. doi: 10.1016/j.celrep.2015.01.049

He, L., Vanlandewijck, M., Mae, M. A., Andrae, J., Ando, K., Del Gaudio, F., et al. (2018). Single-cell RNA sequencing of mouse brain and lung vascular and vessel-associated cell types. *Sci. Data* 5:, 180160.

Hierck, B. P., Van der Heiden, K., Alkemade, F. E., Van de Pas, S., Van Thienen, J. V., Groenendijk, B. C., et al. (2008). Primary cilia sensitize endothelial cells for fluid shear stress. *Dev. Dyn.* 237, 725–735. doi: 10.1002/dvdy.21472

Hikasa, H., Ezan, J., Itoh, K., Li, X., Klymkowsky, M. W., and Sokol, S. Y. (2010). Regulation of TCF3 by Wnt-dependent phosphorylation during vertebrate axis specification. *Dev. Cell* 19, 521–532. doi: 10.1016/j.devcel.2010.09.005

Hirtz, D., and Kirkham, F. J. (2019). Sickle cell disease and stroke. *Pediatr. Neurol.* 95, 34–41.

Hogan, K. A., Ambler, C. A., Chapman, D. L., and Bautch, V. L. (2004). The neural tube patterns vessels developmentally using the VEGF signaling pathway. *Development* 131, 1503–1513. doi: 10.1242/dev.01039

Hupe, M., Li, M. X., Kneitz, S., Davydova, D., Yokota, C., Kele, J., et al. (2017). Gene expression profiles of brain endothelial cells during embryonic development at bulk and single-cell levels. *Sci. Signal* 10:, eaag2476.

Iliff, J. J., Chen, M. J., Plog, B. A., Zeppenfeld, D. M., Soltero, M., Yang, L., et al. (2014). Impairment of glymphatic pathway function promotes tau pathology after traumatic brain injury. *J. Neurosci.* 34, 16180–16193. doi: 10.1523/jneurosci.3020-14.2014

Iliff, J. J., Wang, M., Liao, Y., Plogg, B. A., Peng, W., Gundersen, G. A., et al. (2012). A paravascular pathway facilitates CSF flow through the brain parenchyma and the clearance of interstitial solutes, including amyloid beta. *Sci. Transl Med.* 4:, 147ra111. doi: 10.1126/scitranslmed.3003748

Iomini, C., Tejada, K., Mo, W., Vaananen, H., and Piperno, G. (2004). Primary cilia of human endothelial cells disassemble under laminar shear stress. *J. Cell Biol.* 164, 811–817. doi: 10.1083/jcb.200312133

Jain, R. K. (2003). Molecular regulation of vessel maturation. *Nat. Med.* 9, 685–693. doi: 10.1038/nm0603-685

Jambusaria, A., Hong, Z., Zhang, L., Srivastava, S., Jana, A., Toth, P. T., et al. (2020). Endothelial heterogeneity across distinct vascular beds during homeostasis and inflammation. *Elife* 9:, e51413.

Javaherian, A., and Kriegstein, A. (2009). A stem cell niche for intermediate progenitor cells of the embryonic cortex. *Cereb. Cortex 19 Suppl.* 1, i70–i77.

Jones, T. J., Adapala, R. K., Geldenhuys, W. J., Bursley, C., AbouAlaiwi, W. A., Nauli, S. M., et al. (2012). Primary cilia regulates the directional migration and barrier integrity of endothelial cells through the modulation of hsp27 dependent actin cytoskeletal organization. *J. Cell Physiol.* 227, 70–76. doi: 10.1002/jcp.22704

Kallakuri, S., Yu, J. A., Li, J., Li, Y., Weinstein, B. M., Nicoli, S., et al. (2015). Endothelial cilia are essential for developmental vascular integrity in zebrafish. *J. Am. Soc. Nephrol.* 26, 864–875. doi: 10.1681/asn.2013121314

Kalucka, J., de Rooij, L., Goveia, J., Rohlenova, K., Dumas, S. J., Meta, E., et al. (2020). Single-cell transcriptome atlas of murine endothelial cells. *Cell 180* 76:, e20.

Karakatsani, A., Shah, B., and de Almodovar, C. R. (2019). Blood vessels as regulators of neural stem cell properties. *Front. Mol. Neurosci.* 12:85. doi: 10.3389/fnmol.2019.00085

Kimura, E., Isogai, S., and Hitomi, J. (2015). Integration of vascular systems between the brain and spinal cord in zebrafish. *Dev. Biol.* 406, 40–51. doi: 10.1016/j.ydbio.2015.07.015

Kiss, T., Nyul-Toth, A., Balasubramanian, P., Tarantini, S., Ahire, C., DelFavero, J., et al. (2020). Single-cell RNA sequencing identifies senescent cerebromicrovascular endothelial cells in the aged mouse brain. *Geroscience* 42, 429–444. doi: 10.1007/s11357-020-00177-1

Knobloch, M., and Jessberger, S. (2017). Metabolism and neurogenesis. *Curr. Opin. Neurobiol.* 42, 45–52. doi: 10.1016/j.conb.2016.11.006

Kohn, A. D., and Moon, R. T. (2005). Wnt and calcium signaling: beta-catenin-independent pathways. *Cell Calcium.* 38, 439–446. doi: 10.1016/j.ceca.2005.06.022

Kugler, E. C., van Lessen, M., Daetwyler, S., Chhabria, K., Savage, A. M., Silva, V., et al. (2019). Cerebrovascular endothelial cells form transient Notch-dependent cystic structures in zebrafish. *EMBO Rep.* 20:, e47047.

Kuhl, M., Sheldahl, L. C., Park, M., Miller, J. R., and Moon, R. T. (2000). The Wnt/Ca2+ pathway: a new vertebrate Wnt signaling pathway takes shape. *Trends Genet.* 16, 279–283.

Kuhnert, F., Mancuso, M. R., Shamloo, A., Wang, H. T., Choksi, V., Florek, M., et al. (2010). Essential regulation of CNS angiogenesis by the orphan G protein-coupled receptor GPR124. *Science* 330, 985–989. doi: 10.1126/science.1196554

Lange, C., Storkebaum, E., de Almodovar, C. R., Dewerchin, M., and Carmeliet, P. (2016a). Vascular endothelial growth factor: a neurovascular target in neurological diseases. *Nat. Rev. Neurol.* 12, 439–454. doi: 10.1038/nrneurol.2016.88

Lange, C., Turrero Garcia, M., Decimo, I., Bifari, F., Eelen, G., Quaegebeur, A., et al. (2016b). Relief of hypoxia by angiogenesis promotes neural stem cell differentiation by targeting glycolysis. *EMBO J.* 35, 924–941. doi: 10.15252/embj.201592372

Lee, W., Swarup, S., Chen, J., Ishitani, T., and Verheyen, E. M. (2009). Homeodomain-interacting protein kinases (Hipks) promote Wnt/Wg signaling through stabilization of beta-catenin/Arm and stimulation of target gene expression. *Development* 136, 241–251.

Lenard, A., Ellertsdottir, E., Herwig, L., Krudewig, A., Sauteur, L., Belting, H. G., et al. (2013). In vivo analysis reveals a highly stereotypic morphogenetic pathway of vascular anastomosis. *Dev. Cell* 25, 492–506. doi: 10.1016/j.devcel.2013.05.010

Licht, T., and Keshet, E. (2015). The vascular niche in adult neurogenesis. *Mech. Dev. 138 Pt* 1, 56–62. doi: 10.1016/j.mod.2015.06.001

Liebner, S., Corada, M., Bangsow, T., Babbage, J., Taddei, A., Czupalla, C. J., et al. (2008). Wnt/beta-catenin signaling controls development of the blood-brain barrier. *J. Cell Biol.* 183, 409–417. doi: 10.1083/jcb.200806024

Logan, C. Y., and Nusse, R. (2004). The Wnt signaling pathway in development and disease. *Annu. Rev. Cell Dev. Biol.* 20, 781–810.

Louissaint, A. Jr., Rao, S., Leventhal, C., and Goldman, S. A. (2002). Coordinated interaction of neurogenesis and angiogenesis in the adult songbird brain. *Neuron* 34, 945–960. doi: 10.1016/s0896-6273(02)00722-5

Louveau, A., Herz, J., Alme, M. N., Salvador, A. F., Dong, M. Q., Viar, K. E., et al. (2018). CNS lymphatic drainage and neuroinflammation are regulated by meningeal lymphatic vasculature. *Nat. Neurosci.* 21, 1380–1391. doi: 10.1038/s41593-018-0227-9

Louveau, A., Smirnov, I., Keyes, T. J., Eccles, J. D., Rouhani, S. J., Peske, J. D., et al. (2015). Structural and functional features of central nervous system lymphatic vessels. *Nature* 523, 337–341. doi: 10.1038/nature14432

Lowry, N., Goderie, S. K., Adamo, M., Lederman, P., Charniga, C., Gill, J., et al. (2008). Multipotent embryonic spinal cord stem cells expanded by endothelial factors and Shh/RA promote functional recovery after spinal cord injury. *Exp. Neurol.* 209, 510–522. doi: 10.1016/j.expneurol.2007.09.031

Lustig, B., Jerchow, B., Sachs, M., Weiler, S., Pietsch, T., Karsten, U., et al. (2002). Negative feedback loop of Wnt signaling through upregulation of conductin/axin2 in colorectal and liver tumors. *Mol. Cell Biol.* 22, 1184–1193. doi: 10.1128/mcb.22.4.1184-1193.2002

Luu, V. Z., Chowdhury, B., Al-Omran, M., Hess, D. A., and Verma, S. (2018). Role of endothelial primary cilia as fluid mechanosensors on vascular health. *Atherosclerosis* 275, 196–204. doi: 10.1016/j.atherosclerosis.2018.06.818

Ma, N., and Zhou, J. (2020). Functions of endothelial cilia in the regulation of vascular barriers. *Front. Cell Dev. Biol.* 8:626. doi: 10.3389/fcell.2020.00626

Ma, S., Kwon, H. J., Johng, H., Zang, K., and Huang, Z. (2013). Radial glial neural progenitors regulate nascent brain vascular network stabilization via inhibition of Wnt signaling. *PLoS Biol.* 11:e1001469. doi: 10.1371/journal.pbio.1001469

MacDonald, B. T., Tamai, K., and He, X. (2009). Wnt/beta-catenin signaling: components, mechanisms, and diseases. *Dev. Cell* 17, 9–26. doi: 10.1016/j.devcel.2009.06.016

Malicki, J. J., and Johnson, C. A. (2017). The cilium: cellular antenna and central processing unit. *Trends Cell Biol.* 27, 126–140. doi: 10.1016/j.tcb.2016.08.002

Mancuso, M. R., Kuhnert, F., and Kuo, C. J. (2008). Developmental angiogenesis of the central nervous system. *Lymphat. Res. Biol.* 6, 173–180. doi: 10.1089/lrb.2008.1014

Martowicz, A., Trusohamn, M., Jensen, N., Wisniewska-Kruk, J., Corada, M., Ning, F. C., et al. (2019). Endothelial beta-catenin signaling supports postnatal brain and retinal angiogenesis by promoting sprouting, tip cell formation, and VEGFR (Vascular Endothelial Growth Factor Receptor) 2 expression. *Arterioscler. Thromb. Vasc. Biol.* 39, 2273–2288. doi: 10.1161/atvbaha.119.312749

McMahon, A. P., and Moon, R. T. (1989). Ectopic expression of the proto-oncogene int-1 in Xenopus embryos leads to duplication of the embryonic axis. *Cell* 58, 1075–1084. doi: 10.1016/0092-8674(89)90506-0

Miller, E. C. (2019). Preeclampsia and cerebrovascular disease. *Hypertension* 74, 5–13. doi: 10.1161/hypertensionaha.118.11513

Mlodzik, M. (2002). Planar cell polarization: do the same mechanisms regulate *Drosophila* tissue polarity and vertebrate gastrulation? *Trends Genet.* 18, 564–571. doi: 10.1016/s0168-9525(02)02770-1

Mohyeldin, A., Garzon-Muvdi, T., and Quinones-Hinojosa, A. (2010). Oxygen in stem cell biology: a critical component of the stem cell niche. *Cell Stem Cell* 7, 150–161. doi: 10.1016/j.stem.2010.07.007

Molenaar, M., van de Wetering, M., Oosterwegel, M., Peterson-Maduro, J., Godsave, S., Korinek, V., et al. (1996). XTcf-3 transcription factor mediates beta-catenin-induced axis formation in Xenopus embryos. *Cell* 86, 391–399. doi: 10.1016/s0092-8674(00)80112-9

Montcouquiol, M., Crenshaw, E. B. III, and Kelley, M. W. (2006). Noncanonical Wnt signaling and neural polarity. *Annu. Rev. Neurosci.* 29, 363–386. doi: 10.1146/annurev.neuro.29.051605.112933

Moon, R. T., Campbell, R. M., Christian, J. L., McGrew, L. L., Shih, J., and Fraser, S. (1993). Xwnt-5A: a maternal Wnt that affects morphogenetic movements after overexpression in embryos of Xenopus laevis. *Development* 119, 97–111.

Morris, A. W., Sharp, M. M., Albargothy, N. J., Fernandes, R., Hawkes, C. A., Verma, A., et al. (2016). Vascular basement membranes as pathways for the passage of fluid into and out of the brain. *Acta Neuropathol.* 131, 725–736. doi: 10.1007/s00401-016-1555-z

Nauli, S. M., Kawanabe, Y., Kaminski, J. J., Pearce, W. J., Ingber, D. E., and Zhou, J. (2008). Endothelial cilia are fluid shear sensors that regulate calcium signaling and nitric oxide production through polycystin-1. *Circulation* 117, 1161–1171. doi: 10.1161/circulationaha.107.710111

Nie, K., Molnar, Z., and Szele, F. G. (2010). Proliferation but not migration is associated with blood vessels during development of the rostral migratory stream. *Dev. Neurosci.* 32, 163–172. doi: 10.1159/000301135

Noordermeer, J., Klingensmith, J., Perrimon, N., and Nusse, R. (1994). Dishevelled and armadillo act in the wingless signalling pathway in *Drosophila*. *Nature* 367, 80–83. doi: 10.1038/367080a0

Norris, D. M., and Santoro, M. M. (2018). Before the Pump. *Arterioscler. Thromb. Vasc. Biol.* 38, 2763–2764.

Nusslein-Volhard, C., and Wieschaus, E. (1980). Mutations affecting segment number and polarity in Drosophila. *Nature* 287, 795–801. doi: 10.1038/287795a0

Ottone, C., Krusche, B., Whitby, A., Clements, M., Quadrato, G., Pitulescu, M. E., et al. (2014). Direct cell-cell contact with the vascular niche maintains quiescent neural stem cells. *Nat. Cell Biol.* 16, 1045–1056. doi: 10.1038/ncb3045

Paik, D. T., Tian, L., Williams, I. M., Rhee, S., Zhang, H., Liu, C., et al. (2020). Single-Cell RNA-seq unveils unique transcriptomic signatures of organ-specific endothelial cells. *Circulation* 142, 1848–1862. doi: 10.1161/circulationaha.119.041433

Parr, B. A., Shea, M. J., Vassileva, G., and McMahon, A. P. (1993). Mouse Wnt genes exhibit discrete domains of expression in the early embryonic CNS and limb buds. *Development* 119, 247–261.

Peifer, M., Sweeton, D., Casey, M., and Wieschaus, E. (1994). wingless signal and Zeste-white 3 kinase trigger opposing changes in the intracellular distribution of Armadillo. *Development* 120, 369–380.

Peng, W., Achariyar, T. M., Li, B., Liao, Y., Mestre, H., Hitomi, E., et al. (2016). Suppression of glymphatic fluid transport in a mouse model of Alzheimer's disease. *Neurobiol. Dis.* 93, 215–225. doi: 10.1016/j.nbd.2016.05.015

Picelli, S. (2017). Single-cell RNA-sequencing: the future of genome biology is now. *RNA Biol.* 14, 637–650. doi: 10.1080/15476286.2016.1201618

Pollock, L. M., Perkins, B., and Anand-Apte, B. (2020). Primary cilia are present on endothelial cells of the hyaloid vasculature but are not required for the development of the blood-retinal barrier. *PLoS One* 15:e0225351. doi: 10.1371/journal.pone.0225351

Posokhova, E., Shukla, A., Seaman, S., Volate, S., Hilton, M. B., Wu, B., et al. (2015). GPR124 functions as a WNT7-specific coactivator of canonical beta-catenin signaling. *Cell Rep.* 10, 123–130. doi: 10.1016/j.celrep.2014.12.020

Potter, S. S. (2018). Single-cell RNA sequencing for the study of development, physiology and disease. *Nat. Rev. Nephrol.* 14, 479–492. doi: 10.1038/s41581-018-0021-7

Proulx, K., Lu, A., and Sumanas, S. (2010). Cranial vasculature in zebrafish forms by angioblast cluster-derived angiogenesis. *Dev. Biol.* 348, 34–46. doi: 10.1016/j.ydbio.2010.08.036

Puelles, L., Martinez-Marin, R., Melgarejo-Otalora, P., Ayad, A., Valavanis, A., and Ferran, J. L. (2019). Patterned vascularization of embryonic mouse forebrain, and neuromeric topology of major human subarachnoidal arterial branches: a prosomeric mapping. *Front. Neuroanat.* 13:59. doi: 10.3389/fnana.2019.00059

Raab, S., Beck, H., Gaumann, A., Yuce, A., Gerber, H. P., Plate, K., et al. (2004). Impaired brain angiogenesis and neuronal apoptosis induced by conditional homozygous inactivation of vascular endothelial growth factor. *Thromb. Haemost.* 91, 595–605. doi: 10.1160/th03-09-0582

Radjavi, A., Smirnov, I., Derecki, N., and Kipnis, J. (2014). Dynamics of the meningeal CD4(+) T-cell repertoire are defined by the cervical lymph nodes and facilitate cognitive task performance in mice. *Mol. Psychiatry* 19, 531–533. doi: 10.1038/mp.2013.79

Ramasamy, S. K., Kusumbe, A. P., and Adams, R. H. (2015). Regulation of tissue morphogenesis by endothelial cell-derived signals. *Trends Cell Biol.* 25, 148–157. doi: 10.1016/j.tcb.2014.11.007

Ridley, A. J., Schwartz, M. A., Burridge, K., Firtel, R. A., Ginsberg, M. H., Borisy, G., et al. (2003). Cell migration: integrating signals from front to back. *Science* 302, 1704–1709. doi: 10.1126/science.1092053

Risau, W. (1997). Mechanisms of angiogenesis. *Nature* 386, 671–674.

Rodriguez-Martinez, G., and Velasco, I. (2012). Activin and TGF-beta effects on brain development and neural stem cells. *CNS Neurol. Disord. Drug Targets* 11, 844–855. doi: 10.2174/1871527311201070844

Roman, B. L., Pham, V. N., Lawson, N. D., Kulik, M., Childs, S., Lekven, A. C., et al. (2002). Disruption of acvrl1 increases endothelial cell number in zebrafish cranial vessels. *Development* 129, 3009–3019.

Roose, J., Molenaar, M., Peterson, J., Hurenkamp, J., Brantjes, H., Moerer, P., et al. (1998). The Xenopus Wnt effector XTcf-3 interacts with Groucho-related transcriptional repressors. *Nature* 395, 608–612. doi: 10.1038/26989

Ruhrberg, C., and Bautch, V. L. (2013). Neurovascular development and links to disease. *Cell Mol. Life Sci.* 70, 1675–1684. doi: 10.1007/s00018-013-1277-5

Sabbagh, M. F., Heng, J. S., Luo, C., Castanon, R. G., Nery, J. R., Rattner, A., et al. (2018). Transcriptional and epigenomic landscapes of CNS and non-CNS vascular endothelial cells. *Elife* 7:, e36187.

Seifert, J. R., and Mlodzik, M. (2007). Frizzled/PCP signalling: a conserved mechanism regulating cell polarity and directed motility. *Nat. Rev. Genet.* 8, 126–138. doi: 10.1038/nrg2042

Sheldahl, L. C., Park, M., Malbon, C. C., and Moon, R. T. (1999). Protein kinase C is differentially stimulated by Wnt and Frizzled homologs in a G-protein-dependent manner. *Curr. Biol.* 9, 695–698. doi: 10.1016/s0960-9822(99)80310-8

Si, J., Chen, L., and Xia, Z. (2006). Effects of cervical-lymphatic blockade on brain edema and infarction volume in cerebral ischemic rats. *Chin. J. Physiol.* 49, 258–265.

Siegfried, E., Chou, T. B., and Perrimon, N. (1992). wingless signaling acts through zeste-white 3, the Drosophila homolog of glycogen synthase kinase-3, to regulate engrailed and establish cell fate. *Cell* 71, 1167–1179. doi: 10.1016/s0092-8674(05)80065-0

Siqueira, M., Francis, D., Gisbert, D., Gomes, F. C. A., and Stipursky, J. (2018). Radial glia cells control angiogenesis in the developing cerebral cortex through TGF-beta1 Signaling. *Mol. Neurobiol.* 55, 3660–3675.

Sorriento, D., Santulli, G., Del Giudice, C., Anastasio, A., Trimarco, B., and Iaccarino, G. (2012). Endothelial cells are able to synthesize and release catecholamines both *in vitro* and in vivo. *Hypertension* 60, 129–136. doi: 10.1161/hypertensionaha.111.189605

Strasser, G. A., Kaminker, J. S., and Tessier-Lavigne, M. (2010). Microarray analysis of retinal endothelial tip cells identifies CXCR4 as a mediator of tip cell morphology and branching. *Blood* 115, 5102–5110. doi: 10.1182/blood-2009-07-230284

Szentistvanyi, I., Patlak, C. S., Ellis, R. A., and Cserr, H. F. (1984). Drainage of interstitial fluid from different regions of rat brain. *Am. J. Physiol.* 246, F835–F844.

Tata, M., Ruhrberg, C., and Fantin, A. (2015). Vascularisation of the central nervous system. *Mech. Dev. 138 Pt* 1, 26–36. doi: 10.1016/j.mod.2015.07.001

Tata, M., Wall, I., Joyce, A., Vieira, J. M., Kessaris, N., and Ruhrberg, C. (2016). Regulation of embryonic neurogenesis by germinal zone vasculature. *Proc. Natl. Acad. Sci. U. S. A.* 113, 13414–13419. doi: 10.1073/pnas.1613113113

Ulrich, F., Carretero-Ortega, J., Menendez, J., Narvaez, C., Sun, B., Lancaster, E., et al. (2016). Reck enables cerebrovascular development by promoting canonical Wnt signaling. *Development* 143:, 1055. doi: 10.1242/dev.136507

Ulrich, F., Ma, L. H., Baker, R. G., and Torres-Vazquez, J. (2011). Neurovascular development in the embryonic zebrafish hindbrain. *Dev. Biol.* 357, 134–151. doi: 10.1016/j.ydbio.2011.06.037

Vallon, M., Yuki, K., Nguyen, T. D., Chang, J., Yuan, J., Siepe, D., et al. (2018). WNT7 receptor-ligand interaction enables isoform-specific regulation of Wnt bioavailability. *Cell Rep. 25* 33:, e9.

Vanhollebeke, B., Stone, O. A., Bostaille, N., Cho, C., Zhou, Y., Maquet, E., et al. (2015). Tip cell-specific requirement for an atypical Gpr124- and Reck-dependent Wnt/beta-catenin pathway during brain angiogenesis. *Elife* 4:, e06489.

Vasudevan, A., Long, J. E., Crandall, J. E., Rubenstein, J. L., and Bhide, P. G. (2008). Compartment-specific transcription factors orchestrate angiogenesis gradients in the embryonic brain. *Nat. Neurosci.* 11, 429–439. doi: 10.1038/nn2074

Vion, A. C., Alt, S., Klaus-Bergmann, A., Szymborska, A., Zheng, T., Perovic, T., et al. (2018). Primary cilia sensitize endothelial cells to BMP and prevent excessive vascular regression. *J. Cell Biol.* 217, 1651–1665. doi: 10.1083/jcb.201706151

Vissapragada, R., Contreras, M. A., da Silva, C. G., Kumar, V. A., Ochoa, A., Vasudevan, A., et al. (2014). Bidirectional crosstalk between periventricular endothelial cells and neural progenitor cells promotes the formation of a neurovascular unit. *Brain Res.* 1565, 8–17. doi: 10.1016/j.brainres.2014.03.018

Vlad, A., Rohrs, S., Klein-Hitpass, L., and Muller, O. (2008). The first five years of the Wnt targetome. *Cell Signal.* 20, 795–802. doi: 10.1016/j.cellsig.2007.10.031

Wang, Y., and Nathans, J. (2007). Tissue/planar cell polarity in vertebrates: new insights and new questions. *Development* 134, 647–658. doi: 10.1242/dev.02772

Wu, C. H., Lirng, J. F., Ling, Y. H., Wang, Y. F., Wu, H. M., Fuh, J. L., et al. (2020). Noninvasive characterization of human glymphatics and meningeal lymphatics in an in vivo model of blood-brain barrier leakage. *Ann. Neurol.* 89, 111–124. doi: 10.1002/ana.25928

Zhao, Z., Nelson, A. R., Betsholtz, C., and Zlokovic, B. V. (2015). Establishment and dysfunction of the blood-brain barrier. *Cell* 163, 1064–1078. doi: 10.1016/j.cell.2015.10.067

Zhou, Y., and Nathans, J. (2014). Gpr124 controls CNS angiogenesis and blood-brain barrier integrity by promoting ligand-specific canonical wnt signaling. *Dev. Cell* 31, 248–256. doi: 10.1016/j.devcel.2014.08.018

Zlokovic, B. V. (2005). Neurovascular mechanisms of Alzheimer's neurodegeneration. *Trends Neurosci.* 28, 202–208. doi: 10.1016/j.tins.2005.02.001

**Conflict of Interest:** The authors declare that the research was conducted in the absence of any commercial or financial relationships that could be construed as a potential conflict of interest.

frontiers in Physiology

REVIEW
published: 25 February 2021
doi: 10.3389/fphys.2021.639645

# Vessel Enlargement in Development and Pathophysiology

*Laia Gifre-Renom*[1] *and Elizabeth A. V. Jones*[1,2]*

[1]*Department of Cardiovascular Sciences, Centre for Molecular and Vascular Biology, KU Leuven, Leuven, Belgium,*
[2]*Department of Cardiology, CARIM School for Cardiovascular Diseases, Maastricht University, Maastricht, Netherlands*

From developmental stages until adulthood, the circulatory system remodels in response to changes in blood flow in order to maintain vascular homeostasis. Remodeling processes can be driven by *de novo* formation of vessels or angiogenesis, and by the restructuration of already existing vessels, such as vessel enlargement and regression. Notably, vessel enlargement can occur as fast as in few hours in response to changes in flow and pressure. The high plasticity and responsiveness of blood vessels rely on endothelial cells. Changes within the bloodstream, such as increasing shear stress in a narrowing vessel or lowering blood flow in redundant vessels, are sensed by endothelial cells and activate downstream signaling cascades, promoting behavioral changes in the involved cells. This way, endothelial cells can reorganize themselves to restore normal circulation levels within the vessel. However, the dysregulation of such processes can entail severe pathological circumstances with disturbances affecting diverse organs, such as human hereditary telangiectasias. There are different pathways through which endothelial cells react to promote vessel enlargement and mechanisms may differ depending on whether remodeling occurs in the adult or in developmental models. Understanding the molecular mechanisms involved in the fast-adapting processes governing vessel enlargement can open the door to a new set of therapeutical approaches to be applied in occlusive vascular diseases. Therefore, we have outlined here the latest advances in the study of vessel enlargement in physiology and pathology, with a special insight in the pathways involved in its regulation.

**Keywords: venogenesis, migration, vascular fusion, mechanotransduction, collateral growth, arteriogenesis, vessel enlargement, arterial venous malformation**

OPEN ACCESS

***Edited by:***
*Anna Rita Cantelmo, Université Lille Nord de France, France*

***Reviewed by:***
*Anthony Wayne Orr, Louisiana State University Health Shreveport, United States*
*Stephanie Lehoux, McGill University, Canada*

***Correspondence:**
*Elizabeth A. V. Jones*
*liz.jones@kuleuven.be*

***Specialty section:***
*This article was submitted to Vascular Physiology, a section of the journal Frontiers in Physiology*

***Received:*** *09 December 2020*
***Accepted:*** *01 February 2021*
***Published:*** *25 February 2021*

***Citation:***
*Gifre-Renom L and Jones EAV (2021) Vessel Enlargement in Development and Pathophysiology. Front. Physiol. 12:639645. doi: 10.3389/fphys.2021.639645*

## INTRODUCTION

During development, vascular beds often form as honeycombed shaped capillary plexus that then become perfused and remodel to form a hierarchical vessel structure. One of the most visible changes that occur in this process is the enlargement of both arteries and veins. Vessel enlargement can occur remarkably quickly. In the embryo, this occurs within a single day after the onset of blood flow. As such, vessel enlargement has therapeutic potential in occlusive vascular diseases that slower processes, such as angiogenesis, lack. However, so far, most research on therapeutic strategies has been focused on angiogenesis and significantly less advancement has been made to exploit vessel enlargement as a potential therapy in ischemic diseases. In strokes and heart attacks, for example, local collateral vessels immediately dilate to restore blood flow, but angiogenesis is a latter process in the body's attempt to restore

proper perfusion (Schaper and Ito, 1996). Vessel can dilate on the short term, but can also undergo outward remodeling such that vessel diameter changes are permanent (Silver and Vita, 2006). As such, it is primarily vessel enlargement that prevents excessive cell death.

Though occlusive vascular diseases are important pathologies where inducing vessel enlargement could provide therapeutic benefits, when vessels enlarge ectopically, there can be devastating negative consequences. Arterial-venous malformations (AVMs) are a form of anomalous vessel enlargement where enlarged shunts bypass the capillary bed and directly connect arteries and veins. Because the venous network is then exposed to arterial blood pressure, AVMs are prone to hemorrhage, which can be fatal depending on the organ where they occur. For instance, cerebral AVMs account for 50% of childhood strokes (Meyer-Heim and Boltshauser, 2003). Though AVMs are the most serious example of pathological vessel enlargement, these are not the only example of such a process. Varicose veins also represent a form of pathological vessel enlargement (Jacobs et al., 2017) that can cause itching and discomfort, and are one of the most common reported medical conditions in Western countries (Beebe-Dimmer et al., 2005).

Despite the importance of vessel enlargement, we are just beginning to understand how diameter changes occur. It was initially assumed that vessels enlarged by proliferation and while this may be true in some vascular beds, proliferation is a slow process and therefore could not restore blood flow on the timescales needed after stroke or heart attack. Vessel dilation, followed by outward remodeling can, at least partially, mitigate the slow process of cell proliferation. More recently, however, migration and capillary fusion have been proposed as methods by which a vascular network can increase the diameter of vessels. It is important to note, however, that it is unlikely that any of these processes happen in isolation. As such, vascular networks likely use a combination of means to increase vessel diameters. We therefore review here the processes and pathways by which vessels enlarge, and highlight differences and similarities between vascular development, vasculopathy and enlargement in adult vascular beds.

## MECHANISMS OF VESSEL ENLARGEMENT

Four mechanisms of vessel enlargement have been identified, though the prevalence or relative importance of each of these mechanisms is still not clear. First, endothelial cell migration can lead to the accumulation of cells in one region, leading to regional enlargement of a vessel. Second, smaller vessels can fuse with each other, thereby rapidly increasing the diameter. Vessels can also increase in diameter because of either local proliferation of endothelial cells (third mechanism), or by local hypertrophy of endothelial cells (fourth). Vessel enlargement occurring in developmental vascular networks refers to the enlargement of capillaries to form arterioles/venules. In the adult, vessel enlargement has mostly only been studied with respect to enlargement of larger vessels (arterioles and venules) and of collateral vessels. Differences in the type of vessel which is enlarging can also account for differences in mechanism highlighted below.

### Migration

Migration is currently the most well accepted mechanism for vessel enlargement in developmental models. In this mechanism, vessel enlargement occurs by a reshuffling of existing vessels guided by changes in shear stress. Shear stress is the force per unit area exerted by flow, expressed either in $N/m^2$ (i.e., Pascals) or in $dyne/cm^2$. Shear stress can be thought of as friction against the endothelium. It relates both to the speed of the blood flow and vessel geometry. In the migration paradigm of vessel enlargement, endothelial cells migrate against flow when shear stress levels are decreased compared to physiological normal levels (which are 15 $dyn/cm^2$ in humans or 30 $dyn/cm^2$ in mouse) and stop migrating in the presence of physiological levels (Franco et al., 2015; Tabibian et al., 2020). Therefore, vessels with the lowest flow rates regress increasing the pool of available endothelial cells. Furthermore, because endothelial cells stop migrating in high shear stress vessels, they accumulate in regions of high shear stress (**Figure 1**). This idea was first proposed approximately 20 years ago (Hughes and Chang-Ling, 2000) but gained significantly more interest as imaging technology improved, allowing individual endothelial cell tracking (Udan et al., 2013; Franco et al., 2015).

In support of this mechanism, multiple groups have shown that there is very little proliferation or apoptosis during vessel remodeling and vessel enlargement, either in the retina, in zebrafish embryo or in mouse embryo (Hughes and Chang-Ling, 2000; Udan et al., 2013; Franco et al., 2015). Myosin light chain 2a ($MLC2a$)$^{-/-}$ embryos, which have severely reduced flow and do not undergo vessel enlargement, have the same levels of endothelial cell proliferation and apoptosis as control wild-type embryos (Udan et al., 2013). Furthermore, time-lapse microscopy of developing embryos has shown that there is a stunning amount of endothelial cell migration occurring during vascular remodeling (Sato et al., 2010; Cui et al., 2013). Using a quail embryo that has Yellow Fluorescent Protein (YFP)-labeled endothelial cells, Cui et al. (2013) imaged vitelline artery formation (see especially movie S4). Endothelial cells can be observed migrating against flow, towards the embryo proper, as a mass collective movement. Similarly, using time-lapse microscopy of whole mouse embryos between embryonic day (E) E8.5 and E9.5, Udan et al. (2013) showed that endothelial cells leave low flow capillaries towards enlarging vessels, whereas in the $MLC2a^{-/-}$ mutant embryos, endothelial cells lose their ability to undergo directional migration.

Our group has recently used the migration-induced mechanism of vessel enlargement to develop computational models of remodeling and vessel enlargement (Tabibian et al., 2020). *In vitro*, we found that there is indeed a bell-shaped pattern of migration with respect to shear stress. Endothelial cells do not migrate in static or at extremely low shear stress levels. Endothelial cells exposed to shear stress levels between 0.5 and 5 $dyn/cm^2$ show the highest level of migration, with

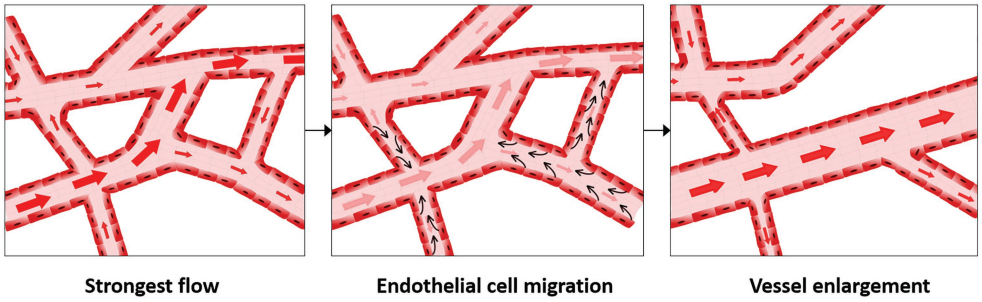


**FIGURE 1 |** Migration-induced vessel enlargement. Under low shear stress, endothelial cells migrate against flow and stop or reduce migration when exposed to shear stresses at or above their shear stress physiological levels. In this way, endothelial cells accumulate in vessels under higher shear stress, leading to vessel enlargement.

a peak at 1 dyn/cm$^2$. Higher shear stress levels return migration rates to static levels (Tabibian et al., 2020). This information was then used to build the computational model where shear-stress levels defined the speed of migration, but the direction of migration was influenced both by the direction of the flow and a requirement for collective cell movement. This alone gave modest predictive ability, which was improved by the addition of growth of avascular regions and, more surprisingly, by the addition of endothelial cell elongation in the direction of flow. Although the role of cell elongation in remodeling is currently unexplored, studies on mice where endothelial cells cannot elongate did not report vessel enlargement defects (Baeyens et al., 2014; Corti et al., 2019). Those results, however, also found that shear stress magnitude is sensed apart from shear stress direction (Baeyens et al., 2014), consistent with our computational results.

In order to migrate against flow, endothelial cells are first polarized against the direction of flow (Franco et al., 2015). Labeling the Golgi and nucleus allows endothelial cell polarization to be visualized. By comparing polarization to predicted flow patterns, endothelial cells were shown to be polarized against flow in the developing retina (Franco et al., 2015). A key player in the maintenance of the endothelial polarization, first identified in the retina, is the primary cilium of endothelial cells (Vion et al., 2018). Primary cilia are present on endothelial cells when exposed to low shear stress, whereas higher levels of shear stress often cause disassembly of the cilia (Iomini et al., 2004; Egorova et al., 2011; Ten Dijke et al., 2012). By a genetic deletion of the essential cilia component intraflagellar transport protein 88 (IFT88), Vion et al. (2018) described a random and premature regression of blood vessels related to an increase in migration and a reduced polarization of the endothelial cells.

The Bone Morphogenetic Protein/Activin receptor-like kinase 1/Endoglin (BMP/ALK1/ENG) pathway is also required for polarized migration in response to flow (**Figure 2**). Mutations in the *ENG* and *ACVRL1* genes (encoding for *ENG* and ALK1) cause Hereditary Hemorrhagic Telangiectasia (HHT), which is a genetic form of AVM development (McAllister et al., 1994; Johnson et al., 1996). Loss of directional migration has been reported for ENG (Jin et al., 2017) and ALK1 (Rochon et al., 2016) in mouse *ENG*-knockouts and in a zebrafish AVM model lacking *ALK1*, respectively. Recently, our group has identified that, under shear stress, SMAD1/5/9 (transcription factors in this pathway) control the expression of the gene (*GJA4*) for the gap junction protein Cx37 (Connexin37; Peacock et al., 2020). We also found that Cx37 has a critical role in the maintenance of the directionality of endothelial cell migration under flow. Interestingly, mechanotransduction by the primary cilium also functions through the ALK1 pathway, with the primary cilium increasing BMP9 responsiveness of endothelial cells under low shear stress, thereby decreasing their migration speed. This may prevent premature vascular regression under low shear stress processes, such as during the initial remodeling of the retinal vascular network (Vion et al., 2018).

Though regressing cells are a source of endothelial cells for enlarging vessels, the venous vascular bed also contributes cells. Notably, proliferation is higher in venous endothelial cells than in arterial endothelial cells (Red-Horse et al., 2010; Ehling et al., 2013) and, therefore, venous cells provide a source of cells for the migration model of vessel enlargement (**Figure 2**). Coup-TFII, which is one of the most important venous transcription factors, can repress the expression of Fms Related Receptor Tyrosine Kinase 1 (*FLT1*; also known as *VEGFR1*, Vascular Endothelial Growth Factor Receptor 1) and *Notch*, thereby promoting endothelial cell proliferation (You et al., 2005; Qin et al., 2010; Chen et al., 2012). In the mouse embryonic heart, for instance, coronary arteries have been shown to form from venous endothelial cells (Su et al., 2018). In the mouse retina, labeling tip cells permitted to observe the integration of the labeled cells in growing arteries, but rarely into the venous vascular bed (Xu et al., 2014; Pitulescu et al., 2017). This has led to the proposal that endothelial cells proliferate in veins, migrate from low shear stress veins through the capillary bed and then ultimately stop migrating in the arterial vascular bed because of high shear stress levels. They therefore accumulate in this region, inducing vessel enlargement (Red-Horse and Siekmann, 2019).

## Fusion

Vessel fusion was first described over three decades ago but has received less attention than other mechanisms of vessel

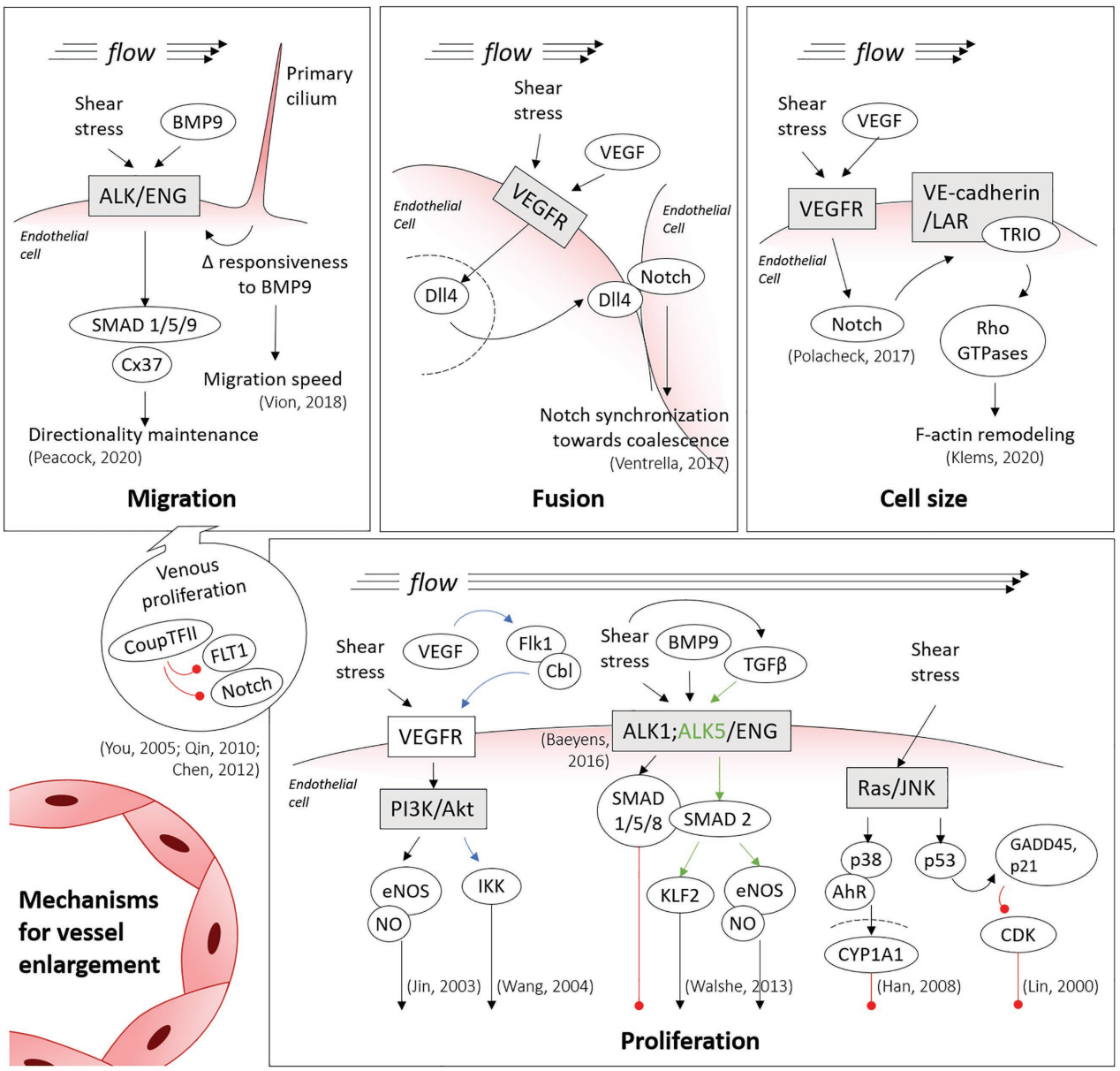


**FIGURE 2 |** Main mechanisms involved in vessel enlargement. Summary of the shear-inducible mechanotransduction pathways involved in migration, fusion, hypertrophy and proliferation of endothelial cells, the processes directing vessel enlargement. Blue and green arrows are colored to clarify the trigger of specific downstream pathways, being shear stress involved in both cases. Red lines denote inhibition (thus, cell cycle arrest, in the proliferation panel). Discontinued lines denote the nuclei membranes.

enlargement. Drake and Little (1995) were first to describe this process. By time-lapsing dorsal aorta development in avian embryos, they showed that a capillary bed initially formed along the length of the embryo proper and that with the onset of blood flow, these capillaries merge together forming larger and larger vessels (**Figure 3A**; Rupp et al., 2004). These observations were further confirmed with the development of transgenic quail embryos that allowed clear visualizations of the forming dorsal aorta [see movies S3 and S6, (Sato et al., 2010)]. Moreover, both the vitelline artery and vitelline vein were also reported to form by fusion of smaller capillaries in these transgenic quails (Sato et al., 2010).

Though the initial reports on fusion mainly focused on the dorsal aorta in avian embryos, this process was later shown to also occur in other models and other vascular beds. In mouse, time-lapse microscopy showed that fusion is the main mechanism by which yolk sac vessel enlarge, leading to periodic jumps in vessel diameter rather than smooth linear increases in vessel diameter (Udan et al., 2013). Here, fusion processes could be identified in the formation of both the

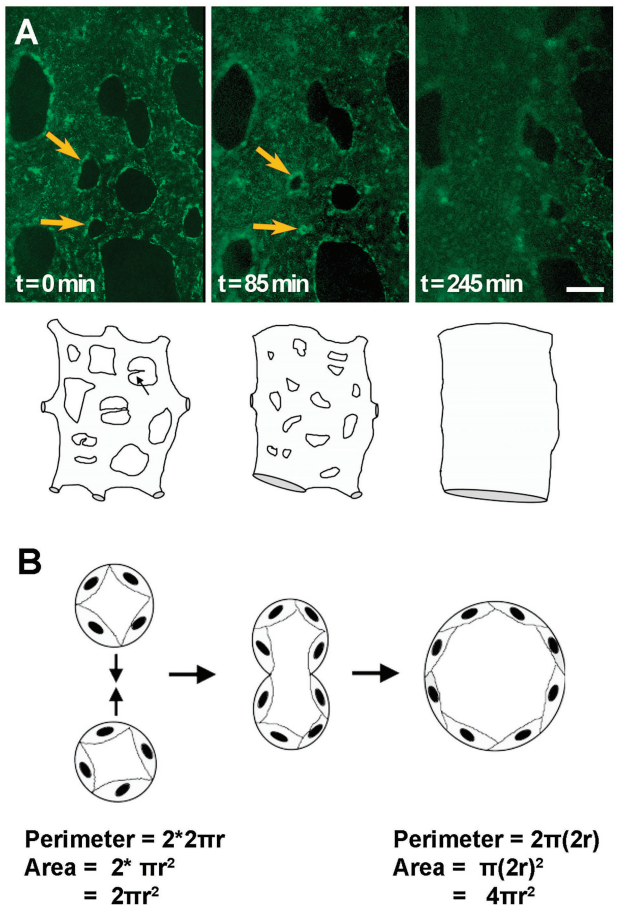


**FIGURE 3 |** Vessel enlargement by fusion. **(A)** Capillary plexus vessels merge to form a larger vessel, as shown by time-lapse microscopy of AcLDL labeled vitelline vessels in quail embryos. Yellow arrows indicate avascular regions that become smaller and smaller until two adjacent vessels fuse. Cartoon exemplifies changes that can be observed by time-lapse microscopy. **(B)** Schematic of the fusion process in transverse view. The same number of cells, or perimeter length, leads to a doubling in the area for flow after fusion. Cartoons adapted from (Drake and Little, 1999).

vitelline artery and the vitelline vein in mouse. Quantification of sprouting/regression/fusion/splitting events during remodeling of the yolk sac vasculature shows that fusion is more common than vessel regression in the embryo, but slightly less common than angiogenesis (Chouinard-Pelletier et al., 2013). The overall number of fusion events is on the same order of magnitude as sprouting and regression events. The coalesce of a capillary bed along the embryonic midline has never been reported for the mouse dorsal aorta formation. However, the Semaphorin 3E (*SEMA3E*)$^{-/-}$ embryo, involved in repulsive endothelial cell guidance, shows a transient phenotype whereby a plexus is present that eventually coalesces to paired dorsal aortae. This suggests that vessel coalescence may be retarded in these mutants and, therefore, observable (Meadows et al., 2013). Vessel enlargement in other organs has also been reported to occur by fusion, or coalescence, of smaller vessels, such as the central pancreatic duct, which develops from smaller capillary vessels joining and fusing into one large diameter vessel (Azizoglu et al., 2016).

Fusion is a much faster process to enlarge a vessel than either migration or proliferation. Within hours, two small vessels can merge leading to a doubling in the radius of the vessel, but a 4-fold increase in the cross-sectional area for flow (**Figure 3B**). This may explain why reports of fusion have been limited to embryonic vascular beds, where remodeling must occur much more rapidly than in more mature systems. It is also possible, thus, that difficulties in detecting fusion prevent its identification in other vascular beds. Morphologically, as vessels fuse, the avascular region between the two vessels becomes smaller and smaller, eventually creating "pillars" of avascular tissue that are identical to the pillars present in intussusceptive angiogenesis. As such, static images cannot differentiate fusion from intussusceptive angiogenesis. Indeed, fusion may only have been identified in embryonic vasculatures because these are the vascular beds where time-lapse microscopy at the resolution of capillaries is possible.

Just as for migration, flow is essential for fusion to occur. In the aforementioned *SEMA3E*$^{-/-}$ mutants, the timing of resolution of the unfused phenotype correlates to the onset of blood flow (Meadows et al., 2013). In normal vascular development, fusion occurs in regions with the highest flow, such as the region where the vitelline artery and vein are forming (Sato et al., 2010; Chouinard-Pelletier et al., 2013; Udan et al., 2013). Unexpectedly, if flow patterns are altered to reduce shear stress, an increased number of fusion events is observed (Chouinard-Pelletier et al., 2013). If shear stress levels are increased instead, the opposite occurs, and less fusion is present. Though these results may appear paradoxical, the increased flow in the region of the forming vitelline artery and vein do not necessarily mean that increased shear stress drives fusion. Shear stress relates not only to the flow velocity but also to geometry of the vessels. If an avascular region between two fusing vessels acts as an obstruction in the middle of a fast-flowing stream, then, as the velocity of that stream increases, shear stress will be increased on the upstream side of the avascular region but decreased on the downstream side (**Figure 4**). As such, gradients of shear stress may drive fusion events rather than just increases in the total amount or velocity of flow.

Given the difficulties in identifying fusion events, very little is known about the mechanism of fusion. There are various phenotypes, however, that present with a hyperfused vascular plexus. Inhibition of Notch in the embryonic yolk sac results in increased number of fusion events (Chouinard-Pelletier et al., 2013; Caolo et al., 2018). The increased amount of fusion observed during Notch inhibition can be rescued by increasing shear stress levels (Caolo et al., 2018). In the chick embryo yolk sac, exogenous vascular endothelial growth factor (VEGF) induced increased vascular fusion (Drake and Little, 1995). Sema3E signaling induces the expression of *sFLT1* (Zygmunt et al., 2011) and, as such, the *SEMA3E*$^{-/-}$ should have reduced VEGF signaling. Though the interplay of VEGF and Notch signaling is well studied for sprouting angiogenesis (Eichmann and Simons, 2012), why they would induce fusion

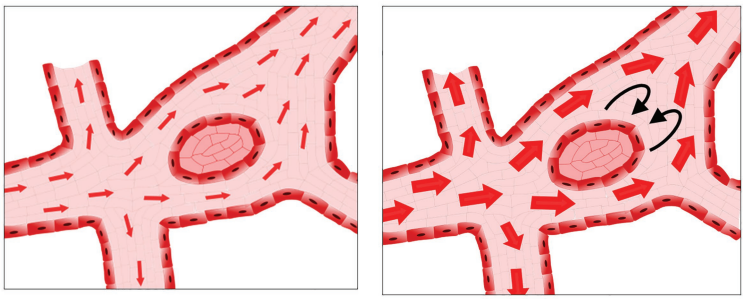

**FIGURE 4 |** Possible low shear stress regions in the presence of increased flow rates. As flow increases, avascular regions can act as obstacles to the flow, resulting in regions of low shear stress and/or recirculation downstream from the avascular region.

in other situations is a mystery. The key may lie in the role of VEGF in synchronizing Notch signaling (**Figure 2**). In somitogenesis, Notch is involved in synchronizing cells such that all cells cycle together and express the same genes together (Jiang et al., 2000). In endothelial cells, levels of Notch targeting genes also oscillate, but in an unsynchronized manner. Under higher levels of VEGF, however, Notch-induced gene expression synchronizes endothelial cells, favoring vessel enlargement rather than extension (Ubezio et al., 2016). The act of favoring "self" (staying together) rather than "other" (extending a sprout) has previously been proposed for the role of Notch target genes in boundary formation (Ventrella et al., 2017). In this model, Notch synchronization would create a situation where vessel coalesce with each other (i.e., fuse), as they prefer adhering to one another rather than remaining separate.

## Proliferation

Though no significant proliferation is observed during vessel enlargement in developmental models, whether the retina or the embryo, this is not the case for vessel enlargement in adult vascular beds. Chronic changes in flow in the adult lead to expansion of collateral blood vessels that restore normal blood flow levels. This process was termed arteriogenesis (Scholz et al., 2001). After partial coronary ligation model, endothelial cell proliferation is observed in enlarging vessels, peaking 3 weeks after implantation of the constrictor (Schaper et al., 1971). In hind limb ischemia models, significant endothelial cell and smooth muscle cell proliferation is observed in the enlarging vessels within 2–3 days of ligation (Scholz et al., 2000). Vessel enlargement by proliferation occurs over a period of days and weeks, not hours. Though endothelial cells are clearly proliferating within the growing arterioles (Scholz et al., 2000), this does not exclude a role for migration in collateral enlargement.

Vascular endothelial growth factor is most well known as a mitogen for endothelial cells proliferation. VEGF acts by binding to VEGF receptors, and this phosphorylates protein kinases that activate downstream Phosphoinositide 3-kinase (PI3K) and Mitogen-activated protein kinase (MAPK) pathways promoting proliferation (**Figure 2**). VEGF expression is triggered by hypoxia. The proliferation process involved in arteriole enlargement, however, does not respond to hypoxia (Deindl et al., 2001). In fact, although experimentally inhibited VEGF in femoral artery ligation (an occlusion model) results in inhibited arteriogenesis (Jacobi et al., 2004; Lloyd et al., 2005; Toyota et al., 2005), *VEGF* is not expressed in the tissue near the growing collaterals (Lee et al., 2004). Thus, although endothelial cells clearly proliferate within the growing arterioles (Scholz et al., 2000), the role of VEGF is unlikely to be needed for this local proliferation. Instead, VEGF may be needed to induce proliferation distal from the site of arteriogenesis, though it is also possible that VEGF could be responsible for the release of blood-marrow derived cells.

In the case of flow-induced remodeling, VEGF itself is also not a necessary ligand to activate PI3K/MAPK signaling pathways. Laminar flow induces a transphosphorylation of VEGF receptor 2 (VEGFR2) that activates the downstream PI3K pathway in a ligand-independent manner (Jin et al., 2003). This leads to the phosphorylation of Akt that has pleiotropic effects on proliferation. Akt phosphorylation by flow is highest at physiological shear stress levels between 10 and 20 dyn/cm$^2$ (Dimmeler et al., 1998; Li et al., 2009), however, these levels of shear stress are known to induce quiescence and not proliferation in endothelial cells. VEGFR2 and Akt phosphorylation are, however, short-lived events that occur within the first 1–2 h of a change in shear stress (Shay-Salit et al., 2002; Guo et al., 2007). Oscillatory flow, which in contrast to unidirectional flow does induce increased proliferation, leads to prolonged VEGFR2 and Akt phosphorylation (Guo et al., 2007). Furthermore, unidirectional flow also activates other factors such as AMP-activated protein kinase (AMPK), which counteract the pro-proliferative signals (Guo et al., 2007).

Shear stress can also modulate endothelial cell proliferation through other signaling pathways. The phosphorylation of endothelial Nitric Oxide Synthase (eNOS) and its increased activity induced by shear stress was one of the first studied effects of mechanotransduction (Buga et al., 1991; Kuchan and Frangos, 1994). Nitric oxide (NO) not only induces vasodilation but also induces proliferation. In vasodilation, NO is produced by endothelial cells, diffuses to smooth muscle cells where it activates soluble guanylyl cyclase by binding to the heme group (Zhao et al., 1999). Estimates vary concerning the concentration at which this occurs, however, most publications have placed

this between 5 and 100 nM (Chen et al., 2008). As a pro-proliferative compound, NO acts by controlling protein activation by reacting with cysteine residues to induce *S*-nitrosylation. NO leads to *S*-nitrosylation of MAPK phosphatase 7 (MKP7), rendering it inactive which then prevents the inactivation of c-Jun N-terminal Kinase 3 (JNK3; Pi et al., 2009). The concentrations at which NO induce proliferation are extremely low, in the pico to nanomolar ranges that occur due to release of NO by macrophages and endothelial cells (Ridnour et al., 2005; Thomas et al., 2008; **Figure 2**). At concentrations in the micromolar range, NO inhibits proliferation and induces cell cycle arrest in several cell types (Gooch et al., 1997; Heller et al., 1999).

Though the ALK1/ENG complex affects endothelial cell migration, this signaling pathway also has a key role in regulating the proliferation of endothelial cells (Goumans et al., 2002; David et al., 2007). The ALK1/ENG complex is, thus, a key component through which shear stress can block endothelial cells from entering the cell cycle (Baeyens et al., 2016; **Figure 2**). By recognizing both BMP9 and flow, the ALK1/ENG complex allows the modulation of vascular morphogenesis in response to flow (Baeyens et al., 2016). Mutations in *SMAD4* and in the Growth differentiation factor 2 (*GDF2*) genes (encoding for SMAD4 and BMP9) had been also reported later on to cause variants of HHT. Both the endothelial-specific ablation of SMAD4 (a transcription factor in the ALK1/ENG pathway) and of ENG show increased proliferation of endothelial cells within the developing shunt (Ola et al., 2018; Tual-Chalot et al., 2020). The later, however, has been described to involve the VEGF signaling pathway (Tual-Chalot et al., 2020).

Transforming Growth Factor-β (TGF-β) is involved in the maintenance of the endothelium in a nonactivated state (Walshe et al., 2009) and protecting it from aberrant permeability and perfusion, and from apoptosis (Walshe et al., 2011). Interestingly, experiments on HUVECs demonstrated that shear stress activates TGF-β, leading to downstream activation of Krüppel-Like Factor 2 (KLF2) and eNOS in an ALK5 dependent manner (Walshe et al., 2013; **Figure 2**). Moreover, TGF-β malfunction through the SMAD signaling pathway has been linked to diverse cerebrovascular diseases related to aberrant endothelial cell proliferation (including HHT), as reviewed by Zhang and Yang (2020).

Flow can also modulate the endothelial cell cycle through other pathways. For example, in bovine aortic endothelial cells, 24 h of laminar shear stress (3–12 dyn/cm$^2$) activated the phosphorylation of p53 protein through the JNK pathway. The increased levels of p53 in turn activated Growth Arrest and DNA Damage 45 (GADD45) and p21 proteins, inhibiting the Cyclin-Dependent Kinase (CDK) and, thus, arresting endothelial cell proliferation (Lin et al., 2000; **Figure 2**). Transcription factor Aryl hydrocarbon receptor (AhR) is also sensitive to shear stress. In this case, laminar shear stress between 6 and 15 dyn/cm$^2$ induced –likely also through the JNK/p38 pathway– the expression and the translocation of AhR into the nucleus. In the nucleus, AhR promotes an increase in Cytochrome P450 Family 1 Subfamily A Member 1 (CYP1A1) expression and the subsequent shear stress-induced arrest of the cell cycle (Han et al., 2008; **Figure 2**).

### Hypertrophy

Endothelial cells have an amazing ability to change their cell size. Vessel enlargement by hypertrophy results in an increase in the size of individual endothelial cells and can extremely rapidly increase vessel diameter. Endothelial cell density in vessels is very high, meaning that there is a large potential for growth purely by altering their size.

In normal embryonic development, no differences in cell density are observed along vessel growth based on somite stage. Nonetheless, between large and small vessels a 30% reduction in endothelial cell density was reported (Udan et al., 2013). The difference, however, was not large enough to explain the difference in vessel diameter, suggesting that size of endothelial cells might be involved. Similarly, in the retina there is no overall change in endothelial cells density as large vessels form, but in this case, the endothelial cell density was not compared between large and small vessels (Franco et al., 2015). In transgenic zebrafish embryos with constitutive or inducible expression of Placental Growth Factor (*PLGF*) under control of a somite muscle-specific promoter (PLGF$^{musc}$), cell size was found to contribute to vessel enlargement but, importantly, alone could not account for the diameter increase (Klems et al., 2020). As such, in normal vascular development as well, endothelial cell hypertrophy appears to contribute to vessel enlargement but never acts alone.

Though endothelial cell size increases appear to play a lesser role in developmental vessel enlargement, this process could still contribute to pathological vessel enlargement. In an AVM model of constitutive expression of active *Notch4*, pathological vessel enlargement occurs not due to an increase in endothelial cell density nor proliferation but, instead, due to an increased size of individual endothelial cells (Murphy et al., 2014). In zebrafish embryos, TRIO (Trio Rho Guanine Nucleotide Exchange Factor) activation, which in turn activates Ras homologous (Rho) GTPases, also leads to increased cell size causing an enlargement in arterial caliber (Klems et al., 2020). Interestingly, these results may be linked because shear-induced Notch activation has been shown to regulate and activate the assembly of a VE-Cadherin/LAR (leukocyte antigen-related protein tyrosine phosphatase)/TRIO complex (Polacheck et al., 2017; **Figure 2**). Other AVM models, such as the endothelial cell specific knockout of ENG (Choi et al., 2014), also present with an increase in endothelial cell size, both in zebrafish and mouse embryos (Sugden et al., 2017). Overall, however, the contribution of cell size changes to vessel growth is rarely assessed.

## ENLARGEMENT OF VEINS

The process of vessel enlargement is referred to as arteriogenesis when it occurs in the mature arterial vascular network, but veins can also increase in diameter. The process of increasing venous diameter is so understudied that it lacks a name, though it is occasionally referred to as venogenesis.

In vascular development, fusion has been reported as the predominant mechanism of venous vessel enlargement in both

mouse and chicken embryos (le Noble et al., 2004; Udan et al., 2013). In the chick embryo, the vitelline vein arises from a region that is genetically arterial before vessel enlargement begins (le Noble et al., 2004). In the developing retina, endothelial specific ablation of Cell Division Control protein 42 (*CDC42* homolog) impairs migration, and enlarged veins and capillaries form without arterial enlargement (Lavina et al., 2018). This increased diameter was attributed to the presence of an increase in the number of endothelial cells per vessel length, without an increase in venous proliferation.

Understanding the process of vein enlargement requires mutants that specifically show changes in the diameter of veins. As such, somatic mutations that lead to venous malformations can be especially informative. Venous malformations are enlarged veins that present with few mural cells. The most well studied somatic mutations in venous malformation are the ones related to the Tyrosine-protein kinase (Tie2) receptor (Limaye et al., 2009; Soblet et al., 2013). Constitutive ablation of *TIE2* leads to embryonic lethality at E10.5 (Sato et al., 1995). If *TIE2* is ablated at later stages, however, arteries continue to form but veins do not (Chu et al., 2016). This is associated with a loss of venous markers [EphB4 (Ephrin type-B receptor 4), APJ (apelin receptor)] without any increase in arterial markers, indicating that this may be a defect in venous specification rather than vessel enlargement. Constitutively active forms of Tie2 that replicate somatic *TIE2* mutations found in venous malformations, cause increased migration but loss of proper polarization in endothelial cells *in vitro* (Cai et al., 2019). However, it is not clear whether loss of proper cell identity or improper migration lead to vessel enlargement in venous malformations.

Though venous malformations arise from veins, some argue that all AVMs originate from venous endothelial cells. In biopsies from patients with telangiectasias, the enlargement of post-capillary venules precedes AVM formation (Braverman et al., 1990). In mouse models, exogenous expression of activated Notch4 induces AVM formation (Murphy et al., 2014). However, when this expression is limited to arteries, no AVMs form (Murphy et al., 2014). Deletion of the ENG only in venous and capillary endothelial cells results in the same rate of AVM formation as for deletion in all endothelial cells (Singh et al., 2020). Conversely, in retinas of an endothelial-specific *ENG* knockout model, imaging of developing AVMs showed that these initiated in arterioles and grew toward the venous vasculature (Jin et al., 2017). Although this would suggest an arterialization of the capillaries, in mouse models of AVM formation, the AVMs themselves express venous markers and downregulate arterial marker (Ola et al., 2018).

Another venous malformation that leads to increased venogenesis is varicose vein development. Though most research on vessel enlargement focuses on the role of shear stress as the stimuli for enlargement, varicose vein development occurs due to defective valves leading to an increase in hydrodynamic pressure (Welkie et al., 1992; Nicolaides et al., 1993). It should be noted, however, that the increased pressure in veins also leads to altered shear stress. On a cellular level, varicose vein development involves activation of endothelial cells leading to immune cell recruitment, increased vessel leakiness and loss of smooth muscle cells (Segiet et al., 2015). Varicose veins have upregulated Notch pathway genes like Delta Like Canonical Notch Ligand 4 (*DLL4*), Hairy/enhancer-of-split related with YRPW motif protein 2 (*HEY2*), and *EPHB2* (Surendran et al., 2016). Smooth muscle cells become enlarged and surrounded by an increased amount of extracellular matrix, suggesting that they de-differentiate into a synthetic phenotype (Wali and Eid, 2001). Matrix Metalloproteinases (MMPs) and Tissue Inhibitors of Metalloproteinases (TIMPs) play an important role in the development of varicose veins. Increases in TIMP-1 levels and in the TIMP/MMP-2 ratio lead to an increase in extracellular matrix deposition and a decrease in degradation processes (Badier-Commander et al., 2000). The mechanism of enlargement for varicose vein is, therefore, much more akin to collateral vessel enlargement than to vessel enlargement in developmental models.

# DIFFERENCES BETWEEN VESSEL ENLARGEMENT IN THE ADULT AND EMBRYO

Vessel enlargement occurs during embryonic development but continues to occur in the adult vascular networks. Any time the vasculature is exposed to a chronic change in flow, the vasculature adapts through either enlargement or inward remodeling to accommodate the altered flow. The most common experimental model for vessel enlargement in the adult is the remodeling of collateral vessels after occlusion, whether by partial occlusion of a coronary artery or by ligation of the femoral or middle cerebral artery. Other models, such as arteriovenous fistulas, have also been used to study the mechanisms of vessel enlargement. Vessel enlargement post-natally is inherently different than in developmental models, such as the retina, since post-natal enlargement requires the degradation of an existing basement membrane as well as the detachment and proliferation of mural cells. Furthermore, the remodeling of adult vessels, such as the collaterals, is initiated by endothelial cell activation, leukocyte invasion, and proliferation of vascular cells (Ma and Bai, 2020). This leads to the question, what parallels exist between vessel enlargement in developmental models and in adult models? And though there may be more than one way in which a vessel enlarges, it is likely that there will be common components from which we can gain significant insight.

## Endothelial Cell Activation

In femoral artery ligation, arteriogenesis occurs far away from where ischemia is occurring (Resnick et al., 2003; Pipp et al., 2004). As such, just as with developmental angiogenesis, it is a process driven by shear stress. Just after coronary occlusion, the endothelial cells in the collateral vessel lose alignment with flow and take on a bulged appearance (Cai and Schaper, 2008). These cells increase DNA synthesis (Schaper et al., 1971; Pasyk et al., 1982) and proliferation, as indicated by

Bromodeoxyuridine (BrdU) incorporation or Ki67 staining (Arras et al., 1998b; Wolf et al., 1998). Interestingly, these are all behaviors associated with low or recirculating shear stress patterns and not with increased shear stress levels. Adult endothelial cells, however, are adapted to the flow to which they are exposed and become activated in response to altered flow (Ward et al., 2020). Furthermore, though physiological shear stress reduces activation and proliferation, when shear levels are extremely elevated (above 30 dyn/cm$^2$ in humans), the response is outward remodeling (Dolan et al., 2013). Thus, difference between developmental and adult remodeling may arise from either one of the following facts. On the one hand, developmental vasculature is naïve and therefore, it is not adapting to its "expected" flow; on the other hand, the stimulus for remodeling is a physiological level of shear stress (i.e., 15 dyn/cm$^2$) for vessel enlargement during development, but an acute non-physiological level of shear stress (above 30 dyn/cm$^2$) in models of vessel enlargement in the adult.

The activated endothelium produces NO that is essential for collateral growth. Both eNOS and iNOS (respectively, endothelial and inducible NOS) are upregulated in remodeling collateral vessel (Cai et al., 2004; Yang et al., 2015). When NO production is inhibited with L-NAME [N(G)-nitro L-arginine methyl ester], there is an almost complete inhibition of collateral enlargement (Eitenmuller et al., 2006; Park et al., 2010). It is not clear, however, whether this is due to a true inhibition of growth or related to increased vasoconstriction (Cai and Schaper, 2008). Endothelial NOS itself is involved in maintaining collateral vessel under physiological conditions. Mice that lack eNOS are born with a normal number of collateral vessels in the brain, but the number of these vessels decreases over the first 6 months of life as compared to age-matched controls (Dai and Faber, 2010). The primary role of NO in vessel enlargement is in the recruitment of immune cells (Park et al., 2010). Delivery of NO donors induces VE-Cadherin disassembly that is necessary for immune cell recruitment. Conversely, NO inhibitor L-NAME prevents increased vessel permeability and immune cell recruitment after vessel occlusion (Yang et al., 2015). Though NO is critical in vessel enlargement in post-natal stages, it has not been extensively investigated during development. The triple knockout of NOS enzymes is born at normal mendelian frequency with no reported vascular defects at birth (Morishita et al., 2005). Conversely, however, culture of E8.5 mouse embryos with the NO inhibitor L-NMMA [N(G)-monomethyl L-arginine] prevents the formation of large vessels in the yolk sac vasculature (Nath et al., 2004). NO influences endothelial cell proliferation (Morbidelli et al., 1996) and migration (Noiri et al., 1998). As such, NO could have a role in several of the mechanisms by which vessel enlarge.

## Immune Cells and Matrix Degradation

Another difference between adult and developmental vessel enlargement is the involvement of immune cells. Immune cells, especially monocytes and macrophages, are essential for adult collateral growth and vessel enlargement in general (Arras et al., 1998a; Voskuil et al., 2003). Inhibiting monocyte recruitment in the adult impairs arteriogenesis during collateral remodeling (Heil et al., 2002, 2004). Recruited monocytes produce Tumor necrosis factor-α (TNF-α) and VEGF, which induces endothelial and smooth muscle cell mitoses (Schaper and Ito, 1996).

Though essential when vessel enlarge post-natally, functional immune cells may not be as present in vessel enlargement occurring just after the onset of flow in the embryo. The first immune cells form at E8.5 in the form of erythromyeloid progenitor and primitive macrophages (Gomez Perdiguero et al., 2015), and no functional role for these progenitors has been established until much later in development. At Hamburger Hamilton stage 18 in avian embryos (equivalent to E12.5–13.5 in mouse), circulating phagocytic cells are recruited to sites of vascular remodeling (Al-Roubaie et al., 2012). In the zebrafish embryo, depletion of myeloid cells using a *pu.1* morpholino inhibits collateral growth in the *gridlock* mutant embryo (Gray et al., 2007). However, both these reports were for embryos at stages much older than the ones that gave the results showing vessel enlargement by migration and/or fusion (Chouinard-Pelletier et al., 2013). The retinal vasculature does form post-natally, when resident myeloid cells are present in the retina (Haupt et al., 2019). Ablation of macrophages using chlodronate liposomes results in a dramatic loss of vascular density, which makes it difficult to assess whether vessel enlargement itself is affected (Checchin et al., 2006).

One of the roles of immune cells in arteriogenesis is to degrade the basement membrane. During arteriogenesis, the elastic lamina is broken down by MMPs to give the vessels room to expand (Haas et al., 2007; Dodd et al., 2011). Inflammatory cells are also an important source of MMPs, as well as of other proteases. Macrophages secrete cytokines that induce MMP expression by endothelial cells (Galis et al., 1994a). Vessel enlargement in response to arteriovenous fistula induces a more than 1700-fold increase in MMP-2, along with a 12–60-fold increase in MMP-9, Membrane-type 1 MMP (MT1-MMP), and TIMP-2 (Sho et al., 2002). These increases correlate to the timing of elastic lamina degradation (Sho et al., 2002). Notably, MMPs are produced as inactive zymogens and, in addition, TIMPs can inhibit their activity. Therefore, increased expression of MMPs does not necessarily indicate increased activity. Indeed, many MMPs are constitutively expressed by endothelial cells and smooth muscle cells (Hanemaaijer et al., 1993; Galis et al., 1994a) but show no enzymatic activity until activated by disease (Galis et al., 1994b, 1995). Though essential in adult remodeling, no single mutant of MMPs has shown defects during embryogenesis. The double mutant of MMP2 and MT1-MMP does die perinatally, with a defect in the formation of vessels with wider diameters (Oh et al., 2004). This is, however, a very late stage of vascular development, after initial vascular remodeling has occurred.

One of the effects of immune cell recruitment and matrix degradation is an increase in permeability. Middle cerebral artery occlusion leads to an increase in permeability in the blood-brain-barrier to large molecules such as fibrinogen, Immunoglobulin G (IgG) or nanoparticles within 2–4 h of the occlusion (Okada et al., 1994; Fischer et al., 2002). Degradation is necessary for this increase in permeability, as inhibiting MMPs

with BB-1101 prevents permeability increases immediately after middle cerebral artery occlusion (Rosenberg et al., 1998).

The presence of this extensive basement membrane is one of the main reasons that post-natal vessel enlargement is unlike to occur by vascular fusion. The presence of extensive matrix and mural cells from the arterioles onward would be a physical barrier for fusion. Hence, vascular fusion could only occur on the capillary level allowing arterioles to grow, which would then have to further increase in diameter by combination with another mechanism.

## CONCLUSION

Vessel enlargement plays a critical role both during development as well as in the adult vasculature, with a high capacity for adapting to flow changes. Through an extremely fast responsiveness and interconnected processes such as fusion, endothelial cell migration and proliferation, vessels reshape in order to accommodate changes in flow rates such as to restore physiological levels. Because these processes are so much present along all the vasculature lifetime, dysregulations may entail critical pathologies. However, more and more pathways and molecular interconnections are being uncovered, shedding light to a better understanding and control over these pathologies.

## AUTHOR CONTRIBUTIONS

LG-R and EAVJ contributed to writing, editing, and making figures. All authors contributed to the article and approved the submitted version.

## FUNDING

This work was supported by the Fonds Wetenschappelijk Onderzoek (G091018N and G0B5920N) and by internal funding from the KU Leuven (IDN/19/031 and C14/19/095). This project has also received funding from the European Union's Horizon 2020 research and innovation program under grant agreement No 848109.

## REFERENCES

Al-Roubaie, S., Hughes, J. H., Filla, M. B., Lansford, R., Lehoux, S., and Jones, E. A. (2012). Time-lapse microscopy of macrophages during embryonic vascular development. *Dev. Dyn.* 241, 1423–1431. doi: 10.1002/dvdy.23835

Arras, M., Ito, W. D., Scholz, D., Winkler, B., Schaper, J., and Schaper, W. (1998a). Monocyte activation in angiogenesis and collateral growth in the rabbit hindlimb. *J. Clin. Invest.* 101, 40–50. doi: 10.1172/JCI119877

Arras, M., Strasser, R., Mohri, M., Doll, R., Eckert, P., Schaper, W., et al. (1998b). Tumor necrosis factor-alpha is expressed by monocytes/macrophages following cardiac microembolization and is antagonized by cyclosporine. *Basic Res. Cardiol.* 93, 97–107. doi: 10.1007/s003950050069

Azizoglu, D. B., Chong, D. C., Villasenor, A., Magenheim, J., Barry, D. M., Lee, S., et al. (2016). Vascular development in the vertebrate pancreas. *Dev. Biol.* 420, 67–78. doi: 10.1016/j.ydbio.2016.10.009

Badier-Commander, C., Verbeuren, T., Lebard, C., Michel, J. B., and Jacob, M. P. (2000). Increased TIMP/MMP ratio in varicose veins: a possible explanation for extracellular matrix accumulation. *J. Pathol.* 192, 105–112. doi: 10.1002/1096-9896(2000)9999:9999<::AID-PATH670>3.0.CO;2-1

Baeyens, N., Larrivee, B., Ola, R., Hayward-Piatkowskyi, B., Dubrac, A., Huang, B., et al. (2016). Defective fluid shear stress mechanotransduction mediates hereditary hemorrhagic telangiectasia. *J. Cell Biol.* 214, 807–816. doi: 10.1083/jcb.201603106

Baeyens, N., Mulligan-Kehoe, M. J., Corti, F., Simon, D. D., Ross, T. D., Rhodes, J. M., et al. (2014). Syndecan 4 is required for endothelial alignment in flow and atheroprotective signaling. *Proc. Natl. Acad. Sci. U. S. A.* 111, 17308–17313. doi: 10.1073/pnas.1413725111

Beebe-Dimmer, J. L., Pfeifer, J. R., Engle, J. S., and Schottenfeld, D. (2005). The epidemiology of chronic venous insufficiency and varicose veins. *Ann. Epidemiol.* 15, 175–184. doi: 10.1016/j.annepidem.2004.05.015

Braverman, I. M., Keh, A., and Jacobson, B. S. (1990). Ultrastructure and three-dimensional organization of the telangiectases of hereditary hemorrhagic telangiectasia. *J. Invest. Dermatol.* 95, 422–427. doi: 10.1111/1523-1747.ep12555569

Buga, G. M., Gold, M. E., Fukuto, J. M., and Ignarro, L. J. (1991). Shear stress-induced release of nitric oxide from endothelial cells grown on beads. *Hypertension* 17, 187–193. doi: 10.1161/01.hyp.17.2.187

Cai, W. J., Kocsis, E., Luo, X., Schaper, W., and Schaper, J. (2004). Expression of endothelial nitric oxide synthase in the vascular wall during arteriogenesis. *Mol. Cell. Biochem.* 264, 193–200. doi: 10.1023/b:mcbi.0000044388.27953.a0

Cai, W., and Schaper, W. (2008). Mechanisms of arteriogenesis. *Acta Biochim. Biophys. Sin.* 40, 681–692. doi: 10.1093/abbs/40.8.681

Cai, Y., Schrenk, S., Goines, J., Davis, G. E., and Boscolo, E. (2019). Constitutive active mutant TIE2 induces enlarged vascular lumen formation with loss of Apico-basal polarity and Pericyte recruitment. *Sci. Rep.* 9:12352. doi: 10.1038/s41598-019-48854-2

Caolo, V., Peacock, H. M., Kasaai, B., Swennen, G., Gordon, E., Claesson-Welsh, L., et al. (2018). Shear stress and VE-cadherin. *Arterioscler. Thromb. Vasc. Biol.* 38, 2174–2183. doi: 10.1161/ATVBAHA.118.310823

Checchin, D., Sennlaub, F., Levavasseur, E., Leduc, M., and Chemtob, S. (2006). Potential role of microglia in retinal blood vessel formation. *Invest. Ophthalmol. Vis. Sci.* 47, 3595–3602. doi: 10.1167/iovs.05-1522

Chen, K., Pittman, R. N., and Popel, A. S. (2008). Nitric oxide in the vasculature: where does it come from and where does it go? A quantitative perspective. *Antioxid. Redox Signal.* 10, 1185–1198. doi: 10.1089/ars.2007.1959

Chen, X., Qin, J., Cheng, C. M., Tsai, M. J., and Tsai, S. Y. (2012). COUP-TFII is a major regulator of cell cycle and notch signaling pathways. *Mol. Endocrinol.* 26, 1268–1277. doi: 10.1210/me.2011-1305

Choi, E. J., Chen, W., Jun, K., Arthur, H. M., Young, W. L., and Su, H. (2014). Novel brain arteriovenous malformation mouse models for type 1 hereditary hemorrhagic telangiectasia. *PLoS One* 9:e88511. doi: 10.1371/journal.pone.0088511

Chouinard-Pelletier, G., Jahnsen, E. D., and Jones, E. A. (2013). Increased shear stress inhibits angiogenesis in veins and not arteries during vascular development. *Angiogenesis* 16, 71–83. doi: 10.1007/s10456-012-9300-2

Chu, M., Li, T., Shen, B., Cao, X., Zhong, H., Zhang, L., et al. (2016). Angiopoietin receptor Tie2 is required for vein specification and maintenance via regulating COUP-TFII. *elife* 5:e21032. doi: 10.7554/eLife.21032

Corti, F., Wang, Y., Rhodes, J. M., Atri, D., Archer-Hartmann, S., Zhang, J., et al. (2019). N-terminal syndecan-2 domain selectively enhances 6-O heparan sulfate chains sulfation and promotes VEGFA165-dependent neovascularization. *Nat. Commun.* 10:1562. doi: 10.1038/s41467-019-09605-z

Cui, C., Filla, M. B., Jones, E. A., Lansford, R., Cheuvront, T., Al-Roubaie, S., et al. (2013). Embryogenesis of the first circulating endothelial cells. *PLoS One* 8:e60841. doi: 10.1371/journal.pone.0060841

Dai, X., and Faber, J. E. (2010). Endothelial nitric oxide synthase deficiency causes collateral vessel rarefaction and impairs activation of a cell cycle gene network during arteriogenesis. *Circ. Res.* 106, 1870–1881. doi: 10.1161/CIRCRESAHA.109.212746

David, L., Mallet, C., Mazerbourg, S., Feige, J. J., and Bailly, S. (2007). Identification of BMP9 and BMP10 as functional activators of the orphan activin receptor-

like kinase 1 (ALK1) in endothelial cells. *Blood* 109, 1953–1961. doi: 10.1182/blood-2006-07-034124

Deindl, E., Buschmann, I., Hoefer, I. E., Podzuweit, T., Boengler, K., Vogel, S., et al. (2001). Role of ischemia and of hypoxia-inducible genes in arteriogenesis after femoral artery occlusion in the rabbit. *Circ. Res.* 89, 779–786. doi: 10.1161/hh2101.098613

Dimmeler, S., Assmus, B., Hermann, C., Haendeler, J., and Zeiher, A. M. (1998). Fluid shear stress stimulates phosphorylation of Akt in human endothelial cells: involvement in suppression of apoptosis. *Circ. Res.* 83, 334–341.

Dodd, T., Jadhav, R., Wiggins, L., Stewart, J., Smith, E., Russell, J. C., et al. (2011). MMPs 2 and 9 are essential for coronary collateral growth and are prominently regulated by p38 MAPK. *J. Mol. Cell. Cardiol.* 51, 1015–1025. doi: 10.1016/j.yjmcc.2011.08.012

Dolan, J. M., Kolega, J., and Meng, H. (2013). High wall shear stress and spatial gradients in vascular pathology: a review. *Ann. Biomed. Eng.* 41, 1411–1427. doi: 10.1007/s10439-012-0695-0

Drake, C. J., and Little, C. D. (1995). Exogenous vascular endothelial growth factor induces malformed and hyperfused vessels during embryonic neovascularization. *Proc. Natl. Acad. Sci. U. S. A.* 92, 7657–7661. doi: 10.1073/pnas.92.17.7657

Drake, C. J., and Little, C. D. (1999). VEGF and vascular fusion: implications for normal and pathological vessels. *J. Histochem. Cytochem.* 47, 1351–1356.

Egorova, A. D., Khedoe, P. P., Goumans, M. J., Yoder, B. K., Nauli, S. M., Ten Dijke, P., et al. (2011). Lack of primary cilia primes shear-induced endothelial-to-mesenchymal transition. *Circ. Res.* 108, 1093–1101. doi: 10.1161/CIRCRESAHA.110.231860

Ehling, M., Adams, S., Benedito, R., and Adams, R. H. (2013). Notch controls retinal blood vessel maturation and quiescence. *Development* 140, 3051–3061. doi: 10.1242/dev.093351

Eichmann, A., and Simons, M. (2012). VEGF signaling inside vascular endothelial cells and beyond. *Curr. Opin. Cell Biol.* 24, 188–193. doi: 10.1016/j.ceb.2012.02.002

Eitenmuller, I., Volger, O., Kluge, A., Troidl, K., Barancik, M., Cai, W. J., et al. (2006). The range of adaptation by collateral vessels after femoral artery occlusion. *Circ. Res.* 99, 656–662. doi: 10.1161/01.RES.0000242560.77512.dd

Fischer, S., Wobben, M., Marti, H. H., Renz, D., and Schaper, W. (2002). Hypoxia-induced hyperpermeability in brain microvessel endothelial cells involves VEGF-mediated changes in the expression of zonula occludens-1. *Microvasc. Res.* 63, 70–80. doi: 10.1006/mvre.2001.2367

Franco, C. A., Jones, M. L., Bernabeu, M. O., Geudens, I., Mathivet, T., Rosa, A., et al. (2015). Dynamic endothelial cell rearrangements drive developmental vessel regression. *PLoS Biol.* 13:e1002125. doi: 10.1371/journal.pbio.1002125

Galis, Z. S., Muszynski, M., Sukhova, G. K., Simon-Morrissey, E., Unemori, E. N., Lark, M. W., et al. (1994a). Cytokine-stimulated human vascular smooth muscle cells synthesize a complement of enzymes required for extracellular matrix digestion. *Circ. Res.* 75, 181–189.

Galis, Z. S., Sukhova, G. K., Lark, M. W., and Libby, P. (1994b). Increased expression of matrix metalloproteinases and matrix degrading activity in vulnerable regions of human atherosclerotic plaques. *J. Clin. Invest.* 94, 2493–2503.

Galis, Z. S., Sukhova, G. K., and Libby, P. (1995). Microscopic localization of active proteases by in situ zymography: detection of matrix metalloproteinase activity in vascular tissue. *FASEB J.* 9, 974–980.

Gomez Perdiguero, E., Klapproth, K., Schulz, C., Busch, K., Azzoni, E., Crozet, L., et al. (2015). Tissue-resident macrophages originate from yolk-sac-derived erythro-myeloid progenitors. *Nature* 518, 547–551. doi: 10.1038/nature13989

Gooch, K. J., Dangler, C. A., and Frangos, J. A. (1997). Exogenous, basal, and flow-induced nitric oxide production and endothelial cell proliferation. *J. Cell. Physiol.* 171, 252–258.

Goumans, M. J., Valdimarsdottir, G., Itoh, S., Rosendahl, A., Sideras, P., and Ten Dijke, P. (2002). Balancing the activation state of the endothelium via two distinct TGF-beta type I receptors. *EMBO J.* 21, 1743–1753. doi: 10.1093/emboj/21.7.1743

Gray, C., Packham, I. M., Wurmser, F., Eastley, N. C., Hellewell, P. G., Ingham, P. W., et al. (2007). Ischemia is not required for arteriogenesis in zebrafish embryos. *Arterioscler. Thromb. Vasc. Biol.* 27, 2135–2141. doi: 10.1161/ATVBAHA.107.143990

Guo, D., Chien, S., and Shyy, J. Y. (2007). Regulation of endothelial cell cycle by laminar versus oscillatory flow: distinct modes of interactions of AMP-activated protein kinase and Akt pathways. *Circ. Res.* 100, 564–571. doi: 10.1161/01.RES.0000259561.23876.c5

Haas, T. L., Doyle, J. L., Distasi, M. R., Norton, L. E., Sheridan, K. M., and Unthank, J. L. (2007). Involvement of MMPs in the outward remodeling of collateral mesenteric arteries. *Am. J. Physiol. Heart Circ. Physiol.* 293, H2429–H2437. doi: 10.1152/ajpheart.00100.2007

Han, Z., Miwa, Y., Obikane, H., Mitsumata, M., Takahashi-Yanaga, F., Morimoto, S., et al. (2008). Aryl hydrocarbon receptor mediates laminar fluid shear stress-induced CYP1A1 activation and cell cycle arrest in vascular endothelial cells. *Cardiovasc. Res.* 77, 809–818. doi: 10.1093/cvr/cvm095

Hanemaaijer, R., Koolwijk, P., Le Clercq, L., de Vree, W. J., and van Hinsbergh, V. W. (1993). Regulation of matrix metalloproteinase expression in human vein and microvascular endothelial cells. Effects of tumour necrosis factor alpha, interleukin 1 and phorbol ester. *Biochem. J.* 296, 803–809. doi: 10.1042/bj2960803

Haupt, F., Krishnasamy, K., Napp, L. C., Augustynik, M., Limbourg, A., Gamrekelashvili, J., et al. (2019). Retinal myeloid cells regulate tip cell selection and vascular branching morphogenesis via notch ligand Delta-like 1. *Sci. Rep.* 9:9798. doi: 10.1038/s41598-019-46308-3

Heil, M., Ziegelhoeffer, T., Pipp, F., Kostin, S., Martin, S., Clauss, M., et al. (2002). Blood monocyte concentration is critical for enhancement of collateral artery growth. *Am. J. Physiol. Heart Circ. Physiol.* 283, H2411–H2419. doi: 10.1152/ajpheart.01098.2001

Heil, M., Ziegelhoeffer, T., Wagner, S., Fernandez, B., Helisch, A., Martin, S., et al. (2004). Collateral artery growth (arteriogenesis) after experimental arterial occlusion is impaired in mice lacking CC-chemokine receptor-2. *Circ. Res.* 94, 671–677. doi: 10.1161/01.RES.0000122041.73808.B5

Heller, R., Polack, T., Grabner, R., and Till, U. (1999). Nitric oxide inhibits proliferation of human endothelial cells via a mechanism independent of cGMP. *Atherosclerosis* 144, 49–57.

Hughes, S., and Chang-Ling, T. (2000). Roles of endothelial cell migration and apoptosis in vascular remodeling during development of the central nervous system. *Microcirculation* 7, 317–333. doi: 10.1080/mic.7.5.317.333

Iomini, C., Tejada, K., Mo, W., Vaananen, H., and Piperno, G. (2004). Primary cilia of human endothelial cells disassemble under laminar shear stress. *J. Cell Biol.* 164, 811–817. doi: 10.1083/jcb.200312133

Jacobi, J., Tam, B. Y., Wu, G., Hoffman, J., Cooke, J. P., and Kuo, C. J. (2004). Adenoviral gene transfer with soluble vascular endothelial growth factor receptors impairs angiogenesis and perfusion in a murine model of hindlimb ischemia. *Circulation* 110, 2424–2429. doi: 10.1161/01.CIR.0000145142.85645.EA

Jacobs, B. N., Andraska, E. A., Obi, A. T., and Wakefield, T. W. (2017). Pathophysiology of varicose veins. *J. Vasc. Surg. Venous Lymphat. Disord.* 5, 460–467. doi: 10.1016/j.jvsv.2016.12.014

Jiang, Y. J., Aerne, B. L., Smithers, L., Haddon, C., Ish-Horowicz, D., and Lewis, J. (2000). Notch signalling and the synchronization of the somite segmentation clock. *Nature* 408, 475–479. doi: 10.1038/35044091

Jin, Y., Muhl, L., Burmakin, M., Wang, Y., Duchez, A. C., Betsholtz, C., et al. (2017). Endoglin prevents vascular malformation by regulating flow-induced cell migration and specification through VEGFR2 signalling. *Nat. Cell Biol.* 19, 639–652. doi: 10.1038/ncb3534

Jin, Z. G., Ueba, H., Tanimoto, T., Lungu, A. O., Frame, M. D., and Berk, B. C. (2003). Ligand-independent activation of vascular endothelial growth factor receptor 2 by fluid shear stress regulates activation of endothelial nitric oxide synthase. *Circ. Res.* 93, 354–363. doi: 10.1161/01.RES.0000089257.94002.96

Johnson, D. W., Berg, J. N., Baldwin, M. A., Gallione, C. J., Marondel, I., Yoon, S. J., et al. (1996). Mutations in the activin receptor-like kinase 1 gene in hereditary haemorrhagic telangiectasia type 2. *Nat. Genet.* 13, 189–195.

Klems, A., van Rijssel, J., Ramms, A. S., Wild, R., Hammer, J., Merkel, M., et al. (2020). The GEF Trio controls endothelial cell size and arterial remodeling downstream of Vegf signaling in both zebrafish and cell models. *Nat. Commun.* 11:5319. doi: 10.1038/s41467-020-19008-0

Kuchan, M. J., and Frangos, J. A. (1994). Role of calcium and calmodulin in flow-induced nitric oxide production in endothelial cells. *Am. J. Phys.* 266, C628–C636.

Lavina, B., Castro, M., Niaudet, C., Cruys, B., Alvarez-Aznar, A., Carmeliet, P., et al. (2018). Defective endothelial cell migration in the absence of Cdc42

leads to capillary-venous malformations. *Development* 145:dev161182. doi: 10.1242/dev.161182

Le Noble, F., Moyon, D., Pardanaud, L., Yuan, L., Djonov, V., Matthijsen, R., et al. (2004). Flow regulates arterial-venous differentiation in the chick embryo yolk sac. *Development* 131, 361–375. doi: 10.1242/dev.00929

Lee, C. W., Stabile, E., Kinnaird, T., Shou, M., Devaney, J. M., Epstein, S. E., et al. (2004). Temporal patterns of gene expression after acute hindlimb ischemia in mice: insights into the genomic program for collateral vessel development. *J. Am. Coll. Cardiol.* 43, 474–482. doi: 10.1016/j.jacc.2003.09.033

Li, M., Stenmark, K. R., Shandas, R., and Tan, W. (2009). Effects of pathological flow on pulmonary artery endothelial production of vasoactive mediators and growth factors. *J. Vasc. Res.* 46, 561–571. doi: 10.1159/000226224

Limaye, N., Wouters, V., Uebelhoer, M., Tuominen, M., Wirkkala, R., Mulliken, J. B., et al. (2009). Somatic mutations in angiopoietin receptor gene TEK cause solitary and multiple sporadic venous malformations. *Nat. Genet.* 41, 118–124. doi: 10.1038/ng.272

Lin, K., Hsu, P. P., Chen, B. P., Yuan, S., Usami, S., Shyy, J. Y., et al. (2000). Molecular mechanism of endothelial growth arrest by laminar shear stress. *Proc. Natl. Acad. Sci. U. S. A.* 97, 9385–9389. doi: 10.1073/pnas.170282597

Lloyd, P. G., Prior, B. M., Li, H., Yang, H. T., and Terjung, R. L. (2005). VEGF receptor antagonism blocks arteriogenesis, but only partially inhibits angiogenesis, in skeletal muscle of exercise-trained rats. *Am. J. Physiol. Heart Circ. Physiol.* 288, H759–H768. doi: 10.1152/ajpheart.00786.2004

Ma, T., and Bai, Y. P. (2020). The hydromechanics in arteriogenesis. *Aging Med.* 3, 169–177. doi: 10.1002/agm2.12101

McAllister, K. A., Grogg, K. M., Johnson, D. W., Gallione, C. J., Baldwin, M. A., Jackson, C. E., et al. (1994). Endoglin, a TGF-beta binding protein of endothelial cells, is the gene for hereditary haemorrhagic telangiectasia type 1. *Nat. Genet.* 8, 345–351.

Meadows, S. M., Ratliff, L. A., Singh, M. K., Epstein, J. A., and Cleaver, O. (2013). Resolution of defective dorsal aortae patterning in Sema3E-deficient mice occurs via angiogenic remodeling. *Dev. Dyn.* 242, 580–590. doi: 10.1002/dvdy.23949

Meyer-Heim, A. D., and Boltshauser, E. (2003). Spontaneous intracranial haemorrhage in children: aetiology, presentation and outcome. *Brain Dev.* 25, 416–421. doi: 10.1016/s0387-7604(03)00029-9

Morbidelli, L., Chang, C. H., Douglas, J. G., Granger, H. J., Ledda, F., and Ziche, M. (1996). Nitric oxide mediates mitogenic effect of VEGF on coronary venular endothelium. *Am. J. Phys.* 270, H411–H415.

Morishita, T., Tsutsui, M., Shimokawa, H., Sabanai, K., Tasaki, H., Suda, O., et al. (2005). Nephrogenic diabetes insipidus in mice lacking all nitric oxide synthase isoforms. *Proc. Natl. Acad. Sci. U. S. A.* 102, 10616–10621. doi: 10.1073/pnas.0502236102

Murphy, P. A., Kim, T. N., Huang, L., Nielsen, C. M., Lawton, M. T., Adams, R. H., et al. (2014). Constitutively active Notch4 receptor elicits brain arteriovenous malformations through enlargement of capillary-like vessels. *Proc. Natl. Acad. Sci. U. S. A.* 111, 18007–18012. doi: 10.1073/pnas.1415316111

Nath, A. K., Enciso, J., Kuniyasu, M., Hao, X. Y., Madri, J. A., and Pinter, E. (2004). Nitric oxide modulates murine yolk sac vasculogenesis and rescues glucose induced vasculopathy. *Development* 131, 2485–2496. doi: 10.1242/dev.01131

Nicolaides, A. N., Hussein, M. K., Szendro, G., Christopoulos, D., Vasdekis, S., and Clarke, H. (1993). The relation of venous ulceration with ambulatory venous pressure measurements. *J. Vasc. Surg.* 17, 414–419.

Noiri, E., Lee, E., Testa, J., Quigley, J., Colflesh, D., Keese, C. R., et al. (1998). Podokinesis in endothelial cell migration: role of nitric oxide. *Am. J. Phys.* 274, C236–C244.

Oh, J., Takahashi, R., Adachi, E., Kondo, S., Kuratomi, S., Noma, A., et al. (2004). Mutations in two matrix metalloproteinase genes, MMP-2 and MT1-MMP, are synthetic lethal in mice. *Oncogene* 23, 5041–5048. doi: 10.1038/sj.onc.1207688

Okada, Y., Copeland, B. R., Fitridge, R., and Koziol, J. A., and Del Zoppo, G. J. (1994). Fibrin contributes to microvascular obstructions and parenchymal changes during early focal cerebral ischemia and reperfusion. *Stroke* 25, 1847–1853.

Ola, R., Kunzel, S. H., Zhang, F., Genet, G., Chakraborty, R., Pibouin-Fragner, L., et al. (2018). SMAD4 prevents flow induced arteriovenous malformations by inhibiting casein kinase 2. *Circulation* 138, 2379–2394. doi: 10.1161/CIRCULATIONAHA.118.033842

Park, B., Hoffman, A., Yang, Y., Yan, J., Tie, G., Bagshahi, H., et al. (2010). Endothelial nitric oxide synthase affects both early and late collateral arterial adaptation and blood flow recovery after induction of hind limb ischemia in mice. *J. Vasc. Surg.* 51, 165–173. doi: 10.1016/j.jvs.2009.08.045

Pasyk, S., Schaper, W., Schaper, J., Pasyk, K., Miskiewicz, G., and Steinseifer, B. (1982). DNA synthesis in coronary collaterals after coronary artery occlusion in conscious dog. *Am. J. Phys.* 242, H1031–H1037.

Peacock, H. M., Tabibian, A., Criem, N., Caolo, V., Hamard, L., Deryckere, A., et al. (2020). Impaired SMAD1/5 Mechanotransduction and Cx37 (Connexin37) expression enable pathological vessel enlargement and shunting. *Arterioscler. Thromb. Vasc. Biol.* 40, e87–e104. doi: 10.1161/ATVBAHA.119.313122

Pi, X., Wu, Y., Ferguson, J. E. 3rd, Portbury, A. L., and Patterson, C. (2009). SDF-1alpha stimulates JNK3 activity via eNOS-dependent nitrosylation of MKP7 to enhance endothelial migration. *Proc. Natl. Acad. Sci. U. S. A.* 106, 5675–5680. doi: 10.1073/pnas.0809568106

Pipp, F., Boehm, S., Cai, W. J., Adili, F., Ziegler, B., Karanovic, G., et al. (2004). Elevated fluid shear stress enhances postocclusive collateral artery growth and gene expression in the pig hind limb. *Arterioscler. Thromb. Vasc. Biol.* 24, 1664–1668. doi: 10.1161/01.ATV.0000138028.14390.e4

Pitulescu, M. E., Schmidt, I., Giaimo, B. D., Antoine, T., Berkenfeld, F., Ferrante, F., et al. (2017). Dll4 and notch signalling couples sprouting angiogenesis and artery formation. *Nat. Cell Biol.* 19, 915–927. doi: 10.1038/ncb3555

Polacheck, W. J., Kutys, M. L., Yang, J., Eyckmans, J., Wu, Y., Vasavada, H., et al. (2017). A non-canonical notch complex regulates adherens junctions and vascular barrier function. *Nature* 552, 258–262. doi: 10.1038/nature24998

Qin, J., Chen, X., Yu-Lee, L. Y., Tsai, M. J., and Tsai, S. Y. (2010). Nuclear receptor COUP-TFII controls pancreatic islet tumor angiogenesis by regulating vascular endothelial growth factor/vascular endothelial growth factor receptor-2 signaling. *Cancer Res.* 70, 8812–8821. doi: 10.1158/0008-5472.CAN-10-0551

Red-Horse, K., and Siekmann, A. F. (2019). Veins and arteries build hierarchical branching patterns differently: bottom-up versus top-down. *BioEssays* 41:e1800198. doi: 10.1002/bies.201800198

Red-Horse, K., Ueno, H., Weissman, I. L., and Krasnow, M. A. (2010). Coronary arteries form by developmental reprogramming of venous cells. *Nature* 464, 549–553. doi: 10.1038/nature08873

Resnick, N., Einav, S., Chen-Konak, L., Zilberman, M., Yahav, H., and Shay-Salit, A. (2003). Hemodynamic forces as a stimulus for arteriogenesis. *Endothelium* 10, 197–206. doi: 10.1080/10623320390246289

Ridnour, L. A., Isenberg, J. S., Espey, M. G., Thomas, D. D., Roberts, D. D., and Wink, D. A. (2005). Nitric oxide regulates angiogenesis through a functional switch involving thrombospondin-1. *Proc. Natl. Acad. Sci. U. S. A.* 102, 13147–13152. doi: 10.1073/pnas.0502979102

Rochon, E. R., Menon, P. G., and Roman, B. L. (2016). Alk1 controls arterial endothelial cell migration in lumenized vessels. *Development* 143, 2593–2602. doi: 10.1242/dev.135392

Rosenberg, G. A., Estrada, E. Y., and Dencoff, J. E. (1998). Matrix metalloproteinases and TIMPs are associated with blood-brain barrier opening after reperfusion in rat brain. *Stroke* 29, 2189–2195.

Rupp, P. A., Czirok, A., and Little, C. D. (2004). alphavbeta3 integrin-dependent endothelial cell dynamics in vivo. *Development* 131, 2887–2897. doi: 10.1242/dev.01160

Sato, Y., Poynter, G., Huss, D., Filla, M. B., Czirok, A., Rongish, B. J., et al. (2010). Dynamic analysis of vascular morphogenesis using transgenic quail embryos. *PLoS One* 5:e12674. doi: 10.1371/journal.pone.0012674

Sato, T. N., Tozawa, Y., Deutsch, U., Wolburg-Buchholz, K., Fujiwara, Y., Gendron-Maguire, M., et al. (1995). Distinct roles of the receptor tyrosine kinases Tie-1 and Tie-2 in blood vessel formation. *Nature* 376, 70–74.

Schaper, W., De Brabander, M., and Lewi, P. (1971). DNA synthesis and mitoses in coronary collateral vessels of the dog. *Circ. Res.* 28, 671–679.

Schaper, W., and Ito, W. D. (1996). Molecular mechanisms of coronary collateral vessel growth. *Circ. Res.* 79, 911–919.

Scholz, D., Cai, W. J., and Schaper, W. (2001). Arteriogenesis, a new concept of vascular adaptation in occlusive disease. *Angiogenesis* 4, 247–257. doi: 10.1023/a:1016094004084

Scholz, D., Ito, W., Fleming, I., Deindl, E., Sauer, A., Wiesnet, M., et al. (2000). Ultrastructure and molecular histology of rabbit hind-limb collateral artery growth (arteriogenesis). *Virchows Arch.* 436, 257–270. doi: 10.1007/s004280050039

Segiet, O. A., Brzozowa-Zasada, M., Piecuch, A., Dudek, D., Reichman-Warmusz, E., and Wojnicz, R. (2015). Biomolecular mechanisms in varicose veins development. *Ann. Vasc. Surg.* 29, 377–384. doi: 10.1016/j.avsg.2014.10.009

Shay-Salit, A., Shushy, M., Wolfovitz, E., Yahav, H., Breviario, F., Dejana, E., et al. (2002). VEGF receptor 2 and the adherens junction as a mechanical transducer in vascular endothelial cells. *Proc. Natl. Acad. Sci. U. S. A.* 99, 9462–9467. doi: 10.1073/pnas.142224299

Sho, E., Sho, M., Singh, T. M., Nanjo, H., Komatsu, M., Xu, C., et al. (2002). Arterial enlargement in response to high flow requires early expression of matrix metalloproteinases to degrade extracellular matrix. *Exp. Mol. Pathol.* 73, 142–153. doi: 10.1006/exmp.2002.2457

Silver, A. E., and Vita, J. A. (2006). Shear-stress-mediated arterial remodeling in atherosclerosis: too much of a good thing? *Circulation* 113, 2787–2789. doi: 10.1161/CIRCULATIONAHA.106.634378

Singh, E., Redgrave, R. E., Phillips, H. M., and Arthur, H. M. (2020). Arterial endoglin does not protect against arteriovenous malformations. *Angiogenesis* 23, 559–566. doi: 10.1007/s10456-020-09731-z

Soblet, J., Limaye, N., Uebelhoer, M., Boon, L. M., and Vikkula, M. (2013). Variable somatic TIE2 mutations in half of sporadic venous malformations. *Mol. Syndromol.* 4, 179–183. doi: 10.1159/000348327

Su, T., Stanley, G., Sinha, R., D'amato, G., Das, S., Rhee, S., et al. (2018). Single-cell analysis of early progenitor cells that build coronary arteries. *Nature* 559, 356–362. doi: 10.1038/s41586-018-0288-7

Sugden, W. W., Meissner, R., Aegerter-Wilmsen, T., Tsaryk, R., Leonard, E. V., Bussmann, J., et al. (2017). Endoglin controls blood vessel diameter through endothelial cell shape changes in response to haemodynamic cues. *Nat. Cell Biol.* 19, 653–665. doi: 10.1038/ncb3528

Surendran, S., Ramegowda, K. S., Suresh, A., Binil Raj, S. S., Lakkappa, R. K., Kamalapurkar, G., et al. (2016). Arterialization and anomalous vein wall remodeling in varicose veins is associated with upregulated FoxC2-Dll4 pathway. *Lab. Investig.* 96, 399–408. doi: 10.1038/labinvest.2015.167

Tabibian, A., Ghaffari, S., Vargas, D. A., Van Oosterwyck, H., and Jones, E. A. V. (2020). Simulating flow induced migration in vascular remodelling. *PLoS Comput. Biol.* 16:e1007874. doi: 10.1371/journal.pcbi.1007874

Ten Dijke, P., Egorova, A. D., Goumans, M. J., Poelmann, R. E., and Hierck, B. P. (2012). TGF-beta signaling in endothelial-to-mesenchymal transition: the role of shear stress and primary cilia. *Sci. Signal.* 5:pt2. doi: 10.1126/scisignal.2002722

Thomas, D. D., Ridnour, L. A., Isenberg, J. S., Flores-Santana, W., Switzer, C. H., Donzelli, S., et al. (2008). The chemical biology of nitric oxide: implications in cellular signaling. *Free Radic. Biol. Med.* 45, 18–31. doi: 10.1016/j.freeradbiomed.2008.03.020

Toyota, E., Warltier, D. C., Brock, T., Ritman, E., Kolz, C., O'malley, P., et al. (2005). Vascular endothelial growth factor is required for coronary collateral growth in the rat. *Circulation* 112, 2108–2113. doi: 10.1161/CIRCULATIONAHA.104.526954

Tual-Chalot, S., Garcia-Collado, M., Redgrave, R. E., Singh, E., Davison, B., Park, C., et al. (2020). Loss of endothelial endoglin promotes high-output heart failure through peripheral arteriovenous shunting driven by VEGF signaling. *Circ. Res.* 126, 243–257. doi: 10.1161/CIRCRESAHA.119.315974

Ubezio, B., Blanco, R. A., Geudens, I., Stanchi, F., Mathivet, T., Jones, M. L., et al. (2016). Synchronization of endothelial Dll4-notch dynamics switch blood vessels from branching to expansion. *elife* 5:e12167. doi: 10.7554/eLife.12167

Udan, R. S., Vadakkan, T. J., and Dickinson, M. E. (2013). Dynamic responses of endothelial cells to changes in blood flow during vascular remodeling of the mouse yolk sac. *Development* 140, 4041–4050. doi: 10.1242/dev.096255

Ventrella, R., Kaplan, N., and Getsios, S. (2017). Asymmetry at cell-cell interfaces direct cell sorting, boundary formation, and tissue morphogenesis. *Exp. Cell Res.* 358, 58–64. doi: 10.1016/j.yexcr.2017.03.024

Vion, A. C., Alt, S., Klaus-Bergmann, A., Szymborska, A., Zheng, T., Perovic, T., et al. (2018). Primary cilia sensitize endothelial cells to BMP and prevent excessive vascular regression. *J. Cell Biol.* 217, 1651–1665. doi: 10.1083/jcb.201706151

Voskuil, M., Van Royen, N., Hoefer, I. E., Seidler, R., Guth, B. D., Bode, C., et al. (2003). Modulation of collateral artery growth in a porcine hindlimb ligation model using MCP-1. *Am. J. Physiol. Heart Circ. Physiol.* 284, H1422–H1428. doi: 10.1152/ajpheart.00506.2002

Wali, M. A., and Eid, R. A. (2001). Smooth muscle changes in varicose veins: an ultrastructural study. *J. Smooth Muscle Res.* 37, 123–135. doi: 10.1540/jsmr.37.123

Walshe, T. E., Dela Paz, N. G., and D'amore, P. A. (2013). The role of shear-induced transforming growth factor-beta signaling in the endothelium. *Arterioscler. Thromb. Vasc. Biol.* 33, 2608–2617. doi: 10.1161/ATVBAHA.113.302161

Walshe, T. E., Dole, V. S., Maharaj, A. S., Patten, I. S., Wagner, D. D., and D'amore, P. A. (2009). Inhibition of VEGF or TGF-{beta} signaling activates endothelium and increases leukocyte rolling. *Arterioscler. Thromb. Vasc. Biol.* 29, 1185–1192. doi: 10.1161/ATVBAHA.109.186742

Walshe, T. E., Leach, L. L., and D'amore, P. A. (2011). TGF-beta signaling is required for maintenance of retinal ganglion cell differentiation and survival. *Neuroscience* 189, 123–131. doi: 10.1016/j.neuroscience.2011.05.020

Ward, A. O., Angelini, G. D., Caputo, M., Evans, P. C., Johnson, J. L., Suleiman, M. S., et al. (2020). NF-kappaB inhibition prevents acute shear stress-induced inflammation in the saphenous vein graft endothelium. *Sci. Rep.* 10:15133. doi: 10.1038/s41598-020-71781-6

Welkie, J. F., Comerota, A. J., Kerr, R. P., Katz, M. L., Jayheimer, E. C., and Brigham, R. A. (1992). The hemodynamics of venous ulceration. *Ann. Vasc. Surg.* 6, 1–4.

Wolf, C., Cai, W. J., Vosschulte, R., Koltai, S., Mousavipour, D., Scholz, D., et al. (1998). Vascular remodeling and altered protein expression during growth of coronary collateral arteries. *J. Mol. Cell. Cardiol.* 30, 2291–2305.

Xu, C., Hasan, S. S., Schmidt, I., Rocha, S. F., Pitulescu, M. E., Bussmann, J., et al. (2014). Arteries are formed by vein-derived endothelial tip cells. *Nat. Commun.* 5:5758. doi: 10.1038/ncomms6758

Yang, B., Cai, B., Deng, P., Wu, X., Guan, Y., Zhang, B., et al. (2015). Nitric oxide increases arterial endotheial permeability through mediating VE-cadherin expression during arteriogenesis. *PLoS One* 10:e0127931. doi: 10.1371/journal.pone.0127931

You, L. R., Lin, F. J., Lee, C. T., Demayo, F. J., Tsai, M. J., and Tsai, S. Y. (2005). Suppression of notch signalling by the COUP-TFII transcription factor regulates vein identity. *Nature* 435, 98–104. doi: 10.1038/nature03511

Zhang, Y., and Yang, X. (2020). The roles of TGF-beta signaling in cerebrovascular diseases. *Front. Cell Dev. Biol.* 8:567682. doi: 10.3389/fcell.2020.567682

Zhao, Y., Brandish, P. E., Ballou, D. P., and Marletta, M. A. (1999). A molecular basis for nitric oxide sensing by soluble guanylate cyclase. *Proc. Natl. Acad. Sci. U. S. A.* 96, 14753–14758.

Zygmunt, T., Gay, C. M., Blondelle, J., Singh, M. K., Flaherty, K. M., Means, P. C., et al. (2011). Semaphorin-PlexinD1 signaling limits angiogenic potential via the VEGF decoy receptor sFlt1. *Dev. Cell* 21, 301–314. doi: 10.1016/j.devcel.2011.06.033

**Conflict of Interest:** The authors declare that the research was conducted in the absence of any commercial or financial relationships that could be construed as a potential conflict of interest.

frontiers in Physiology

ORIGINAL RESEARCH
published: 02 March 2021
doi: 10.3389/fphys.2020.623769

# Endothelial Cell Orientation and Polarity Are Controlled by Shear Stress and VEGF Through Distinct Signaling Pathways

*Anne-Clémence Vion[1,2]*, Tijana Perovic[1], Charlie Petit[1], Irene Hollfinger[1], Eireen Bartels-Klein[1], Emmanuelle Frampton[3], Emma Gordon[3,4], Lena Claesson-Welsh[4] and Holger Gerhardt[1,5,6]**

[1] Integrative Vascular Biology Laboratory, Max Delbruck Center for Molecular Medicine, Berlin, Germany, [2] Université de Nantes, CNRS, INSERM, l'institut du thorax, Nantes, France, [3] Institute for Molecular Bioscience, The University of Queensland, Brisbane, QLD, Australia, [4] Beijer and Science for Life Laboratories, Rudbeck Laboratory, Department of Immunology, Genetics and Pathology, Uppsala University, Uppsala, Sweden, [5] DZHK (German Center for Cardiovascular Research), Berlin, Germany, [6] Berlin Institute of Health (BIH), Berlin, Germany

OPEN ACCESS

**Edited by:**
Anna Rita Cantelmo,
Université Lille Nord de France, France

**Reviewed by:**
Stephan Huveneers,
Amsterdam University Medical Center (UMC), Netherlands
Elizabeth Anne Vincent Jones,
KU Leuven, Belgium

***Correspondence:**
Anne-Clémence Vion
anne-clemence.vion@univ-nantes.fr
Holger Gerhardt
holger.gerhardt@mdc-berlin.de

**Specialty section:**
This article was submitted to Vascular Physiology, a section of the journal Frontiers in Physiology

**Received:** 30 October 2020
**Accepted:** 08 December 2020
**Published:** 02 March 2021

**Citation:**
Vion A-C, Perovic T, Petit C, Hollfinger I, Bartels-Klein E, Frampton E, Gordon E, Claesson-Welsh L and Gerhardt H (2021) Endothelial Cell Orientation and Polarity Are Controlled by Shear Stress and VEGF Through Distinct Signaling Pathways. Front. Physiol. 11:623769. doi: 10.3389/fphys.2020.623769

Vascular networks form, remodel and mature under the influence of multiple signals of mechanical or chemical nature. How endothelial cells read and interpret these signals, and how they integrate information when they are exposed to both simultaneously is poorly understood. Here, we show using flow-induced shear stress and VEGF-A treatment on endothelial cells *in vitro*, that the response to the magnitude of a mechanical stimulus is influenced by the concentration of a chemical stimulus, and vice versa. By combining different flow levels and different VEGF-A concentrations, front-rear polarity of endothelial cells against the flow direction was established in a flow and VEGF-A dose-response while their alignment with the flow displayed a biphasic response depending on the VEGF-A dose (perpendicular at physiological dose, aligned at no or pathological dose of VEGF-A). The effect of pharmaceutical inhibitors demonstrated that while VEGFR2 is essential for both polarity and orientation establishment in response to flow with and without VEGF-A, different downstream effectors were engaged depending on the presence of VEGF-A. Thus, Src family inhibition (c-Src, Yes, Fyn together) impaired alignment and polarity without VEGF-A while FAK inhibition modified polarity and alignment only when endothelial cells were exposed to VEGF-A. Studying endothelial cells in the aortas of $VEGFR2^{Y949F}$ mutant mice and $SRC^{iEC-KO}$ mice confirmed the role of VEGFR2 and specified the role of c-SRC *in vivo*. Endothelial cells of $VEGFR2^{Y949F}$ mutant mice lost their polarity and alignment while endothelial cells from $SRC^{iEC-KO}$ mice only showed reduced polarity. We propose here that VEGFR2 is a sensor able to integrate chemical and mechanical information simultaneously and that the underlying pathways and mechanisms activated will depend on the co-stimulation. Flow alone shifts VEGFR2 signaling toward a Src family pathway activation and a junctional effect (both *in vitro* and *in vivo*) while flow and VEGF-A together shift VEGFR2 signaling toward focal adhesion activation (*in vitro*) both modifying cell responses that govern orientation and polarity.

**Keywords: endothelial cell, shear stress, VEGF, blood flow, signaling/signaling pathways**

## INTRODUCTION

During embryonic development, all vertebrates initially establish a primitive network of vessels that subsequently remodels into a hierarchical vascular structure. This involves the creation of a primary vascular plexus that expands by sprouting angiogenesis (Isogai et al., 2003; Potente et al., 2011) followed by vascular remodeling to adapt vessel organization, shape and size; in its course, superfluous and inefficient segments are pruned away by active regression (Franco et al., 2015). The cellular and molecular regulation of this process is influenced by blood flow, hypoxia and metabolism. In this context, cells need to respond appropriately to both mechanical and chemical cues to ensure healthy tissue development and homeostasis.

Endothelial cells (ECs), which constitute the inner layer of vessels, are in particular under constant mechanical strains exerted by blood flow. Interestingly, ECs are able to sense small variations in the direction, magnitude, and regularity of blood flow–induced shear stress (Wang et al., 2013; Givens and Tzima, 2016) and respond to such changes by controlling their number, shape and movement (Culver and Dickinson, 2010; Baeyens et al., 2016a). Adaptation of ECs to flow is critical for both the development and the maintenance of a well-functioning cardiovascular system, as modification of capillary patterning allows for efficient oxygen and nutrient supply, while inward and outward remodeling of main arteries maintains appropriate blood pressure over the entire body (Baeyens et al., 2015). Physiological shear stress level, as found when the network is mature will favor EC elongation and orientation parallel to the flow direction. Furthermore, the Golgi of EC will position itself upstream of the nucleus, thus pointing against the flow direction (Franco et al., 2015) indicating their current migratory direction.

ECs are also well equipped to sense hypoxia. Hypoxic conditions drive the expression of vascular endothelial growth factors (VEGFs) by the surrounding tissues, which initiates endothelial sprouting through binding and activation of VEGF receptors (VEGFRs). Signaling downstream of these receptors is essential for vascular morphogenesis, as they control processes such as EC migration, proliferation and vessel permeability (Simons et al., 2016) and can influence arterial differentiation (Carmeliet and Tessier-Lavigne, 2005).

A long-standing question in developmental and cell biology relates to how cells integrate mechanical and chemical signals to orchestrate the morphogenic behaviors that ensure adequate tissue patterning. When looking at the receptors and signaling cascades implicated in both flow and chemical responses in ECs, it is clear that they are largely redundant and involve the same players (Jin et al., 2003; Koch and Claesson-Welsh, 2012). This suggests a cooperative or competitive action of chemical and mechanical stimuli during vascular bed formation, patterning, maturation and maintenance. In this context, VEGFR2 signaling is one of the most interesting examples. VEGFR2 is essential for VEGF-A-driven biological effects (Koch et al., 2011). It becomes activated and phosphorylated on tyrosine residues in response to VEGF-A: Y951, Y1059, Y1175, and Y1214 (human sequence numbers) (Matsumoto et al., 2005). The Y951 phosphosite (Y949 in mouse VEGFR2) presents a specific binding site for the T cell-specific adaptor which is implicated in VEGF-A-induced permeability, by regulating VEGFR2-dependent SRC signaling pathway at EC junctions (Sun et al., 2012). The Y1059 residues, located on the tyrosine kinase activation loop, are required for full kinase activity (Koch et al., 2011). The phosphorylated Y1175 (Y1173 in mouse VEGFR2) binds phospholipase Cg, which is of importance for endothelial extracellular-signal-regulated kinase ERK1/2 pathway activation (Takahashi et al., 2001). A phenylalanine knock-in mouse $Vegfr2^{Y1173F/Y1173F}$ is embryonically lethal due to an arrest in EC development (Sakurai et al., 2005). Interestingly this phosphosite has also been described to be activated by flow, independently of VEGF, activating ERK1/2 and JNK pathways as well as eNOS (Chen et al., 1999; Jin et al., 2003). It has also been shown to activate NFκB both *in vitro* (Tzima et al., 2005; Coon et al., 2015) and *in vivo* (Baeyens et al., 2015). Finally, VEGFR2 Y1214 signaling induces activation of ERK1/2 and Akt pathways required for c-Myc-dependent gene regulation, endothelial proliferation, and vessel stability (Testini et al., 2019).

## MATERIALS AND METHODS

### Mice and Treatments

The following mouse strains were used: $VEGFR^{Y949F}$ mice (knock-in of phenylalanine (F) to replace the tyrosine (Y) at position 949 of VEGFR2 (Li et al., 2016) and c-Src-flox, Cdh5-CreERT2 mice designated as $SRC^{iEC-KO}$ mice (Cdh5-CreERT2 mice were provided by Ralf Adams (MPI, Muünster, Germany) (Kogata et al., 2006; Wang et al., 2010). c-Src-floxed mice were delivered from the Nice Mice, National Resource Center for Mutant Mice, Model Animal Research Center, China) (Schimmel et al., 2020). Mice were maintained at the Uppsala University under standard husbandry conditions. All animal work was approved by the Uppsala University board of animal experimentation (permit 5.2.18-8927-16). To induce Cre-mediated deletion, tamoxifen (Sigma-Aldrich) was injected i.p. (100 μg) at P1, P2 and P3. Aortas were then collected at P6 onward. The investigators were blinded to genotype during experiments.

### Metatarsal Assay

Metatarsals were isolated from E16.5 mice using a protocol adapted from Song et al. (2015). After dissection, one metatarsal per well was placed in a μ-Plate 24 well ibiTreat plate with a 1.5 polymer coverslip (Ibidi) and left in 170 μl of MEM-alpha (Gibco) with 10% FCS and 1% penicillin/streptomycin (Sigma). After 3 days, media were replaced with 300 μl MEM-alpha + 10% FCS + 1% pen/strep per well and media changed every 48 h. To induce Cre activity, cells were treated with 1 μM of 4-hydroxytamoxifen (Sigma) after 5 days. After 14 days, metatarsals were fixed in 4% PFA in PBS for 20 min and antibodies were added in 3% Triton X-100, 1% Tween and 0.5% BSA in PBS.

The following antibodies were used: GM130 (ref 560066, mouse, 1:500, BD Biosciences), ERG (ref ab92513, rabbit, 1:500, Abcam).

## Cell Culture and Microfluidic Chamber Experiments

HUVECs (passage 2–6; PromoCell) were routinely cultured in EBM-Bulletkit (Promocell). For flow experiments including static condition leading to WB lysate collection or immunofluorescence from **Figures 2**, **3**, cells were cultured on 0.2% gelatin-coated slides (Menzel Glazer) and unidirectional laminar shear stress was applied using peristaltic pumps (Gilson) connected to a glass reservoir (ELLIPSE) and the chamber containing the slide. This device allows the circulation of 10 ml of medium on the slides, static slides has been exposed to 10 ml of medium without any medium circulation. For flow experiments under high shear stress (**Figure 4**) and immunofluorescence staining, cells were cultured on 0.2% gelatin-coated 0.4 ibidi slides (IBIDI) and unidirectional laminar shear stress was applied using the pumping system and control unit form IBIDI, allowing the circulation of 10 ml of medium as for the peristaltic system.

Local shear stress was calculated using Poiseuille's law and averaged to 2 (Low SS) or 20 dyn/cm$^2$ (High SS). For VEGF-A treatment, cells were exposed to shear stress for 24 h using EBM media (Promocell) without VEGF-A supplement and co-stimulated with 0, 0.5, 10 or 200, ng/ml of human VEGF-A165 (PeproTech ref 450-32) under the different flow conditions. For inhibition experiments, VEGFR2 inhibitors (SU1498, 1.5 μM; ZM323881, 4 nM), Src family inhibitor (SU6656, 500 nM), FAK inhibitor (PND-1186, 3 nM) and p38 inhibitor (SB203580, 1 μM) were added to the media 30 min prior flow start. Control condition were treated with DMSO diluted at 1/1,000 as all inhibitor used.

## Western Blotting

HUVECs were washed with cold PBS and scraped off in M-PER (Mammalian Protein Extraction Reagent; Thermo Fisher Scientific) completed protease and phosphatase inhibitors (Roche). Lysates were centrifuged and protein supernatant was quantified using the Lowry protein assay (Bio-Rad). Lysates were mixed with reducing sample buffer for electrophoresis and subsequently transferred onto polyvinylidene fluoride membranes. Equal loading was checked using Ponceau red solution. Membranes were incubated with primary antibodies (see below). After incubation with secondary antibodies (1:3,000; GE Healthcare), immunodetection was performed using an enhanced chemiluminescence kit (SuperSignal West Dura; Pierce), and bands were revealed using the Las-4000 imaging system. After initial immunodetection, membranes were stripped of antibodies, probed with total form of the phosphorylated form when suitable (PXL) and then reprobed with anti–GAPDH antibody. Values reported from Western blots were obtained by band density analysis using FIJI (ImageJ) and expressed as the ratio of the protein of interest to GAPDH or as the ratio of phosphorylated form to total form of the protein of interest. The following antibodies were used: GAPDH (ref MAB374, goat; 1:10,000; Millipore), VEGFR2 (ref 2479, rabbit, 1:1,000; cell signaling), p1175-VEGFR2 (ref 3770, rabbit, 1:1,000; cell signaling), p951-VEGFR2 (ref 2471, rabbit, 1:1,000; cell signaling), VE-cadherin (ref ab33168, rabbit, 1:1,000; abcam), p685-VE-cadherin (ref ab119785, rabbit, 1:1,000; abcam), ZO-1(ref 61-7300, rabbit, 1:1,000; Thermo Fisher Scientific), FAK (ref 3285, rabbit, 1:1,000; cell signaling), Claudin5 (ref 34-1600, rabbit, 1:1,000; Invitrogen), Paxillin (ref 610051, rabbit, 1:1,000; BD Biosciences), p118-Paxillin (ref 2541, rabbit, 1:1,000; cell signaling).

## Immunofluorescence Staining

HUVECs were fixed with 4% PFA in PBS for 10 min at room temperature (RT). Blocking/permeabilization was performed using blocking buffer consisting of 5% BSA (Sigma-Aldrich), 0.5% Triton X-100 (Sigma-Aldrich), 0.01% sodium deoxycholate (Sigma-Aldrich), and 0.02% sodium azide (Sigma-Aldrich) in PBS at pH 7.4 for 45 min at RT. Primary antibodies were incubated at the desired concentration in 1:1 Blocking buffer/PBS at RT for 2 h and secondary antibodies were incubated at the desired concentration in 1:1 blocking buffer/PBS for 1 h at RT. Aortas were fixed with 4% PFA in PBS overnight at 4°C. Blocking/permeabilization was performed using blocking buffer consisting of 1% FBS, 3% BSA (Sigma-Aldrich), 0.5% Triton X-100 (Sigma-Aldrich), 0.01% sodium deoxycholate (Sigma-Aldrich), and 0.02% sodium azide (Sigma-Aldrich) in PBS at pH 7.4 for 1 h at RT. Primary antibodies were incubated at the desired concentration in 1:1 Blocking buffer/PBS overnight at 4°C and secondary antibodies were incubated at the desired concentration in 1:1 blocking buffer/PBS for 2 h at RT. DAPI (Sigma-Aldrich, 1/10,000, 5 min) was used for nuclear labeling. Cells and aortas were mounted in Mowiol. The following antibodies were used *in vitro*: VE-cadherin (ref sc-6458, goat; 1:100; Santa cruz), ZO-1 (ref 61-7300, rabbit, 1:500; Thermo Fisher Scientific), GM130 (ref 610822, mouse, 1:1,000;BD Biosciences). The following antibodies were used *in vivo*: GOLPH4 (ref ab28049, rabbit; 1:500; Abcam), VE–cadherin (ref 555289; rat; 1/100; BD Biosciences).

## Microscope Image Acquisition

Images from fluorescently labeled HUVECs were acquired using a LSM 700 upright microscope equipped with a Plan-Apochromat 20×/0.8 NA Ph2 objective. Images were taken at room temperature using Zen 2.3 software. Bright-field images were taken using a Leica DMIL LED microscope equipped with a 10×/0.22 NA Ph1 objective and a CCD camera (DFC3000 G). Images were acquired at room temperature while the cells were still in their culture medium using LAS X software (Leica). Images of aortas were taken using a LSM 780 inverted microscope (Zeiss) equipped with a Plan-Apochromat 20×/0.8 NA Ph2 objective or with a Plan-Apochromat 63×/1.4 NA DIC objective. The microscope was equipped with a photon multiplier tube detector. Images were taken at room temperature using Zen 2.3 software (Zeiss). Images of metatarsals were acquired using a LSM 710 inverted microscope equipped with Plan-Apochromat 10×/0.45 NA and 20×/0.8 NA objectives. For all animal experiments, the investigators were unaware of the genotypes of the animals while acquiring images.

## Cell Junction Activity Analysis

Cell junction morphology analysis was done in HUVECs stained for VE-cadherin using the patch and classified Matlab code previously developed by Bentley et al. (2014) adapted for 2D images. Two status were defined: activated vs. stabilized, and divided into 3 level: from low to high. Activated junctions were defined as serrated or reticular and stabilized as straight thick junctions. Each image taken was divided into small pieces of images allowing to visualized only a portion of the junction and these small images were presented blindly and randomly to the user who then classified the junction accordingly. This technic ensured an unbiased analysis of the junctions regarding the treatment and regarding the global shape of the cell.

## Flow-Induced Orientation Analysis

To analyze the orientation of cells, we calculated the angle formed between the vector of the flow direction (obtained by knowledge of flow direction within the slide) and the "orientation vector" given by orientation of the main axe of each cell. Each value for each cell is then used to plot the hemi-roses presented in **Figure 2A**. To plot the bar graphs presented in **Figures 2B**, **4B**, **5B**, **6B** the cells were classified in 2 categories: aligned with the flow direction, and not aligned with the flow direction. For *in vitro* experiment, aligned with the flow was defined as an absolute value of angle between 0 and 45°, not aligned with the flow as an absolute value of angle between 45 and 90°; for *in vivo* experiments, aligned with the flow was defined as an absolute value of angle between 0 and 15° and not aligned with the flow as an absolute value of angle between 15 and 90°. Angle calculation and roses presentation was done automatically using a homemade Matlab script validated on the first experiment by a comparison to hand calculation with FIJI.

## Flow-Induced Polarity Analysis

To analyze the polarization of cells, we calculated the angle formed between the vector of the flow direction (obtained by knowledge of flow direction within the slide) and the "golgi vector" given by the line from the center of the nucleus to the center of the Golgi. Of note, static experiments are not exposed to flow and therefor calculation has been made using an arbitrary direction given by the geometry of the ibidi slide. Each value for each cell is then used to plot the roses presented in **Figure 2C**. To plot the bar graphs presented in **Figures 2D**, **4D**, **5D**, **6D**, the cells were classified in 3 categories: against the flow direction, sided to the flow direction and with the flow direction. For *in vitro* experiment, with the flow was defined as an absolute value of angle between 0 and 45°, sided as an absolute value of angle between 45 and 135° and against the flow as an absolute value of angle between 135 and 180°; for *in vivo* experiment with the flow was defined as an absolute value of angle between 0 and 30°, sided as an absolute value of angle between 30 and 150° and against the flow as an absolute value of angle between 150 and 180°. Angle calculation and roses presentation was done automatically using a homemade Matlab script validated on the first experiment by a comparison to hand calculation with FIJI. Metatarsal polarity analysis was performed using FIJI with values defined as for *in vivo* experimental values (with: 0–30°, sided: 30–150°, and against: 150–180°).

## Statistical Analysis

Statistical analysis was performed using GraphPad Prism software. For *in vitro* and *in vivo* experiments, two-way ANOVA (data distribution was assumed to be normal) were used, followed by a Tukey test or a Fisher LSD test when conditions were considered experimentally independent. Details of the statistical test used for each experiment can be found in the figure legends. The investigators were blinded to genotype during experiments and quantification.

# EXPERIMENTAL APPROACH

To study how physical forces and growth factors jointly influence front-rear polarity and cell elongation toward the flow direction (alignment/orientation), we subjected ECs to either static conditions, low or high shear stress (SS, 2 or 20 dyn/cm$^2$ for 24 h) and to different VEGF-A concentrations ranging from physiological (0.5 and 10 ng/mL) to pathological (200 ng/mL) levels. Cell orientation refers to the long axis of ECs as they adopt their prototypical elongated cell shape under the influence of blood flow *in vivo*, or equivalent shear stress induced by medium flow *in vitro*. Alignment in this context depicts whether this long-axis of the ECs is aligned with the direction of the flow. Similarly, front-rear polarity is also assessed in relation to the flow direction. Unlike elongation or alignment, the polarity vector assigns a front and a rear to the cell, in a way that is normally associated with dynamic movement of cells in a certain direction. When they migrate, many cell types, including ECs, position their centrosome and Golgi ahead of the nucleus in the direction of migration. Therefore, determining the center of mass of the Golgi in relation to the center of mass of the cell nucleus delivers a vector that can be used as a proxy for front-rear polarity of migrating cells. Recent work illustrated that ECs under flow *in vivo* and *in vitro* follow the same principle as they orientate and migrate against the direction of flow during vascular remodeling (Kupfer et al., 1982; Franco et al., 2015). We therefore determined the Golgi-nucleus vector to establish front-rear polarity under all conditions of SS and growth factor stimulation. Throughout the analysis below, cell alignment and polarity in relation to the direction of flow will serve as reference system for the phenotypical flow response of ECs (**Figure 1**).

As the polarized movement of ECs requires junctional rearrangements and turnover, both during angiogenic sprouting and vascular remodeling under flow (Koch et al., 2011; Conway et al., 2013; Neto et al., 2018), we also assessed endothelial junctional patterns under the various conditions. Previous studies classified junctional features that correlate with junctional dynamics and VE-cadherin turnover (Bentley et al., 2014), providing a useful quantitative framework for the assessment of flow and growth factor effects. We used this classification tool adapted for a 2D layer to evaluate junctional activity in our different *in vitro* conditions. We complemented these results with biochemical analysis of VE-cadherin phosphorylation on Tyrosine 685, which contributes

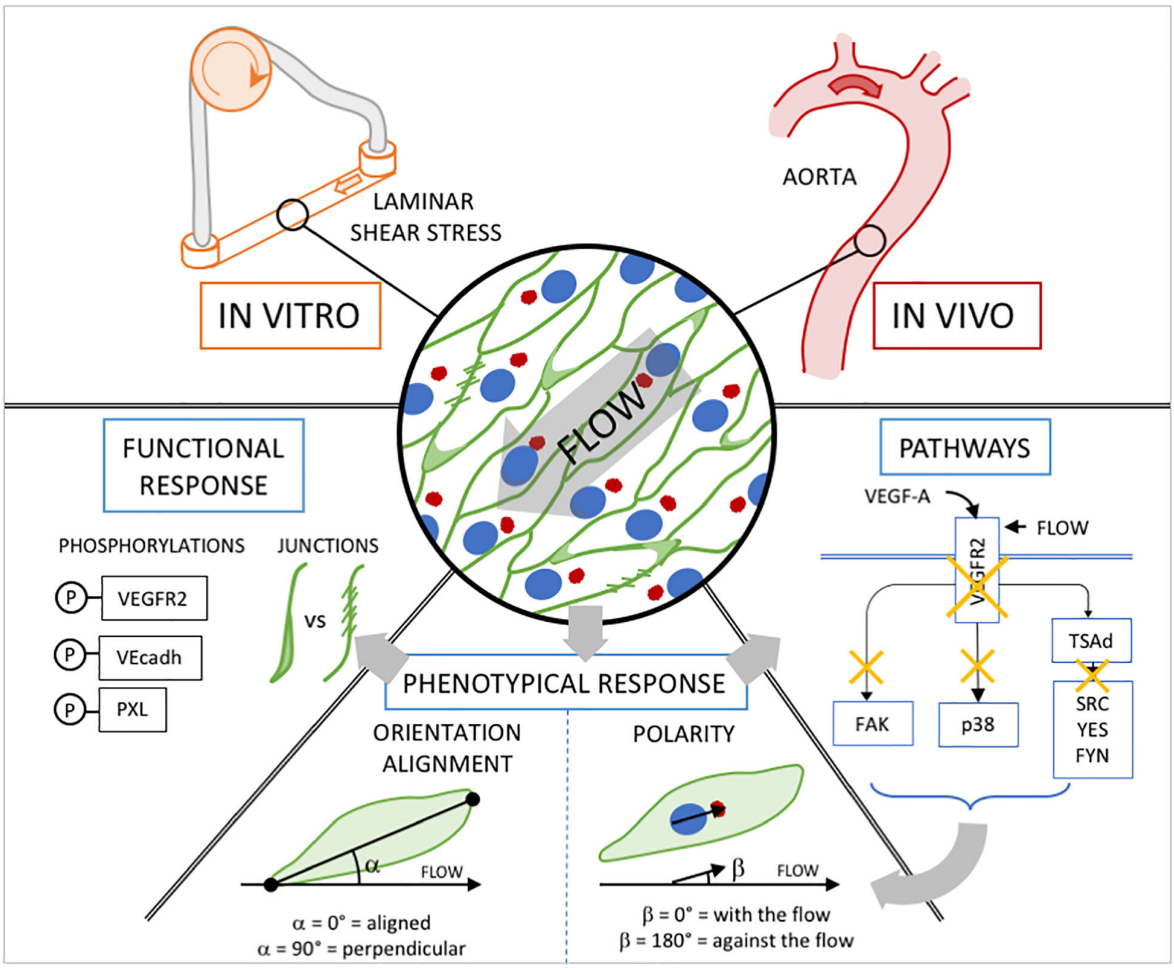


**FIGURE 1 |** Experimental approach. *In vitro*, We subjected ECs to either static condition, low or high shear stress (SS, 2 or 20 dyn/cm$^2$ for 24 h) and to different VEGF-A concentrations ranging from physiological (0.5 and 10ng/mL) to pathological (200 ng/mL) levels. *In vivo*, we used the linear part of aorta which is exposed to high SS and free from VEGF-A influence. **Phenotypical response:** Cell orientation/alignment refers to the long axis of ECs as they adopt their prototypical elongated cell shape under the influence of blood flow *in vivo*, or equivalent shear stress induced by medium's flow *in vitro*. Determining the center of mass of the golgi in relation to the center of mass of the cell nucleus delivers a vector used as a proxy for front-rear polarity of migrating cells. **Functional response:** biochemical analysis of VEGFR2 phosphorylation on Tyrosine 1175 and 951; VE-cadherin phosphorylation on Tyrosine 685; Paxillin phosphorylation on Tyrosine 118. classification of junction type through VE-cadherin staining. **Pathways:** inhibition through drug treatment (*in vitro*) or Knock-Out strategies (*in vivo*) and analysis of the phenotypical response.

to VE-cadherin internalization (Orsenigo et al., 2012). Since VEGFR2 is a flow sensor (Tzima et al., 2005) when associated to PECAM and VE-cadherin, in addition to its VEGF-A receptor activity, we then employed biochemical analysis to study its activation. We exposed ECs to selective inhibitor treatments to identify pathway activity patterns and their relevance for the different aspects of the endothelial phenotypical response to flow. Finally, we validated our results using an *in vivo* approach. The aorta is exposed to high SS (similar level as used in our *in vitro* experiments) in its linear, thoracic part and free from VEGF-A influence. In this model, ECs forming the linear part are highly elongated and aligned with the flow direction and mostly polarized against the flow. In contrast EC display rounded shape and random alignment in the aortic arch exposed to turbulent flow generating low SS (Gimbrone and García-Cardeña, 2013). We took advantage of these aortic characteristics to assess EC alignment in deficient mice models to validate our *in vitro* finding on phenotypical response to flow (**Figure 1**).

## RESULTS

### Combination of Flow Exposure and VEGF-A Treatment Modifies Endothelial Cell Orientation and Polarity

As VEGF-A induces proliferation of ECs (Koch et al., 2011), we first controlled whether our experimental condition influenced cell density and therefore the analyses. In all conditions, static, low SS (2 dyn/cm2), or high SS (20 dyn/cm$^2$), VEGF-A (0.5–200 ng/ml) did not affect the EC number

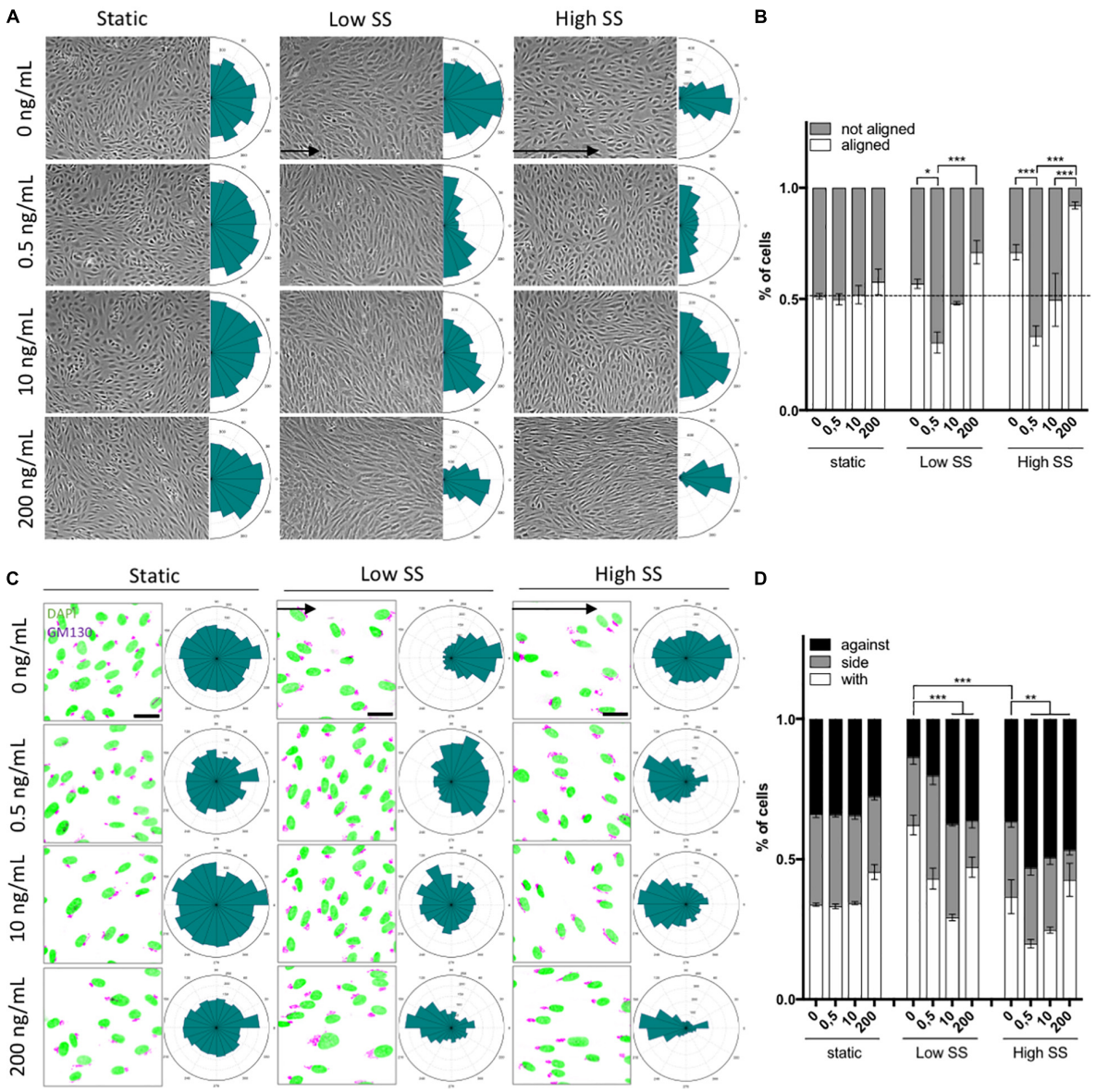


**FIGURE 2 |** Dose-dependent effect of shear stress and VEGF-A concentration on cell orientation and polarity. **(A)** Representative picture (phase contrast) of endothelial cells exposed to shear stress for 24 h (static: 0 dyn/cm$^2$; Low SS: 3 dyn/cm$^2$; High SS: 20 dyn/cm$^2$) and associated orientation quantification shown as circular plots ($N$ = 3; between 1,500 and 3,000 cells analyzed). **(B)** Quantification of percentage of cells aligned with the flow direction (in between 45° around the flow axis, $N$ = 3, between 1,500 and 3,000 cells analyzed), Data presented as Mean + SEM. **(C)** Representative picture (Immunofluorescence) of endothelial cells exposed to shear stress for 24 h (Low SS: 3 dyn/cm$^2$; High SS: 20 dyn/cm$^2$) (scale bars: 30 μm). **(D)** Quantification of golgi position around the nucleus compared to the flow direction ($N$ = 3; with: in between 0 and 45° around the flow axis, side: 45–135°, against: 135–180°; between 1,500 and 3,000 cells analyzed). Two-way ANOVA; Tukey's *post hoc*, $^*p < 0.05$; $^{**}p < 0.01$; $^{***}p < 0.001$.

(**Supplementary Figure 1A**). Both high and low SS exposure reduced the number of cells to about 75% of that in the static conditions. Alignment analyses showed that the ECs main axis in static condition (no flow, 0 dyn/cm$^2$) was randomly distributed, with no effect of VEGF-A addition (**Figures 2A,B**). The only effect observed was an increase in cell elongation after treating ECs with 200 ng/mL of VEGF-A (**Supplementary Figure 1B**).

Low SS (2 dyn/cm$^2$, no VEGF-A) had no effect on cell alignment, which remained random. VEGF-A addition (0.5 ng/ml) to low SS promoted alignment perpendicular to the flow direction while treatment with 200 ng/ml VEGF-A promoted EC alignment with the flow (**Figures 2A,B**). This showed that the effect of VEGF-A under low SS was biphasic, dependent on the dose used.

High SS itself (20 dyn/cm$^2$, no VEGF-A) enhanced alignment with the flow. VEGF-A addition (0.5 ng/ml) to high SS made ECs align perpendicular to the flow direction. At high VEGF-A concentrations (200 ng/ml), alignment with the flow was

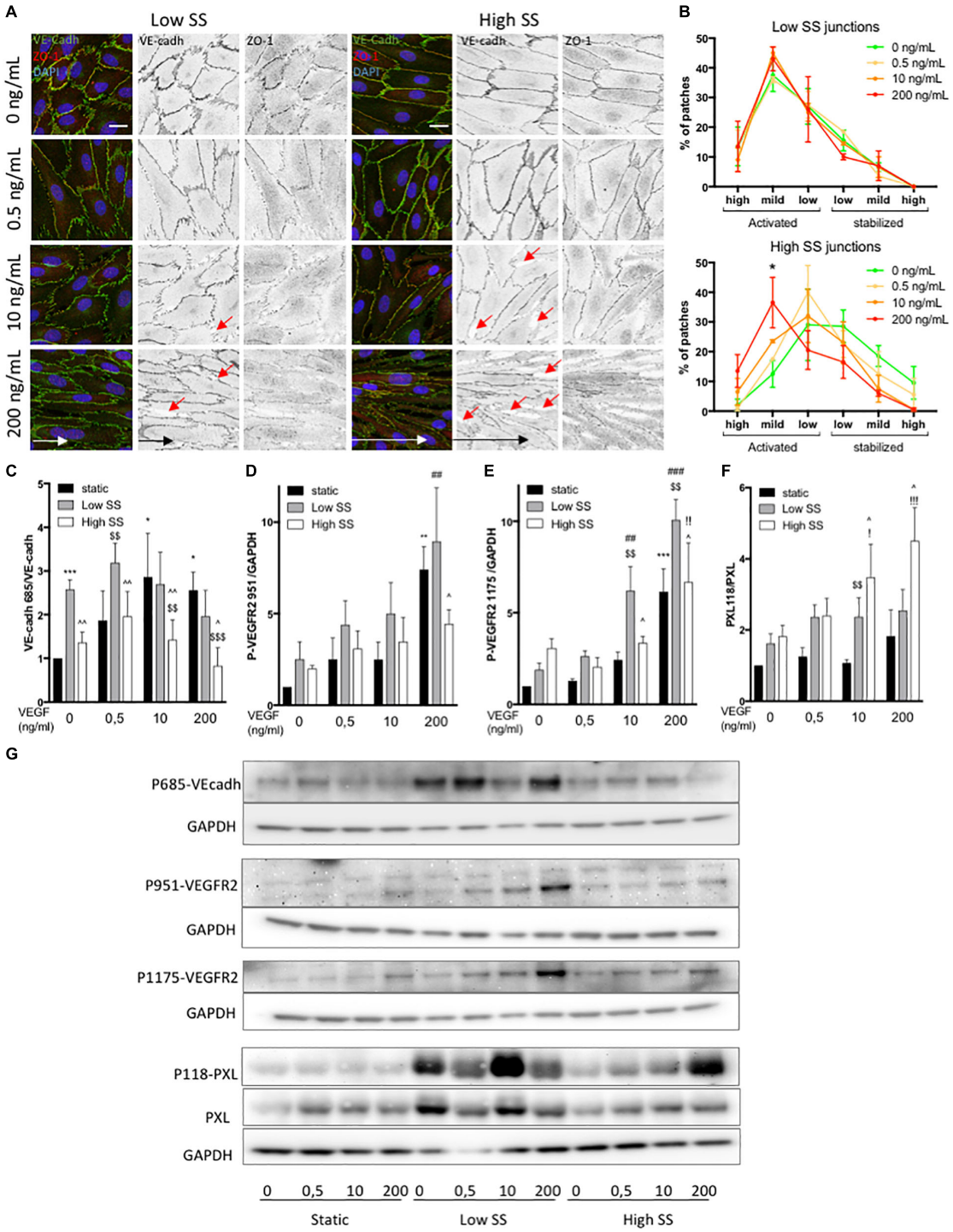


**FIGURE 3 |** Effect of flow and VEGF-A combination on VEGFR2, junctional and focal adhesion activity. **(A)** Representative picture (Immunofluorescence) of endothelial cells exposed to shear stress for 24 h (Low SS: 3 dyn/cm$^2$; High SS: 20 dyn/cm$^2$). Red arrows indicate gaps in the ECs monolayer **(B)** Quantification of junction status based on their morphology ($N$ = 3; 100 patches analyzed blinded by images, 5–8 images per N) (scale bars: 20 μm, same magnification for all images). **(C)** WB analysis of VE-cadherin phosphorylation, $N$ = 5, **(D)** WB analysis of VEGFR2 phosphorylation on Tyr951. $N$ = 4 **(E)** WB analysis of VEGFR2 phosphorylation on Tyr1175. $N$ = 4 **(F)** WB analysis of Paxilllin phosphorylation on Tyr118. $N$ = 4 **(G)** WB representative images. Data presented as Mean + SEM. Two-way ANOVA; Fisher LSD test, $^{*}p < 0.05$; $^{**}p < 0.01$; $^{***}p < 0.001$ compared to static 0 VEGF; $^{\#\#}p < 0.01$; $^{\#\#\#}p < 0.001$ (compared to LSS 0 VEGF); $^{!!}p < 0.01$ (compared to HSS 0 VEGF); $^{\$\$}p < 0.01$; $^{\$\$\$}p < 0.001$ compared to static from the same VEGF concentration; $^{\wedge\wedge}p < 0.05$; $^{\wedge\wedge\wedge}p < 0.01$ compared to Low SS from the same VEGF concentration.

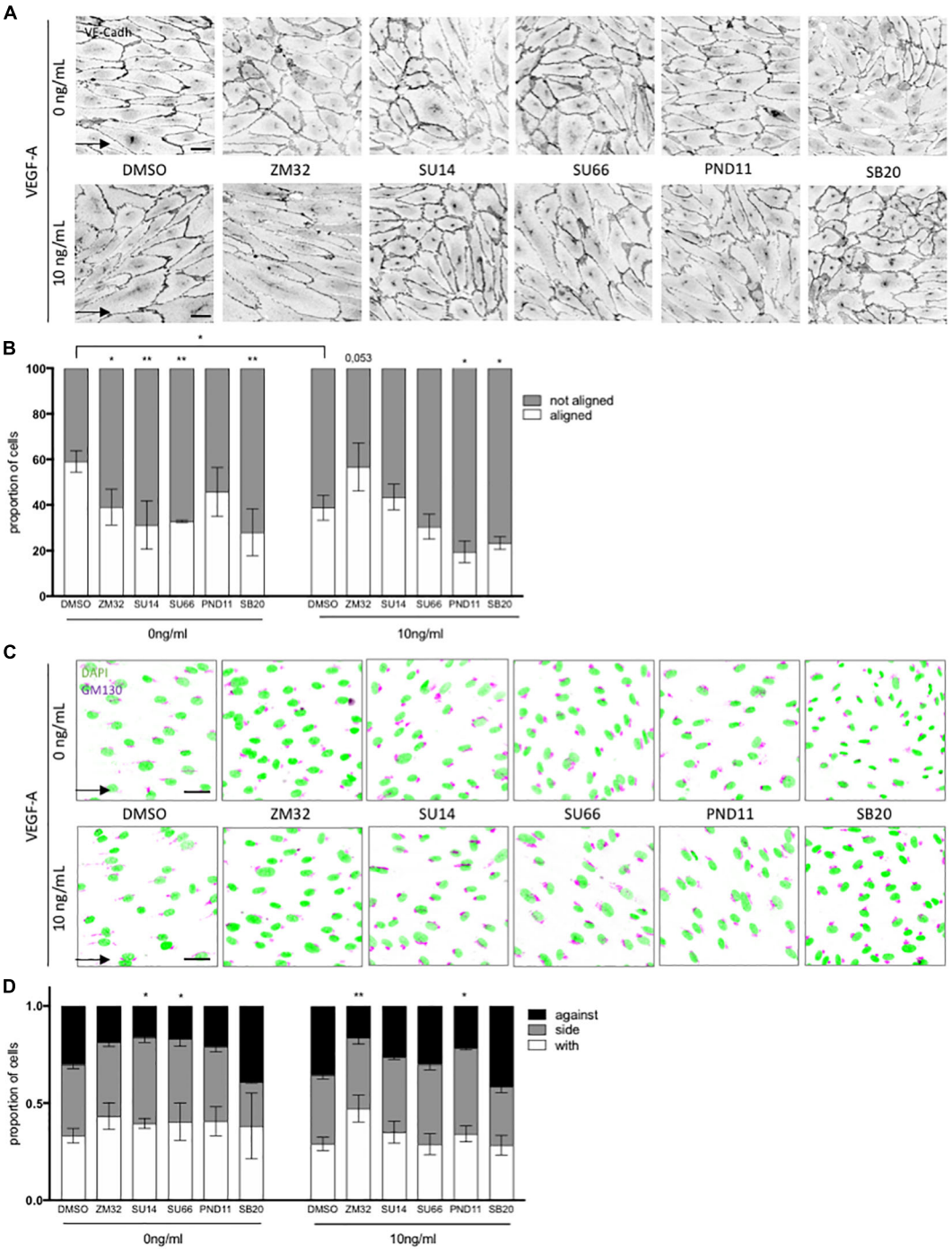


**FIGURE 4 |** Pathways involved in flow and VEGF responses. **(A)** Representative picture of junction (VE-cadherin mentioned as VE-cadh) of endothelial cells exposed to shear stress for 24 h (High SS: 20 dyn/cm$^2$) without or with inhibitors (scale bars: 40 $\mu$m, same magnification for all images). **(B)** Quantification of percentage of cells aligned with the flow direction (in between 30° around the flow axis. DMSO, $N = 5$, inhibitors $N = 3$). **(C)** Representative picture polarity of endothelial cells exposed to shear stress for 24 h (High SS: 20 dyn/cm$^2$) without or with inhibitors (scale bars: 40 $\mu$m, same magnification for all images). **(D)** Quantification of golgi position around the nucleus compared to the flow direction (DMSO, $N = 5$, inhibitors $N = 3$. with: in between 0 and 45∘ around the flow axis, side: 45–135°, against: 135–180°). Arrow represents flow direction (High SS). Two-way ANOVA; $^*p < 0.05$; $^{**}p < 0.01$; $^{***}p < 0.001$. VEGFR2 inhibitors (SU1498, 1.5 mM; ZM323881, 4 nM), Src family inhibitor (SU6656, 500 nM), FAK inhibitor (PND-1186, 3 nM) and p38 inhibitor (SB203580, 1 mM) were added to the media 30 min prior flow start.

increased, as observed under low SS (**Figures 2A,B**) but even more pronounced.

When assessing polarity, ECs in static culture remained randomly polarized in the absence and presence of VEGF-A (**Figures 2C,D**). At low SS in the absence of VEGF-A, ECs polarized in the direction "with" the flow, meaning that their Golgi was mostly placed behind the nucleus compared to the flow direction. On the contrary, high SS triggered a partial polarization against the flow. In both low and high SS, VEGF-A promoted polarity against the flow, in a dose-response manner: the higher the VEGF-A concentration, the better cells polarized against the flow (**Figures 2C,D**).

Taken together, these data show that ECs align and orient themselves relative to flow by integrating chemical and flow conditions and that the magnitude of the stimuli direct the response. With the more pronounced combined stimulation, ECs aligned efficiently and polarized against the flow.

## Combination of Flow Exposure and VEGF-A Treatment Affects VEGFR2 Phosphorylation, Adherens Junction Stability and Focal Adhesion Activity

We then looked at cell adherens junctions. Under static conditions, VE-cadherin staining and quantification of stabilized (straight) and activated (serrated) junctions did not show any effect of VEGF-A treatment after 24 h (**Supplementary Figures 2A,B**). ZO-1 appeared localized at the junction for all VEGF-A concentration (**Supplementary Figure 2A**). Some discontinuities in the adherens junctions were observed at 200 ng/mL (**Supplementary Figure 2**, red arrow). This was not associated to a change in VE-cadherin and ZO-1 protein levels upon SS and VEGF-A exposure (**Supplementary Figures 3B,C**).

Upon low SS alone (no VEGF-A), ECs showed a high level of activated/serrated junctions (**Figures 3A,B**). VEGF-A treatment had no additional effect on junction activation which remained high. In contrast, high SS induced stabilization/straightening of the junctions and increasing the concentration of VEGF-A correlated with an increase in serrated VE-cadherin junctions (**Figures 3A,B**). Junctional ZO-1 was higher in ECs exposed to high SS than in ECs exposed to low SS (**Figure 3A**). VEGF-A treatment induced a loss of this junctional ZO-1 both under low and high SS (**Figure 2A**). Additionally, both under low and high SS, high VEGF-A concentrations (10 and 200 ng/mL) led to loosening of the adherens junctions, which displayed increased number of gaps in the endothelial layer (indicated as red arrows on **Figure 3A**), to a higher extent at high SS.

To better understand the junctional modifications, we analyzed VE-cadherin phosphorylation on Tyrosine 685, which contributes to VE-cadherin internalization (Orsenigo et al., 2012). Under static condition, VEGF-A treatment increased VEcadh$^{Y685}$ level in a dose dependent manner (**Figures 3C,G**). ECs exposed to low SS have high VE-cadherin phosphorylation level independently of VEGF-A concentration (**Figures 3C,G**), matching the observation of high level of serrated junction in this flow condition. VEcadh$^{Y685}$ levels remained low under high SS independently of VEGF-A concentration and despite increasing serrated junctions.

Since VEGFR2 is a flow sensor (Tzima et al., 2005) when associated to PECAM and VE-cadherin in addition to its VEGF-A receptor activity, we evaluated its phosphorylation status in our conditions. First, we confirmed that both tyrosine 1175 and 951 were phosphorylated in a dose-response manner upon VEGF-A treatment under static conditions (**Figures 3D,E,G**). VEGFR2 expression was stable in static condition but significantly increased in response to flow in the absence of VEGF-A (**Supplementary Figure 3A**). Of note, high VEGF-A treatment (200 ng/mL) slightly but significantly decreased VEGFR2 expression, suggesting modification in protein turn over. VEGFR2$^{Y1175}$ phosphorylation level was increased by SS (**Figures 3E,G**) in the absence of VEGF-A, with high SS inducing more VEGFR2$^{Y1175}$ phosphorylation than low SS. In comparison, VEGFR2$^{Y951}$ phosphorylation was increased by SS but at an equivalent level between low and high SS (**Figures 3D,G**). When ECs were exposed to low SS, VEGF-A treatment strongly increased VEGFR2$^{Y951}$ and VEGFR2$^{Y1175}$ phosphorylation in a dose-response manner while this effect was not present (VEGFR2$^{Y951}$) or mild (VEGFR2$^{Y1175}$) when ECs were exposed to high SS (**Figures 3D,G**).

As VEGFR2 activation can also affect focal adhesion formation (Pietilä et al., 2019), we then checked the expression levels of FAK and Paxillin and the phosphorylation level of Paxillin on tyrosine 118, which controls focal adhesion turn over, affinity to FAK and cell migration (López-Colomé et al., 2017). FAK and Paxillin displayed stable expression over all of the tested conditions (**Figure 3F** and **Supplementary Figure 3F**). Paxillin$^{Y118}$ phosphorylation was activated by both low and high SS in the absence of VEGF-A compared to static condition (**Figures 3F,G**). At low SS, increasing VEGF-A concentration did not significantly change Paxillin$^{Y118}$ phosphorylation level. In contrast, at high SS, VEGF-A treatment increased it in a dose-response manner (**Figures 3F,G**).

Combined, these data show that low flow induced an "activated" junctional morphology and phosphorylation of VEGFR2 and VE-cadherin; these effects were further augmented by VEGF-A. In contrast, high flow combined with VEGF-A preferentially induced focal adhesion signaling.

## VEGFR2 Is Involved in Orientation and Polarity Responses Through Different Signaling Cascades

In order to understand better how activation of VEGFR2 contributed to focal adhesion or adherens junction turn-over in our setting and what was the role of each one in orientation and polarity, respectively, we exposed ECs to pharmacological inhibitors targeting the known pathways downstream of VEGFR2 activation. We decided to focus on the condition that displayed the clearest dichotomic effects of flow and VEGF-A on polarity and alignment respectively, namely high SS with or without 10 ng/mL of VEGF-A.

VEGFR2 inhibition by SU1498 and ZM323881 (two different kinases inhibitor with a high selectivity for VEGFR2 but targeting

different downstream effectors) had a strong effect on cell elongation and alignment with the flow in absence of VEGF-A; ECs were less elongated (**Supplementary Figure 4**) and lost their alignment with the flow (**Figures 4A,B**). Surprisingly, SU1498 had no significant effect on cell alignment and elongation in presence of VEGF-A (**Figures 4A,B** and **Supplementary Figure 4**) and ZM323881 tended to restore alignment with the flow in presence of VEGF-A. VEGFR2 inhibition also impaired ECs polarization against the flow both without (SU1498) and with VEGF-A (ZM323881) (**Figures 4C,D**).

We then inhibited SRC family kinases members (SU6656), FAK (PND-1186) and p38 (SB203580) in order to target pathways responsible for ECs cellular processes implicated in adhesion and migration. SRC family kinases inhibition significantly reduced ECs alignment with the flow and polarity against the flow in the absence of VEGF-A but had no effect in presence of VEGF-A. In contrast, FAK inhibition significantly impaired alignment with the flow and polarity against the flow only when ECs were exposed to VEGF-A (**Figures 3A–D**) but not when VEGF-A was absent. This demonstrated that cell orientation and polarity were under the control of different pathways in the presence or absence of VEGF-A. Interestingly, p38 inhibition which prevents stress activation and migration of ECs, blocked EC alignment and elongation both with and without VEGF-A, but had no effect on cell polarity; ECs remained partially polarized against the flow as in control condition (**Figures 4A–D** and **Supplementary Figure 4**).

These data support the notion that alignment in response to flow is dependent on VEGFR2 and that alignment and polarity are differently regulated by pathways downstream of VEGFR2.

## VEGFR2 and SRC Control Endothelial Cell Orientation and Polarity *in vivo* in Matures Arteries

As SRC family kinases inhibition impaired ECs response to flow in the absence of VEGF-A *in vitro*, we evaluated the relevance of the VEGFR2—SRC pathway *in vivo*. First, As VEGFR2-949 phosphorylation by VEGF stimulation recruits activated Src to EC junctions to phosphorylate VE-cadherin, we analyzed the aortas of VEGFR2$^{Y949F}$ mutant mice. We observed that ECs from the aorta of VEGFR2$^{Y949F}$ mutant mice lost their alignment in response to flow (**Figure 5A**) and had a reduced cell length (**Supplementary Figures 5A,B**), similar to what we observed *in vitro* following treatment with the VEGFR2 inhibitor ZM323881 (**Supplementary Figure 4**). Loss of VEGFR2 phosphorylation on this specific site also impaired polarity of ECs against the flow; the proportion of ECs well polarized against the flow was decreased compared to control mice (**Figure 5C**). To study whether this effect was associated specifically with SRC and not YES or FYN *in vivo*, we assessed alignment and polarity of ECs in aortas of mice lacking endothelial SRC (SRC$^{iEC-KO}$ mice).

Cell shape and junction morphology was similarly affected in SRC$^{iEC-KO}$ aortas as in VEGFR2$^{Y949F}$aortas. Surprisingly, however, EC alignment with the flow was not impaired in SRC$^{iEC-KO}$ aortas (**Figures 6A,B**) nor was there any effect on EC length (**Supplementary Figure 5B**). Nevertheless, polarity against the flow was reduced in SRC$^{iEC-KO}$ mice compared to control (**Figures 6C,D**) similarly to VEGFR2$^{Y949F}$ mutant mice. Finally, to confirm the flow specificity of these observations, we used an *ex vivo* sprouting assay from mouse metatarsals (Song et al., 2015; Schimmel et al., 2020), which reproduced angiogenesis in a "no flow" but high growth factor condition. Polarity of ECs at the tip position was not altered in metatarsal explants from SRC$^{iEC-KO}$ mice compared to control mice (**Supplementary Figure 6**). These results indicate that SRC activity is not generally required for ECs to polarize, but selectively involved in flow induced cell polarity.

In conclusion, the *in vitro* and *in vivo* data agree on the importance of VEGFR2, specifically through pY951 signaling, in endothelial cell alignment and polarity. Moreover, the Src pathway regulates polarity but not alignment of ECs.

# DISCUSSION

In the past decade, many efforts have been made to elucidate how mechanical forces and chemical signals contribute to vascular formation and patterning. Several mechano-sensory pathways controlling cell shape (Levesque and Nerem, 1985; Wojciak-Stothard and Ridley, 2003; Noria et al., 2004), polarity (Franco et al., 2015; Kwon et al., 2016) and migration (Baeyens et al., 2016b; Rochon et al., 2016) during vascular patterning have been described and the basic cellular and molecular mechanisms controlling angiogenesis have been well characterized (Potente et al., 2011; Potente and Mäkinen, 2017). Nevertheless, how ECs integrate signals coming from both mechanical and chemical stimuli at the same time is not well understood, despite its importance in physiology and pathology. Here, we observed that these signals can have synergistic or antagonistic effects depending on the feature observed.

We first confirm that VEGF-A treatment increases cell elongation, VEGFR2$^{Y1175}$, VEGFR2$^{Y951}$ and VEcadh$^{Y685}$ phosphorylation levels in a dose dependent manner under static condition, as expected from the literature (Simons et al., 2016; Cao et al., 2017). We also observe already described effects of low SS and high SS on cell alignment (Chien, 2007; Wang et al., 2013), junctions aspect (Chiu and Chien, 2011) and changes in VEGFR2$^{Y1175}$ phosphorylation (Jin et al., 2003) in the absence of VEGF-A. However, beyond these observations, we also identify new features associated with the combination of flow and VEGF-A. Polarity against the flow is established in a dose-response to VEGF-A both under low and high SS, but only high SS could trigger polarity against the flow without VEGF-A. Furthermore, alignment displays a biphasic response depending on the VEGF-A level (aligned without VEGF or at pathologically high dose of VEGF-A, but perpendicular to flow at physiological levels of VEGF-A). This indicates that orientation and polarity are controlled by different mechanisms. Interestingly, the effect of VEGF-A on polarity under high SS was seen even from the lowest concentrations used (0.5 ng/mL) while a higher concentration (10 ng/ml) was required to reach the same percentage of polarity against the flow at low SS. This suggests that both parameters mutually control the cells' sensitivity to

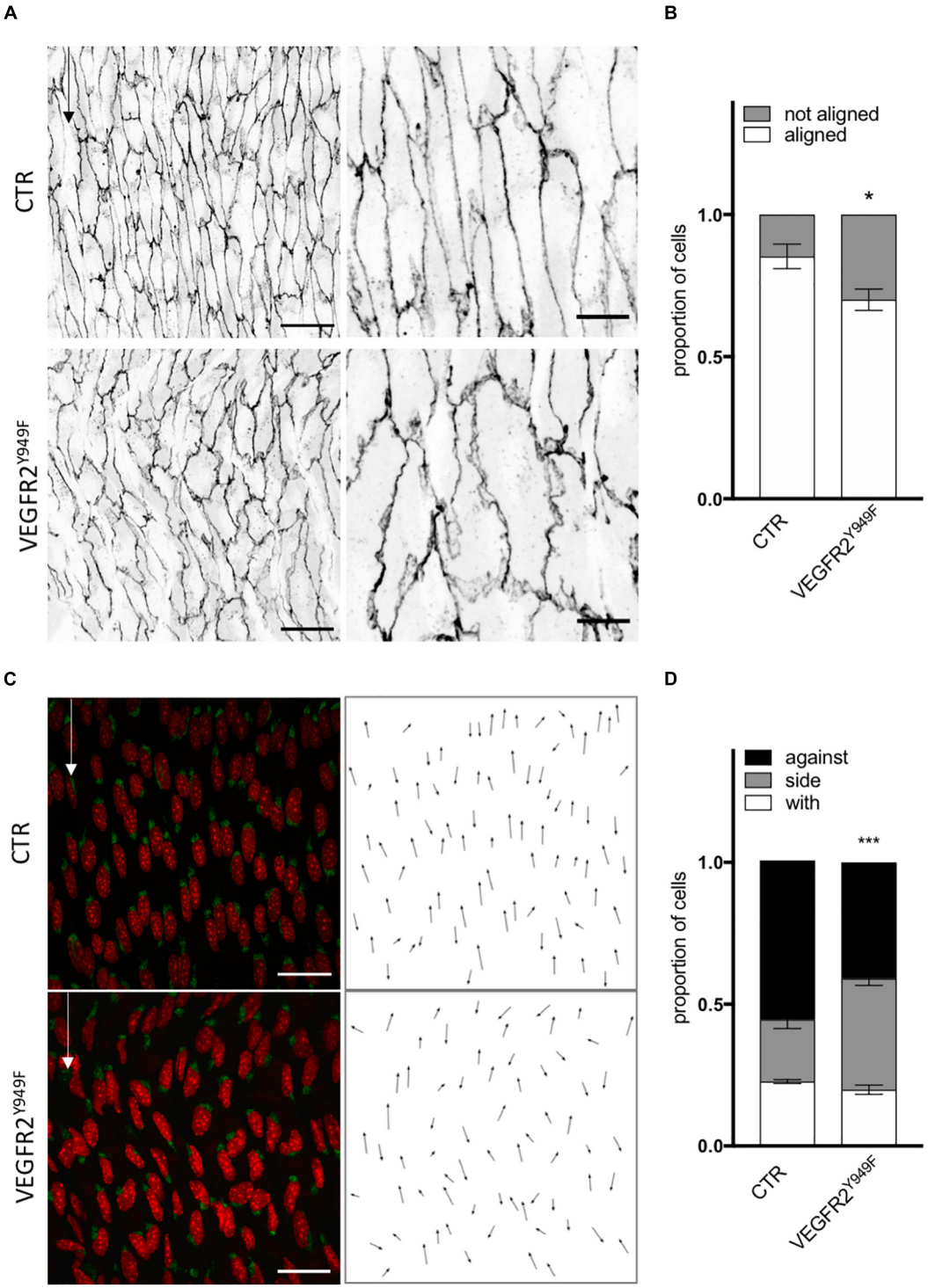


**FIGURE 5 |** VEGFR2 mutation impaired cell orientation and cell polarity *in vivo*. **(A)** Representative images of VE-cadherin staining of endothelial cell from the aortas of littermate P6 pups (CTR) or carrying VEGFR2 mutation (Y949F) (scale bars: 25 and 10 μm, respectively). **(B)** Quantification of cells aligned with the flow direction (in between 15° around the flow axe, *N* = 5, Data presented as Mean + SEM. **(C)** Representative images of golgi staining of endothelial cell from the aortas of P6 pups littermate (CTR) or carrying VEGFR2 mutation (Y949F) (scale bars: 25 μm). **(D)** Quantification of golgi position around the nucleus compared to the flow direction (*N* = 5; with: in between 0 and 30° around the flow axe, side: 30–150°, against: 150–180°). Two-way ANOVA; Tukey's *post hoc*, $^{*}p < 0.05$; $^{***}p < 0.001$.

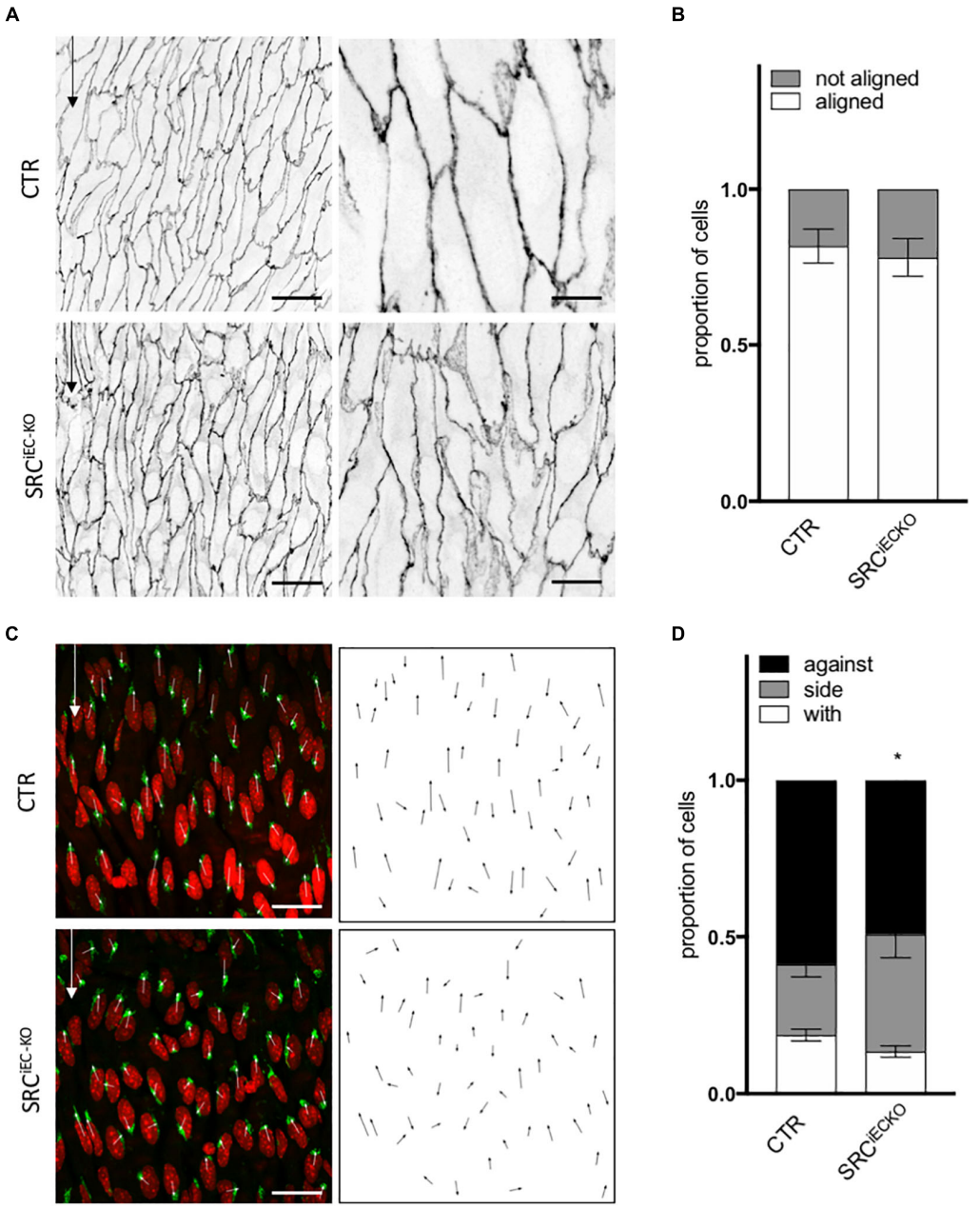


**FIGURE 6 |** SRC deletion in ECs mutation impaired cell orientation and cell polarity *in vivo*. **(A)** Representative images of VE-cadherin staining of endothelial cell from the aortas of P6 pups littermate (CTR) or deleted for SRC in ECs ($SRC^{iEC-KO}$) (scale bars: 25 and 10 μm, respectively). **(B)** Quantification of cells aligned with the flow direction (in between 15° around the flow axe, WT, $N = 6$; KO, $N = 7$, Data presented as Mean + SEM. **(C)** Representative images of golgi staining of endothelial cell from the aortas of P6 pups littermate (CTR) or deleted for SRC in ECs ($SRC^{iEC-KO}$) (scale bars: 25 μm). **(D)** Quantification of golgi position around the nucleus compared to the flow direction (WT, $N = 6$; KO, $N = 7$; with: in between 0 and 30° around the flow axe, side: 30–150°, against: 150–180°). Two-way ANOVA; Tukey's *post hoc*, $^{*}p < 0.05$; $^{***}p < 0.001$.

the other. Shear Stress modifies the sensitivity to VEGF-A, but VEGF-A in turn also affect the cell's ability to respond to flow.

When inhibiting VEGFR2, the effects of both SS and VEGF-A on alignment and polarity are lost suggesting that VEGFR2 could be the hub controlling these responses. The effect of SU1498 on polarity was significant only in the absence of VEGF-A, whereas ZM323881 significantly affected polarity only with VEGF-A. Studies using these inhibitors highlight their selectivity for VEGFR2 but also show that SU1498 prevents ERK1/2 signaling cascade (Boguslawski et al., 2004) while ZM323881 inhibits rather p38 and Rac1 pathways (Whittles et al., 2002; Garrett et al., 2007). Altogether this suggests that these inhibitors might differently restrict pathways downstream of VEGFR2 that contribute to polarity establishment with or without VEGF-A.

Inhibiting downstream effectors of VEGFR2, namely FAK and SRC family members, uncovered that the orientation and polarity of ECs are controlled differently in the presence or absence of VEGF-A. Without VEGF-A, alignment with the flow and polarity against the flow are dependent on SRC family activity while in the presence of VEGF-A, alignment and polarity against the flow are dependent on FAK activity. Interestingly, p38 inhibition only impaired alignment with the flow, not polarity which remains mostly against the flow. In this context, p38 inhibition suggests that ECs can establish and modify their planar polarity without changing their cell shape.

These conclusions are further supported by our *in vivo* analysis, as VEGFR2 phosphorylation at Y951 contributes to ECs alignment with the flow and polarity against the flow in the absence of VEGF-A. By genetically deleting SRC specifically in ECs, we highlight that SRC is essential for polarity control but not for alignment, although this was expected from our inhibitor experiments *in vitro*. Interestingly, the inhibitor used *in vitro* has a strong affinity toward Yes and Fyn, the two other SRC family members. While Yes and Fyn are structurally highly similar to SRC, evidence for their distinct roles in the endothelium are currently emerging (Eliceiri et al., 1999; Gordon et al., 2016; Schimmel et al., 2020). Combining our *in vivo* and *in vitro* results, we can propose that loss of SRC impairs endothelial polarity against the flow, which is not compensated by Fyn or Yes. Loss of SRC had no effect on ECs alignment *in vivo* suggesting that this feature could be under the control of Yes or Fyn. Further work will need to establish the exact contribution of Yes and Fyn to the alignment of ECs in response to flow. In the same line as for the p38 inhibition *in vitro*, we highlight that polarity and alignment can occur independently, but here showing that change in cell shape does not required planar polarity establishment.

By pointing their Golgi better against the flow at high SS, ECs display a cellular organization that is characteristic for their migration against the flow. In both SS conditions, VEGF-A will cause an activation that will enable ECs to adjust their junctions and basal adhesions more dynamically and polarize better against the flow even if exposed to a lower unidirectional force. Whether polarity always correlates with cell displacement (migration), however, remains unclear. Two hypotheses arise from the increased polarity against the flow; the first one is that ECs are indeed migrating better against the flow at high SS or with VEGF-A addition, the second would be that while ECs polarize against the flow at high SS or with VEGF-A, they migrate very little due to high counteracting apical forces.

Both hypotheses raise the question of tension sensing and balance between basal and lateral forces. Force transmission occurs through different structures in ECs (Campinho et al., 2020; Gordon et al., 2020); cell-cell junctions and cell adhesions to the matrix have been both well described as mechano-sensitive elements. In our study, the structural changes of VE-cadherin junctions do not correlate with alteration of VEcadh$^{Y685}$ phosphorylation, suggesting that other junctional players are involved. Interestingly ZO-1 has been shown to control endothelial cell-cell tension and its loss, while loosening tension in-between cells favors focal adhesion formation (Tornavaca et al., 2015) and therefore reinforces basal adhesion. In our setting, ZO-1 localization at junctions is specifically decreased by VEGF-A when ECs are exposed to SS compared to static condition and could be the missing player explaining the visual modifications of adherens junctions. Additionally, increased Paxillin phosphorylation also correlates with the loss of junctional ZO-1. Together with our observation, this supports our hypothesis that tension forces in between ECs could be highly different in between our different *in vitro* conditions. VEGF-A addition under SS, would trigger loss of cell-cell tension (lateral) while increasing cell-matrix tension (basal). This effect of VEGF-A appears to be more pronounced at high SS compared to low SS.

Another situation where ECs adapt their shape and polarity is when they migrate to close a wound. In such a case, driven by the first row of cells directly in contact with the free edge, ECs polarize collectively and migrate toward the wound. In that situation, the origin of the signal is different from a flow situation. In a wound assay, most cells are not exposed to the free edge and receive an indirect cue for migration through force transmission via the lateral junctions. Recent work from Carvalho et al. (2019) shows that by decreasing VE-cadherin tension (therefore lateral forces) in between cells, ECs failed to collectively polarize toward the wound. Under flow, every cell is independently exposed to the same directional signal: SS at their apical side. Combining these facts and observations allows to hypothesize that the origin of the mechanical signal and its way of transmission in-between cells is crucial to determine if loosening of the lateral tension will lead to loss or reinforcement of polarity. In the case of a wound closure, loosening junctions decreases collective polarity toward the wound because ECs distant from the wound become blind to its location. In our settings, loosening junctions increases polarity against the flow because ECs become more capable of detecting flow direction as signal from the lateral junctions does not interfere with the apical cue each cell perceive.

Interestingly, while testing inhibitor effects on polarity and alignment under high SS, we find that SRC family inhibition is efficient only without VEGF-A, i.e., a situation in which ZO-1 is present at the junctions and phospho-Paxillin is low, lateral tension should be high and basal tension low. In contrast, FAK inhibition is efficient only with VEGF-A, a situation in which ZO-1 is delocalized from the junctions and phospho-Paxillin is high, suggesting low lateral tension and high basal tension. Therefore, it is tempting to speculate that rather than having different pathways controlling polarity and alignment independently, the same pathways could be in charge of polarity and alignment, but their relative contribution would vary depending on the presence or absence of VEGF-A. SRC family members would participate when VEGF-A is absent and FAK pathways would take over once VEGF-A is present to loosen the junction.

Finally, modification in flow sensitivity in ECs has been ascribed to the mechanosensitive complex formed by VEGFRs-PECAM-VE-cadherin (Baeyens et al., 2015), and in particular to the ratio of VEGFR3 or VEGFR2 engaged in this complex, thus modifying at which range of SS ECs align with the flow. Here we show that the joint presence of flow and VEGF-A can also act as a lever to influence ECs alignment and polarity mostly through changes in the balance of the different VEGFR2 phospho-sites that become activated. Whether or not alignment and polarity go

precisely through the same type of complex and if VEGFR3 could also play a role will need to be demonstrated.

## DATA AVAILABILITY STATEMENT

The raw data supporting the conclusions of this article will be made available by the authors, without undue reservation, to any qualified research.

## ETHICS STATEMENT

The animal study was reviewed and approved by the Uppsala University board of animal experimentation (permit 5.2.18-8927-16).

## AUTHOR CONTRIBUTIONS

A-CV designed the study, performed experiments, analyzed the results, and wrote the manuscript. TP and CP performed the experiments and analyzed the results. EB-K, IH, and EF performed the experiments. EG performed the experiments and reviewed the manuscript. LC-W provided the mice, designed the *in vivo* study, and reviewed the manuscript. HG designed the study and wrote the manuscript. All authors contributed to the article and approved the submitted version.

## FUNDING

This work was supported by the German Centre for Cardiovascular Research, the German Ministry of Education and Research, the Fondation pour la Recherche Medical (ARF20170938625) (A-CV), the European Research Council consolidator grant 311719 Reshape (HG), the Knut and Alice Wallenberg foundation project grant and Wallenberg Scholar grant (KAW 20150030 and KAW 2015.0275 to LC-W), and the Fondation Leducq transatlantic network of excellence grant in neurovascular disease (17 CVD 03, HG and LC-W). EG was supported by the Wenner-Gren Foundation Postdoctoral Fellowship.

## ACKNOWLEDGMENTS

We thank Dr. Anna Szymborska for helpful comments on the manuscript.

## SUPPLEMENTARY MATERIAL

The Supplementary Material for this article can be found online at: https://www.frontiersin.org/articles/10.3389/fphys.2020.623769/full#supplementary-material

**Supplementary Figure 1 |** VEGF-A treatment does not affect cell number but increases cell elongation. **(A)** Quantification of endothelial cells number under flow and VEGF-A. **(B)** Quantification of aspect ratio (length of main axis/length of short axis) of endothelial cells under flow and VEGF-A. $N = 3$, between 1,500 and 3,000 cells analyzed. $N = 3$, around 1,500 cells analyzed. Data presented as Mean + SEM. Two-way ANOVA; Tukey's *post hoc*, $^{***}p < 0.001$ compared to static 0 VEGF; $^{\#\#\#}p < 0.001$ (compared to LSS 0 VEGF); $^{!!!}p < 0.001$ (compared to HSS 0 VEGF).

**Supplementary Figure 2 |** VEGF treatment does not change junctions activation under static condition. **(A)** Representative picture (Immunofluorescence) of endothelial cells exposed to VEGF-A for 24 h. Red arrows indicate gaps in the ECs monolayer **(B)** Quantification of junction status based on their morphology ($N = 3$; 100 patches analyzed blinded by images, 5–8 images per N).

**Supplementary Figure 3 |** Proteins expression upon flow and VEGF treatment. **(A)** VEGFR2 expression assessed by WB, $N = 6$. **(B)** ZO1 expression assessed by WB, $N = 3$. **(C)** VE-cadherin expression assessed by WB, $N = 5$. **(D)** FAK expression assessed by WB, $N = 5$. ANOVA followed by Tukey *post Hoc*; $^{*}p < 0.05$; $^{**}p < 0.01$. **(E)** Representative pictures of the quantified WB.

**Supplementary Figure 4 |** Inhibitors effect on cell elongation. Quantification of aspect ratio (length of main axis/length of short axis) of endothelial cells under high SS with or without VEGF-A (10 ng/mL) and with or without inhibitors (DMSO, $N = 5$, inhibitors $N = 3$) One-way ANOVA; Tukey's *post hoc*, $^{***}p < 0.001$ compared to DMSO 0 VEGF; $^{\#\#\#}p < 0.001$ compared to DMSO 10 VEGF.

**Supplementary Figure 5 |** VEGFR2 mutation impairs cell length but not SRC deletion *in vivo*. **(A)** Quantification of ECs length in the aortas of P6 pups littermate (CTR) or carrying VEGFR2 mutation (Y949F). $N = 5$ **(B)** Distribution of cell length. $N = 5$ **(C)** Quantification of ECs length in the aortas of P6 pups littermate (CTR) or deleted for SRC in ECs ($SRC^{iEC-KO}$). $N = 3$–5 **(D)** Distribution of cell length. Unpaired *T*-Test; $^{***}p < 0.001$.

**Supplementary Figure 6 |** ECs polarity is not impaired during directional sprouting upon loss of c-Src. Representative images and quantification of polarity of ECs sprouting out of metatarsal *ex vivo*. With means that ECs polarize in the direction of the sprout (0–30°); side, ECs present their golgi on the side of the cell (30–150°); against, ECs polarize in the opposite direction of the sprout (150–180°). $N = 294$ cells analyzed from 12 metatarsals from 2 independent experiments.

**Supplementary Table 1 |** *p*-Values for each comparison for **Figures 2B,D**. Two-way ANOVA; Tukey's *post hoc*, $^{*}p < 0.05$; $^{**}p < 0.01$; $^{***}p < 0.001$. Gray lines: statistics presented on the graphs. Bold: significant difference.

**Supplementary Table 2 |** *p*-Values for each comparison for **Figures 3C–F**. Two-way ANOVA; Fisher LSD. $^{*}p < 0.05$; $^{**}p < 0.01$; $^{***}p < 0.001$. Gray lines: statistics presented on the graphs. Bold: significant difference.

## REFERENCES

Baeyens, N., Bandyopadhyay, C., Coon, B. G., Yun, S., and Schwartz, M. A. (2016a). Endothelial fluid shear stress sensing in vascular health and disease. *J. Clin. Invest.* 126, 821–828. doi: 10.1172/jci83083

Baeyens, N., Larrivée, B., Ola, R., Hayward-Piatkowskyi, B., Dubrac, A., Huang, B., et al. (2016b). Defective fluid shear stress mechanotransduction mediates hereditary hemorrhagic telangiectasia. *J. Cell Biol.* 214, 807–816. doi: 10.1083/jcb.201603106

Baeyens, N., Nicoli, S., Coon, B. G., Ross, T. D., Van den Dries, K., Han, J., et al. (2015). Vascular remodeling is governed by a VEGFR3-dependent fluid shear stress set point. *eLife* 4:e04645.

Bentley, K., Franco, C. A., Philippides, A., Blanco, R., Dierkes, M., Gebala, V., et al. (2014). The role of differential VE-cadherin dynamics in cell rearrangement during angiogenesis. *Nat. Cell Biol.* 16, 309–321. doi: 10.1038/ncb2926

Boguslawski, G., McGlynn, P. W., Harvey, K. A., and Kovala, A. T. (2004). SU1498, an inhibitor of vascular endothelial growth factor receptor 2, causes accumulation of phosphorylated ERK kinases and inhibits their activity in vivo and in vitro. *J. Biol. Chem.* 279, 5716–5724. doi: 10.1074/jbc.m308625200

Campinho, P., Vilfan, A., and Vermot, J. (2020). Blood flow forces in shaping the vascular system: a focus on endothelial cell behavior. *Front. Physiol.* 11:552. doi: 10.3389/fphys.2020.00552

Cao, J., Ehling, M., März, S., Seebach, J., Tarbashevich, K., Sixta, T., et al. (2017). Polarized actin and VE-cadherin dynamics regulate junctional remodelling and cell migration during sprouting angiogenesis. *Nat. Commun.* 8:2210.

Carmeliet, P., and Tessier-Lavigne, M. (2005). Common mechanisms of nerve and blood vessel wiring. *Nature* 436, 193–200. doi: 10.1038/nature03875

Carvalho, J. R., Chia, M., Dufton, N., Almagro, L. O., Conway, D. E., Randi, A. M., et al. (2019). Non-canonical Wnt signaling regulates junctional mechanocoupling during angiogenic collective cell migration. *eLife* 8:e45853.

Chen, K. D., Li, Y. S., Kim, M., Li, S., Yuan, S., Chien, S., et al. (1999). Mechanotransduction in response to shear stress. Roles of receptor tyrosine kinases, integrins, and Shc. *J. Biol. Chem.* 274, 18393–18400. doi: 10.1074/jbc.274.26.18393

Chien, S. (2007). Mechanotransduction and endothelial cell homeostasis: the wisdom of the cell. *Am. J. Physiol. Heart Circ. Physiol.* 292, H1209–H1224.

Chiu, J.-J., and Chien, S. (2011). Effects of disturbed flow on vascular endothelium: pathophysiological basis and clinical perspectives. *Physiol. Rev.* 91, 327–387. doi: 10.1152/physrev.00047.2009

Conway, D. E., Breckenridge, M. T., Hinde, E., Gratton, E., Chen, C. S., Schwartz, M. A., et al. (2013). Fluid shear stress on endothelial cells modulates mechanical tension across VE-cadherin and PECAM-1. *Curr. Biol.* 23, 1024–1030. doi: 10.1016/j.cub.2013.04.049

Coon, B. G., Baeyens, N., Han, J., Budatha, M., Ross, T. D., Fang, J. S., et al. (2015). Intramembrane binding of VE-cadherin to VEGFR2 and VEGFR3 assembles the endothelial mechanosensory complex. *J. Cell Biol.* 208, 975–986. doi: 10.1083/jcb.201408103

Culver, J. C., and Dickinson, M. E. (2010). The effects of hemodynamic force on embryonic development. *Microcirculation* 17, 164–178. doi: 10.1111/j.1549-8719.2010.00025.x

Eliceiri, B. P., Paul, R., Schwartzberg, P. L., Hood, J. D., Leng, J., Cheresh, D. A., et al. (1999). Selective requirement for Src kinases during VEGF-induced angiogenesis and vascular permeability. *Mol. Cell* 4, 915–924. doi: 10.1016/s1097-2765(00)80221-x

Franco, C. A., Jones, M. L., Bernabeu, M. O., Geudens, I., Mathivet, T., Rosa, A., et al. (2015). Dynamic endothelial cell rearrangements drive developmental vessel regression. *PLoS Biol.* 13:e1002125. doi: 10.1371/journal.pbio.1002125

Garrett, T. A., Van Buul, J. D., and Burridge, K. (2007). VEGF-induced Rac1 activation in endothelial cells is regulated by the guanine nucleotide exchange factor Vav2. *Exp. Cell Res.* 313, 3285–3297. doi: 10.1016/j.yexcr.2007.05.027

Gimbrone, M. A., and García-Cardeña, G. (2013). Vascular endothelium, hemodynamics, and the pathobiology of atherosclerosis. *Cardiovasc. Pathol.* 22, 9–15. doi: 10.1016/j.carpath.2012.06.006

Givens, C., and Tzima, E. (2016). Endothelial mechanosignaling: does one sensor fit all? *Antioxid. Redox Signal.* 25, 373–388. doi: 10.1089/ars.2015.6493

Gordon, E., Schimmel, L., and Frye, M. (2020). The importance of mechanical forces for *in vitro* endothelial cell biology. *Front. Physiol.* 11:684. doi: 10.3389/fphys.2020.00684

Gordon, E. J., Fukuhara, D., Weström, S., Padhan, N., Sjöström, E. O., van Meeteren, L., et al. (2016). The endothelial adaptor molecule TSAd is required for VEGF-induced angiogenic sprouting through junctional c-Src activation. *Sci. Signal.* 9:ra72. doi: 10.1126/scisignal.aad9256

Isogai, S., Lawson, N. D., Torrealday, S., Horiguchi, M., and Weinstein, B. M. (2003). Angiogenic network formation in the developing vertebrate trunk. *Development* 130, 5281–5290. doi: 10.1242/dev.00733

Jin, Z.-G., Ueba, H., Tanimoto, T., Lungu, A. O., Frame, M. D., Berk, B. C., et al. (2003). Ligand-independent activation of vascular endothelial growth factor receptor 2 by fluid shear stress regulates activation of endothelial nitric oxide synthase. *Circ. Res.* 93, 354–363. doi: 10.1161/01.res.0000089257.94002.96

Koch, S., and Claesson-Welsh, L. (2012). Signal transduction by vascular endothelial growth factor receptors. *Cold Spring Harb. Perspect. Med.* 2:a006502. doi: 10.1101/cshperspect.a006502

Koch, S., Tugues, S., Li, X., Gualandi, L., and Claesson-Welsh, L. (2011). Signal transduction by vascular endothelial growth factor receptors. *Biochem. J.* 437, 169–183. doi: 10.1042/bj20110301

Kogata, N., Arai, Y., Pearson, J. T., Hashimoto, K., Hidaka, K., Koyama, T., et al. (2006). Cardiac ischemia activates vascular endothelial cadherin promoter in both preexisting vascular cells and bone marrow cells involved in neovascularization. *Circ. Res.* 98, 897–904. doi: 10.1161/01.res.0000218193.51136.ad

Kupfer, A., Louvard, D., and Singer, S. J. (1982). Polarization of the Golgi apparatus and the microtubule-organizing center in cultured fibroblasts at the edge of an experimental wound. *Proc. Natl. Acad. Sci. U.S.A.* 79, 2603–2607. doi: 10.1073/pnas.79.8.2603

Kwon, H.-B., Wang, S., Helker, C. S., Rasouli, S. J., Maischein, H. M., Offermanns, S., et al. (2016). In vivo modulation of endothelial polarization by Apelin receptor signalling. *Nat. Commun.* 7:11805.

Levesque, M. J., and Nerem, R. M. (1985). The elongation and orientation of cultured endothelial cells in response to shear stress. *J. Biomech. Eng.* 107, 341–347. doi: 10.1115/1.3138567

Li, X., Padhan, N., Sjöström, E. O., Roche, F. P., Testini, C., Honkura, N., et al. (2016). VEGFR2 pY949 signalling regulates adherens junction integrity and metastatic spread. *Nat. Commun.* 7:11017.

López-Colomé, A. M., Lee-Rivera, I., Benavides-Hidalgo, R., and López, E. (2017). Paxillin: a crossroad in pathological cell migration. *J. Hematol. Oncol.* 10:50.

Matsumoto, T., Bohman, S., Dixelius, J., Berge, T., Dimberg, A., Magnusson, P., et al. (2005). VEGF receptor-2 Y951 signaling and a role for the adapter molecule TSAd in tumor angiogenesis. *EMBO J.* 24, 2342–2353. doi: 10.1038/sj.emboj.7600709

Neto, F., Klaus-Bergmann, A., Ong, Y. T., Alt, S., Vion, A. C., Szymborska, A., et al. (2018). YAP and TAZ regulate adherens junction dynamics and endothelial cell distribution during vascular development. *eLife* 7:e31037.

Noria, S., Xu, F., McCue, S., Jones, M., Gotlieb, A. I., Langille, B. L., et al. (2004). Assembly and reorientation of stress fibers drives morphological changes to endothelial cells exposed to shear stress. *Am. J. Pathol.* 164, 1211–1223. doi: 10.1016/s0002-9440(10)63209-9

Orsenigo, F., Giampietro, C., Ferrari, A., Corada, M., Galaup, A., Sigismund, S., et al. (2012). Phosphorylation of VE-cadherin is modulated by haemodynamic forces and contributes to the regulation of vascular permeability in vivo. *Nat. Commun.* 3:1208.

Pietilä, I., Van Mourik, D., Tamelander, A., Kriz, V., Claesson-Welsh, L., Tengholm, A., et al. (2019). Temporal dynamics of VEGFA-induced VEGFR2/FAK co-localization depend on SHB. *Cells* 8:1645. doi: 10.3390/cells8121645

Potente, M., Gerhardt, H., and Carmeliet, P. (2011). Basic and therapeutic aspects of angiogenesis. *Cell* 146, 873–887. doi: 10.1016/j.cell.2011.08.039

Potente, M., and Mäkinen, T. (2017). Vascular heterogeneity and specialization in development and disease. *Nat. Rev. Mol. Cell Biol.* 18, 477–494. doi: 10.1038/nrm.2017.36

Rochon, E. R., Menon, P. G., and Roman, B. L. (2016). Alk1 controls arterial endothelial cell migration in lumenized vessels. *Development* 143, 2593–2602. doi: 10.1242/dev.135392

Sakurai, Y., Ohgimoto, K., Kataoka, Y., Yoshida, N., and Shibuya, M. (2005). Essential role of Flk-1 (VEGF receptor 2) tyrosine residue 1173 in vasculogenesis in mice. *Proc. Natl. Acad. Sci. U.S.A.* 102, 1076–1081. doi: 10.1073/pnas.0404984102

Schimmel, L., Fukuhara, D., Richards, M., Jin, Y., Essebier, P., Frampton, E., et al. (2020). c-Src controls stability of sprouting blood vessels in the developing retina independently of cell-cell adhesion through focal adhesion assembly. *Development* 147:dev185405. doi: 10.1242/dev.185405

Simons, M., Gordon, E., and Claesson-Welsh, L. (2016). Mechanisms and regulation of endothelial VEGF receptor signalling. *Nat. Rev. Mol. Cell Biol.* 17, 611–625. doi: 10.1038/nrm.2016.87

Song, W., Fhu, C. W., Ang, K. H., Liu, C. H., Johari, N. A., Lio, D., et al. (2015). The fetal mouse metatarsal bone explant as a model of angiogenesis. *Nat. Protoc.* 10, 1459–1473. doi: 10.1038/nprot.2015.097

Sun, Z., Li, X., Massena, S., Kutschera, S., Padhan, N., Gualandi, L., et al. (2012). VEGFR2 induces c-Src signaling and vascular permeability in vivo via the adaptor protein TSAd. *J. Exp. Med.* 209, 1363–1377. doi: 10.1084/jem.20111343

Takahashi, T., Yamaguchi, S., Chida, K., and Shibuya, M. A. (2001). single autophosphorylation site on KDR/Flk-1 is essential for VEGF-A-dependent

activation of PLC-gamma and DNA synthesis in vascular endothelial cells. *EMBO J.* 20, 2768–2778. doi: 10.1093/emboj/20.11.2768

Testini, C., Smith, R. O., Jin, Y., Martinsson, P., Sun, Y., Hedlund, M., et al. (2019). Myc-dependent endothelial proliferation is controlled by phosphotyrosine 1212 in VEGF receptor-2. *EMBO Rep.* 20:e47845.

Tornavaca, O., Chia, M., Dufton, N., Almagro, L. O., Conway, D. E., Randi, A. M., et al. (2015). ZO-1 controls endothelial adherens junctions, cell-cell tension, angiogenesis, and barrier formation. *J. Cell Biol.* 208, 821–838. doi: 10.1083/jcb.201404140

Tzima, E., Irani-Tehrani, M., Kiosses, W. B., Dejana, E., Schultz, D. A., Engelhardt, B., et al. (2005). A mechanosensory complex that mediates the endothelial cell response to fluid shear stress. *Nature* 437, 426–431. doi: 10.1038/nature03952

Wang, C., Baker, B. M., Chen, C. S., and Schwartz, M. A. (2013). Endothelial cell sensing of flow direction. *Arterioscler. Thromb. Vasc. Biol.* 33, 2130–2136. doi: 10.1161/atvbaha.113.301826

Wang, Y., Nakayama, M., Pitulescu, M. E., Schmidt, T. S., Bochenek, M. L., Sakakibara, A., et al. (2010). Ephrin-B2 controls VEGF-induced angiogenesis and lymphangiogenesis. *Nature* 465, 483–486. doi: 10.1038/nature09002

Whittles, C. E., Pocock, T. M., Wedge, S. R., Kendrew, J., Hennequin, L. F., Harper, S. J., et al. (2002). ZM323881, a novel inhibitor of vascular endothelial growth factor-receptor-2 tyrosine kinase activity. *Microcirculation* 9, 513–522. doi: 10.1038/sj.mn.7800164

Wojciak-Stothard, B., and Ridley, A. J. (2003). Shear stress-induced endothelial cell polarization is mediated by Rho and Rac but not Cdc42 or PI 3-kinases. *J. Cell Biol.* 161, 429–439. doi: 10.1083/jcb.200210135

**Conflict of Interest:** The authors declare that the research was conducted in the absence of any commercial or financial relationships that could be construed as a potential conflict of interest.

frontiers in Physiology

REVIEW
published: 05 March 2021
doi: 10.3389/fphys.2021.622615

# The Normal and Brain Tumor Vasculature: Morphological and Functional Characteristics and Therapeutic Targeting

*Joris Guyon[1†], Candice Chapouly[2†], Laetitia Andrique[1,3], Andreas Bikfalvi[1*] and Thomas Daubon[4*‡]*

[1] INSERM, LAMC, U1029, University Bordeaux, Pessac, France, [2] INSERM, Biology of Cardiovascular Diseases, U1034, University Bordeaux, Pessac, France, [3] VoxCell 3D Plateform, UMS TBMcore 3427, Bordeaux, France, [4] University Bordeaux, CNRS, IBGC, UMR 5095, Bordeaux, France

Glioblastoma is among the most common tumor of the central nervous system in adults. Overall survival has not significantly improved over the last decade, even with optimizing standard therapeutic care including extent of resection and radio- and chemotherapy. In this article, we review features of the brain vasculature found in healthy cerebral tissue and in glioblastoma. Brain vessels are of various sizes and composed of several vascular cell types. Non-vascular cells such as astrocytes or microglia also interact with the vasculature and play important roles. We also discuss *in vitro* engineered artificial blood vessels which may represent useful models for better understanding the tumor–vessel interaction. Finally, we summarize results from clinical trials with anti-angiogenic therapy alone or in combination, and discuss the value of these approaches for targeting glioblastoma.

**Keywords: brain, glioblastoma, blood vessels, astrocyte, antiangiogenic therapy, vascular tissue engineering**

OPEN ACCESS

***Edited by:***
*Sara Petrillo,*
*University of Turin, Italy*

***Reviewed by:***
*Maria Rodriguez Aburto,*
*University College Cork, Ireland*
*Nicolas Santander,*
*University of California,*
*San Francisco, United States*

***Correspondence:**
*Thomas Daubon*
*thomas.daubon@u-bordeaux.fr*
*Andreas Bikfalvi*
*andreas.bikfalvi@u-bordeaux.fr*

*†These authors share first authorship*

*‡Lead Author*

***Specialty section:***
*This article was submitted to Vascular Physiology, a section of the journal Frontiers in Physiology*

***Received:*** *28 October 2020*
***Accepted:*** *25 January 2021*
***Published:*** *05 March 2021*

***Citation:***
*Guyon J, Chapouly C, Andrique L, Bikfalvi A and Daubon T (2021) The Normal and Brain Tumor Vasculature: Morphological and Functional Characteristics and Therapeutic Targeting. Front. Physiol. 12:622615. doi: 10.3389/fphys.2021.622615*

## INTRODUCTION

In vertebrates, vessels are built of an internal layer made of endothelial cells which are in contact with the blood and of mural cells that are composed of either smooth muscle cells (larger vessels) or pericytes (in capillaries). In the brain, blood vessels are tightly organized and participate in blood and brain tissue exchange via the blood–brain barrier (BBB).

Within the brain tumor vasculature, two different types of vessels are found, vessels formed by angiogenesis (neoangiogenic vessels) and preexisting vessels which may be co-opted by tumor cells (co-opted vessels). Anti-angiogenic strategies have been developed for targeting the brain tumor vasculature (Lakka and Rao, 2008). Unfortunately, clinical trials were not crowned with success (Chinot et al., 2014). A contributing factor is represented by a shift of tumor cells to a co-optive mode induced by anti-angiogenic therapy which contributes to tumor spread and development (Griveau et al., 2018).

In this article, we discuss the characteristics and specific features of the normal and brain tumor vasculature. We will also include in our discussion *in vitro* constructed artificial blood vessels by tissue engineering which represent an interesting tool to study tissue–vessel interactions and may also be useful in the tumor context. Finally, we will review some recent clinical studies using anti-angiogenic drugs in glioblastoma.

## THE BLOOD–BRAIN BARRIER

In a healthy individual, the central nervous system (CNS) parenchyma is protected from the peripheral circulation by the BBB. This barrier comprises a network of blood vessels made of endothelial cells with unique features (**Figure 1** – healthy brain). Endothelial cells at the BBB act as gatekeepers to control soluble factors and immune cell trafficking into the vessel wall and underlying tissues, and both the transcellular and paracellular pathways are involved in this process.

### The Paracellular Pathway

The paracellular pathway is modulated by the coordinated opening and closure of endothelial cell–cell junctions which involves a complex rearrangement of endothelium-specific transmembrane tight/adherens junction proteins and the related cytoskeleton. CNS tight junctions are primarily formed by Claudin5 and Occludin, and are coupled with the Zonula Occludens intracellular proteins (ZO1, ZO2, and ZO3) which form a scaffold between these transmembrane proteins and the actin cytoskeleton. Other Claudins may be involved in controlling endothelial cell paracellular barrier properties, as Claudin5 downregulation only leads to small size molecule leakage at the BBB (Nitta et al., 2003). Claudin1, Claudin3, and Claudin12 have been identified as potential candidates, but their role still needs to be clarified (Ohtsuki et al., 2008; Daneman et al., 2010a; Kooij et al., 2014). Members of the immunoglobulin superfamily, notably CAMs (PECAM1, ICAM1, and VCAM1), JAMs (JAM1–3), and Nectin proteins, clustered at CNS endothelial intercellular contacts, promote homotypic cell–cell adhesion and regulate inflammatory cell transmigration at the BBB (Del Maschio et al., 1999). Recent literature suggested that tricellular contacts, where the corners of three cells meet, can also be found in CNS endothelial cells. Specifically, tricellulin and angulin-1/lipolysis-stimulated lipoprotein receptor (LSR) were shown to participate to BBB paracellular control of plasmatic protein and immune cell trafficking (Iwamoto et al., 2014; Sohet et al., 2015). Importantly, tight junctions cannot be dissociated from adherent junctions in regulating BBB tightness; CNS endothelial adherent junctions are characterized by homophilic cadherin (VE-cadherin and *N*-cadherin) interactions controlling cell adhesion. Adherent junctions are linked to the cytoskeleton *via* their binding partner β-catenin and participate to BBB tightness through phosphorylation, cleavage, and internalization, or by modulating Claudin5 expression level (Meng and Takeichi, 2009).

### The Transcellular Pathway

Aside from the paracellular pathway, brain nutrient intake and CNS toxin removal are highly regulated by solute transporters and receptor-mediated transcytosis at the BBB, and inflammatory cells are actively prevented from crossing the BBB by low levels of immune receptors that normally permit immune trafficking.

Specifically, the cerebral endothelium expresses a number of specific solute transporters to facilitate the carrier-mediated transport of glucose (glucose transporters: GLUT1), amino acids (cationic amino acid transporters: CAT1, CAT3), monocarboxylic acids (monocarboxylate transporters: MCT1), hormones (thyroid hormone transporters: MCT8), fatty acids (fatty acid transporters: FATP-1), nucleotides (nucleoside transporters: ENT1, ENT2), ions (organic anion and organic cation transporters), amines, choline, and vitamins, which are otherwise excluded from the brain due to the paracellular pathway (Sweeney et al., 2019). Efflux mechanisms also contribute to barrier functions, with ATP-binding cassette transporters (P-gp: MDR1), breast cancer resistance protein (BCRP), and multidrug resistance-associated proteins (MRP 1–5) hydrolyzing ATP to actively pump drugs and their conjugates, xenobiotics, endogenous metabolites, and nucleosides across the luminal side of blood vessels into the circulation (Mahringer and Fricker, 2016; Sweeney et al., 2019).

Selective peptides and even large proteins can enter the brain by binding to receptors on endothelial cells via endocytosis (receptor-mediated transcytosis) (leptin receptors, transferrin receptors, and insulin receptors) (Preston et al., 2014). The BBB is characterized by extremely low rates of vesicular transport (transcytosis) which limits the transcellular passage across CNS barriers. It has been recently reported that the major facilitator superfamily domain containing 2a (Mfsd2a) is selectively expressed in CNS blood vessels and actively participates to BBB homeostasis by suppressing transcytosis in CNS endothelial cells (Ben-Zvi et al., 2014). Mfsd2a is located upstream of Caveolin-1 (Cav-1) (Chow and Gu, 2017), which is involved in regulating endothelial permeability, angiogenesis, and leukocyte diapedesis (Zhao et al., 2014), and VE-cadherin/catenin complex targets Cav-1 to endothelial cell junctions leading to BBB breakdown under permeability conditions (Kronstein et al., 2012).

These features exist within the majority of the CNS capillary population. However, it is worth noting that some regions of the CNS display a leaky BBB. These regions are grouped together under the term "circumventricular organs" which are regions of the brain sensing blood-borne signals. Morphologically, in the circumventricular organs, the capillaries are fenestrated with discontinuous tight junctions and thinner endothelial cells which contain more vesicles than capillaries of other parts of the CNS (Coomber and Stewart, 1985). This permits the two-way exchange of metabolic information: the delivery of neuro-hormones into the bloodstream by secretory organs and the sensing of blood-borne molecules by neurons in sensory organs. However, within the circumventricular organs, there is no direct passage of blood-borne substances in the parenchyma due to the presence of outer basement membrane but also astrocytes and tanycytes (ependymal cells sharing common features with radial glial cells and astrocytes) which are considered alternative CNS barriers (Langlet et al., 2013). The peculiar organization of the BBB within the circumventricular organs leads us to approach the CNS vascular barrier system from another angle by acknowledging its complex architecture which is not just a vascular endothelium. Indeed, it is more proper to consider it as a multi-cellular neurovascular unit comprising notably astrocytes, pericytes, basement membranes as well as blood vessels.

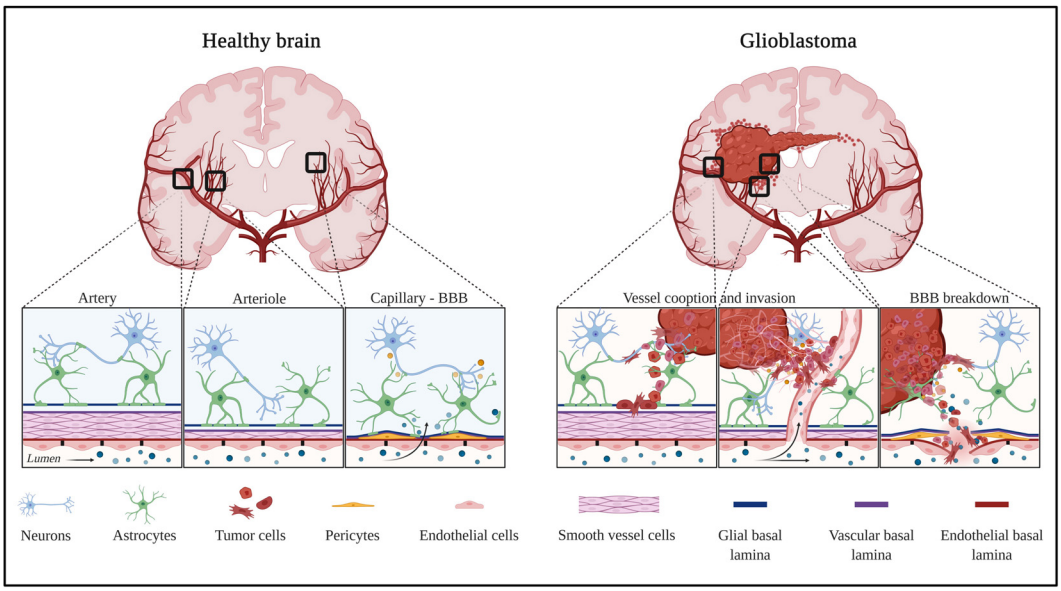


**FIGURE 1 |** Healthy and tumor brain vascular architecture: focus on artery, arteriole, and capillary. **Left panel:** in a healthy brain vasculature, endothelial cell monolayer is surrounded by a smooth muscle coat in arteries and arterioles, and is replaced by pericytes in the capillaries. The perivascular space is delimited by the vascular basement membrane and glial basement membrane. This space gradually diminished and the two basement membranes enter in direct contact to astrocytes endfeet. Molecules diffuse or are transported at the capillary level. **Right panel:** GBM is a highly angiogenic and infiltrative tumor. Cells invade along blood vessels to support tumor growth (co-option). GBM displaces astrocytes endfeet and alters pericyte stability, leading to perivascular niches and cell evasion. Created with Biorender.com.

## THE NEUROVASCULAR UNIT, A MULTI-CELLULAR CNS-BARRIER STRUCTURE

A wealth of literature published during the last decades has enabled a change in the vision of the BBB, leading to the concept of a multi-cellular CNS-barrier structure. Indeed, substantial intercellular communication occurs between vascular cells (endothelial cells and pericytes) and the adjoining glia (Iadecola, 2017). More specifically, to enter the CNS from the vasculature, soluble factors and immune cells must traverse the endothelial BBB and the adjacent pericyte layer. Once soluble factors and immune cells penetrate the BBB, they circulate within the perivascular space, a region surrounding the basal surface of the endothelial cell wall, to reach the CNS parenchyma by passing through the glia limitans composed of the parenchymal basement membrane and the astrocyte endfeet (Engelhardt and Coisne, 2011; Engelhardt and Ransohoff, 2012).

### Pericytes

Pericytes, strategically positioned along capillaries, play a critical role in the multi-cellular CNS barrier structure. Indeed, pericytes, sandwiched between endothelial cells and astrocytes, are dynamically and synergistically engaged in interactions with neighboring cells to maintain homeostasis of the CNS (**Figure 1** – healthy brain). Pericytes are notably involved in the regulation of cerebral blood flow, neurovascular coupling and BBB homeostasis.

A role for pericytes in the regulation of microcirculatory blood flow has long been suspected (Armulik et al., 2011; Hall et al., 2014; Sweeney et al., 2016). Recent work demonstrated that pericytes synchronize microvascular blood flow dynamics and neurovascular coupling *via* nanotube-like processes called inter-pericyte tunneling nanotubes (IP-TNTs) which connect two pericytes on separate capillaries to form a functional network (Alarcon-Martinez et al., 2020). Pericytes are also part of the neurovascular unit and are most firmly attached to brain capillaries. They are involved in a crosstalk between endothelial cells and the surrounding cerebral tissue. Notably, it has been reported that pericytes interact with endothelial cells via specific adhesion sites that represent peg-and-socket junctions in the presence of *N*-cadherin (Sweeney et al., 2016), the single cell adhesion receptor CD146 (Chen et al., 2017), adhesion plaques containing fibronectin (Courtoy and Boyles, 1983), Connexin43 gap junctions (Cuevas et al., 1984), and even tight junctions (Larson et al., 1987). In a mouse model lacking pericyte coverage at the microvascular level, BBB integrity is compromised because of the transcellular barrier specific dysfunction (Sweeney et al., 2016) but also because of the loss of astrocytic endfeet polarization (Armulik et al., 2010). While pericytes are necessary for maintaining BBB integrity, astrocytic endfeets are also major actors in CNS barrier homeostasis.

### Astrocytes

Astrocytes represent an important population of glial cells in the CNS and astrocytic endfeet create a thick continuous layer that covers BBB microvessels called the glia limitans

(Mathiisen et al., 2010) (**Figure 1** – healthy brain). Neural precursor cells represent the primary source of astrocytes which develop at late gestation stages in mammals (Daneman et al., 2010b; Cheslow and Alvarez, 2016). Therefore, it is commonly accepted that if astrocytes do not play a major role in BBB establishment, they strongly impact BBB maturation and maintenance.

Reducing the vascular coverage of the population of astrocytes and astrocytic endfeet in the early postnatal cerebral cortex leads to the formation of microvessels with an abnormally large diameter (Ma et al., 2012). In addition, astrocytes are actively involved in the production of the basement membrane embedding the glia limitans. Knocking down elements of the basement membrane results in the disruption of Aquaporin4 (AQP4) channel enrichment at the astrocytic endfeet membrane (Brightman, 2002; Lien et al., 2012; Menezes et al., 2014). This leads to BBB permeability and associated brain edema (Nagelhus and Ottersen, 2013).

Astrocytes maintain BBB integrity *via* the secretion of soluble factors. Astrocytes improve endothelial barrier function in co-culture or after administration of conditioned medium to CNS endothelial mono-culture (Igarashi et al., 1999; Alvarez et al., 2011; Podjaski et al., 2015). Astrocytes secrete soluble factors notably Sonic Hedgehog (Shh) (Alvarez et al., 2011), retinoic acid (RA) (Mizee et al., 2014), glial-derived neurotrophic factor (GDNF) (Igarashi et al., 1999), and angiopoietin 1 (Ang-1) (Suri et al., 1996; Pfaff et al., 2006) which reduce permeability.

Blood–brain barrier integrity in the cerebellum, spinal cord, and olfactory bulbs relies on astrocyte-derived Wnt-like ligand Norrin which interacts with the endothelial Frizzled4 receptor. Knocking down the Norrin/Frizzled4 signaling leads to BBB defects through β-catenin–dependent transcriptional regulation (Zhou et al., 2014).

Astrocytes also express members of the ephrin receptor (EphR)/ephrin family (Nestor et al., 2007) which may impact BBB homeostasis. Notably, EphA4 receptor is expressed by glial cells especially around blood vessels in the adult marmoset (Goldshmit et al., 2014). EphA4 also plays a role in vascular formation and guidance during CNS development in mice. The proper interaction between the EphA4 receptor and its astrocytic ephrinA5 ligand is necessary for the development of a normal vascular system in the hippocampus of adult mice (Goldshmit et al., 2006; Hara et al., 2010).

Hence, based on these strong arguments, it is now recognized that the vascular component in the CNS is inseparably linked to glial and neuronal partners. Therefore, it is necessary to consider the neurovascular unit as a whole (and not only the BBB) in vascular pathophysiology and targeted therapeutic strategies.

## Glioblastoma Disrupts The Normal Brain Architecture And Molecular Interactions

### Basic Characteristics of Glioblastoma

Diffuse gliomas are brain tumors classified into IDH1mut and WT tumors (Louis et al., 2016). Glioblastomas (grade IV gliomas) are generally IDH WT tumors and represent the most aggressive form with an extremely poor prognosis. It is now admitted that glioblastoma (GBM) are mainly derived from neural stem cells, giving rise to transformed cells with astrocytic, neuronal, or oligodendrocytic characteristics (Alcantara Llaguno et al., 2009; Zong et al., 2012). Accumulation of genetic mutations, alterations, and amplifications play a central role in the transformation of healthy neural stem cells. Typical alterations in primary GBM are represented by amplification or mutation of PTEN, NF1, CDKN2A/B, and RB genes, or homozygous deletion or mutation of MDM2, CDK4, EGFR, PDGFRα, and PI3K genes. Typical histopathological features of GBM comprise highly proliferative cells with multinuclei, areas of necrosis surrounded by pseudopalisading cells, and endothelial cell proliferation with numerous clusters of blood vessels forming so-called glomeruloid structures. In 1938, Scherer highlighted several modes of GBM invasion: interstitial invasion, white matter tract invasion, and perivascular invasion (Scherer, 1940). GBM invasion relies on genetic alterations such as overexpression, amplification, deletion, or mutation in focal adhesion kinase (FAK) and phosphatidylinositol 3-kinase (PI3K) pathways. Activation of growth factors and their receptors are mainly involved in promoting invasion. These include CD44, integrins, osteonectin (SPARC), transforming growth factor (TGF)α/β, and receptors for platelet-derived growth factor (PDGF), fibroblast growth factor (FGF-2), and epidermal growth factor (EGF). Extracellular matrix components such as thrombospondins, laminins, or fibronectin are also overexpressed in GBM and their inhibition reduces invasiveness of GBM cells (Serres et al., 2014; Chouleur et al., 2020). Indeed, we and others characterized the role of thrombospondin-1 (which was primarily described as anti-angiogenic molecule) in GBM development and invasion (Daubon et al., 2019).

Glioblastoma is the most common brain tumor in Europe, in the United States, or in China, with more than 50% of glioma cases each year, and with an incidence of 3.2 per 100,000 people each year in the United States. Increasing incidence in populations from several countries were observed, suggested by authors as consequences of environmental or lifestyle factors (Philips et al., 2018). The 5-year overall survival (OS) rate is very low of only 5.1%, even with standard-of-care treatment (large tumor resection, chemo- and radiotherapy, so-called Stupp protocol). GBM are often only diagnosed at an advanced stage of the disease and often only detected when patients present symptoms (headaches, seizures, memory loss, loss of movements, cognitive impairments, and language dysfunctions). The poor response to therapy is partially explained by high intratumor heterogeneity, leaky and tortuous blood vessels in the central part, and intact BBB surrounding invasive cells, which leads to difficulties for therapeutic molecules to reach these sites (**Figure 1** – glioblastoma).

## Metabolic Interactions Between GBM Cells and the Endothelium

Glioblastoma is considered as one of the most glycolytic human tumors. High glycolytic flux drive production of pyruvate from glucose, and then pyruvate into lactate by lactate dehydrogenases, to regenerate $NAD^+$ to support glycolytic flux by fulfilling the

demand for ATP and other metabolic precursors. As previously described in striated muscles and also in the brain, lactate is, in turn, retro-converted into pyruvate by oxygenated tumor cells to feed oxidative metabolism. This phenomenon was described in the seminal publication of Pellerin et al. (1998) as lactate shuttle between astrocytes and neurons. Vegran et al. (2011) also demonstrated a lactate shuttle between tumor cells and endothelial cells, mainly *via* endothelial monocarboxylate transporter 1 (MCT1). More recently, MCT1 was also identified as a key mediator of lactate signaling between glioma cells and brain endothelial cells (Miranda-Gonçalves et al., 2017). Targeting symbiotic metabolism between GBM and endothelial cells may represent an interesting therapeutic strategy.

## Involvement of Pericytes and Astrocytes in Glioblastoma Vascular Pathophysiology

The chronic hyper-permeability of blood vessels is a hallmark of glioblastoma. We focus herein our attention on the role of pericytes and astrocytes in disrupting the BBB in glioblastoma.

### Role of Pericytes

Glioblastoma vessels are characterized by numerous structural and functional abnormalities, including altered association between endothelial cells and pericytes. These dysfunctional, unstable vessels contribute to hypoxia, interstitial fluid pressure, and enhanced susceptibility to metastatic invasion (Barlow et al., 2013). An interesting feature of glioblastoma pericytes is that they represent one of the active cell components of the perivascular niche. It has been reported that cancer stem cells, which are closely associated with tumor vessels, trans-differentiate into endothelial cells or pericytes (Wang et al., 2010; Cheng et al., 2013), a phenomenon described as vasculogenic mimicry (VM). VM was also shown to be promoted by tumor-associated macrophages (TAMs) by increasing the expression of cyclooxygenase 2 in the tumor cells (Rong et al., 2016) and has been associated with poor patient prognosis. However, the significance of VM in GBM is still debated and not universally accepted. Furthermore, tumor-derived pericytes exhibit specific genetic alterations that allow for discrimination between them and normal pericytes (Cheng et al., 2013), which may be relevant for diagnosis and therapy. Finally, pericytes were shown to promote evasion from the anti-tumor immune response favoring tumor growth (**Figure 1** – glioblastoma). Glioblastoma-dependent immunosuppressive function in pericytes is mediated by the expression of anti-inflammatory molecules such as IL-10, TGF-β, and MHC-II (Valdor et al., 2017).

### Role of Astrocytes

Reactive astrocytes are an integral part of the glioblastoma micro-environment and are characterized by hypertrophy, upregulation of intermediate filaments (vimentin and glial fibrillary acidic protein), and increase in proliferation. The role of reactive astrocytes in the pathophysiology of glioblastoma has been widely documented in the literature. Astrocyte–glioma crosstalk was shown to drive migration, proliferation, and invasion of glioblastoma (Guan et al., 2018). However, only few works focused on the contribution of astrocytes to the aberrant organization of the BBB in these tumors.

The participation of astrocytes to BBB permeability in glioblastoma is documented by the loss of astrocytic endfeet polarity which is characterized by Aquaporin-4 (AQP4) redistribution to membrane domains apart from endfeet areas (Kröger et al., 2004). This re-localization is probably due to the degradation of the proteoglycan agrin by the matrix metalloproteinase 3 (MMP3). Consequently, the water transport is compromised leading to edema. This, in turn, may drive BBB breakdown characterized by disrupted tight junctions leading to the development of vasogenic edema. However, how the loss of polarity is linked to the disturbance of microvascular tight junctions is still not understood (Wolburg et al., 2012). Using a clinically relevant mouse model of glioblastoma, it has been shown that tumor cells populate the perivascular space of preexisting vessels and displace astrocytic endfeet from endothelial or mural cells. This leads to abnormal BBB permeability and loss of astrocyte-mediated gliovascular coupling which pave the way for glioma cells to take control of vascular tone regulation (Watkins et al., 2014). This phenomenon, known as blood vessel co-option, is a strategy for glioblastoma to invade distant sites of the brain parenchyma (**Figure 1** – glioblastoma). Vessel co-opting GBM cells directly obtain oxygen and nutrients from the blood. The interactions with the vascular niche stimulate proliferation and self-renewal of GBM cells.

There is still much to explore as reactive astrocytes have already been identified as key players impacting the state of the BBB in various diseases (Liebner et al., 2018). They are likely to also play an important role in vessel hyper-permeability of GBM.

# VASCULAR TISSUE ENGINEERING AND ITS POTENTIAL FOR THE STUDY OF GBM–VESSEL INTERACTIONS

The tumor vasculature is critically involved in GBM development. This has led to clinical trials using anti-angiogenic drugs but with mixed results (Chinot et al., 2014). It has been postulated that anti-angiogenic treatment may impact tumor cell behavior by shifting them from an angiogenic to a co-optive behavior (Griveau et al., 2018). Thus, it is important to better understand more rigorously how tumor cells and vessels interact. A number of experimental models have been proposed in this context.

There are two classic and widely used models to study the role of the vasculature in tumor growth: the *in vivo* chick chorio-allantoic membrane (CAM) assay (Lokman et al., 2012) and the *in vivo* mouse/rodent graft model (Eklund et al., 2013). These two models are based on grafting tumor cells on the membrane of a growing chicken or in a specific site in mouse. If the chick model follows to some extent better the 3R rule (replacement, reduction, and refinement; Aske and Waugh, 2017) as considered as less sentient living beings due to not fully active nervous system, it is nevertheless necessary to develop alternative models that are closer to the human situation.

During the last decade, tissue engineering led to the development of artificial vessels which can be used for tissue vascularization in a 3D environment. These *in vitro* models may represent a promising alternative to animal models.

Regarding studies related to tumor–vessel interactions, it is important to note that cancer cells are involved in two phenomena: inducing vessel sprouting (angiogenesis) and transmigrating through the blood vessel wall (endothelial cells, smooth muscle cells, and matrix) for dissemination. The latter phenomenon is difficult to study in both CAM and mouse models. It is therefore necessary to develop *in vitro* models that are closer to the human situation. During the last decade, tissue engineering led to the development of artificial human vessels which can be used for tissue vascularization in a 3D environment. These *in vitro* models, which harbor all the histological components of a blood vessel (lumen, endothelium, smooth muscle cells, and matrix), must also retain its mechanical properties such as liquid-tightness, perfusability, and contractility.

## Tissue-Engineered Blood Vessels

Since the 1950s, synthetic tubes were the first choice for vascular reconstruction and grafts in patients with cardiovascular diseases. These conducts were made of polymer materials like expanded polytetrafluoroethylene (ePTFE), polyethylene terephthalate (Dacron), and polyurethane (Kannan et al., 2005), but all the functional characteristics of a blood vessel were not maintained in these tubes: they were not contractile and are not immune to thrombosis or inflammation. Motivated by these limitations, the development of 3D tissue-engineered blood vessels (TEBVs) has progressed significantly over the past two decades. Indeed, TEBVs tend to better match the biomechanical properties and the physiological responses of healthy blood vessels.

Tissue-engineered blood vessels can be not only used for vascular grafts but also for mechanistical studies related to the tumor–vessel interaction. For all the aforementioned reasons, engineering of artificial blood vessels is not an easy task and has been for a long time restricted to big diameter arteries (>6 mm) (Niu et al., 2014), and were usually made of synthetic polymers without endothelial of smooth muscle cell. Recently, efforts have been made to produce smaller blood vessels (<2 mm) by the use of various approaches (Song et al., 2018) (**Figure 2A**).

The production of tubular structures is achieved by three commonly used techniques: sheet rolling, tubular molding, and direct scaffolding. The sheet rolling technique is based on the creation of a sheet with the biomaterial of your choice and on the rolling of several sheets together for generating a tubular structure (Peck et al., 2011). Weinberg and Bell (1986) first described the use of a tubular mold that was filled with the desired cells and matrix. Finally, most of the biopolymers can be directly injected in a tubular form by direct scaffolding, but the major issue for all these techniques is the long-term culture of blood vessel. As an example, two pioneered groups (Roger Kamn and Lance Munn) developed in 2011 and 2012 microfluidic channels surrounded by 3D hydrogels using microfabricated silicone molds (Song and Munn, 2011; Shin et al., 2012). The point was to put endothelial cells in 2D culture on top of these hydrogels to mimic vessel sprouting and invasion inside a tissue. These models were subsequently improved by mixing stroma and tumor cells inside the hydrogel for tumor angiogenesis studies. A recent paper by Andrique et al. (2019) used a co-extrusion microfluidic device to produce small-diameter artificial vessels (<500 μm) with both endothelial and smooth muscle cells, surrounded by a scaffold made of biocompatible alginate polymer. These "vesseloids" are rapidly formed (only 1 day of culture) easy to handle, perfusable, liquid-tight, and retain their vascular functions (contractility, response to inflammatory stimuli) (**Figure 2B**). Vesseloids may be used as trunks for angiogenic sprouts to emerge which are useful for organ or tumor vascularization.

## Controlled Microenvironment in 3D *in vitro* Models

3D co-culture systems including tumors cells, endothelial cells (blood vessels), and other micro-environmental components have emerged for reproducing tumor–stroma interactions. It was shown that tissue stiffness modulate tumor growth and nutrient transport (Massa et al., 2017). This is critical and must be considered for drug testing in cancer therapy. The major advantage of 3D co-culture models relies on the fact that various parameters can be controlled: type and density of the ECM components (e.g., Matrigel, collagen, PEG, fibronectin, and gelatin methacryloyl), stiffness, hypoxia and gas exchange, and the inclusion of various cell types such as macrophages, astrocytes, or vascular cells.

3D systems, which do not include the vascular component, already improve phenotypic properties, gene expression, and drug response. The importance of the environment in drug delivery testing was already highlighted by Seo et al. (2014). They explained that new anti-cancer drugs are usually tested in 2D tissue culture which neglects the complexity of the 3D micro-environment (Langhans, 2018). The development of 3D *in vitro* tissue-engineered models will help to refine the drug response and contribute to the improvement of anti-cancer therapies. More recently, striking differences in gene expression between 2D and 3D culture of GBM have been reported (Ma et al., 2018) which mirrored the phenotypic differences. This is in agreement with another study (Chaicharoenaudomrung et al., 2020) where GBM cells were cultured in Ca-alginate 3D scaffolds before next-generation sequencing (Illumina), and this uncovered cellular pathways (Map kinase, autophagy, and cell metabolism) for 3D different to 2D cultures. Musah-Eroje and Watson (2019) developed a new 3D model of GBM which seems to more accurately reflect the complexity of the GBM micro-environment. Compared with regular 2D cultures or spheroids, they showed that GBM cells in the3D model were more resistant to temozolomide and that this resistance was potentiated by hypoxia. One unresolved issue regarding 3D brain organoid models is the lack of functional vascularization. Recently, Cakir et al. (2019) developed with success *in vitro* functional vasculature-like networks in human cortical organoids (hCOs) from human embryonic

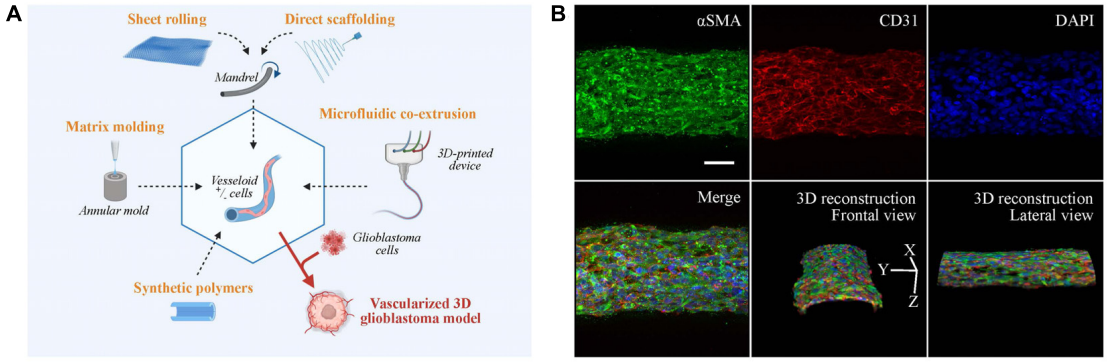


**FIGURE 2 |** Vascular models in neuro-oncology research. **(A)** Fabrication strategies for engineering artificial vessels. Vascular models are synthesized by rolling, molding, scaffolding, or microfluidic co-extrusion using biomaterials with/without cells. Addition of glioblastoma cells creates a vascularized tumor model. **(B)** Confocal imaging of vesseloid (scale bar: 50 μm). Nuclei in blue (DAPI), αSMA in green, and endothelial marker in red (CD31). On top and merge panels, images correspond to a maximal intensity projection along the *z*-axis. Other panels are 3D-image reconstructions.

stem cells (hESCs). In this work, endothelial reprogramming in hCOs induced the formation of organoids with vascular-like structures. These vascular structures are functional and exhibit BBB characteristics. Close to this work, a recent model of vascularized human cortical organoids (vOrganoids) was developed by Shi et al. (2020) (Vascularized human cortical organoids (vOrganoids) model cortical development *in vivo* 2020 PLOS One). These vOrganoids (human cortical cell types with vasculature structure) presented bidirectional electrical transmission trough functional synapses, and their transplantation in the mouse cortex resulted in the survival of the graft. All these innovative 3D models represent useful models for studies related to physiology or pathology and may be useful as a model for therapeutic studies.

## 3D Co-Culture Models of Tumor and Endothelial Cells

The ultimate step of these 3D tumor models is the inclusion of endothelial and/or pericytes/smooth muscle cells to mimic blood vessels to produce vascularized tissues. A number of these works were done in tumor types other than glioblastoma. For example, Silvestri et al. (2020) developed a tissue-engineered model of a 3D co-culture of microvessels and mammary tumor organoids. They first fabricated a collagen gel scaffold with cylindrical channels filled with endothelial cells as a microvessel device. After perfusion and verification of the microvessels permeability, mammary tumor organoids were introduced inside of the 3D collagen scaffold and tumor cell–endothelial cell interactions were analyzed by live imaging. Others went further and developed a tri-culture metastatic model of breast cancer (Cui et al., 2020). By stereolithography 3D printing, a complex tripartite tissue was created which is composed of bone, vessels, and breast cancer cells. This model was used to study mechanisms of bone metastasis. Wang et al. (2014) have developed a 3D model to observe tumor invasion with high spatial and temporal resolution. Furthermore, intravasation and extravasation were observed at high spatial resolution using microvessels embedded in collagen 3D matrix and mixed with cancer cells (Langhans, 2018). As for glioblastoma, McCoy et al. (2019) generated GBM spheroids of uniform size distribution, and embedded them into collagen hydrogels to investigate GBM invasion into the ECM of the perivascular niche. They also showed by co-culturing endothelial and GBM cells that GBM cells have a high stemness potential and invasion capacity dependent on IL-8 signaling. Thus, tumor vasculature models may be very useful to shed light into the complex interactions between the vasculature and tumor cells.

# REVIVAL OF ANTI-ANGIOGENIC THERAPY: COMBINATION WITH OTHER DRUGS

## Anti-Angiogenic Background

To date, bevacizumab is the only anti-angiogenic drug admitted for GBM management. Based on the results of three different clinical studies (**Table 1**), bevacizumab was approved by the Food and Drug Administration (FDA), the Japanese Ministry of Health, Labour and Welfare (MHLW), and other countries as a combination treatment with standard therapy and as a single agent for relapsed or progressive GBM after previous therapy. However, the OS was not prolongated in these studies; bevacizumab showed nevertheless some benefit in decreasing the use of corticosteroids, the adverse effects of which impair patient's quality of life. However, the European Medicine Agency (EMA) has not approved its indication, estimating that the benefit–risk assessment is not in favor of its prescription in the management of GBM. This is also supported by the National Institute for Health and Care Excellence (NICE) guidelines (NICE, 2018). It is important to emphasize that bevacizumab cannot be used a month before and after brain surgery. This must be considered when using this treatment. Of note, the pharmacokinetics and bioavailability of bevacizumab is limited since it cannot cross the intact BBB which is nevertheless partially disrupted to allow drug penetration to some extent.

**TABLE 1 |** Pivotal clinical trials supporting the approval indication.

| Study name or ID | Design | Treatment arms | Median PFS (1) vs (2) | Median OS (1) vs (2) |
|---|---|---|---|---|
| AVAglio (NCT00943826) (Chinot et al., 2014) (new dig GBM) | Randomized, double-blinded, placebo-controlled Phase III (N = 921) | (1) RT + TMZ + Placebo (*N* = 463) (2) RT + TMZ + Bev (*N* = 458) | *6.2 (6.0–7.5) vs. 10.6 (10.0–11.4) months; HR = 0.64 (0.55–0.74); $p < 0.001$ | *16.7 (15.4–18.4) vs. 16.8 (15.5–18.5) months; HR = 0.88 (0.76–1.02); $p = 0.1$ |
| RTOG0825 (NCT00884741) (new dig GBM) | Randomized, double-blinded, placebo-controlled Phase III (*N* = 637) | (1) RT + TMZ + Placebo (*N* = 317) (2) RT + TMZ + Bev (*N* = 320) | *7.3 (5.6–7.9) vs. 10.7 (10.0–12.2) months; HR = 0.79 (0.66–0.94); $p = 0.004$ | *16.1 (14.8–18.7) vs. 15.7 14.2–16.8) months; HR = 1.13 (0.93–1.37); $p = 0.11$ |
| EORTC26101 (NCT01290939) (Wick et al., 2017) (recurrent GBM) | Randomized Phase III (*N* = 437) | (1) Lomustine alone (*N* = 149) (2) Lomustine + Bev (*N* = 288) | #1.5 (1.5–2.5) vs. 4.2 (3.7–4.3) months; HR = 0.49 (0.39–0.61); $p < 0.001$ | *8.6 (7.6–10.4) vs. 9.1 (8.1–10.1) months; HR = 0.95 (0.74–1.21); $p = 0.65$ |

*RT, radiotherapy; TMZ, temozolomide; Bev, bevacizumab; PFS, progression-free survival; OS, overall survival. *Primary outcome measure. #Secondary outcome measure.*

## Revival of Bevacizumab and Anti-Angiogenic Therapy

Bevacizumab alone is certainly not a curative treatment for GBM and this raises ethical issues related to the benefit–risk of this treatment between the improvement of the patients' quality of life and frequent occurrence of serious side effects. Security data of clinical trials, as pharmacovigilance studies, have shown frequent and serious cardiovascular effects (hemorrhages, thromboembolic events, and heart failure) and hematological disorders (neutropenia, leukopenia, and thrombocytopenia) (Chinot et al., 2014; Gilbert et al., 2014; Wick et al., 2017). On theoretical grounds, the use of anti-angiogenic drugs may be justified due to physiopathological consideration (high expression of VEGF, BBB dysfunction, edema leading to hemorrhages, cognitive impairment, tumor growth, and cell invasion). Better outcomes may be observed when anti-angiogenic therapy is combined with inhibitors of tumor cell invasion or in combination with immunotherapy as documented in some studies (Kang et al., 2015; Piao et al., 2016; Gravina et al., 2017; Daubon et al., 2019).

A short review of the last-5-years published clinical trials is shown in **Table 2**, using the following parameters from PubMed: key words = Glioblastoma AND Antiangiogenic; filters = Abstract available, Clinical Trial; date = between 2015 and 2020. As no clinical trials of phase III were found, articles related to phase II studies, describing new associations or new indications with bevacizumab or new individual anti-angiogenic drugs, were selected if median progression-free survival (mPFS) or the median overall survival (mOS) outcomes were available and if the trial was referenced in https://clinicaltrials.gov/. mPFS and mOS reflect more robust outcomes than response rate. Eighteen clinical trials were found using these inclusion criteria.

## New Investigations for Bevacizumab

Certain populations are under-represented in global clinical trials. This has led to the investigation of the efficacy of bevacizumab in newly diagnosed GBM (nGBM) in the elderly (ARTE, Wirsching et al., 2018 and ATAG, Reyes-Botero et al., 2018 studies) and in pediatric populations (HERBY study, Grill et al., 2018). The ARTE study showed that when radiotherapy associated with bevacizumab, it did not prolong mOS compared with radiotherapy only (12.2 vs 12.1 months; HR = 1.09; $p = 0.75$). However, mPFS was favorable with bevacizumab in restricted *per* protocol analyses (7.6 vs 4.8 months; HR = 0.36; $p = 0.001$) (Wirsching et al., 2018). In combination with temozolomide, bevacizumab seemed active in the ATAG study and had an acceptable adverse effect profile (Reyes-Botero et al., 2018). As for the pediatric population, adjunction of bevacizumab to the current therapy did not improve mOS (18.3 vs 20.3 months; HR = 1.23; $p = 0.46$) (Grill et al., 2018). The results in the pediatric population differ from adults, and, thus, further research is needed.

## New Associations With Bevacizumab

Glioblastomas are associated with increased stimulation of different signaling pathways. Trials have been run with bevacizumab combined with molecules interfering with these pathways. The association of bevacizumab with BKM 120–buparlisib, an oral PI3K inhibitor, did not improve outcome (mPFS: 2.8 to 5.3 months; mOS: 6.6 to 10.8 months) and increased the adverse drug effect profile (Hainsworth et al., 2019). In another study, mOS in the arm of bevacizumab combined with dasatinib, a Src signaling inhibitor, is similar to the placebo arm (7.3 vs 7.9 months; HR = 0.92; $p = 0.7$) (Galanis et al., 2019). In two trials, addition with bevacizumab to the histone deacetylase inhibitors vorinostat (Ghiaseddin et al., 2018) and panobinostat (Lee et al., 2015) failed to improve outcome compared with control (mPFS: 3.7 and 5 months; mOS: 10.4 and 9 months, respectively). When bevacizumab is combined with onartuzumab, a monovalent MET inhibitor, it did also not improve patient outcome versus bevacizumab plus placebo alone (mPFS: 3.9 vs 2.9 months; HR = 1.06; $p = 0.74$ and mOS: 8.8 vs 12.6 months; HR = 1.45; $p = 0.14$) (Cloughesy et al., 2017). The GLARIUS trial aimed to study the association of bevacizumab with irinotecan, a topoisomerase 1 inhibitor, comparing with temozolomide alone in nGBM with un-methylated MGMT

**TABLE 2 |** Phase II clinical trials recently published.

| Study name or ID | Indication | Design | Treatment arms | Outcomes (months) | |
|---|---|---|---|---|---|
| | | | | mPFS | mOS |
| NCT01349660 (Hainsworth et al., 2019) | Relapsed or refractory GBM following first-line therapy | Non-randomized, single group assignment, open label (*N* = 76) | BKM 120 (buparlisib) *per os* + Bev (1) Prior anti-angiogenic therapy (*N* = 19) (2) Without previous anti-angiogenic therapy (*N* = 57) | *(1)* 2.8 (1.6–5.3) *(2)* 5.3 (3.6–9.2) | #*(1)* 6.6 (4.0–14.6) #*(2)* 10.8 (9.2–13.5) |
| NCT01753713 (Sharma et al., 2019) | Recurrent or progressive GBM following first-line therapy | Non-randomized, parallel assignment, open label (*N* = 33) | (1) Dovitinib *per os* in anti-angiogenic naïve patients (*N* = 19) (2) Dovitinib *per os* in progressed GBM on previous anti-angiogenic therapy (*N* = 14) | #*(1)* 2.0 (1.3–3.7) #*(2)* 1.8 (0.9–1.8) | #*(1)* 8.0 (4.4–11.7) #*(2)* 4.3 (2.6–6.7) |
| NCT00892177 | Recurrent or progressive GBM | Randomized, parallel assignment, double blinded (*N* = 12(1) | *(1)* Bev + dasatinib *per os* (*N* = 83) *(2)* Bev + placebo (*N* = 38) | | #*(1)* 7.3 (6.2–9.7) vs. *(2)* 7.9 (6.6–11.3); HR = 0.92 (0.61–1.4); *p* = 0.7 |
| REGOMA (NCT02926222) (Lombardi et al., 2019) | Relapsed GBM after surgery | Randomized, parallel assignment, open label (*N* = 119) | *(1)* Regorafenib *per os* (*N* = 59) *(2)* Lomustine *per os* (*N* = 60) | | **(1)* 7.4 (5.8–12.0) vs *(2)* 5.6 (4.7–7.3); HR = 0.5 (0.33–0.75); *p* = 0.0009 |
| ARTE (NCT01443676) (Wirsching et al., 2018) | Newly diagnosed GBM in elderly patients | Randomized. parallel assignment, open label (*N* = 75) | *(1)* RT (*N* = 25) *(2)* RT + Bev (*N* = 50) | #*(1)* 4.8 vs *(2)* 7.6; HR = 0.36 (0.20–0.65); *p* = 0.001 | **(1)* 12.1 vs *(2)* 12.2; HR = 1.09 (0.63–1.89); *p* = 0.75 |
| ATAG (NCT02898012)(Reyes-Botero et al., 2018) | GBM in elderly patients with a Karnofsky performance status < 70 | Non-randomized, single group assignment, open label (*N* = 66) | TMZ + Bev (*N* = 66) | #3.8 (3.2–4.8) | *6 (4.8–6.9) |
| HERBY (NCT01390948) (Grill et al., 2018) | Newly diagnosed GBM in pediatric and adolescent patients | Randomized, parallel assignment, open label (*N* = 12(1) | *(1)* RT + TMZ (*N* = 59) *(2)* RT + TMZ + Bev (*N* = 62) | | #*(1)* 20.3 (14.8–33.8) vs. *(2)* 18.3 (16.2–25.7); HR = 1.23 (0.72–2.09); *p* = 0.46 |
| NRG/RTOG (NCT01609790) (Reardon et al., 2018) | Recurrent GBM | Randomized, parallel assignment, double blinded (*N* = 115) | *(1)* Bev + placebo (*N* = 58) *(2)* Bev + trebananib (*N* = 57) | #*(1)* 4.8 (3.8–7.1) vs. *(2)* 4.2 (3.7–5.6); HR = 1.51 (1.02–2.24); *p* = 0.04 | #*(1)* 11.5 (8.4–14.2) vs *(2)* 7.5 (6.8–10.1); HR = 1.46 (0.95–2.27); *p* = 0.09 |
| NCT01738646 (Ghiaseddin et al., 2018) | Recurrent GBM | Non-randomized, single group assignment, open label (*N* = 40) | Bev + vorinostat (*N* = 40) | #3.7 (2.9–4.8) | #10.4 (7.6–12.8) |
| NCT00704288 (Cloughesy et al., 2018) | Recurrent or progressive GBM following previous anti-angiogenic therapy | Non-randomized, single group assignment, open label (*N* = 222) | Cabozantinib *per os* (*N* = 70) *(1)* 140 mg/day (*N* = 12) *(2)* 100 mg/day (*N* = 58) | #2.3 overall (1) 3.3– 2) 2.3 | #4.6 (3.0–5.6) overall (1) 4.1– 2) 4.6 |
| NCT00704288 (Wen et al., 2018) | Recurrent or refractory GBM following non–anti-angiogenic therapy | Non-randomized, single group assignment, open label (*N* = 222) | Cabozantinib *per os* (*N* = 152) *(1)* 140 mg/day (*N* = 34) *(2)* 100 mg/day (*N* = 118) | #3.7 overall | #(1) 7.7 #2) 10.4 |
| GO27819 (NCT01632228) (Cloughesy et al., 2017) | Recurrent GBM | Randomized, parallel assignment, double blinded (*N* = 129) | *(1)* Bev + onartuzumab (*N* = 64) *(2)* Bev + placebo (*N* = 65) | **(1)* 3.9 vs. *(2)* 2.9; HR = 1.06 (0.72–1.56); *p* = 0.74 | #*(1)* 8.8 vs. *(2)* 12.6; HR = 1.45 (0.88–2.37); *p* = 0.14 |
| NCT01846871 (Kalpathy-Cramer et al., 2017) | Recurrent GBM | Non-randomized, single group assignment, open label (*N* = 10) | Tivozanib | #2.3 (1.5–4) | #8.1 (5.2–12.5) |

*(Continued)*

**TABLE 2** | Continued

| Study name or ID | Indication | Design | Treatment arms | Outcomes (months) | |
|---|---|---|---|---|---|
| | | | | mPFS | mOS |
| NCT01067469 (Weathers et al., 2016) | Recurrent GBM | Randomized, single group assignment, open label (*N* = 69) | *(1)* Bev (*N* = 36) *(2)* Bev low doses + lomustine (*N* = 33) | **(1)* 4.11 (2.96–5.55) **(2)* 4.34 (2.96–8.34) | #*(1)* 8.3 (6.42–11.58) #*(2)* 9.6 (6.26–16.73) |
| GLARIUS (NCT00967330) (Herrlinger et al., 2016) | Newly diagnosed GBM and a non-methylated MGMT promoter | Randomized, parallel assignment, open label (*N* = 182) | *(1)* Bev + irinotecan (*N* = 122) *(2)* TMZ (*N* = 60) | #*(1)* 9.7 (8.7–10.8) vs. *(2)* 6.0 (2.7–6.2); HR = 0.59 (0.42–0.82); *p* = 0.001 | #*(1)* 16.6 (15.4–18.4) vs. *(2)* 17.3 (14.8–20.4); HR = 0.96 (0.68–1.35); *p* = 0.83 |
| NCT00667394 | Recurrent GBM | Non-randomized, parallel assignment, open label (N = 41) | Bev + tandutinib | ¤4.1 | ¤11 |
| NCT00720356 (Raizer et al., 2016) | Newly diagnosed GBM and a non-methylated MGMT promoter | Non-randomized, single-group assignment, open label (*N* = 46) | Bev + erlotinib | ¤9.2 (6.4–11.3) | *13.2 (10.8–19.6) |
| NCT00859222 (Lee et al., 2015) | Recurrent GBM | Non-randomized, single group assignment, open label (*N* = 24) | Bev + panobinostat | #5 (3–9) | #9 (6–19) |

*mPFS, median progression-free survival; mOS, median overall survival; Bev, bevacizumab; RT, radiotherapy; TMZ, temozolomide.*
**Primary outcome measure. #Secondary outcome measure. ¤Post hoc analysis.*

promoter. This resulted in a superior mPFS with the drug combination (9.7 vs 6.0 months; HR = 0.59; $p = 0.001$) without improving mOS (16.6 vs 17.3 months; HR = 0.96; $p = 0.83$) (Herrlinger et al., 2016).

Another strategy aims at an additive effect by targeting both the vasculature and tumor cells and by combining bevacizumab with inhibitors of other growth factor pathways. Trebananib is a Fc fusion protein that targets Ang1 and Ang2; however, its association with bevacizumab failed to improve outcome when compared with bevacizumab plus placebo alone (mPFS: 4.2 vs 4.8 months, HR = 1.51, $p = 0.04$; and mOS 7.5 vs 11.5 months, HR = 1.46, $p = 0.09$) (Reardon et al., 2018). The association between bevacizumab and tandutinib, an oral FLT3, c-Kit, and PGDFRβ inhibitor, showed some benefit (*post hoc* mPFS: 4.1 months; *post hoc* mOS: 11 months) but showed a high toxicity (Odia et al., 2016). One trial with patients presenting a nGBM with an unmethylated MGMT promoter investigated the combination with erlotinib, an EGFR tyrosine kinase inhibitor. This association did not also increase survival (mOS: 13.2 months – estimated mOS should have reached 17.9 months to show an increase in survival) (Raizer et al., 2016). This indicates that, during these last 5 years, no new drug combination with bevacizumab showed substantial clinical benefit and even increased toxicity. Furthermore, when comparing the use of low doses of bevacizumab to standard doses in patients with rGBM, it did not improve survival (mPFS: 4.34 vs 4.11 months; mOS: 9.6 vs 8.3 months) (Weathers et al., 2016).

Combination with immunotherapy also did not provide significant benefit. Recently nivolumab was investigated in a phase III randomized clinical trial with or without bevacizumab in patients with rGBM; nivolumab arm did not improve mOS [9.8 (8.2–11.8) vs 10.0 (9.0–11.8) months; HR = 1.04 (0.83–1.30), $p = 0.76$] and showed a lower mPFS [1.5 (1.5–1.6) vs 3.5 (2.9–4.6) months; HR = 1.97 (1.57–2.48), $p > 0.001$] (Reardon et al., 2020).

## New Anti-Angiogenic Drugs

Bevacizumab is the first representative of a drug family that interfered with the VEGF pathway. Others are represented by VEGF receptor tyrosine kinase inhibitors. A great advantage of these drugs is the oral administration which increases the patient's observance. In 2013, a phase III clinical trial studied the efficacy of cediranib, VEGFR, PDGFR, and c-Kit inhibitor, in combination with lomustine versus lomustine alone in patients with rGBM, but results did not show improvement of PFS (Batchelor et al., 2013). In a trial that compared dovitinib, a FGFR and VEGFR inhibitor, as second-line treatment after prior anti-angiogenic therapy by bevacizumab, no efficacy in prolonging mPFS (1.8 vs 2 months) was seen (Sharma et al., 2019). Tivozanib also showed limited activity in rGBM (mPFS: 2.3 months; mOS: 8.1 months), but the patient number in the trial ($N = 10$) was low (Kalpathy-Cramer et al., 2017). Two studies on cabozantinib, which inhibits MET and VEGFR2, on a global population did show some positive outcome in the rGBM group not treated previously with anti-angiogenic drugs (mPFS: 2.3 and 3.7 months; mOS: 4.6 and 10.4 months) (Cloughesy et al., 2018; Wen et al., 2018). Furthermore, the REGOMA study showed encouraging therapeutic benefit with regorafenib compared with lomustine alone (mOS: 7.4 vs 5.6 months; HR = 0.5; $p < 0.001$) (Lombardi et al., 2019).

## Drug Delivery

Therapy development for GBM is challenging. This is due to resistances to radio- and chemotherapy because of the presence of glioblastoma stem-like cells (Safa et al., 2015). Furthermore, the CNS is composed of natural barriers which impair drug delivery

into the brain. As such, the BBB allows the passive transport of gas and liposoluble molecules. BBB's tight junctions regulate, furthermore, paracellular transport.

Current pharmacological treatments for GBM are administered systemically by intravenous injection or orally. Oral route simplifies patient treatment by proposing several pharmaceutical options. Parenteral route allows a short action period and a controlled dosage. However, tissue diffusion into the brain is hampered and toxic side effects occur because of their systemic action and the possibility to reach the brain tissue only when the BBB is altered. To overcome these problems, permeability of drugs can be enhanced by increasing liposolubility or integrating them into liposomes or nanocarriers. On the other hand, BBB can be temporarily disrupted by therapeutic ultrasound whereas a hyperosmotic disruption did not improve the drug penetration (Kobrinsky et al., 1999; Idbaih et al., 2019).

Another possibility is to administer topically medicinal products using injectable or implantable devices with sustained drug release. Local delivery strategies aim at increasing the concentration of the drug at the tumor site, at decreasing alterations related to enzymatic metabolization, and at reducing the systemic side effects. After surgery, the resection cavity represents an accessible implantation site near non-surgically resectable cells. The only approved strategy by the FDA for nGBM and rGBM is the carmustine-impregnated biodegradable Gliadel wafer. However, these implants did not improve outcomes and presented higher local toxicity (brain edema, seizures) (De Bonis et al., 2012). Hydrogels are a 3D matrix composed of a hydrophilic polymer network. Injectable hydrogel is a reservoir-system similar to soft tissue that can contain a large panel of drugs able to diffuse into the surrounding tissue (Basso et al., 2018). Antineoplastic drugs can be administered directly into the cavity or in the cerebrospinal fluid via an intrathecal injection device (Ommaya reservoir) for therapeutic delivery (Ommaya, 1984). However, the drug concentration decreases as the diffusion distance increases, and thus, this approach is of limited use in highly infiltrating tumors. Moreover, long-term use of these medical devices may cause complications including infections and hemorrhages. Convection-enhanced delivery has been developed to increase local delivery by enhancing diffusion by a bulk flow to maintain a pressure gradient (Bobo et al., 1994). Despite an acceptable safety profile, this method did not improve clinical outcomes of patient with GBM (Oberoi et al., 2016). An alternative method is the use of the intranasal delivery, which is non-invasive because of the anatomical proximity of these structures. Intranasal administration of a telomerase inhibitor in a rat model extended animal survival (Hashizume et al., 2008).

## Perspectives for Anti-Angiogenic Drugs

There are new avenues to be explored for anti-vascular therapy. They can be used to enhance the activity of other therapies. For example, local hypoxia induced by bevacizumab could activate evofosfamide, a hypoxia-activated alkylating prodrug (Duan et al., 2008). Evofosmamide was studied on a phase I clinical trial for the treatment of rGBM following previous bevacizumab therapy, and results appeared to be favorable for being studied in a phase II trial (Brenner et al., 2018). Furthermore, anti-angiogenic therapy could be of more benefit in some GBM subgroups. In a retrospective study of the AVAglio Trial, it has been shown that bevacizumab treatment led to a prolongation of OS of 4.3 months compared with placebo (17.1 vs 12.8 months; multivariable HR = 0.42; $p$ = 0.001) in patients with proneural and IDH-1 wild-type nGBM (Sandmann et al., 2015). To date, the use of anti-angiogenic drugs should preferably be part of personalized care for patients.

# GENERAL CONCLUSION

The vasculature plays an important role in the brain in normal and pathological conditions. In this article, we reviewed some recent literature on this subject. In a healthy tissue, endothelial cells are considered gatekeepers in all vessel types, for controlling diffusion of soluble factors or immune cells, by using para- or transcellular pathways. In GBM, however, vessels present maturation defect and chronic hyper-permeability, leading to vessel leakage, and poor vessel perfusion and delivery of nutrients. Pericytes and astrocytes have a central role in controlling physiology of normal and GBM NVUs. Pericytes, which are positioned along capillaries, help GBM cells to invade distant sites along blood vessels, as observed for reactive astrocytes. Importantly, GBM cells displace the astrocytic endfeet during co-option, disrupting endothelial cell junctions, and participating in blood leakage and hemorrhage.

The tumor–vessel interaction can also be modeled using *in vitro* bioengineered blood vessels. For now, no perfect 3D co-culture model exists. However, recent efforts have been made at developing 3D artificial vessels and 3D co-culture models using co-cultures of cancer cells and artificial blood vessels. Regarding vascularized 3D GBM models, researchers departed from 2D co-cultures to spheroids and are now able to reproduce small brain organoids with or without a functional vascular network. The main challenge for brain organoids is the co-culture of multiple cell types including neurons, astrocytes, oligodendrocytes, and microglia (Cakir et al., 2019). Another difficulty is the reconstruction of a tissue resembling to the human brain with microglia and six cortical layers (Heide et al., 2018) which exhibits the functional characteristics of the human brain such as neuronal networks and functional synapses (Shi et al., 2020). Moreover, the presence of a stabilized functional vascular network is also critical which requires the improvement of the current models for better recapitulating the physiopathology of these models.

3D co-culture models of blood vessels have been recently developed which may be used as vascularization trunks for tumor models. 3D models are much more relevant to study these interactions because they better recapitulate cell behavior and also better mirror *in vivo* gene expression and signaling. 3D co-culture models represent an attractive alternative to animal models and may be used in drug screening to identify better therapies.

Anti-angiogenic therapy in GBM did not meet the initial high expectations when tested in clinical trials. There was no real clinical benefit in newly diagnosed and recurrent GBM (maybe with exception of regorafenib). However, if clinical trials allow to obtain a global vision of the therapeutic effect, they do not consider patient subgroups. When considered, this may allow a more precise vision of the therapeutic response. Another drawback is variable study design and the criteria for determining progression. Radiologic response criteria such as Macdonald or RANO criteria may be misleading in monitoring clinical responses to anti-angiogenic therapy. Thus, this is still not the end of the road for anti-angiogenic therapy in GBM and more promising data from clinical trials are expected to come.

## AUTHOR CONTRIBUTIONS

All authors listed have made a substantial, direct, and intellectual contribution to the work, and approved it for publication.

## ACKNOWLEDGMENTS

This work was supported by Fondation ARC 2020, Ligue Contre le Cancer (Comité de la Gironde), ARTC, Plan Cancer 2021, INCA PLBIO, the Region Nouvelle Aquitaine. JG is a recipient of fellowship from the Toulouse University Hospital (CHU Toulouse).

## REFERENCES

Alarcon-Martinez, L., Villafranca-Baughman, D., Quintero, H., Kacerovsky, J. B., Dotigny, F., Murai, K. K., et al. (2020). Interpericyte tunnelling nanotubes regulate neurovascular coupling. *Nature* 585, 1–5. doi: 10.1038/s41586-020-2589-x

Alcantara Llaguno, S., Chen, J., Kwon, C. H., Jackson, E. L., Li, Y., Burns, D. K., et al. (2009). Malignant astrocytomas originate from neural stem/progenitor cells in a somatic tumor suppressor mouse model. *Cancer Cell* 15, 45–56. doi: 10.1016/j.ccr.2008.12.006

Alvarez, J. I., Dodelet-Devillers, A., Kebir, H., Ifergan, I., Fabre, P. J., Terouz, S., et al. (2011). The Hedgehog pathway promotes blood-brain barrier integrity and CNS immune quiescence. *Science* 334, 1727–1731. doi: 10.1126/science.1206936

Andrique, L., Recher, G., Alessandri, K., Pujol, N., Feyeux, M., Bon, P., et al. (2019). A model of guided cell self-organization for rapid and spontaneous formation of functional vessels. *Sci. Adv.* 5:eaau6562. doi: 10.1126/sciadv.aau6562

Armulik, A., Genové, G., and Betsholtz, C. (2011). Pericytes: developmental, physiological, and pathological perspectives, problems, and promises. *Dev. Cell* 21, 193–215. doi: 10.1016/j.devcel.2011.07.001

Armulik, A., Genové, G., Mäe, M., Nisancioglu, M. H., Wallgard, E., Niaudet, C., et al. (2010). Pericytes regulate the blood-brain barrier. *Nature* 468, 557–561.

Aske, K. C., and Waugh, C. A. (2017). Expanding the 3R principles: more rigour and transparency in research using animals. *EMBO Rep.* 18, 1490–1492. doi: 10.15252/embr.201744428

Barlow, K. D., Sanders, A. M., Soker, S., Ergun, S., and Metheny-Barlow, L. J. (2013). Pericytes on the tumor vasculature: jekyll or hyde? *Cancer Microenviron. Off. J. Int. Cancer Microenviron. Soc.* 6, 1–17. doi: 10.1007/s12307-012-0102-2

Basso, J., Miranda, A., Nunes, S., Cova, T., Sousa, J., Vitorino, C., et al. (2018). Hydrogel-based drug delivery nanosystems for the treatment of brain tumors. *Gels* 4:62. doi: 10.3390/gels4030062

Batchelor, T. T., Mulholland, P., Neyns, B., Nabors, L. B., Campone, M., Wick, A., et al. (2013). Phase III randomized trial comparing the efficacy of cediranib as monotherapy, and in combination with lomustine, versus lomustine alone in patients with recurrent glioblastoma. *J. Clin. Oncol.* 31, 3212–3218. doi: 10.1200/jco.2012.47.2464

Ben-Zvi, A., Lacoste, B., Kur, E., Andreone, B. J., Mayshar, Y., Yan, H., et al. (2014). Mfsd2a is critical for the formation and function of the blood–brain barrier. *Nature* 509, 507–511. doi: 10.1038/nature13324

Bobo, R. H., Laske, D. W., Akbasak, A., Morrison, P. F., Dedrick, R. L., and Oldfield, E. H. (1994). Convection-enhanced delivery of macromolecules in the brain. *Proc. Natl. Acad. Sci. U.S.A.* 91, 2076–2080.

Brenner, A., Zuniga, R., Sun, J. D., Floyd, J., Part, C. P., Kroll, S., et al. (2018). Hypoxia-activated evofosfamide for treatment of recurrent bevacizumab-refractory glioblastoma: a phase I surgical study. *Neuro-Oncol.* 20, 1231–1239. doi: 10.1093/neuonc/noy015

Brightman, M. W. (2002). The brain's interstitial clefts and their glial walls. *J. Neurocytol.* 31, 595–603.

Cakir, B., Xiang, Y., Tanaka, Y., Kural, M. H., Parent, M., Kang, Y. J., et al. (2019). Engineering of human brain organoids with a functional vascular-like system. *Nat. Methods* 16, 1169–1175. doi: 10.1038/s41592-019-0586-5

Chaicharoenaudomrung, N., Kunhorm, P., Promjantuek, W., Rujanapun, N., Heebkaew, N., Soraksa, N., et al. (2020). Transcriptomic profiling of 3D glioblastoma tumoroids for the identification of mechanisms involved in anticancer drug resistance. *In Vivo* 34, 199–211. doi: 10.21873/invivo.11762

Chen, J., Luo, Y., Hui, H., Cai, T., Huang, H., Yang, F., et al. (2017). CD146 coordinates brain endothelial cell–pericyte communication for blood–brain barrier development. *Proc. Natl. Acad. Sci. U.S.A.* 114, E7622–E7631.

Cheng, L., Huang, Z., Zhou, W., Wu, Q., Donnola, S., Liu, J. K., et al. (2013). Glioblastoma stem cells generate vascular pericytes to support vessel function and tumor growth. *Cell* 153, 139–152. doi: 10.1016/j.cell.2013.02.021

Cheslow, L., and Alvarez, J. I. (2016). Glial-endothelial crosstalk regulates blood–brain barrier function. *Curr. Opin. Pharmacol.* 26, 39–46. doi: 10.1016/j.coph.2015.09.010

Chinot, O. L., Wick, W., Mason, W., Henriksson, R., Saran, F., Nishikawa, R., et al. (2014). Bevacizumab plus radiotherapy–temozolomide for newly diagnosed glioblastoma. *N. Engl. J. Med.* 370, 709–722.

Chouleur, T., Tremblay, M. L., and Bikfalvi, A. (2020). Mechanisms of invasion in glioblastoma. *Curr. Opin. Oncol.* 32, 631–639. doi: 10.1097/cco.0000000000000679

Chow, B. W., and Gu, C. (2017). Gradual suppression of transcytosis governs functional blood-retinal barrier formation. *Neuron* 93, 1325–1333.e3.

Cloughesy, T., Finocchiaro, G., Belda-Iniesta, C., Recht, L., Brandes, A. A., Pineda, E., et al. (2017). Randomized, double-blind, placebo-controlled, multicenter Phase II study of onartuzumab plus bevacizumab versus placebo plus bevacizumab in patients with recurrent glioblastoma: efficacy, safety, and hepatocyte growth factor and O6-Methylguanine-DNA Methyltransferase biomarker analyses. *J. Clin. Oncol. Off. J. Am. Soc. Clin. Oncol.* 35, 343–351. doi: 10.1200/jco.2015.64.7685

Cloughesy, T. F., Drappatz, J., de Groot, J., Prados, M. D., Reardon, D. A., Schiff, D., et al. (2018). Phase II study of cabozantinib in patients with progressive glioblastoma: subset analysis of patients with prior antiangiogenic therapy. *Neuro-Oncol.* 20, 259–267. doi: 10.1093/neuonc/nox151

Coomber, B. L., and Stewart, P. A. (1985). Morphometric analysis of CNS microvascular endothelium. *Microvasc. Res.* 30, 99–115. doi: 10.1016/0026-2862(85)90042-1

Courtoy, P. J., and Boyles, J. (1983). Fibronectin in the microvasculature: localization in the pericyte-endothelial interstitium. *J. Ultrastruct. Res.* 83, 258–273. doi: 10.1016/s0022-5320(83)90133-8

Cuevas, P., Gutierrez-Diaz, J. A., Reimers, D., Dujovny, M., Diaz, F. G., and Ausman, J. I. (1984). Pericyte endothelial gap junctions in human cerebral capillaries. *Anat. Embryol. (Berl.)* 170, 155–159. doi: 10.1007/bf00319000

Cui, H., Esworthy, T., Zhou, X., Hann, S. Y., Glazer, R. I., Li, R., et al. (2020). Engineering a novel 3D printed vascularized tissue model for investigating breast cancer metastasis to bone. *Adv. Healthc. Mater.* 9:e1900924.

Daneman, R., Zhou, L., Agalliu, D., Cahoy, J. D., Kaushal, A., and Barres, B. A. (2010a). The mouse blood-brain barrier transcriptome: a new resource for

understanding the development and function of brain endothelial cells. *PLoS One* 5:e13741. doi: 10.1371/journal.pone.0013741

Daneman, R., Zhou, L., Kebede, A. A., and Barres, B. A. (2010b). Pericytes are required for blood-brain barrier integrity during embryogenesis. *Nature* 468, 562–566. doi: 10.1038/nature09513

Daubon, T., Léon, C., Clarke, K., Andrique, L., Salabert, L., Darbo, E., et al. (2019). Deciphering the complex role of thrombospondin-1 in glioblastoma development. *Nat. Commun.* 10:1146.

De Bonis, P., Anile, C., Pompucci, A., Fiorentino, A., Balducci, M., Chiesa, S., et al. (2012). Safety and efficacy of Gliadel wafers for newly diagnosed and recurrent glioblastoma. *Acta Neurochir. (Wien)* 154, 1371–1378. doi: 10.1007/s00701-012-1413-2

Del Maschio, A., De Luigi, A., Martin-Padura, I., Brockhaus, M., Bartfai, T., Fruscella, P., et al. (1999). Leukocyte recruitment in the cerebrospinal fluid of mice with experimental meningitis is inhibited by an antibody to junctional adhesion molecule (Jam). *J. Exp. Med.* 190, 1351–1356. doi: 10.1084/jem.190.9.1351

Duan, J.-X., Jiao, H., Kaizerman, J., Stanton, T., Evans, J. W., Lan, L., et al. (2008). Potent and highly selective hypoxia-activated achiral phosphoramidate mustards as anticancer drugs. *J. Med. Chem.* 51, 2412–2420. doi: 10.1021/jm701028q

Eklund, L., Bry, M., and Alitalo, K. (2013). Mouse models for studying angiogenesis and lymphangiogenesis in cancer. *Mol. Oncol.* 7, 259–282. doi: 10.1016/j.molonc.2013.02.007

Engelhardt, B., and Coisne, C. (2011). Fluids and barriers of the CNS establish immune privilege by confining immune surveillance to a two-walled castle moat surrounding the CNS castle. *Fluids Barriers CNS* 8:4.

Engelhardt, B., and Ransohoff, R. M. (2012). Capture, crawl, cross: the T cell code to breach the blood-brain barriers. *Trends Immunol.* 33, 579–589. doi: 10.1016/j.it.2012.07.004

Galanis, E., Anderson, S. K., Twohy, E. L., Carrero, X. W., Dixon, J. G., Tran, D. D., et al. (2019). A phase 1 and randomized, placebo-controlled phase 2 trial of bevacizumab plus dasatinib in patients with recurrent glioblastoma: alliance/North Central Cancer Treatment Group N0872. *Cancer* 125, 3790–3800. doi: 10.1002/cncr.32340

Ghiaseddin, A., Reardon, D., Massey, W., Mannerino, A., Lipp, E. S., Herndon, J. E. I. I., et al. (2018). Phase II study of bevacizumab and vorinostat for patients with recurrent World Health Organization grade 4 malignant glioma. *Oncologist* 23, 157–e21. doi: 10.1634/theoncologist.2017-0501

Gilbert, M. R., Dignam, J. J., Armstrong, T. S., Wefel, J. S., Blumenthal, D. T., Vogelbaum, M. A., et al. (2014). A randomized trial of bevacizumab for newly diagnosed glioblastoma. *N. Engl. J. Med.* 370, 699–708. doi: 10.1056/NEJMoa1308573

Goldshmit, Y., Galea, M. P., Bartlett, P. F., and Turnley, A. M. (2006). EphA4 regulates central nervous system vascular formation. *J. Comp. Neurol.* 497, 864–875. doi: 10.1002/cne.21029

Goldshmit, Y., Homman-Ludiye, J., and Bourne, J. A. (2014). EphA4 is associated with multiple cell types in the marmoset primary visual cortex throughout the lifespan. *Eur. J. Neurosci.* 39, 1419–1428. doi: 10.1111/ejn.12514

Gravina, G. L., Mancini, A., Marampon, F., Colapietro, A., Delle Monache, S., Sferra, R., et al. (2017). The brain-penetrating CXCR4 antagonist, PRX177561, increases the antitumor effects of bevacizumab and sunitinib in preclinical models of human glioblastoma. *J. Hematol. Oncol.* 10:5. doi: 10.1186/s13045-016-0377-8

Grill, J., Massimino, M., Bouffet, E., Azizi, A. A., McCowage, G., Cañete, A., et al. (2018). Phase II, open-label, randomized, multicenter trial (HERBY) of bevacizumab in pediatric patients with newly diagnosed high-grade glioma. *J. Clin. Oncol. Off. J. Am. Soc. Clin. Oncol.* 36, 951–958. doi: 10.1200/JCO.2017.76.0611

Griveau, A., Seano, G., Shelton, S. J., Kupp, R., Jahangiri, A., Obernier, K., et al. (2018). A glial signature and Wnt7 signaling regulate glioma-vascular interactions and tumor microenvironment. *Cancer Cell* 33, 874.e–889.e. doi: 10.1016/j.ccell.2018.03.020

Guan, X., Hasan, M. N., Maniar, S., Jia, W., and Sun, D. (2018). Reactive astrocytes in glioblastoma multiforme. *Mol. Neurobiol.* 55, 6927–6938. doi: 10.1007/s12035-018-0880-8

Hainsworth, J. D., Becker, K. P., Mekhail, T., Chowdhary, S. A., Eakle, J. F., Wright, D., et al. (2019). Phase I/II study of bevacizumab with BKM120, an oral PI3K inhibitor, in patients with refractory solid tumors (phase I) and relapsed/refractory glioblastoma (phase II). *J. Neurooncol.* 144, 303–311. doi: 10.1007/s11060-019-03227-7

Hall, C. N., Reynell, C., Gesslein, B., Hamilton, N. B., Mishra, A., Sutherland, B. A., et al. (2014). Capillary pericytes regulate cerebral blood flow in health and disease. *Nature* 508, 55–60. doi: 10.1038/nature13165

Hara, Y., Nomura, T., Yoshizaki, K., Frisén, J., and Osumi, N. (2010). Impaired hippocampal neurogenesis and vascular formation in ephrin-A5-deficient mice. *Stem Cells Dayt. Ohio* 28, 974–983. doi: 10.1002/stem.427

Hashizume, R., Ozawa, T., Gryaznov, S. M., Bollen, A. W., Lamborn, K. R., et al. (2008). New therapeutic approach for brain tumors: Intranasal delivery of telomerase inhibitor GRN163. *Neuro-Oncol.* 10, 112–120. doi: 10.1215/15228517-2007-052

Heide, M., Huttner, W. B., and Mora-Bermúdez, F. (2018). Brain organoids as models to study human neocortex development and evolution. *Curr. Opin. Cell Biol.* 55, 8–16. doi: 10.1016/j.ceb.2018.06.006

Herrlinger, U., Schäfer, N., Steinbach, J. P., Weyerbrock, A., Hau, P., Goldbrunner, R., et al. (2016). Bevacizumab plus irinotecan versus temozolomide in newly diagnosed O6-methylguanine-DNA methyltransferase nonmethylated glioblastoma: the randomized GLARIUS trial. *J. Clin. Oncol. Off. J. Am. Soc. Clin. Oncol.* 34, 1611–1619. doi: 10.1200/JCO.2015.63.4691

Iadecola, C. (2017). The neurovascular unit coming of age: a journey through neurovascular coupling in health and disease. *Neuron* 96, 17–42. doi: 10.1016/j.neuron.2017.07.030

Idbaih, A., Canney, M., Belin, L., Desseaux, C., Vignot, A., Bouchoux, G., et al. (2019). Safety and feasibility of repeated and transient blood–brain barrier disruption by pulsed ultrasound in patients with recurrent glioblastoma. *Clin. Cancer Res.* 25, 3793–3801. doi: 10.1158/1078-0432.CCR-18-3643

Igarashi, Y., Utsumi, H., Chiba, H., Yamada-Sasamori, Y., Tobioka, H., Kamimura, Y., et al. (1999). Glial cell line-derived neurotrophic factor induces barrier function of endothelial cells forming the blood-brain barrier. *Biochem. Biophys. Res. Commun.* 261, 108–112. doi: 10.1006/bbrc.1999.0992

Iwamoto, N., Higashi, T., and Furuse, M. (2014). Localization of angulin-1/LSR and tricellulin at tricellular contacts of brain and retinal endothelial cells in vivo. *Cell Struct. Funct.* 39, 1–8. doi: 10.1247/csf.13015

Kalpathy-Cramer, J., Chandra, V., Da, X., Ou, Y., Emblem, K. E., Muzikansky, A., et al. (2017). Phase II study of tivozanib, an oral VEGFR inhibitor, in patients with recurrent glioblastoma. *J. Neurooncol.* 131, 603–610. doi: 10.1007/s11060-016-2332-5

Kang, W., Kim, S. H., Cho, H. J., Jin, J., Lee, J., Joo, K. M., et al. (2015). Talin1 targeting potentiates anti-angiogenic therapy by attenuating invasion and stem-like features of glioblastoma multiforme. *Oncotarget* 6, 27239–27251. doi: 10.18632/oncotarget.4835

Kannan, R. Y., Salacinski, H. J., Butler, P. E., Hamilton, G., and Seifalian, A. M. (2005). Current status of prosthetic bypass grafts: a review. *J. Biomed. Mater. Res. B Appl. Biomater.* 74B, 570–581. doi: 10.1002/jbm.b.30247

Kobrinsky, N. L., Packer, R. J., Boyett, J. M., Stanley, P., Shiminski-Maher, T., Allen, J. C., et al. (1999). Etoposide with or without mannitol for the treatment of recurrent or primarily unresponsive brain tumors: a Children's Cancer Group Study, CCG-9881. *J. Neurooncol.* 45, 47–54. doi: 10.1023/A:1006333811437

Kooij, G., Kopplin, K., Blasig, R., Stuiver, M., Koning, N., Goverse, G., et al. (2014). Disturbed function of the blood-cerebrospinal fluid barrier aggravates neuro-inflammation. *Acta Neuropathol. (Berl.)* 128, 267–277. doi: 10.1007/s00401-013-1227-1

Kröger, S., Wolburg, H., and Warth, A. (2004). Redistribution of aquaporin-4 in human glioblastoma correlates with loss of agrin immunoreactivity from brain capillary basal laminae. *Acta Neuropathol. (Berl.)* 107, 311–318. doi: 10.1007/s00401-003-0812-0

Kronstein, R., Seebach, J., Grossklaus, S., Minten, C., Engelhardt, B., Drab, M., et al. (2012). Caveolin-1 opens endothelial cell junctions by targeting catenins. *Cardiovasc. Res.* 93, 130–140. doi: 10.1093/cvr/cvr256

Lakka, S. S., and Rao, J. S. (2008). Antiangiogenic therapy in brain tumors. *Expert Rev. Neurother.* 8, 1457–1473. doi: 10.1586/14737175.8.10.1457

Langhans, S. A. (2018). Three-dimensional in vitro cell culture models in drug discovery and drug repositioning. *Front. Pharmacol.* 9:6. doi: 10.3389/fphar.2018.00006

Langlet, F., Mullier, A., Bouret, S. G., Prevot, V., and Dehouck, B. (2013). Tanycyte-like cells form a blood-cerebrospinal fluid barrier in the circumventricular

organs of the mouse brain. *J. Comp. Neurol.* 521, 3389–3405. doi: 10.1002/cne.23355

Larson, D. M., Carson, M. P., and Haudenschild, C. C. (1987). Junctional transfer of small molecules in cultured bovine brain microvascular endothelial cells and pericytes. *Microvasc. Res.* 34, 184–199. doi: 10.1016/0026-2862(87)90052-5

Lee, E. Q., Reardon, D. A., Schiff, D., Drappatz, J., Muzikansky, A., Grimm, S. A., et al. (2015). Phase II study of panobinostat in combination with bevacizumab for recurrent glioblastoma and anaplastic glioma. *Neuro-Oncol.* 17, 862–867. doi: 10.1093/neuonc/nou350

Liebner, S., Dijkhuizen, R. M., Reiss, Y., Plate, K. H., Agalliu, D., and Constantin, G. (2018). Functional morphology of the blood–brain barrier in health and disease. *Acta Neuropathol. (Berl.)* 135, 311–336. doi: 10.1007/s00401-018-1815-1

Lien, C. F., Mohanta, S. K., Frontczak-Baniewicz, M., Swinny, J. D., Zablocka, B., and Górecki, D. C. (2012). Absence of glial α-dystrobrevin causes abnormalities of the blood-brain barrier and progressive brain edema. *J. Biol. Chem.* 287, 41374–41385. doi: 10.1074/jbc.M112.400044

Lokman, N. A., Elder, A. S. F., Ricciardelli, C., and Oehler, M. K. (2012). Chick chorioallantoic membrane (CAM) assay as an in vivo model to study the effect of newly identified molecules on ovarian cancer invasion and metastasis. *Int. J. Mol. Sci.* 13, 9959–9970. doi: 10.3390/ijms13089959

Lombardi, G., De Salvo, G. L., Brandes, A. A., Eoli, M., Rudà, R., Faedi, M., et al. (2019). Regorafenib compared with lomustine in patients with relapsed glioblastoma (REGOMA): a multicentre, open-label, randomised, controlled, phase 2 trial. *Lancet Oncol.* 20, 110–119. doi: 10.1016/S1470-2045(18)30675-2

Louis, D. N., Perry, A., Reifenberger, G., von Deimling, A., Figarella-Branger, D., Cavenee, W. K., et al. (2016). The 2016 World Health Organization classification of tumors of the central nervous system: a summary. *Acta Neuropathol. (Berl.)* 131, 803–820. doi: 10.1007/s00401-016-1545-1

Ma, L., Zhang, B., Zhou, C., Li, Y., Li, B., Yu, M., et al. (2018). The comparison genomics analysis with glioblastoma multiforme (GBM) cells under 3D and 2D cell culture conditions. *Colloids Surf. B Biointerfaces* 172, 665–673. doi: 10.1016/j.colsurfb.2018.09.034

Ma, S., Kwon, H. J., and Huang, Z. (2012). A functional requirement for astroglia in promoting blood vessel development in the early postnatal brain. *PLoS One* 7:e48001. doi: 10.1371/journal.pone.0048001

Mahringer, A., and Fricker, G. (2016). ABC transporters at the blood-brain barrier. *Expert Opin. Drug Metab. Toxicol.* 12, 499–508. doi: 10.1517/17425255.2016.1168804

Massa, S., Sakr, M. A., Seo, J., Bandaru, P., Arneri, A., Bersini, S., et al. (2017). Bioprinted 3D vascularized tissue model for drug toxicity analysis. *Biomicrofluidics* 11:044109. doi: 10.1063/1.4994708

Mathiisen, T. M., Lehre, K. P., Danbolt, N. C., and Ottersen, O. P. (2010). The perivascular astroglial sheath provides a complete covering of the brain microvessels: an electron microscopic 3D reconstruction. *Glia* 58, 1094–1103. doi: 10.1002/glia.20990

McCoy, M. G., Nyanyo, D., Hung, C. K., Goerger, J. P., Zipfel, W. R., Williams, R. M., et al. (2019). Endothelial cells promote 3D invasion of GBM by IL-8-dependent induction of cancer stem cell properties. *Sci. Rep.* 9:9069. doi: 10.1038/s41598-019-45535-y

Menezes, M. J., McClenahan, F. K., Leiton, C. V., Aranmolate, A., Shan, X., and Colognato, H. (2014). The extracellular matrix protein laminin α2 regulates the maturation and function of the blood-brain barrier. *J. Neurosci. Off. J. Soc. Neurosci.* 34, 15260–15280. doi: 10.1523/JNEUROSCI.3678-13.2014

Meng, W., and Takeichi, M. (2009). Adherens junction: molecular architecture and regulation. *Cold Spring Harb. Perspect. Biol.* 1:a002899. doi: 10.1101/cshperspect.a002899

Miranda-Gonçalves, V., Bezerra, F., Costa-Almeida, R., Freitas-Cunha, M., Soares, R., Martinho, O., et al. (2017). Monocarboxylate transporter 1 is a key player in glioma-endothelial cell crosstalk. *Mol. Carcinog.* 56, 2630–2642. doi: 10.1002/mc.22707

Mizee, M. R., Nijland, P. G., van der Pol, S. M., Drexhage, J. A., van Het Hof, B., Mebius, R., et al. (2014). Astrocyte-derived retinoic acid: a novel regulator of blood-brain barrier function in multiple sclerosis. *Acta Neuropathol. (Berl.)* 128, 691–703. doi: 10.1007/s00401-014-1335-6

Musah-Eroje, A., and Watson, S. (2019). A novel 3D in vitro model of glioblastoma reveals resistance to temozolomide which was potentiated by hypoxia. *J. Neurooncol.* 142, 231–240. doi: 10.1007/s11060-019-03107-0

Nagelhus, E. A., and Ottersen, O. P. (2013). Physiological roles of aquaporin-4 in brain. *Physiol. Rev.* 93, 1543–1562. doi: 10.1152/physrev.00011.2013

Nestor, M. W., Mok, L.-P., Tulapurkar, M. E., and Thompson, S. M. (2007). Plasticity of neuron-glial interactions mediated by astrocytic EphARs. *J. Neurosci. Off. J. Soc. Neurosci.* 27, 12817–12828. doi: 10.1523/JNEUROSCI.2442-07.2007

NICE (2018). *Recommendations | Brain Tumours (Primary) and Brain Metastases in Adults | Guidance | NICE*. Available online at: https://www.nice.org.uk/guidance/ng99/chapter/Recommendations (accessed July 11, 2018).

Nitta, T., Hata, M., Gotoh, S., Seo, Y., Sasaki, H., Hashimoto, N., et al. (2003). Size-selective loosening of the blood-brain barrier in claudin-5-deficient mice. *J. Cell Biol.* 161, 653–660. doi: 10.1083/jcb.200302070

Niu, G., Sapoznik, E., and Soker, S. (2014). Bioengineered blood vessels. *Expert Opin. Biol. Ther.* 14, 403–410. doi: 10.1517/14712598.2014.880419

Oberoi, R. K., Parrish, K. E., Sio, T. T., Mittapalli, R. K., Elmquist, W. F., and Sarkaria, J. N. (2016). Strategies to improve delivery of anticancer drugs across the blood–brain barrier to treat glioblastoma. *Neuro-Oncol.* 18, 27–36. doi: 10.1093/neuonc/nov164

Odia, Y., Sul, J., Shih, J. H., Kreisl, T. N., Butman, J. A., Iwamoto, F. M., et al. (2016). A Phase II trial of tandutinib (MLN 518) in combination with bevacizumab for patients with recurrent glioblastoma. *CNS Oncol.* 5, 59–67. doi: 10.2217/cns-2015-0010

Ohtsuki, S., Yamaguchi, H., Katsukura, Y., Asashima, T., and Terasaki, T. (2008). mRNA expression levels of tight junction protein genes in mouse brain capillary endothelial cells highly purified by magnetic cell sorting. *J. Neurochem.* 104, 147–154.

Ommaya, A. K. (1984). Implantable devices for chronic access and drug delivery to the central nervous system. *Cancer Drug Deliv.* 1, 169–179. doi: 10.1089/cdd.1984.1.169

Peck, M., Dusserre, N., McAllister, T. N., and L'Heureux, N. (2011). Tissue engineering by self-assembly. *Mater. Today* 14, 218–224. doi: 10.1016/S1369-7021(11)70117-1

Pellerin, L., Pellegri, G., Bittar, P. G., Charnay, Y., Bouras, C., Martin, J. L., et al. (1998). Evidence supporting the existence of an activity-dependent astrocyte-neuron lactate shuttle. *Dev. Neurosci.* 20, 291–299. doi: 10.1159/000017324

Pfaff, D., Fiedler, U., and Augustin, H. G. (2006). Emerging roles of the Angiopoietin-Tie and the ephrin-Eph systems as regulators of cell trafficking. *J. Leukoc. Biol.* 80, 719–726. doi: 10.1189/jlb.1105652

Philips, A., Henshaw, D. L., Lamburn, G., and O'Carroll, M. J. (2018). Brain tumours: rise in glioblastoma multiforme incidence in England 1995–2015 suggests an adverse environmental or lifestyle factor. *J. Environ. Public Health* 2018, 1–10. doi: 10.1155/2018/7910754 doi: 10.1155/2018/2170208 doi: 10.1155/2018/2170208

Piao, Y., Park, S. Y., Henry, V., Smith, B. D., Tiao, N., Flynn, D. L., et al. (2016). Novel MET/TIE2/VEGFR2 inhibitor altiratinib inhibits tumor growth and invasiveness in bevacizumab-resistant glioblastoma mouse models. *Neuro-Oncol.* 18, 1230–1241. doi: 10.1093/neuonc/now030

Podjaski, C., Alvarez, J. I., Bourbonniere, L., Larouche, S., Terouz, S., Bin, J. M., et al. (2015). Netrin 1 regulates blood–brain barrier function and neuroinflammation. *Brain* 138, 1598–1612. doi: 10.1093/brain/awv092

Preston, J. E., Joan Abbott, N., and Begley, D. J. (2014). Transcytosis of macromolecules at the blood-brain barrier. *Adv. Pharmacol. San Diego Calif.* 71, 147–163. doi: 10.1016/bs.apha.2014.06.001

Raizer, J. J., Giglio, P., Hu, J., Groves, M., Merrell, R., Conrad, C., et al. (2016). A phase II study of bevacizumab and erlotinib after radiation and temozolomide in MGMT unmethylated GBM patients. *J. Neurooncol.* 126, 185–192. doi: 10.1007/s11060-015-1958-z

Reardon, D. A., Brandes, A. A., Omuro, A., Mulholland, P., Lim, M., Wick, A., et al. (2020). Effect of nivolumab vs bevacizumab in patients with recurrent glioblastoma: the checkmate 143 phase 3 Randomized clinical trial. *JAMA Oncol.* 6:1003. doi: 10.1001/jamaoncol.2020.1024

Reardon, D. A., Lassman, A. B., Schiff, D., Yunus, S. A., Gerstner, E. R., Cloughesy, T. F., et al. (2018). Phase 2 and biomarker study of trebananib, an angiopoietin-blocking peptibody, with and without bevacizumab for patients with recurrent glioblastoma. *Cancer* 124, 1438–1448. doi: 10.1002/cncr.31172

Reyes-Botero, G., Cartalat-Carel, S., Chinot, O. L., Barrie, M., Taillandier, L., Beauchesne, P., et al. (2018). Temozolomide plus bevacizumab in elderly patients with newly diagnosed glioblastoma and poor performance status:

an ANOCEF Phase II trial (ATAG). *Oncologist* 23, 524–e44. doi: 10.1634/theoncologist.2017-0689

Rong, X., Huang, B., Qiu, S., Li, X., He, L., and Peng, Y. (2016). Tumor-associated macrophages induce vasculogenic mimicry of glioblastoma multiforme through cyclooxygenase-2 activation. *Oncotarget* 7, 83976–83986. doi: 10.18632/oncotarget.6930

Safa, A. R., Saadatzadeh, M. R., Cohen-Gadol, A. A., Pollok, K. E., and Bijangi-Vishehsaraei, K. (2015). Glioblastoma stem cells (GSCs) epigenetic plasticity and interconversion between differentiated non-GSCs and GSCs. *Genes Dis.* 2, 152–163. doi: 10.1016/j.gendis.2015.02.001

Sandmann, T., Bourgon, R., Garcia, J., Li, C., Cloughesy, T., Chinot, O. L., et al. (2015). Patients with proneural glioblastoma may derive overall survival benefit from the addition of bevacizumab to first-line radiotherapy and temozolomide: retrospective analysis of the AVAglio trial. *J. Clin. Oncol. Off. J. Am. Soc. Clin. Oncol.* 33, 2735–2744. doi: 10.1200/JCO.2015.61.5005

Scherer, H. J. (1940). THE FORMS OF GROWTH IN GLIOMAS AND THEIR PRACTICAL SIGNIFICANCE. *Brain* 63, 1–35. doi: 10.1093/brain/63.1.1

Seo, B. R., DelNero, P., and Fischbach, C. (2014). In vitro models of tumor vessels and matrix: engineering approaches to investigate transport limitations and drug delivery in cancer. *Adv. Drug Delivery Rev.* 6, 205–216. doi: 10.1016/j.addr.2013.11.011

Serres, E., Debarbieux, F., Stanchi, F., Maggiorella, L., Grall, D., Turchi, L., et al. (2014). Fibronectin expression in glioblastomas promotes cell cohesion, collective invasion of basement membrane in vitro and orthotopic tumor growth in mice. *Oncogene* 33, 3451–3462. doi: 10.1038/onc.2013.305

Sharma, M., Schilero, C., Peereboom, D. M., Hobbs, B. P., Elson, P., Stevens, G. H. J., et al. (2019). Phase II study of Dovitinib in recurrent glioblastoma. *J. Neurooncol.* 144, 359–368. doi: 10.1007/s11060-019-03236-6

Shi, Y., Sun, L., Wang, M., Liu, J., Zhong, S., Li, R., et al. (2020). Vascularized human cortical organoids (vOrganoids) model cortical development in vivo. *PLoS Biol.* 18:e3000705. doi: 10.1371/journal.pbio.3000705

Shin, Y., Han, S., Jeon, J. S., Yamamoto, K., Zervantonakis, I. K., Sudo, R., et al. (2012). Microfluidic assay for simultaneous culture of multiple cell types on surfaces or within hydrogels. *Nat. Protoc.* 7, 1247–1259. doi: 10.1038/nprot.2012.051

Silvestri, V. L., Henriet, E., Linville, R. M., Wong, A. D., Searson, P. C., and Ewald, A. J. (2020). A tissue-engineered 3D microvessel model reveals the dynamics of mosaic vessel formation in breast cancer. *Cancer Res.* 80:canres.1564.2019. doi: 10.1158/0008-5472.CAN-19-1564

Sohet, F., Lin, C., Munji, R. N., Lee, S. Y., Ruderisch, N., Soung, A., et al. (2015). LSR/angulin-1 is a tricellular tight junction protein involved in blood-brain barrier formation. *J. Cell Biol.* 208, 703–711. doi: 10.1083/jcb.201410131

Song, H.-H. G., Rumma, R. T., Ozaki, C. K., Edelman, E. R., and Chen, C. S. (2018). Vascular tissue engineering: progress, challenges, and clinical promise. *Cell Stem Cell* 22, 340–354. doi: 10.1016/j.stem.2018.02.009

Song, J. W., and Munn, L. L. (2011). Fluid forces control endothelial sprouting. *Proc. Natl. Acad. Sci. U.S.A.* 108, 15342–15347. doi: 10.1073/pnas.1105316108

Suri, C., Jones, P. F., Patan, S., Bartunkova, S., Maisonpierre, P. C., Davis, S., et al. (1996). Requisite role of angiopoietin-1, a ligand for the TIE2 receptor, during embryonic angiogenesis. *Cell* 87, 1171–1180. doi: 10.1016/s0092-8674(00)81813-9

Sweeney, M. D., Ayyadurai, S., and Zlokovic, B. V. (2016). Pericytes of the neurovascular unit: key functions and signaling pathways. *Nat. Neurosci.* 19, 771–783. doi: 10.1038/nn.4288

Sweeney, M. D., Zhao, Z., Montagne, A., Nelson, A. R., and Zlokovic, B. V. (2019). Blood-brain barrier: from physiology to disease and back. *Physiol. Rev.* 99, 21–78.

Valdor, R., García-Bernal, D., Bueno, C., Ródenas, M., Moraleda, J. M., Macian, F., et al. (2017). Glioblastoma progression is assisted by induction of immunosuppressive function of pericytes through interaction with tumor cells. *Oncotarget* 8, 68614–68626. doi: 10.18632/oncotarget.19804

Vegran, F., Boidot, R., Michiels, C., Sonveaux, P., and Feron, O. (2011). Lactate influx through the endothelial cell monocarboxylate transporter MCT1 supports an NF- B/IL-8 pathway that drives tumor angiogenesis. *Cancer Res.* 71, 2550–2560. doi: 10.1158/0008-5472.can-10-2828

Wang, R., Chadalavada, K., Wilshire, J., Kowalik, U., Hovinga, K. E., Geber, A., et al. (2010). Glioblastoma stem-like cells give rise to tumour endothelium. *Nature* 468, 829–833. doi: 10.1038/nature09624

Wang, X.-Y., Jin, Z. H., Gan, B. W., Lv, S. W., Xie, M., and Huang, W. H. (2014). Engineering interconnected 3D vascular networks in hydrogels using molded sodium alginate lattice as the sacrificial template. *Lab. Chip* 14, 2709–2716. doi: 10.1039/c4lc00069b

Watkins, S., Robel, S., Kimbrough, I. F., Robert, S. M., Ellis-Davies, G., Sontheimer, H., et al. (2014). Disruption of astrocyte–vascular coupling and the blood–brain barrier by invading glioma cells. *Nat. Commun.* 5:4196.

Weathers, S.-P., Han, X., Liu, D. D., Conrad, C. A., Gilbert, M. R., Loghin, M. E., et al. (2016). A randomized phase II trial of standard dose bevacizumab versus low dose bevacizumab plus lomustine (CCNU) in adults with recurrent glioblastoma. *J. Neurooncol.* 129, 487–494. doi: 10.1007/s11060-016-2195-9

Weinberg, C. B., and Bell, E. (1986). A blood vessel model constructed from collagen and cultured vascular cells. *Science* 231, 397–400. doi: 10.1126/science.2934816

Wen, P. Y., Drappatz, J., de Groot, J., Prados, M. D., Reardon, D. A., Schiff, D., et al. (2018). Phase II study of cabozantinib in patients with progressive glioblastoma: subset analysis of patients naive to antiangiogenic therapy. *Neuro-Oncol* 20, 249–258. doi: 10.1093/neuonc/nox154

Wick, W., Gorlia, T., Bendszus, M., Taphoorn, M., Sahm, F., Harting, I., et al. (2017). Lomustine and bevacizumab in progressive glioblastoma. *N. Engl. J. Med.* 377, 1954–1963.

Wirsching, H.-G., Tabatabai, G., Roelcke, U., Hottinger, A. F., Jörger, F., Schmid, A., et al. (2018). Bevacizumab plus hypofractionated radiotherapy versus radiotherapy alone in elderly patients with glioblastoma: the randomized, open-label, phase II ARTE trial. *Ann. Oncol. Off. J. Eur. Soc. Med. Oncol.* 29, 1423–1430.

Wolburg, H., Noell, S., Fallier-Becker, P., Mack, A. F., and Wolburg-Buchholz, K. (2012). The disturbed blood–brain barrier in human glioblastoma. *Mol. Aspects Med.* 33, 579–589.

Zhao, Y.-L., Song, J.-N., and Zhang, M. (2014). Role of caveolin-1 in the biology of the blood-brain barrier. *Rev. Neurosci.* 25, 247–254.

Zhou, Y., Wang, Y., Tischfield, M., Williams, J., Smallwood, P. M., Rattner, A., et al. (2014). Canonical WNT signaling components in vascular development and barrier formation. *J. Clin. Invest.* 124, 3825–3846.

Zong, H., Verhaak, R. G., and Canoll, P. (2012). The cellular origin for malignant glioma and prospects for clinical advancements. *Expert Rev. Mol. Diagn.* 12, 383–394.

**Conflict of Interest:** The authors declare that the research was conducted in the absence of any commercial or financial relationships that could be construed as a potential conflict of interest.

frontiers in Physiology

REVIEW
published: 09 March 2021
doi: 10.3389/fphys.2021.624928

# Heterogeneity and Dynamics of Vasculature in the Endocrine System During Aging and Disease

*Sina Stucker, Jessica De Angelis and Anjali P. Kusumbe**

*Tissue and Tumor Microenvironments Group, Kennedy Institute of Rheumatology, Nuffield Department of Orthopaedics, Rheumatology and Musculoskeletal Sciences (NDORMS), University of Oxford, Oxford, United Kingdom*

The endocrine system consists of several highly vascularized glands that produce and secrete hormones to maintain body homeostasis and regulate a range of bodily functions and processes, including growth, metabolism and development. The dense and highly vascularized capillary network functions as the main transport system for hormones and regulatory factors to enable efficient endocrine function. The specialized capillary types provide the microenvironments to support stem and progenitor cells, by regulating their survival, maintenance and differentiation. Moreover, the vasculature interacts with endocrine cells supporting their endocrine function. However, the structure and niche function of vasculature in endocrine tissues remain poorly understood. Aging and endocrine disorders are associated with vascular perturbations. Understanding the cellular and molecular cues driving the disease, and age-related vascular perturbations hold potential to manage or even treat endocrine disorders and comorbidities associated with aging. This review aims to describe the structure and niche functions of the vasculature in various endocrine glands and define the vascular changes in aging and endocrine disorders.

**Keywords: endocrine system, vascular niche, aging, vasculature, pancreas**

OPEN ACCESS

***Edited by:***
*Sara Petrillo,*
*University of Turin, Italy*

***Reviewed by:***
*Mihaela Gherghiceanu,*
*Victor Babes National Institute of Pathology (INCDVB), Romania*
*Jamila H. Siamwala,*
*Brown University, United States*

****Correspondence:***
*Anjali P. Kusumbe*
*anjali.kusumbe@kennedy.ox.ac.uk*

***Specialty section:***
*This article was submitted to Vascular Physiology, a section of the journal Frontiers in Physiology*

***Received:*** *01 November 2020*
***Accepted:*** *09 February 2021*
***Published:*** *09 March 2021*

***Citation:***
*Stucker S, De Angelis J and Kusumbe AP (2021) Heterogeneity and Dynamics of Vasculature in the Endocrine System During Aging and Disease. Front. Physiol. 12:624928. doi: 10.3389/fphys.2021.624928*

## INTRODUCTION

The endocrine system is vital for efficient function and communication between different parts of the body and maintenance of homeostasis (Chrousos, 2007). It consists of various organs and glands including the gonads, pancreas and pituitary-, thyroid-, and adrenal- glands. Endocrine organs secrete signals, known as hormones, that are essential for maintaining the homeostasis. Many hormones in the body act on various organs, regulating a wide range of basic bodily functions. For instance, metabolic activities of muscle, adipose tissue, liver and other organs are regulated by insulin, adrenaline and noradrenaline. Sex development and characteristics are regulated by sex hormones such as testosterone and estrogen. Angiotensin and renin regulate blood pressure and renal filtration (Hiller-Sturmhöfel and Bartke, 1998; Kolka and Bergman, 2012; Maurer et al., 2016).

Hormones are transported via the bloodstream to reach their target tissues and cells. When binding to their target receptors, they induce an intracellular signaling cascade that triggers specific cellular responses.

The hypothalamus controls the production and secretion of numerous hormones in the pituitary gland via neuroendocrine signals. These pituitary hormones are subsequently released into the

bloodstream and transported to target glands where they, in turn, trigger the release of hormones that affect organ function. Constant feedback mechanisms along this axis enable the regulation of hormone levels to maintain a stable system. Once hormones from target glands reach a certain concentration in the blood, this initiates a negative feedback loop that inhibits further hormone release in the hypothalamus and pituitary gland (Fliers et al., 2014; Keller-Wood, 2015; Ortiga-Carvalho et al., 2016). There are several regulatory hormonal cascades that rely on feedback mechanisms, including the hypothalamic-pituitary-thyroidal (HPT) or hypothalamic-pituitary-adrenal (HPA) axis (Hiller-Sturmhöfel and Bartke, 1998). Within these axes, hypothalamic releasing hormones such as thyrotropin-releasing hormone (TRH) and corticotrophin-releasing hormone (CRH) stimulate the pituitary gland to produce thyrotropin-stimulating hormone (TSH) and adrenocorticotrophic hormone (ACTH). TSH and ACTH then act on their respective target glands. TSH stimulates the release of thyroid hormones, while ACTH promotes adrenal cortisol production. Both cortisol and ACTH feedback on the hypothalamus and pituitary gland by inhibiting hypothalamic and pituitary hormone release and modulating pituitary and target gland sensitivity to hypothalamic releasing hormones and pituitary hormones, respectively (Hiller-Sturmhöfel and Bartke, 1998; Houshyar et al., 2001). In addition, increased plasma levels of corticosterone and ACTH reduce whole brain expression of glucocorticoid receptors (Houshyar et al., 2001).

The vasculature constitutes the primary transport system for hormones and is crucial for endocrine signaling. The endothelium poses a structural and functional barrier for hormone transport to their target cells. Specific changes in blood vessels (e.g., blood volume and pressure) can affect the release of certain hormones that, themselves can also modulate the endothelium and its function, for instance via controlling the production of growth factors and other hormones that regulate angiogenesis (Hiller-Sturmhöfel and Bartke, 1998; Clapp et al., 2009; Kolka and Bergman, 2012). Vasoactive hormones such as insulin (Tack et al., 1996), estradiol (Gilligan et al., 1994) and testosterone (Yue et al., 1995) are able to modulate the vessel diameter by inducing vasodilation or -constriction, thereby modulating the vascular surface area for exchange (Kolka and Bergman, 2012). The endothelium itself possesses an endocrine function and is often considered as part of the endocrine system. For instance, endothelial cells (EC) release various vasoactive signals such as a nitric oxide (NO) that cause vasorelaxation or vasoconstriction (Henderson and Henderson, 1995).

Most hormones are released in pulses that cause rapid or episodic increase in circulating concentrations. This is important for regulation of target cell function. This pulsatile pattern of hormone release relies on tight temporal control of hormone secretion and entry into the bloodstream (Marie et al., 2011). This is achieved by a complex interplay between the endothelium and endocrine cell that ensures precise temporal uptake and transport of hormones by the blood vessels (Marie et al., 2011). However, the structure and function of the microvasculature in many endocrine glands remain poorly understood. Therefore, this review aims to describe the structure and function of blood vessels in different endocrine glands. Secondly, this review will define vascular perturbations in aging and various endocrine disorders.

## ANATOMY, STRUCTURE, AND HETEROGENEITY OF BLOOD VESSELS IN THE ENDOCRINE GLANDS

Endocrine glands are typically supplied by larger vessels that give rise to a dense network of capillaries. This microvascular network enables close interaction between endocrine cells and the vasculature (Henderson and Moss, 1985; Augustin and Koh, 2017). The specialized microvascular endothelium of endocrine glands is highly permeable to allow rapid hormone release and response to changes in homeostasis (LeCouter et al., 2001). Several endocrine glands, including thyroid and pituitary gland, contain fenestrated capillaries with intracellular pores of varying permeability that enable the exchange of nutrients, hormones and small peptides. Sinusoidal capillaries have larger gaps between ECs that enable the free exchange of water, plasma proteins and other larger solutes. In sinusoidal vessels, the blood flow decelerates to prolong the time of exchange between blood and interstitial fluid (Augustin and Koh, 2017).

Despite advances in understanding the specialization of the vasculature in organs such as liver and bone (Ding et al., 2014; Kusumbe et al., 2014, 2016; Augustin and Koh, 2017), the specialized structure and function of the vascular system in endocrine organs remains elusive. In the following paragraphs, we will briefly describe the anatomical structure of various endocrine glands, including afferent and efferent large vessels and the small capillaries.

### Testis

The testes are part of the male reproductive system. Their main functions include testosterone production and spermatogenesis, which is essential for male fertility. Among other functions, testosterone regulates testicular blood flow and vasomotion (Damber et al., 1992; Collin et al., 1993). The testis is comprised of multiple lobules containing two distinct compartments that are closely interconnected. The interstitial compartment that makes up around 15% of the human testicular volume contains Leydig cells (LCs) that are the main source of testosterone (Maddocks and Setchell, 1988; Ilacqua et al., 2018). The avascular tubular compartment, comprised of convoluted seminiferous tubules, occupies approximately 60-80% of the total testicular volume in humans and is the location of spermatogenesis (Ilacqua et al., 2018). In these tubules, nutrients are transported via the interstitial fluid, the formation of which is regulated by interstitial vessel permeability (Sharpe, 1983; Park et al., 2018). Also, the tubular compartment also contains germ cells and Sertoli cells (SCs) that reside in the basal membrane, extending into the lumen of the seminiferous tubuli. SCs promote germ cell maturation and adult sperm production and form the blood-testis barrier via expression of specialized tight junctional molecules (Ilacqua et al., 2018).

Testicular blood supply is provided via the testicular artery that originates from the abdominal aorta. Each lobule is supplied with blood via one main artery that branches into an elaborate bed of intratesticular arteries and capillaries between the seminiferous tubules. Testicular microvasculature is closely linked to seminiferous tubules and interstitial clusters of LCs (Ergün et al., 1994). Arterioles are enwrapped by LCs and branch into capillaries that innervate the wall of the seminiferous tubules, adapting to the coiling of the tubules (Ergün et al., 1994). Upon leaving the tubular wall, capillaries continue as post-capillary venules that enter an intricate network of veins wrapped around the testicular artery. This intertubular capillary network unites into the testicular vein. The testicular vein leaves the testis, draining into the inferior vena cava and the renal vein (Harrison and Barclay, 1948; Lupiáñz et al., 2012).

The major functions of the testicular vasculature include the regulation of testicular temperature and the transport of nutrients, metabolites and hormones. It transports pituitary gonadotropins to promote testicular spermatogenesis and testosterone production. Conversely, testosterone is transported to various target tissues throughout the body (Lupiáñz et al., 2012; Ilacqua et al., 2018). Moreover, testicular hormones regulate hypothalamic and pituitary output in classically defined feedback mechanisms (Matsumoto and Bremner, 1987; Roser, 2008).

In mammals, testicular microvessels are locally regulated via vasomotion, which is important for testicular function by affecting blood flow, transvascular fluid exchange and interstitial fluid formation (Collin et al., 2000; Lysiak et al., 2000). In combination with the high oxygen consumption due to spermatogenesis demands, the testicular environment contains low oxygen levels. In line with this, rat and mouse testis show constitutive expression of the transcription factor hypoxia-induced factor-1 (HIF-1) that is stabilized under hypoxic conditions and regulates oxygen homeostasis (Powell et al., 2002; Lysiak et al., 2009; Colli et al., 2019). Hypertension has been shown to impair testicular vasomotion, alter vascular morphology and increase HIF-1 expression in rats, suggesting a drop of oxygen levels in hypertensive rat testes (Colli et al., 2019). Moreover, hypertensive rats showed increased vascular endothelial growth factor (VEGF) levels and decreased sperm concentration and quality, indicating an essential role for blood pressure and vasomotion in testicular function (Colli et al., 2019). Additionally, ECs are essential for maintaining the spermatogonial stem cell (SSC) niche, with testicular endothelial cells expressing organ specific growth factors that are essential for maintaining SSC self-renewal. Disruption of key signaling pathways of testicular endothelial cells, such as in down syndrome, can lead to reduced fertility (Bhang et al., 2018).

## Ovary

The ovaries are the female gonads located on either side of the uterus. Anatomically, the ovary can be divided into three zones, the cortex, medulla and hilus. The blood supply in ovaries is provided via the ovarian artery that anastomoses with a branch of the uterine artery. The ovarian artery splits into smaller arterial branches that penetrate the hilus and medulla. Medullary arteries and arterioles show pronounced coiling and branching and form a plexus from which smaller arterioles originate that penetrate the cortex, forming a dense and highly fenestrated vascular network. Ovarian arteries and arterioles are accompanied by veins that merge into the ovarian vein at the hilus. The left ovarian vein drains into the renal vein, and the right ovarian vein drains into the vena cava (Clement, 1987; Kozik, 2000).

Anatomically, the ovary contains a large number of growing follicles in the cortex and medulla that modulate the vasculature according to their changing needs during follicular development (Brown and Russell, 2014). Within each follicle, angiogenesis is regulated independently, forming an individual capillary network (Fraser, 2006). Compared to the relative quiescent nature of the vascular system in the adult, the follicular vasculature is remarkably active, exhibiting dynamic changes in angiogenesis, vascular permeability and blood flow during different stages of the ovarian cycle. Before ovulation, the dominant follicle exhibits increased blow flow and follicular size (Acosta et al., 2003), whereas angiogenesis and vascularity peaks during the formation of the corpus luteum (CL) after ovulation (Brown and Russell, 2014). This continuous cyclic remodeling of the vascular system is crucial for follicular and luteal development and normal ovarian function (Augustin et al., 1995; Brown and Russell, 2014).

Four-dimensional time-lapse imaging of gonad vascularization shows a sex-specific pattern of gonadal vasculature. In the XY gonad, mesonephric blood vessels break down and release mesonephric ECs that migrate into the developing testis to form the major testicular artery. These mechanisms correlate with a rapid morphogenesis and change in direction of testicular blood flow and may increase testicular blood flow to enhance testosterone export during secondary sex determination (Brennan et al., 2002; Coveney et al., 2008). In contrast, the ovary is relatively quiescent. The ovarian vasculature grows from pre-existing vessels independently of mesonephric vasculature (Brennan et al., 2002; Coveney et al., 2008). VEGFA-VEGFR2 signaling plays an important role in gonadal morphogenesis and vasculogenesis and angiogenesis, promoting EC survival, differentiation and migration (Bott et al., 2006, 2010). In the ovary, VEGFA is expressed in granulosa and theca cells in ovarian follicles, and pharmacological inhibition of VEGFA signaling drastically reduces ovarian vascular density by 94% and disrupts follicular development (McFee et al., 2009). Similar experiments in rat testis demonstrate VEGFA expression in SCs. Here, inhibition of VEGFA signaling results in a 90% reduction of vascular density and inhibition of seminiferous tube formation *in vitro* (Bott et al., 2006). Collectively, these studies highlight the importance of VEFA in gonadal morphogenesis and vascularization. During fertility treatment, the ovaries can respond to Human Chorionic Gonadotropin to upregulate VEGF, increasing vascular permeability in ECs, leading to Ovarian hyperstimulation syndrome (Albert et al., 2002; Fang et al., 2020).

## Thyroid Gland

The thyroid gland is one of the largest endocrine glands in the human body and resides in the lower neck, anterolaterally to the trachea and larynx. It is composed of a left and a

right lobe interconnected by an isthmus (Ozgur et al., 2011; Policeni et al., 2012). Blood supply to the thyroid gland is provided by two pairs of inferior and superior thyroid arteries that branch from the thyrocervical arteries and the external carotid arteries, respectively (Loevner, 1996). These inferior and superior thyroid arteries have many anastomoses, creating a rich basket-like capillary network around thyroid follicles (Fujita and Murakami, 1974; Cozzolino et al., 2005). The venous system is formed by a venal plexus that drains blood into the internal jugular vein (via the superior and middle thyroid veins) and the brachiocephalic vein (via the inferior thyroid vein) (Loevner, 1996; Policeni et al., 2012).

Thyroid microvasculature is heavily fenestrated with distinct clusters of fenestrations and depends on VEGF signaling. Inhibition of VEGF via administration of AG013736, a small molecule inhibitor of VEGFRs drastically reduced both capillary vascularity and fenestrations in adult mouse thyroids (Inai et al., 2004; Kamba et al., 2006). Furthermore, thyroid capillaries are supported pericytes that express NG2 or PDGFRβ and consistently wrap along the length of capillaries (Kamba et al., 2006).

The core function of the thyroid gland is the production of essential thyroid hormones, including triiodothyronine ($T_3$) and thyroxine ($T_4$), that are important in metabolic processes. Thyroid hormone secretion is mediated via feedback mechanisms along the hypothalamic-pituitary axis. TRH from the hypothalamus stimulates the release of a TSH by the pituitary that acts on the thyroid gland, promoting the thyroid hormone secretion (Loevner, 1996; Policeni et al., 2012). In the bloodstream, $T_3$ and $T_4$ are transported in their form by carrier proteins such as thyroxine-binding globulin and albumin. Only small fractions of of $T_3$ and $T_4$ exist in an unbound, active form. While $T_4$ is produced entirely in the thyroid gland, only a small proportion of $T_3$ is synthesized here, whereby the majority of $T_3$ synthesis takes place peripherally via conversion of $T_4$ (Loevner, 1996; Vita et al., 2019).

## Pituitary Gland

The pituitary gland, also called hypophysis, is an endocrine gland attached at the base of the hypothalamus. Despite its small size of approximately 10mm, it is essential to maintain homeostasis and hormonal balance and functions as the central endocrine regulator. Anatomically, the pituitary gland consists of two compartments that act as independent endocrine organs with distinct cytology, outputs and regulation (Amar and Weiss, 2003). The adenohypophysis, composed of epithelial cells, consists of the anterior lobe and the pituitary stalk or infundibulum that connects the pituitary gland to the brain. The neurohypophysis describes the posterior lobe that is derived from neural ectoderm. The anterior and posterior lobes are is connected via the pars intermedia (Amar and Weiss, 2003).

The adenohypophysis contains acini with five types of endocrine cells, including corticotropic, somatotropic, mammotropic, gonadotropic and thyrotropic cells that produce ACTH, growth hormone (GH), prolactin (PRL), luteinizing hormone (LH) and follicle-stimulating hormone (FSH), and TSH, respectively (Larkin and Ansorge, 2000). Although most pituitary acini contain a mixture of these endocrine cell types, cellular distribution is not random. While acini in the lateral lobe contain mostly somatotrophs and lactotrophs, corticotrophs are located primarily in the center of the adenohypophysis (Larkin and Ansorge, 2000). The center of the acini is occupied by non-hormone producing follicular-stellate (FS) cells that have extended processes between the endocrine cells and are thought to act as stem cells that give rise to endocrine cells (Horvath and Kovacs, 2002).

The adenohypophysis is considered the most highly vascularized mammalian tissue and is mainly supplied by a set of superior hypophyseal arteries (SHAs) that originate from the internal carotid artery (Page, 1982; Amar and Weiss, 2003). The SHA branches into smaller arteries that anastomose with branches from the contralateral SHA, forming a rich primary plexus of fenestrated capillaries at the top of the pituitary stalk. The fenestrated capillaries merge into venules that subsequently drain into larger portal veins that advance into the anterior lobe to form a secondary plexus. This secondary plexus then drains into efferent lateral hypophyseal veins (Daniel, 1966). Adenohypophyseal hormones in the second plexus can also reflux to the primary plexus to modulate their own synthesis via feedback mechanisms (Page, 1982; Amar and Weiss, 2003).

The neurohypophysis exhibits a very different histology compared to the nested organization of endocrine cells in the adenohypophysis. Instead, it contains axons from hypothalamic neurons, forming a hypothalamic-hypophyseal tract. These axon terminals release their neurosecretory products, including oxytocin and vasopressin and are surrounded by elongated pituicytes (Larkin and Ansorge, 2000; Le Tissier et al., 2017). The neurohypophysis is supplied by a set of inferior hypophyseal arteries (IHAs) that divide into ascending and descending branches that anastomose with the branches on the contralateral side, forming an arterial ring that receives neurosecretory products from the axon terminals (Page, 1982; Lechan and Toni, 2000; Amar and Weiss, 2003).

## Adrenal Gland

The adrenal glands are in the retroperitoneum, located above the kidneys. Through the production of two major types of hormones, catecholamines and steroids, they are an important regulator of metabolic, immune and cardiovascular processes. The adrenal gland can be divided into the cortex and medulla which have distinct histology and function.

The adrenal cortex contains adrenocortical cells that are organized into three subzones (zona glomerulosa, zona fasciculata, zona reticularis). These cortical subzones exhibit characteristic histology and secrete different steroid hormones (Idelman, 1970; Miller and Auchus, 2011; Sun et al., 2018). The zona glomerulosa produces mineralocorticoids that are involved in the regulation of blood pressure and electrolyte balance. Endocrine cells in the zona fasciculata are the source of glucocorticoids which play an important role in metabolism and immune response. Glucocorticoid secretion is regulated by the hypothalamic-pituitary-adrenal (HPA) axis that includes hypothalamic CRH. CRH stimulates pituitary corticotropes to secrete ACTH that ultimately regulates adrenal steroidogenesis.

The zona reticularis secretes androgens. In contrast, the adrenal medulla produces catecholamine hormones, including epinephrine, also known as adrenaline, and norepinephrine that drive the stress response (Bassett and West, 1997; Vinson, 2016; Sun et al., 2018).

The left and right adrenal glands are supplied by the left renal artery and the inferior phrenic artery, respectively. These arteries form an arteriolar plexus that branches into smaller vessels, innervating the medulla and draining into a central vein (Murakami et al., 1989; Bassett and West, 1997). The cortex is supplied by vessels that arise from the capsular plexus and anastomose in the zona glomerulosa. This anastomotic network flows into sinusoidal capillaries that continue through the zona fasciculata before draining into larger sinusoids in the zona reticularis that run into the central vein (Idelman, 1970; Vinson et al., 1985; Bassett and West, 1997).

## Pancreas

The pancreatic gland contains small lobules, containing both endocrine and exocrine tissue and plays a crucial role in digestion and glucose homeostasis. The majority of pancreatic cells are exocrine and are organized in acini that release bicarbonate and digestive enzymes into the duodenum. Endocrine cells makeup only 1-2% of the pancreatic tissue and are clustered in islets of Langerhans scattered throughout the exocrine tissue (In't Veld and Marichal, 2010). Endocrine islet cells can be divided into subtypes including α-, β-, δ-, and PP-cells that secrete distinct metabolic-regulating hormones including glucagon, insulin, somatostatin and pancreatic peptide, respectively (Ballian and Brunicardi, 2007).

The islets of Langerhans are embedded within a dense network of specialized microvessels that is distinct from that of the exocrine pancreas (Goldstein and Davis, 1968; Ballian and Brunicardi, 2007; Olerud et al., 2009). The vascular system in these islets is crucial for islet function and intercellular communication between endocrine and exocrine cells (Ballian and Brunicardi, 2007) and is supported by NG2 or PDGFRβ-expressing pericytes (Kamba et al., 2006). The capillary network in pancreatic islets highly expresses VEGFR2 and VEGFR3 and is dependent on VEGF signaling. Inhibiting VEGF signaling leads to a drastic vascular regression of islet capillaries in adult mice (Kamba et al., 2006). This capillary loss can also be observed in multiple other endocrine glands, including the adrenal, pituitary and thyroid glands. In contrast, the vascular density of many other organs such as heart, brain, retina, lung and skeletal muscle did not show significant changes. These findings indicate a large proportion of VEGF-vascular beds in the endocrine system of adult mice (Kamba et al., 2006).

Under basal conditions, islets are hyperperfused, enabling adjustment to insulin secretion under constant blood flow (Johansson et al., 2005). Each islet is innervated by one to five afferent arterioles that branch into a network of capillaries surrounding endocrine cells to enable a sufficient supply of oxygen and nutrients (Brunicardi et al., 1996). Depending on islet size, venous blood exits either directly into veins or drains into the insulo-portal system to perfuse exocrine pancreatic tissue. In turn, the exocrine tissue can also deliver blood to islets, indicating a bilateral communication between endocrine and exocrine pancreatic tissue (Murakami et al., 1992; Ballian and Brunicardi, 2007).

In rodents, islets show a topographical cytoarchitecture and microcirculation. Blood flows to the islet core, where mostly β-cells reside and exits through venules in the periphery (Murakami et al., 1993; Ballian and Brunicardi, 2007). The human islets of Langerhans, however, do not show a cellular topography. Instead, α-, β-, and δ- cells are scattered throughout the islets without significant clustering (Cabrera et al., 2006). In both humans and rodents, the majority of β-cells are aligned along capillaries, and vascular cells and are organized in a 'rosette-like' structure (Bonner-Weir, 1988; Cabrera et al., 2006; Bonner-Weir et al., 2015).

Furthermore, β-cells exhibit a high degree of phenotypic and functional heterogeneity with multiple studies reporting variations in size, granularity, membrane potential, glucose responsiveness and, insulin secretion (Dean and Matthews, 1968; Cabrera et al., 2006; Wojtusciszyn et al., 2008; Katsuta et al., 2012; Roscioni et al., 2016). This β-cell heterogeneity depends on differences in the pancreatic microenvironment that is created, in part, by distinct islet vascularization and blood perfusion patterns (Ellenbroek et al., 2013). Whole-mount imaging and three-dimensional analysis of islet vascular architecture demonstrate changes in vascularization depending on size and location within the pancreas. For example, larger islets have more vascular penetration points than smaller islets, and central islets are supplied by larger vessels, while peripheral islets may receive capillaries in a polarized fashion (El-Gohary et al., 2012; Roscioni et al., 2016). Likewise, islets also differ in blood perfusion and can be divided into low-blood perfused islets with low oxygen consumption and high blood perfused islets with high oxygen consumption. Multiple *in vivo* studies demonstrate increased β-cell proliferation, insulin secretion and stress susceptibility in high-blood compared to low-blood perfused islets (Olsson and Carlsson, 2011; Lau et al., 2012; Ullsten et al., 2015). ECs from pancreatic islets bidirectionally communicate with β-cells to increase glucose medicated insulin secretion (Johansson et al., 2009). Changes in islet vasculature can influence β-cell mass and are linked with diabetes (Staels et al., 2019).

Alonside vasculature, islets are innervated by the autonomic nervous system that controls islets architecture and maturation. Of interest, genetically or pharmacologically induced ablation of the sympathetic nerve fibers in mice, significantly alters islet architecture and impairs insulin secretion and glucose tolerance (Borden et al., 2013). In contrast to murine islets, human islets are sparsely innervated by autonomic axons, suggesting an indirect regulation of hormone secretion by via sympathetic control of local blood (Rodriguez-Diaz et al., 2011).

# NICHE FUNCTIONS OF BLOOD VESSELS IN THE ENDOCRINE SYSTEM

The microvascular blood vessel network plays an essential role in tissue development and function via its ability to transport nutrients and oxygen to all tissues throughout the body. The

local microvasculature in endocrine glands interacts with local endocrine cells to maintain their function and homeostasis (Colin et al., 2013). ECs achieve this through the secretion of a variety of paracrine factors such as growth factors and cytokines, collectively termed angiocrine signals. Angiocrine signals are crucial for stem and progenitor cell maintenance, differentiation, and function (Colmone and Sipkins, 2008).

This vascular microenvironment is also referred to as vascular niche, and has been described in different organs and tissues. Vascular microenvironments are involved in a wide range of physiological and pathological processes (Augustin and Koh, 2017). In the bone marrow, ECs have been identified as a critical component in the maintenance of the hematopoietic stem cell (HSC) niche (Hooper et al., 2009; Morrison and Scadden, 2014). Here, ECs show a striking morphological and functional diversity and growing evidence suggests an organotypic function of endothelium that regulates development and homeostasis. This diversity enables them to adapt to local needs and supports distinct tissue-specific functions (LeCouter et al., 2001; Cleaver and Melton, 2003; Nolan et al., 2013). However, the role of vascular niches in the endocrine system remains incompletely understood. In the following section, we will describe the niche functions of the vasculature in different endocrine glands (**Table 1**).

## Angiocrine Factors in Testis

In the testis, the convoluted seminiferous tubules are surrounded by interstitial tissue that contains blood vessels, LCs and other perivascular cells. The basal compartment of the seminiferous tubules contains spermatogonia in various stages of differentiation, including spermatogonial stem cells (SSCs) that are crucial for spermatogenesis and fertility (Desjardins and Ewing, 1993; Russell et al., 1993; Ogawa et al., 2005). These SSCs reside in a specialized stem cell niche that is, at least partially, maintained by testicular endothelial cells (TECs). TECs produce several factors to support SSCs survival and maintenance, including glial cell line-derived neurotrophic factor (GDNF) (Kubota et al., 2004; Bhang et al., 2018). Endothelial GDNF production is mediated via fibroblast growth factor 2 (FGF-2) and fibroblast growth factor receptor 1 (FGFR1) signaling that activates the calcineurin pathway. Transplantation of TECs in chemotherapy-treated mice restored spermatogenesis, demonstrating an important role for TECs in SSC self-renewal and testicular regeneration (Bhang et al., 2018).

LCs contribute to SSC maintenance by expression colony-stimulating factor 1 receptor (CSF1R) that promotes SSC self-renewal (Oatley et al., 2009; **Figure 1**). Time-lapse imaging of GFP-labeled undifferentiated spermatogonia demonstrates a preferential localization of undifferentiated spermatogonia near intertubular vessels and interstitial LCs (Yoshida et al., 2007). Upon differentiation, spermatogonia move away from intertubular vessels, dispersing throughout the basal compartment of the seminiferous tubules. This relocation of spermatgonia is accompanied by a vascular reorganization. Transplantation of seminiferous tubules triggers the formation of vasculature with SSCs localizing along with the newly established vascular pattern in the graft (Yoshida et al., 2007; Yoshida, 2018). This demonstrates a crucial role for interstitial cells and vessels in SSC maintenance and stem cell niche establishment.

Within the seminiferous tubules, somatic SCs also express GDNF and have been implicated in SSC niche formation. SSC transplantation into host mice with polythiouracil (PTU)-induced increase in SC numbers enhanced vascular niches. Transplanting SSCs from PTU-treated donors into normal recipients significantly increased SSCs numbers by more than 3-fold, indicating a key role for SCs in regulating SSC and niche abundance (Oatley et al., 2011).

Fetal testis provides a perivascular microenvironment for multipotent progenitor cells (Kumar and DeFalco, 2018). These perivascular multipotent progenitor cells are Notch-active and Nestin-positive and give rise to several interstitial cell types, including LCs, pericytes and smooth muscle cells. Vascular inhibition disrupts Notch signaling in these progenitors, stimulating excessive LC differentiation. Thus, angiocrine Notch signals crucially regulate the balance of LC differentiation, highlighting the importance of the vasculature for interstitial progenitor cell maintenance (Kumar and DeFalco, 2018).

## Vascular Microenvironments in Ovary

Ovarian function depends on the periodic growth regression of the ovarian vasculature and variations in blood flow rate. Ovarian vasculature provides blood and nutrients to follicles and the CL and regulates steroid production. Small follicles are avascular and rely on the stromal vasculature (Mariana Di et al., 2018). Beyond the primary stage, follicle growth requires the formation of an individual capillary network in the thecal layer of each follicle. Vessel formation and regression are mediated via angiogenic factors such as VEGFA, platelet-derived growth factor (PDGF), angiopoietins (Angs) and thrombospondin-1 (TSP-1) that stimulate EC proliferation, migration, and vascular stability (Tamanini and De Ambrogi, 2004; Nilsson et al., 2006; Yang and Fortune, 2007; Abramovich et al., 2009; **Figure 1**). Multiple studies demonstrate that inhibition of angiogenesis via blockade of VEGFA signaling or administration of antiangiogenic compounds, disrupts follicular growth and ovulation, and completely inhibits CL vascularization (Ferrara et al., 1998; Wulff et al., 2002; Kuhnert et al., 2008; Robinson et al., 2009). Preovulatory follicles show an increased Ang1:Ang2 ratio (Hayashi et al., 2004) and Ang2 injection into monkey follicles delayed follicle maturation and inhibited ovulation by disrupting EC-pericyte interactions (Xu and Stouffer, 2005). Perivascular cells in the endocrine system can be marked by perivascular markers such as platelet-derived growth factor receptor β (PDGFRβ), NG2 and α-SMA. A recent deep imaging study by Chen et al. (2020b) visualized PDGFRβ and NG2 and α-SMA expressing perivascular cells in multiple glands of the endocrine system in both rodents and humans.

The antiangiogenic factor TSP-1 is upregulated during follicular atresia in marmoset monkeys and has been suggested to play an important role in follicular breakdown via the inhibition of angiogenesis (Thomas et al., 2008).

**TABLE 1 |** Vascular niche associated factors in the endocrine system in homeostasis, aging, and endocrine disorders.

| Sl. No | Factor/Signal | Function | Cell Type | Condition | References |
|---|---|---|---|---|---|
| 1 | Angiopoietin-1 | Angiogenesis, ovarian follicular development, ovulation | ECs, follicular cells | | Xu and Stouffer, 2005; Abramovich et al., 2009 |
| 2 | Angiotensin-1 | Aldosterone release | Adrenocortical cells | | Rosolowsky and Campbell, 1994; Ansurudeen et al., 2006 |
| 3 | CSFR1 | SSC renewal | SSC | | Oatley et al., 2009 |
| 4 | EG-VEGF | EC proliferation, migration and fenestration | ECs | | LeCouter et al., 2001 |
| 5 | Endothelin | Aldosterone and corticosterone release, insulin secretion | Adrenocortical cells, β-cells | | Rosolowsky and Campbell, 1994; Belloni et al., 1996; Gregersen et al., 1996 |
| 6 | Ezh2 | β-cell expansion | β-cells | Aging | Chen et al., 2011 |
| 7 | FGF-2 | Mediation of endothelial GDNF, corpus luteum vascularization | ECs | | Berisha et al., 2000; Bhang et al., 2018 |
| 8 | Fibronectin, laminin, collagen | β-cell proliferation, insulin gene expression | β-cells | | Kaido et al., 2004; Nikolova et al., 2006 |
| 9 | GDNF | SSC survival and maintenance | SSCs | | Kubota et al., 2004; Bhang et al., 2018 |
| 10 | Gja1 | Pancreatic islet capillary maintenance | ECs | Aging | Chen et al., 2020b |
| 11 | Glucocorticoids | Inhibition of angiogenesis, TSP-1 production | ECs | Aging | Logie et al., 2010; Yang et al., 2018 |
| 12 | HIF-1α | Angiogenesis, VEGFA secretion, oxygen homeostasis | ECs | Hypertension | Gérard et al., 2009; Lysiak et al., 2009; Colli et al., 2019 |
| 13 | HGF | β-cell proliferation | β-cells | | Johansson et al., 2006 |
| 14 | ICAM-1 | Inflammation, immune cell recruitment | Immune cells | Aging | Chen et al., 2020b |
| 15 | Jagged1 | Pituitary stem cell maintenance | Pituitary stem cells | | Tando et al., 2013 |
| 16 | MMPs | Periovulatory basement membrane breakdown, EC invasion, ECM remodeling, fibrosis | ECM | Aging, diabetes | Kano et al., 2005; Su et al., 2008; Almaça et al., 2014 |
| 17 | Nitric oxide | Vasodilation, corticosterone and aldosterone production | ECs, adrenocortical cells | Diabetes, aging | Marin et al., 1999; Romero Maritza et al., 2008 |
| 18 | NOTCH2 | Perivascular progenitor maintenance | Perivascular progenitor cells | | Kumar and DeFalco, 2018 |
| 19 | p53 | Insulin resistance, inflammation, lypolysis | Adipocytes | Obesity | Minamino et al., 2009; Vergoni et al., 2016 |
| 20 | PDGFβ | EC proliferation and migration, pericyte activation, β-cell maintenance | ECs, pericytes, β-cells | PCOS | Nilsson et al., 2006; Woad et al., 2009; Chen et al., 2020b |
| 21 | Smad | Thyroid development, EC differentiation | Thyrocytes, ECs | | Hick et al., 2013; Villacorte et al., 2016 |
| 22 | TGF-β1 | β-cell maintenance, angiogenesis | β-cells, follicular cells | PCOS | Tal et al., 2013; Liu et al., 2015; Jiang et al., 2018 |
| 23 | Thy-1 | Ovarian follicular growth, cellular differentiation | Granulosa cells | | Bukovský et al., 1995 |
| 24 | TSP-1 | Inhibition of angiogenesis, TGF-β1 activation | ECs | PCOS | Crawford et al., 1998; Thomas et al., 2008; Liu et al., 2015 |
| 25 | VEGFA | Angiogenesis, ovarian follicular growth, corpus luteum vascularization, seminiferous tube formation | ECs | Aging | Ferrara et al., 1998; Berisha et al., 2000; Klein et al., 2000; Bott et al., 2006; Yang and Fortune, 2007; McFee et al., 2009 |
| 26 | VEGFR2 | Fenestrae formation, follicular cell proliferation | ECs, follicular cells | | Jang et al., 2017 |

During ovulation, the basement membrane is broken down, enabling EC and pericyte invasion and rapid vascularization of the developing CL. This vascularization is likely mediated by VEGFA and FGF2 that accumulates before ovulation in the later stages of follicular development (Berisha et al., 2000; Robinson et al., 2009). Periovulatory breakdown of the basement membrane requires proteases that degrade components of the extracellular matrix (ECM). In line with this, the metalloproteinase ADAMTS1 is transiently upregulated in ECs (Su et al., 2008; Robinson et al., 2009). Matrix metalloproteinases (MMPs) are also produced by pericytes that are activated by luteal PDGF-signaling (Kano et al., 2005; Robinson et al., 2009; Woad et al., 2009).

ECs and pericytes also play an important role in the maintenance of ovarian stem cells (OSCs). In adult ovaries, OSCs give rise to germ and granulosa cells and reside in a stem cell niche in the ovarian surface epithelium (Bukovsky et al., 2004; Flesken-Nikitin et al., 2013). Within this niche, vascular pericytes facilitate the formation of secondary germ cells. These germ cells migrate towards cortical vessels that transport them to granulosa cell nests in the lower cortex to form primordial follicles (Bukovsky, 2011). In addition, pericytes

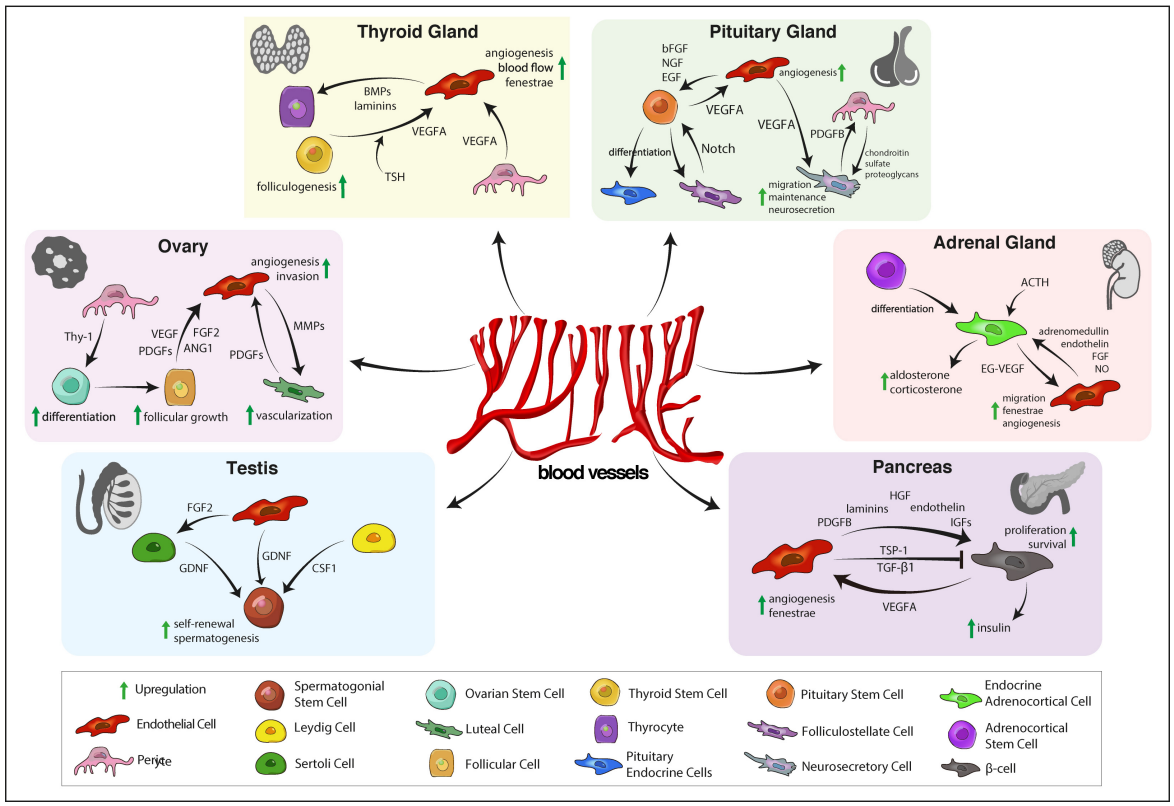


**FIGURE 1 |** Vascular niche functions in the endocrine system. In the testis, ECs release various endocrine signals to maintain SSCs and spermatogenesis. OSC maintenance is supported by pericytes. During follicular and luteal stages of the cycle, growth factors regulate periodic growth and regression of ovarian vasculature that is needed for follicular and luteal development. In the thyroid, angiogenic signals from TSCs and pericytes regulate angiogenesis, endothelial fenestrae formation that is important for thyrocyte function. Pituitary ECs and pericytes promote maintenance and function of neurosecretory cells in the neurohypophysis and pituitary stem cells in the adenohypophysis. Angiocrine signals also regulate endocrine function of the adrenal cortex, that, in turn, promotes angiogenesis via the endocrine gland-specific growth factor EG-VEGF. In the pancreas, reciprocal interaction between ECs and β-cells is required for angiogenesis and insulin secretion. EC, endothelial cell; SSC, spermatogonial stem cell; FGF2, fibroblast growth factor 2; GDNF, glial cell line-derived neurotrophic factor; CSF-1, colony-stimulating factor 1; OSC, ovarian stem cell; PDGF, platelet-derived growth factor, VEGF, vascular endothelial growth factor; ANG1, angiopoietin 1; MMP, matrix metalloproteinase; TSC, thyroid stem cell; TSH, thyrotropin-releasing hormone; BMP, bone morphogenetic protein; bFGF, basic fibroblast growth factor; NGF, nerve growth factor; EGF, epidermal growth factor; EG-VEGF, endocrine gland-derived vascular endothelial growth factor; NO, nitric oxide; HGF, hepatocyte growth factor; IGF, insulin-like growth factor; TSP-1, thrombospondin-1; TGF-β1, transforming growth factor β1.

release the morphoregulatory Thy-1 differentiation protein, that is associated with cellular differentiation and macrophage presence. Thy-1 is released among granulosa cells to initiate the growth of resting follicles (Bukovský et al., 1995; Bukovsky, 2011).

## Vascular Niches in Thyroid Gland

In the thyroid gland, follicular cells and surrounding capillaries form an angiofollicular unit to control endocrine thyroid function (Gérard et al., 2002; Colin et al., 2013). Independent of TSH stimulation, angiofollicular units can induce microvascular responses to preserve thyroid hormone synthesis. For instance, when intracellular iodine levels drop, follicular cells increase HIF-1α expression, which is accompanied by an increase in ROS generation, stabilizing HIF-1α. The subsequent increase of follicular VEGFA secretion activates neighboring ECs and pericytes, resulting in microvascular expansion and elevated blood flow (Gérard et al., 2009; Colin et al., 2013). Furthermore, genetic depletion of VEGFR2 and pharmacological blockade of VEGFA or VEGFR2 in mice demonstrates that endothelial VEGFA-VEGFR2 signaling promotes fenestrae formation and follicular cell proliferation (Jang et al., 2017; **Figure 1**).

In adult thyroids, thyroid stem cells constitute a very small proportion of thyroid cells. They maintain their proliferation and differentiation ability, enabling regeneration of thyrocytes and reconstruction of thyroid follicles (Thomas et al., 2006; Lan et al., 2007; Gibelli et al., 2009). Folliculogenesis requires the formation of an epithelial basement membrane which is controlled by bone morphogenetic protein (BMP)-Smad signaling in thyrocytes and EC invasion into the developing thyroid (Hick et al., 2013; Villacorte et al., 2016). BMP-Smad signaling also regulates VEGFA expression in thyroid progenitors. Thyroid-specific double knockout of Smad1 and Smad5 impairs thyroid development, follicle architecture, endothelial differentiation and basement membrane assembly. Conditioned medium from embryonic endothelial progenitor

cells (eEPCs) rescues the observed defects in folliculogenesis. Normal folliculogenesis further requires laminins and type IV collagens that are produced by endothelial and epithelial components of the angiofollicular unit (Hick et al., 2013; Villacorte et al., 2016). These findings suggest a reciprocal communication between ECs and thyrocytes that creates a folliculogenic microenvironment.

## Vascular Microenvironments in Pituitary Gland

In the pituitary gland, hormone secretion is regulated by neuroendocrine signals from the hypothalamus and peripheral endocrine feedback mechanisms. The adult pituitary is able to adapt relative and absolute numbers of cells from its different endocrine cell types, enabling high adaptability of hormonal output/input responses to changing physiological demands (Levy, 2002; Fauquier et al., 2008). Therefore, adult adenohypophysis harbors various stem and progenitor cell populations. A small SOX2 and SOX9 expressing population of multipotent pituitary stem and progenitor cells gives rise to all pituitary endocrine cell types and parenchymal folliculostellate cells (Andoniadou et al., 2013; Rizzoti et al., 2013). In rodents, SOX2-positive pituitary stem and progenitor cells are mainly located in the marginal cell layer but can also be found in clusters scattered throughout the parenchyma of the adenohypophysis (Fauquier et al., 2008). A majority (85%) of SOX2-positive pituitary stem and progenitor cells express calcium-binding protein B (S100β) and produce various growth and angiogenic factors including VEGF (Ferrara et al., 1987; Gospodarowicz and Lau, 1989; Yoshida et al., 2011). S100β-positive cells in the marginal cell layer niche of transgenic S100β-GFP mice also express Notch receptors and ligands that are important for stem and progenitor cell maintenance (Tando et al., 2013).

Within these marginal cell layer and parenchymal niches, stem cells are regulated by growth factors such as basic fibroblast growth factor (bFGF), epidermal growth factor (EGF) and nerve growth factor (NGF) (Chen et al., 2006; Yoshida et al., 2016). Immunostaining for endothelial and stem cell markers further suggests the existence of a perivascular MSC population, as it has been shown in other organs such as the bone marrow (Garcia-Lavandeira et al., 2009, 2015; Méndez-Ferrer et al., 2010).

In the neurohypophysis, axon terminals store neurosecretory granules containing PDGF-β that may activate pericytes that highly express PDGFRβ. This may induce a shape conversion of these pericytes that can extend their processes to increase vascular protrusions, leading to a reorganization of the perivascular space in the neurohypophysis (Miyata, 2017; Nishikawa et al., 2017; **Figure 1**). Inhibition of VEGF-signaling decreased the density of neurosecretory axonal terminals and reduced the contact with the vasculature, indicating an important role in axonal maintenance. The neurohypophysis further shows an expression of chondroitin sulfate proteoglycans, that act as perivascular substrates for neuronal migration, indicating an important role for pericytes in support and migration of neural stem and progenitor cells (Morita et al., 2010; Furube et al., 2014).

## Blood Vessel-Derived Signals in Adrenal Gland

The adrenal medulla is the place of catecholamine production and mainly consists of chromaffin cells in close association with the medullary endothelium. Coculturing adrenal medulla-derived PC12 cells with bovine adrenal medullary ECs, stimulated chromaffin differentiation of PC12 cells, indicating an important role for ECs in organ-specific differentiation of the adrenal medulla (Mizrachi et al., 1990).

The adrenal cortex represents the site of steroid hormone production and contains various types of steroidogenic cells originating from self-renewing populations of undifferentiated somatic stem cell progenitors (Mitani et al., 2003). Ki67 labeling and BrdU pulse-chase labeling experiments show that these somatic stem cell progenitors are located in the outer cortex, where the majority of cell proliferation takes place. Subsequently, cells move inwardly along the cortical subzones towards the medulla (McNicol and Duffy, 1987; Chang et al., 2013). At the border to the medulla, they are eliminated by apoptosis (Zajicek et al., 1986; Carsia et al., 1996; Chang et al., 2013).

The dense fenestrated adrenocortical capillaries enable close contact of endocrine cells and ECs, which is important for paracrine signaling between vasculature and endocrine tissue (Thomas et al., 2003). Stimulation of human adrenocortical cells (in HUVEC conditioned medium) with angiotensin II or FSK significantly increases aldosterone release and sensitizes adrenocortical endocrine cells to angiotensin II stimulation (Ansurudeen et al., 2006). Since HUVEC conditioned medium contains a variety of angiocrine factors, the precise mechanisms of this effect remain largely unknown (Kanczkowski et al., 2017). Earlier studies demonstrate that EC-derived signals such as NO, endothelin and adrenomedullin stimulate aldosterone and corticosterone production in adrenocortical cells (Rosolowsky and Campbell, 1994; Belloni et al., 1996; Ehrhart-Bornstein et al., 1998; Rosolowsky et al., 1999). This stimulation may be mediated by NO-regulated activation of cyclic adenosine monophosphate (cAMP) (Ansurudeen et al., 2009). Another study suggests the involvement of a yet unknown protein of 3 KDa that may increase aldosterone secretion through activation of the protein kinase C (PKC) pathway (Rosolowsky and Campbell, 1994). Recently, endothelial FGF has also been associated with the β-catenin-induced adrenocortical activity (Schwafertz et al., 2017).

In turn, high levels of adrenocortical hormones such as glucocorticoids and catecholamines in the adrenal microenvironment can also influence vascular function. For instance, high plasma steroid levels have been shown to stimulate and sustain endothelial production of developmental endothelial locus-1 (Del-1), that is associated with adrenal inflammation (Kanczkowski et al., 2013).

Steroidogenic glands express a special endocrine gland-derived VEGF, termed EG-VEGF (LeCouter et al., 2001; **Figure 1**). Despite its structural distinction form VEGFA, EG-VEGF has a similar function. EG-VEGF induces proliferation, migration and fenestration in endocrine gland-derived ECs and promotes extensive angiogenesis while showing no effect on other ECs (e.g., HUVECs, human dermal microvascular cells, adult bovine aortic and bovine

brain capillary cells) and non-EC types (pericytes, vascular smooth muscle cells, fibroblasts and keratinocytes), highlighting the tissue-specific regulation of vascular proliferation and differentiation (LeCouter et al., 2001).

## Vascular Niches in Pancreas

Endocrine pancreatic islets are vascularized by a dense and highly branched network of capillaries, whereas the surrounding tissue contains thinner quiescent capillaries (Zhou et al., 1996; Gorczyca et al., 2010). Islet ECs are characterized by distinct expression of cell surface markers that distinguishes them from the surrounding exocrine tissue (Yao et al., 2005). These markers include nephrin (Zanone et al., 2005), TSP-1, endostatin and the proteinase inhibitor alpha-1 that maintains their low proliferation rate (Lou et al., 1999; Cantaluppi et al., 2006; Mattsson et al., 2006). A recently identified subtype of islet capillaries is positive for CD31 and ESM-1 and shows high expression of Endomucin. This vessel subtype secretes growth factors involved in β-cell survival and maintenance, including Pdgfa, Pdgfb, Igf1, Igf2, Cxcl12 and stem cell factor (SCF) (Chen et al., 2020b).

ECs can directly affect β-cell function. For instance, islet capillaries can upregulate insulin secretion and promote β-cell survival via secretion of soluble factors and ECM proteins such as laminins, fibronectin and collagen in a $\beta_1$-integrin-dependent manner (Kaido et al., 2004; Nikolova et al., 2006; **Figure 1**). Treatment of VEGF-A deficient mutant islets with vascular laminins rescued impaired β-cell proliferation and lead to an upregulation of insulin gene expression (Nikolova et al., 2006). These beneficial effects were reduced when treating mutant islets with an anti-β1-integrin blocking antibody (Nikolova et al., 2006). Endothelial upregulation of hepatocyte growth factor (HGF) in response to increased insulin and VEGFA levels promotes β-cell proliferation (Crawford et al., 1998; Johansson et al., 2006). In addition, endothelial production of the vasoconstrictor endothelin-1 promotes insulin secretion (Gregersen et al., 1996). Furthermore, distinct expression of EC junctional adherence and cell adhesion molecules such as E-cadherin and neuronal cell adhesion molecule (NCAM) has been shown to correlate with β-cell insulin secretion and may contribute to functional β-cell heterogeneity (Domenico et al., 2007; Karaca et al., 2009; Roscioni et al., 2016).

In contrast, TSP-1 functions as a negative regulator of angiogenesis and β-cell proliferation (via activation of transforming growth factor (TGF)-β1, that maintains β-cells in a non-proliferative state) (Crawford et al., 1998; Jiang et al., 2018). However, sustained depletion of TSP-1 impairs β-cell function due to insufficient TGF-β1 activation (Olerud et al., 2008; Olerud et al., 2011).

Islet β-cells exhibit an abundance of VEGFA expression that is required for the formation of the islet-specific microvascular network, specifically promoting the development of fenestrae (Lammert et al., 2003). β-cell-specific inactivation of VEGFA significantly decreased vascularity, and β-cell mass in islets of Rip-Cre;$VEGF^{fl/fl}$ mice (Brissova et al., 2006; Iwashita et al., 2007). These findings were recapitulated by EC-specific knockout of the VEGFA receptor VEGFR2 in $Vegfr2^{i\Delta EC}$ mice, significantly decreasing the density of islet capillaries, β-cell numbers and insulin production (Chen et al., 2020b). These findings demonstrate a close reciprocal relationship between islet vasculature and endocrine β-cell function (Olerud et al., 2009).

# AGING OF THE ENDOCRINE SYSTEM AND ENDOCRINE TISSUES

Aging represents a major stress factor on cellular function and increases the risk of age-related diseases and mortality. It is a complex facet that remains incompletely understood. In the endocrine system, aging induces endocrine changes that affect overall health, metabolism, fertility, cognition, and cardiovascular risk (Traub and Santoro, 2010; Vitale et al., 2013).

According to the "geroscience hypothesis," aging is the common major risk factor underlying multiple chronic diseases (Kennedy et al., 2014; Khosla et al., 2020). Therefore, manipulating the fundamental mechanisms of aging may prevent or alleviate these chronic diseases. The mechanisms of aging can be divided into nine, highly interconnected hallmarks, including genomic instability, epigenetic alteration, telomere attrition, exhaustion of stem cells and cellular senescence (López-Otín et al., 2013; Khosla et al., 2020). Senescent cells typically exhibit gene expression changes, loss of proliferative potential and often develop a senescence-associated secretory phenotype (SASP) (Tchkonia et al., 2013). SASP includes excessive production of inflammatory cytokines that affect stem and progenitor cell function, growth factors and vasopressors, that, in turn, induce inflammation and tissue damage (Coppé et al., 2006; Xu et al., 2015; Khosla et al., 2020).

Cellular senescence also impairs mitochondrial function and reduction of oxygen, leading to the excessive formation of reactive oxygen species (ROS). Elevated ROS levels induce oxidative damage and are associated with increased cytokine levels and chronic, subclinical inflammation, further impairing cellular function (Vitale et al., 2013). In the following sections, we will summarize age-related changes in the endocrine system and their known consequences.

## Age-Dependent Changes in Testis

Aging is associated with a decline in testicular function, whereby both mice and humans exhibit decreased serum testosterone levels and spermatogenesis (Chen et al., 1994; Harman et al., 2001). Testosterone is crucial for endothelial function and regulates vasodilation via upregulation of vascular androgen receptors and production of endothelial-derived NO (Chou et al., 1996; Hanke et al., 2001). Multiple studies have found a link between sex steroid hormone deficiency and endothelial dysfunction (Marin et al., 1999; Sader et al., 2003; Hougaku et al., 2006). For instance, castrated rats showed reduced expression and activity of endothelial NOS that was restored upon testosterone treatment (Marin et al., 1999). Furthermore, reduced testosterone levels cause arterial stiffness (Hougaku et al., 2006),

impair arterial reactivity and sexual function (Aversa et al., 2011) and increase the risk and severity of cardiovascular disease and mortality (Khaw et al., 2007; Haring et al., 2010; Li L. et al., 2012), suggesting a protective effect of normal testosterone levels against atherosclerosis.

In contrast to testosterone, FSH and LH levels gradually increase with age, further promoting reduced testosterone secretion (Veldhuis et al., 1992). Increased gonadotropin levels may also reflect the reduced secretion of androgen and estrogen from LCs observed in elderly males. In addition, SCs exhibit reduced secretion of inhibin B, indicating an age-related decline in SC function (Tenover et al., 1988). This age-related hypogonadism is associated with decreased muscle mass and strength and bone density to which testosterone treatment has been identified to reverse these effects (Snyder, 2001).

Moreover, aged testes exhibit increased ROS production by LC mitochondria, inhibiting steroidogenesis (Chen et al., 2001). Low testicular ROS levels have important physiological functions in the testis, contributing to the maintenance of LC proliferation and function and regulating spermatozoa maturation (Griveau and Lannou, 1997; Tai and Ascoli, 2011). However, age-related increase of ROS levels impairs steroidogenesis via the inhibition of steroidogenic enzyme expression and suppression of mitochondrial cholesterol transfer that initiates steroidogenesis (Lee et al., 2009). Furthermore, testicular aging also damages seminiferous tubules and impairs sperm motility and viability and consequently reduces male fertility (Nakamura et al., 2010; Vitale et al., 2013; **Figure 2**). High ROS levels can result in oxidation of unesterified fatty acids that are very abundant in the cell membrane of spermatozoa, making them highly sensitive to oxidative stress (de Lamirande et al., 1997). Rodent models of aging show increased Ink4a/Arf expression in multiple tissues, including testis and ovaries (Krishnamurthy et al., 2004). The Ink4a/Arf locus encodes the cell cycle inhibitor p16INK4a and can be used as a biomarker of mammalian aging.

## Age-Associated Changes in Ovarian Tissue

During the process of ovarian aging, the pool of oocytes and follicles decreases in quantity and quality (Broekmans et al., 2009; **Figure 2**). Since ovarian follicular cells represent an important source of steroid hormones, continuous reduction of follicle numbers with age induces ovarian cycle irregularity and impairs female fertility (Michael and Ramkumar, 2016).

In addition, oocyte maturation worsens with age, while the rate of DNA fragmentation and concomitant apoptotic potential increases (Fujino et al., 1996; Tatone et al., 2006). Morphometric follicle analysis demonstrates aged follicles to precociously enter the growth phase compared to younger follicles (Westergaard et al., 2007). This altered follicular growth may contribute to the qualitative and quantitative decline in ovarian follicles with age (Tatone et al., 2008). Ultimately, the pool of follicles is exhausted, and the menstrual cycle can no longer be sustained during menopause (Faddy et al., 1992). Age-related reduced oocyte quality can result in aneuploidy of embryos, fetal death and miscarriages (Andersen et al., 2000; Pellestor et al., 2003). According to the telomere theory of reproductive senescence, aged oocytes may also be susceptible to telomere shortening due to a decline in telomerase activity, impairing fertility and reproduction (Keefe et al., 2005). Inducing telomere shortening in TR-/- mice lacking telomerase activity disrupts meiosis and embryonic cell cycles and promotes embryonic apoptosis (Liu et al., 2002). In women undergoing *in vitro* fertilization, telomere length in oocytes predicts embryo fragmentation, which functions as a marker for apoptosis (Keefe et al., 2005).

Furthermore, reduced follicle quality and ovarian function during aging are associated with oxidative stress. Multiple studies demonstrate increased ROS levels in granulosa cells and oocytes, concomitant with increased levels of mitochondrial DNA deletions and reduced expression of antioxidant enzymes (Seifer et al., 2002; Tatone et al., 2006; Yamada-Fukunaga et al., 2013). Endogenous ROS are required for oocyte maturation, steroidogenesis and CL function and are produced by immune cells and preovulatory follicles to induce ovulation (Shkolnik et al., 2011). However, age-associated accumulation of cyclically produced ROS may lead to DNA damage, telomere shortening and ovarian aging (Behrman et al., 2001; Liu et al., 2003). In line with this, antioxidants such as melatonin (Zhang et al., 2019), coenzyme Q10 (Ben-Meir et al., 2015), and C-phycocyanin (Li et al., 2016) have an anti-aging effect on murine oocytes by regulating mitochondrial function. They reduce ROS levels, reverse the decline of oocyte quality and quantity and restore fertility during reproductive aging.

The age-related drop of follicle numbers also reduces the production of estrogen and progesterone, causing bone loss, hot flashes and other age-related conditions (Finkelstein et al., 2008; Michael and Ramkumar, 2016). Estrogens are known to have a vasodilative effect and pharmacological inhibition of aromatase impaired flow-mediated vasodilation, demonstrating an important regulatory role for endogenous estrogens in endothelial function (English et al., 2001; Lew et al., 2003). Interestingly, multiple studies demonstrate a protective role for estrogens against oxidative stress and aging. Female rats show significantly lower mitochondrial ROS production than male rats and ovariectomy increased oxidative stress levels to those seen in male rats. This could be prevented by estrogen replacement therapy (Borrás et al., 2003). Similarly, estrogens upregulate the expression of antioxidant enzymes and longevity-associated genes via MAPK and NFkB activation (Jose et al., 2011).

## Aging in Thyroid Gland

In the thyroid gland, aging is associated with a decrease in tissue volume and secretion of thyroid hormones while increasing the prevalence of various thyroid diseases (Mariotti et al., 1993, 1995). In elderly individuals without thyroid disease, TSH secretion and serum levels are increased while $T_4$ levels remain unchanged (Bremner et al., 2012) and aged mice show decreased serum thyroid hormone levels (da Costa et al., 2001). These findings suggest an age-associated disruption of negative feedback pathways on the hypothalamus-pituitary-thyroid axis (Jansen et al., 2015). Hypothyroidism and increased TSH

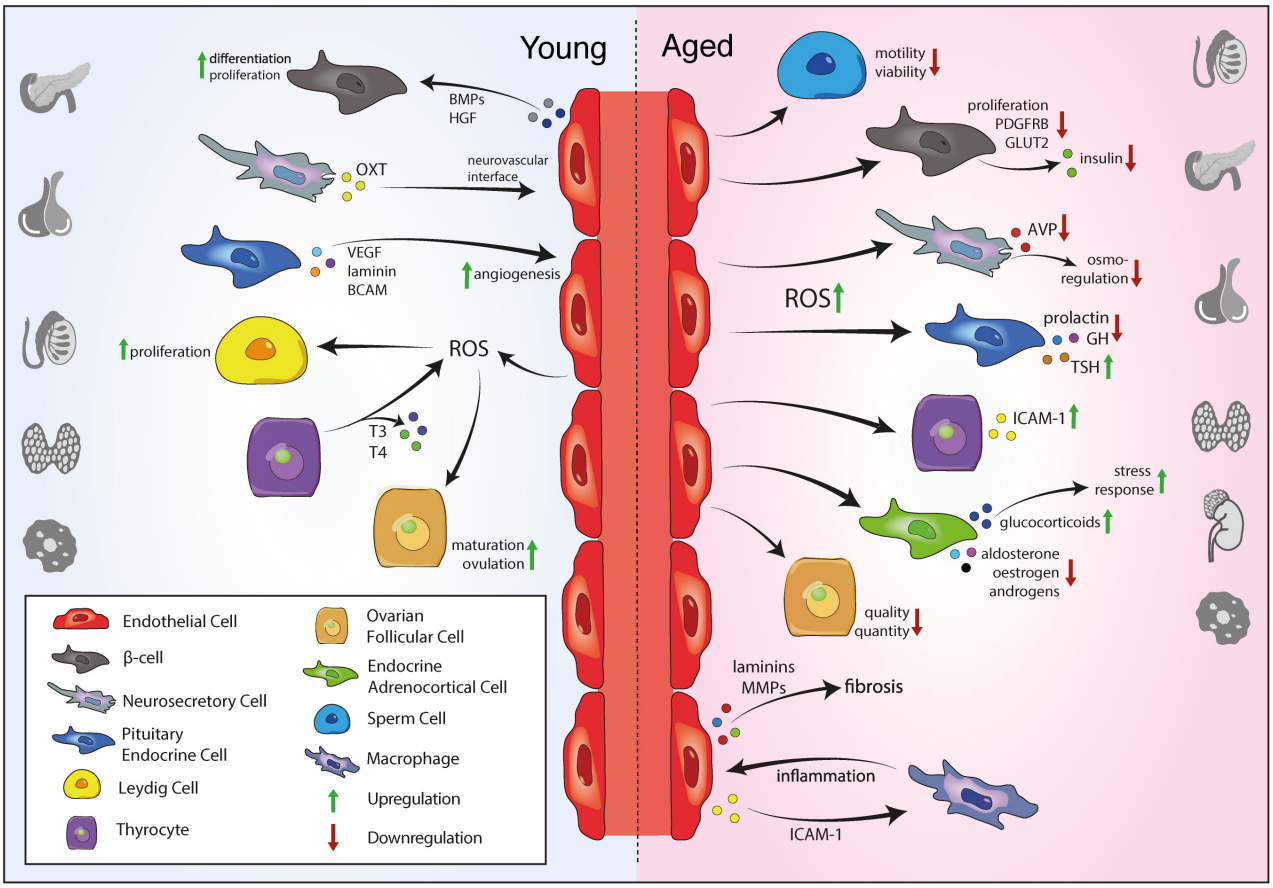


**FIGURE 2 |** Vascular niche function in the endocrine system during aging. Young ECs secrete angiocrine signals to promote proliferation of endocrine cells and support endocrine function. In the young endocrine system, ECs produce low ROS levels that support Leydig cell proliferation in the testis and promote ovulation OSC maturation in the ovaries. Angiogenic growth factors from pituitary endocrine cells and others promote angiogenesis. Upon aging, endothelial ROS production increases, impairing sperm cell motility, quality and quantity of follicular cells in the ovary and proliferation and hormone production of various endocrine cells, including pancreatic β-cells and endocrine cells and neurosecretory axon terminals in the pituitary gland. In contrast, elevated ROS levels increase the production of inflammatory mediators such ICAM-1 in the thyroid and increases the release of glucocorticoids from the adrenal cortex, promoting the stress response. EC, endothelial cell; ROS, reactive oxygen species; T3, triiodothyronine; T4, thyroxine; VEGF, vascular endothelial growth factor; BCAM, basal cell adhesion molecule; OXT, oxytocin; BMP, bone morphogenetic protein; HGF, hepatocyte growth factor; AVP, arginine vasopressin; GH, growth hormone; TSH, thyroid stimulating hormone; ICAM-1, intercellular adhesion molecule 1; MMP, matrix metalloproteinase.

levels are associated with cognitive impairments (Hogervorst et al., 2008), depression (Medici et al., 2014) increased fracture risk (Blum et al., 2015), cardiovascular disease and mortality (Rodondi et al., 2010). Surprisingly, several studies demonstrate an association between age-related hypothyroidism and longevity in mice and humans (Ooka and Shinkai, 1986; Atzmon et al., 2009; Corsonello et al., 2010; Rozing et al., 2010). However, the mechanisms underlying this association remain unclear.

Thyrocytes produce large amounts of $H_2O_2$ to synthesize thyroid hormones, that results in thyrocytes being constantly subjected to ROS. Protection of thyrocytes against excessive ROS relies on an antioxidant system that is dysregulated in aging, causing an imbalance between ROS and antioxidants that may damage thyroid morphology and function (Vitale et al., 2013). For instance, thyroid levels of the antioxidant selenium decrease with age and may increase thyroid vulnerability to oxidative stress (Akbaraly et al., 2007; **Figure 2**). Increased ROS levels and oxidative stress also contributes to the development of thyroid autoimmune diseases through fragmentation of thyroglobulin and increased expression of intercellular adhesion molecule 1 (ICAM-1) by thyrocytes (Duthoit et al., 2001; Burek and Rose, 2008).

## Age-Related Modulations in Pituitary Gland

Pituitary hormone secretion exhibits complex and heterogeneous changes during aging (van den Beld et al., 2018; **Figure 2**). Aging is associated with a progressive decline in pituitary function, due to endocrine deficiency, that, in turn, may contribute to senescence (Vitale et al., 2013). Furthermore, aged pituitary glands show an accumulation of oxidative products that further contributes to aging (Kondo et al., 2001). Increased levels of radicals are also found in the hypothalamus of aging rats,

concomitant with reduced antioxidant capacity as measured by glutathione peroxidase activity (Rodrigues Siqueira et al., 2005). These findings suggest an imbalance of oxidant production and antioxidant protection that may cause oxidative damage to cells of the HP axis (Rodrigues Siqueira et al., 2005; Vitale et al., 2013). In addition, aging increases apoptosis of endocrine cells in the adenohypophysis, contributing to impaired hormone production (Nessi et al., 1995).

For instance, pituitary aging decreases GH pulses, causing GH deficiency and decreasing insulin-like growth factor 1 (IGF-1) production (Aimaretti et al., 2003). GH secretion during exercise, sleep and fasting declines with age, particularly in company with abdominal visceral adiposity (Broglio et al., 2003; Veldhuis et al., 2011; Veldhuis, 2013). Moreover, GH activity is positively associated with age-related dysfunction of white adipose tissue and senescent cell accumulation (Stout et al., 2014). Aged GH-deficient and GH-resistant mice with homozygous deletion of the GH receptor (GHR-/-) exhibit increased levels of circulating GH, reduced age-related lipid redistribution and senescent cell burden.

Prolaction secretion in pituitary mammotrophs becomes more irregular in aged men (Kok et al., 2004; Roelfsema et al., 2012).

In contrast, pituitary TSH secretion increases with age and multiple population-based cohort studies demonstrate an association of increased TSH levels with longevity (Atzmon et al., 2009; Rozing et al., 2010; Bremner et al., 2012; Waring et al., 2012). However, confounding factor such as decreased exercise, reduced caloric intake or glucocorticoid exposure may suppress TSH levels during aging (Veldhuis, 2013).

Similar to TSH levels, gonadotropin levels gradually increase in aging men (FSH and LH) and premenopausal women (FSH) (Tenover et al., 1988; Sowers et al., 2008). Aging is also linked to more acidic and sialylated FSH isoforms with a higher half-life and lower *in vitro* bioactivity (Loreti et al., 2009). High FSH levels have been shown to promote osteoclast differentiation and bone resorption in mice (Sun et al., 2006). Genetic deletion of the FSHβ subunit (FSHβ-/- mice) or FSH receptor (FSHR-/- mice) protects against bone loss despite severe hypogonadism, demonstrating a contribution of FSH in hypogonadal bone loss (Iqbal et al., 2006; Sun et al., 2006).

The effects of aging on the stress-responsive HPA-axis remain controversial. Unstressed mean levels of ACTH are reported to remain unchanged, decrease or increase with age (Veldhuis, 2013). These discrepant findings may be indicative of the presence of confounding factors such as alterations in intra-abdominal adipose tissue. Adipose tissue has been shown to increase plasma ACTH levels and impair adrenal sensitivity to ACTH (Ferdinand et al., 2012). In the neurohypophysis, arginine vasopressin (AVP) secretion increases with age (Terwel et al., 1992; Greenwood et al., 2018). Systemically AVP triggers water reabsorption in the kidneys. Therefore, age-related changes in AVP secretion disrupt osmoregulation and water homeostasis (Veldhuis, 2013). Moreover, aging downregulates renal expression of the AVP receptor V2 and the water channel aquaporin 2 in Fischer 344 and Brown-Norway F1 hybrid rats, impairing renal concentrating ability (Tian et al., 2004).

## Age-Dependent Changes in Adrenal Gland

Aging of the adrenal gland is associated with a gradual, sustained increase in glucocorticoids (Yiallouris et al., 2019; **Figure 2**). This age-related glucocorticoid overload may be caused by increased hippocampal oxidative stress and decreased negative feedback control over the HPA axis that is regulated by glucocorticoid and mineralocorticoid receptors on the hippocampus, hypothalamus and pituitary gland (Kobayashi et al., 2009; Vitale et al., 2013). According to the 'glucocorticoid vulnerability hypothesis', these age-related disruptions of the HPA-axis lead to long-term exposure to increased glucocorticoid levels that subsequently causes cognitive impairments (Cheryl, 2008), perhaps contributing to the development of age-related neurodegenerative diseases (Yiallouris et al., 2019). Chronically enhanced glucocorticoid levels also delay and impair the recovery from stressful stimuli in aging (Sapolsky et al., 1983; Lorens et al., 1990; Segar et al., 2009). Moreover, aged adrenals exhibit reduced efficiency of the antioxidant defence system, that may further enhance oxidative damage and senescence (Azhar et al., 1995).

In contrast, other adrenocortical hormones such as aldosterone and the precursor of estrogens and androgens, DHEA, progressively decrease during aging (Hegstad et al., 1983; Orentreich et al., 1984; Labrie et al., 1997) and this decrease is linked to an increased risk in the development of cardiovascular mortality and mental health impairments (Yiallouris et al., 2019). Decreased aldosterone levels are associated with reduced renin activity (Hegstad et al., 1983; Yiallouris et al., 2019). However, the mechanisms underlying these decreases remain unclear. Aging also reduces adrenal androgen production and steroidogenesis. Excessive adrenal ROS levels may cause increased lipid peroxidation and subsequent oxidative damage of cell membranes, particularly in steroidogenic cells that contain high levels of lipids (Azhar et al., 1995; Traub and Santoro, 2010).

## Age-Dependent Changes in Pancreatic Tissue

The pancreas shows an age-related decline of endocrine function that leads to an impairment in glucose homeostasis and metabolism. Aging impairs islet β-cell function and insulin secretion (**Figure 2**), while simultaneously increasing insulin resistance (Chen et al., 1985; Christina et al., 2009) and the incidence of type 2 diabetes (DeFronzo, 1981). The age-dependent decline in insulin secretion is, in part, caused by a decrease of β-cell sensitivity to incretin stimulation (Chang and Halter, 2003), loss of Sirt1-mediated glucose stimulated insulin secretion (Ramsey et al., 2008), decreased expression of β-cell glucose transporter 2 (GLUT2) (Ihm et al., 2007), decreased mitochondrial function and increased oxidative stress (Cooksey et al., 2004).

Chronically increased ROS levels contribute to decreased proliferation and regeneration and increased apoptosis of β-cells and failure in β-cell function (Maedler et al., 2006; Gu et al., 2012; Vitale et al., 2013). Pancreatic β-cells exhibit a low antioxidant defense capacity, rendering them highly sensitive to oxidative stress (Rashidi et al., 2009). In addition, aging decreases the

activity of antioxidant enzymes (e.g., total superoxide dismutase, CuZn superoxide dismutase and glutathione peroxidase), further increasing the ROS burden (Gu et al., 2012). Moreover, aging reduces β-cell levels of PDGFR. PDGFR signaling promotes age-dependent β-cell proliferation via Erk1/2 phosphorylation and activation of the histone methyltransferase Ezh2. Ezh2 levels are decreased in aged β-cells, impairing β-cell replication (Chen et al., 2011). In line with this, conditional Cre-mediated *Pdgfra* knockout (RIP-Cre; $Pdgfra^{fl/fl}$ mice) prevented β-cell expansion and regeneration, while targeted activation of human PDGFRα in β-cells (RIP-Cre; R26-$PDGFRA^{D842V}$) stimulates Erk1/2 phosphorylation and promotes Ezh2-mediated β-cell expansion (Chen et al., 2011).

## VASCULAR PERTURBATIONS DURING AGING OF THE ENDOCRINE SYSTEM

Aging represents a major stress factor for the tissue microenvironment, impairing vascular morphology and function. Vascular aging and its consequences have been extensively studied in the bone marrow microenvironment, demonstrating impaired angiogenesis, vascular integrity and HSC niche function (Kusumbe et al., 2014; Poulos et al., 2017; Singh et al., 2019). In contrast, vascular aging of the endocrine system remains poorly understood. Defining age-related vascular changes in the endocrine system is important to understand mechanisms that drive aging. This may facilitate the rejuvenation of endocrine tissue by manipulation of the vasculature (Almaça et al., 2014).

Vascular aging in the endocrine system is associated with inflammation and fibrosis (**Figure 2**). For instance, aged pancreatic islet vasculature exhibits increased macrophage density and upregulated expression of inflammatory markers such as ICAM-1 (Almaça et al., 2014). These findings are supported by a recent deep imaging study, revealing increased numbers of perivascular macrophages and fibroblasts in aged endocrine glands (Chen et al., 2020b). Aged pancreatic islets also contain more laminin and exhibit accumulation of fibrotic material in the ECM of islet vasculature (Chen et al., 2020b). In addition, aging increases the expression of MMP genes that are involved in ECM remodeling and fibrosis (Almaça et al., 2014). These findings demonstrate that aging causes inflammation and fibrosis of islet vasculature, threatening islet function. Interestingly, transplantation of aged pancreatic islets into the eye of young mice with diabetes lead to graft revascularization with healthy vessels, islet cell proliferation and restoration of glucose tolerance (Almaça et al., 2014), suggesting vascular aging as a driving force in the age-related decline of pancreas function.

Using deep imaging of endocrine glands and 3D spatial proteomic data, a recent study demonstrates various age-related vascular changes in the endocrine system (Chen et al., 2020b). Aging decreases arterial numbers and microvascular density in pancreas, testis and thyroid in mice and humans. This is accommodated by an abundance of hypoxic regions. Through increasing gap junctions, aging specifically leads to a decline of an islet capillary subpopulation involved in β-cell maintenance and pancreatic angiogenesis. The decline of this subpopulation correlates with a decline in β-cell proliferation during aging. Reactivation of this subpopulation restores β-cell numbers and self-renewal (Chen et al., 2020b).

Furthermore, aging reduces ovarian vascularization and perifollicular blood flow as measured by power doppler ultrasound assessment of aged ovaries (Ng et al., 2004; Costello et al., 2006). This decline of ovarian vascularity results in a reduced supply of oxygen, nutrients and signaling molecules (Tatone et al., 2008; Li Q. et al., 2012). Regulation of follicular development and oocyte quality relies on adequate vascular supply of nutrients and signals mainly provided by perifollicular vascularization (Li Q. et al., 2012). Consequently, reduced oxygen supply is associated with an aged oocyte phenotype and decreased fertilization and developmental potential of oocytes (Van Blerkom et al., 1997; Huey et al., 1999). Aged ovaries also show upregulated VEGF levels likely as an attempt to compensate for hypoxia (Friedman et al., 1997; Klein et al., 2000; Tatone et al., 2008; Fujii and Nakayama, 2010).

Similar to ovarian aging, aged testis exhibit reduced blood flow and perfusion rate. These changes are accompanied by alterations in arterial resistance and microvascular structure, including impaired vasoconstriction in response to noradrenaline and collapse of peritubular capillary networks (Takizawa and Hatakeyama, 1978; Dominguez et al., 2011). In line with this, testicular microvascular oxygen pressure decreases with age. Oxygen transport from testicular microvasculature to the interstitium requires a certain pressure gradient for diffusion. Therefore, this age-associated decline of microvascular oxygen may limit diffusional $O_2$ transport from microvessels to testicular mitochondria and hypoxic regions, thereby impairing testicular function (Dominguez et al., 2011).

## VASCULAR DYSREGULATION DURING ENDOCRINE DISORDERS

Despite altering endocrine function and vasculature, aging also constitutes a major risk factor for endocrine disorders such as diabetes, osteoporosis and vascular disease (Khosla et al., 2020). Diabetes mellitus is one of the most commonly diagnosed endocrine disorders. It describes a group of chronic metabolic disorders characterized by persistent high blood sugar levels (hyperglycemia) caused by insulin resistance, inadequate secretion of insulin or excessive secretion of glucagon (Lipscombe and Hux, 2007; Blair, 2016). Three-dimensional analysis of the pancreas vasculature demonstrated reduced islet vasculature and vascular branch points in nonobese diabetic (NOD) mice compared to wild-type mice. In addition, NOD mice show reduced numbers of islets and β-cell mass, suggesting a crucial role of the complex inter-islet vascular network to maintain islet function and hormone transport (El-Gohary et al., 2012).

Furthermore, diabetes is associated with many comorbidities and vascular complications that are considered the leading cause of morbidity and mortality. These vascular complications

include atherosclerosis, hypertension, cardiovascular disease and endothelial dysfunction (Domingueti et al., 2016). Platelets of diabetic patients show increased aggregation and adhesiveness. This platelet hyperactivity triggers and promotes atherosclerosis (Tschoepe et al., 1990, 1995; Yngen et al., 2004). In the arterial vasculature, MMP-mediated degradation of ECM proteins is downregulated, which increases ECM disposition and leads to pathological vascular remodeling (Portik-Dobos et al., 2002). Endothelial dysfunction is linked to increased vascular arginase expression and activity and reduced endothelial production of vasodilating NO. Arginase competes with endothelial NO synthase (eNOS) for its substrate arginine. This reduces arginine availability to eNOS, leading to decreased NO production and impaired vasorelaxation. Instead, superoxide production increases, inducing oxidative stress measured by elevated levels of lipid peroxidation (Tawfik et al., 2006; Romero Maritza et al., 2008).

Insulin resistance, a hallmark of type 2 diabetes, is associated with obesity. Insulin resistance and obesity interact in a complex system and induce a range of metabolic and proinflammatory changes that impair vascular function and structure, increasing the risk of vascular complications (Tounian et al., 2001; Ho et al., 2011; DeMarco et al., 2015; Camastra et al., 2017; Petrie et al., 2018). Activation of the cell-cycle regulator and tumor suppressor protein p53 in adipose tissue crucially contributes to insulin resistance and is linked to obesity.

In Ay mice, ectopic expression of agouti peptide induces excessive calorie intake via disruption of the melanocortin pathway, inducing senescence-like changes in adipose tissue including an accumulation of oxidative stress increased inflammatory cytokine production and activity of senescence-associated beta-galactosidase (Minamino et al., 2009). A similar study with C57BL6/J mice on a high-fat diet supports these findings, demonstrating increased DNA oxidation, DNA damage, reduced telomere length and increased p53 pathway activation in adipocytes (Vergoni et al., 2016). Targeted inhibition of p53 in adipose tissue in $Trp53^{loxP/loxP}$ Fabp4-Cre mice reduces inflammatory cytokine production and improves insulin resistance, while pharmacological activation of p53 stimulates lipolysis and reduces insulin-induced transport of glucose, thereby enhancing inflammation and inducing insulin resistance (Minamino et al., 2009; Vergoni et al., 2016).

A recent study by Avram and colleagues developed a digital biomarker for type 2 diabetes using smartphone-measured photoplethysmography (PPG), that measures heart rate and peripheral blood oxygen saturation (Avram et al., 2020). Here, they developed a deep neural network that analyses smartphone-measured PPG recordings to predict type 2 diabetes development independent of other comorbidities.

Central diabetes insipidus (CDI) describes a deficiency of the hormone AVP, leading to excessive thirst and production of dilute urine. CDI is often caused by degeneration of hypothalamic neurons and is associated with reduced local arterial blood flow and abnormal blood supply to the posterior lobe of the pituitary gland (Maghnie et al., 2004).

Besides diabetes, polycystic ovarian syndrome (PCOS) is considered one of the most prevalent endocrine disorders and is characterized by hyperandrogenism, oligomenorrhea or amenorrhea and ovarian cysts. PCOS is often accommodated by comorbidities such as cardiovascular disease, type-2 diabetes and infertility (Mariana Di et al., 2018). Ovaries of women with PCOS exhibit multiple vascular anomalies that affect follicular blood supply, including increased VEGF levels, blood flow rate and stromal vascularization (Agrawal et al., 1998; Abd El Aal et al., 2005; Alcázar and Kudla, 2012). Ultrasound assessment of ovarian morphology and blood flow in PCOS patients revealed enlarged ovarian size that correlated with increased insulin levels (Carmina et al., 2005). Moreover, increased ovarian blood flow in PCOS patients correlated with elevated levels of testosterone, estradiol and VEGF (Agrawal et al., 1998; Carmina et al., 2005). Increased TGFβ levels and bioavailability may facilitate ovarian angiogenesis and fibrosis in PCOS (Tal et al., 2013; Liu et al., 2015). Furthermore, PDGF-β levels are reportedly decreased in PCOS (Scotti et al., 2014; Di Pietro et al., 2015). Besides stimulating angiogenesis, PDGFRβ signaling is involved in regulating early folliculogenesis (Pinkas et al., 2008). Therefore, decreased ovarian PDGF-β levels may contribute to deregulated angiogenesis and abnormal accumulation of primordial follicles (Scotti et al., 2014).

Cushing's disease describes the overproduction of glucocorticoids caused by ACTH-secreting pituitary tumors. Immunohistochemical studies revealed a decreased microvascular density and increased vessel diameter in pituitary adenomas (Turner et al., 2000; Takano et al., 2014). Glucocorticoids are known to inhibit angiogenesis and increase TSP-1 levels (Logie et al., 2010; Yang et al., 2018), suggesting that ACTH-secreting tumors may alter vascular architecture. Cushing's disease is associated with hypercorticism, which is a major cause of glucocorticoid-induced osteoporosis (GIO) (Bolanowski et al., 2015). GIO, in turn, is associated with additional vascular changes such as a decline of PDGF-β levels and bone-specific type H vessels, impairing both angiogenesis and osteogenesis (Yang et al., 2018).

During a process termed endothelial-mesenchymal transition (EndMT), ECs are able to acquire a myofibroblastic or mesenchymal phenotype that includes a loss of cell-cell junctions and the acquisition of migratory and invasive properties (Lin et al., 2012). ECs lose their endothelial markers and express mesenchymal markers such as fibroblast-specific protein 1 (FSP1) and α-smooth muscle actin. This mesenchymal phenotype also includes a loss of cell-cell junctions and the acquisition of migratory and invasive properties. This type of transdifferentiation causes multiple morphological changes and contributes to many pathological processes and diseases, including fibrosis and tumor progression (Zeisberg et al., 2007b; Lin et al., 2012). Using lineage tracing experiments, ECs have been found to undergo EndMT and contribute to the progression of cardiac fibrosis (Zeisberg et al., 2007b). This process is mediated by TGF-β1 and Smad3-signaling that stimulates endothelial proliferation and is able to induce the acquisition of a fibroblast-like phenotype (Zeisberg et al., 2007a,b). In streptozotocin-induced diabetic mice, ECs undergo EndMT and begin to express

the fibroblast marker endothelin-1 (ET-1) which itself promotes cardiac fibrosis and heart failure via EndMT-associated fibroblast accumulation (Widyantoro et al., 2010). EndMT has also been identified as a mechanism in the early development of renal fibrosis in diabetic mice. Genetic lineage tracing demonstrated a significant proportion of renal myofibroblasts of endothelial origin in streptozotocin-induced diabetic Tie2-Cre;LoxP-EGFP mice (Li et al., 2009). Furthermore, there is evidence for EndMT as a source of cancer-associated fibroblasts that play an important role in tumor progression and affect the tumor microenvironment through the secretion of ECM molecules and paracrine factors (Lin et al., 2012). In tumors of Tie2-cre; R26Rosa-lox-Stop-lox-LacZ mice, that labels all EC-derived cells with LacZ (β-galactosidase), a portion of FSP1+ and αSMA+ cells were LacZ positive, indicating an endothelial origin of these fibroblasts (Zeisberg et al., 2007a).

## BONE: VASCULAR HETEROGENEITY, AGING, AND ENDOCRINE FUNCTIONS

The vasculature of the skeletal system is crucial for delivering nutrients and oxygen to the stem and progenitor cells that reside in specialized vascular niches in the bone marrow (BM). Moreover, BM ECs secrete a variety of angiocrine signals to maintain resident stem cells and regulate bone angiogenesis, osteogenesis and hematopoiesis (Colmone and Sipkins, 2008; Sivan et al., 2019; Stucker et al., 2020). BM ECs show a remarkable heterogeneity based on the distinct expression pattern of vascular cell surface markers such as CD31 (Pecam-1), Endomucin and E-selectin (Winkler et al., 2012; Kusumbe et al., 2014). The most abundant vessels in the BM are fenestrated sinusoidal type L vessels that express low Endomucin and CD31 levels (Kusumbe et al., 2014). Type H endothelium, a vessel subtype that is mainly found in metaphyseal BM near the growth plate, is characterized by high expression of these two markers. Type H vessels are directly connected to arterioles and contain higher oxygen levels and blood flow rate than type L vessels, thereby creating distinct vascular niches in the BM (Kusumbe et al., 2014; Duarte et al., 2018). BM ECs are associated with distinct perivascular cell types that contribute to specialized vascular niches for hematopoietic stem cells (HSCs). Arterioles and type H vessels are supported by pericytes that express PDGFRβ and NG2, whereas sinusoidal type L endothelium is surrounded by CXCL12-abundant reticular (CAR) cells and perivascular LepR+ cells (Sugiyama et al., 2006; Ding et al., 2012; Kunisaki et al., 2013). Furthermore, type H endothelium is associated with osteoprogenitors and couples osteogenesis to angiogenesis by expressing osteogenic and angiogenic factors such as VEGF, PDGF-β and HIF-1α (Kusumbe et al., 2014; Romeo et al., 2019; Rumney et al., 2019; Chen et al., 2020a).

Skeletal aging induces significant morphological changes in BM endothelium, including decreased vascular integrity and increased leakiness (Poulos et al., 2017; Stucker et al., 2020). Aged BM exhibits a significant reduction in arteriolar and type H vessels as well as PDGFRβ-expressing pericytes (Kusumbe et al., 2014, 2016; Singh et al., 2019). This age-related decline of type H endothelium is accompanied by a reduction of osteoprogenitors, subsequently resulting in decreased osteogenesis and bone density (Kusumbe et al., 2016). Metabolic changes in aged endothelium include increased hypoxia and ROS levels that impair angiogenesis (Poulos et al., 2017). Furthermore, BM aging reduces endothelial expression of CXCL12, SCF, and other signals that are essential for HSC maintenance and homeostasis (Kusumbe et al., 2016; Poulos et al., 2017).

The continuous renewal of the skeletal system suggests that bone homeostasis is interlinked with energy metabolism (Karsenty, 2006). This was demonstrated by the discovery that the skeletal system was capable of secreting a range of hormones that are important for energy metabolism and fertility. Osteocalcin (OCN) secreted from osteoblasts modulates a range of physiological parameters. OCN controls glucose-stimulated insulin secretion and proliferation of β-cells in the pancreas. Moreover, OCN signals to the muscle, live and adipocytes to regulate insulin sensitivity (Lee et al., 2007). OCN secreted from the bone is important in male fertility in mice and humans by increasing testosterone synthesis in LCs (Oury et al., 2011). Osteocalcin regulates murine and human fertility through a pancreas-bone-testis axis (Oury et al., 2013a). Male and female Ocn-null mice show docility and a reduction in spatial learning, which was shown to be due to OCN being able to cross the blood-brain barrier to stimulate hippocampal development and neurotransmitter synthesis (Oury et al., 2013b).

Fibroblast growth factor 23 (FGF23) is produced by osteocytes to regulate 1-alpha-hydroxylase, serum phosphate and para-thyroid hormone (PTH), providing an important signal in phosphate metabolism in the kidney to regulate renal homeostasis (Urakawa et al., 2006; Ben-Dov et al., 2007; Karsenty and Olson, 2016). It has recently been shown that lipocalin (LPN) specifically secreted from osteoblasts regulates food intake in mice (Mosialou et al., 2017). Furthermore, the function of regulation lipocalin is conserved in higher-order primates to regulate hunger (Petropoulou et al., 2020).

## CONCLUSION

The endocrine system consists of various glands that produce and secrete hormones to regulate a wide range of physiological processes and maintain the homeostasis. As hormone transport takes place via the bloodstream, endocrine glands are vascularized with a dense microvascular network (Hiller-Sturmhöfel and Bartke, 1998). This dense vascularization pattern is crucial for sensing changes in blood composition and transporting hormones and regulatory signals (Katoh, 2003; Jang et al., 2017). Moreover, the microvasculature provides a microenvironment that harbors stem and progenitor cells, regulating their survival, maintenance and differentiation. This vascular niche also interacts with endocrine cells to support and maintain efficient gland function (Ballian and Brunicardi, 2007; Colin et al., 2013).

Aging of the endocrine system significantly alters the vascular network of the endocrine system, decreasing vascular density and function. This vascular decline disrupts the blood and disrupts

the tissue microenvironment, amalgamating in impairment of endocrine gland function. Thereby, vascular changes and associated microenvironmental alterations in the aging endocrine system may contribute to tissue aging and may be involved in the pathogenesis of various endocrine disorders.

## AUTHOR CONTRIBUTIONS

SS wrote the original draft. SS and JD revised the review. AK designed the review structure and edited the manuscript. All authors contributed to the article and approved the submitted version.

## FUNDING

AK was supported by the Medical Research Council (CDA: MR/P02209X/1), European Research Council (StG: metaNiche, 805201), Leuka (2017/JGF/001), The Royal Society (RG170326), Kennedy Trust for Rheumatology Research (KENN 15 16 09), and John Fell Fund OUP Research Fund (161/061).

## REFERENCES

Abd El Aal, D. E. M., Mohamed, S. A., Amine, A. F., and Meki, A.-R. M. A. (2005). Vascular endothelial growth factor and insulin-like growth factor-1 in polycystic ovary syndrome and their relation to ovarian blood flow. *Eur. J. Obstetr. Gynecol. Reprod. Biol.* 118, 219–224. doi: 10.1016/j.ejogrb.2004.07.024

Abramovich, D., Rodriguez Celin, A., Hernandez, F., Tesone, M., and Parborell, F. (2009). Spatiotemporal analysis of the protein expression of angiogenic factors and their related receptors during folliculogenesis in rats with and without hormonal treatment. *Reproduction* 137, 309–320. doi: 10.1530/rep-08-0130

Acosta, T. J., Hayashi, K. G., Ohtani, M., and Miyamoto, A. (2003). Local changes in blood flow within the preovulatory follicle wall and early corpus luteum in cows. *Reproduction* 125, 759–767.

Agrawal, R., Conway, G., Sladkevicius, P., Tan, S. L., Engmann, L., Payne, N., et al. (1998). Serum vascular endothelial growth factor and Doppler blood flow velocities in in vitro fertilization: relevance to ovarian hyperstimulation syndrome and polycystic ovaries. *Fertil. Steril.* 70, 651–658. doi: 10.1016/S0015-0282(98)00249-0

Aimaretti, G., Corneli, G., Baldelli, R., Di Somma, C., Gasco, V., Durante, C., et al. (2003). Diagnostic reliability of a single IGF-I measurement in 237 adults with total anterior hypopituitarism and severe GH deficiency. *Clin. Endocrinol.* 59, 56–61. doi: 10.1046/j.1365-2265.2003.01794.x

Akbaraly, N. T., Hininger-Favier, I., Carrière, I., Arnaud, J., Gourlet, V., Roussel, A.-M., et al. (2007). Plasma selenium over time and cognitive decline in the elderly. *Epidemiology* 18, 52–58.

Albert, C., Garrido, N., Mercader, A., Rao, C. V., Remohí, J., Simón, C., et al. (2002). The role of endothelial cells in the pathogenesis of ovarian hyperstimulation syndrome. *Mol. Hum. Reprod.* 8, 409–418. doi: 10.1093/molehr/8.5.409

Alcázar, J. L., and Kudla, M. J. (2012). Ovarian stromal vessels assessed by spatiotemporal image correlation–high definition flow in women with polycystic ovary syndrome: a case–control study. *Ultrasound Obstetr. Gynecol.* 40, 470–475. doi: 10.1002/uog.11187

Almaça, J., Molina, J., Arrojo, E., Drigo, R., Abdulreda, M. H., Jeon, W. B., et al. (2014). Young capillary vessels rejuvenate aged pancreatic islets. *Proc. Natl. Acad. Sci. U.S.A.* 111, 17612–17617. doi: 10.1073/pnas.1414053111

Amar, A. P., and Weiss, M. H. (2003). Pituitary anatomy and physiology. *Neurosurg. Clin. N. Am.* 14, 11–23. doi: 10.1016/s1042-3680(02)00017-7

Andersen, A.-M. N., Wohlfahrt, J., Christens, P., Olsen, J., and Melbye, M. (2000). Maternal age and fetal loss: population based register linkage study. *BMJ* 320:1708. doi: 10.1136/bmj.320.7251.1708

Andoniadou, C. L., Matsushima, D., Mousavy Gharavy, S. N., Signore, M., Mackintosh, A. I., Schaeffer, M., et al. (2013). Sox2(+) stem/progenitor cells in the adult mouse pituitary support organ homeostasis and have tumor-inducing potential. *Cell Stem Cell* 13, 433–445. doi: 10.1016/j.stem.2013.07.004

Ansurudeen, I., Kopprasch, S., Ehrhart-Bornstein, M., Willenberg, H. S., Krug, A. W., Funk, R. H. W., et al. (2006). Vascular-adrenal Niche - endothelial cell-mediated sensitization of human adrenocortical cells to Angiotensin II. *Horm. Metab. Res.* 38, 476–480. doi: 10.1055/s-2006-948136

Ansurudeen, I., Willenberg, H. S., Kopprasch, S., Krug, A. W., Ehrhart-Bornstein, M., and Bornstein, S. R. (2009). Endothelial factors mediate aldosterone release via PKA-independent pathways. *Mol. Cell Endocrinol.* 300, 66–70. doi: 10.1016/j.mce.2008.11.020

Atzmon, G., Barzilai, N., Hollowell, J. G., Surks, M. I., and Gabriely, I. (2009). Extreme longevity is associated with increased serum thyrotropin. *J. Clin. Endocrinol. Metab.* 94, 1251–1254. doi: 10.1210/jc.2008-2325

Augustin, H. G., Braun, K., Telemenakis, I., Modlich, U., and Kuhn, W. (1995). Ovarian angiogenesis. Phenotypic characterization of endothelial cells in a physiological model of blood vessel growth and regression. *Am. J. Pathol.* 147, 339–351.

Augustin, H. G., and Koh, G. Y. (2017). Organotypic vasculature: from descriptive heterogeneity to functional pathophysiology. *Science* 357:eaal2379. doi: 10.1126/science.aal2379

Aversa, A., Bruzziches, R., Francomano, D., Greco, E., Migliaccio, S., and Lenzi, A. (2011). The role of steroids in endothelial function in the aging male. *US Endocrinol.* 7, 145–149. doi: 10.17925/USE.2011.07.02.145

Avram, R., Olgin, J. E., Kuhar, P., Hughes, J. W., Marcus, G. M., Pletcher, M. J., et al. (2020). A digital biomarker of diabetes from smartphone-based vascular signals. *Nat. Med.* 26, 1576–1582. doi: 10.1038/s41591-020-1010-5

Azhar, S., Cao, L., and Reaven, E. (1995). Alteration of the adrenal antioxidant defense system during aging in rats. *J. Clin. Invest.* 96, 1414–1424. doi: 10.1172/JCI118177

Ballian, N., and Brunicardi, F. C. (2007). Islet vasculature as a regulator of endocrine pancreas function. *World J. Surg.* 31, 705–714. doi: 10.1007/s00268-006-0719-8

Bassett, J. R., and West, S. H. (1997). Vascularization of the adrenal cortex: its possible involvement in the regulation of steroid hormone release. *Microsc. Res. Techn.* 36, 546–557. doi: 10.1002/(SICI)1097-0029(19970315)36:6<546::AID-JEMT11<3.0.CO;2-O

Behrman, H. R., Kodaman, P. H., Preston, S. L., and Gao, S. (2001). Oxidative stress and the ovary. *J. Soc. Gynecol. Invest.* 8, S40–S42. doi: 10.1016/s1071-5576(00)00106-4

Belloni, A. S., Rossi, G. P., Andreis, P. G., Neri, G., Albertin, G., Pessina, A. C., et al. (1996). Endothelin adrenocortical secretagogue effect is mediated by the B receptor in rats. *Hypertension* 27, 1153–1159. doi: 10.1161/01.hyp.27.5.1153

Ben-Dov, I. Z., Galitzer, H., Lavi-Moshayoff, V., Goetz, R., Kuro-o, M., Mohammadi, M., et al. (2007). The parathyroid is a target organ for FGF23 in rats. *J. Clin. Invest.* 117, 4003–4008. doi: 10.1172/JCI32409

Ben-Meir, A., Burstein, E., Borrego-Alvarez, A., Chong, J., Wong, E., Yavorska, T., et al. (2015). Coenzyme Q10 restores oocyte mitochondrial function and fertility during reproductive aging. *Aging cell* 14, 887–895. doi: 10.1111/acel.12368

Berisha, B., Schams, D., Kosmann, M., Amselgruber, W., and Einspanier, R. (2000). Expression and localisation of vascular endothelial growth factor and basic fibroblast growth factor during the final growth of bovine ovarian follicles. *J. Endocrinol.* 167, 371–382. doi: 10.1677/joe.0.1670371

Bhang, D. H., Kim, B.-J., Kim, B. G., Schadler, K., Baek, K.-H., Kim, Y. H., et al. (2018). Testicular endothelial cells are a critical population in the germline stem cell niche. *Nat. Commun.* 9:4379. doi: 10.1038/s41467-018-06881-z

Blair, M. (2016). Diabetes mellitus review. *Urol. Nurs.* 36, 27–36.

Blum, M. R., Bauer, D. C., Collet, T. H., Fink, H. A., Cappola, A. R., da Costa, B. R., et al. (2015). Subclinical thyroid dysfunction and fracture risk: a meta-analysis. *JAMA* 313, 2055–2065. doi: 10.1001/jama.2015.5161

Bolanowski, M., Halupczok, J., and Jawiarczyk-Przybyłowska, A. (2015). Pituitary disorders and osteoporosis. *Int. J. Endocrinol.* 2015:206853. doi: 10.1155/2015/206853

Bonner-Weir, S. (1988). Morphological evidence for pancreatic polarity of β-Cell within islets of langerhans. *Diabetes* 37:616. doi: 10.2337/diab.37.5.616

Bonner-Weir, S., Sullivan, B. A., and Weir, G. C. (2015). Human islet morphology revisited: human and rodent islets are not so different after all. *J. Histochem. Cytochem.* 63, 604–612. doi: 10.1369/0022155415570969

Borden, P., Houtz, J., Leach, S. D., and Kuruvilla, R. (2013). Sympathetic innervation during development is necessary for pancreatic islet architecture and functional maturation. *Cell Rep.* 4, 287–301. doi: 10.1016/j.celrep.2013.06.019

Borrás, C., Sastre, J., García-Sala, D., Lloret, A., Pallardó, F. V., and Viña, J. (2003). Mitochondria from females exhibit higher antioxidant gene expression and lower oxidative damage than males. *Free Radic. Biol. Med.* 34, 546–552. doi: 10.1016/S0891-5849(02)01356-4

Bott, R. C., Clopton, D. T., Fuller, A. M., McFee, R. M., Lu, N., McFee, R. M., et al. (2010). KDR-LacZ-expressing cells are involved in ovarian and testis-specific vascular development, suggesting a role for VEGFA in the regulation of this vasculature. *Cell Tissue Res.* 342, 117–130. doi: 10.1007/s00441-010-1038-9

Bott, R. C., McFee, R. M., Clopton, D. T., Toombs, C., and Cupp, A. S. (2006). Vascular endothelial growth factor and kinase domain region receptor are involved in both seminiferous cord formation and vascular development during testis morphogenesis in the Rat1. *Biol. Reprod.* 75, 56–67. doi: 10.1095/biolreprod.105.047225

Bremner, A. P., Feddema, P., Leedman, P. J., Brown, S. J., Beilby, J. P., Lim, E. M., et al. (2012). Age-related changes in thyroid function: a longitudinal study of a community-based cohort. *J. Clin. Endocrinol. Metab.* 97, 1554–1562. doi: 10.1210/jc.2011-3020

Brennan, J., Karl, J., and Capel, B. (2002). Divergent vascular mechanisms downstream of sry establish the arterial system in the XY Gonad. *Dev. Biol.* 244, 418–428. doi: 10.1006/dbio.2002.0578

Brissova, M., Shostak, A., Shiota, M., Wiebe, P. O., Poffenberger, G., Kantz, J., et al. (2006). Pancreatic islet production of vascular endothelial growth factor–a is essential for islet vascularization, revascularization, and function. *Diabetes* 55, 2974–2985. doi: 10.2337/db06-0690

Broekmans, F. J., Soules, M. R., and Fauser, B. C. (2009). Ovarian aging: mechanisms and clinical consequences. *Endoc. Rev.* 30, 465–493. doi: 10.1210/er.2009-0006

Broglio, F., Benso, A., Castiglioni, C., Gottero, C., Prodam, F., Destefanis, S., et al. (2003). The endocrine response to ghrelin as a function of gender in humans in young and elderly subjects. *J. Clin. Endocrinol. Metab.* 88, 1537–1542. doi: 10.1210/jc.2002-021504

Brown, H. M., and Russell, D. L. (2014). Blood and lymphatic vasculature in the ovary: development, function and disease. *Hum. Reprod. Update* 20, 29–39. doi: 10.1093/humupd/dmt049

Brunicardi, F. C., Stagner, J., Bonner-Weir, S., Wayland, H., Kleinman, R., Livingston, E., et al. (1996). Microcirculation of the islets of langerhans. long beach veterans administration regional medical education center symposium. *Diabetes* 45, 385–392. doi: 10.2337/diab.45.4.385

Bukovsky, A. (2011). Ovarian stem cell niche and follicular renewal in mammals. *Anat. Rec.* 294, 1284–1306. doi: 10.1002/ar.21422

Bukovský, A., Caudle, M. R., Keenan, J. A., Wimalasena, J., Foster, J. S., and Van Meter, S. E. (1995). Quantitative evaluation of the cell cycle-related retinoblastoma protein and localization of Thy-1 differentiation protein and macrophages during follicular development and atresia, and in human corpora lutea. *Biol. Reprod.* 52, 776–792. doi: 10.1095/biolreprod52.4.776

Bukovsky, A., Caudle, M. R., Svetlikova, M., and Upadhyaya, N. B. (2004). Origin of germ cells and formation of new primary follicles in adult human ovaries. *Reprod. Biol. Endocrinol.* 2:20. doi: 10.1186/1477-7827-2-20

Burek, C. L., and Rose, N. R. (2008). Autoimmune thyroiditis and ROS. *Autoimmun. Rev.* 7, 530–537. doi: 10.1016/j.autrev.2008.04.006

Cabrera, O., Berman, D. M., Kenyon, N. S., Ricordi, C., Berggren, P. O., and Caicedo, A. (2006). The unique cytoarchitecture of human pancreatic islets has implications for islet cell function. *Proc. Natl. Acad. Sci. U.S.A.* 103, 2334–2339. doi: 10.1073/pnas.0510790103

Camastra, S., Vitali, A., Anselmino, M., Gastaldelli, A., Bellini, R., Berta, R., et al. (2017). Muscle and adipose tissue morphology, insulin sensitivity and beta-cell function in diabetic and nondiabetic obese patients: effects of bariatric surgery. *Sci. Rep.* 7:9007. doi: 10.1038/s41598-017-08444-6

Cantaluppi, V., Biancone, L., Romanazzi, G. M., Figliolini, F., Beltramo, S., Ninniri, M. S., et al. (2006). Antiangiogenic and immunomodulatory effects of rapamycin on islet endothelium: relevance for islet transplantation. *Am. J. Transplant.* 6, 2601–2611. doi: 10.1111/j.1600-6143.2006.01534.x

Carmina, E., Orio, F., Palomba, S., Longo, R. A., Lombardi, G., and Lobo, R. A. (2005). Ovarian size and blood flow in women with polycystic ovary syndrome and their correlations with endocrine parameters. *Fertil. Steril.* 84, 413–419. doi: 10.1016/j.fertnstert.2004.12.061

Carsia, R. V., Macdonald, G. J., Gibney, J. A., Tilly, K. I., and Tilly, J. L. (1996). Apoptotic cell death in the rat adrenal gland: an in vivo and in vitro investigation. *Cell Tissue Res.* 283, 247–254. doi: 10.1007/s004410050535

Chang, A. M., and Halter, J. B. (2003). Aging and insulin secretion. *Am. J. Physiol. Endocrinol. Metab.* 284, E7–E12. doi: 10.1152/ajpendo.00366.2002

Chang, S.-P., Morrison, H. D., Nilsson, F., Kenyon, C. J., West, J. D., and Morley, S. D. (2013). Cell proliferation, movement and differentiation during maintenance of the adult mouse adrenal cortex. *PLoS One* 8:e81865. doi: 10.1371/journal.pone.0081865

Chen, H., Cangello, D., Benson, S., Folmer, J., Zhu, H., Trush, M. A., et al. (2001). Age-related increase in mitochondrial superoxide generation in the testosterone-producing cells of Brown Norway rat testes: relationship to reduced steroidogenic function? *Exp. Gerontol.* 36, 1361–1373. doi: 10.1016/S0531-5565(01)00118-8

Chen, H., Gu, X., Liu, Y., Wang, J., Wirt, S. E., Bottino, R., et al. (2011). PDGF signalling controls age-dependent proliferation in pancreatic β-cells. *Nature* 478, 349–355. doi: 10.1038/nature10502

Chen, H., Hardy, M. P., Huhtaniemi, I., and Zirkin, B. R. (1994). Age-related decreased Leydig cell testosterone production in the brown Norway rat. *J. Androl.* 15, 551–557.

Chen, J., Crabbe, A., Van Duppen, V., and Vankelecom, H. (2006). The notch signaling system is present in the postnatal pituitary: marked expression and regulatory activity in the newly discovered side population. *Mol. Endocrinol.* 20, 3293–3307. doi: 10.1210/me.2006-0293

Chen, J., Hendriks, M., Chatzis, A., Ramasamy, S. K., and Kusumbe, A. P. (2020a). Bone vasculature and bone marrow vascular niches in health and disease. *J. Bone Min. Res.* 35, 2103–2120. doi: 10.1002/jbmr.4171

Chen, J., Lippo, L., Labella, R., Tan, S. L., Marsden, B. D., Dustin, M. L., et al. (2020b). Decreased blood vessel density and endothelial cell subset dynamics during ageing of the endocrine system. *EMBO J.* 40:e105242. doi: 10.15252/embj.2020105242

Chen, M., Bergman, R. N., Pacini, G., Porte, D. Jr. (1985). Pathogenesis of age-related glucose intolerance in man: insulin resistance and decreased beta-cell function. *J. Clin. Endocrinol. Metab.* 60, 13–20. doi: 10.1210/jcem-60-1-13

Cheryl, D. C. (2008). Chronic stress-induced hippocampal vulnerability: the glucocorticoid vulnerability hypothesis. *Rev. Neurosci.* 19, 395–412. doi: 10.1515/REVNEURO.2008.19.6.395

Chou, T. M., Sudhir, K., Hutchison, S. J., Ko, E., Amidon, T. M., Collins, P., et al. (1996). Testosterone induces dilation of canine coronary conductance and resistance arteries in vivo. *Circulation* 94, 2614–2619. doi: 10.1161/01.cir.94.10.2614

Christina, R., Saskia, E., Irene, E., Bruno, S., Markus, W. B., Peter, P. N., et al. (2009). Impaired islet turnover in human donor pancreata with aging. *Eur. J. Endocrinol.* 160, 185–191. doi: 10.1530/EJE-08-0596

Chrousos, G. P. (2007). Organization and integration of the endocrine system: the arousal and sleep perspective. *Sleep Med. Clin.* 2, 125–145. doi: 10.1016/j.jsmc.2007.04.004

Clapp, C., Thebault, S., Jeziorski, M. C., Martínez, and De La Escalera, G. (2009). Peptide hormone regulation of angiogenesis. *Physiol. Rev.* 89, 1177–1215. doi: 10.1152/physrev.00024.2009

Cleaver, O., and Melton, D. A. (2003). Endothelial signaling during development. *Nat. Med.* 9, 661–668. doi: 10.1038/nm0603-661

Clement, P. B. (1987). "Anatomy and histology of the ovary," in *Blaustein's Pathology of the Female Genital Tract*, ed. R. J. Kurman (New York, NY: Springer), 438–470.

Colin, I. M., Denef, J.-F., Lengelé, B., Many, M.-C., and Gérard, A.-C. (2013). Recent insights into the cell biology of thyroid angiofollicular units. *Endocr. Rev.* 34, 209–238. doi: 10.1210/er.2012-1015

Colli, L. G., Belardin, L. B., Echem, C., Akamine, E. H., Antoniassi, M. P., Andretta, R. R., et al. (2019). Systemic arterial hypertension leads to decreased semen quality and alterations in the testicular microcirculation in rats. *Sci. Rep.* 9:11047. doi: 10.1038/s41598-019-47157-w

Collin, O., Bergh, A., Damber, J. E., and Widmark, A. (1993). Control of testicular vasomotion by testosterone and tubular factors in rats. *J. Reprod. Fertil.* 97, 115–121. doi: 10.1530/jrf.0.0970115

Collin, O., Zupp, J. L., and Setchell, B. P. (2000). Testicular vasomotion in different mammals. *Asian J. Androl.* 2, 297–300.

Colmone, A., and Sipkins, D. A. (2008). Beyond angiogenesis: the role of endothelium in the bone marrow vascular niche. *Transl. Res.* 151, 1–9. doi: 10.1016/j.trsl.2007.09.003

Cooksey, R. C., Jouihan, H. A., Ajioka, R. S., Hazel, M. W., Jones, D. L., Kushner, J. P., et al. (2004). Oxidative stress, beta-cell apoptosis, and decreased insulin secretory capacity in mouse models of hemochromatosis. *Endocrinology* 145, 5305–5312. doi: 10.1210/en.2004-0392

Coppé, J. P., Kauser, K., Campisi, J., and Beauséjour, C. M. (2006). Secretion of vascular endothelial growth factor by primary human fibroblasts at senescence. *J. Biol. Chem.* 281, 29568–29574. doi: 10.1074/jbc.M603307200

Corsonello, A., Montesanto, A., Berardelli, M., De Rango, F., Dato, S., Mari, V., et al. (2010). A cross-section analysis of FT3 age-related changes in a group of old and oldest-old subjects, including centenarians' relatives, shows that a down-regulated thyroid function has a familial component and is related to longevity. *Age Age.* 39, 723–727. doi: 10.1093/ageing/afq116

Costello, M. F., Shrestha, S. M., Sjoblom, P., McNally, G., Bennett, M. J., Steigrad, S. J., et al. (2006). Power doppler ultrasound assessment of the relationship between age and ovarian perifollicular blood flow in women undergoing in vitro fertilization treatment. *J. Assist. Reprod. Genet.* 23, 359–365. doi: 10.1007/s10815-006-9067-8

Coveney, D., Cool, J., Oliver, T., and Capel, B. (2008). Four-dimensional analysis of vascularization during primary development of an organ, the gonad. *Proc. Natl. Acad. Sci. U.S.A.* 105:7212. doi: 10.1073/pnas.0707674105

Cozzolino, M. F., Pereira, K. F., and Chopard, R. P. (2005). Analysis of thyroid gland microvascularization in rats induced by ingestion of potassium bromide: a scanning electron microscopy study. *Ann. Anat.* 187, 71–76. doi: 10.1016/j.aanat.2004.08.004

Crawford, S. E., Stellmach, V., Murphy-Ullrich, J. E., Ribeiro, S. M., Lawler, J., Hynes, R. O., et al. (1998). Thrombospondin-1 is a major activator of TGF-beta1 in vivo. *Cell* 93, 1159–1170. doi: 10.1016/s0092-8674(00)81460-9

da Costa, V. M., Moreira, D. G., and Rosenthal, D. (2001). Thyroid function and aging: gender-related differences. *J. Endocrinol.* 171, 193–198. doi: 10.1677/joe.0.1710193

Damber, J. E., Maddocks, S., Widmark, A., and Bergh, A. (1992). Testicular blood flow and vasomotion can be maintained by testosterone in Leydig cell-depleted rats. *Int. J. Androl.* 15, 385–393. doi: 10.1111/j.1365-2605.1992.tb01353.x

Daniel, P. M. (1966). The blood supply of the hypothalamus and pituitary glanD. *Br. Med. Bull.* 22, 202–208. doi: 10.1093/oxfordjournals.bmb.a070474

de Lamirande, E., Jiang, H., Zini, A., Kodama, H., and Gagnon, C. (1997). Reactive oxygen species and sperm physiology. *Rev. Reprod.* 2, 48–54. doi: 10.1530/ror.0.0020048

Dean, P. M., and Matthews, E. K. (1968). Electrical activity in pancreatic islet cells. *Nature* 219, 389–390. doi: 10.1038/219389a0

DeFronzo, R. A. (1981). Glucose intolerance and aging. *Diabetes Care* 4, 493–501. doi: 10.2337/diacare.4.4.493

DeMarco, V. G., Habibi, J., Jia, G., Aroor, A. R., Ramirez-Perez, F. I., Martinez-Lemus, L. A., et al. (2015). Low-dose mineralocorticoid receptor blockade prevents western diet-induced arterial stiffening in female mice. *Hypertension* 66, 99–107. doi: 10.1161/hypertensionaha.115.05674

Desjardins, C., and Ewing, L. (1993). *Cell and Molecular Biology of the Testis*. Oxford: Oxford University Press.

Di Pietro, M., Parborell, F., Irusta, G., Pascuali, N., Bas, D., Bianchi, M. S., et al. (2015). Metformin regulates ovarian angiogenesis and follicular development in a female polycystic ovary syndrome rat model. *Endocrinology* 156, 1453–1463. doi: 10.1210/en.2014-1765

Ding, B. S., Cao, Z., Lis, R., Nolan, D. J., Guo, P., Simons, M., et al. (2014). Divergent angiocrine signals from vascular niche balance liver regeneration and fibrosis. *Nature* 505, 97–102. doi: 10.1038/nature12681

Ding, L., Saunders, T. L., Enikolopov, G., and Morrison, S. J. (2012). Endothelial and perivascular cells maintain haematopoietic stem cells. *Nature* 481, 457–462. doi: 10.1038/nature10783

Domenico, B., Dominique, G. R., and Philippe, A. H. (2007). Differential expression of E-cadherin at the surface of rat β-cells as a marker of functional heterogeneity. *J. Endocrinol.* 194, 21–29. doi: 10.1677/JOE-06-0169

Domingueti, C. P., Dusse, L. M., Carvalho, M., de Sousa, L. P., Gomes, K. B., and Fernandes, A. P. (2016). Diabetes mellitus: the linkage between oxidative stress, inflammation, hypercoagulability and vascular complications. *J. Diabetes Complic.* 30, 738–745. doi: 10.1016/j.jdiacomp.2015.12.018

Dominguez, J. M., Davis, R. T., McCullough, D. J., Stabley, J. N., and Behnke, B. J. (2011). Aging and exercise training reduce testes microvascular Po2 and alter vasoconstrictor responsiveness in testicular arterioles. *Am. J. Physiol. Regul. Integr. Comp. Physiol.* 301, R801–R810. doi: 10.1152/ajpregu.00203.2011

Duarte, D., Hawkins, E. D., Akinduro, O., Ang, H., De Filippo, K., Kong, I. Y., et al. (2018). Inhibition of endosteal vascular niche remodeling rescues hematopoietic stem cell loss in AML. *Cell Stem Cell* 22, 64.e6–77.e6. doi: 10.1016/j.stem.2017.11.006

Duthoit, C., Estienne, V., Giraud, A., Durand-Gorde, J.-M., Rasmussen, ÅK., Feldt-Rasmussen, U., et al. (2001). Hydrogen peroxide-induced production of a 40 kDa immunoreactive thyroglobulin fragment in human thyroid cells: the onset of thyroid autoimmunity? *Biochem. J.* 360, 557–562. doi: 10.1042/bj3600557

Ehrhart-Bornstein, M., Hinson, J. P., Bornstein, S. R., Scherbaum, W. A., and Vinson, G. P. (1998). Intraadrenal interactions in the regulation of adrenocortical steroidogenesis. *Endocr. Rev.* 19, 101–143. doi: 10.1210/edrv.19.2.0326

El-Gohary, Y., Sims-Lucas, S., Lath, N., Tulachan, S., Guo, P., Xiao, X., et al. (2012). Three-dimensional analysis of the islet vasculature. *Anat. Rec.* 295, 1473–1481. doi: 10.1002/ar.22530

Ellenbroek, J. H., Töns, H. A., de Graaf, N., Loomans, C. J., Engelse, M. A., Vrolijk, H., et al. (2013). Topologically heterogeneous beta cell adaptation in response to high-fat diet in Mice. *PLoS One* 8:e56922. doi: 10.1371/journal.pone.0056922

English, K. M., Jones, R. D., Jones, T. H., Morice, A. H., and Channer, K. S. (2001). Gender differences in the vasomotor effects of different steroid hormones in rat pulmonary and coronary arteries. *Horm. Metab. Res.* 33, 645–652. doi: 10.1055/s-2001-18689

Ergün, S., Stingl, J., and Holstein, A. F. (1994). Microvasculature of the human testis in correlation to Leydig cells and seminiferous tubules. *Andrologia* 26, 255–262. doi: 10.1111/j.1439-0272.1994.tb00799.x

Faddy, M. J., Gosden, R. G., Gougeon, A., Richardson, S. J., and Nelson, J. F. (1992). Accelerated disappearance of ovarian follicles in mid-life: implications for forecasting menopause. *Hum. Reprod.* 7, 1342–1346. doi: 10.1093/oxfordjournals.humrep.a137570

Fang, L., Li, Y., Wang, S., Li, Y., Chang, H. M., Yi, Y., et al. (2020). TGF-β1 induces VEGF expression in human granulosa-lutein cells: a potential mechanism for the pathogenesis of ovarian hyperstimulation syndrome. *Exp. Mol. Med.* 52, 450–460. doi: 10.1038/s12276-020-0396-y

Fauquier, T., Rizzoti, K., Dattani, M., Lovell-Badge, R., and Robinson, I. C. A. F. (2008). SOX2-expressing progenitor cells generate all of the major cell types in the adult mouse pituitary gland. *Proc. Natl. Acad. Sci. U.S.A.* 105, 2907–2912. doi: 10.1073/pnas.0707886105

Ferdinand, R., Hanno, P., Daniel, M. K., and Johannes, D. V. (2012). Diminished adrenal sensitivity and ACTH efficacy in obese premenopausal women. *Eur. J. Endocrinol.* 167, 633–642. doi: 10.1530/EJE-12-0592

Ferrara, N., Chen, H., Davis-Smyth, T., Gerber, H. P., Nguyen, T. N., Peers, D., et al. (1998). Vascular endothelial growth factor is essential for corpus luteum angiogenesis. *Nat. Med.* 4, 336–340. doi: 10.1038/nm0398-336

Ferrara, N., Schweigerer, L., Neufeld, G., Mitchell, R., and Gospodarowicz, D. (1987). Pituitary follicular cells produce basic fibroblast growth factor. *Proc. Natl. Acad. Sci. U.S.A.* 84, 5773–5777. doi: 10.1073/pnas.84.16.5773

Finkelstein, J. S., Brockwell, S. E., Mehta, V., Greendale, G. A., Sowers, M. R., Ettinger, B., et al. (2008). Bone mineral density changes during the menopause

transition in a multiethnic cohort of women. *J. Clin. Endocrinol. Metab.* 93, 861–868. doi: 10.1210/jc.2007-1876

Flesken-Nikitin, A., Hwang, C.-I., Cheng, C.-Y., Michurina, T. V., Enikolopov, G., and Nikitin, A. Y. (2013). Ovarian surface epithelium at the junction area contains a cancer-prone stem cell niche. *Nature* 495, 241–245. doi: 10.1038/nature11979

Fliers, E., Kalsbeek, A., and Boelen, A. (2014). Beyond the fixed setpoint of the hypothalamus-pituitary-thyroid axis. *Eur. J. Endocrinol.* 171, R197–R208. doi: 10.1530/eje-14-0285

Fraser, H. M. (2006). Regulation of the ovarian follicular vasculature. *Reprod. Biol. Endocrinol.* 4, 18–18. doi: 10.1186/1477-7827-4-18

Friedman, C. I., Danforth, D. R., Herbosa-Encarnacion, C., Arbogast, L., Alak, B. M., and Seifer, D. B. (1997). Follicular fluid vascular endothelial growth factor concentrations are elevated in women of advanced reproductive age undergoing ovulation induction. *Fertil. Steril.* 68, 607–612. doi: 10.1016/S0015-0282(97)00278-1

Fujii, E. Y., and Nakayama, M. (2010). The measurements of RAGE, VEGF, and AGEs in the plasma and follicular fluid of reproductive women: the influence of aging. *Fertil. Steril.* 94, 694–700. doi: 10.1016/j.fertnstert.2009.03.029

Fujino, Y., Ozaki, K., Yamamasu, S., Ito, F., Matsuoka, I., Hayashi, E., et al. (1996). DNA fragmentation of oocytes in aged mice. *Hum. Reprod.* 11, 1480–1483. doi: 10.1093/oxfordjournals.humrep.a019421

Fujita, H., and Murakami, T. (1974). Scanning electron microscopy on the distribution of the minute blood vessels in the thyroiod gland of the dog, rat and rhesus monkey. *Arch. Histol. Jpn.* 36, 181–188. doi: 10.1679/aohc1950.36.181

Furube, E., Mannari, T., Morita, S., Nishikawa, K., Yoshida, A., Itoh, M., et al. (2014). VEGF-dependent and PDGF-dependent dynamic neurovascular reconstruction in the neurohypophysis of adult mice. *J. Endocrinol.* 222, 161–179. doi: 10.1530/joe-14-0075

Garcia-Lavandeira, M., Diaz-Rodriguez, E., Bahar, D., Garcia-Rendueles, A. R., Rodrigues, J. S., Dieguez, C., et al. (2015). Pituitary cell turnover: from adult stem cell recruitment through differentiation to death. *Neuroendocrinology* 101, 175–192. doi: 10.1159/000375502

Garcia-Lavandeira, M., Quereda, V., Flores, I., Saez, C., Diaz-Rodriguez, E., Japon, M. A., et al. (2009). A GRFa2/Prop1/stem (GPS) cell niche in the pituitary. *PLoS One* 4:e4815. doi: 10.1371/journal.pone.0004815

Gérard, A. C., Many, M. C., Daumerie, C., Costagliola, S., Miot, F., DeVijlder, J. J., et al. (2002). Structural changes in the angiofollicular units between active and hypofunctioning follicles align with differences in the epithelial expression of newly discovered proteins involved in iodine transport and organification. *J. Clin. Endocrinol. Metab.* 87, 1291–1299. doi: 10.1210/jcem.87.3.8278

Gérard, A. C., Poncin, S., Audinot, J. N., Denef, J. F., and Colin, I. M. (2009). Iodide deficiency-induced angiogenic stimulus in the thyroid occurs via HIF- and ROS-dependent VEGF-A secretion from thyrocytes. *Am. J. Physiol. Endocrinol. Metab.* 296, E1414–E1422. doi: 10.1152/ajpendo.90876.2008

Gibelli, B., El-Fattah, A., Giugliano, G., Proh, M., and Grosso, E. (2009). Thyroid stem cells–danger or resource? *Acta Otorhinolaryngol. Italica* 29, 290–295.

Gilligan, D. M., Badar, D. M., Panza, J. A., Quyyumi, A. A., et al. (1994). Acute vascular effects of estrogen in postmenopausal women. *Circulation* 90, 786–791. doi: 10.1161/01.cir.90.2.786

Goldstein, M. B., and Davis, E. A. Jr. (1968). The three dimensional architecture of the islets of Langerhans. *Acta Anat.* 71, 161–171. doi: 10.1159/000143183

Gorczyca, J., Litwin, J. A., Pitynski, K., and Miodonski, A. J. (2010). Vascular system of human fetal pancreas demonstrated by corrosion casting and scanning electron microscopy. *Anat. Sci. Int.* 85, 235–240. doi: 10.1007/s12565-010-0084-4

Gospodarowicz, D., and Lau, K. (1989). Pituitary follicular cells secrete both vascular endothelial growth factor and follistatin. *Biochem. Biophys. Res. Commun.* 165, 292–298. doi: 10.1016/0006-291x(89)91068-1

Greenwood, M. P., Greenwood, M., Romanova, E. V., Mecawi, A. S., Paterson, A., Sarenac, O., et al. (2018). The effects of aging on biosynthetic processes in the rat hypothalamic osmoregulatory neuroendocrine system. *Neurobiol. Aging* 65, 178–191. doi: 10.1016/j.neurobiolaging.2018.01.008

Gregersen, S., Thomsen, J. L., Brock, B., and Hermansen, K. (1996). Endothelin-1 stimulates insulin secretion by direct action on the islets of Langerhans in mice. *Diabetologia* 39, 1030–1035. doi: 10.1007/BF00400650

Griveau, J. F., and Lannou, D. L. (1997). Reactive oxygen species and human spermatozoa: physiology and pathology. *Int. J. Androl.* 20, 61–69. doi: 10.1046/j.1365-2605.1997.00044.x

Gu, Z., Du, Y., Liu, Y., Ma, L., Li, L., Gong, Y., et al. (2012). Effect of aging on islet beta-cell function and its mechanisms in Wistar rats. *Age* 34, 1393–1403. doi: 10.1007/s11357-011-9312-7

Hanke, H., Lenz, C., Hess, B., Spindler, K.-D., and Weidemann, W. (2001). Effect of testosterone on plaque development and androgen receptor expression in the arterial vessel wall. *Circulation* 103, 1382–1385. doi: 10.1161/01.CIR.103.10.1382

Haring, R., Völzke, H., Steveling, A., Krebs, A., Felix, S. B., Schöfl, C., et al. (2010). Low serum testosterone levels are associated with increased risk of mortality in a population-based cohort of men aged 20-79. *Eur. Heart J.* 31, 1494–1501. doi: 10.1093/eurheartj/ehq009

Harman, S. M., Metter, E. J., Tobin, J. D., Pearson, J., and Blackman, M. R. (2001). Longitudinal effects of aging on serum total and free testosterone levels in healthy men. Baltimore longitudinal study of aging. *J. Clin. Endocrinol. Metab.* 86, 724–731. doi: 10.1210/jcem.86.2.7219

Harrison, R. G., and Barclay, A. E. (1948). The distribution of the testicular artery (internal spermatic artery) to the human testis. *Br. J. Urol.* 20, 57–66. doi: 10.1111/j.1464-410x.1948.tb10711.x

Hayashi, K.-G., Berisha, B., Matsui, M., Schams, D., and Miyamoto, A. (2004). Expression of mRNA for the angiopoietin-tie system in granulosa cells during follicular development in cows. *J. Reprod. Dev.* 50, 477–480. doi: 10.1262/jrd.50.477

Hegstad, R., Brown, R. D., Jiang, N.-S., Kao, P., Weinshilboum, R. M., Strong, C., et al. (1983). Aging and aldosterone. *Am. J. Med.* 74, 442–448. doi: 10.1016/0002-9343(83)90971-3

Henderson, J., and Henderson, I. W. (1995). The endocrine function of the vascular endothelium. *J. Biol. Educ.* 29, 104–109. doi: 10.1080/00219266.1995.9655428

Henderson, J. R., and Moss, M. C. (1985). A morphometric study of the endocrine and exocrine capillaries of the pancreas. *Q. J. Exp. Physiol.* 70, 347–356.

Hick, A.-C., Delmarcelle, A.-S., Bouquet, M., Klotz, S., Copetti, T., Forez, C., et al. (2013). Reciprocal epithelial:endothelial paracrine interactions during thyroid development govern follicular organization and C-cells differentiation. *Dev. Biol.* 381, 227–240. doi: 10.1016/j.ydbio.2013.04.022

Hiller-Sturmhöfel, S., and Bartke, A. (1998). The endocrine system: an overview. *Alcohol Health Res. World* 22, 153–164.

Ho, C. T., Lin, C. C., Hsu, H. S., Liu, C. S., Davidson, L. E., Li, T. C., et al. (2011). Arterial stiffness is strongly associated with insulin resistance in Chinese–a population-based study (Taichung Community Health Study, TCHS). *J. Atheroscler. Thromb.* 18, 122–130. doi: 10.5551/jat.5686

Hogervorst, E., Huppert, F., Matthews, F. E., and Brayne, C. (2008). Thyroid function and cognitive decline in the MRC cognitive function and ageing study. *Psychoneuroendocrinology* 33, 1013–1022. doi: 10.1016/j.psyneuen.2008.05.008

Hooper, A. T., Butler, J. M., Nolan, D. J., Kranz, A., Iida, K., Kobayashi, M., et al. (2009). Engraftment and reconstitution of hematopoiesis is dependent on VEGFR2-mediated regeneration of sinusoidal endothelial cells. *Cell Stem Cell* 4, 263–274. doi: 10.1016/j.stem.2009.01.006

Horvath, E., and Kovacs, K. (2002). Folliculo-stellate cells of the human pituitary: a type of adult stem cell? *Ultrastruct. Pathol.* 26, 219–228. doi: 10.1080/01913120290104476

Hougaku, H., Fleg, J. L., Najjar, S. S., Lakatta, E. G., Harman, S. M., Blackman, M. R., et al. (2006). Relationship between androgenic hormones and arterial stiffness, based on longitudinal hormone measurements. *Am. J. Physiol. Endocrinol. Metab.* 290, E234–E242. doi: 10.1152/ajpendo.00059.2005

Houshyar, H., Galigniana, M. D., Pratt, W. B., and Woods, J. H. (2001). Differential responsivity of the hypothalamic-pituitary-adrenal axis to glucocorticoid negative-feedback and corticotropin releasing hormone in rats undergoing morphine withdrawal: possible mechanisms involved in facilitated and attenuated stress responses. *J. Neuroendocrinol.* 13, 875–886. doi: 10.1046/j.1365-2826.2001.00714.x

Huey, S., Abuhamad, A., Barroso, G., Hsu, M.-I., Kolm, P., Mayer, J., et al. (1999). Perifollicular blood flow doppler indices, but not follicular pO, pCO2, or pH,

predict oocyte developmental competence in in vitro fertilization. *Fertil. Steril.* 72, 707–712. doi: 10.1016/S0015-0282(99)00327-1

Idelman, S. (1970). "Ultrastructure of the mammalian adrenal cortex," in *International Review of Cytology*, eds G. H. Bourne, J. F. Danlelli, and K. W. Jeon (Cambridge, MA: Academic Press), 181–281.

Ihm, S. H., Moon, H. J., Kang, J. G., Park, C. Y., Oh, K. W., Jeong, I. K., et al. (2007). Effect of aging on insulin secretory function and expression of beta cell function-related genes of islets. *Diabetes Res. Clin. Pract.* 77(Suppl. 1), S150–S154. doi: 10.1016/j.diabres.2007.01.049

Ilacqua, A., Francomano, D., and Aversa, A. (2018). ""The physiology of the testis,"," in *Principles of Endocrinology and Hormone Action*, eds A. Belfiore and D. LeRoith (Cham: Springer International Publishing), 455–491.

Inai, T., Mancuso, M., Hashizume, H., Baffert, F., Haskell, A., Baluk, P., et al. (2004). Inhibition of vascular endothelial growth factor (VEGF) signaling in cancer causes loss of endothelial fenestrations, regression of tumor vessels, and appearance of basement membrane ghosts. *Am. J. Pathol.* 165, 35–52. doi: 10.1016/S0002-9440(10)63273-7

In't Veld, P., and Marichal, M. (2010). "Microscopic anatomy of the human islet of langerhans," in *The Islets of Langerhans*, ed. M. S. Islam (Dordrecht: Springer), 1–19.

Iqbal, J., Sun, L., Kumar, T. R., Blair, H. C., and Zaidi, M. (2006). Follicle-stimulating hormone stimulates TNF production from immune cells to enhance osteoblast and osteoclast formation. *Proc. Natl. Acad. Sci. U.S.A.* 103, 14925–14930. doi: 10.1073/pnas.0606805103

Iwashita, N., Uchida, T., Choi, J. B., Azuma, K., Ogihara, T., Ferrara, N., et al. (2007). Impaired insulin secretion in vivo but enhanced insulin secretion from isolated islets in pancreatic beta cell-specific vascular endothelial growth factor-A knock-out mice. *Diabetologia* 50, 380–389. doi: 10.1007/s00125-006-0512-0

Jang, J. Y., Choi, S. Y., Park, I., Park, D. Y., Choe, K., Kim, P., et al. (2017). VEGFR2 but not VEGFR3 governs integrity and remodeling of thyroid angiofollicular unit in normal state and during goitrogenesis. *EMBO Mol. Med.* 9, 750–769. doi: 10.15252/emmm.201607341

Jansen, S. W., Akintola, A. A., Roelfsema, F., van der Spoel, E., Cobbaert, C. M., Ballieux, B. E., et al. (2015). Human longevity is characterised by high thyroid stimulating hormone secretion without altered energy metabolism. *Sci. Rep.* 5, 11525–11525. doi: 10.1038/srep11525

Jiang, Y., Fischbach, S., and Xiao, X. (2018). The role of the TGFβ receptor signaling pathway in adult beta cell proliferation. *Int. J. Mol. Sci.* 19:3136. doi: 10.3390/ijms19103136

Johansson, A., Lau, J., Sandberg, M., Borg, L. A., Magnusson, P. U., and Carlsson, P. O. (2009). Endothelial cell signalling supports pancreatic beta cell function in the rat. *Diabetologia* 52, 2385–2394. doi: 10.1007/s00125-009-1485-6

Johansson, M., Carlsson, P. O., Bodin, B., Andersson, A., Källskog, O., and Jansson, L. (2005). Acute effects of a 50% partial pancreatectomy on total pancreatic and islet blood flow in rats. *Pancreas* 30, 71–75.

Johansson, M., Mattsson, G., Andersson, A., Jansson, L., and Carlsson, P. O. (2006). Islet endothelial cells and pancreatic beta-cell proliferation: studies in vitro and during pregnancy in adult rats. *Endocrinology* 147, 2315–2324. doi: 10.1210/en.2005-0997

Jose, V., Juan, G., Raul, L.-G., Khira, M. A., Mariona, J., and Consuelo, B. (2011). Females live longer than males: role of oxidative stress. *Curr. Pharmaceut. Design* 17, 3959–3965. doi: 10.2174/138161211798764942

Kaido, T., Yebra, M., Cirulli, V., and Montgomery, A. M. (2004). Regulation of human beta-cell adhesion, motility, and insulin secretion by collagen IV and its receptor alpha1beta1. *J. Biol. Chem.* 279, 53762–53769. doi: 10.1074/jbc.M411202200

Kamba, T., Tam, B. Y. Y., Hashizume, H., Haskell, A., Sennino, B., Mancuso, M. R., et al. (2006). VEGF-dependent plasticity of fenestrated capillaries in the normal adult microvasculature. *Am. J. Physiol. Heart Circ. Physiol.* 290, H560–H576. doi: 10.1152/ajpheart.00133.2005

Kanczkowski, W., Chatzigeorgiou, A., Grossklaus, S., Sprott, D., Bornstein, S. R., and Chavakis, T. (2013). Role of the endothelial-derived endogenous anti-inflammatory factor Del-1 in inflammation-mediated adrenal gland dysfunction. *Endocrinology* 154, 1181–1189. doi: 10.1210/en.2012-1617

Kanczkowski, W., Sue, M., and Bornstein, S. R. (2017). The adrenal gland microenvironment in health, disease and during regeneration. *Hormones (Athens)* 16, 251–265. doi: 10.14310/horm.2002.1744

Kano, M. R., Morishita, Y., Iwata, C., Iwasaka, S., Watabe, T., Ouchi, Y., et al. (2005). VEGF-A and FGF-2 synergistically promote neoangiogenesis through enhancement of endogenous PDGF-B-PDGFRbeta signaling. *J. Cell Sci.* 118(Pt 16), 3759–3768. doi: 10.1242/jcs.02483

Karaca, M., Castel, J., Tourrel-Cuzin, C., Brun, M., Géant, A., Dubois, M., et al. (2009). Exploring functional β-Cell heterogeneity in vivo using PSA-NCAM as a specific marker. *PLoS One* 4:e5555. doi: 10.1371/journal.pone.0005555

Karsenty, G. (2006). Convergence between bone and energy homeostases: leptin regulation of bone mass. *Cell Metab.* 4, 341–348. doi: 10.1016/j.cmet.2006.10.008

Karsenty, G., and Olson, E. N. (2016). Bone and muscle endocrine functions: unexpected paradigms of inter-organ communication. *Cell* 164, 1248–1256. doi: 10.1016/j.cell.2016.02.043

Katoh, R. (2003). Angiogenesis in endocrine glands: special reference to the expression of vascular endothelial growth factor. *Microsc. Res. Techn.* 60, 181–185. doi: 10.1002/jemt.10256

Katsuta, H., Aguayo-Mazzucato, C., Katsuta, R., Akashi, T., Hollister-Lock, J., Sharma, A. J., et al. (2012). Subpopulations of GFP-marked mouse pancreatic β-Cells differ in size, granularity, and insulin secretion. *Endocrinology* 153, 5180–5187. doi: 10.1210/en.2012-1257

Keefe, D. L., Franco, S., Liu, L., Trimarchi, J., Cao, B., Weitzen, S., et al. (2005). Telomere length predicts embryo fragmentation after in vitro fertilization in women—toward a telomere theory of reproductive aging in women. *Am. J. Obstetr. Gynecol.* 192, 1256–1260. doi: 10.1016/j.ajog.2005.01.036

Keller-Wood, M. (2015). Hypothalamic-pituitary–adrenal axis-feedback control. *Compr. Physiol.* 5, 1161–1182. doi: 10.1002/cphy.c140065

Kennedy, B. K., Berger, S. L., Brunet, A., Campisi, J., Cuervo, A. M., Epel, E. S., et al. (2014). Geroscience: linking aging to chronic disease. *Cell* 159, 709–713. doi: 10.1016/j.cell.2014.10.039

Khaw, K. T., Dowsett, M., Folkerd, E., Bingham, S., Wareham, N., Luben, R., et al. (2007). Endogenous testosterone and mortality due to all causes, cardiovascular disease, and cancer in men: European prospective investigation into cancer in Norfolk (EPIC-Norfolk) Prospective Population Study. *Circulation* 116, 2694–2701. doi: 10.1161/circulationaha.107.719005

Khosla, S., Farr, J. N., Tchkonia, T., and Kirkland, J. L. (2020). The role of cellular senescence in ageing and endocrine disease. *Nat. Rev. Endocrinol.* 16, 263–275. doi: 10.1038/s41574-020-0335-y

Klein, N. A., Battaglia, D. E., Woodruff, T. K., Padmanabhan, V., Giudice, L. C., Bremner, W. J., et al. (2000). Ovarian follicular concentrations of activin, follistatin, inhibin, insulin-like growth factor I (IGF-I), IGF-II, IGF-binding protein-2 (IGFBP-2), IGFBP-3, and vascular endothelial growth factor in spontaneous menstrual cycles of normal women of advanced reproductive age. *J. Clin. Endocrinol. Metab.* 85, 4520–4525. doi: 10.1210/jcem.85.12.7056

Kobayashi, N., Machida, T., Takahashi, T., Takatsu, H., Shinkai, T., Abe, K., et al. (2009). Elevation by oxidative stress and aging of hypothalamic-pituitary-adrenal activity in rats and its prevention by Vitamin E. *J. Clin. Biochem. Nutr.* 45, 207–213. doi: 10.3164/jcbn.09-33

Kok, P., Roelfsema, F., Frölich, M., Meinders, A. E., and Pijl, H. (2004). Prolactin release is enhanced in proportion to excess visceral fat in obese women. *J. Clin. Endocrinol. Metab.* 89, 4445–4449. doi: 10.1210/jc.2003-032184

Kolka, C. M., and Bergman, R. N. (2012). The barrier within: endothelial transport of hormones. *Physiology* 27, 237–247. doi: 10.1152/physiol.00012.2012

Kondo, T., Ohshima, T., and Ishida, Y. (2001). Age-dependent expression of 8-hydroxy-2'-deoxyguanosine in human pituitary gland. *Histochem. J.* 33, 647–651. doi: 10.1023/A:1016354417834

Kozik, W. (2000). [Arterial vasculature of ovaries in women of various ages in light of anatomic, radiologic and microangiographic examinations]. *Ann. Acad. Med. Stetin.* 46, 25–34.

Krishnamurthy, J., Torrice, C., Ramsey, M. R., Kovalev, G. I., Al-Regaiey, K., Su, L., et al. (2004). Ink4a/Arf expression is a biomarker of aging. *J. Clin. Invest.* 114, 1299–1307. doi: 10.1172/jci22475

Kubota, H., Avarbock, M. R., and Brinster, R. L. (2004). Growth factors essential for self-renewal and expansion of mouse spermatogonial stem cells. *Proc. Natl. Acad. Sci. U.S.A.* 101, 16489–16494. doi: 10.1073/pnas.0407063101

Kuhnert, F., Tam, B. Y., Sennino, B., Gray, J. T., Yuan, J., Jocson, A., et al. (2008). Soluble receptor-mediated selective inhibition of VEGFR and PDGFRbeta signaling during physiologic and tumor angiogenesis. *Proc. Natl. Acad. Sci. U.S.A.* 105, 10185–10190. doi: 10.1073/pnas.0803194105

Kumar, D. L., and DeFalco, T. (2018). A perivascular niche for multipotent progenitors in the fetal testis. *Nat. Commun.* 9:4519. doi: 10.1038/s41467-018-06996-3

Kunisaki, Y., Bruns, I., Scheiermann, C., Ahmed, J., Pinho, S., Zhang, D., et al. (2013). Arteriolar niches maintain haematopoietic stem cell quiescence. *Nature* 502, 637–643. doi: 10.1038/nature12612

Kusumbe, A. P., Ramasamy, S. K., and Adams, R. H. (2014). Coupling of angiogenesis and osteogenesis by a specific vessel subtype in bone. *Nature* 507, 323–328. doi: 10.1038/nature13145

Kusumbe, A. P., Ramasamy, S. K., Itkin, T., Mäe, M. A., Langen, U. H., Betsholtz, C., et al. (2016). Age-dependent modulation of vascular niches for haematopoietic stem cells. *Nature* 532, 380–384. doi: 10.1038/nature17638

Labrie, F., Bélanger, A., Cusan, L., Gomez, J. L., and Candas, B. (1997). Marked decline in serum concentrations of adrenal C19 sex steroid precursors and conjugated androgen metabolites during aging. *J. Clin. Endocrinol. Metab.* 82, 2396–2402. doi: 10.1210/jcem.82.8.4160

Lammert, E., Gu, G., McLaughlin, M., Brown, D., Brekken, R., Murtaugh, L. C., et al. (2003). Role of VEGF-A in vascularization of pancreatic islets. *Curr. Biol.* 13, 1070–1074. doi: 10.1016/s0960-9822(03)00378-6

Lan, L., Cui, D., Nowka, K., and Derwahl, M. (2007). Stem cells derived from goiters in adults form spheres in response to intense growth stimulation and require thyrotropin for differentiation into thyrocytes. *J. Clin. Endocrinol. Metab.* 92, 3681–3688. doi: 10.1210/jc.2007-0281

Larkin, S., and Ansorge, O. (2000). *Development and Microscopic Anatomy of the Pituitary Gland*. South Dartmouth, MA: MDText.com Inc.

Lau, J., Svensson, J., Grapensparr, L., Johansson, Å, and Carlsson, P. O. (2012). Superior beta cell proliferation, function and gene expression in a subpopulation of rat islets identified by high blood perfusion. *Diabetologia* 55, 1390–1399. doi: 10.1007/s00125-012-2476-6

Le Tissier, P., Campos, P., Lafont, C., Romanò, N., Hodson, D. J., and Mollard, P. (2017). An updated view of hypothalamic-vascular-pituitary unit function and plasticity. *Nat. Rev. Endocrinol.* 13, 257–267. doi: 10.1038/nrendo.2016.193

Lechan, R. M., and Toni, R. (2000). *Functional Anatomy of the Hypothalamus and Pituitary*. South Dartmouth, MA: MDText.com Inc.

LeCouter, J., Kowalski, J., Foster, J., Hass, P., Zhang, Z., Dillard-Telm, L., et al. (2001). Identification of an angiogenic mitogen selective for endocrine gland endothelium. *Nature* 412, 877–884. doi: 10.1038/35091000

Lee, N. K., Sowa, H., Hinoi, E., Ferron, M., Ahn, J. D., Confavreux, C., et al. (2007). Endocrine regulation of energy metabolism by the skeleton. *Cell* 130, 456–469. doi: 10.1016/j.cell.2007.05.047

Lee, S.-Y., Gong, E.-Y., Hong, C. Y., Kim, K.-H., Han, J.-S., Ryu, J. C., et al. (2009). ROS inhibit the expression of testicular steroidogenic enzyme genes via the suppression of Nur77 transactivation. *Free Radic. Biol. Med.* 47, 1591–1600. doi: 10.1016/j.freeradbiomed.2009.09.004

Levy, A. (2002). Physiological implications of pituitary trophic activity. *J. Endocrinol.* 174, 147–155. doi: 10.1677/joe.0.1740147

Lew, R., Komesaroff, P., Williams, M., Dawood, T., and Sudhir, K. (2003). Endogenous estrogens influence endothelial function in young men. *Circ. Res.* 93, 1127–1133. doi: 10.1161/01.RES.0000103633.57225.BC

Li, J., Qu, X., and Bertram, J. F. (2009). Endothelial-myofibroblast transition contributes to the early development of diabetic renal interstitial fibrosis in streptozotocin-induced diabetic mice. *Am. J. Pathol.* 175, 1380–1388. doi: 10.2353/ajpath.2009.090096

Li, L., Guo, C.-Y., Jia, E.-Z., Zhu, T.-B., Wang, L.-S., Cao, K.-J., et al. (2012). Testosterone is negatively associated with the severity of coronary atherosclerosis in men. *Asian J. Androl.* 14, 875–878. doi: 10.1038/aja.2012.95

Li, Q., Geng, X., Zheng, W., Tang, J., Xu, B., and Shi, Q. (2012). Current understanding of ovarian aging. *Sci. China Life Sci.* 55, 659–669. doi: 10.1007/s11427-012-4352-5

Li, Y. J., Han, Z., Ge, L., Zhou, C. J., Zhao, Y. F., Wang, D. H., et al. (2016). C-phycocyanin protects against low fertility by inhibiting reactive oxygen species in aging mice. *Oncotarget* 7, 17393–17409. doi: 10.18632/oncotarget.8165

Lin, F., Wang, N., and Zhang, T.-C. (2012). The role of endothelial–mesenchymal transition in development and pathological process. *IUBMB Life* 64, 717–723. doi: 10.1002/iub.1059

Lipscombe, L. L., and Hux, J. E. (2007). Trends in diabetes prevalence, incidence, and mortality in Ontario, Canada 1995–2005: a population-based study. *Lancet* 369, 750–756. doi: 10.1016/S0140-6736(07)60361-4

Liu, L., Blasco, M. A., Trimarchi, J. R., and Keefe, D. L. (2002). An Essential role for functional telomeres in mouse germ cells during fertilization and early development. *Dev. Biol.* 249, 74–84. doi: 10.1006/dbio.2002.0735

Liu, L., Trimarchi, J. R., Navarro, P., Blasco, M. A., and Keefe, D. L. (2003). Oxidative stress contributes to arsenic-induced telomere attrition, chromosome instability, and apoptosis. *J. Biol. Chem.* 278, 31998–32004.

Liu, M., Gao, J., Zhang, Y., Li, P., Wang, H., Ren, X., et al. (2015). Serum levels of TSP-1, NF-kappaB and TGF-beta1 in polycystic ovarian syndrome (PCOS) patients in northern China suggest PCOS is associated with chronic inflammation. *Clin. Endocrinol.* 83, 913–922. doi: 10.1111/cen.12951

Loevner, L. A. (1996). Imaging of the thyroid gland. *Semin. Ultrasound CT MRI* 17, 539–562. doi: 10.1016/S0887-2171(96)90003-7

Logie, J. J., Ali, S., Marshall, K. M., Heck, M. M., Walker, B. R., and Hadoke, P. W. (2010). Glucocorticoid-mediated inhibition of angiogenic changes in human endothelial cells is not caused by reductions in cell proliferation or migration. *PLoS One* 5:e14476. doi: 10.1371/journal.pone.0014476

López-Otín, C., Blasco, M. A., Partridge, L., Serrano, M., and Kroemer, G. (2013). The hallmarks of aging. *Cell* 153, 1194–1217. doi: 10.1016/j.cell.2013.05.039

Lorens, S. A., Hata, N., Handa, R. J., Van de Kar, L. D., Guschwan, M., Goral, J., et al. (1990). Neurochemical, endocrine and immunological responses to stress in young and old Fischer 344 male rats. *Neurobiol. Aging* 11, 139–150. doi: 10.1016/0197-4580(90)90047-4

Loreti, N., Ambao, V., Juliato, C. T., Machado, C., Bahamondes, L., and Campo, S. (2009). Carbohydrate complexity and proportion of serum FSH isoforms reflect pituitary–ovarian activity in perimenopausal women and depot medroxyprogesterone acetate users. *Clin. Endocrinol.* 71, 558–565. doi: 10.1111/j.1365-2265.2009.03559.x

Lou, J., Triponez, F., Oberholzer, J., Wang, H., Yu, D., Buhler, L., et al. (1999). Expression of alpha-1 proteinase inhibitor in human islet microvascular endothelial cells. *Diabetes* 48, 1773–1778. doi: 10.2337/diabetes.48.9.1773

Lupiáñz, D. G., Real, F. M., Dadhich, R. K., Carmona, F. D., Burgos, M., Barrionuevo, F. J., et al. (2012). Pattern and density of vascularization in mammalian testes, ovaries, and ovotestes. *J. Exp. Zool. B Mol. Dev. Evol.* 318, 170–181. doi: 10.1002/jez.b.22000

Lysiak, J. J., Kirby, J. L., Tremblay, J. J., Woodson, R. I., Reardon, M. A., Palmer, L. A., et al. (2009). Hypoxia-inducible factor-1alpha is constitutively expressed in murine Leydig cells and regulates 3beta-hydroxysteroid dehydrogenase type 1 promoter activity. *J. Androl.* 30, 146–156. doi: 10.2164/jandrol.108.006155

Lysiak, J. J., Nguyen, Q. A., and Turner, T. T. (2000). Fluctuations in rat testicular interstitial oxygen tensions are linked to testicular vasomotion: persistence after repair of torsion. *Biol. Reprod.* 63, 1383–1389. doi: 10.1095/biolreprod63.5.1383

Maddocks, S., and Setchell, B. P. (1988). The physiology of the endocrine testis. *Oxf. Rev. Reprod. Biol.* 10, 53–123.

Maedler, K., Schumann, D. M., Schulthess, F., Oberholzer, J., Bosco, D., Berney, T., et al. (2006). Aging correlates with decreased β-Cell proliferative capacity and enhanced sensitivity to apoptosis. *Diabetes* 55, 2455–2462. doi: 10.2337/db05-1586

Maghnie, M., Altobelli, M., Di Iorgi, N., Genovese, E., Meloni, G., Manca-Bitti, M. L., et al. (2004). Idiopathic central diabetes insipidus is associated with abnormal blood supply to the posterior pituitary gland caused by vascular impairment of the inferior hypophyseal artery system. *J. Clin. Endocrinol. Metab.* 89, 1891–1896. doi: 10.1210/jc.2003-031608

Mariana, Di, P., Natalia, P., Fernanda, P., and Dalhia, A. (2018). Ovarian angiogenesis in polycystic ovary syndrome. *Reproduction* 155, R199–R209. doi: 10.1530/REP-17-0597

Marie, S., David, J. H., Chrystel, L., and Patrice, M. (2011). Endocrine cells and blood vessels work in tandem to generate hormone pulses. *J. Mol. Endocrinol.* 47, R59–R66. doi: 10.1530/JME-11-0035

Marin, R., Escrig, A., Abreu, P., and Mas, M. (1999). Androgen-dependent nitric oxide release in rat penis correlates with levels of constitutive nitric oxide synthase isoenzymes. *Biol. Reprod.* 61, 1012–1016. doi: 10.1095/biolreprod61.4.1012

Mariotti, S., Barbesino, G., Caturegli, P., Bartalena, L., Sansoni, P., Fagnoni, F., et al. (1993). Complex alteration of thyroid function in healthy centenarians. *J. Clin. Endocrinol. Metab.* 77, 1130–1134. doi: 10.1210/jcem.77.5.8077303

Mariotti, S., Franceschi, C., Cossarizza, A., and Pinchera, A. (1995). The aging thyroid. *Endocr. Rev.* 16, 686–715. doi: 10.1210/edrv-16-6-686

Matsumoto, A. M., and Bremner, W. J. (1987). 4Endocrinology of the hypothalamic-pituitary-testicular axis with particular reference to the hormonal control of spermatogenesis. *Baillière's Clin. Endocrinol. Metab.* 1, 71–87. doi: 10.1016/S0950-351X(87)80053-8

Mattsson, G., Danielsson, A., Kriz, V., Carlsson, P. O., and Jansson, L. (2006). Endothelial cells in endogenous and transplanted pancreatic islets: differences in the expression of angiogenic peptides and receptors. *Pancreatology* 6, 86–95. doi: 10.1159/000090027

Maurer, A. J., Lissounov, A., Knezevic, I., Candido, K. D., and Knezevic, N. N. (2016). Pain and sex hormones: a review of current understanding. *Pain Manag.* 6, 285–296. doi: 10.2217/pmt-2015-0002

McFee, R. M., Artac, R. A., McFee, R. M., Clopton, D. T., Smith, R. A. L., Rozell, T. G., et al. (2009). Inhibition of vascular endothelial growth factor receptor signal transduction blocks follicle progression but does not necessarily disrupt vascular development in perinatal rat ovaries1. *Biol. Reprod.* 81, 966–977. doi: 10.1095/biolreprod.109.078071

McNicol, A. M., and Duffy, A. E. (1987). A study of cell migration in the adrenal cortex of the rat using bromodeoxyuridine. *Cell Tissue Kinet.* 20, 519–526. doi: 10.1111/j.1365-2184.1987.tb01361.x

Medici, M., Direk, N., Visser, W. E., Korevaar, T. I., Hofman, A., Visser, T. J., et al. (2014). Thyroid function within the normal range and the risk of depression: a population-based cohort study. *J. Clin. Endocrinol. Metab.* 99, 1213–1219. doi: 10.1210/jc.2013-3589

Méndez-Ferrer, S., Michurina, T. V., Ferraro, F., Mazloom, A. R., Macarthur, B. D., Lira, S. A., et al. (2010). Mesenchymal and haematopoietic stem cells form a unique bone marrow niche. *Nature* 466, 829–834. doi: 10.1038/nature09262

Michael, C. V., and Ramkumar, M. (2016). Positive and negative effects of cellular senescence during female reproductive aging and pregnancy. *J. Endocrinol.* 230, R59–R76. doi: 10.1530/JOE-16-0018

Miller, W. L., and Auchus, R. J. (2011). The molecular biology, biochemistry, and physiology of human steroidogenesis and its disorders. *Endocr. Rev.* 32, 81–151. doi: 10.1210/er.2010-0013

Minamino, T., Orimo, M., Shimizu, I., Kunieda, T., Yokoyama, M., Ito, T., et al. (2009). A crucial role for adipose tissue p53 in the regulation of insulin resistance. *Nat. Med.* 15, 1082–1087. doi: 10.1038/nm.2014

Mitani, F., Mukai, K., Miyamoto, H., Suematsu, M., and Ishimura, Y. (2003). The undifferentiated cell zone is a stem cell zone in adult rat adrenal cortex. *Biochim. Biophys. Acta* 1619, 317–324. doi: 10.1016/s0304-4165(02)00490-7

Miyata, S. (2017). Advances in understanding of structural reorganization in the hypothalamic neurosecretory system. *Front. Endocrinol.* 8:275. doi: 10.3389/fendo.2017.00275

Mizrachi, Y., Naranjo, J. R., Levi, B. Z., Pollard, H. B., and Lelkes, P. I. (1990). PC12 cells differentiate into chromaffin cell-like phenotype in coculture with adrenal medullary endothelial cells. *Proc. Natl. Acad. Sci. U.S.A.* 87, 6161–6165. doi: 10.1073/pnas.87.16.6161

Morita, S., Oohira, A., and Miyata, S. (2010). Activity-dependent remodeling of chondroitin sulfate proteoglycans extracellular matrix in the hypothalamo-neurohypophysial system. *Neuroscience* 166, 1068–1082. doi: 10.1016/j.neuroscience.2010.01.041

Morrison, S. J., and Scadden, D. T. (2014). The bone marrow niche for haematopoietic stem cells. *Nature* 505, 327–334. doi: 10.1038/nature12984

Mosialou, I., Shikhel, S., Liu, J. M., Maurizi, A., Luo, N., He, Z., et al. (2017). MC4R-dependent suppression of appetite by bone-derived lipocalin 2. *Nature* 543, 385–390. doi: 10.1038/nature21697

Murakami, T., Fujita, T., Miyake, T., Ohtsuka, A., Taguchi, T., and Kikuta, A. (1993). The insulo-acinar portal and insulo-venous drainage systems in the pancreas of the mouse, dog, monkey and certain other animals: a scanning electron microscopic study of corrosion casts. *Arch. Histol. Cytol.* 56, 127–147. doi: 10.1679/aohc.56.127

Murakami, T., Fujita, T., Taguchi, T., Nonaka, Y., and Orita, K. (1992). The blood vascular bed of the human pancreas, with special reference to the insulo-acinar portal system. Scanning electron microscopy of corrosion casts. *Arch. Histol. Cytol.* 55, 381–395. doi: 10.1679/aohc.55.381

Murakami, T., Oukouchi, H., Uno, Y., Ohtsuka, A., and Taguchi, T. (1989). Blood vascular beds of rat adrenal and accessory adrenal glands, with special reference to the corticomedullary portal system: a further scanning electron microscopic study of corrosion casts and tissue specimens. *Arch. Histol. Cytol.* 52, 461–476. doi: 10.1679/aohc.52.461

Nakamura, B. N., Lawson, G., Chan, J. Y., Banuelos, J., Cortés, M. M., Hoang, Y. D., et al. (2010). Knockout of the transcription factor NRF2 disrupts spermatogenesis in an age-dependent manner. *Free Radic. Biol. Med.* 49, 1368–1379. doi: 10.1016/j.freeradbiomed.2010.07.019

Nessi, A. C., De Hoz, G., Tanoira, C., Guaraglia, E., and Consens, G. (1995). Pituitary physiological and ultrastructural changes during aging. *Endocrine* 3, 711–716. doi: 10.1007/BF03000202

Ng, E. H. Y., Chan, C. C. W., Yeung, W. S. B., and Ho, P. C. (2004). Effect of age on ovarian stromal flow measured by three-dimensional ultrasound with power Doppler in Chinese women with proven fertility. *Hum. Reprod.* 19, 2132–2137. doi: 10.1093/humrep/deh387

Nikolova, G., Jabs, N., Konstantinova, I., Domogatskaya, A., Tryggvason, K., Sorokin, L., et al. (2006). The vascular basement membrane: a niche for insulin gene expression and β Cell proliferation. *Dev. Cell* 10, 397–405. doi: 10.1016/j.devcel.2006.01.015

Nilsson, E. E., Detzel, C., and Skinner, M. K. (2006). Platelet-derived growth factor modulates the primordial to primary follicle transition. *Reproduction* 131, 1007–1015. doi: 10.1530/rep.1.00978

Nishikawa, K., Furube, E., Morita, S., Horii-Hayashi, N., Nishi, M., and Miyata, S. (2017). Structural reconstruction of the perivascular space in the adult mouse neurohypophysis during an osmotic stimulation. *J. Neuroendocrinol.* 29. doi: 10.1111/jne.12456

Nolan, D. J., Ginsberg, M., Israely, E., Palikuqi, B., Poulos, M. G., James, D., et al. (2013). Molecular signatures of tissue-specific microvascular endothelial cell heterogeneity in organ maintenance and regeneration. *Dev. Cell* 26, 204–219. doi: 10.1016/j.devcel.2013.06.017

Oatley, J. M., Oatley, M. J., Avarbock, M. R., Tobias, J. W., and Brinster, R. L. (2009). Colony stimulating factor 1 is an extrinsic stimulator of mouse spermatogonial stem cell self-renewal. *Development* 136, 1191–1199. doi: 10.1242/dev.032243

Oatley, M. J., Racicot, K. E., and Oatley, J. M. (2011). Sertoli cells dictate spermatogonial stem cell niches in the mouse testis1. *Biol. Reprod.* 84, 639–645. doi: 10.1095/biolreprod.110.087320

Ogawa, T., Ohmura, M., and Ohbo, K. (2005). The niche for spermatogonial stem cells in the mammalian testis. *Int. J. Hematol.* 82, 381–388. doi: 10.1532/ijh97.05088

Olerud, J., Johansson, Å, and Carlsson, P.-O. (2009). Vascular niche of pancreatic islets. *Exp. Rev. Endocrinol. Metab.* 4, 481–491. doi: 10.1586/eem.09.25

Olerud, J., Johansson, M., Lawler, J., Welsh, N., and Carlsson, P.-O. (2008). Improved vascular engraftment and graft function after inhibition of the angiostatic factor thrombospondin-1 in mouse pancreatic islets. *Diabetes* 57, 1870–1877. doi: 10.2337/db07-0724

Olerud, J., Mokhtari, D., Johansson, M., Christoffersson, G., Lawler, J., Welsh, N., et al. (2011). Thrombospondin-1: an islet endothelial cell signal of importance for β-cell function. *Diabetes* 60, 1946–1954. doi: 10.2337/db10-0277

Olsson, R., and Carlsson, P.-O. (2011). A low-oxygenated subpopulation of pancreatic islets constitutes a functional reserve of endocrine cells. *Diabetes* 60, 2068–2075. doi: 10.2337/db09-0877

Ooka, H., and Shinkai, T. (1986). Effects of chronic hyperthyroidism on the lifespan of the rat. *Mech. Ageing Dev.* 33, 275–282. doi: 10.1016/0047-6374(86)90052-7

Orentreich, N., Brind, J. L., Rizer, R. L., and Vogelman, J. H. (1984). Age changes and sex differences in serum dehydroepiandrosterone sulfate concentrations throughout adulthood. *J. Clin. Endocrinol. Metab.* 59, 551–555. doi: 10.1210/jcem-59-3-551

Ortiga-Carvalho, T. M., Chiamolera, M. I., Pazos-Moura, C. C., and Wondisford, F. E. (2016). Hypothalamus-pituitary-thyroid axis. *Compr. Physiol.* 6, 1387–1428. doi: 10.1002/cphy.c150027

Oury, F., Ferron, M., Huizhen, W., Confavreux, C., Xu, L., Lacombe, J., et al. (2013a). Osteocalcin regulates murine and human fertility through a pancreas-bone-testis axis. *J. Clin. Invest.* 123, 2421–2433. doi: 10.1172/jci65952

Oury, F., Khrimian, L., Denny, C. A., Gardin, A., Chamouni, A., Goeden, N., et al. (2013b). Maternal and offspring pools of osteocalcin influence

brain development and functions. *Cell* 155, 228–241. doi: 10.1016/j.cell.2013.08.042

Oury, F., Sumara, G., Sumara, O., Ferron, M., Chang, H., Smith, C. E., et al. (2011). Endocrine regulation of male fertility by the skeleton. *Cell* 144, 796–809. doi: 10.1016/j.cell.2011.02.004

Ozgur, Z., Celik, S., Govsa, F., and Ozgur, T. (2011). Anatomical and surgical aspects of the lobes of the thyroid glands. *Eur. Arch. Oto Rhino Laryngol.* 268, 1357–1363. doi: 10.1007/s00405-011-1502-5

Page, R. B. (1982). Pituitary blood flow. *Am. J. Physiol. Endocrinol. Metab.* 243, E427–E442. doi: 10.1152/ajpendo.1982.243.6.E427

Park, S. A., Jeong, S., Choe, Y. H., and Hyun, Y.-M. (2018). Sensing of vascular permeability in inflamed vessel of live animal. *J. Anal. Methods Chem.* 2018:5797152. doi: 10.1155/2018/5797152

Pellestor, F., Andréo, B., Arnal, F., Humeau, C., and Demaille, J. (2003). Maternal aging and chromosomal abnormalities: new data drawn from in vitro unfertilized human oocytes. *Hum. Genet.* 112, 195–203. doi: 10.1007/s00439-002-0852-x

Petrie, J. R., Guzik, T. J., and Touyz, R. M. (2018). Diabetes, hypertension, and cardiovascular disease: clinical insights and vascular mechanisms. *Can. J. Cardiol.* 34, 575–584. doi: 10.1016/j.cjca.2017.12.005

Petropoulou, P.-I., Mosialou, I., Shikhel, S., Hao, L., Panitsas, K., Bisikirska, B., et al. (2020). Lipocalin-2 is an anorexigenic signal in primates. *eLife* 9:e58949. doi: 10.7554/eLife.58949

Pinkas, H., Fisch, B., Rozansky, G., Felz, C., Kessler-Icekson, G., Krissi, H., et al. (2008). Platelet-derived growth factors (PDGF-A and -B) and their receptors in human fetal and adult ovaries. *Mol. Hum. Reprod.* 14, 199–206. doi: 10.1093/molehr/gan011

Policeni, B. A., Smoker, W. R. K., and Reede, D. L. (2012). Anatomy and embryology of the thyroid and parathyroid glands. *Semin. Ultrasound CT MRI* 33, 104–114. doi: 10.1053/j.sult.2011.12.005

Portik-Dobos, V., Anstadt, M. P., Hutchinson, J., Bannan, M., and Ergul, A. (2002). Evidence for a matrix metalloproteinase induction/activation system in arterial vasculature and decreased synthesis and activity in diabetes. *Diabetes* 51:3063. doi: 10.2337/diabetes.51.10.3063

Poulos, M. G., Ramalingam, P., Gutkin, M. C., Llanos, P., Gilleran, K., Rabbany, S. Y., et al. (2017). Endothelial transplantation rejuvenates aged hematopoietic stem cell function. *J. Clin. Invest.* 127, 4163–4178. doi: 10.1172/jci93940

Powell, J. D., Elshtein, R., Forest, D. J., and Palladino, M. A. (2002). Stimulation of hypoxia-inducible factor-1 alpha (HIF-1alpha) protein in the adult rat testis following ischemic injury occurs without an increase in HIF-1alpha messenger RNA expression. *Biol. Reprod.* 67, 995–1002. doi: 10.1095/biolreprod.101.002576

Ramsey, K. M., Mills, K. F., Satoh, A., and Imai, S. (2008). Age-associated loss of Sirt1-mediated enhancement of glucose-stimulated insulin secretion in beta cell-specific Sirt1-overexpressing (BESTO) mice. *Aging Cell* 7, 78–88. doi: 10.1111/j.1474-9726.2007.00355.x

Rashidi, A., Kirkwood, T. B. L., and Shanley, D. P. (2009). Metabolic evolution suggests an explanation for the weakness of antioxidant defences in beta-cells. *Mech. Age. Dev.* 130, 216–221. doi: 10.1016/j.mad.2008.12.007

Rizzoti, K., Akiyama, H., and Lovell-Badge, R. (2013). Mobilized adult pituitary stem cells contribute to endocrine regeneration in response to physiological demand. *Cell Stem Cell* 13, 419–432. doi: 10.1016/j.stem.2013.07.006

Robinson, R. S., Woad, K. J., Hammond, A. J., Laird, M., Hunter, M. G., and Mann, G. E. (2009). Angiogenesis and vascular function in the ovary. *Reproduction* 138, 869–881. doi: 10.1530/rep-09-0283

Rodondi, N., den Elzen, W. P. J., Bauer, D. C., Cappola, A. R., Razvi, S., Walsh, J. P., et al. (2010). Subclinical hypothyroidism and the risk of coronary heart disease and mortality. *JAMA* 304, 1365–1374. doi: 10.1001/jama.2010.1361

Rodrigues Siqueira, I., Fochesatto, C., da Silva, Torres, I. L., Dalmaz, C., and Alexandre Netto, C. (2005). Aging affects oxidative state in hippocampus, hypothalamus and adrenal glands of Wistar rats. *Life Sci.* 78, 271–278. doi: 10.1016/j.lfs.2005.04.044

Rodriguez-Diaz, R., Abdulreda, Midhat, H., Formoso, Alexander, L., Gans, I., et al. (2011). Innervation patterns of autonomic axons in the human endocrine pancreas. *Cell Metab.* 14, 45–54. doi: 10.1016/j.cmet.2011.05.008

Roelfsema, F., Pijl, H., Keenan, D. M., and Veldhuis, J. D. (2012). Prolactin secretion in healthy adults is determined by gender, age and body mass index. *PLoS One* 7:e31305. doi: 10.1371/journal.pone.0031305

Romeo, S. G., Alawi, K. M., Rodrigues, J., Singh, A., Kusumbe, A. P., and Ramasamy, S. K. (2019). Endothelial proteolytic activity and interaction with non-resorbing osteoclasts mediate bone elongation. *Nat. Cell Biol.* 21, 430–441. doi: 10.1038/s41556-019-0304-7

Romero Maritza, J., Platt Daniel, H., Tawfik Huda, E., Labazi, M., El-Remessy Azza, B., Bartoli, M., et al. (2008). Diabetes-induced coronary vascular dysfunction involves increased arginase activity. *Circ. Res.* 102, 95–102. doi: 10.1161/CIRCRESAHA.107.155028

Roscioni, S. S., Migliorini, A., Gegg, M., and Lickert, H. (2016). Impact of islet architecture on β-cell heterogeneity, plasticity and function. *Nat. Rev. Endocrinol.* 12, 695–709. doi: 10.1038/nrendo.2016.147

Roser, J. F. (2008). Regulation of testicular function in the stallion: an intricate network of endocrine, paracrine and autocrine systems. *Anim. Reprod. Sci.* 107, 179–196. doi: 10.1016/j.anireprosci.2008.05.004

Rosolowsky, L. J., and Campbell, W. B. (1994). Endothelial cells stimulate aldosterone release from bovine adrenal zona glomerulosa cells. *Am. J. Physiol.* 266(1 Pt 1), E107–E117. doi: 10.1152/ajpendo.1994.266.1.E107

Rosolowsky, L. J., Hanke, C. J., and Campbell, W. B. (1999). Adrenal capillary endothelial cells stimulate aldosterone release through a protein that is distinct from endothelin. *Endocrinology* 140, 4411–4418. doi: 10.1210/endo.140.10.7060

Rozing, M. P., Houwing-Duistermaat, J. J., Slagboom, P. E., Beekman, M., Frölich, M., de Craen, A. J. M., et al. (2010). Familial longevity is associated with decreased thyroid function. *J. Clin. Endocrinol. Metab.* 95, 4979–4984. doi: 10.1210/jc.2010-0875

Rumney, R. M. H., Lanham, S. A., Kanczler, J. M., Kao, A. P., Thiagarajan, L., Dixon, J. E., et al. (2019). In vivo delivery of VEGF RNA and protein to increase osteogenesis and intraosseous angiogenesis. *Sci. Rep.* 9:17745. doi: 10.1038/s41598-019-53249-4

Russell, L. D., Ettlin, R. A., Hikim, A. P. S., and Clegg, E. D. (1993). Histological and histopathological evaluation of the testis. *Int. J. Androl.* 16, 83–83. doi: 10.1111/j.1365-2605.1993.tb01156.x

Sader, M. A., Griffiths, K. A., Skilton, M. R., Wishart, S. M., Handelsman, D. J., and Celermajer, D. S. (2003). Physiological testosterone replacement and arterial endothelial function in men. *Clin. Endocrinol.* 59, 62–67. doi: 10.1046/j.1365-2265.2003.01796.x

Sapolsky, R. M., Krey, L. C., and McEwen, B. S. (1983). The adrenocortical stress-response in the aged male rat: impairment of recovery from stress. *Exp. Gerontol.* 18, 55–64. doi: 10.1016/0531-5565(83)90051-7

Schwafertz, C., Schinner, S., Kühn, M. C., Haase, M., Asmus, A., Mülders-Opgenoorth, B., et al. (2017). Endothelial cells regulate β-catenin activity in adrenocortical cells via secretion of basic fibroblast growth factor. *Mol. Cell Endocrinol.* 441, 108–115. doi: 10.1016/j.mce.2016.11.015

Scotti, L., Parborell, F., Irusta, G., De Zuñiga, I., Bisioli, C., Pettorossi, H., et al. (2014). Platelet-derived growth factor BB and DD and angiopoietin1 are altered in follicular fluid from polycystic ovary syndrome patients. *Mol. Reprod. Dev.* 81, 748–756. doi: 10.1002/mrd.22343

Segar, T. M., Kasckow, J. W., Welge, J. A., and Herman, J. P. (2009). Heterogeneity of neuroendocrine stress responses in aging rat strains. *Physiol. Behav.* 96, 6–11. doi: 10.1016/j.physbeh.2008.07.024

Seifer, D. B., DeJesus, V., and Hubbard, K. (2002). Mitochondrial deletions in luteinized granulosa cells as a function of age in women undergoing in vitro fertilization. *Fertil. Steril.* 78, 1046–1048. doi: 10.1016/s0015-0282(02)04214-0

Sharpe, R. M. (1983). Local control of testicular function. *Q. J. Exp. Physiol.* 68, 265–287. doi: 10.1113/expphysiol.1983.sp002723

Shkolnik, K., Tadmor, A., Ben-Dor, S., Nevo, N., Galiani, D., and Dekel, N. (2011). Reactive oxygen species are indispensable in ovulation. *Proc. Natl. Acad. Sci. U.S.A.* 108:1462. doi: 10.1073/pnas.1017213108

Singh, A., Veeriah, V., Xi, P., Labella, R., Chen, J., Romeo, S. G., et al. (2019). Angiocrine signals regulate quiescence and therapy resistance in bone metastasis. *JCI Insight* 4:e125679. doi: 10.1172/jci.insight.125679

Sivan, U., De Angelis, J., and Kusumbe, A. P. (2019). Role of angiocrine signals in bone development, homeostasis and disease. *Open Biol.* 9, 190144. doi: 10.1098/rsob.190144

Snyder, P. J. (2001). Effects of age on testicular function and consequences of testosterone treatment1. *J. Clin. Endocrinol. Metab.* 86, 2369–2372. doi: 10.1210/jcem.86.6.7602

Sowers, M. F. R., Eyvazzadeh, A. D., McConnell, D., Yosef, M., Jannausch, M. L., Zhang, D., et al. (2008). Anti-mullerian hormone and inhibin B in the definition of ovarian aging and the menopause transition. *J. Clin. Endocrinol. Metab.* 93, 3478–3483. doi: 10.1210/jc.2008-0567

Staels, W., Heremans, Y., Heimberg, H., and De Leu, N. (2019). VEGF-A and blood vessels: a beta cell perspective. *Diabetologia* 62, 1961–1968. doi: 10.1007/s00125-019-4969-z

Stout, M. B., Tchkonia, T., Pirtskhalava, T., Palmer, A. K., List, E. O., Berryman, D. E., et al. (2014). Growth hormone action predicts age-related white adipose tissue dysfunction and senescent cell burden in mice. *Aging* 6, 575–586. doi: 10.18632/aging.100681

Stucker, S., Chen, J., Watt, F. E., and Kusumbe, A. P. (2020). Bone angiogenesis and vascular niche remodeling in stress, aging, and diseases. *Front. Cell Dev. Biol.* 8:602269. doi: 10.3389/fcell.2020.602269

Su, S. C., Mendoza, E. A., Kwak, H. I., and Bayless, K. J. (2008). Molecular profile of endothelial invasion of three-dimensional collagen matrices: insights into angiogenic sprout induction in wound healing. *Am. J. Physiol. Cell Physiol.* 295, C1215–C1229. doi: 10.1152/ajpcell.00336.2008

Sugiyama, T., Kohara, H., Noda, M., and Nagasawa, T. (2006). Maintenance of the hematopoietic stem cell pool by CXCL12-CXCR4 chemokine signaling in bone marrow stromal cell niches. *Immunity* 25, 977–988. doi: 10.1016/j.immuni.2006.10.016

Sun, L., Peng, Y., Sharrow, A. C., Iqbal, J., Zhang, Z., Papachristou, D. J., et al. (2006). FSH directly regulates bone mass. *Cell* 125, 247–260. doi: 10.1016/j.cell.2006.01.051

Sun, N., Wu, Y., Nanba, K., Sbiera, S., Kircher, S., Kunzke, T., et al. (2018). High-resolution tissue mass spectrometry imaging reveals a refined functional anatomy of the human adult adrenal gland. *Endocrinology* 159, 1511–1524. doi: 10.1210/en.2018-00064

Tack, C. J., Schefman, A. E., Willems, J. L., Thien, T., Lutterman, J. A., and Smits, P. (1996). Direct vasodilator effects of physiological hyperinsulin-aemia in human skeletal muscle. *Eur. J. Clin. Invest.* 26, 772–778. doi: 10.1046/j.1365-2362.1996.2020551.x

Tai, P., and Ascoli, M. (2011). Reactive Oxygen Species (ROS) play a critical role in the cAMP-Induced activation of ras and the phosphorylation of ERK1/2 in leydig cells. *Mol. Endocrinol.* 25, 885–893. doi: 10.1210/me.2010-0489

Takano, S., Akutsu, H., Hara, T., Yamamoto, T., and Matsumura, A. (2014). Correlations of vascular architecture and angiogenesis with pituitary adenoma histotype. *Int. J. Endocrinol.* 2014:989574. doi: 10.1155/2014/989574

Takizawa, T., and Hatakeyama, S. (1978). Age-associated changes in microvasculature of human adult testis. *Acta Pathol. Jpn.* 28, 541–554. doi: 10.1111/j.1440-1827.1978.tb00894.x

Tal, R., Seifer, D. B., Shohat-Tal, A., Grazi, R. V., and Malter, H. E. (2013). Transforming growth factor-beta1 and its receptor soluble endoglin are altered in polycystic ovary syndrome during controlled ovarian stimulation. *Fertil. Steril.* 100, 538–543. doi: 10.1016/j.fertnstert.2013.04.022

Tamanini, C., and De Ambrogi, M. (2004). Angiogenesis in developing follicle and corpus luteum. *Reprod. Domest. Anim.* 39, 206–216. doi: 10.1111/j.1439-0531.2004.00505.x

Tando, Y., Fujiwara, K., Yashiro, T., and Kikuchi, M. (2013). Localization of Notch signaling molecules and their effect on cellular proliferation in adult rat pituitary. *Cell Tissue Res.* 351, 511–519. doi: 10.1007/s00441-012-1532-3

Tatone, C., Amicarelli, F., Carbone, M. C., Monteleone, P., Caserta, D., Marci, R., et al. (2008). Cellular and molecular aspects of ovarian follicle ageing. *Hum. Reprod. Update* 14, 131–142. doi: 10.1093/humupd/dmm048

Tatone, C., Carbone, M. C., Falone, S., Aimola, P., Giardinelli, A., Caserta, D., et al. (2006). Age-dependent changes in the expression of superoxide dismutases and catalase are associated with ultrastructural modifications in human granulosa cells. *Mol. Hum. Reprod.* 12, 655–660. doi: 10.1093/molehr/gal080

Tawfik, H. E., El-Remessy, A. B., Matragoon, S., Ma, G., Caldwell, R. B., and Caldwell, R. W. (2006). Simvastatin improves diabetes-induced coronary endothelial dysfunction. *J. Pharmacol. Exp. Therap.* 319, 386–395. doi: 10.1124/jpet.106.106823

Tchkonia, T., Zhu, Y., van Deursen, J., Campisi, J., and Kirkland, J. L. (2013). Cellular senescence and the senescent secretory phenotype: therapeutic opportunities. *J. Clin. Invest.* 123, 966–972. doi: 10.1172/jci64098

Tenover, J. S., McLachlan, R. I., Dahl, K. D., Burger, H. G., Kretser, D. M. D., and Bremner, W. J. (1988). Decreased serum inhibin levels in normal elderly men: evidence for a decline in sertoli cell function with aging. *J. Clin. Endocrinol. Metab.* 67, 455–459. doi: 10.1210/jcem-67-3-455

Terwel, D., Markerink, M., and Jolles, J. (1992). Age-related changes in concentrations of vasopressin in the central nervous system and plasma of the male Wistar rat. *Mech. Ageing Dev.* 65, 127–136. doi: 10.1016/0047-6374(92)90029-d

Thomas, F. H., Wilson, H., Silvestri, A., and Fraser, H. M. (2008). Thrombospondin-1 expression is increased during follicular atresia in the primate ovary. *Endocrinology* 149, 185–192. doi: 10.1210/en.2007-0835

Thomas, M., Kéramidas, M., Monchaux, E., and Feige, J.-J. (2003). Role of adrenocorticotropic hormone in the development and maintenance of the adrenal cortical vasculature. *Microsc. Res. Techn.* 61, 247–251. doi: 10.1002/jemt.10333

Thomas, T., Nowka, K., Lan, L., and Derwahl, M. (2006). Expression of endoderm stem cell markers: evidence for the presence of adult stem cells in human thyroid glands. *Thyroid* 16, 537–544. doi: 10.1089/thy.2006.16.537

Tian, Y., Serino, R., and Verbalis, J. G. (2004). Downregulation of renal vasopressin V2 receptor and aquaporin-2 expression parallels age-associated defects in urine concentration. *Am. J. Physiol. Renal Physiol.* 287, F797–F805. doi: 10.1152/ajprenal.00403.2003

Tounian, P., Aggoun, Y., Dubern, B., Varille, V., Guy-Grand, B., Sidi, D., et al. (2001). Presence of increased stiffness of the common carotid artery and endothelial dysfunction in severely obese children: a prospective study. *Lancet* 358, 1400–1404. doi: 10.1016/s0140-6736(01)06525-4

Traub, M. L., and Santoro, N. (2010). Reproductive aging and its consequences for general health. *Ann. N. Y. Acad. Sci.* 1204, 179–187. doi: 10.1111/j.1749-6632.2010.05521.x

Tschoepe, D., Driesch, E., Schwippert, B., Nieuwenhuis, H. K., and Gries, F. A. (1995). Exposure of adhesion molecules on activated platelets in patients with newly diagnosed IDDM is not normalized by near-normoglycemia. *Diabetes* 44, 890–894. doi: 10.2337/diab.44.8.890

Tschoepe, D., Roesen, P., Kaufmann, L., Schauseil, S., Kehrel, B., Ostermann, H., et al. (1990). Evidence for abnormal platelet glycoprotein expression in diabetes mellitus. *Eur. J. Clin. Invest.* 20, 166–170. doi: 10.1111/j.1365-2362.1990.tb02264.x

Turner, H. E., Nagy, Z., Gatter, K. C., Esiri, M. M., Harris, A. L., and Wass, J. A. H. (2000). Angiogenesis in pituitary adenomas and the normal pituitary gland. *J. Clin. Endocrinol. Metab.* 85, 1159–1162. doi: 10.1210/jcem.85.3.6485

Ullsten, S., Lau, J., and Carlsson, P.-O. (2015). Vascular heterogeneity between native rat pancreatic islets is responsible for differences in survival and revascularisation post transplantation. *Diabetologia* 58, 132–139. doi: 10.1007/s00125-014-3385-7

Urakawa, I., Yamazaki, Y., Shimada, T., Iijima, K., Hasegawa, H., Okawa, K., et al. (2006). Klotho converts canonical FGF receptor into a specific receptor for FGF23. *Nature* 444, 770–774. doi: 10.1038/nature05315

Van Blerkom, J., Antczak, M., and Schrader, R. (1997). The developmental potential of the human oocyte is related to the dissolved oxygen content of follicular fluid: association with vascular endothelial growth factor levels and perifollicular blood flow characteristics. *Hum. Reprod.* 12, 1047–1055. doi: 10.1093/humrep/12.5.1047

van den Beld, A. W., Kaufman, J.-M., Zillikens, M. C., Lamberts, S. W. J., Egan, J. M., and van der Lely, A. J. (2018). The physiology of endocrine systems with ageing. *Lancet Diabetes Endocrinol.* 6, 647–658. doi: 10.1016/S2213-8587(18)30026-3

Veldhuis, J. D. (2013). Changes in pituitary function with ageing and implications for patient care. *Nat. Rev. Endocrinol.* 9, 205–215. doi: 10.1038/nrendo.2013.38

Veldhuis, J. D., Roelfsema, F., Keenan, D. M., and Pincus, S. (2011). Gender, age, body mass index, and IGF-I individually and jointly determine distinct GH dynamics: analyses in one hundred healthy adults. *J. Clin. Endocrinol. Metab.* 96, 115–121. doi: 10.1210/jc.2010-1669

Veldhuis, J. D., Urban, R. J., Lizarralde, G., Johnson, M. L., and Iranmanesh, A. (1992). Attenuation of luteinizing hormone secretory burst amplitude as a proximate basis for the hypoandrogenism of healthy aging in men. *J. Clin. Endocrinol. Metab.* 75, 707–713. doi: 10.1210/jcem.75.3.1517359

Vergoni, B., Cornejo, P. J., Gilleron, J., Djedaini, M., Ceppo, F., Jacquel, A., et al. (2016). DNA damage and the activation of the p53 pathway mediate alterations in metabolic and secretory functions of adipocytes. *Diabetes* 65, 3062–3074. doi: 10.2337/db16-0014

Villacorte, M., Delmarcelle, A.-S., Lernoux, M., Bouquet, M., Lemoine, P., Bolsée, J., et al. (2016). Thyroid follicle development requires Smad1/5- and endothelial cell-dependent basement membrane assembly. *Development* 143, 1958–1970. doi: 10.1242/dev.134171

Vinson, G. P. (2016). Functional zonation of the adult mammalian adrenal cortex. *Front. Neurosci.* 10:238–238. doi: 10.3389/fnins.2016.00238

Vinson, G. P., Pudney, J. A., and Whitehouse, B. J. (1985). The mammalian adrenal circulation and the relationship between adrenal blood flow and steroidogenesis. *J. Endocrinol.* 105, 285–294. doi: 10.1677/joe.0.1050285

Vita, R., Di Bari, F., Perelli, S., Capodicasa, G., and Benvenga, S. (2019). Thyroid vascularization is an important ultrasonographic parameter in untreated Graves' disease patients. *J. Clin. Transl. Endocrinol.* 15, 65–69. doi: 10.1016/j.jcte.2019.01.001

Vitale, G., Salvioli, S., and Franceschi, C. (2013). Oxidative stress and the ageing endocrine system. *Nat. Rev. Endocrinol.* 9, 228–240. doi: 10.1038/nrendo.2013.29

Waring, A. C., Arnold, A. M., Newman, A. B., Bùžková, P., Hirsch, C., and Cappola, A. R. (2012). Longitudinal changes in thyroid function in the oldest old and survival: the cardiovascular health study all-stars study. *J. Clin. Endocrinol. Metab.* 97, 3944–3950. doi: 10.1210/jc.2012-2481

Westergaard, C. G., Byskov, A. G., and Andersen, C. Y. (2007). Morphometric characteristics of the primordial to primary follicle transition in the human ovary in relation to age. *Hum. Reprod.* 22, 2225–2231. doi: 10.1093/humrep/dem135

Widyantoro, B., Emoto, N., Nakayama, K., Anggrahini, D. W., Adiarto, S., Iwasa, N., et al. (2010). Endothelial cell-derived endothelin-1 promotes cardiac fibrosis in diabetic hearts through stimulation of endothelial-to-mesenchymal transition. *Circulation* 121, 2407–2418. doi: 10.1161/circulationaha.110.938217

Winkler, I. G., Barbier, V., Nowlan, B., Jacobsen, R. N., Forristal, C. E., Patton, J. T., et al. (2012). Vascular niche E-selectin regulates hematopoietic stem cell dormancy, self renewal and chemoresistance. *Nat. Med.* 18, 1651–1657. doi: 10.1038/nm.2969

Woad, K. J., Hammond, A. J., Hunter, M., Mann, G. E., Hunter, M. G., and Robinson, R. S. (2009). FGF2 is crucial for the development of bovine luteal endothelial networks in vitro. *Reproduction* 138, 581–588. doi: 10.1530/rep-09-0030

Wojtusciszyn, A., Armanet, M., Morel, P., Berney, T., and Bosco, D. (2008). Insulin secretion from human beta cells is heterogeneous and dependent on cell-to-cell contacts. *Diabetologia* 51, 1843–1852. doi: 10.1007/s00125-008-1103-z

Wulff, C., Wilson, H., Wiegand, S. J., Rudge, J. S., and Fraser, H. M. (2002). Prevention of thecal angiogenesis, antral follicular growth, and ovulation in the primate by treatment with vascular endothelial growth factor Trap R1R2. *Endocrinology* 143, 2797–2807. doi: 10.1210/endo.143.7.8886

Xu, F., and Stouffer, R. L. (2005). Local delivery of angiopoietin-2 into the preovulatory follicle terminates the menstrual cycle in rhesus monkeys. *Biol. Reprod.* 72, 1352–1358. doi: 10.1095/biolreprod.104.037143

Xu, M., Palmer, A. K., Ding, H., Weivoda, M. M., Pirtskhalava, T., White, T. A., et al. (2015). Targeting senescent cells enhances adipogenesis and metabolic function in old age. *eLife* 4:e12997. doi: 10.7554/eLife.12997

Yamada-Fukunaga, T., Yamada, M., Hamatani, T., Chikazawa, N., Ogawa, S., Akutsu, H., et al. (2013). Age-associated telomere shortening in mouse oocytes. *Reprod. Biol. Endocrinol.* 11:108. doi: 10.1186/1477-7827-11-108

Yang, M. Y., and Fortune, J. E. (2007). Vascular endothelial growth factor stimulates the primary to secondary follicle transition in bovine follicles in vitro. *Mol. Reprod. Dev.* 74, 1095–1104. doi: 10.1002/mrd.20633

Yang, P., Lv, S., Wang, Y., Peng, Y., Ye, Z., Xia, Z., et al. (2018). Preservation of type H vessels and osteoblasts by enhanced preosteoclast platelet-derived growth factor type BB attenuates glucocorticoid-induced osteoporosis in growing mice. *Bone* 114, 1–13. doi: 10.1016/j.bone.2018.05.025

Yao, V. J., Ozawa, M. G., Trepel, M., Arap, W., McDonald, D. M., and Pasqualini, R. (2005). Targeting pancreatic islets with phage display assisted by laser pressure catapult microdissection. *Am. J. Pathol.* 166, 625–636. doi: 10.1016/s0002-9440(10)62283-3

Yiallouris, A., Tsioutis, C., Agapidaki, E., Zafeiri, M., Agouridis, A. P., Ntourakis, D., et al. (2019). Adrenal aging and its implications on stress responsiveness in humans. *Front. Endocrinol.* 10:54. doi: 10.3389/fendo.2019.00054

Yngen, M., Östenson, C. G., Hu, H., Li, N., Hjemdahl, P., and Wallén, N. H. (2004). Enhanced P-selectin expression and increased soluble CD40 Ligand in patients with Type 1 diabetes mellitus and microangiopathy: evidence for platelet hyperactivity and chronic inflammation. *Diabetologia* 47, 537–540. doi: 10.1007/s00125-004-1352-4

Yoshida, S. (2018). Open niche regulation of mouse spermatogenic stem cells. *Dev. Growth Differ.* 60, 542–552. doi: 10.1111/dgd.12574

Yoshida, S., Kato, T., and Kato, Y. (2016). Regulatory system for stem/progenitor cell niches in the adult rodent pituitary. *Int. J. Mol. Sci.* 17:75. doi: 10.3390/ijms17010075

Yoshida, S., Kato, T., Yako, H., Susa, T., Cai, L. Y., Osuna, M., et al. (2011). Significant quantitative and qualitative transition in pituitary stem / progenitor cells occurs during the postnatal development of the rat anterior pituitary. *J. Neuroendocrinol.* 23, 933–943. doi: 10.1111/j.1365-2826.2011.02198.x

Yoshida, S., Sukeno, M., and Nabeshima, Y.-I. (2007). A vasculature-associated niche for undifferentiated spermatogonia in the mouse testis. *Science* 317:1722. doi: 10.1126/science.1144885

Yue, P., Chatterjee, K., Beale, C., Poole-Wilson, P. A., and Collins, P. (1995). Testosterone relaxes rabbit coronary arteries and aorta. *Circulation* 91, 1154–1160. doi: 10.1161/01.cir.91.4.1154

Zajicek, G., Ariel, I., and Arber, N. (1986). The streaming adrenal cortex: direct evidence of centripetal migration of adrenocytes by estimation of cell turnover rate. *J. Endocrinol.* 111, 477–482. doi: 10.1677/joe.0.1110477

Zanone, M. M., Favaro, E., Doublier, S., Lozanoska-Ochser, B., Deregibus, M. C., Greening, J., et al. (2005). Expression of nephrin by human pancreatic islet endothelial cells. *Diabetologia* 48, 1789–1797. doi: 10.1007/s00125-005-1865-5

Zeisberg, E. M., Potenta, S., Xie, L., Zeisberg, M., and Kalluri, R. (2007a). Discovery of endothelial to mesenchymal transition as a source for carcinoma-associated fibroblasts. *Cancer Res.* 67, 10123–10128. doi: 10.1158/0008-5472.Can-07-3127

Zeisberg, E. M., Tarnavski, O., Zeisberg, M., Dorfman, A. L., McMullen, J. R., Gustafsson, E., et al. (2007b). Endothelial-to-mesenchymal transition contributes to cardiac fibrosis. *Nat. Med.* 13, 952–961. doi: 10.1038/nm1613

Zhang, L., Zhang, Z., Wang, J., Lv, D., Zhu, T., Wang, F., et al. (2019). Melatonin regulates the activities of ovary and delays the fertility decline in female animals via MT1/AMPK pathway. *J. Pineal Res.* 66:e12550. doi: 10.1111/jpi.12550

Zhou, Z. G., Gao, X. H., Wayand, W. U., Xiao, L. J., and Du, Y. (1996). Pancreatic microcirculation in the monkey with special reference to the blood drainage system of Langerhans islets: light and scanning electron microscopic study. *Clin. Anat.* 9, 1–9. doi: 10.1002/(sici)1098-235319969:1<1::Aid-ca1<3.0.Co;2-m

**Conflict of Interest:** The authors declare that the research was conducted in the absence of any commercial or financial relationships that could be construed as a potential conflict of interest.

frontiers in Physiology

PERSPECTIVE
published: 31 March 2021
doi: 10.3389/fphys.2021.642812

# Human Induced Pluripotent Stem Cell-Derived Brain Endothelial Cells: Current Controversies

*Tyler M. Lu[1,2], José Gabriel Barcia Durán[1], Sean Houghton[1], Shahin Rafii[1], David Redmond[1]* and Raphaël Lis[1,2]**

[1] Division of Regenerative Medicine, Department of Medicine, Ansary Stem Cell Institute, Weill Cornell Medicine, New York, NY, United States, [2] Ronald O. Perelman and Claudia Cohen Center for Reproductive Medicine, Weill Cornell Medicine, New York, NY, United States

Brain microvascular endothelial cells (BMECs) possess unique properties that are crucial for many functions of the blood-brain-barrier (BBB) including maintenance of brain homeostasis and regulation of interactions between the brain and immune system. The generation of a pure population of putative brain microvascular endothelial cells from human pluripotent stem cell sources (iBMECs) has been described to meet the need for reliable and reproducible brain endothelial cells *in vitro*. Human pluripotent stem cells (hPSCs), embryonic or induced, can be differentiated into large quantities of specialized cells in order to study development and model disease. These hPSC-derived iBMECs display endothelial-like properties, such as tube formation and low-density lipoprotein uptake, high transendothelial electrical resistance (TEER), and barrier-like efflux transporter activities. Over time, the *de novo* generation of an organotypic endothelial cell from hPSCs has aroused controversies. This perspective article highlights the developments made in the field of hPSC derived brain endothelial cells as well as where experimental data are lacking, and what concerns have emerged since their initial description.

**Keywords: induced pluripotent stem cells, endothelial cell, epithelial cell, cell fate and differentiation, misclassification, brain–blood barrier (BBB), disease modeling**

OPEN ACCESS

***Edited by:***
*Tullio Genova,*
*University of Turin, Italy*

***Reviewed by:***
*Alla B. Salmina,*
*Krasnoyarsk State Medical University, Russia*
*Bingmei M. Fu,*
*City College of New York (CUNY), United States*

****Correspondence:***
*David Redmond*
*dar2042@med.cornell.edu*
*Raphaël Lis*
*ral2020@med.cornell.edu*

***Specialty section:***
*This article was submitted to Vascular Physiology, a section of the journal Frontiers in Physiology*

***Received:*** *16 December 2020*
***Accepted:*** *08 March 2021*
***Published:*** *31 March 2021*

***Citation:***
*Lu TM, Barcia Durán JG, Houghton S, Rafii S, Redmond D and Lis R (2021) Human Induced Pluripotent Stem Cell-Derived Brain Endothelial Cells: Current Controversies. Front. Physiol. 12:642812. doi: 10.3389/fphys.2021.642812*

## INTRODUCTION

The latest efforts to develop drugs targeting neurodegeneration and neurological disorders have been met with disappointment in recent clinical trials. The relative ineffectiveness of those drugs has incited the scientific community to develop better pre-clinical models by improving human cell-based models to capture the complexity of the brain. While the discovery of induced pluripotent stem cells and subsequent generation of brain organoids has advanced innovative avenues, these brain organoids are still rudimentary, lacking primordial non-neuronal cell types of the central nervous system (CNS) like microglia and most importantly functional blood vessels. During embryonic development, endothelial cells (ECs) acquire unique organ-specific molecular and cellular specializations that are crucial for the formation of the blood-brain-barrier (BBB) and therefore the maintenance of brain homeostasis. Human pluripotent stem cells (hPSCs), embryonic or induced, have been used in an effort to generate large quantities of specialized cells for development studies and disease modeling. The use of hPSCs to generate a pure population of

these specialized brain microvascular ECs (iBMECs) has been described to meet the need for a reliable and reproducible *in vitro* BBB model. Specifically, it has been reported that hPSC-derived iBMECs display EC-like properties including tube formation, low density lipoprotein uptake, high transendothelial electrical resistance (TEER), and select barrier-like transporter activity. Over time, this *de novo* generation of an organotypic endothelial cell from hPSCs has aroused controversies. This perspective article highlights the developments made in the field of hPSC derived brain endothelial cells as well as where experimental data are lacking, and what concerns have emerged since their initial description.

## FROM GENERIC TO CNS SPECIFIC ENDOTHELIAL CELLS

Brain endothelial cells plays an essential role in the development of a multicellular vascular structure separating the central nervous system (CNS) from the peripheral blood circulation (Bär, 1980; Risau and Wolburg, 1990; Engelhardt, 2003). In mammals, this process begins when cells originating from the mesoderm, known as angioblasts, enter the head region and form the perineural vascular plexus (PNVP) which will go on to encompass the neural tube by mid-gestation. None of the microvasculature in the CNS is derived from the neuroectoderm but instead, new vessels sprout from the existing PNVP into the developing neuroectoderm (Risau and Wolburg, 1990; Engelhardt, 2003). This process is highly regulated, occurring at precise stages of embryonic development, thus leading to the formation of a reproducible pattern of neuro-vasculature in all mammals (Aird, 2007a,b).

Initial signs for CNS angiogenesis and induction of BBB traits are given by the neural microenvironment on embryonic day E10 in mice (Obermeier et al., 2013). Endothelial cell progenitors from the PNVP infiltrate the neuroectoderm following a gradient of vascular endothelial growth factor (VEGF), resulting in the development of nascent "leaky" or "immature" blood vessels (Potente et al., 2011). Activation of the Wnt/β-catenin pathway in these nascent blood vessels triggers the expression of genes critical for the formation of the BBB. Wnt ligands secreted by the neural microenvironment bind to a set of receptors expressed by the endothelial cells (Frizzled, LRP5, LRP6) to elicit the expression of GLUT1, DR6, and TROY (Stenman et al., 2008; Tam et al., 2012). Furthermore, G-protein coupled receptor 124 (GPR124) seems to be essential for barrier genesis in the brain as it acts as an endothelial specific co-activator of Wnt/β-catenin signaling in the BBB (Kuhnert et al., 2010; Anderson et al., 2011; Cullen et al., 2011). By day E15 an embryonic BBB is formed in mice (Daneman et al., 2010; Ben-Zvi et al., 2014); however, the exact timing of BBB formation in human development and whether humans are born with a fully mature BBB remains unclear (Saunders et al., 2013).

This primitive BBB further mature by recruiting pericytes to the developing blood vessels. This step is critical to ensure proper BBB formation and function (Armulik et al., 2010; Bell et al., 2010; Daneman et al., 2010; Vanlandewijck et al., 2018). A recent study deconvoluted the complexity of the endothelial responses to pericytes at the single cell level (Andaloussi Mae et al., 2020). Activation of endothelial TIE2 signaling by ANGPT2 secreted by pericytes reinforce endothelial arterio-venous zonation, angiogenic quiescence and a limited set of BBB functions. It was also shown that the last component of the BBB, astrocytes, support the endothelial cells in acquiring BBB attributes and barrier properties (Alvarez et al., 2011).

## ORGANOTYPIC PROPERTIES OF BRAIN MICROVASCULAR ENDOTHELIAL CELLS

The major endothelial transport systems, ions channels and GPCRs are described in detail elsewhere (Daneman and Prat, 2015; Vanlandewijck et al., 2018; Hariharan et al., 2020). The unique cellular junction molecules expressed by brain endothelial cells are briefly discussed below.

The BBB is lined with specialized endothelial cells (EC) known as brain microvascular endothelial cells (BMEC) that possess intercellular tight junctions (TJs), lack fenestrations, and greatly limit transcytosis. BMECs, acting in conjunction with various neural cell types and non-cellular elements, form the BBB which regulates the dynamic transfer of select molecules into and out of the CNS (Zlokovic, 2008; Daneman et al., 2009; Daneman, 2012). These properties are achieved through the presence of distinctive TJs exhibiting a high *trans*-endothelial electrical resistance (TEER) *in vivo* and reduced caveolar-mediated transport, along with the presence of selective transporters. Due to their significant structural and functional overlap, most of the current understanding of endothelial cell TJs has been derived from examination of their epithelial counterparts (MDCK, CACO2, and ECV304) (Garberg et al., 2005). However, BBB-endothelial TJs hold many unique attributes which may be more akin to ECs of other organs when paracellular permeability and dynamic regulation are evaluated under pathophysiological conditions.

The establishment and maintenance of BBB TJs are governed by mainly three transmembrane proteins: Claudins, Occludin, and Junction Adhesion Proteins (JAM). The Claudin family is comprised of at least 24 member proteins which contain two extracellular loops responsible for homophilic interaction as well as establishing a link with claudins of contiguous endothelial cells. This homophilic interaction forms the primary seal of the TJ *in vivo* (Piontek et al., 2008) with Claudin -1, -3, -5, and -12 initially thought to be expressed by BBB-forming ECs. While some studies showed immunostaining against Claudin-1 at the BBB in rodent models (Liebner et al., 2000), it has since been shown that it is not expressed by BBB-forming ECs (Pfeiffer et al., 2011). Likewise, while some research groups have reported that brain microvasculature expresses Claudin-3 (Wolburg et al., 2003), others could not reproduce or confirm this observation (Kominsky et al., 2007; Steinemann et al., 2016). The generation of a Claudin-$3^{-/-}$ mice demonstrated that the junctional immunostaining

produced by anti-Claudin-3 antibodies in mouse brain ECs *in situ* and *in vitro* is not due to the presence of Claudin-3 but rather to an endothelial junctional antigen that is still present in brain ECs of Claudin-$3^{-/-}$ mice (Castro Dias et al., 2019). Of note, it is now known that Claudin-1 and -3 are selectively expressed by the epithelium of the choroid plexus (Steinemann et al., 2016). Thus, these contradictory observations emphasize the contentious reliability of assessing Claudin protein expression in BBB TJs though their transcript expression still remain an important measure of cell specific tight junctions.

Another barrier property of the BBB lies in their ability to restrict immune cell infiltration to the CNS as BMECs generally has a low expression of leucocyte adhesion molecules during homeostatic conditions (Reese and Karnovsky, 1967; Brightman and Reese, 1969; Westergaard and Brightman, 1973). Immune cell trafficking across the BBB during pathophysiological conditions have been extensively studied in animal models of neuroinflammatory disease. These studies highlight the unique interaction of immune cells with BMECs which is regulated by a sequential cascade of different signaling pathways involving various adhesion molecules. BMECs harbor unique intrinsic properties which allow them to adapt and respond to inflammatory cues and thereby regulate immune cell trafficking through the BBB. BMECs exposed to TNFα, IL-1β, and IL-6 have shown increased paracellular permeability as well as acquiring an activated phenotype (de Vries et al., 1996).

These phenotypical modifications, unique to the vascular cells, are mainly characterized by an induced expression of endothelial cellular adhesion molecules that are critical for the recruitment of circulating leukocytes to sites of inflammation. The importance of ICAM-1 in regulating leukocyte recruitment during neuroinflammation has been highlighted in different animal models using both ICAM-1-null mice and ICAM-1-blocking antibodies (Zhang Rui et al., 1995; Kitagawa et al., 1998). An *in vivo* study in mice showed that E-selectin deficiency exert a neuroprotective effect characterized by reduced inflammation and neuronal apoptosis (Ma et al., 2012). Additionally, genetic P-selectin knock-in mice show increased BBB permeability and stroke injury (Kisucka et al., 2009). Hence, any BMEC cultured *in vitro* must be able to phenocopy this response to inflammatory stimuli in order to be considered physiologically relevant BBB model.

## A BRIEF OVERVIEW OF *IN VITRO* BLOOD BRAIN BARRIER MODELS

The development of *in vitro* models has accelerated mechanical studies on the BBB as well as large scale screening of drugs with potential to penetrate the brain, with some limitations. Many studies have been conducted using primary BMEC isolated from various animal tissues, most commonly bovine, porcine, and rodent (Dehouck et al., 1990; Gaillard et al., 2001; Deli et al., 2005; Roux and Couraud, 2005; Zhang et al., 2006; Burek et al., 2012; Yusof et al., 2014; Helms et al., 2016; Veszelka et al., 2018). BMECs isolated from larger animal models generally possess higher TEER, at around 800 $\Omega.cm^2$ (Rubin et al., 1991), and low permeability due to high expression of junctional markers such as claudin-5, ZO-1, and occludin (Rubin et al., 1991; Cecchelli et al., 2007; Cohen-Kashi Malina et al., 2009; Patabendige et al., 2013). In particular, bovine and porcine brain ECs can be isolated in large quantities with ease; as a result, they have become the preferred choice for many permeability and transcytosis studies. Rodent brain ECs, specifically mouse or rat, have also been widely used as an *in vitro* model of the BBB with some groups developing immortalized cell lines (Roux et al., 1994; Wagner and Risau, 1994; Burek et al., 2012) and others discovering the use of Puromycin to increase the purity of primary isolations (Perrière et al., 2005; Calabria et al., 2006). Brain ECs these models generally possess lower TEER (under 300 $\Omega.cm^2$) (Daneman et al., 2010) but offer an avenue for BBB studies in transgenic models. Models using rodent brain ECs also provide the opportunity for large cohort studies and cells which can be targeted by many established antibodies.

These animal BMECs have also been studied in many co-culture conditions allowing for the discovery of many important cellular interactions between BMECs, astrocytes, and pericytes in the neurovascular microenvironment (Gaillard et al., 2001; Coisne et al., 2005; Garberg et al., 2005; Nakagawa et al., 2007; Helms et al., 2010, 2012; Liu et al., 2014). These co-culture models also possess higher TEER with the larger animal models exceeding 2,500 $\Omega.cm^2$ in some studies (Helms et al., 2014). Over time, BBB models developed using these various animal cell lines have demonstrated well-characterized permeability phenotypes and physiological similarities to human BMECs (Warren et al., 2009; Shawahna et al., 2011; Uchida et al., 2011; Hoshi et al., 2013). For instance, bovine co-culture models possess highly differentiated junctions which allow for various permeability and junction modulation assays using drug compounds (Wolburg et al., 1994; Gaillard and de Boer, 2000; Schaddelee et al., 2003; Boveri et al., 2006; Bohara et al., 2014). Rodent co-culture conditions utilizing single or multiple neural cell types have been shown to successfully mimic the neurovascular unit and even induce certain BBB phenotypes such as elevated TEER *in vitro* which has been validated by small molecule permeability screening (Coisne et al., 2005; Nakagawa et al., 2007, 2009; Abbott et al., 2012; Watson et al., 2013). Animal BBB models have provided a wealth of insight into various aspects of BBB physiology and pathology with a large amount of cross-validation between models. However, recent advances in the field have illuminated aspects in which animal models are lacking such as precise reproducibility with certain models showing a wide range of varied TEER and junctional phenotypes between laboratories (Schaddelee et al., 2003; Helms et al., 2014).

In an effort to generate a completely homologous model for clinical research and drug development, human primary BMECs have also been used in *in vitro* BBB models but are difficult to procure in sufficient numbers for experimental purposes (Bernas et al., 2010). Though human BMECs have provided a useful model for the study of many developmental and

regulatory neurovascular pathways, the ethical questions and general restrictions placed on obtaining healthy human brain tissue along with low BMEC yields during isolation places a substantial limitation on their use in *in vitro* studies (Bernas et al., 2010). In addition, often times human BMECs offered by commercial vendors lack detailed documentation as to the isolation and sourcing of the cells, creating concerns over their use in many physiological models (Helms et al., 2016). The barrier properties and endothelial identity of primary BMECs are also not well maintained *in vitro* for extended periods of time, rendering them suboptimal for a number of potential BBB assays (Helms et al., 2016).

In order to overcome these limitations, immortalized human BMEC lines were established (Stins et al., 2001; Weksler et al., 2005; Rahman et al., 2016). These cells provided researchers with a model of human BMECs which was easy to use and had less batch variation availability issues. However, immortalized human BMECs also lose many of their brain specific EC attributes and produce a sub-physiologic TEER *in vitro* making them ineffective for functional studies (Urich et al., 2012; Weksler et al., 2013; Helms et al., 2016). It has also been reported that expression of endothelial tight junction specific *CLDN5* is significantly lower in immortalized human BMECS than *in vivo*. Taken together, BMECs originating from either animal or human tissue origins lose some of their organotypic phenotypes when cultured *in vitro* (Urich et al., 2012; Weksler et al., 2013). The use of all the previously mentioned brain endothelial cells in various mono- and co-culture conditions has highlighted the need for a stable *in vitro* BBB model possessing both vascular endothelial and barrier phenotypes (Helms et al., 2016).

## HUMAN PLURIPOTENT STEM CELL DIFFERENTIATION AS A POSSIBLE ALTERNATIVE

Recently, Lippmann et al. (2012) have reported the generation of a pure population of putative BMECs from pluripotent stem cell sources (iBMECs) has been described to meet the need for a reliable and reproducible *in vitro* human BBB model. Human pluripotent stem cells, embryonic or induced, can differentiate into large quantities of specialized cells in order to study development and model disease. iBMECs are generated primarily through directed differentiation of pluripotent stem cells into both neural and endothelial progenitors followed by selective purification. Under these differentiation culture conditions, it is proposed that the neural cell types provide a microenvironmental cues that coax the emerging endothelial progenitors toward a BBB-specific phenotype as they further differentiate into ECs (Lippmann et al., 2012). Later iterations of this protocol reported that adding retinoic acid or inhibiting GSK3 during this neuro-endothelial differentiation process would enhance the yield and fidelity of these putative iBMECs (Lippmann et al., 2014; Qian et al., 2017; Faley et al., 2019). Additionally, others have developed a more defined serum-free method which aimed to improve the consistency of differentiated iBMECs while decreasing the overall length of the differentiation process (Hollmann et al., 2017; Neal et al., 2019) (**Table 1**). Regardless of the method used, these iBMECs display endothelial-like properties, such as tube formation and low-density lipoprotein uptake, high TEER ($\geq$800 $\Omega.cm^2$), and barrier-like efflux transporter activities (Stebbins et al., 2016; Appelt-Menzel et al., 2017; Canfield et al., 2017; Hollmann et al., 2017; Lim et al., 2017; Stebbins Matthew et al., 2017; Vatine et al., 2017; Delsing et al., 2018; Sances et al., 2018). They have also been reported to express select BMEC marker transcripts such as *PECAM1, CDH5,* and *CLDN5,* among other BBB-specific markers (Qian et al., 2017; Vatine et al., 2017, 2019; Lee et al., 2018; Faley et al., 2019; Martins Gomes et al., 2019; Linville et al., 2020).

iBMECs generated using the original neuro-endothelial differentiation and subsequent protocols have quickly been adopted as a robust and viable source of human BMECs in many different *in vitro* studies of the BBB. At their inception, iBMECs were primarily used as a monoculture system to recapitulate the BBB in two-dimensional cell culture conditions. The cells were described to replicate barrier and transporter phenotypes present in the BBB *in vivo* in a cell-autonomous manner as well as respond to signaling from other neural cell types and microenvironmental changes. iBMECs cocultured with astrocytes and/or pericytes have been reported to have increased TEER to above 1,500 $\Omega.cm^2$ as well as expression of certain transporters and receptors present in the BBB such as *SLC2A1*, *BCRP*, *MRP1*, and *LRP1* (Lippmann et al., 2012, 2014; Canfield et al., 2017; Qian et al., 2017; Vatine et al., 2017, 2019). Some groups have concluded that not only does the vascular endothelial identity of iBMECs remain stable in co-culture but that these conditions aid in the maturation of iBMECs into a more functional BBB model defined in large part by a decrease in dextran permeability through the barrier model.

Unsurprisingly, culturing these cells on a 2-D surface, regardless of the extra cellular matrix used, places observable limitations on cell–cell interactions including movement of secreted factors in the dish. These limitations would eventually lead to iBMECs being adapted to three-dimensional BBB models including various brain "organ-on-chip" models designed to have iBMECs interacting with various other cell types in 3-D (Sances et al., 2018; Faley et al., 2019). Some of these models also allow for flow to be introduced to the cells, further mimicking *in vivo* conditions (DeStefano et al., 2017; Vatine et al., 2019). Many groups have used 3-D iBMEC based models to further study the BBB under more physiologically relevant conditions; reporting data on permeability, gene expression, and barrier properties of iBMECs (Vatine et al., 2019; Linville et al., 2020). Over time, the use of both 2-D and 3-D iBMEC-based BBB models has led to many conclusions regarding the properties and functions of brain specific ECs which has added a lot of data to the field of BBB research. As a result of these reports, iBMECs have been widely accepted for use as a brain specific EC in many *in vitro* systems to assess BBB properties and function in homeostatic and disease models (Lippmann et al., 2012, 2013, 2014; Wilson et al., 2015; Stebbins et al., 2016; Appelt-Menzel et al., 2017; Canfield et al., 2017; Hollmann et al., 2017; Lim et al., 2017; Qian et al., 2017; Stebbins Matthew et al., 2017; Vatine et al., 2017, 2019;

**TABLE 1 |** Major iterations of hPSC-derived iBMEC protocols.

| Year | References | Protocol | Changes vs. 2012 | Cell line/Maintenance | Differentiation media | QPCR | Antibodies | Barrier assays | Transporters/ transcytosis |
|---|---|---|---|---|---|---|---|---|---|
| 2012 | Lippmann et al. (2012). Nature biotechnology | (1) Prior diff cells are passaged on Matrigel (mTESR1 for 2–3 days.<br>(2). Media is switched to lack of FGF (UM) for 5–7 days.<br>(3). Switch to EC media human Endothelial Serum-Free Medium (Invitrogen) supplemented with 20 ng/mL bFGF and 1% platelet-poor plasma derived bovine serum32 (PDS; Biomedical Technologies, Inc.).<br>(4) 1–2 days of EC medium treatment, cells were dissociated with dispase (2 mg/mL; Invitrogen) and plated onto 12-well tissue culture polystyrene plates and maintained in EC media. | NA | ES line: H9, IPS: IMR90-4, iPS-DF19-9-11T33, iPS-DF6-9-9T. Irradiated MEFS, DMEMF12 20%KOSR, 1xMEM, 1mM-lglutamine, 4ng.ml bFGF | UM = lack of FGF and EC = Endothelial Serum-Free Medium (Invitrogen) supplemented with 20 ng/mL bFGF and 1% platelet-poor plasma derived bovine serum32 (PDS; Biomedical Technologies, Inc.) | PECAM1, CDH5, vWF, LDLR, LRP1, INSR, LEPR, BCAM, TFRC, AGER, STRA6, SLC7A5, SLC1A1, SLC38A5, SLC16A1, SLC2A1, ABCB1, ABCG2, ABCC1, ABCC2, ABCC4, and ABCC5. PLVAP, SLC21A14, FST, FZD7, FZD4, FZD6, STRA6, LEF1, APCDD1, SLC2A1, ABCB1 control: GAPDH, NO EC CONTROL | PECAM-1 (Rabbit, Thermo Fisher) CLAUDIN-5 (Mouse, Invitrogen) Occludin (Mouse, Invitrogen) *P*-glycoprotein (Mouse, Thermo Fisher) GLUT-1a (Rabbit antiserum) VE-Cadherin (Mouse, SCBT) Nestin (Rabbit, Millipore) βIII tubulin (Rabbit, Sigma) βcatenin (FITC-conjugated Mouse, BD Biosciences) Wnt7a FISH Wnt7b FISH GFAP (Polyclonal Rabbit, Dako) aSMA (Mouse, American Research Products) | TEER, coculture with rat astrocytes | Inulin, sucrose, glucose, vincristine, colchicine, prazosin, diazepam, rodhamine 123 ((cyclosporine). No EC control |

*(Continued)*

**TABLE 1 |** Continued

| Year | References | Protocol | Changes vs. 2012 | Cell line/Maintenance | Differentiation media | QPCR | Antibodies | Barrier assays | Transporters/ transcytosis |
|---|---|---|---|---|---|---|---|---|---|
| 2014 | Lippmann et al. (2014)Lippmann et al., . Scientific reports | (1) Prior diff cells are passaged on Matrigel (mTESR1 for 2–3 days. (2). Media is switched to lack of FGF (UM) for 5–7 days. (3). Switch to EC media human Endothelial Serum-Free Medium (Invitrogen) supplemented with 20 ng/mL bFGF and 1% platelet-poor plasma derived bovine serum32 (PDS; Biomedical Technologies, Inc.). (4). 1–2 days of EC medium treatment, cells were dissociated with dispase (2 mg/mL; Invitrogen) and plated onto 12-well tissue culture polystyrene plates and maintained in EC media (RA | Addition of Retinoic Acid on day 6 use of versene to dissociate the cells instead of dispase, results in less debris | IMR90-4 and DF19-9-11T iPSCs and H9 hESCs in mTESR or 2012 | UM = lack of FGF and EC = Endothelial Serum-Free Medium (Invitrogen) supplemented with 20 ng/mL bFGF and 1% platelet-poor plasma derived bovine serum32 (PDS; Biomedical Technologies, Inc.) + RA | ABCB1, ABCG2, ABCC1, ABCC2, ABCC5, and STRA6 | PECAM-1 (Rabbit, Thermo Scientific) GLUT-1 (Mouse, Thermo Scientific) Occludin (Mouse, Life Technologies) CLAUDIN-5 (Mouse, Life Technologies) VE-Cadherin (Mouse, SCBT) E-Cadherin (Goat, R&D Systems) *P*-glycoprotein (Mouse, Life Technologies) BCRP (Mouse, Millipore) MRP1 (Mouse, Millipore) GFAP (Rabbit, Dako) βIII tubulin (Rabbit, Sigma) Nestin (Mouse, Millipore) αSMA (Mouse, American Research Products) PDGFRβ (Rabbit, Cell Signaling) | TEER, coculture with NPC astrocytes, neurons and primary pericytes | DOXO, rhodamine DCFDA |

*(Continued)*

**TABLE 1 |** Continued

| Year | References | Protocol | Changes vs. 2012 | Cell line/Maintenance | Differentiation media | QPCR | Antibodies | Barrier assays | Transporters/ transcytosis |
|---|---|---|---|---|---|---|---|---|---|
| 2017 | Qian et al. (2017). Science advances | 6 (μM of CHIR on D0-1, he medium was removed and cells were transitioned to DeSR2 (DeSR1 plus B27 supplement) for another 5 days with daily medium changes. At day 6, cells were switched to hECSR1 medium [human endothelial serum-free medium (hESFM) supplemented with basic fibroblast growth factor (bFGF, 20 ng/ml), 10 (M RA, and B27] to induce RA signaling in the hPSC-derived endothelial progenitors in an attempt to drive the specification to BMECs. Cells were maintained in this medium for 2 days. At day 8, cells were replated onto a Matrigel-coated substrate in hECSR1, and at day 9, the medium was switched to hECSR2 (hECSR1 lacking RA and bFGF). | Accutase instead of Versene | Human iPSCs [iPS(IMR90)-4 (*72*), iPS-DF 19-9-11T (*73*), and hESCs (H9) (*29*)] were maintained on Matrigel (Corning)–coated surfaces in mTeSR1 | 6 μM CHIR99021 (Selleckchem) in DeSR1: DMEM/Ham's F12 (Thermo Fisher Scientific), 1× MEM-NEAA (Thermo Fisher Scientific), 0.5× GlutaMAX (Thermo Fisher Scientific), and 0.1 mM β-mercaptoethanol (Sigma). After 24 h, the medium was changed to DeSR2: DeSR1 plus 1× B27 (Thermo Fisher Scientific) every day for another 5 days. At day 6, the medium was switched to hECSR1: hESFM (Thermo Fisher Scientific) supplemented with bFGF (20 ng/ml), 10 μM RA, and 1× B27 | | Brachyury (R&D Systems) PAX2 (SCBT) CD31 (Thermo Fisher) VE-Cadherin (SCBT) vWF (Dako) VEGFR2 (SCBT) CLAUDIN-5 (Invitrogen) Occludin (Invitrogen) ZO-1 (Invitrogen) GLUT-1 (Thermo Fisher) PGP (Thermo Fisher) BCRP (Millipore) MRP1 (Millipore) OCT3/4 (SCBT) TRA-1-60 (SCBT) NANOG (SCBT) ICAM-1 (R&D Systems) | "We also compared the differentiation reproducibility with that of the previously reported UM protocol (33). Although both methods produce BMECs capable of substantial barrier formation from multiple hPSC lines, BMECs differentiated from H9 hESCs and 19-9-11 iPSCs using the defined method exhibited higher TEERs and lower batch-to-batch variation." | Efflux transporter activities were measured by the intracellular accumulation of (G) rhodamine 123, (H) Hoechst, and (I) DCFDA, substrates for Pgp, BCRP, and MRP, respectively. CsA, Ko143, and MK571 were used as specific inhibitors of Pgp, BCRP, and MRP, respectively |

*(Continued)*

**TABLE 1 |** Continued

| Year | References | Protocol | Changes vs. 2012 | Cell line/Maintenance | Differentiation media | QPCR | Antibodies | Barrier assays | Transporters/ transcytosis |
|---|---|---|---|---|---|---|---|---|---|
| 2017 | Hollmann et al. (2017). Fluids barriers CNS | Modified 2014 protocol | E8 and E6 media, E6 for 4 days then continued as Lippmann et al. (2014) protocol. | MR90-4 iPSCs CC3 iPSCs, CD12 iPSCs, and SM14 iPSCs in growth factor-reduced Matrigel (VWR) in E8 medium | E8 medium was prepared by adding 100 μL of human insulin solution (Sigma-Aldrich), 500 μL of 10 mg/mL of human holo-transferrin (R&D Systems), 500 μL of 100 μg/mL human basic fibroblast growth factor (bFGF; PeproTech), and 500 μL of 2 μg/mL TGFβ1 (PeproTech) to 500 mL of E4. The final concentrations are 2.14 mg/L insulin, 100 μg/L bFGF, 2 μg/L TGFβ1, and 10.7 mg/L holo-transferrin E6 medium was prepared by adding 100 μL of human insulin solution and 500 μL of 10 mg/mL of human holo-transferrin to 500 mL of E4. The final concentrations are 2.14 mg/L insulin and 10.7 mg/L holo-transferrin UM and EC same as 2–14 | | PECAM-1 (Rabbit, Thermo Scientific) GLUT-1 (Mouse, Thermo Scientific) OCCLUDIN (Mouse, Thermo Scientific) CLAUDIN-5 (Mouse, Thermo Scientific) VE-Cadherin (Goat, R&D Systems) GFAP (Rabbit, Dako) PDGFR-B (Rabbit, SCBT) NG2 (Mouse, SCBT) αSMA (Mouse, SCBT) | TEER | Intracellular accumulation of rhodamine 123 (a Pgp substrate) was evaluated in the absence of bFGF and RA. Cells were incubated with 10 μM PSC833 or 10 μM MK-571 for 1 h at 37°C. They were then incubated for an additional house with 10 μM rhodamine 123 or 10 μM H2DCFDA. |

*A summary of the original hPSC-derived iBMEC protocol (Lippmann et al., 2012) as well as the major adaptations made in subsequent studies (Lippmann et al., 2014; Hollmann et al., 2017; Qian et al., 2017) highlighting the key changes and experimental conditions used in each study.*

Delsing et al., 2018; Lee et al., 2018; Sances et al., 2018; Faley et al., 2019; Martins Gomes et al., 2019; Linville et al., 2020).

## CONFLICTING REPORTS OF IBMEC VASCULAR CELL IDENTITY

Cellular identity is multifaceted and is usually determined by a combination of transcriptional, translational and functional phenotypes presented by a cell. This concept is particularly important for PSC-derived cell types, as directed differentiation to a target cell may yield a heterogenous population where the target cell type is less frequent or lacking in canonical lineage-specific genes that can have a tremendous impact on the overall efficacy of the cell as an *in vitro* model. Moreover, there is an existing concern regarding the standards by which cells engineered *in vitro* are validated against their primary counterparts in native tissues (Daley, 2015). These concerns stem from reports using only a small number of transcriptional or protein markers, limited or peripheral functional assays, and global RNA expression analyses which taken together can lead to a misguided identification of the cell type produced *in vitro*.

The characterization of iBMECs has been dominated by their *in vitro* barrier properties which has largely been based off the TEER measurements of these cells in monolayer conditions (Stebbins et al., 2016). Expression of barrier specific genes such as *ZO-1* and *OCLN* have also served as a standard to bolster this barrier phenotype though these and many other tight junction marker genes expressed by iBMECs are not canonically specific to vascular ECs (Acharya et al., 2004; Hwang et al., 2013). Over time, some studies have started to present conflicting data regarding the cellular identity of these cells (Delsing et al., 2018; Lu et al., 2019; Vatine et al., 2019). Given that organ specific models rely heavily on cell specific responses to stimuli or cell–cell interactions which can differ widely depending on cell type, concerns over iBMEC cellular identity presents a major problem with their use in *in vitro* BBB models.

As the BBB is principally a vascular structure, it is imperative that iBMECs are phenotypically, transcriptionally and functionally analogous to definitive ECs which make up the BBB. Recently, there have been several reports demonstrating certain incongruencies in the cellular identity of iBMECs. Delsing et al. (2018) demonstrated that iBMECs generated from the neuro-endothelial differentiation expressed a considerably lower level of key endothelial marker genes in both mono and co-culture conditions when compared to other hPSC derived ECs or primary human BMECs. This study reported the presence of PECAM1, ZO-1, CLDN-5, VWF, and other endothelial markers in protein staining of iBMECs as well as hPSC derived ECs of a different protocol. However, the bulk RNA sequencing data reported a statistically significant decrease in mRNA expression of *PECAM1*, *CDH5*, *CLDN5*, and *VWF*, in iBMECs relative to the other ECs tested. The study went on to show that iBMECs express *CLDN4*, *CLDN6*, and *CLDN7* indicating the presence of an epithelial cell junction. Taken together, this data led the group to conclude that iBMECs possess somewhat of a mixed phenotype (Delsing et al., 2018).

In Lu et al. (2019), our group conducted an in-depth characterization of iBMECs using a combinatorial analysis of protein and RNA expression comparing iBMECs from previously published work to their own. Our analysis also included multiple primary endothelial cell controls as well as hPSC derived ECs generated using a another previously published protocol (James et al., 2010). Initial microscopy and fluorescence activated cell sorting (FACS) revealed a lack of PECAM1 and CDH5 protein expression in iBMECs compared to the other ECs used in this study. EPCAM protein expression is also demonstrated in exclusively the iBMECs using the same assays. To validate these results, we performed a meta-analysis of bulk RNA sequencing data comparing their own iBMECs to previously published RNA transcriptomes obtained from the NCBI Gene Expression Omnibus (GEO).

We were able to demonstrate that not only were their iBMECs transcriptionally equivalent with previously published iBMECs but also that all iBMECs lacked a canonical EC transcriptional profile and conversely expressed many genes normally related to an epithelial cell lineage such as *EPCAM*, *KRT8*, *KRT19*, *SPP1*, and *FREM2*. These results were confirmed by single-cell RNA sequencing which also showed iBMECs to be a homogenous epithelial cell population lacking a vascular EC identity. An absence of key EC transcription factor (TF) and marker genes was observed in both RNA sequencing platforms, concerns over the validity of the previously established protein expression data becomes apparent. iBMECs used in this study were shown to be transcriptionally identical to those previously published which mean that positive protein expression data could be due to non-specific binding by monoclonal antibodies, especially in the case of proteins from large homologous families such as Claudins (Krause et al., 2015). In summary, this study concludes that though iBMECs present a tight junction phenotype with high TEER, their cellular identity is severely lacking in congruency to vascular ECs making them unsuitable for use as an *in vitro* model of the human BBB (Lu et al., 2019) (**Table 2**).

**TABLE 2 |** hPSC-derived iBMECs are not phenotypically comparable to primary human BMECs.

| | **hPSC-Derived BMEC *in vitro*** | **Primary Human BMEC *in vitro*** |
|---|---|---|
| Surface marker profile | PECAM1$^-$ CDH5$^-$ EPCAM$^+$ | PECAM1$^+$ CDH5$^+$ EPCAM$^-$ |
| Claudin family repertoire | Claudin-4, Claudin-6, Claudin-7 | Claudin-5 |
| Barrier properties | High junctional electrical resistance | Low junctional electrical resistance |
| Inflammatory response | No canonical vascular response observed | VCAM-1, ICAM-2, E-Selectin upregulation |
| Significant media differences | Serum free (or 1% platelet poor bovine serum) | Fetal bovine serum; SB431542 |
| Extracellular matrix | Fibronectin/collagen IV mixture | Gelatin |

*An overview of crucial differences between hPSC-derived iBMECs and primary human BMECs illustrating major differences in cellular phenotype as well as in vitro culture conditions.*

Using many of the same bulk RNA endothelial and epithelial control samples from the GEO repository as Lu et al. (2019), and their own iBMECs, Vatine et al. (2019) performed a meta-analysis as well. iBMECs in this study were seeded in an organ-chip device in which the authors claim they establish a hollow vessel-like structure. A Principal Component Analysis (PCA) of their dataset revealed that iBMECs clustered closest to some of the endothelial controls. However, the lung epithelial cell libraries used in this analysis were prepared using total RNA without ribosomal depletion, while the rest of the dataset consisted of samples that were both polyA-primed and depleted of their ribosomal transcripts. Such a discrepancy in library preparation methods is likely to have caused a significant bias in this PCA; in fact, sample divergence across PC1 was exclusively due to the presence of ribosomal transcripts. Still, this meta-analysis also reported the presence of many epithelial cell transcripts in iBMEC samples, reinforcing previous conclusions about the presence of a non-vascular epithelial cell identity in these cells. This study goes on to introduce iBMEC organ-chips to different levels of laminar flow and co-culture with various hPSC-derived neural cell types. Bulk RNA sequencing of iBMECs in each of these conditions revealed a number of differences in expression of the *CLDN* gene family (**Figure 1**) as well as junction related genes (**Figure 2**) which the authors used to conclude that certain conditions allowed for the functional maturation of iBMECs (Vatine et al., 2019).

Importantly, these changes in expression levels were reported in relative terms for each transcript after normalization across samples that did not include an EC control. The FPKM values for some of the genes reported varied with statistical significance across conditions (*CLDN4*, *CLDN6*, *HIF1A*, and *CAV1*); however, some of these statistically significant differences denoted changes in FPKM values of less than 1 (*CLDN5*, *CLDN10*) stipulating an overall lack of function difference in gene expression. Interestingly, differences in FPKM values of greater than 20 occurs exclusively in genes more closely related to an epithelial lineage, reinforcing the notion of an epithelial phenotype in iBMECs. Differences in FPKM of some marker genes were also shown to be not significantly different between samples even though the Row *Z*-score demonstrates a large difference in expression. Moreover, the average FPKM of some of these marker genes across all samples was under 0.1 indicating that

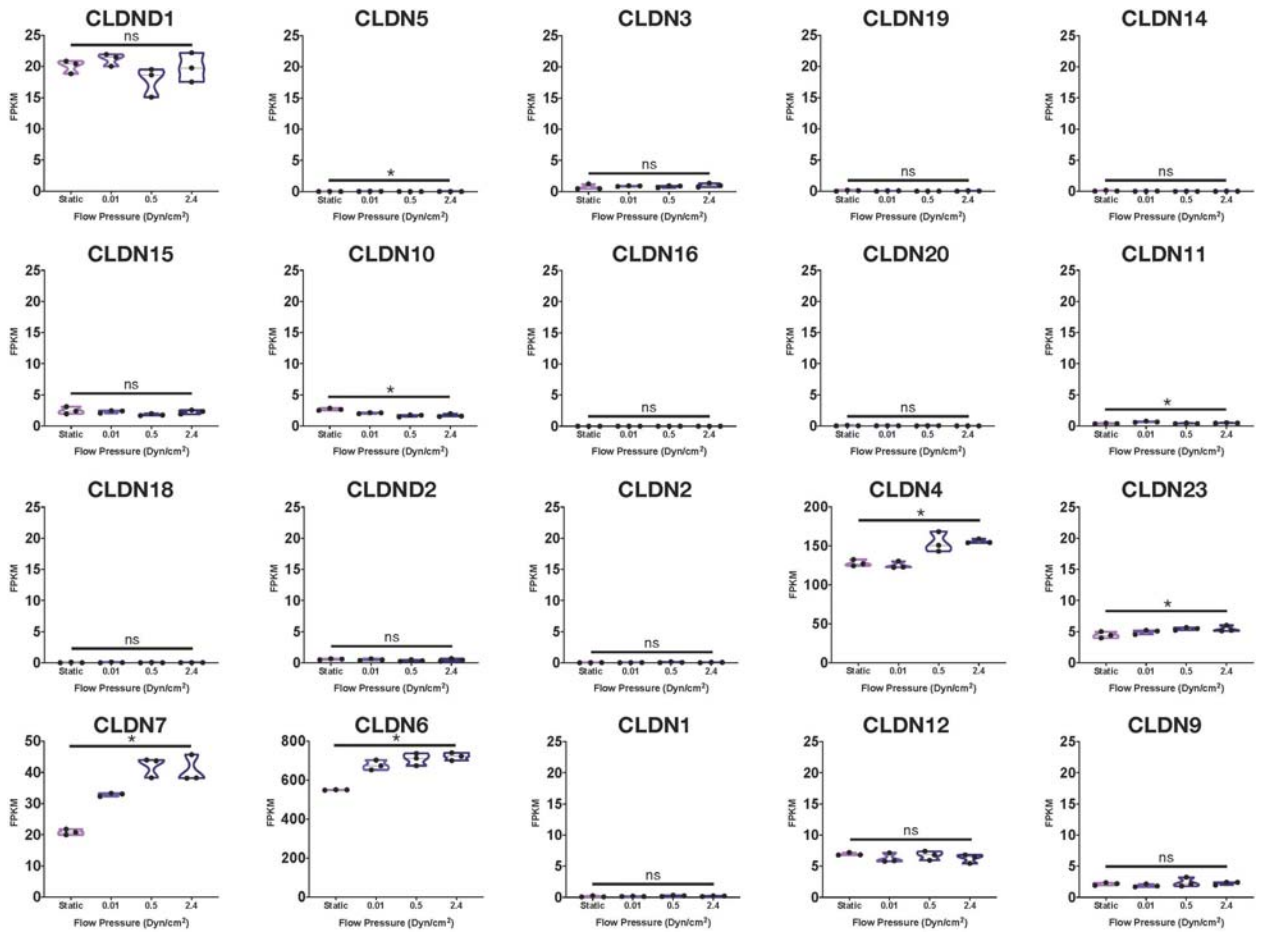


**FIGURE 1 |** Claudin family RNA expression in iBMECs under sheer stress. Violin plots of Claudin family gene expression in iBMEC organ-chip samples at various flow pressures adapted from data provided by Vatine et al. (2019) (significance indicates $p$-value $< 0.05$).

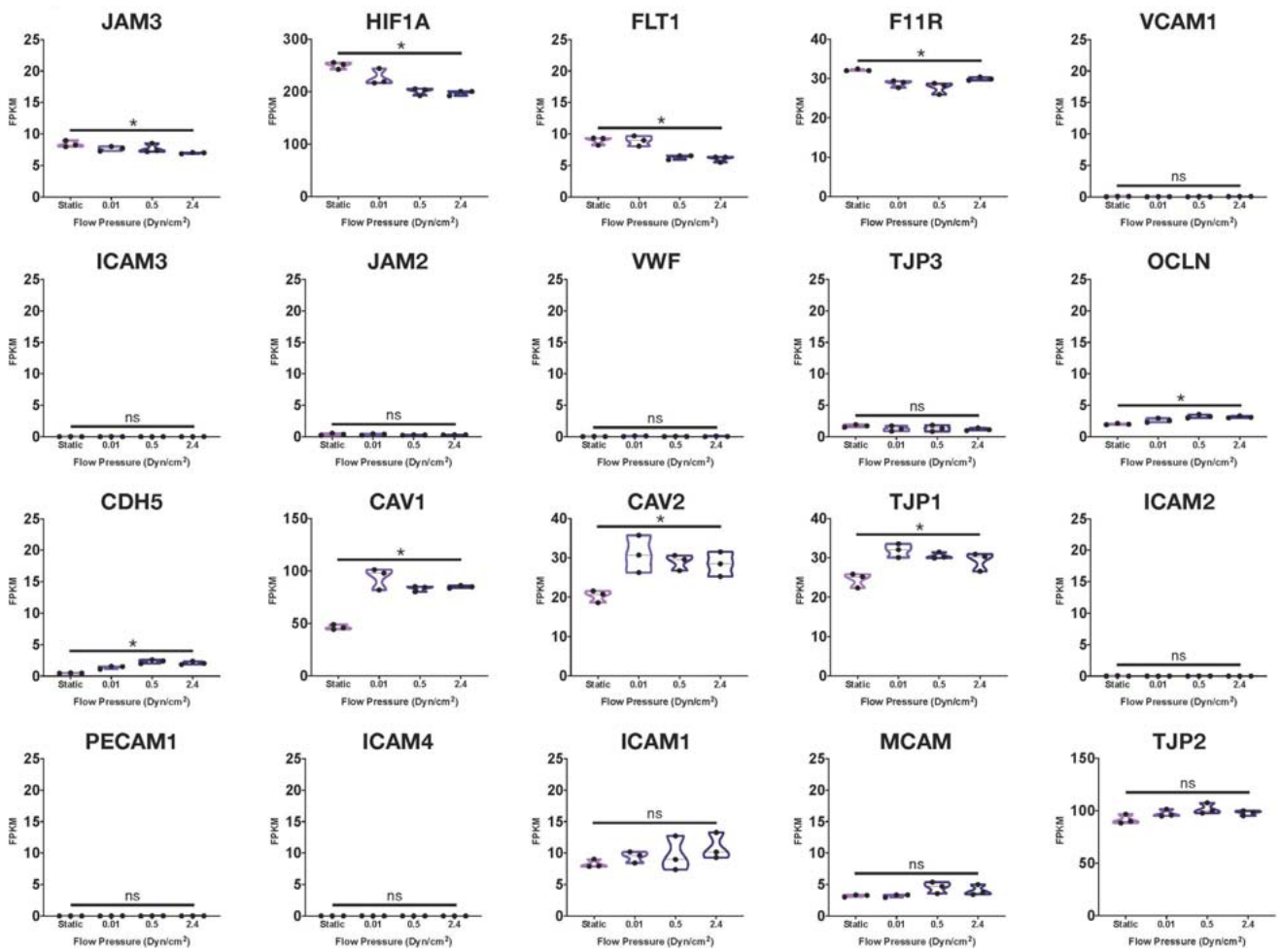


**FIGURE 2 |** Junctional-related gene RNA expression in iBMECs under sheer stress. Violin plots of junctional-related gene expression in iBMEC organ-chip samples at various flow pressures adapted from data provided by Vatine et al. (2019). Genes were defined as junctional-related according to the referenced study (significance indicates $p$-value $< 0.05$).

the genes are barely expressed and unlikely to undergo any translation (Hart et al., 2013). Interpretation of near zero FPKM values as functional expression of a gene could lead to incorrect assumptions of cell identity and functional phenotypes.

The lack of a functional vascular endothelial identity in iBMECs is further reinforced in a study by Martins Gomes et al. (2019) in their study focusing on their use as a disease model for *Neisseria meningitidis* (*Nm*) infection of the brain. While characterizing the response of iBMECs to inflammatory factors brought on by *Nm* infection, the group notes no difference in VCAM-1 or E-Selectin RNA expression which shows a lack of an EC specific response to inflammatory stimuli. Nishihara et al. (2020) further bolsters these results with their study in which they assess immune cell interactions with iBMECs. They characterized the inflammatory response of iBMECs generated with the established method (Lippmann et al., 2014) and those generated using the later adapted chemically defined method (Qian et al., 2017). Interestingly, it was shown that iBMECs differentiated using either method did not stain positive for ICAM-2, VCAM-1, E-selectin, or P-Selectin (Nishihara et al., 2020). ICAM-1 upregulation was only reported upon removal of retinoic acid, which was previously described to contribute greatly to the development of a vascular EC identity in these cells (Lippmann et al., 2014), from the differentiation process. The group ultimately concluded that iBMECs generated from any of these protocols lack expression of many vascular cell adhesion molecules and are not well suited for modeling immune cell interactions in the BBB.

## POSSIBLE MEANS FOR INDUCTION OF VASCULAR BBB PHENOTYPE IN HPSC-DERIVED CELLS *IN VITRO*

Before a functional hPSC-derived vascular BBB model can be developed, stable hPSC-derived vascular ECs must be generated. In a recent study (Lu et al., 2021), our group demonstrated that a vascular fate can be induced in iBMECs through

introduction of certain EC-specific ETS TFs (*ETV2*, *ERG,* and *FLI1*). These reprogrammed cells (rECs) harbor an EC transcriptomic profile, retaining a $PECAM1^{+}CDH5^{+}KDR^{+}$ EC immunophenotype during passaging and expansion. Purified rECs can respond to inflammatory stimuli (i.e., TNF-α) and permeabilizing agents (i.e., VEGF-A and anti-VE-cadherin antibody) in a manner congruent with vascular ECs. rECs were also shown to be capable of forming tubes *in vivo* using an immunocompromised mouse model, whereas iBMECs derived from the same hPSCs could not. This strategy of transcription factor reprogramming establishes a vascular EC identity in cells that otherwise lacked any phenotypic and functional aspects of bona fide ECs. However, further work is required to generate a reliable brain specific EC and that this only represents a crucial step toward the generation of true brain ECs suitable for *in vitro* modeling of physiological and pharmaceutical studies of the BBB.

In addition to the co-culture systems referenced above, numerous culture conditions have been demonstrated to improve BBB phenotypes *in vitro*. Some groups were able to show that neural cell conditioned media could increase barrier resistance and decrease permeability in BMEC monolayers (Siddharthan et al., 2007; Puech et al., 2018). Others have used cytokines and small molecules in the culture medium to modify barrier and vascular phenotypes these ECs. As previously mentioned, de Vries et al. (1996) demonstrated that exposure to cytokines such as TNF-α, IL1-β, and IL-6 induces an overall decline in TEER across rat brain EC monolayers. Schulze et al. (1997) later showed that Lysophosphatidic Acid increases tight junction permeability in porcine brain ECs. In contrast, a study from Roudnicky et al. (2020b) has indicated that the ALK5 inhibitor RepSox could modulate EC barrier stability. These studies all support the notion that microenvironmental queues play a large role in the homeostatic regulation of BMECs and adjustments to culture conditions will largely affect the overall function of an *in vitro* BBB model.

Moving on from culture conditions, intrinsic transcriptional regulation may also be critical for the establishment of a vascular BBB model. A separate Roudnicky et al. (2020a) study was able to demonstrate that synergistic overexpression of TFs including *SOX18*, *TAL1*, *SOX7,* and *ETS1* can enhance certain properties in EC such as barrier function. Their work shows that hPSC-derived ECs transduced with these TFs have increased transmembrane electrical resistance and tight junction protein expression while also decreasing paracellular transport (Roudnicky et al., 2020a). Taken together, this data suggests transcription factor overexpression could eventually be used in conjunction with chemomodulation in order to directly generate

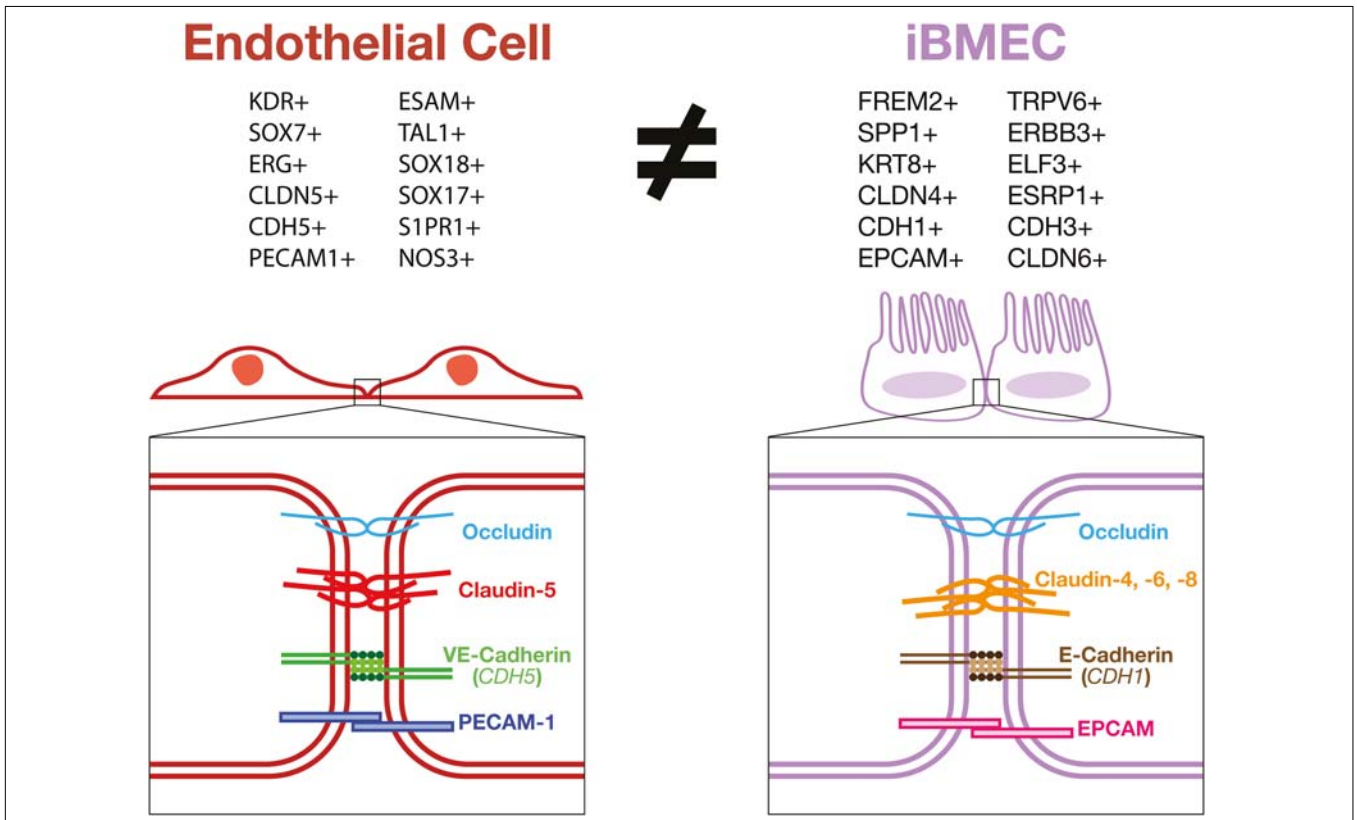


**FIGURE 3 |** iBMECs do not possess an endothelial transcriptional profile or vascular junctional components. iBMECs are shown to lack expression of phenotypical markers of a vascular EC lineage while expressing many epithelial cell lineage genes by bulk and single-cell RNA sequencing methods. The junctional components in iBMECs are also incongruent with canonical EC junctions leading to very serious concerns as to the efficacy of their use in an *in vitro* vascular BBB model.

brain-specific ECs from hPSCs which could be suitable for *in vitro* BBB models.

## CONCLUDING REMARKS

Over the past decade many groups have aimed to advance the study of the BBB by developing *in vitro* models attempting to mimic the physiological complexity of the BBB *in vivo*. Many difficulties have arisen during the course of these efforts as such models must phenocopy the high TEER observed *in vivo* as well as the intricate cellular transport mechanisms that are hallmarks of the BBB. It has been demonstrated that BBB traits are not intrinsic to brain specific ECs, but rather the result of a dynamic interplay with their microenvironment including multiple cell types such as astrocytes and pericytes. Consequently, primary brain ECs lose their barrier properties, especially high TEER, when cultured *in vitro*. Many laboratories have attempted to resolve this issue by developing various *in vitro* BBB models using neural cell co-cultures consisting of ECs, pericytes, and astrocytes. These models also include pluripotent stem cell differentiation methods as well as brain organoids and 'organ-on-a-chip' approaches.

Validation of these *in vitro* models relies mainly on using TEER and expression of tight junction proteins as a determinant of barrier function. Using these measurements as a proxy for functional BBB-specific tight junctions presents some limitations since it can only measure the paracellular junctions. The BBB has many transcellular permeability functions that are imperative for its function which cannot be measured in this way. Additionally, high TEER and many of the junctional proteins used to validate brain EC identity have been demonstrated in other non-endothelial cell types such as epithelial cells. ECs have also been shown to possess a polarized morphology (Lizama and Zovein, 2013) similar to epithelial cells, however, these morphological and junctional characteristics do not suggest that epithelial cells can be used interchangeably with ECs in *in vitro* vascular barrier models. Other problems may also have arisen from assigning a vascular EC identity to hPSC-derived cells based on the expression of a restricted set of brain EC markers. False positive results of EC identity can occur in these cases due to antibody cross-reactivity with proteins present in the cell sample that are not specific to ECs. As shown, iBMECs may demonstrate a high TEER *in vitro* and express certain non-vascular specific junctional genes, however, they lack many functional phenotypes intrinsic to ECs. By not responding to inflammatory stimuli in an EC specific manner, their use in many models would yield results misrepresenting the *in vivo* BBB (**Figure 3**).

Taken altogether, the data presented by recent studies (Delsing et al., 2018; Lu et al., 2019; Martins Gomes et al., 2019; Vatine et al., 2019; Nishihara et al., 2020) contradict the vascular cellular identity of iBMECs and instead demonstrate that these cells might be of an epithelial lineage. iBMECs have been shown to lack expression of key EC marker genes such as *PECAM1*, *CDH5*, *CLDN5,* and *VWF* while also expressing epithelial cell genes including *EPCAM*, *FREM2,* and *CLDN4*. Expression of genes such as E-Selectin, VCAM-1, P-Selectin were also shown to be completely unaffected by inflammatory stimuli further decreasing the possibility for these cells to be used as a functional model of the BBB *in vitro*. This leads to the possibility that the barrier function observed in iBMECs could in fact more closely resemble an epithelial cell barrier such as the choroid plexus or intestinal epithelial barrier. As these cells lack a canonical vascular EC phenotype, the use of current protocols to generate iBMECs as prototypical human BBB model could results in inaccurate physiological studies and screening for misguided druggable targets or treatments with potential ineffective clinical outcomes. Thus, the application of a rigorous and thorough characterization of stem cell-derived products using the latest available technologies such as single cell multi-omics and metabolomics should be necessary, rather than facultative, for the development of faithful disease models and safe cell-based therapies.

## DATA AVAILABILITY STATEMENT

The original contributions generated for this study are included in the article/supplementary material, further inquiries can be directed to the corresponding authors.

## AUTHOR CONTRIBUTIONS

All authors listed have made a substantial, direct and intellectual contribution to the work, and approved it for publication.

## REFERENCES


Abbott, N. J., Dolman, D. E., Drndarski, S., and Fredriksson, S. M. (2012). An improved in vitro blood-brain barrier model: rat brain endothelial cells co-cultured with astrocytes. *Methods Mol. Biol.* 814, 415–430.

Acharya, P., Beckel, J., Ruiz, W. G., Wang, E., Rojas, R., Birder, L., et al. (2004). Distribution of the tight junction proteins ZO-1, occludin, and claudin-4, -8, and -12 in bladder epithelium. *Am. J. Physiol. Renal. Physiol.* 287, F305–F318. doi: 10.1152/ajprenal.00341.2003

Aird, W. C. (2007a). Phenotypic heterogeneity of the endothelium: I. Structure, function, and mechanisms. *Circ. Res.* 100, 158–173.

Aird, W. C. (2007b). Phenotypic heterogeneity of the endothelium: II. Representative vascular beds. *Circ. Res.* 100, 174–190. doi: 10.1161/01.RES.0000255690.03436.ae

Alvarez, J. I., Dodelet-Devillers, A., Kebir, H., Ifergan, I., Fabre, P. J., Terouz, S., et al. (2011). The Hedgehog pathway promotes blood-brain barrier integrity and CNS immune quiescence. *Science* 334, 1727–1731. doi: 10.1126/science.1206936

Andaloussi Mae, M., He, L., Nordling, S., Vazquez-Liebanas, E., Nahar, K., Jung, B., et al. (2020). Single-cell analysis of blood-brain barrier response to pericyte loss. *Circ. Res.* 128, e46–e62. doi: 10.1161/CIRCRESAHA.120.317473

Anderson, K. D., Pan, L., Yang, X.-m, Hughes, V. C., Walls, J. R., Dominguez, M. G., et al. (2011). Angiogenic sprouting into neural tissue requires Gpr124, an orphan G protein-coupled receptor. *Proc. Natl. Acad. Sci. U.S.A.* 108, 2807–2812. doi: 10.1073/pnas.1019761108

Appelt-Menzel, A., Cubukova, A., Günther, K., Edenhofer, F., Piontek, J., Krause, G., et al. (2017). Establishment of a human blood-brain barrier co-culture model

mimicking the neurovascular unit using induced pluri- and multipotent stem cells. *Stem Cell Rep.* 8, 894–906. doi: 10.1016/j.stemcr.2017.02.021

Armulik, A., Genove, G., Mae, M., Nisancioglu, M. H., Wallgard, E., Niaudet, C., et al. (2010). Pericytes regulate the blood-brain barrier. *Nature* 468, 557–561. doi: 10.1038/nature09522

Bär, T. (1980). The vascular system of the cerebral cortex. *Adv. Anat. Embryol. Cell Biol.* 59, I-VI, 1-62. doi: 10.1007/978-3-642-67432-7

Bell, R. D., Winkler, E. A., Sagare, A. P., Singh, I., LaRue, B., Deane, R., et al. (2010). Pericytes control key neurovascular functions and neuronal phenotype in the adult brain and during brain aging. *Neuron* 68, 409–427. doi: 10.1016/j.neuron.2010.09.043

Ben-Zvi, A., Lacoste, B., Kur, E., Andreone, B. J., Mayshar, Y., Yan, H., et al. (2014). Mfsd2a is critical for the formation and function of the blood-brain barrier. *Nature* 509, 507–511. doi: 10.1038/nature13324

Bernas, M. J., Cardoso, F. L., Daley, S. K., Weinand, M. E., Campos, A. R., Ferreira, A. J., et al. (2010). Establishment of primary cultures of human brain microvascular endothelial cells to provide an in vitro cellular model of the blood-brain barrier. *Nat. Protoc.* 5, 1265–1272. doi: 10.1038/nprot.2010.76

Bohara, M., Kambe, Y., Nagayama, T., Tokimura, H., Arita, K., and Miyata, A. (2014). C-type natriuretic peptide modulates permeability of the blood-brain barrier. *J. Cereb. Blood Flow Metab.* 34, 589–596. doi: 10.1038/jcbfm.2013.234

Boveri, M., Kinsner, A., Berezowski, V., Lenfant, A. M., Draing, C., Cecchelli, R., et al. (2006). Highly purified lipoteichoic acid from gram-positive bacteria induces in vitro blood-brain barrier disruption through glia activation: role of pro-inflammatory cytokines and nitric oxide. *Neuroscience* 137, 1193–1209. doi: 10.1016/j.neuroscience.2005.10.011

Brightman, M. W., and Reese, T. S. (1969). Junctions between intimately apposed cell membranes in the vertebrate brain. *J. Cell Biol.* 40, 648–677.

Burek, M., Salvador, E., and Förster, C. Y. (2012). Generation of an immortalized murine brain microvascular endothelial cell line as an in vitro blood brain barrier model. *J. Vis. Exp.* 66:e4022. doi: 10.3791/4022

Calabria, A. R., Weidenfeller, C., Jones, A. R., de Vries, H. E., and Shusta, E. V. (2006). Puromycin-purified rat brain microvascular endothelial cell cultures exhibit improved barrier properties in response to glucocorticoid induction. *J. Neurochem.* 97, 922–933. doi: 10.1111/j.1471-4159.2006.03793.x

Canfield, S. G., Stebbins, M. J., Morales, B. S., Asai, S. W., Vatine, G. D., Svendsen, C. N., et al. (2017). An isogenic blood-brain barrier model comprising brain endothelial cells, astrocytes and neurons derived from human induced pluripotent stem cells. *J. Neurochem.* 140, 874–888. doi: 10.1111/jnc.13923

Castro Dias, M., Coisne, C., Lazarevic, I., Baden, P., Hata, M., Iwamoto, N., et al. (2019). Claudin-3-deficient C57BL/6J mice display intact brain barriers. *Sci. Rep.* 9:203. doi: 10.1038/s41598-018-36731-3

Cecchelli, R., Berezowski, V., Lundquist, S., Culot, M., Renftel, M., Dehouck, M. P., et al. (2007). Modelling of the blood-brain barrier in drug discovery and development. *Nat. Rev. Drug Discov.* 6, 650–661. doi: 10.1038/nrd2368

Cohen-Kashi Malina, K., Cooper, I., and Teichberg, V. I. (2009). Closing the gap between the in-vivo and in-vitro blood-brain barrier tightness. *Brain Res.* 1284, 12–21. doi: 10.1016/j.brainres.2009.05.072

Coisne, C., Dehouck, L., Faveeuw, C., Delplace, Y., Miller, F., Landry, C., et al. (2005). Mouse syngenic in vitro blood-brain barrier model: a new tool to examine inflammatory events in cerebral endothelium. *Lab. Invest.* 85, 734–746. doi: 10.1038/labinvest.3700281

Cullen, M., Elzarrad, M. K., Seaman, S., Zudaire, E., Stevens, J., Yang, M. Y., et al. (2011). GPR124, an orphan G protein-coupled receptor, is required for CNS-specific vascularization and establishment of the blood–brain barrier. *Proc. Natl. Acad. Sci. U.S.A.* 108:5759. doi: 10.1073/pnas.1017192108

Daley, G. Q. (2015). Stem cells and the evolving notion of cellular identity. *Philos. Trans. R. Soc. Lond. B Biol. Sci.* 370:20140376. doi: 10.1098/rstb.2014.0376

Daneman, R. (2012). The blood–brain barrier in health and disease. *Ann. Neurol.* 72, 648–672. doi: 10.1002/ana.23648

Daneman, R., Agalliu, D., Zhou, L., Kuhnert, F., Kuo, C. J., and Barres, B. A. (2009). Wnt/β-catenin signaling is required for CNS, but not non-CNS, angiogenesis. *Proc. Natl. Acad. Sci. U.S.A.* 106, 641–646. doi: 10.1073/pnas.0805165106

Daneman, R., and Prat, A. (2015). The blood-brain barrier. *Cold Spring Harb. Perspect. Biol.* 7:a020412. doi: 10.1101/cshperspect.a020412

Daneman, R., Zhou, L., Kebede, A. A., and Barres, B. A. (2010). Pericytes are required for blood-brain barrier integrity during embryogenesis. *Nature* 468, 562–566. doi: 10.1038/nature09513

de Vries, H. E., Blom-Roosemalen, M. C., van Oosten, M., de Boer, A. G., van Berkel, T. J., Breimer, D. D., et al. (1996). The influence of cytokines on the integrity of the blood-brain barrier in vitro. *J. Neuroimmunol.* 64, 37–43. doi: 10.1016/0165-5728(95)00148-4

Dehouck, M. P., Méresse, S., Delorme, P., Fruchart, J. C., and Cecchelli, R. (1990). An easier, reproducible, and mass-production method to study the blood-brain barrier in vitro. *J. Neurochem.* 54, 1798–1801. doi: 10.1111/j.1471-4159.1990.tb01236.x

Deli, M. A., Abrahám, C. S., Kataoka, Y., and Niwa, M. (2005). Permeability studies on in vitro blood-brain barrier models: physiology, pathology, and pharmacology. *Cell. Mol. Neurobiol.* 25, 59–127. doi: 10.1007/s10571-004-1377-8

Delsing, L., Donnes, P., Sanchez, J., Clausen, M., Voulgaris, D., Falk, A., et al. (2018). Barrier properties and transcriptome expression in human iPSC-derived models of the blood-brain barrier. *Stem Cells* 36, 1816–1827. doi: 10.1002/stem.2908

DeStefano, J. G., Xu, Z. S., Williams, A. J., Yimam, N., and Searson, P. C. (2017). Effect of shear stress on iPSC-derived human brain microvascular endothelial cells (dhBMECs). *Fluids Barriers CNS* 14:20. doi: 10.1186/s12987-017-0068-z

Engelhardt, B. (2003). Development of the blood-brain barrier. *Cell Tissue Res.* 314, 119–129. doi: 10.1007/s00441-003-0751-z

Faley, S. L., Neal, E. H., Wang, J. X., Bosworth, A. M., Weber, C. M., Balotin, K. M., et al. (2019). iPSC-derived brain endothelium exhibits stable, long-term barrier function in perfused hydrogel scaffolds. *Stem Cell Rep.* 12, 474–487. doi: 10.1016/j.stemcr.2019.01.009

Gaillard, P. J., and de Boer, A. G. (2000). Relationship between permeability status of the blood-brain barrier and in vitro permeability coefficient of a drug. *Eur. J. Pharm. Sci.* 12, 95–102. doi: 10.1016/s0928-0987(00)00152-4

Gaillard, P. J., Voorwinden, L. H., Nielsen, J. L., Ivanov, A., Atsumi, R., Engman, H., et al. (2001). Establishment and functional characterization of an in vitro model of the blood-brain barrier, comprising a co-culture of brain capillary endothelial cells and astrocytes. *Eur. J. Pharm. Sci.* 12, 215–222. doi: 10.1016/s0928-0987(00)00123-8

Garberg, P., Ball, M., Borg, N., Cecchelli, R., Fenart, L., Hurst, R. D., et al. (2005). In vitro models for the blood-brain barrier. *Toxicol. In Vitro* 19, 299–334. doi: 10.1016/j.tiv.2004.06.011

Hariharan, A., Weir, N., Robertson, C., He, L., Betsholtz, C., and Longden, T. A. (2020). The ion channel and GPCR toolkit of brain capillary pericytes. *Front. Cell. Neurosci.* 14:601324. doi: 10.3389/fncel.2020.601324

Hart, T., Komori, H. K., LaMere, S., Podshivalova, K., and Salomon, D. R. (2013). Finding the active genes in deep RNA-seq gene expression studies. *BMC Genomics* 14:778. doi: 10.1186/1471-2164-14-778

Helms, H. C., Abbott, N. J., Burek, M., Cecchelli, R., Couraud, P.-O., Deli, M. A., et al. (2016). In vitro models of the blood-brain barrier: an overview of commonly used brain endothelial cell culture models and guidelines for their use. *J. Cereb. Blood Flow Metab.* 36, 862–890. doi: 10.1177/0271678X16630991

Helms, H. C., Hersom, M., Kuhlmann, L. B., Badolo, L., Nielsen, C. U., and Brodin, B. (2014). An electrically tight in vitro blood-brain barrier model displays net brain-to-blood efflux of substrates for the ABC transporters, P-gp, Bcrp and Mrp-1. *AAPS J.* 16, 1046–1055. doi: 10.1208/s12248-014-9628-1

Helms, H. C., Madelung, R., Waagepetersen, H. S., Nielsen, C. U., and Brodin, B. (2012). In vitro evidence for the brain glutamate efflux hypothesis: brain endothelial cells cocultured with astrocytes display a polarized brain-to-blood transport of glutamate. *Glia* 60, 882–893. doi: 10.1002/glia.22321

Helms, H. C., Waagepetersen, H. S., Nielsen, C. U., and Brodin, B. (2010). Paracellular tightness and claudin-5 expression is increased in the BCEC/astrocyte blood-brain barrier model by increasing media buffer capacity during growth. *AAPS J.* 12, 759–770. doi: 10.1208/s12248-010-9237-6

Hollmann, E. K., Bailey, A. K., Potharazu, A. V., Neely, M. D., Bowman, A. B., and Lippmann, E. S. (2017). Accelerated differentiation of human induced pluripotent stem cells to blood–brain barrier endothelial cells. *Fluids Barriers CNS* 14:9. doi: 10.1186/s12987-017-0059-0

Hoshi, Y., Uchida, Y., Tachikawa, M., Inoue, T., Ohtsuki, S., and Terasaki, T. (2013). Quantitative atlas of blood-brain barrier transporters, receptors, and tight junction proteins in rats and common marmoset. *J. Pharm. Sci.* 102, 3343–3355. doi: 10.1002/jps.23575

Hwang, I., An, B. S., Yang, H., Kang, H. S., Jung, E. M., and Jeung, E. B. (2013). Tissue-specific expression of occludin, zona occludens-1, and junction adhesion

molecule A in the duodenum, ileum, colon, kidney, liver, lung, brain, and skeletal muscle of C57BL mice. *J. Physiol. Pharmacol.* 64, 11–18.

James, D., Nam, H.-s, Seandel, M., Nolan, D., Janovitz, T., Tomishima, M., et al. (2010). Expansion and maintenance of human embryonic stem cell–derived endothelial cells by TGFβ inhibition is Id1 dependent. *Nat. Biotechnol.* 28:161. doi: 10.1038/nbt.1605

Kisucka, J., Chauhan, A. K., Zhao, B.-Q., Patten, I. S., Yesilaltay, A., Krieger, M., et al. (2009). Elevated levels of soluble P-selectin in mice alter blood-brain barrier function, exacerbate stroke, and promote atherosclerosis. *Blood* 113, 6015–6022. doi: 10.1182/blood-2008-10-186650

Kitagawa, K., Matsumoto, M., Mabuchi, T., Yagita, Y., Ohtsuki, T., Hori, M., et al. (1998). Deficiency of intercellular adhesion molecule 1 attenuates microcirculatory disturbance and infarction size in focal cerebral ischemia. *J. Cereb. Blood Flow Metab.* 18, 1336–1345. doi: 10.1097/00004647-199812000-00008

Kominsky, S. L., Tyler, B., Sosnowski, J., Brady, K., Doucet, M., Nell, D., et al. (2007). Clostridium perfringens enterotoxin as a novel-targeted therapeutic for brain metastasis. *Cancer Res.* 67, 7977–7982. doi: 10.1158/0008-5472.CAN-07-1314

Krause, G., Protze, J., and Piontek, J. (2015). Assembly and function of claudins: structure–function relationships based on homology models and crystal structures. *Semin. Cell Dev. Biol.* 42, 3–12. doi: 10.1016/j.semcdb.2015.04.010

Kuhnert, F., Mancuso, M. R., Shamloo, A., Wang, H.-T., Choksi, V., Florek, M., et al. (2010). Essential regulation of CNS angiogenesis by the orphan G protein-coupled receptor GPR124. *Science* 330, 985–989. doi: 10.1126/science.1196554

Lee, C. A. A., Seo, H. S., Armien, A. G., Bates, F. S., Tolar, J., and Azarin, S. M. (2018). Modeling and rescue of defective blood-brain barrier function of induced brain microvascular endothelial cells from childhood cerebral adrenoleukodystrophy patients. *Fluids Barriers CNS* 15:9. doi: 10.1186/s12987-018-0094-5

Liebner, S., Fischmann, A., Rascher, G., Duffner, F., Grote, E. H., Kalbacher, H., et al. (2000). Claudin-1 and claudin-5 expression and tight junction morphology are altered in blood vessels of human glioblastoma multiforme. *Acta Neuropathol.* 100, 323–331. doi: 10.1007/s004010000180

Lim, R. G., Quan, C., Reyes-Ortiz, A. M., Lutz, S. E., Kedaigle, A. J., Gipson, T. A., et al. (2017). Huntington's disease iPSC-derived brain microvascular endothelial cells reveal WNT-mediated angiogenic and blood-brain barrier deficits. *Cell Rep.* 19, 1365–1377. doi: 10.1016/j.celrep.2017.04.021

Linville, R. M., DeStefano, J. G., Nerenberg, R. F., Grifno, G. N., Ye, R., Gallagher, E., et al. (2020). Long-term cryopreservation preserves blood–brain barrier phenotype of iPSC-derived brain microvascular endothelial cells and three-dimensional microvessels. *Mol. Pharm.* 17, 3425–3434. doi: 10.1021/acs.molpharmaceut.0c00484

Lippmann, E. S., Al-Ahmad, A., Azarin, S. M., Palecek, S. P., and Shusta, E. V. (2014). A retinoic acid-enhanced, multicellular human blood-brain barrier model derived from stem cell sources. *Sci. Rep.* 4:4160. doi: 10.1038/srep04160

Lippmann, E. S., Al-Ahmad, A., Palecek, S. P., and Shusta, E. V. (2013). Modeling the blood–brain barrier using stem cell sources. *Fluids Barriers CNS* 10:2. doi: 10.1186/2045-8118-10-2

Lippmann, E. S., Azarin, S. M., Kay, J. E., Nessler, R. A., Wilson, H. K., Al-Ahmad, A., et al. (2012). Derivation of blood-brain barrier endothelial cells from human pluripotent stem cells. *Nat. Biotechnol.* 30:783. doi: 10.1038/nbt.2247

Liu, H., Li, Y., Lu, S., Wu, Y., and Sahi, J. (2014). Temporal expression of transporters and receptors in a rat primary co-culture blood-brain barrier model. *Xenobiotica* 44, 941–951. doi: 10.3109/00498254.2014.919430

Lizama, C. O., and Zovein, A. C. (2013). Polarizing pathways: balancing endothelial polarity, permeability, and lumen formation. *Exp. Cell Res.* 319, 1247–1254. doi: 10.1016/j.yexcr.2013.03.028

Lu, T. M., Houghton, S., Magdeldin, T., Durán, J. G. B., Minotti, A. P., Snead, A., et al. (2021). Pluripotent stem cell-derived epithelium misidentified as brain microvascular endothelium requires ETS factors to acquire vascular fate. *Proc. Natl. Acad. Sci. U.S.A.* 118:e2016950118. doi: 10.1073/pnas.2016950118

Lu, T. M., Redmond, D., Magdeldin, T., Nguyen, D.-H. T., Snead, A., Sproul, A., et al. (2019). Human induced pluripotent stem cell-derived neuroectodermal epithelial cells mistaken for blood-brain barrier-forming endothelial cells. *bioRxiv* [Preprint]. doi: 10.1101/699173 bioRxiv: 699173,

Ma, X. J., Cheng, J. W., Zhang, J., Liu, A. J., Liu, W., Guo, W., et al. (2012). E-selectin deficiency attenuates brain ischemia in mice. *CNS Neurosci. Ther.* 18, 903–908. doi: 10.1111/cns.12000

Martins Gomes, S. F., Westermann, A. J., Sauerwein, T., Hertlein, T., Forstner, K. U., Ohlsen, K., et al. (2019). Induced pluripotent stem cell-derived brain endothelial cells as a cellular model to study *Neisseria meningitidis* infection. *Front. Microbiol.* 10:1181. doi: 10.3389/fmicb.2019.01181

Nakagawa, S., Deli, M. A., Kawaguchi, H., Shimizudani, T., Shimono, T., Kittel, A., et al. (2009). A new blood-brain barrier model using primary rat brain endothelial cells, pericytes and astrocytes. *Neurochem. Int.* 54, 253–263. doi: 10.1016/j.neuint.2008.12.002

Nakagawa, S., Deli, M. A., Nakao, S., Honda, M., Hayashi, K., Nakaoke, R., et al. (2007). Pericytes from brain microvessels strengthen the barrier integrity in primary cultures of rat brain endothelial cells. *Cell. Mol. Neurobiol.* 27, 687–694. doi: 10.1007/s10571-007-9195-4

Neal, E. H., Marinelli, N. A., Shi, Y., McClatchey, P. M., Balotin, K. M., Gullett, D. R., et al. (2019). A simplified, fully defined differentiation scheme for producing blood-brain barrier endothelial cells from human iPSCs. *Stem Cell Rep.* 12, 1380–1388. doi: 10.1016/j.stemcr.2019.05.008

Nishihara, H., Gastfriend, B. D., Soldati, S., Perriot, S., Mathias, A., Sano, Y., et al. (2020). Advancing human induced pluripotent stem cell-derived blood-brain barrier models for studying immune cell interactions. *FASEB J.* 34, 16693–16715. doi: 10.1096/fj.202001507RR

Obermeier, B., Daneman, R., and Ransohoff, R. M. (2013). Development, maintenance and disruption of the blood-brain barrier. *Nat. Med.* 19, 1584–1596. doi: 10.1038/nm.3407

Patabendige, A., Skinner, R. A., Morgan, L., and Abbott, N. J. (2013). A detailed method for preparation of a functional and flexible blood-brain barrier model using porcine brain endothelial cells. *Brain Res.* 1521, 16–30. doi: 10.1016/j.brainres.2013.04.006

Perrière, N., Demeuse, P., Garcia, E., Regina, A., Debray, M., Andreux, J. P., et al. (2005). Puromycin-based purification of rat brain capillary endothelial cell cultures. Effect on the expression of blood-brain barrier-specific properties. *J. Neurochem.* 93, 279–289. doi: 10.1111/j.1471-4159.2004.03020.x

Pfeiffer, F., Schafer, J., Lyck, R., Makrides, V., Brunner, S., Schaeren-Wiemers, N., et al. (2011). Claudin-1 induced sealing of blood-brain barrier tight junctions ameliorates chronic experimental autoimmune encephalomyelitis. *Acta Neuropathol.* 122, 601–614. doi: 10.1007/s00401-011-0883-2

Piontek, J., Winkler, L., Wolburg, H., Muller, S. L., Zuleger, N., Piehl, C., et al. (2008). Formation of tight junction: determinants of homophilic interaction between classic claudins. *FASEB J.* 22, 146–158. doi: 10.1096/fj.07-8319com

Potente, M., Gerhardt, H., and Carmeliet, P. (2011). Basic and therapeutic aspects of angiogenesis. *Cell* 146, 873–887. doi: 10.1016/j.cell.2011.08.039

Puech, C., Hodin, S., Forest, V., He, Z., Mismetti, P., Delavenne, X., et al. (2018). Assessment of HBEC-5i endothelial cell line cultivated in astrocyte conditioned medium as a human blood-brain barrier model for ABC drug transport studies. *Int. J. Pharm.* 551, 281–289. doi: 10.1016/j.ijpharm.2018.09.040

Qian, T., Maguire, S. E., Canfield, S. G., Bao, X., Olson, W. R., Shusta, E. V., et al. (2017). Directed differentiation of human pluripotent stem cells to blood-brain barrier endothelial cells. *Sci. Adv.* 3:e1701679. doi: 10.1126/sciadv.1701679

Rahman, N. A., Rasil, A. N. H. M., Meyding-Lamade, U., Craemer, E. M., Diah, S., Tuah, A. A., et al. (2016). Immortalized endothelial cell lines for in vitro blood–brain barrier models: a systematic review. *Brain Res.* 1642, 532–545. doi: 10.1016/j.brainres.2016.04.024

Reese, T. S., and Karnovsky, M. J. (1967). Fine structural localization of a blood-brain barrier to exogenous peroxidase. *J. Cell Biol.* 34, 207–217. doi: 10.1083/jcb.34.1.207

Risau, W., and Wolburg, H. (1990). Development of the blood-brain barrier. *Trends Neurosci.* 13, 174–178. doi: 10.1016/0166-2236(90)90043-A

Roudnicky, F., Kim, B. K., Lan, Y., Schmucki, R., Küppers, V., Christensen, K., et al. (2020a). Identification of a combination of transcription factors that synergistically increases endothelial cell barrier resistance. *Sci. Rep.* 10:3886. doi: 10.1038/s41598-020-60688-x

Roudnicky, F., Zhang, J. D., Kim, B. K., Pandya, N. J., Lan, Y., Sach-Peltason, L., et al. (2020b). Inducers of the endothelial cell barrier identified through -edited hPSC-endothelial cells. *Proc. Natl. Acad. Sci. U.S.A.* 117:19854. doi: 10.1073/pnas.1911532117

Roux, F., and Couraud, P. O. (2005). Rat brain endothelial cell lines for the study of blood-brain barrier permeability and transport functions. *Cell. Mol. Neurobiol.* 25, 41–58. doi: 10.1007/s10571-004-1376-9

Roux, F., Durieu-Trautmann, O., Chaverot, N., Claire, M., Mailly, P., Bourre, J. M., et al. (1994). Regulation of gamma-glutamyl transpeptidase and alkaline phosphatase activities in immortalized rat brain microvessel endothelial cells. *J. Cell. Physiol.* 159, 101–113. doi: 10.1002/jcp.1041590114

Rubin, L. L., Hall, D. E., Porter, S., Barbu, K., Cannon, C., Horner, H. C., et al. (1991). A cell culture model of the blood-brain barrier. *J. Cell Biol.* 115, 1725–1735. doi: 10.1083/jcb.115.6.1725

Sances, S., Ho, R., Vatine, G., West, D., Laperle, A., Meyer, A., et al. (2018). Human iPSC-Derived endothelial cells and microengineered organ-chip enhance neuronal development. *Stem Cell Rep.* 10, 1222–1236. doi: 10.1016/j.stemcr.2018.02.012

Saunders, N. R., Daneman, R., Dziegielewska, K. M., and Liddelow, S. A. (2013). Transporters of the blood-brain and blood-CSF interfaces in development and in the adult. *Mol. Aspects Med.* 34, 742–752. doi: 10.1016/j.mam.2012.11.006

Schaddelee, M. P., Voorwinden, H. L., van Tilburg, E. W., Pateman, T. J., Ijzerman, A. P., Danhof, M., et al. (2003). Functional role of adenosine receptor subtypes in the regulation of blood-brain barrier permeability: possible implications for the design of synthetic adenosine derivatives. *Eur. J. Pharm. Sci.* 19, 13–22. doi: 10.1016/s0928-0987(03)00034-4

Schulze, C., Smales, C., Rubin, L. L., and Staddon, J. M. (1997). Lysophosphatidic acid increases tight junction permeability in cultured brain endothelial cells. *J. Neurochem.* 68, 991–1000. doi: 10.1046/j.1471-4159.1997.68030991.x

Shawahna, R., Uchida, Y., Declèves, X., Ohtsuki, S., Yousif, S., Dauchy, S., et al. (2011). Transcriptomic and quantitative proteomic analysis of transporters and drug metabolizing enzymes in freshly isolated human brain microvessels. *Mol. Pharm.* 8, 1332–1341. doi: 10.1021/mp200129p

Siddharthan, V., Kim, Y. V., Liu, S., and Kim, K. S. (2007). Human astrocytes/astrocyte-conditioned medium and shear stress enhance the barrier properties of human brain microvascular endothelial cells. *Brain Res.* 1147, 39–50. doi: 10.1016/j.brainres.2007.02.029

Stebbins, M. J., Wilson, H. K., Canfield, S. G., Qian, T., Palecek, S. P., and Shusta, E. V. (2016). Differentiation and characterization of human pluripotent stem cell-derived brain microvascular endothelial cells. *Methods* 101, 93–102. doi: 10.1016/j.ymeth.2015.10.016

Stebbins Matthew, J., Lippmann Ethan, S., Faubion Madeline, G., Daneman, R., Palecek Sean, P., and Shusta Eric, V. (2017). Activation of RARα, RARγ, or RXRα increases barrier tightness in human induced pluripotent stem cell-derived brain endothelial cells. *Biotechnol. J.* 13:1700093. doi: 10.1002/biot.201700093

Steinemann, A., Galm, I., Chip, S., Nitsch, C., and Maly, I. P. (2016). Claudin-1, -2 and -3 are selectively expressed in the epithelia of the choroid plexus of the mouse from early development and into adulthood while Claudin-5 is restricted to endothelial cells. *Front. Neuroanat.* 10:16. doi: 10.3389/fnana.2016.00016

Stenman, J. M., Rajagopal, J., Carroll, T. J., Ishibashi, M., McMahon, J., and McMahon, A. P. (2008). Canonical Wnt signaling regulates organ-specific assembly and differentiation of CNS vasculature. *Science* 322, 1247–1250. doi: 10.1126/science.1164594

Stins, M. F., Badger, J., and Sik Kim, K. (2001). Bacterial invasion and transcytosis in transfected human brain microvascular endothelial cells. *Microb. Pathog.* 30, 19–28. doi: 10.1006/mpat.2000.0406

Tam, S. J., Richmond, D. L., Kaminker, J. S., Modrusan, Z., Martin-McNulty, B., Cao, T. C., et al. (2012). Death receptors DR6 and TROY regulate brain vascular development. *Dev. Cell* 22, 403–417. doi: 10.1016/j.devcel.2011.11.018

Uchida, Y., Ohtsuki, S., Katsukura, Y., Ikeda, C., Suzuki, T., Kamiie, J., et al. (2011). Quantitative targeted absolute proteomics of human blood–brain barrier transporters and receptors. *J. Neurochem.* 117, 333–345. doi: 10.1111/j.1471-4159.2011.07208.x

Urich, E., Lazic, S. E., Molnos, J., Wells, I., and Freskgård, P. O. (2012). Transcriptional profiling of human brain endothelial cells reveals key properties crucial for predictive in vitro blood-brain barrier models. *PLoS One* 7:e38149. doi: 10.1371/journal.pone.0038149

Vanlandewijck, M., He, L., Mae, M. A., Andrae, J., Ando, K., Del Gaudio, F., et al. (2018). A molecular atlas of cell types and zonation in the brain vasculature. *Nature* 554, 475–480. doi: 10.1038/nature25739

Vatine, G. D., Al-Ahmad, A., Barriga, B. K., Svendsen, S., Salim, A., Garcia, L., et al. (2017). Modeling psychomotor retardation using iPSCs from MCT8-deficient patients indicates a prominent role for the blood-brain barrier. *Cell Stem Cell* 20, 831–843.e835. doi: 10.1016/j.stem.2017.04.002

Vatine, G. D., Barrile, R., Workman, M. J., Sances, S., Barriga, B. K., Rahnama, M., et al. (2019). Human iPSC-derived blood-brain barrier chips enable disease modeling and personalized medicine applications. *Cell Stem Cell* 24, 995–1005.e1006. doi: 10.1016/j.stem.2019.05.011

Veszelka, S., Tóth, A., Walter, F. R., Tóth, A. E., Gróf, I., Mészáros, M., et al. (2018). Comparison of a rat primary cell-based blood-brain barrier model with epithelial and brain endothelial cell lines: gene expression and drug transport. *Front. Mol. Neurosci.* 11:166. doi: 10.3389/fnmol.2018.00166

Wagner, E. F., and Risau, W. (1994). Oncogenes in the study of endothelial cell growth and differentiation. *Semin. Cancer Biol.* 5, 137–145.

Warren, M. S., Zerangue, N., Woodford, K., Roberts, L. M., Tate, E. H., Feng, B., et al. (2009). Comparative gene expression profiles of ABC transporters in brain microvessel endothelial cells and brain in five species including human. *Pharmacol. Res.* 59, 404–413. doi: 10.1016/j.phrs.2009.02.007

Watson, P. M., Paterson, J. C., Thom, G., Ginman, U., Lundquist, S., and Webster, C. I. (2013). Modelling the endothelial blood-CNS barriers: a method for the production of robust in vitro models of the rat blood-brain barrier and blood-spinal cord barrier. *BMC Neurosci* 14:59. doi: 10.1186/1471-2202-14-59

Weksler, B., Romero, I. A., and Couraud, P. O. (2013). The hCMEC/D3 cell line as a model of the human blood brain barrier. *Fluids Barriers CNS* 10:16. doi: 10.1186/2045-8118-10-16

Weksler, B. B., Subileau, E. A., Perrière, N., Charneau, P., Holloway, K., Leveque, M., et al. (2005). Blood-brain barrier-specific properties of a human adult brain endothelial cell line. *FASEB J.* 19, 1872–1874. doi: 10.1096/fj.04-3458fje

Westergaard, E., and Brightman, M. W. (1973). Transport of proteins across normal cerebral arterioles. *J. Comp. Neurol.* 152, 17–44. doi: 10.1002/cne.901520103

Wilson, H. K., Canfield, S. G., Hjortness, M. K., Palecek, S. P., and Shusta, E. V. (2015). Exploring the effects of cell seeding density on the differentiation of human pluripotent stem cells to brain microvascular endothelial cells. *Fluids Barriers CNS* 12:13. doi: 10.1186/s12987-015-0007-9

Wolburg, H., Neuhaus, J., Kniesel, U., Krauss, B., Schmid, E. M., Ocalan, M., et al. (1994). Modulation of tight junction structure in blood-brain barrier endothelial cells. Effects of tissue culture, second messengers and cocultured astrocytes. *J. Cell Sci.* 107(Pt 5), 1347–1357.

Wolburg, H., Wolburg-Buchholz, K., Kraus, J., Rascher-Eggstein, G., Liebner, S., Hamm, S., et al. (2003). Localization of claudin-3 in tight junctions of the blood-brain barrier is selectively lost during experimental autoimmune encephalomyelitis and human glioblastoma multiforme. *Acta Neuropathol.* 105, 586–592. doi: 10.1007/s00401-003-0688-z

Yusof, S. R., Avdeef, A., and Abbott, N. J. (2014). In vitro porcine blood-brain barrier model for permeability studies: pCEL-X software pKa(FLUX) method for aqueous boundary layer correction and detailed data analysis. *Eur. J. Pharm. Sci.* 65, 98–111. doi: 10.1016/j.ejps.2014.09.009

Zhang, Y., Li, C. S., Ye, Y., Johnson, K., Poe, J., Johnson, S., et al. (2006). Porcine brain microvessel endothelial cells as an in vitro model to predict in vivo blood-brain barrier permeability. *Drug Metab. Dispos.* 34, 1935–1943. doi: 10.1124/dmd.105.006437

Zhang Rui, L., Chopp, M., Jiang, N., Tang Wen, X., Prostak, J., Manning Anthony, M., et al. (1995). Anti–intercellular adhesion molecule–1 antibody reduces ischemic cell damage after transient but not permanent middle cerebral artery occlusion in the wistar rat. *Stroke* 26, 1438–1443. doi: 10.1161/01.STR.26.8.1438

Zlokovic, B. V. (2008). The blood-brain barrier in health and chronic neurodegenerative disorders. *Neuron* 57, 178–201. doi: 10.1016/j.neuron.2008.01.003

**Conflict of Interest:** The authors declare that the research was conducted in the absence of any commercial or financial relationships that could be construed as a potential conflict of interest.

frontiers in Physiology

REVIEW
published: 12 April 2021
doi: 10.3389/fphys.2021.640061

# The Oncogene Transcription Factor EB Regulates Vascular Functions

*Gabriella Doronzo[1,2], Elena Astanina[1,2] and Federico Bussolino[1,2]**

*[1] Department of Oncology, University of Torino, Candiolo, Italy, [2] Laboratory of Vascular Oncology, Candiolo Cancer Institute-IRCCS-FPO, Candiolo, Italy*

Transcription factor EB (TFEB) represents an emerging player in vascular biology. It belongs to the bHLH-leucine zipper transcription factor microphthalmia family, which includes microphthalmia-associated transcription factor, transcription factor E3 and transcription factor EC, and is known to be deregulated in cancer. The canonical transcriptional pathway orchestrated by TFEB adapts cells to stress in all kinds of tissues by supporting lysosomal and autophagosome biogenesis. However, emerging findings highlight that TFEB activates other genetic programs involved in cell proliferation, metabolism, inflammation and immunity. Here, we first summarize the general principles and mechanisms by which TFEB activates its transcriptional program. Then, we analyze the current knowledge of TFEB in the vascular system, placing particular emphasis on its regulatory role in angiogenesis and on the involvement of the vascular unit in inflammation and atherosclerosis.

**Keywords: angiogenesis, embryo, cell cycle, autophagy, inflammation**

OPEN ACCESS

***Edited by:***
*Luca Munaron, University of Turin, Italy*

***Reviewed by:***
*Serena Zacchigna, International Centre for Genetic Engineering and Biotechnology, Italy*
*Ilaria Cascone, Université Paris-Est Créteil Val de Marne, France*
*Lena Claesson-Welsh, Uppsala University, Sweden*

***Correspondence:**
*Federico Bussolino*
*Federico.bussolino@unito.it*

***Specialty section:***
*This article was submitted to Vascular Physiology, a section of the journal Frontiers in Physiology*

***Received:*** *10 December 2020*
***Accepted:*** *17 March 2021*
***Published:*** *12 April 2021*

***Citation:***
*Doronzo G, Astanina E and Bussolino F (2021) The Oncogene Transcription Factor EB Regulates Vascular Functions. Front. Physiol. 12:640061. doi: 10.3389/fphys.2021.640061*

## INTRODUCTION

The vascular unit is characterized by endothelial cells (ECs) lying on a basal membrane, where pericytes are embedded. Located at the interface between the bloodstream and tissues, the vascular unit orchestrates bidirectional information by integrating humoral, mechanical and cellular cues during the embryonic organogenesis process and in adults; this unit also plays a role in communicable and non-communicable diseases (Peng et al., 2019). Consequently, the vascular unit and, in particular, ECs undergo different genetic programs (Mantovani et al., 1997) regulated by specific transcription factors that adjust the transcriptional landscape to properly respond to different pathophysiological stimuli (De Val and Black, 2009; Park et al., 2013; Vanlandewijck et al., 2018).

Emerging evidence underlines autophagy as a key cellular mechanism involved in vessel development and physiological and pathological angiogenesis (Schaaf et al., 2019). Moreover, autophagy occurs on the basis of dynamic EC responses to changing environments, angiogenic cues, or intrinsic and extrinsic insults or injuries (such as metabolic stress, redox homeostasis and hypoxia). Activation of endothelial autophagy, as in other cell types, is mediated by different signaling pathways that are capable of regulating the autophagy-related gene complex, which controls various stages of the process as well as autophagosome formation and elongation, vesicle trafficking, and autophagosome lysosome fusion (Choi et al., 2013).

Transcription factor EB (TFEB) belongs to the microphthalmia (MiT) gene family of bHLH-leucine zipper transcription factors, which includes microphthalmia-associated transcription factor (MITF), TFE3 and TFEC. It was originally described to be translocated in a subset of renal

carcinomas (Argani et al., 2005) and deregulated in melanomas and several carcinomas (Astanina et al., 2020). The current findings clearly support the existence of a canonical pathway by which TFEB acts as a master regulator of lysosomal and autophagosome biogenesis and represents a molecular tool to adapt cells to stress, including starvation and energy depletion (Sardiello et al., 2009; Napolitano and Ballabio, 2016; Saftig and Puertollano, 2020). TFEB directly promotes the transcription of some genes directly involved in autophagy (*ATG9, UVRAG, VPS11, VPS18, and WIPI)* and regulates autophagic flux (Settembre et al., 2011). Furthermore, it controls the expression of genes that orchestrate the expression, localization, entrance, influx, and performance of lysosomal and non-lysosomal enzymes participating in the destruction of cellular macromolecules (Sardiello et al., 2009; Palmieri et al., 2011; Settembre et al., 2011). In addition, TFEB can promote lysosomal exocytosis, allowing cargo secretion through fusion to the cell membrane (Medina et al., 2015).

In addition to the canonical pathway, new results definitively demonstrate wider regulatory activities encompassing metabolism, immunity, angiogenesis and inflammation, which are not necessarily associated with autophagy [see the following reviews: (Napolitano and Ballabio, 2016; Astanina et al., 2020; Irazoqui, 2020; Yu et al., 2020)] and refer to non-canonical pathways.

This review summarizes our current understanding of the functions of TFEB in regulating EC activities in embryos and adults (**Figure 1**).

## STRUCTURE OF TFEB

Transcription factor EB is a transcription factor with low tissue and cellular specificity that is widely expressed in fetuses and adults (Napolitano and Ballabio, 2016). The DNA-binding region is characterized by a helix-loop-helix (HLH) and a leucine zipper domain (Zip) flanked by an upstream basic region that is able to recognize an E-box sequence (CAYGTG) in the promoter regions of targeted genes (Carr and Sharp, 1990; Fisher et al., 1991; Palmieri et al., 2011; Doronzo et al., 2019). The Zip domain is essential for homodimerization or heterooligomerization with other MiT genes. The TFEB structure is also characterized by a glutamine- and proline-rich domain, which has poorly described functions that are discussed in **Box 1**.

## MECHANISMS INVOLVED IN TFEB ACTIVATION

Transcription factor EB is localized in the cytosol in an inactive state induced mainly by the phosphorylation of specific amino acid residues and translocates to the nucleus to start specific transcriptional programs when dephosphorylated (**Figure 2**).

The expression of TFEB is transcriptionally regulated by several factors, including androgen receptor (Shang et al., 2020), peroxisome proliferator-activated receptor-γ coactivator 1α (PPARGC1α), retinoid X receptor-α (RXRα), the peroxisome proliferator-activated receptor-α (PPARα) complex (Salma et al., 2017; Byun et al., 2020), cAMP response element-binding protein (CREB), the CREB-regulated transcription coactivator 2 complex (Seok et al., 2014), ETS2 (Ma et al., 2016), Krüppel-like factor 2 (KLF2) (Song et al., 2019), MYC (Annunziata et al., 2019), XBP1 (Zhang Z. et al., 2020) and TFEB itself (Settembre et al., 2011).

Interestingly, some of these transcription factors (PPARGC1α, CREB, and MYC) are involved in the metabolic regulation and reprogramming observed in stressed conditions and cancer (Stine et al., 2015; Dubois et al., 2017; Berdeaux and Hutchins, 2019).

A wide number of transcription factors promoting TFEB activation indicate that it might participate in many biological functions, but the external cues regulating TFEB transcription and activation are poorly investigated. However, the available findings strongly indicate that TFEB regulates energy homeostasis under the direct or indirect control of the two metabolic sensors mTOR and AMP-activated protein kinase (AMPK) both in physiological and pathologic settings.

The most defined system, which restricts TFEB to the cytosol, thus blocking its nuclear translocation, is represented by mTORC1 (Roczniak-Ferguson et al., 2012; Settembre et al., 2012; Palmieri et al., 2017; Vega-Rubin-de-Celis et al., 2017) and Rag GTPases, which localize both mTORC1 and TFEB itself on the cytosolic surface of lysosomes and degrade TFEB (Settembre et al., 2012; Martina and Puertollano, 2013; Petit et al., 2013; Di Malta et al., 2017). Therefore, when cells are fed, activated mTORC1 regulates anabolic pathways and phosphorylates TFEB, impeding its nuclear translocation.

Activated protein kinase exerts a mirrored function. In the absence of nutrient availability, AMPK promotes the dephosphorylation of TFEB and its translocation to the nucleus (Collodet et al., 2019; El-Houjeiri et al., 2019). At present, this dephosphorylation mechanism is unknown.

In addition to phosphorylation, other posttranslational modifications, including dephosphorylation (Settembre et al., 2011, 2012; Roczniak-Ferguson et al., 2012; Ferron et al., 2013; Medina et al., 2015; Li et al., 2016; Palmieri et al., 2017; Vega-Rubin-de-Celis et al., 2017; Hsu et al., 2018; Martina and Puertollano, 2018; Zhang et al., 2018), acetylation/deacetylation (Miller et al., 2005; Bao et al., 2016; Wang et al., 2020) and sumoylation (Napolitano et al., 2020), regulate nuclear-cytosolic shuttling and nuclear activity (**Box 2**).

## A PARADIGMATIC EXAMPLE OF THE MULTIFACETED ROLE OF TFEB IN PATHOLOGY: CANCER

The regulatory role of mTOR and AMPK on TFEB is part of the complex metabolic scenario occurring in cancer. TFEB is deactivated by mTORC1 under the condition of nutrient availability *via* its cytoplasmic retention but also controls mTORC1 lysosomal recruitment, which is required for its activation, creating a mechanism for transducing the information of the cell energy environment into the switch between anabolic and catabolic pathways (Perera et al., 2015;

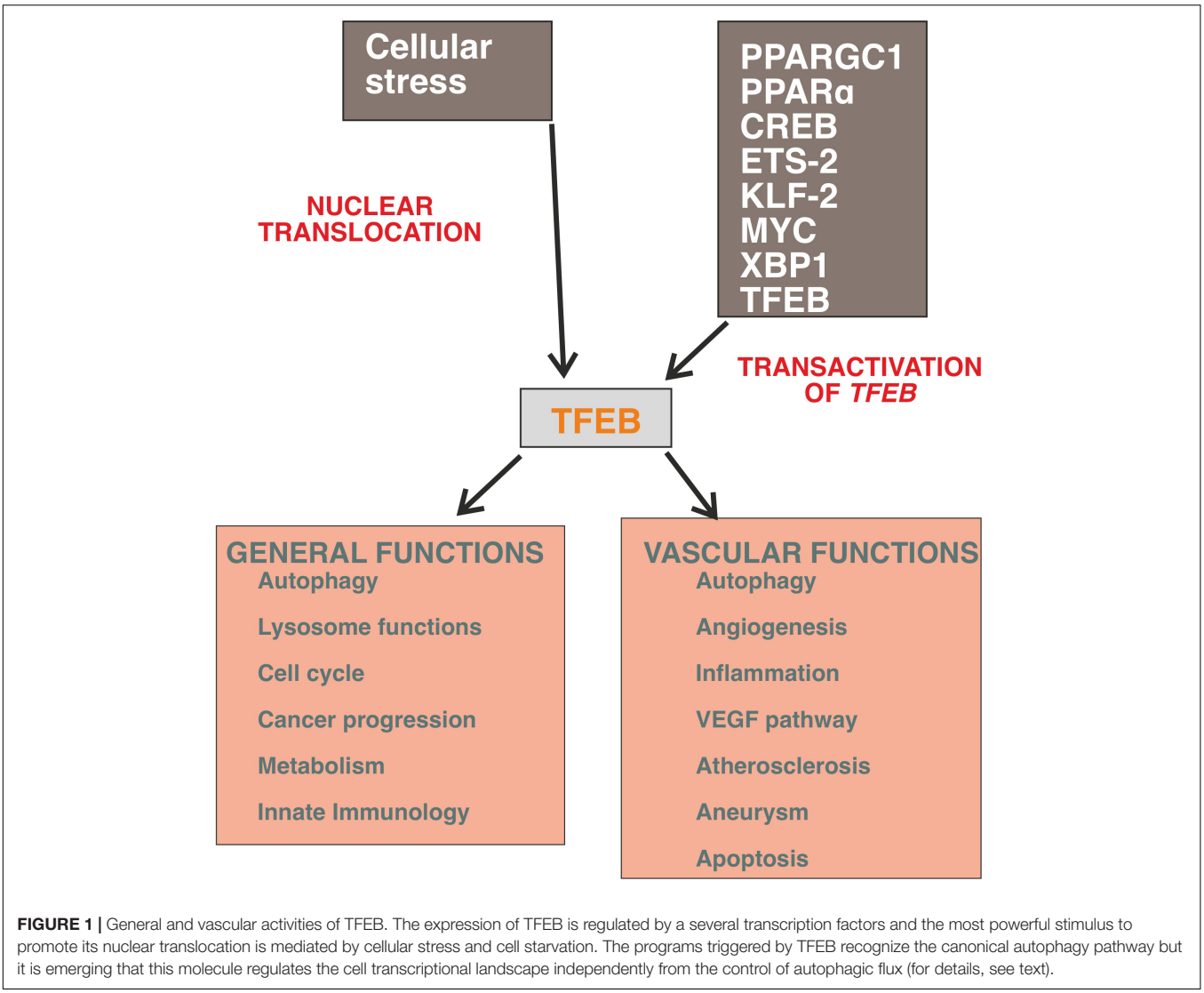


**FIGURE 1 |** General and vascular activities of TFEB. The expression of TFEB is regulated by a several transcription factors and the most powerful stimulus to promote its nuclear translocation is mediated by cellular stress and cell starvation. The programs triggered by TFEB recognize the canonical autophagy pathway but it is emerging that this molecule regulates the cell transcriptional landscape independently from the control of autophagic flux (for details, see text).

Di Malta et al., 2017; Li et al., 2019). Upregulation of TFEB in several cancers, such as pancreatic adenocarcinoma, melanoma, renal cell carcinoma colorectal cancer and non-small cell lung cancer (Davis et al., 2010; Liang et al., 2010; Giatromanolaki et al., 2015; Li et al., 2019), promotes cancer progression *via* mTORC1 hyperactivation signaling to promote cell proliferation and boost autophagy, producing an intracellular pool of nutrients, most importantly amino acids, and thus supporting cancer growth. Moreover, in pancreatic cancer, TFEB-induced autophagic activation leads to cancer progression *via* increased migration and metastasis of cancer cells due to endocytosis of Itgα5 and disassembly of adhesion machinery (He et al., 2018). The autophagy-independent function of TFEB was demonstrated in breast cancer, where TFEB inhibited apoptosis by regulating DNA repair mechanisms (Slade et al., 2020). More evidence supports a role for TFEB in the tumor microenvironment. In tumor-associated macrophages, TFEB acts as a major switch of both canonical and non-canonical pathways, leading to attenuation of the tumor-supporting phenotype. TFEB inhibits STAT3 activation, thus suppressing the production of an array of tumor-associated macrophage effector molecules and blocking the transcription of PPARγ, inhibiting the downstream expression of proinflammatory cytokines and HIF1α. Moreover, TFEB-induced increases in autophagic and lysosomal activity disactivate inflammasomes and degrade the HIF1α protein, thereby halting the hypoxic response associated with cancer progression (Li et al., 2020).

## TFEB REGULATES VASCULAR FUNCTIONS

### TFEB and Angiogenesis in Embryos and Adults

Mouse mutants have suggested that Tfeb functions as a modulator of endothelial activities related to angiogenesis in both

**BOX 1 |** Structure of TFEB (**Figure 2**).

TFEB has been highly conserved throughout evolution and is present in flies, fishes, avians, and mammals (Steingrímsson et al., 1998; Hallsson et al., 2004; Lister et al., 2011; Lapierre et al., 2013), exhibiting similar genomic organization and structural features. Human TFEB is constituted by 476 amino acids and has a mass of ~53 kDa. *TFEB* spans approximately 51,000 bp and is located on chromosome 6, whereas mouse Tfeb (475 amino acids) is on chromosome 17 and extends over 55,000 bp. Genomic organization analysis of the human gene unveiled the presence of nine exons, each of which is spliced to the common coding exons 2–9 (Kuiper et al., 2004). This organization generates a 2,364 bp mRNA transcript consisting of two non-coding exons and eight coding exons, with a 302-bp 5′ UTR followed by a start codon in exon 3 and a stop codon in exon 10, followed by a 621 bp 3′ UTR. Seven alternative mRNAs with the same translational start site at exon 2 have been described with differential and restricted tissue distributions (Kuiper et al., 2004; Vu et al., 2021). The mouse TFEB protein is 94% identical to its human ortholog, sharing domain structure organization and posttranslational modification sites (Steingrímsson et al., 2004).

As the other member of the MiT gene family, the bHLH (position 235–288) and Zip (position 298–319) domains establish the DNA binding region. The activation domain (AD) is mapped at position 156–165 and predicts a binding site for the transcriptional coactivator p300 (Muhle-Goll et al., 1994). In the absence of DNA, a tetramer-sized form of TFEB is formed that dissociates to bind added DNA as a dimer (Fisher et al., 1991; Muhle-Goll et al., 1994). The TFEB structure also contains a N-terminus glutamine-rich region (position 10–44) encompassing the binding site of Rag C and a C-terminal proline-rich region (position 366–414) with undetermined functions. Of note, this domain is also present in TFE3, where it has activating functions (Artandi et al., 1995). The abilities of TFEB to promote autophagy and lysosome biogenesis are mediated by a palindromic consensus sequence (GTCACGTGAC) overlapping the E-Box sequence, named the coordinated lysosomal expression and regulation motif (CLEAR) (Sardiello et al., 2009; Palmieri et al., 2011; Settembre et al., 2011).

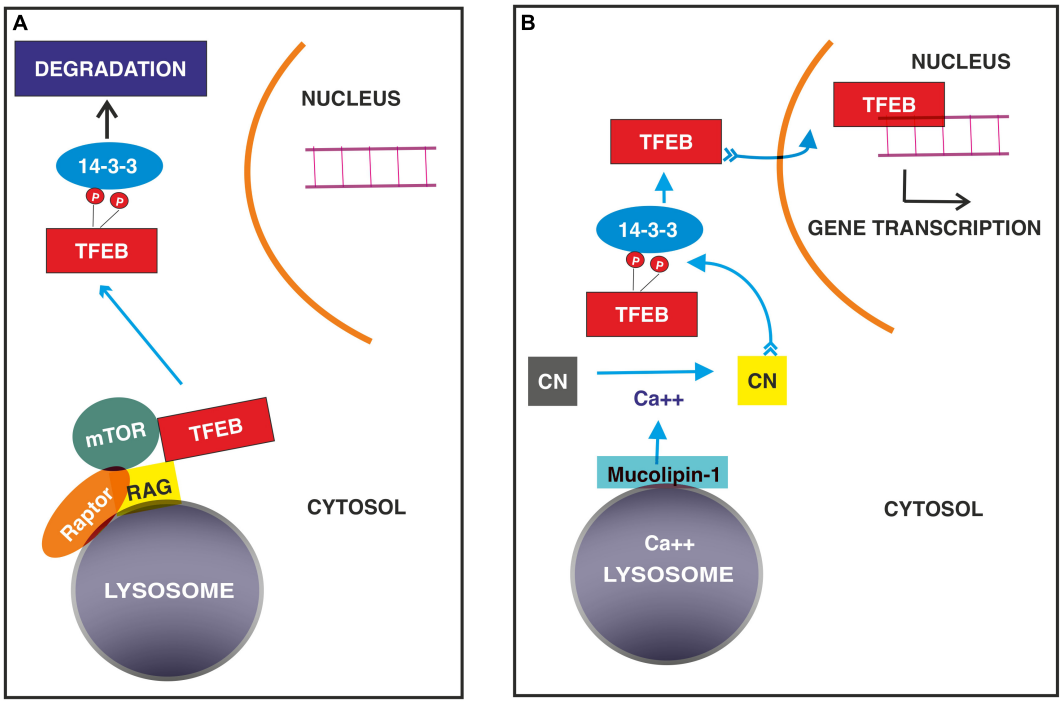


**FIGURE 2 |** Signaling mechanisms regulating TFEB nuclear translocation in normal **(A)** and stressed conditions **(B)**. **(A)** TFEB binds GTP- RagGTPase on the surface of lysosome followed by the recruitment of Raptor and mTOR. This complex allows the phosphorylation of TFEB, which interacts with 14-3-3 adaptor with subsequent degradation. **(B)** In stressed conditions, calcium ions released from lysosomes through mucolipin 1 channel activates the protein phosphatase calcineurin, (CN) which dephosphorylates TFEB, allowing its nuclear translocation.

embryos (Steingrímsson et al., 1998; Doronzo et al., 2019) and adult animals (Fan et al., 2018; Doronzo et al., 2019).

In wild-type mice, Tfeb is expressed at low levels in E8.5- to 10.5-day-old embryos, while it is highly expressed in labyrinthine trophoblasts from 8.5-day-old placentas. In *Tfeb* null mice, vascular invasion of the labyrinthine trophoblast layer by the embryo is blocked, and capillaries stop in the chorion. In contrast, maternal sinuses invade the placenta, although they are fewer and smaller than normal. Other defects of extraembryonic tissue are not evident. Interestingly, these placental vascular defects precede embryonic lethality, suggesting that the observed lethality is caused by placental defects, which are then instrumental in inducing hypoxia and cell necrosis (Steingrímsson et al., 1998). Mechanistically, *Tfeb* null mice express lower trophoblast levels of vascular endothelial growth factor (VEGF) A than wild-type mice, supporting that Tfeb directly or indirectly controls the expression of this angiogenic inducer (Steingrímsson et al., 1998).

The specific endothelial deletion of *Tfeb* is lethal at E10.5, with vascular alterations explained by defects in the remodeling of the primitive vascular plexus. Vessels appear irregular and dilated with reduced branching and impairment of invasion into intersomitic tissue. Furthermore, the yolk sac appears poorly vascularized and exhibits a hypoxic area (Doronzo et al., 2019).

**BOX 2 |** Posttranslational modifications regulate TFEB transcriptional activity (**Table 1**).

**TFEB phosphorylation**

TFEB phosphorylation is required for the control of both nuclear entry and export. The phosphorylation of Ser 122, 142, and 211 (Settembre et al., 2011, 2012; Martina et al., 2012; Roczniak-Ferguson et al., 2012; Vega-Rubin-de-Celis et al., 2017) is required for TFEB degradation, while Ser 462, 463, 466, 467 and 469 likely favor its activation, as inferred from the observation that the substitution of these residues with phosphomimetic aspartate forces TFEB nuclear translocation (Peña-Llopis et al., 2011). Many phosphorylation events occur at the lysosomal surface and are mediated by mTORC1. (Roczniak-Ferguson et al., 2012; Settembre et al., 2012; Palmieri et al., 2017; Vega-Rubin-de-Celis et al., 2017). The first 30 amino acid residues of TFEB bind Rag GTPase in the GTP active binding configuration (Martina and Puertollano, 2013) and allow its localization on the cytosolic membrane of lysosomes (Settembre et al., 2012; Martina and Puertollano, 2013; Petit et al., 2013; Di Malta et al., 2017). This interaction is crucial for the recruitment of mTOR and Raptor (regulatory associated protein of mTOR) and promote mTOR-dependent TFEB phosphorylation.

Once Ser 211 is phosphorylated, TFEB is released from the lysosomal surface and bound by the 14-3-3 scaffold protein, rendering it inactive in the cytosol (Settembre et al., 2011, 2012; Roczniak-Ferguson et al., 2012; Vega-Rubin-de-Celis et al., 2017). Phosphorylation of Ser 142 and 211 induce the degradation of TFEB through the ubiquitin-proteasome pathway (Sha et al., 2017), while Ser 122 enhances the effect of phosphorylated Ser 211 (Vega-Rubin-de-Celis et al., 2017).

In low nutrient conditions, the Rag GTPase in the GTP-active configuration is inactivated by two GTPase-activating proteins named GATOR 1 and Folliculin, resulting in the release of mTOR in the cytosol (Saxton and Sabatini, 2017).

In addition to mTOR, extracellular signal-regulated kinase (ERK) 2, mitogen-activated protein kinase kinase kinase 3 (MAP3K3), glycogen synthase kinase (GSK)3β, protein kinase Cβ (Ferron et al., 2013) and AKT (Palmieri et al., 2017) recognize TFEB as a substrate and differentially regulate its fate. ERK2 (Settembre et al., 2011, 2012), GSK 3β (Li et al., 2016) and AKT (Palmieri et al., 2017) contribute to TFEB retention in the cytosol, protein kinase Cβ stabilizes TFEB and cooperates with mTOR (Ferron et al., 2013), and MAP3K3 antagonizes TFEB phosphorylation by mTORC1(Hsu et al., 2018).

A particular mechanism is played by phosphatase calcineurin, which is activated by calcium released from lysosomes in stressed conditions and dephosphorylates TFEB at Ser 211 and 142, thus inducing its nuclear translocation (Medina et al., 2015). Similarly, protein phosphatase 2A activated by oxidative stress dephosphorylates TFEB at the Ser 109, 114, 122 and 211 residues (Martina and Puertollano, 2018.

Phosphorylation is also involved in regulating the export of TFEB from the nucleus to the cytosol when its transcriptional activity needs to be interrupted. A hydrophobic nuclear export sequence has been mapped at residues 129–152 and encompasses Ser 142 and 138. Interestingly, the phosphorylation of Ser 142 by mTOR or ERK2 primes the nuclear export sequence for phosphorylation by GSK β at Ser 138, achieving an efficient nuclear export through exportin-1 (Li et al., 2018; Napolitano et al., 2018). Finally, TFEB activates the transcription of cyclin−dependent kinase (CDK) 4 (Doronzo et al., 2019), which may phosphorylate TFEB at Ser 142, thus allowing its nuclear export (Yin et al., 2020) and damping TFEB-mediated cell cycle activation (Brady et al., 2018; Doronzo et al., 2019).

**TFEB acetylation and deacetylation**

TFEB contains some Lys residues, which are substrates of acetylating and deacetylating enzymes, and acetylation appears to inhibit TFEB dimerization and its capability to bind the promoter regions of target genes (Wang et al., 2020). In microglia, the deacetylating enzyme sirtuin-1 binds and deacetylates TFEB at the Lys116 residue, thus increasing its transcriptional function (Bao et al., 2016). In contrast, in cancer cell lines, inhibitors of histone deacetylases indirectly favor acetylation of Lys 91, 103, 116, and 430 at the nuclear level (Zhang et al., 2018) and increase TFEB transcriptional activity. Finally, it has been reported that histone deacetylase can bind the *TFEB* promoter to inhibit its expression (Annunziata et al., 2019). The data available are partially conflicting and might suggest that the effects of these posttranslational modifications depend on the cellular context.

When *Tfeb* is deleted in all tissues (Steingrímsson et al., 1998), homozygous null mice die between E9.5 and E11.5 and exhibit characteristics of general and diffuse cell damage, particularly at somites, neural tubes, ganglia and mesenchyme.

Alterations in the VEGF pathway were further highlighted in conditional and endothelium-specific Tfeb knockout mice. In this model, endothelial *Tfeb* deletion after birth results in impairment of the maturation of retinal and renal vasculature because the EC cycle is blocked by the reduced expression of cyclin−dependent kinase (CDK) 4, which is under the direct transcriptional control of TFEB (Doronzo et al., 2019). As a consequence, the phosphorylation of the retinoblastoma protein is reduced, blocking the nuclear translocation of E2F to transcribe genes necessary for the S−phase of the cell cycle (Doronzo et al., 2019). Of note, the ability of TFEB to regulate the cell cycle independent of the autophagy pathway is not restricted to ECs, as it is observed in other cell types (Brady et al., 2018; Pastore et al., 2020; Pisonero-Vaquero et al., 2020). In an attempt to restore the cell cycle, ECs lacking TFEB overexpress VEGF receptor (R)2, but this process is ineffective in restoring cell proliferation. This cell response is not mediated by a direct effect of TFEB on VEGFR2 transcription because its promoter does not exhibit any specific binding site. In contrast, TFEB transactivates the intragenic miR-15a/16-1 cluster, which limits the stability of the VEGFR2 transcript (Chamorro-Jorganes et al., 2011; Chan et al., 2013). In the absence of this posttranscriptional regulatory mechanism, *VEGFR2* mRNA is stabilized, thus promoting receptor accumulation (Doronzo et al., 2019). However, the signaling properties of VEGFR2 rely on not only the catalytic activity of the kinase domain but also its trafficking, which is instrumental for its performance (Simons et al., 2016). TFEB represses *MYO1C*, an unconventional myosin protein, which promotes VEGFR2 delivery to the plasma membrane (Tiwari et al., 2013). The regulated activity of VEGFR2 in ECs requires its internalization, trafficking to endosomes, and either transport to lysosomes for degradation or recycling back to the plasma membrane (Simons et al., 2016). In TFEB knockdown cells, the reduced and increased amounts of miR-15a/16-1 and MYO1C, respectively, result in the overexpression of VEGFR2 on the plasma membrane, which shows low signaling activity (Doronzo et al., 2019) that is most likely dependent on defects in receptor trafficking. **Figure 3** summarizes the multiple effects induced by TFEB deletion in ECs.

In ECs, autophagic flux is controlled at the transcriptional level by NF-kB (Zeng et al., 2016; Leonard et al., 2019) and FOXO (Liu et al., 2015). It has also been recently reported that TFEB controls autophagy in ECs. This activity has been associated with the angiogenic response in ischemic skeletal muscle. Capillary ECs overexpressing TFEB respond to limb ischemia by promoting angiogenesis and improving tissue blood perfusion. In contrast, this proangiogenic activity is blunted in ECs devoid of TFEB. The angiogenic response is mediated by an increase

**TABLE 1 |** Posttranslational modifications of TFEB *.

| Aminoacid Residue | Enzyme | Effect |
|---|---|---|
| Ser 3 | Phosphorylation by MAP3K3 | Inhibit Ser 211 phosphorylation mediated by mTORC1 |
| Ser 122 | Phosphorylation by mTOR | Cytosolic retention |
| Ser 134 | Phosphorylation by GSK3 | Cytosolic retention |
| Ser 138 | Phosphorylation by GSK3 | Cytosolic retention and export from nucleus |
| Ser 142 | Phosphorylation by mTOR, Erk 1/2 | Cytosolic retention |
| Ser 142 | Nuclear phosphorylation by CDK4 or CDK6 | Nuclear export |
| Ser 211 | Phosphorylation by mTOR | Cytosolic retention and 14-3-3 binding site |
| Ser 462 | Phosphorylation by PKC | Stabilization of TFEB |
| Ser 463 | Phosphorylation by PKC | Stabilization of TFEB |
| Ser 467 | Phosphorylation by PKC | Stabilization of TFEB |
| Ser 467 | Phosphorylation by AKT | Cytosolic retention |
| Ser 469 | Phosphorylation by PKC | Stabilization of TFEB |
| Lys 116 | Deacetylation by Sirtuin-1 | Increase of transcriptional activity |
| Lys 116 | Acetylation by GCN5 | Suppression of transcriptional activity |
| Lys 274 | Acetylation by GCN5 | Suppression of transcriptional activity |
| Lys 279 | Acetylation by GCN5 | Suppression of transcriptional activity |

**CDK4 and CDK6 also phosphorylate Ser 114 and Thr 331 but without any specific effect (Yin et al., 2020).*

in autophagic genes and activation of AMP-activated protein kinase signaling, as inferred by pharmacological inhibition or genetic silencing (Fan et al., 2018). The role of autophagy in angiogenesis represents a mechanism by which ECs can accommodate the metabolic changes required to support their migration and proliferation (Schaaf et al., 2019). Furthermore, autophagy represents a mechanism by which angiostatic signals are transferred from the extracellular matrix. For instance, the secreted proteoglycan decorin exerts antiangiogenic activity by activating autophagy in ECs (Torres et al., 2017), and this effect is mediated by TFEB. In this context, the nuclear translocation of TFEB relies on the catalytic activity of VEGFR2, as inferred by the use of tyrosine kinase inhibitors, which halt decorin-mediated TFEB activation (Neill et al., 2017).

## TFEB Controls an Inflammatory Program in ECs

Recently, some studies have highlighted the anti-inflammatory role of TFEB in ECs (Lu et al., 2017; Song et al., 2019). Laminar shear stress, known to protect against atherosclerosis but not oscillatory shear stress, induces TFEB activation. ECs exposed to laminar flow express more TFEB than those exposed to static conditions by a mechanism mediated by Krüppel-like factor 2, which is a shear stress-responsive factor. TFEB overexpression results in a reduction in the synthesis of inflammatory cytokines and adhesive molecules and in the adhesiveness of circulating monocytes in response to an inflammatory stimulus. This phenotype is reverted by TFEB knockdown. These effects are independent of autophagic flux but rely on the suppressive activity of the NF-kB pathway. TFEB inhibits IκB kinase activity, leading to reduced p65 nuclear translocation (Song et al., 2019). Furthermore, the overexpression of TFEB in human ECs isolated from cord veins transactivates the antioxidant enzymes heme oxygenase-1 and superoxide dismutase 2 (Lu et al., 2017). In parallel, the overexpression of TFEB reduces the production of radical oxygen species, whereas TFEB knockdown has the opposite effect (Lu et al., 2017). A similar event was reported in cardiac endothelial cells subjected to ischemia/reperfusion both *in vitro* and *in vivo* (Zhang Y.J. et al., 2020). However, in this model, $NAD^+$-dependent TFEB expression recovers the autophagic flux damaged by ischemic injury and prevents apoptosis. The antiapoptotic effect of TFEB was further investigated in vascular smooth muscle cell (VSMC)-selective *Tfeb* knockout mice and in human and mouse aortic aneurysm samples. TFEB binds the promoter of BCL2 in VSMCs, enhances its transcription and halts apoptosis. However, in this experimental setting, the antiapoptotic effect of TFEB was independent of autophagic flux because knockdown of the autophagic gene *ATG7* did not abolish its antiapoptotic effect (Lu et al., 2020).

## TFEB and the Atherosclerotic Process

Autophagy in both vascular ECs and VSMCs is a protective and prosurvival mechanism aimed at combating many pathophysiological stimuli, including oxidized low-density lipoproteins, reactive oxygen species, inflammatory stimuli, shear stress and hypoxia (De Meyer et al., 2015; Jiang, 2016). However, autophagy can exert a dangerous effect when the pathological stimulus burden is dominant (De Meyer et al., 2015; Jiang, 2016).

A paradigmatic example of this bimodal function in vascular pathology is atherosclerosis (Martinet and De Meyer, 2009; De Meyer et al., 2015). Autophagy is involved in promoting reverse cholesterol transport from macrophages infiltrating the vessel wall and protecting plaque cells from middle injuries, thereby favoring plaque stability (Ouimet et al., 2011). However, when oxidative stress and turbulent blood flow worsen, the autophagic response is insufficient to remove altered macromolecules and organelles (e.g., mitochondria). Damage to mitochondria and lysosome membranes results in the release of cytochrome c, mtDNA (Tumurkhuu et al., 2016) and acidic hydrolases (Wen and Weak, 2007) and in the subsequent activation of apoptosis, impairment of autophagosome formation and accumulation of insoluble ceroids constituted by proteins precipitated with oxidized lipids (Wen and Weak, 2007). The compromised autophagic flux in ECs and infiltrating macrophages results in the reduction of antithrombotic function of the vessel wall and in plaque instability.

In the atherosclerotic process, TFEB activation likely aims to revert the impairment of autophagic flux, as described in lysosomal storage diseases (Parenti et al., 2015). The potential role of TFEB in eliminating insoluble ceroids was demonstrated both *in vitro* and *in vivo*. Specifically,

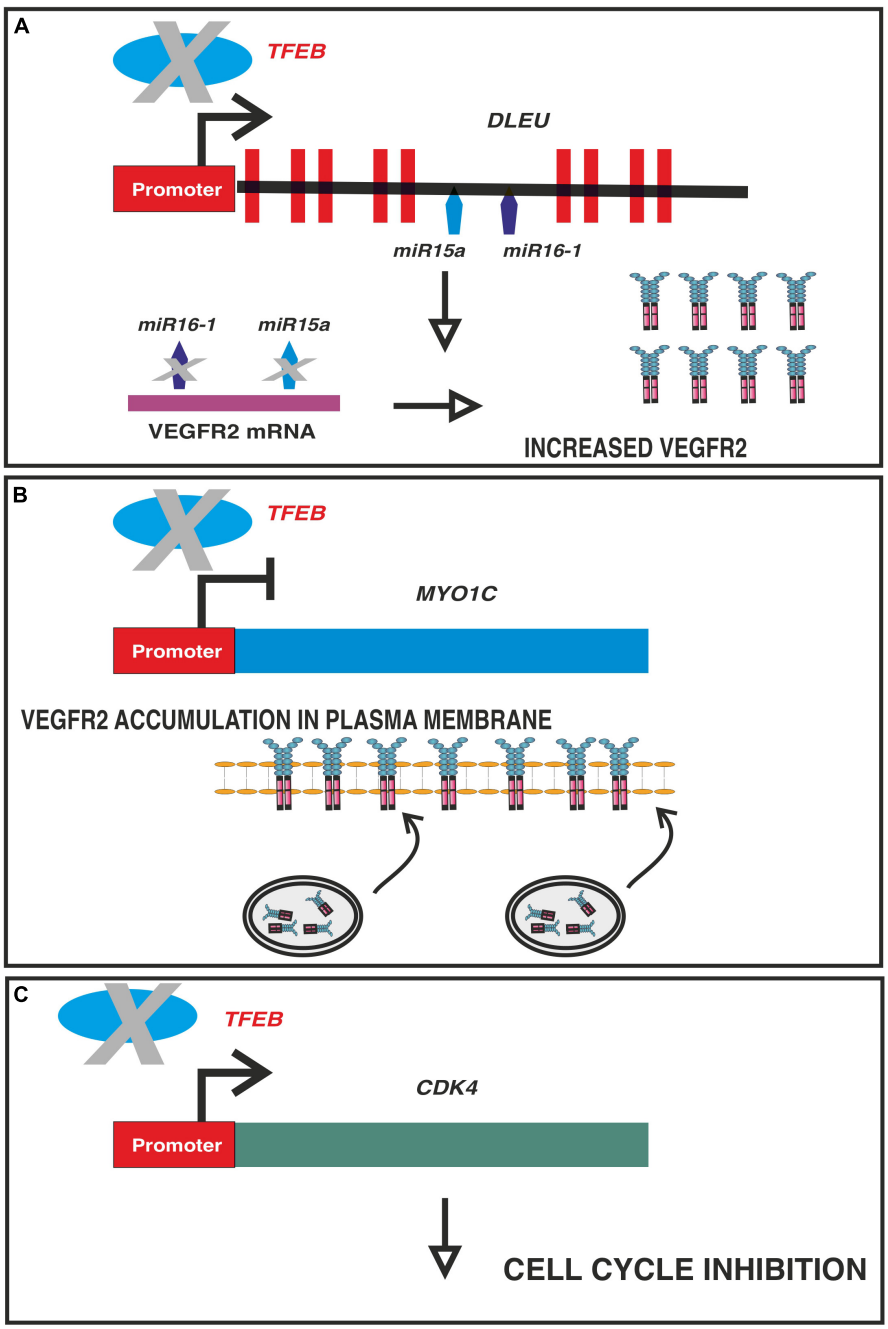


**FIGURE 3 |** Multiple effects of TFEB deletion on ECs. In vascular ECs, TFEB directly binds and regulate the promoters of: **(A)** *DLEU2*, which encodes miR-15a/16-1 cluster **(A,B)** *MYO1C* and **(C)** *CDK4*. Panel **(A)**: in absence of TFEB the post-transcriptional regulation of VEGFR2 mediated by miR-15a-5p and miR-16-5p is impaired leading to an increased stabilization of the transcript. Panel **(B)**: TFEB is a repressor of *MYO1C*, an unconventional myosin involved in VEGFR2 exocytosis. In absence of TFEB, the expression of this gene is increased and more VEGFR2 is available and transported to plasma membrane through Rab4 $^{+}$ exocytic vesicles. As a consequence the receptor recycling is impaired with a reduced efficiency of signaling machinery. Panel **(C)**: TFEB transactivates *CDK4* and the consequence of its deletion is the cell cycle in G1 phase.

induction of lysosomal biogenesis by overexpression of TFEB in macrophages rescues ceroid-induced lysosome dysfunction, defers inflammasome activation, enhances cholesterol efflux, and reduces the *in vivo* progression of atherosclerotic disease in proatherogenic ApoE-null mice (Emanuel et al., 2014; Sergin et al., 2017). Interestingly, sorting nexin 10, a protein involved in regulating endosome trafficking, accumulates in atherosclerotic plaques and inhibits TFEB nuclear translocation by promoting AKT-dependent phosphorylation. Deletion of this protein in atherosclerotic

macrophages suppresses the AKT pathway and increases the nuclear translocation of TFEB (You et al., 2020).

The inhibitory effect of TFEB on the atherosclerotic process was confirmed by findings obtained in VSMCs. In this cell type, oxidized lipoproteins inhibit the transcription of TFEB, which is counteracted by overexpression of stearoyl−coenzyme A desaturase−1, an integral protein anchored in the endoplasmic reticulum membrane. Overexpression of this enzyme inhibits the differentiation of VSMCs in foam cells and increases TFEB nuclear translocation (Pi et al., 2019). In mice maintained on a high-fat diet and subjected to partial carotid ligation, VSMCs undergo neointima formation, which is a hallmark of atherosclerotic plaques. The proliferation of VSMCs is dependent on the inhibition of TFEB-mediated autophagic flux and blocked by TFEB reactivation (Wang et al., 2019).

## CONCLUSION AND PERSPECTIVES

Current knowledge regarding the TFEB regulation of the vascular system is in its infancy, but the emerging results regarding its molecular and biological activities in other cellular types envisage its potential effects on many physiopathological conditions involving the vasculature, from cancer to inflammatory, metabolic and neurodegenerative diseases. However, to truly understand the budding role of TFEB in vascular medicine, several issues must be faced and solved. First, it is necessary to increase our knowledge of TFEB in vascular processes characterized by the activation of autophagy, such as pulmonary arterial hypertension, Fabry disease, pathological angiogenesis, atherosclerosis, chronic and acute ischemic disorders, and aneurysms. Because autophagy is associated with the endoplasmic reticulum stress response, which has an emerging role in vascular homeostasis (Battson et al., 2017), it might be relevant to understand how this stress response is regulated by TFEB in the vasculature. Interestingly, TFEB has been reported to transactivate the unfolded protein response and activate transcription factor 4 in retinal cells (Martina et al., 2016), which are key players in this pathway.

Second, TFEB is likely a hub of an undefined transcription factor network, which dynamically shapes the transcriptional landscape in a cellular context-dependent manner. To date, these transcriptional circuits have been poorly investigated (Astanina et al., 2020) and raise the question of whether other genetic programs are orchestrated or modulated by TFEB in addition to the well-established canonical autophagy process. Furthermore, elucidating the correlation between the level of TFEB activation in the vasculature and the type of transcriptional response is important to understand the extent to which TFEB will be a druggable target. A paradigmatic example is provided by hypoxia-inducible factor, which determines the features of gene expression according to the harshness of hypoxia (Pouysségur et al., 2006). Third, new findings on the effects of TFEB on key mechanisms of vascular homeostasis, such as endothelial metabolism, endothelial-mesenchymal transition, the cell cycle and cell motility, might open new translational opportunities.

## AUTHOR CONTRIBUTIONS

EA wrote the sections on the general aspect of TFEB biology. FB inspired the review and supervised the final version. GD wrote the sections related to the vascular functions of TFEB. All authors contributed to the article and approved the submitted version.

## FUNDING

This work was supported by AIRC—Associazione Italiana Per la Ricerca sul Cancro (grant 22910), Regione Piemonte (grant A1907A, Deflect), Fondazione CRT, Ministero dell'Universita' e della Ricerca (PRIN 2017, grant 2017237P5X), FPRC 5xmille 2016 MIUR (Biofilm) and ERA-Net Transcan-2 (grant TRS-2018–00000689) to FB.

## REFERENCES

Annunziata, I., van de Vlekkert, D., Wolf, E., Finkelstein, D., Neale, G., Machado, E., et al. (2019). MYC competes with MiT/TFE in regulating lysosomal biogenesis and autophagy through an epigenetic rheostat. *Nat. Commun.* 10:3623. doi: 10.1038/s41467-019-11568-0

Argani, P., Laé, M., Hutchinson, B., Reuter, V. E., Collins, M. H., Perentesis, J., et al. (2005). Renal carcinomas with the t(6;11)(p21;q12): clinicopathologic features and demonstration of the specific alpha-TFEB gene fusion by immunohistochemistry, RT-PCR, and DNA PCR. *Am. J. Surg. Pathol.* 29, 230–240.

Artandi, S. E., Merrell, K., Avitahl, N., Wong, K. K., and Calame, K. (1995). TFE3 contains two activation domains, one acidic and the other proline-rich, that synergistically activate transcription. *Nucleic Acids Res.* 23, 3865–3871. doi: 10.1093/nar/23.19.3865

Astanina, E., Bussolino, F., and Doronzo, G. (2020). Multifaceted activities of transcription factor eb in cancer onset and progression. *Mol. Oncol.* 15, 327–346. doi: 10.1002/1878-0261.12867

Bao, J., Zheng, L., Zhang, Q., Li, X., Zhang, X., Li, Z., et al. (2016). Deacetylation of TFEB promotes fibrillar Aβ degradation by upregulating lysosomal biogenesis in microglia. *Protein Cell* 7, 417–433. doi: 10.1007/s13238-016-0269-2

Battson, M. L., Lee, D. M., and Gentile, C. L. (2017). Endoplasmic reticulum stress and the development of endothelial dysfunction. *Am. J. Physiol. Heart Circ. Physiol.* 312, H355–H367. doi: 10.1152/ajpheart.00437.2016

Berdeaux, R., and Hutchins, C. (2019). Anabolic and pro-metabolic functions of CREB-CRTC in skeletal muscle: advantages and obstacles for type 2 diabetes and cancer cachexia. *Front. Endocrinol.* 10:535. doi: 10.3389/fendo.2019.00535

Brady, O. A., Jeong, E., Martina, J. A., Pirooznia, M., Tunc, I., and Puertollano, R. (2018). The transcription factors TFE3 and TFEB amplify p53 dependent transcriptional programs in response to DNA damage. *Elife* 7:e40856. doi: 10.7554/eLife.40856

Byun, S., Seok, S., Kim, Y. C., Zhang, Y., Yau, P., Iwamori, N., et al. (2020). Fasting-induced FGF21 signaling activates hepatic autophagy and lipid degradation via JMJD3 histone demethylase. *Nat. Commun.* 11:807. doi: 10.1038/s41467-020-14384-z

Carr, C. S., and Sharp, P. A. (1990). A helix-loop-helix protein related to the immunoglobulin E box-binding proteins. *Mol. Cell. Biol.* 10, 4384–4388. doi: 10.1128/mcb.10.8.4384

Chamorro-Jorganes, A., Araldi, E., Penalva, L. O., Sandhu, D., Fernández-Hernando, C., and Suárez, Y. (2011). MicroRNA-16 and microRNA-424 regulate cell-autonomous angiogenic functions in endothelial cells via targeting vascular endothelial growth factor receptor-2 and fibroblast growth factor

receptor-1. *Arterioscler. Thromb. Vasc. Biol.* 31, 2595–2606. doi: 10.1161/ATVBAHA.111.236521

Chan, L. S., Yue, P. Y., Wong, Y. Y., and Wong, R. N. (2013). MicroRNA-15b contributes to ginsenoside-Rg1-induced angiogenesis through increased expression of VEGFR-2. *Biochem. Pharmacol.* 86, 392–400. doi: 10.1016/j.bcp.2013.05.006

Choi, A. M., Ryter, S. W., and Levine, B. (2013). Autophagy in human health and disease. *N. Engl. J. Med.* 368, 1845–1846. doi: 10.1056/NEJMc1303158

Collodet, C., Foretz, M., Deak, M., Bultot, L., Metairon, S., Viollet, B., et al. (2019). AMPK promotes induction of the tumor suppressor FLCN through activation of TFEB independently of mTOR. *FASEB J.* 33, 12374–12391. doi: 10.1096/fj.201900841R

Davis, I. J., Hsi, B. L., Arroyo, J. D., Vargas, S. O., Yeh, Y. A., Motyckova, G., et al. (2010). Cloning of an Alpha-TFEB fusion in renal tumors harboring the t(6;11)(p21;q13) chromosome translocation. *Proc. Natl. Acad. Sci. U.S.A.* 100, 6051–6056. doi: 10.1073/pnas.0931430100

De Meyer, G. R., Grootaert, M. O., Michiels, C. F., Kurdi, A., Schrijvers, D. M., and Martinet, W. (2015). Autophagy in vascular disease. *Circ. Res.* 116, 468–479. doi: 10.1161/CIRCRESAHA.116.303804

De Val, S., and Black, B. L. (2009). Transcriptional control of endothelial cell development. *Dev. Cell* 16, 180–195. doi: 10.1016/j.devcel.2009.01.014

Di Malta, C., Siciliano, D., Calcagni, A., Monfregola, J., Punzi, S., Pastore, N., et al. (2017). Transcriptional activation of RagD GTPase controls mTORC1 and promotes cancer growth. *Science* 356, 1188–1192. doi: 10.1126/science.aag2553

Doronzo, G., Astanina, E., Corà, D., Chiabotto, G., Comunanza, V., Noghero, A., et al. (2019). TFEB controls vascular development by regulating the proliferation of endothelial cells. *EMBO J.* 38:e98250. doi: 10.15252/embj.201798250

Dubois, V., Eeckhoute, J., Lefebvre, P., and Staels, B. (2017). Distinct but complementary contributions of PPAR isotypes to energy homeostasis. *J. Clin. Invest.* 127, 1202–1214. doi: 10.1172/JCI88894

El-Houjeiri, L., Possik, E., Vijayaraghavan, T., Paquette, M., Martina, J. A., Kazan, J. M., et al. (2019). The transcription factors TFEB and TFE3 Link the FLCN-AMPK signaling axis to innate immune response and pathogen resistance. *Cell Rep.* 26, 3613–3628.e6. doi: 10.1016/j.celrep.2019.02.102

Emanuel, R., Sergin, I., Bhattacharya, S., Turner, J., Epelman, S., Settembre, C., et al. (2014). Induction of lysosomal biogenesis in atherosclerotic macrophages can rescue lipid-induced lysosomal dysfunction and downstream sequelae. *Arterioscler. Thromb. Vasc. Biol.* 34, 1942–1952. doi: 10.1161/ATVBAHA.114.303342

Fan, Y., Lu, H., Liang, W., Garcia-Barrio, M. T., Guo, Y., Zhang, J., et al. (2018). Endothelial TFEB (Transcription Factor EB) positively regulates postischemic angiogenesis. *Circ. Res.* 122, 945–957. doi: 10.1161/CIRCRESAHA.118.312672

Ferron, M., Settembre, C., Shimazu, J., Lacombe, J., Kato, S., Rawlings, D. J., et al. (2013). A RANKL-PKCβ-TFEB signaling cascade is necessary for lysosomal biogenesis in osteoclasts. *Genes Dev.* 27, 955–969. doi: 10.1101/gad.213827.113

Fisher, D. E., Carr, C. S., Parent, L. A., and Sharp, P. A. (1991). TFEB has DNA-binding and oligomerization properties of a unique helix-loop-helix/leucine-zipper family. *Genes Dev.* 5, 2342–2352. doi: 10.1101/gad.5.12a.2342

Giatromanolaki, A., Kalamida, D., Sivridis, E., Karagounis, I. V., Gatter, K. C., Harris, A. L., et al. (2015). Increased expression of transcription factor EB (TFEB) is associated with autophagy, migratory phenotype and poor prognosis in non-small cell lung cancer. *Lung Cancer* 90, 98–105. doi: 10.1016/j.lungcan.2015.07.008

Hallsson, J. H., Haflidadóttir, B. S., Stivers, C., Odenwald, W., Arnheiter, H., Pignoni, F., et al. (2004). The basic helix-loop-helix leucine zipper transcription factor Mitf is conserved in *Drosophila* and functions in eye development. *Genetics* 167, 233–241. doi: 10.1534/genetics.167.1.233

He, R., Wang, M., Zhao, C., Shen, M., Yu, Y., He, L., et al. (2018). TFEB-driven autophagy potentiates TGF-β induced migration in pancreatic cancer cells. *J. Exp. Clin. Cancer Res.* 38:340. doi: 10.1186/s13046-019-1343-4

Hsu, C. L., Lee, E. X., Gordon, K. L., Paz, E. A., Shen, W. C., Ohnishi, K., et al. (2018). MAP4K3 mediates amino acid-dependent regulation of autophagy via phosphorylation of TFEB. *Nat. Commun.* 9:942. doi: 10.1038/s41467-018-03340-7

Irazoqui, J. E. (2020). Key roles of MiT transcription factors in innate immunity and inflammation. *Trends Immunol.* 41, 157–171. doi: 10.1016/j.it.2019.12.003

Jiang, F. (2016). Autophagy in vascular endothelial cells. *Clin. Exp. Pharmacol. Physiol.* 43, 1021–1028. doi: 10.1111/1440-1681.12649

Kuiper, R. P., Schepens, M., Thijssen, J., Schoenmakers, E. F., and van Kessel, A. G. (2004). Regulation of the MiTF/TFE bHLH-LZ transcription factors through restricted spatial expression and alternative splicing of functional domains. *Nucleic Acids Res.* 32, 2315–2322. doi: 10.1093/nar/gkh571

Lapierre, L. R., De Magalhaes Filho, C. D., McQuary, P. R., Chu, C. C., Visvikis, O., Chang, J. T., et al. (2013). The TFEB orthologue HLH-30 regulates autophagy and modulates longevity in *Caenorhabditis elegans*. *Nat. Commun.* 4:2267. doi: 10.1038/ncomms3267

Leonard, A., Millar, M. W., Slavin, S. A., Bijli, K. M., Dionisio Santos, D. A., Dean, D. A., et al. (2019). Critical role of autophagy regulator Beclin1 in endothelial cell inflammation and barrier disruption. *Cell. Signal.* 61, 120–129. doi: 10.1016/j.cellsig.2019.04.013

Li, L., Friedrichsen, H. J., Andrews, S., Picaud, S., Volpon, L., Ngeow, K., et al. (2018). A TFEB nuclear export signal integrates amino acid supply and glucose availability. *Nat. Commun.* 9:2685. doi: 10.1038/s41467-018-04849-7

Li, S., Song, Y., Quach, C., Guo, H., Jang, G. B., Maazi, H., et al. (2019). Transcriptional regulation of autophagy-lysosomal function in BRAF-driven melanoma progression and chemoresistance. *Nat. Commun.* 10:1693. doi: 10.1038/s41467-019-09634-8

Li, Y., Hodge, J., Liu, Q., Wang, J., Wang, Y., Evans, T. D., et al. (2020). TFEB is a master regulator of tumor-associated macrophages in breast cancer. *J. Immunother. Cancer* 8:e000543. doi: 10.1136/jitc-2020-000543

Li, Y., Xu, M., Ding, X., Yan, C., Song, Z., Chen, L., et al. (2016). Protein kinase C controls lysosome biogenesis independently of mTORC1. *Nat. Cell Biol.* 18, 1065–1077. doi: 10.1038/ncb3407

Liang, J., Jia, X., Wang, K., and Zhao, N. (2010). High expression of TFEB is associated with aggressive clinical features in colorectal cancer. *Onco Targets Ther.* 11, 8089–8098. doi: 10.2147/OTT.S180112

Lister, J. A., Lane, B. M., Nguyen, A., and Lunney, K. (2011). Embryonic expression of zebrafish MiT family genes tfe3b, tfeb, and tfec. *Dev. Dyn.* 240, 2529–2538. doi: 10.1002/dvdy.22743

Liu, J., Bi, X., Chen, T., Zhang, Q., Wang, S. X., Chiu, J. J., et al. (2015). Shear stress regulates endothelial cell autophagy via redox regulation and Sirt1 expression. *Cell Death Dis.* 6:e1827. doi: 10.1038/cddis.2015.193

Lu, H., Fan, Y., Qiao, C., Liang, W., Hu, W., Zhu, T., et al. (2017). TFEB inhibits endothelial cell inflammation and reduces atherosclerosis. *Sci. Signal.* 10:eaah4214. doi: 10.1126/scisignal.aah4214

Lu, H., Sun, J., Liang, W., Chang, Z., Rom, O., Zhao, Y., et al. (2020). Cyclodextrin prevents abdominal aortic aneurysm via activation of vascular smooth muscle cell transcription factor EB. *Circulation* 142, 483–498. doi: 10.1161/CIRCULATIONAHA.119.044803

Ma, S., Fang, Z., Luo, W., Yang, Y., Wang, C., Zhang, Q., et al. (2016). The C-ETS2-TFEB axis promotes neuron survival under oxidative stress by regulating lysosome activity. *Oxid. Med. Cell. Longev.* 2016:4693703. doi: 10.1155/2016/4693703

Mantovani, A., Bussolino, F., and Introna, M. (1997). Cytokine regulation of endothelial cell function: from molecular level to the bedside. *Immunol. Today* 18, 231–240.

Martina, J. A., Chen, Y., Gucek, M., and Puertollano, R. (2012). MTORC1 functions as a transcriptional regulator of autophagy by preventing nuclear transport of TFEB. *Autophagy* 8, 903–914. doi: 10.4161/auto.19653

Martina, J. A., Diab, H. I., Brady, O. A., and Puertollano, R. (2016). TFEB and TFE3 are novel components of the integrated stress response. *EMBO J.* 35, 479–495. doi: 10.15252/embj.201593428

Martina, J. A., and Puertollano, R. (2013). Rag GTPases mediate amino acid-dependent recruitment of TFEB and MITF to lysosomes. *J. Cell Biol.* 200, 475–491. doi: 10.1083/jcb.201209135

Martina, J. A., and Puertollano, R. (2018). Protein phosphatase 2A stimulates activation of TFEB and TFE3 transcription factors in response to oxidative stress. *J. Biol. Chem.* 293, 12525–12534. doi: 10.1074/jbc.RA118.003471

Martinet, W., and De Meyer, G. R. (2009). Autophagy in atherosclerosis: a cell survival and death phenomenon with therapeutic potential. *Circ. Res.* 104, 304–317. doi: 10.1161/CIRCRESAHA.108.188318

Medina, D. L., Paola, S. Di, Peluso, I., Armani, A., De Stefani, D., Venditti, R., et al. (2015). Lysosomal calcium signalling regulates autophagy through calcineurin and TFEB. *Nat. Cell Biol.* 17, 288–299. doi: 10.1038/ncb3114

Miller, A. J., Levy, C. I, Davis, J., Razin, E., and Fisher, D. E. (2005). Sumoylation of MITF and its related family members TFE3 and TFEB. *J. Biol. Chem.* 280, 146–155. doi: 10.1074/jbc.M411757200

Muhle-Goll, C., Gibson, T., Schuck, P., Schubert, D., Nalis, D., Nilges, M., et al. (1994). The dimerization stability of the HLH-LZ transcription protein family is modulated by the leucine zippers: a CD and NMR study of TFEB and c-Myc. *Biochemistry* 33, 11296–11306. doi: 10.1021/bi00203a027

Napolitano, G., and Ballabio, A. (2016). TFEB at a glance. *J. Cell Sci.* 129, 2475–2481. doi: 10.1242/jcs.146365

Napolitano, G., Esposito, A., Choi, H., Matarese, M., Benedetti, V., Di Malta, C., et al. (2018). mTOR-dependent phosphorylation controls TFEB nuclear export. *Nat. Commun.* 9:3312. doi: 10.1038/s41467-018-05862-6

Napolitano, G., Malta, C. Di, Esposito, A., de Arauju, M. E. G., Pece, S., Bertalot, G., et al. (2020). A substrate-specific mTORC1 pathway underlies Birt-Hogg-Dubé syndrome. *Nature* 585, 597–602. doi: 10.1038/s41586-020-2444-0

Neill, T., Sharpe, C., Owens, R. T., and Iozzo, R. V. (2017). Decorin-evoked paternally expressed gene 3 (PEG3) is an upstream regulator of the transcription factor EB (TFEB) in endothelial cell autophagy. *J. Biol. Chem.* 292, 16211–16220. doi: 10.1074/jbc.M116.769950

Ouimet, M., Franklin, V., Mak, E., Liao, X., Tabas, I., and Marcel, Y. (2011). Autophagy regulates cholesterol efflux from macrophage foam cells via lysosomal acid lipase. *Cell Metab.* 13, 655–667.

Palmieri, M., Impey, S., Kang, H., di Ronza, A., Pelz, C., Sardiello, M., et al. (2011). Characterization of the CLEAR network reveals an integrated control of cellular clearance pathways. *Hum. Mol. Genet.* 20, 3852–3866. doi: 10.1093/hmg/ddr306

Palmieri, M., Pal, R., Nelvagal, H. R., Lotfi, P., Stinnett, G. R., Seymour, M. L., et al. (2017). mTORC1-independent TFEB activation via Akt inhibition promotes cellular clearance in neurodegenerative storage diseases. *Nat. Commun.* 8:14338. doi: 10.1038/ncomms14338

Parenti, G., Andria, G., and Ballabio, A. (2015). Lysosomal storage diseases: from pathophysiology to therapy. *Annu. Rev. Med.* 66, 471–486. doi: 10.1146/annurev-med-122313-085916

Park, C., Kim, T. M., and Malik, A. B. (2013). Transcriptional regulation of endothelial cell and vascular development. *Circ. Res.* 112, 1380–1400. doi: 10.1161/CIRCRESAHA.113.301078

Pastore, N., Huynh, T., Herz, N. J., Calcagni', A., Klisch, T. J., Brunetti, L., et al. (2020). TFEB regulates murine liver cell fate during development and regeneration. *Nat. Commun.* 11:2461. doi: 10.1038/s41467-020-16300-x

Peña-Llopis, S., Vega-Rubin-de-Celis, S., Schwartz, J. C., Wolff, N. C., Tran, T. A., Zou, L., et al. (2011). Regulation of TFEB and V-ATPases by mTORC1. *EMBO J.* 30, 3242–3258. doi: 10.1038/emboj.2011.257

Peng, Z., Shu, B., Zhang, Y., and Wang, M. (2019). Endothelial response to pathophysiological stress. *Arterioscler. Thromb. Vasc. Biol.* 39, e233–e243. doi: 10.1161/ATVBAHA.119.312580

Perera, R. M., Stoykova, S., Nicolay, B. N., Ross, K. N., Fitamant, J., Boukhali, M., et al. (2015). Transcriptional control of autophagy-lysosome function drives pancreatic cancer metabolism. *Nature* 524, 361–365. doi: 10.1038/nature14587

Petit, C. S., Roczniak-Ferguson, A., and Ferguson, S. M. (2013). Recruitment of folliculin to lysosomes supports the amino acid-dependent activation of Rag GTPases. *J. Cell Biol.* 202, 1107–1122. doi: 10.1083/jcb.201307084

Pi, H., Wang, Z., Liu, M., Deng, P., Yu, Z., Zhou, Z., et al. (2019). SCD1 activation impedes foam cell formation by inducing lipophagy in oxLDL-treated human vascular smooth muscle cells. *J. Cell. Mol. Med.* 23, 5259–5269. doi: 10.1111/jcmm.14401

Pisonero-Vaquero, S., Soldati, C., Cesana, M., Ballabio, A., and Medina, D. L. (2020). TFEB modulates p21/WAF1/CIP1 during the DNA damage response. *Cells* 9:1186. doi: 10.3390/cells9051186

Pouysségur, J., Dayan, F., and Mazure, N. M. (2006). Hypoxia signalling in cancer and approaches to enforce tumour regression. *Nature* 441, 437–443. doi: 10.1038/nature04871

Roczniak-Ferguson, A., Petit, C. S., Froehlich, F., Qian, S., Ky, J., Angarola, B., et al. (2012). The transcription factor TFEB links mTORC1 signaling to transcriptional control of lysosome homeostasis. *Sci. Signal.* 5:ra42. doi: 10.1126/scisignal.2002790

Saftig, P., and Puertollano, R. (2020). How lysosomes sense, integrate, and cope with stress. *Trends Biochem. Sci.* 46, 97–112. doi: 10.1016/j.tibs.2020.09.004

Salma, N., Song, J. S., Kawakami, A., Devi, S. P., Khaled, M., Cacicedo, J. M., et al. (2017). Tfe3 and Tfeb transcriptionally regulate peroxisome proliferator-activated receptor γ2 expression in adipocytes and mediate adiponectin and glucose levels in mice. *Mol. Cell. Biol.* 37, e608–e616. doi: 10.1128/MCB.00608-16

Sardiello, M., Palmieri, M., di Ronza, A., Medina, D. L., Valenza, M., Gennarino, V. A., et al. (2009). A gene network regulating lysosomal biogenesis and function. *Science* 325, 473–477. doi: 10.1126/science.1174447

Saxton, R. A., and Sabatini, D. M. (2017). mTOR signaling in growth, metabolism, and disease. *Cell* 168, 960–976. doi: 10.1016/j.cell.2017.02.004

Schaaf, M. B., Houbaert, D., Meçe, O., and Agostinis, P. (2019). Autophagy in endothelial cells and tumor angiogenesis. *Cell Death Differ.* 26, 665–779. doi: 10.1038/s41418-019-0287-8

Seok, S., Fu, T., Choi, S. E., Li, Y., Zhu, R., Kumar, S., et al. (2014). Transcriptional regulation of autophagy by an FXR-CREB axis. *Nature* 516, 108–111. doi: 10.1038/nature13949

Sergin, I., Evans, T., Zhang, X., Bhattacharya, S., Stokes, C., Song, E., et al. (2017). Exploiting macrophage autophagy-lysosomal biogenesis as a therapy for atherosclerosis. *Nat. Commun.* 8:15750.

Settembre, C., Di Malta, C., Polito, V. A., Garcia Arencibia, M., Vetrini, F., Erdin, S., et al. (2011). TFEB links autophagy to lysosomal biogenesis. *Science* 332, 1429–1433. doi: 10.1126/science.1204592

Settembre, C., Zoncu, R., Medina, D. L., Vetrini, F., Erdin, S., Huynh, T., et al. (2012). A lysosome-to-nucleus signalling mechanism senses and regulates the lysosome via mTOR and TFEB. *EMBO J.* 31, 1095–1108. doi: 10.1038/emboj.2012.32

Sha, Y., Rao, L., Settembre, C., Ballabio, A., and Eissa, N. T. (2017). STUB1 regulates TFEB-induced autophagy-lysosome pathway. *EMBO J.* 36, 2544–2552. doi: 10.15252/embj.201796699

Shang, D., Wang, L., Klionsky, D. J., Cheng, H., and Zhou, R. (2020). Sex differences in autophagy-mediated diseases: toward precision medicine. *Autophagy* 17, 1–12. doi: 10.1080/15548627.2020.1752511

Simons, M., Gordon, E., and Claesson-Welsh, L. (2016). Mechanisms and regulation of endothelial VEGF receptor signalling. *Nat. Rev. Mol. Cell Biol.* 17, 611–625. doi: 10.1038/nrm.2016.8

Slade, L., Biswas, D., Ihionu, F., El Hiani, Y., Kienesberger, P. C., and Pulinilkunnil, T. (2020). A lysosome independent role for TFEB in activating DNA repair and inhibiting apoptosis in breast cancer cells. *Biochem. J.* 477, 137–160. doi: 10.1042/BCJ20190596

Song, W., Zhang, C. L., Gou, L., He, L., Gong, Y. Y., Qu, D., et al. (2019). Endothelial TFEB (Transcription Factor EB) Restrains IKK (IκB Kinase)-p65 pathway to attenuate vascular inflammation in diabetic db/db mice. *Arterioscler. Thromb. Vasc. Biol.* 39, 719–730. doi: 10.1161/ATVBAHA.119.312316

Steingrímsson, E., Copeland, N. G., and Jenkins, N. A. (2004). Melanocytes and the microphthalmia transcription factor network. *Annu. Rev. Genet.* 38, 365–411. doi: 10.1146/annurev.genet.38.072902.092717

Steingrímsson, E., Tessarollo, L., Reid, S. W., Jenkins, N. A., and Copeland, N. G. (1998). The bHLH-Zip transcription factor Tfeb is essential for placental vascularization. *Development* 125, 4607–4616.

Stine, Z. E., Walton, Z. E., Altman, B. J., Hsieh, A. L., and Dang, C. V. (2015). MYC, metabolism, and cancer. *Cancer Discov.* 5, 1024–1039. doi: 10.1158/2159-8290.CD-15-05

Tiwari, A., Jung, J. J., Inamdar, S. M., Nihalani, D., and Choudhury, A. (2013). The myosin motor Myo1c is required for VEGFR2 delivery to the cell surface and for angiogenic signaling. *Am. J. Physiol. Heart Circ. Physiol.* 304, H687–H696. doi: 10.1152/ajpheart.00744.2012

Torres, A., Gubbiotti, M. A., and Iozzo, R. V. (2017). Decorin-inducible Peg3 evokes beclin 1-mediated autophagy and thrombospondin 1-mediated angiostasis. *J. Biol. Chem.* 292, 5055–5069. doi: 10.1074/jbc.M116.753632

Tumurkhuu, G., Shimada, K., Dagvadorj, J., Crother, T., Zhang, W., Luthringer, D., et al. (2016). Ogg1 -dependent DNA repair regulates NLRP3 inflammasome and prevents atherosclerosis. *Circ. Res.* 119, e76–e90.

Vanlandewijck, M., He, L., Mäe, M. A., Andrae, J., Ando, K., Del Gaudio, F., et al. (2018). A molecular atlas of cell types and zonation in the brain vasculature. *Nature* 554, 475–480. doi: 10.1038/nature25739

Vega-Rubin-de-Celis, S., Peña-Llopis, S., Konda, M., and Brugarolas, J. (2017). Multistep regulation of TFEB by MTORC1. *Autophagy* 13, 464–472. doi: 10.1080/1554

Vu, H. N., Dilshat, R., Fock, V., and Steingrímsson, E. (2021). User guide to MiT-TFE isoforms and post-translational modifications. *Pigment Cell Melanoma Res.* 34, 13–27. doi: 10.1111/pcmr.12922

Wang, Y., Huang, Y., Liu, J., Zhang, J., Xu, M., You, Z., et al. (2020). Acetyltransferase GCN5 regulates autophagy and lysosome biogenesis by targeting TFEB. *EMBO Rep.* 21:e48335. doi: 10.15252/embr.201948335

Wang, Y. T., Li, X., Chen, J., McConnell, B. K., Chen, L., Li, P. L., et al. (2019). Activation of TFEB ameliorates dedifferentiation of arterial smooth muscle cells and neointima formation in mice with high-fat diet. *Cell Death Dis.* 10:676. doi: 10.1038/s41419-019-1931-4

Wen, Y., and Weak, D. (2007). Low density lipoprotein undergoes oxidation within lysosomes in cells. *Circ. Res.* 100, 1337–1343.

Yin, Q., Jian, Y., Xu, M., Huang, X., Wang, N., Liu, Z., et al. (2020). CDK4/6 regulate lysosome biogenesis through TFEB/TFE3. *J. Cell Biol.* 219:e201911036. doi: 10.1083/jcb.201911036

You, Y., Bao, W., Zhang, S., Li, H., Li, H., Dang, W., et al. (2020). Sorting Nexin 10 mediates metabolic reprogramming of macrophages in atherosclerosis through the Lyn-dependent TFEB signaling pathway. *Circ. Res.* 127, 534–549.

Yu, S., Wang, Z., Ding, L., and Yang, L. (2020). The regulation of TFEB in lipid homeostasis of non-alcoholic fatty liver disease: molecular mechanism and promising therapeutic targets. *Life Sci.* 246:117418. doi: 10.1016/j.lfs.2020.117418

Zeng, M., Wei, X., Wu, Z., Li, W., Zheng, Y., Li, B., et al. (2016). Simulated ischemia/reperfusion-induced p65-Beclin 1-dependent autophagic cell death in human umbilical vein endothelial cells. *Sci. Rep*. 6:37448. doi: 10.1038/srep37448

Zhang, J., Wang, J., Zhou, Z., Park, J. E., Wang, L., Wu, S., et al. (2018). Importance of TFEB acetylation in control of its transcriptional activity and lysosomal function in response to histone deacetylase inhibitors. *Autophagy* 14, 1043–1059. doi: 10.1080/15548627.2018.1447290

Zhang, Y. J., Zhang, M., Zhao, X., Shi, K., Ye, M., Tian, J., et al. (2020). NAD+ administration decreases microvascular damage following cardiac ischemia/reperfusion by restoringautophagic fux. *Basic Res. Cardiol.* 115:57. doi: 10.1007/s00395-020-0817-z

Zhang, Z., Qian, Q., Li, M., Shao, F., Ding, W. X., Lira, V. A., et al. (2020). The unfolded protein response regulates hepatic autophagy by sXBP1-mediated activation of TFEB. *Autophagy* 1–15. doi: 10.1080/15548627.2020.1788889

**Conflict of Interest:** The authors declare that the research was conducted in the absence of any commercial or financial relationships that could be construed as a potential conflict of interest.

# Advantages of publishing in Frontiers

**OPEN ACCESS**
Articles are free to read for greatest visibility and readership

**FAST PUBLICATION**
Around 90 days from submission to decision

**HIGH QUALITY PEER-REVIEW**
Rigorous, collaborative, and constructive peer-review

**TRANSPARENT PEER-REVIEW**
Editors and reviewers acknowledged by name on published articles

**Frontiers**
Avenue du Tribunal-Fédéral 34
1005 Lausanne | Switzerland

**Visit us:** www.frontiersin.org
**Contact us:** frontiersin.org/about/contact

**REPRODUCIBILITY OF RESEARCH**
Support open data and methods to enhance research reproducibility

**DIGITAL PUBLISHING**
Articles designed for optimal readership across devices

**FOLLOW US**
@frontiersin

**IMPACT METRICS**
Advanced article metrics track visibility across digital media

**EXTENSIVE PROMOTION**
Marketing and promotion of impactful research

**LOOP RESEARCH NETWORK**
Our network increases your article's readership